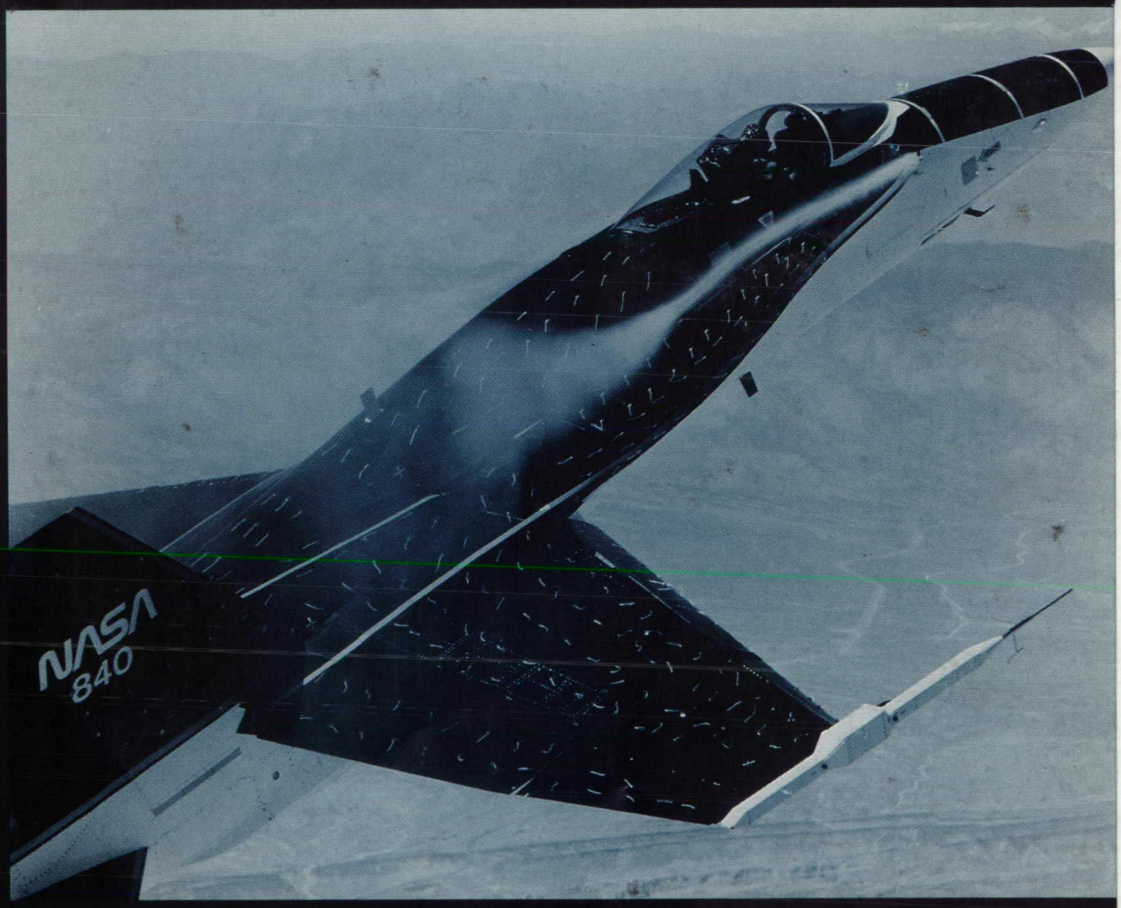
NASA-TM-103850

RESEARCH AND TECHNOLOGY 1990



(NASA-TM-103850) RESEARCH AND TECHNOLOGY, 1990 (NASA) 487 p
N92-33948
Unclas
G3/99 0115126

NASA

Ames Research Center

ORIGINAL PAGE
BLACK AND WHITE PHOTOGRAPH



Shown in flight at high angle of attack, the F-18 High Alpha Research Vehicle is one of many research programs at Ames Research Center.

Smoke is being emitted near the wing to highlight the vortical flows of air that buffet the vertical tails of the aircraft.
(See page 227.)

RESEARCH AND TECHNOLOGY 1990

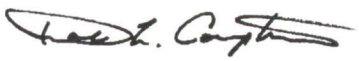
National Aeronautics and Space Administration
Ames Research Center, Moffett Field, California

Foreword

Each year, brief summaries of selected achievements at both the Ames-Moffett and Ames-Dryden sites of Ames Research Center are compiled as a NASA Technical Memorandum.

This year's report, Research and Technology 1990, presents some of the challenging work recently accomplished in the areas of Aerospace Systems, Flight Operations and Research, Aerophysics, and Space Research. Here, you can sample the scope and diversity of the research that is now being conducted and obtain a view of the stimulating research challenges of the future.

If you wish further information on any of the Ames research and technology programs, please call the number(s) at the end of each article.



DALE L. COMPTON
Director

ORIGINAL CONTAINS
COLOR ILLUSTRATIONS

Aerospace Systems Directorate

Page

Aircraft Technology Division

Assessing Tilt-Rotor Technology: A Total Logistics Cost Approach 1
Larry Alton

Potential Use of Tilt Rotor in Canadian Aviation 2
Larry Alton

The Civil Tilt-Rotor Aircraft's Potential in Developing Economies 3
Larry Alton

Infrared Imaging of STOVL Flow Fields for Computational Fluid Dynamics Code Validation 4
Larry Birckelbaw

UH-60 Optical Data Base Management System 5
M. Bondi

Tilt-Wing Simulation Study 6
L. Corliss

Reduced Takeoff Roll for Short Takeoff Transport Aircraft 7
Joseph C. Eppel

QSRA Controls and Display Experiments 8
J. Franklin, Joseph C. Eppel

Design Synthesis of High-Speed Transport Aircraft 9
Thomas L. Galloway, Paul Gelhausen

High-Speed Tilt-Rotor Feasibility Study 10
Thomas L. Galloway, David R. Schleicher

Aircraft Synthesis Program Institute 12
Paul Gelhausen

Modal Analysis of UH-60A Instrumented Rotor Blades 13
Karen S. Hamade, Robert M. Kufeld

Passive Chlorophyll Detector 15
Leonard Haslim, Paul McDonough

Biodegradable Deicing Fluids 16
Leonard Haslim, Paul McDonough

Blue Ice 17
Leonard Haslim, Paul McDonough

Electro-Expulsive Deicing System 18
Leonard Haslim, Paul McDonough

Safety Seat Cushion 19
Leonard Haslim, Paul McDonough

Puma Airloads Correlation 20
Francisco Hernandez

Multiple Instruction Multiple Data Parallel Processing 22
Gary Hill

Aerospace Systems Directorate (continued)

Page

Aircraft Technology Division (continued)

UH-60A Pressure Blade Calibration 23
B. Kufeld

UH-60A Flight Project Development 24
Paul Loschke

UH-60 Instrument Positioning System 25
Paul Loschke, M. Aoyagi

XV-15/Advanced-Technology Blades Flight Investigations 26
Martin Maisel, J. Brent Wellman

Improved Calculation of Sensitivity for Structural Parameter Identification 27
H. Miura, M. K. Chargin

V/STOL Aircraft Design Synthesis 28
Jim Phillips, Tom Galloway

Hypersonic Aircraft Geometry Modeling 29
Cathy Roberts, Jeff V. Bowles

High-Speed Rotorcraft Technology Studies 31
Peter D. Talbot

Investigation of Jet-Induced Effects in Hover 33
Douglas A. Wardwell, Daniel B. Levin, Demo J. Giulianetti

Acoustic Laboratory Data Acquisition System (ALDAS) 35
Michael Watts

Civil Tilt-Rotor Study 36
John Zuk

Full-Scale Aerodynamics Research Division

Full-Scale Tilt-Rotor Performance 37
Mike Derby

Fully Coupled Structural Deformations and Computational Fluid Dynamics 38
Fort Felker

Shadowgraph Flow Visualization of Rotor Wakes 39
Alexandra Frerking, Jeffrey Light

Computation of Rotor Aerodynamic Loads in Forward Flight 40
Ruth Heffernan

Dynamic Characteristics of Bell M412 Pylon and Model 576 Test Stand 41
Mohammed Hoque

Dynamic Characteristics of the Simulated Rotor Test Apparatus 43
Mohammed Hoque, Randy Peterson

Advanced Bearingless Rotor Research with Active Controls 45
Stephen Jacklin

Bell 412 Pressure/Acceleration-Instrumented Rotor 46
Stephen Jacklin

Aerospace Systems Directorate (continued)

Page

Full-Scale Aerodynamics Research Division (continued)

Individual Blade-Control Research Program 47
Stephen Jacklin

Real-Time Rotor Identification Methods 48
Stephen Jacklin

Study of Aeroelastic Problems Using Active Controls 50
Stephen Jacklin

System Identification of Rotor State Dynamics 51
Stephen Jacklin

Rotating Sensor Data for Rotor State Identification and Control 53
Stephen Jacklin, Ruth Heffernan, Mohammed Hoque

The Trailed-Rotor Concept in Cruise Configuration 55
Jeffrey Johnson, Stephen Swanson

Calculating Blade-Vortex-Interaction Aerodynamics and Noise by the Kirchoff Method 56
Cahit Kitaplioglu

Calculating Blade-Vortex Interaction by Navier-Stokes Procedures 57
Cahit Kitaplioglu

Small-Scale Study of Rotor Blade-Vortex Interaction Acoustics 59
Cahit Kitaplioglu

General Time-Domain Unsteady Aerodynamics of Rotors 60
Benton Lau

Soft Hub for Bearingless Rotors 61
Benton Lau

Lynx Helicopter Flight-Test Correlation 63
Benton Lau, Alex Louie

Panel Method Calculation of Tilt-Rotor Download 64
Johnson Lee

Comparison of Helicopter Vibration Controllers 65
Jane Leyland

Tait-Bryan Angles Required for Diagonalizing a Real Symmetric (3 × 3) Rank-Two Tensor 66
Jane Leyland

Scale Model (0.658) V-22 Rotor and Wing Performance 67
Jeffrey Light

Navier-Stokes Tilt-Rotor Download Research 68
Jeffrey Light

Rotor Blade Optimization in Hover 70
Jeffrey Light

Semispan Scale-Model V-22 Hover Download Test 71
Jeffrey Light, Alexandra Frerking

Helicopter Drag Reduction Program 72
Dan Martin

Direct Periodic Solutions of Rotor Free-Wake Calculations 73
Wayne Miller

Aerospace Systems Directorate (continued)

Page

Full-Scale Aerodynamics Research Division (continued)

Evaluation of Acoustic Model of Ducts 75
Marianne Mosher

Tilt-Rotor Aircraft Aeroacoustics 76
Marianne Mosher

Active Control to Alleviate Rotor-Blade Stall 77
Khanh Nguyen

Advanced Helicopter Rotor Analysis Code 78
Khanh Nguyen

Bearingless Rotor Correlation Study 80
Khanh Nguyen

Rotor Aeroelastic Response Analysis for Emergency Power Loss 81
Khanh Nguyen

Large-Rotor Test Apparatus Development 82
Tom Norman, Jeffrey Johnson

Rotorcraft Aerodynamic Interaction Program 84
Tom Norman, Gloria Yamauchi

Modern Four-Bladed Rotor Research in the 40- by 80-Foot Wind Tunnel 85
Tom Norman, Sesi Kottapalli, Jane Leyland

Rotorcraft Aeroelastic Stability Program 87
Randy Peterson, Benton Lau

Light Helicopter Risk Reduction and Demonstration/Validation Program 88
Randy Peterson, Larry Young

Testing of Large Ram-Air-Inflated Wings 89
James C. Ross

Short Takeoff and Vertical Landing CFD Validation Studies 91
Karlin R. Roth

Modern Four-Bladed Rotor Research in the 80- by 120-Foot Wind Tunnel 93
Patrick Shinoda

Correlation of Measured Tail-Rotor Acoustics with ROTONET Predictions 94
David Signor, Martin Hagen

Steady/Dynamic Rotor Balance for the Ames Rotor Test Apparatus 96
David Signor, Johannes M. van Aken

In-Flight Rotorcraft Acoustics Program 97
David Signor, Gloria Yamauchi, Marianne Mosher

Results of Full-Scale Testing of E-7A Ejector-Lift, Vectored-Thrust Aircraft 98
Brian Smith

Aerodynamic Interaction between Vortical Wakes and Lifting Two-Dimensional Bodies 100
Paul Stremel

Direct Solution of the Velocity-Vorticity Formulation 101
Paul Stremel

Aerospace Systems Directorate (continued)

Page

Full-Scale Aerodynamics Research Division (continued)

Zonal Flow Analysis Method 102
Paul Stremel

Stopped Rotor/Disk High-Speed Rotorcraft Research 103
Stephen Swanson, Robert Stroub

Tilt-Rotor Whirl-Flutter Alleviation 105
Jan van Aken

Stability Analysis of Tilt Rotors in the National Full-Scale Aerodynamics Complex 106
Jan van Aken, Ruth Heffernan

Particle Image Velocimetry Applied to Rotor Aerodynamics 107
Alan J. Wadcock

Tilt-Rotor Aeroacoustic Model Research Program 108
Larry Young

Information Sciences Division

Approximate Reasoning-Based Intelligent Control 109
Hamid Berenji

Principal Investigator in a Box 110
Silvano Colombano, Irving Statler, Mike Compton

Advanced Automation: An Assessment of Processing Requirements 112
Gloria Davis

Integrated Planning, Scheduling, and Control 113
Mark Drummond

Control Systems Group Summary 115
Brian Glass

Optical Image Processing and Control 116
Charles Jorgensen

Optimization of Multiprocessor Computing 117
Charles Jorgensen

Scientific Modeling Assistant Project 118
Richard M. Keller, Michael H. Sims

GEMPLAN/COLLAGE Multi-Agent Planning Systems 120
Amy Lansky, Andrew Philpot

Comparison of Microprocessors for Space Station Freedom 122
Yuan-Kwei Liu

Fault-Tolerant Systems 123
F. Ann Patterson-Hine, David L. Iverson

Photonics and Optical Processing 124
Max Reid

Parallel Systems Research 125
Nancy Sliwa

Aerospace Systems Directorate (continued)

Page

Information Sciences Division (continued)

Differential Thermal Analyzer: Gas Chromatograph Autonomous Controller 126
David E. Thompson, Deepak Kulkarni, Richard Levinson

Space Shuttle Ground Processing Scheduling 127
Monte Zweben

Aerospace Human Factors Research Division

Learning Receptor Positions 128
Albert J. Ahumada, Jr.

Networks for Image Acquisition, Processing, and Display 129
Albert J. Ahumada, Jr., Andrew B. Watson

Geographical Orientation 130
Vernol Battiste

Human-Centered Aircraft Automation Philosophy 131
Charles E. Billings, E. James Hartzell

Traffic-Alert Collision Avoidance System 132
Sheryl L. Chappell, Charles E. Billings

Space Habitability Research Program 133
Yvonne A. Clearwater, E. James Hartzell

Circadian Rhythms and Performance of Flight Crews 134
Linda J. Connell, E. James Hartzell

Perspective Displays to Aid in Low-Visibility Curved Approaches 135
Nancy S. Dorighi, Stephen R. Ellis

Integrated Rendezvous and Proximity-Operations Displays 136
Stephen R. Ellis

Virtual Interactive Environment Workstation 137
Stephen R. Ellis, Michael W. McGreevy

Human Performance Issues with Sensor Imagery 138
David C. Foyle, Mary K. Kaiser

Innovative Flight Training Methods 139
Sandra G. Hart

Pilot Behavior and Workload Management Program 140
Sandra G. Hart

Knowledge Organization and Information Transfer Research 141
E. James Hartzell

Visual Flight-Path Control Research 142
Walter W. Johnson, C. T. Bennett

Crew Factors beyond the Flight Deck 143
Barbara G. Kanki, E. James Hartzell

Crew Factors in Aircrew Performance 144
Barbara G. Kanki, E. James Hartzell

Aerospace Systems Directorate (continued)

Page

Aerospace Human Factors Research Division (continued)

Crew Resource Management Research 145
Barbara G. Kanki, E. James Hartzell

Socio-Organizational Influences on Team Performance 146
Barbara G. Kanki, E. James Hartzell

Image Fusion 147
James O. Larimer

Modeling of Cockpit Display Visibility 148
James O. Larimer

Filling in the Retinal Image 149
James O. Larimer, Jennifer Gille

Information Management and Transfer 150
Sandra C. Lozito, Sheryl L. Chappell

Visualization for Planetary Exploration 151
Michael W. McGreevy

Optimal Image Combination Rules for Heads-Up Display 152
Jeffrey B. Mulligan

Flight Management System Human Factors 153
Everett A. Palmer, Sheryl L. Chappell

Error-Tolerant Cockpit Systems 154
Everett A. Palmer, Asaf Degani

Development of a Touch-Panel Operated Electronic Checklist 155
Everett A. Palmer, Asaf Degani

Human Factors of Flight-Deck Checklists: The Normal Checklist 156
Everett A. Palmer, Asaf Degani

Human Factors of Advanced Technology Transport Aircraft 157
Everett A. Palmer, E. James Hartzell

Process Measures of Pilot Behavior: Methods and Tools 158
Everett A. Palmer, E. James Hartzell

Computational Models of Human Cognition: Modeling the NASA Test Director 159
Roger W. Remington

Aviation Safety Reporting System 160
William D. Reynard, E. James Hartzell

Individual Crew Factors in Flight Operations: In-Flight Sleep 162
Mark R. Rosekind

Pilot Decision-Making 163
Robert J. Shively

Army-NASA Aircrew/Aircraft Integration Program 164
Barry R. Smith

Aviation Display Design 166
Barry R. Smith

Dynamic Anthropometric Modeling 167
Barry R. Smith

Aerospace Systems Directorate (continued)

Page

Aerospace Human Factors Research Division (continued)

Symbolic Operator Model 168
Barry R. Smith

Visibility Modeling Tool 169
Barry R. Smith

Motion Processing in Man and Machine 170
Andrew B. Watson

Perceptual Components Architecture 171
Andrew B. Watson

Pyramid Image Codes 172
Andrew B. Watson

Three-Dimensional Auditory Display Systems 173
Elizabeth M. Wenzel

Flight Systems and Simulation Research Division

An Exact Linear-Error Attitude Control Law 175
Ralph Bach, Jr., Russell Paielli

Field-Based Passive Ranging Using Matched Velocity Filters 176
Yair Barniv

Obstacle-Avoidance Guidance and Control 177
Victor Cheng

Automatic Nap-of-the Earth Flight Simulation 179
Richard A. Coppenbarger

Final Approach Spacing Tool 181
Tom Davis, Heinz Erzberger, Chris Brinton

Civil Tilt-Rotor Airworthiness Criteria 182
W. Decker

Design of Automation System for Terminal-Area Air Traffic Control 183
Heinz Erzberger

RASCAL In-Flight Simulator 185
M. Eshow, J. V. Lebacqz, D. C. Watson, W. Hindson

Control Research on the V/STOL Research Aircraft 186
John D. Foster

Control-System Concepts and Design Criteria for STOVL Aircraft 188
J. Franklin

Four-Dimensional Aircraft/Air Traffic Control Operations Study 189
Steven Green

Terminal-Area Operations with the NAVSTAR Global Positioning System 191
B. David McNally, Thomas Schultz

Display and Guidance Improvements for AV-8B Harrier 193
Vernon Merrick, Ernesto Moralez

Aerospace Systems Directorate (continued)

Page

Flight Systems and Simulation Research Division (continued)

Optimal Scheduling/Sequencing of Aircraft Traffic 195
Frank Neuman

In-Flight Display Research for Hovering and Landing 197
Jeffery A. Schroeder, Vernon K. Merrick

Validation of Vision-Based Obstacle-Detection Algorithms Using Flight Data 199
Phillip Smith, Banavar Sridhar

Integrated Stereo/Motion Vision for Obstacle Detection 201
Banavar Sridhar, Ray Suorsa

Laboratory for Vision-Based Detection Research 203
Raymond Suorsa, Banavar Sridhar

Computer Aiding for Low-Altitude Helicopter Flight Project 205
Harry N. Swenson

Rotorcraft Flight-Control Design Methods 207
Marc D. Takahashi

Rotorcraft System Identification 208
Mark B. Tischler

Helicopter Stick Dynamics Investigations 209
D. Watson, J. Schroeder

Helicopter Yaw Response Requirements 210
Matthew S. Whalley

Separation of Turbulence and Maneuver Loads from Airline Flight Records 212
R. C. Wingrove, R. E. Bach, Jr.

Dryden Flight Research Facility Directorate

Page

Research Engineering Division

F-16XL Supersonic Laminar Flow Control Research 215
Bianca T. Anderson

Propulsive Techniques for Emergency Control 217
Frank W. Burcham, Glenn B. Gilyard

Flight-Test Results of the X-29A at High Angle of Attack 218
Robert Clarke

Thermoelastic Vibration Testing 220
Michael W. Kehoe

Pegasus "Add-On" Hypersonic Flight Experiments 222
Greg Noffz, Robert Curry

Advanced Multidisciplinary Analysis 224
Kevin L. Petersen, Kajal K. Gupta

F-18 High Angle-of-Attack Research Vehicle Vortex Flow Field Results 227
David M. Richwine, David F. Fisher

Computer-Aided Systems Testing 229
Joel R. Sitz

Western Aeronautical Test Range Color-Alphanumeric Panel Display Processing System 231
James Skultety

Scientific and Technical Electronic Publishing System 233
Gene Waltman

Western Aeronautical Test Range Shared Memory System 235
Duane Wheaton

Aerophysics Directorate

Page

Aerodynamics Division

Navier-Stokes Simulation of Flow Through a Highly Contoured Diffuser Inlet 237
Wei J. Chyu, Daniel P. Bencze

Sonic Boom Pressure Signature Computations Using Euler Codes 239
Susan E. Cliff-Hovey

Aircraft Aerodynamics Using Solution-Adaptive Unstructured Grids 241
Jahed Djomehri, Larry Erickson

Euler Computations of a Generic Fighter 243
Aga M. Goodsell

Sonic Boom Prediction Using TranAir 245
Michael D. Madson

Unstructured Euler Flow Solutions Using Hexahedral Cell Refinement 247
John E. Melton, Scott D. Thomas, Gelsomina Cappuccio

Computation of Induced Drag for Elliptical and Crescent-Shaped Wings 248
Stephen C. Smith

Fluid Dynamics Division

Three-Dimensional Laser Doppler Velocimeter for Supersonic Turbulent Flows 250
James L. Brown

Finite-Difference Algorithms for Computational Acoustics 251
Sanford Davis

Separating Flow Study 253
Dave Driver

Turbulence Modeling Near Solid Boundaries 254
Paul Durbin

Nonlinear Sonic Boom Prediction Method 255
Thomas A. Edwards

Aeroelastic Responses Associated with Vortical Flows 256
Guru P. Guruswamy

Laser Doppler Velocimeter for Three-Dimensional Near-Surface Measurements 258
Dennis Johnson

Structure of the Turbulent Separated Flow Behind a Backward-Facing Step 260
Srba Jovic

Three-Dimensional Instability of Rotating Flows with Oscillating Axial Strain 261
N. Mansour

Simultaneous Temperature and Density Measurements in Air Using Laser-Induced Fluorescence 262
Robert McKenzie

Transition to Turbulence in a Mixing Layer 263
Robert D. Moser, Michael M. Rogers

Computational Fluid Dynamics Impact on Turbomachinery Design 265
A. A. Rangwalla

Aerophysics Directorate (continued)

Page

Fluid Dynamics Division (continued)

Computational High-Alpha F-18 Aerodynamics 266
Yehia Rizk, Ken Gee, Lewis B. Schiff

Pre-Processor for Three-Dimensional Elliptic Grid Generation 267
Reese L. Sorenson

Computational Study of Pneumatic Forebody Flow Control 268
Domingo Tavella, Ken Gee, Lewis B. Schiff

An Efficient Supersonic Wind Tunnel Drive System for Mach 2.5 Flows 269
Stephen W. D. Wolf, James A. Laub, Lyndell S. King

Efficient Algorithm for Viscous Incompressible Flows 271
Seokkwan Yoon, Dochan Kwak

Thermosciences Division

A Three-Dimensional Self-Adaptive Grid Code 272
Carol Davies, Ethiraj Venkatapathy

Direct Particle Simulation of Coupled Vibration-Dissociation 274
Brian L. Haas, Iain D. Boyd, Donald Baganoff, William J. Feiereisen

Low-Density Silica Fiber Ablators 276
William D. Henline

Nonequilibrium Hydrogen-Air Reaction in Nozzle Recombination 278
Seung-Ho Lee, John Cavolowsky

Very-High-Temperature Heat Shield Material Development 280
Daniel J. Rasky

Prediction of Hydrogen Recombination Rates 282
David Schwenke

Measurements of Relaxation Rate Parameters in a Shock Tube 284
Surendra Sharma

Computational Analysis of Plume-Induced Separation 286
Ethiraj Venkatapathy

Space Research Directorate

Page

Advanced Life Support Division

Characterizing Crop Plan Performance for Regenerative Life Support Technology 287
David Bubenheim

Hydrocarbon Contamination on Polytetrafluoroethylene Exposed to Oxygen Atoms 289
Morton Golub, Ted Wydeven

Benefits of Recycling (Loop Closure) in a Space Habitat 291
Mark Hightower

A Fiber-Optic-Based Total Organic Carbon Sensor 294
John W. Hines, Jeff Roe, Christopher Miles

Salad Machine: A Vegetable Production Unit for Long-Duration Space Missions 295
Mark Kliss, Bob MacElroy

Life Support Database System 298
William E. Likens

A Direct Interface Fusible Heat Sink for Astronaut Cooling 300
Curtis Lomax

An Experimental and Computational Study of Unsteady Facilitated Transport 301
Ted Wydeven, Alicia Yum, Sanford Davis

Space Projects Division

High Purity GaAs as a Far-Infrared Photoconductor 302
Jam Farhoomand

Compressed Video for Remote Animal Monitoring 303
Robert W. Jackson, Richard F. Haines

Space Qualified ^{3}He Cooler 304
Peter Kittel

Low-Background and Radiation Environment Evaluation of Infrared Detector Arrays 305
Mark McKelvey

Biological Research Laboratory for Space Station Freedom 306
Joel Sperans, Roger D. Arno, John J. Givens

Earth System Science Division

Pilot Land Data System 308
Gary Angelici, L. Popovici, Jay Skiles, C. Wong

A Cryogenic Absorption Cell for Gas Phase Spectroscopy 309
Charles Chackerian, Jr., James E. McGee

Computer Simulations Help Unravel Origins of Tropospheric Ozone Hill 310
Robert Chatfield

Boundary Delineation of Agricultural Lands by Graphics Workstations 311
Tom Cheng , Robert Slye, Matt Ma, Gary Angelici

Space Research Directorate (continued)

Page

Earth System Science Division (continued)

Remote Sensing and Paleoecology 313
Hector D'Antoni

Airborne Arctic Stratospheric Expedition Results 315
Steve Hipskind, Estelle Condon

Estimating Regional Carbon Flux in High Latitude Ecosystems 316
Gerald Livingston, Leslie A. Morrissey, James R. Podolske

Contributions of Tropical Forests and Land Use Change to Global Nitrous Oxide Emissions 318
Pamela Matson, Carol Volkmann, Tina Billow

Remote Sensing of Canopy Chemistry and Herbivory in Mangrove Forests 319
David L. Peterson, Roy A. Armstrong

Regional Extrapolation of Ecosystem Models of Evapotranspiration and Net Primary Production 320
David L. Peterson, Jennifer Dungan

Advanced Technology for Remote Sensing the Biochemical Content of Plant Canopies 321
David L. Peterson, Scott G. Hubbard

Oregon Transect Ecosystem Research Project 322
David L. Peterson, Michael A. Spanner, Pamela A. Matson, Lee Johnson, Gary Angelici, Jay Skiles, Jennifer Dungan, Tina Billow

NASA Remote Sensing Links Dinosaur Extinction to Asteroid Impact 324
Kevin O. Pope, Adriana C. Ocampo, Charles E. Duller

Advanced Aircraft for Earth Science 325
Philip B. Russell, Max Loewenstein, Steven Wegener

Remote Sensing Data Prove Useful for Disease Vector Modeling 326
Joan S. Salute, Byron L. Wood

Airborne Tropospheric Chemistry Studies 327
Hanwant B. Singh

Telescience as a Tool for ER-2 Investigators 328
Steven S. Wegener

Modeling Forest Fire Smoke Plumes 329
Douglas L. Westphal, Owen B. Toon

Advanced Automation of Mass Spectrometric Systems for Life Support Systems 331
Carla M. Wong, Peter T. Palmer

Search for Extraterrestrial Intelligence Office

Implementation of Signal Processing Algorithms in the Search for Extraterrestrial Intelligence 332
D. Kent Cullers, Peter Backus

Space Research Directorate (continued)

Page

Life Science Division

Gravitational Effects on Regional Distribution of Calcium in the Adult Human Skeleton 333
Sara Arnaud

Perceptual and Behavioral Adaptation to Altered Gravitational-Inertial Forces 335
M. M. Cohen, R. Welch

Autogenic-Feedback Training: Countermeasure for Orthostatic Intolerance 338
P. Cowings

Autogenic-Feedback Training: Preventing Space Motion Sickness on SL-J 339
P. Cowings

Autogenic-Feedback Training: Aid to Cockpit Peak Performance 340
P. Cowings

Investigating Neural Adaptation to Altered Gravity 341
N. Daunton, F. D'Amelio, R. Fox, M. Corcoran, M. Ross, L-C. Wu

Astronaut Rehydration Fluid Formulations 343
J. Greenleaf, L. Keil

Exercise as a Countermeasure of Muscle Wasting in Long-Term Hindlimb Suspension 346
R. Grindeland

Physiologic Mechanisms of Fluid Shifts in Humans During Acute, Simulated Microgravity 348
A. R. Hargens, S. E. Parazynski, M. Aratow

Lower Body Negative Pressure Provides Load Bearing for Humans Exposed to Microgravity 349
A. R. Hargens, R. T. Whalen, D. E. Watenpaugh, G. Murthy, D. F. Schwandt

Gravity and Skeletal Growth 350
E. Morey-Holton

Effects of 24 Hours of Reloading on Bone Metabolism after 6 or 11 Days of Hindlimb Unloading 351
E. Morey-Holton, C. Cone, D. Bikle

Neurocomputer Development Based on Experimental Data at the Vestibular Research Facility 352
A. J. Pellionisz, D. L. Tomko

Biological Neural Networks as a Basis for Improved Computer Technology and Chip Design 354
M. Ross

The Role of Visual-Vestibular Interactions in the Perception of Motion 355
L. Stone

Gravity Receptor Physiology Research at the Vestibular Research Facility 356
D. L. Tomko

Vestibular Research Facility for Ground-Based Studies 357
D. L. Tomko, T. Wynn

Postflight Fainting, Blood Pressure Control, and Countermeasures 358
Joan Vernikos

Adaptation to Altered Gravito-Inertial Environments 359
R. Welch, M. M. Cohen

Space Research Directorate (continued)

Page

Life Science Division (continued)

Influence of Physical Activity Level on Bone Density 360
R. Whalen, T. Tamanaha, T. Hutchinson

Musculoskeletal Loading with Lower Body Negative Pressure 361
R. T. Whalen, A. R. Hargens, D. E. Watenpaugh, D. F. Schwandt

Space Life Sciences Payloads Office

Characterization of Neurospora Circadian Rhythms Experiment 363
Randy Berthold

Growth Hormone Concentration and Distribution in Plants 364
Randy Berthold

Spacelab Life Sciences-1: 1990 Events 365
Bonnie P. Dalton

Space Science Division

Astrophysical Simulation and Analysis Facility 366
Louis Allamandola, Farid Salama, Scott Sandford, William Schutte, Robert Walker

Search for Planet Formation Debris Signatures 368
Dana E. Backman, Fred C. Witteborn

Detection of Nanophase Lepidocrocite in Iron-Smectite Mars Soil Analog Materials 370
Amos Banin, David F. Blake

Global Properties of the Heliosphere 372
A. Barnes, P. Gazis, J. Mihalov

Plasma Environment of Venus 374
A. Barnes, P. Gazis, J. Mihalov

Stable Isotope Analysis Using Tunable Diode Laser Spectroscopy 375
Joe Becker, Todd Sauke

Phase Relationships in Low-Temperature Mixed Ices 376
David Blake, Louis J. Allamandola

Robotic Telescope Search for Other Planetary Systems 378
William J. Borucki

Search for Venusian Lightning 379
William J. Borucki, John W. Dyer, James R. Phillips, Phan Pham

Long Duration Exposure Facility Post-Retrieval Evaluation of Exobiology Interests 380
T. E. Bunch

Polycyclic Aromatic Hydrocarbon Molecules around Evolved Stars 382
Richard H. Buss, Jr., Alexander Tielens

Sedimentary Records of Atmospheric O_2 Levels 384
D. E. Canfield

Sulfate Reduction in Modern and Ancient Sediments 385
D. E. Canfield, D. J. Des Marais

Space Research Directorate (continued)

Page

Space Science Division (continued)

High Molecular Weight Polycyclic Aromatic Hydrocarbons and Fullerenes in Carbonaceous Meteorites 387
Sherwood Chang, Etta Peterson

Organic Material on Solar System Bodies 390
Dale Cruikshank

Particle Gas Dynamics in the Protoplanetary Nebula 391
Jeffrey N. Cuzzi

Planetary Ring Dynamics and Morphology 392
Jeffrey N. Cuzzi

Microbial Mats, Stromatolites, and the Rise of Molecular Oxygen in Earth's Early Atmosphere 394
David J. Des Marais

Planetary Protection Issues and the Future Exploration of Mars 396
Don L. DeVincenzi

Far Infrared Emission from the Galactic Center Filaments 397
Ed Erickson, Sean Colgan, Jan Simpson

Stratospheric Observatory for Infrared Astronomy 399
Ed Erickson, Ted Dunham, Jackie Davidson

Exobiology Intact Capture Experiment 401
Mark Fonda, Glenn Carle

Olivine—Surprises from Below the Continents 402
Friedemann Freund, Minoru M. Freund, François Batllo, Rodney C. LeRoy

Schroedinger's Radial Equation: Solution by Extrapolation 404
David Goorvitch, David C. Galant

Molecular and Atomic Shocks in the Interstellar Medium 405
Michael R. Haas, Ed Erickson, David J. Hollenbach

Mars Climate Studies 407
Robert M. Haberle

Evolution of the ATP Synthase Complex 408
Lawrence Hochstein, Helga Stan-Lotter

Center for Star Formation Studies 410
David Hollenbach

Small-Particle Research on Space Station Freedom 411
Judith Huntington, David Stratton, Mark Fonda

An Isotopic Signature of Carbon Cycling in Paleoenvironments 413
Linda L. Jahnke, Roger E. Simmons, David J. DesMarais

Prebiotic Polynucleotide Synthesis: Hot or Cold? 414
Anastassia Kanavarioti, Sherwood Chang

Use of the Shuttle External Tank as a Gamma-Ray Imaging Telescope 416
David G. Koch

Small Explorer Mission to Measure Chemical Species Important in Star Formation Processes 417
David G. Koch, David Hollenbach

Space Research Directorate (continued)

Page

Space Science Division (continued)

Microvolume Metastable Ionization Detector for Analyzing Planetary Atmospheres 418
Dan Kojiro, Fritz Woeller, Nori Takeuchi, Don Humphry

Severe Downslope Windstorms on Mars 419
Julio A. Magalhães, Richard E. Young

Biomarkers and the Search for Extinct Life on Mars 420
Rocco Mancinelli, Lisa White

Definition of Exobiology Experiments for Future Mars Missions 421
Rocco Mancinelli, Lisa White

Wind Tunnel Experiments Enable Prediction of Magellan Spacecraft Findings 424
John R. Marshall

Titan's Atmosphere 425
Christopher P. McKay, James B. Pollack, Jonathan I. Lunine, Régis Courtin

Impact Constraints on the Environment for Chemical Evolution and the Continuity of Life 426
Verne R. Oberbeck, Guy Fogleman

Prebiotic Chemistry in Clouds 427
Verne R. Oberbeck, John Marshall, Thomas Shen

Comet Ice and Dust Gas Chromatograph Instrument 428
Bonnie O'Hara

Spectroscopy and Reactivity of Mineral Analogs of Martian Soil 429
Jim Orenberg, Ted Roush

Cavities in Liquids and Hydrophobic Solubilities 431
Andrew Pohorille, Lawrence R. Pratt

Development of the Mid-Infrared Spectrometer for the Infrared Telescope in Space 432
T. L. Roellig

Evolution of Biological Carbon Fixation and the Search for Life on Mars 433
Lynn J. Rothschild

Experimental Study of Aerosol Formation in Titan's Atmosphere 434
Thomas W. Scattergood

Mineral Crystals as Biomarkers in the Search for Life on Mars 436
Deborah E. Schwartz, Rocco L. Mancinelli

Silicone Gas Chromatographic Column Development 437
Thomas Shen

A Planetary Rings Data Center 440
Mark R. Showalter, Jeffrey N. Cuzzi

Mineralogy of Mercury, the Moon, and Asteroids 441
Ann L. Sprague

Physics of the Lunar Alkali Atmosphere 442
Ann L. Sprague

Telepresence for Planetary Exploration 443
Carol Stoker, Michael McGreevy, Christopher McKay, Owen Gwynne

Space Research Directorate (continued)

Page

Space Science Division (continued)

Science Strategy for Human Exploration of Mars 445
Carol Stoker, Christopher McKay, Robert Haberle, Owen Gwynne

An Instrumentation Technique to Measure Water Vapor in the Martian Atmosphere 446
José Valentin, Kirsten Hall, John Phillips

Galileo Mission to Jupiter 448
Richard E. Young

Xenon Fractionation in Porous Planetesimals 449
Kevin Zahnle, James B. Pollack, James F. Kasting

Appendix

Color Plates 451

Assessing Tilt-Rotor Technology: A Total Logistics Cost Approach

Larry Alton

The feasibility and competitive potential of tilt-rotor aircraft technology in the short-haul passenger transportation market is studied through optimization of transport systems combining tilt-rotor and turboprop service. A total logistics cost function whose arguments are tilt-rotor frequency, turboprop frequency, tilt-rotor market shares, and, in one case, the number of vertiports, is used.

When the system involves one center city vertiport and one airport at the city periphery, total cost may be minimized when the tilt-rotor market share is either greater than 50% or zero. Conditions when the tilt rotor is definitely feasible and definitely infeasible are represented by functional relationships between (1) the difference in per-seat aircraft operating cost and the ratio of per-flight aircraft operating cost, and (2) the parameters which reflect the size of the market, traveler valuations of the cost of airport/vertiport access, and traveler valuations of time spent waiting for flights. Curves relating optimal tilt-rotor market share to tilt-rotor per-seat operating cost exhibit discontinuities as the optimum shifts from exclusive tilt-rotor service, to mixed service, to exclusive turboprop service.

When multiple vertiports are allowed, the optimum number is almost always 10 or less and, for most markets, less than 4. However, the total logistics cost is fairly insensitive to the number of vertiports, so long as frequencies at any given number are set to their optimum values. Even under extreme conditions, when the optimum number of vertiports is 16, the multiple vertiport system market share is, in most cases, only marginally greater than that of a system involving just one vertiport.

However, the multiple vertiport system is better able to compensate for constraints on tilt-rotor aircraft size. This is particularly important because the sizes receiving the most consideration are smaller than what would be optimum for markets of several hundred passengers or more. If at all possible, however, the nominal civil tilt-rotor aircraft should be increased in size and be "stretchable" in order to reduce total aircraft operating cost.

Ames-Moffett contact: L. Alton
(415) 604-5887 or FTS 464-5887
Headquarters program office: OAET

Potential Use of the Tilt Rotor in Canadian Aviation

Larry Alton

This investigation describes the aviation system in Canada as it relates to the potential applicability of tilt-rotor aircraft technology and infrastructure characteristics. Commuter service in two corridors, the Vancouver-Victoria route on the west coast and the heavily traveled Montreal-Toronto corridor in eastern Canada, are examined.

The operation of air service from the near-downtown Toronto STOLport and from the Victoria-Vancouver downtown heliport facilities are studied. The emergency medical services, search and rescue, and natural resources development sectors are described with regard to the needs that tilt-rotor technology could uniquely meet in these areas. The airport construction program in isolated communities of northern Quebec and possible tilt-rotor service in northern regions are reviewed.

The federal and provincial governments' financial support policy regarding the aeronautical industry is to encourage the establishment and expansion of businesses in the field of aeronautics and to make possible the acquisition of new technology. This policy has implications for the tilt-rotor program. The tilt rotor's speed, range, all-terrain accessibility, noise characteristics, and infrastructure requirements offer significant advantages in Canada.

Ames-Moffett contact: L. Alton
(415) 604-5887 or FTS 464-5887
Headquarters program office: OAET

The Civil Tilt-Rotor Aircraft's Potential in Developing Economies

Larry Alton

The operational demonstration of tilt-rotor technology by the Bell-Boeing V-22 Osprey team for the U.S. military in 1989 aroused worldwide interest throughout the civilian aviation community. Combining the speed and safety of fixed-wing airplanes with the landing and takeoff flexibility of helicopters, this new technology appears to have the potential of revolutionizing the air transportation services industry.

The civil tilt rotor is analyzed as a new transportation technology with the potential for changing one of the key economic factors linked to third world economic development. It is contended that (1) efficient, and lower cost, transport services are a necessary, but not sufficient, condition for the economic development of third world countries, and (2) the civil tilt-rotor (CTR) technology capabilities and operating costs can provide improved, and lower cost, transport services than have heretofore been available to third world countries. It is also argued that a case study of potential CTR use among the nations of the Caribbean Basin region appears to offer both analytical and empirical support to these contentions.

Analysis indicates that normal market mechanisms are adequate for developing air cargo services using the CTR's capabilities. The separation of benefits and costs involved in CTR air passenger service, however, may require new institutional arrangements if its widespread adoption is to occur.

Tilt-rotor technology could make an important contribution to the economic development of third world countries. Whether this contribution occurs, however, depends largely on creating necessary political and institutional arrangements and adapting international barriers to travel and commerce (such as customs and immigration procedures) to the CTR's potential.

Ames-Moffett contact: L. Alton
(415) 604-5887 or FTS 464-5887
Headquarters program office: OAET

Infrared Imaging of STOVL Flow Fields for Computational Fluid Dynamics Code Validation

Larry Birckelbaw

During takeoff, landing, and hover, the vectored engine exhaust jets of vertical takeoff and landing (VTOL) and short takeoff and vertical landing (STOVL) aircraft undergo complicated interactions with both the ground and the aircraft surfaces. These interactions can create a number of effects that are detrimental to the aircraft and the runway surface. These include a dramatic loss of lift at low altitude (known as "suck-down"), a loss of engine thrust owing to reingestion of hot exhaust gases, potential engine damage resulting from the ingestion of foreign objects made airborne by the exhaust jet energy, excessive heating of the airframe, and damage to the runway surface by the hot, high-velocity impinging jet.

Work is under way at Ames Research Center to model exhaust jet flow fields using advanced computational fluid dynamics (CFD) codes. In one effort, a Navier-Stokes solution for the complete flow field about a Harrier YAV-8B in a typical landing approach configuration is being obtained.

Before these advanced CFD methods can be employed to design future advanced VTOL or STOVL configurations, it is necessary to validate the codes using experimentally obtained data. However, because of the scale and complexity of the flow fields about VTOL and STOVL aircraft, it is not practical to obtain sufficient validation data using conventional wind-tunnel or flight-test instrumentation techniques.

Infrared (IR) imaging provides a means of obtaining large amounts of detailed data about these flow fields in a totally non-intrusive manner. Real-time flow-field images with sufficient detail to resolve both the small-scale flow structures and the surface heating effects have been obtained by using a dual-wavelength infrared scanning system. These infrared images provide qualitative insight into the basic nature of the flow field.

Efforts are under way to develop IR enhancement techniques that will permit a quantitative infared image temperature comparison with the CFD-predicted flow-field temperatures. These efforts are being conducted as part of a cooperative grant with Virginia Polytechnic Institute. Initially, a small-scale proof-of-concept hot-jet test was conducted to compare thermocouple temperature measurements with enhanced IR image temperature data. The favorable comparisons of the temperature data demonstrated the feasibility of the enhancement technique. Further refinements of the procedure are under way, and will result in improved accuracy and speed.

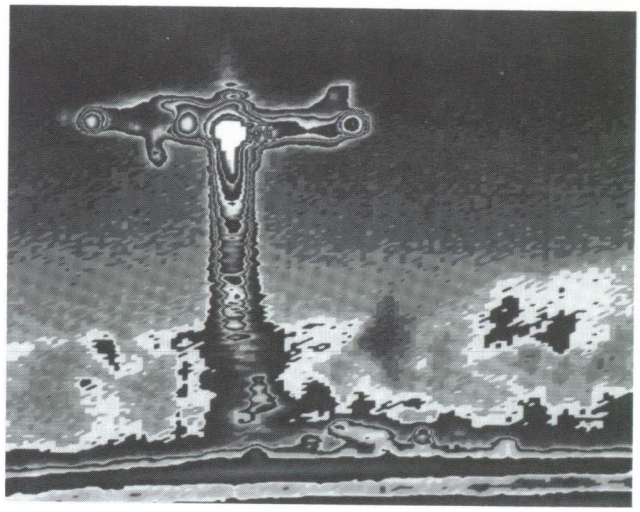


Fig. 1. Infrared image of YAV-8B Harrier in hover (see color plate 1 in Appendix)

Initial IR imaging of the Ames YAV-8B Harrier is presented in the figure, which shows the potential capability of the method. An extensive infrared imaging test of the YAV-8B is planned for the summer of 1991. Infrared data will be recorded while the Harrier performs a variety of landing, takeoff, and hover maneuvers. These maneuvers will be viewed both from a ground-based position and from a hovering helicopter. This test will provide CFD validation data for both the jet flow field about the Harrier and the resulting runway heating.

Ames-Moffett contact: L. Birckelbaw
(415) 604-5042 or FTS 464-5042
Headquarters program office: OAET

UH-60 Optical Data Base Management System

M. Bondi

A NASA engineer sits at his terminal and types a few short lines. In seconds his screen displays plots of flight-test data for one test point selected from a massive data base covering many flights. He types a few more lines and is presented a spectral analysis of a function of several variables. He sees a result that confirms his hunch about the effect of rotor-induced vibration.

To check the result, he runs the same analysis for another test point from a different flight. He calls a colleague at Princeton University to tell him about it. The colleague logs onto the Ames computer via a modem and views the same results on his screen, then checks them for other test points. Meanwhile, other engineers are investigating different aspects of the same and other data bases, using the same tools—TRENDS (Tilt Rotor Engineering Data Management System) and the new laser-optical jukebox.

This scenario is reality at Ames today. A state-of-the-art optical data-base management system has been developed specifically for the UH-60 Rotor Airloads Program, but it will have broader applications in the future.

The UH-60 Airloads Project engineers have been provided unassisted, interactive, and immediate access to approximately 50 gigabytes of UH-60 data, while still allowing further TRENDS support of another 30 gigabytes for other data bases. The optical jukebox system can store 134 laser-optical disks and has four disk drives providing very high density storage/unit volume. It is about the same size but a little taller than a normal four-drawer file cabinet (see the figure). The productivity of the system is enhanced by the caching of disk data onto a magnetic disk automatically, thereby allowing the four optical disk drives to service 8 or even 12 users, essentially simultaneously. Each 5 1/4-inch laser-optical disk has a capacity of 600 megabytes of write-once-read-many (WORM) storage. It is believed that this jukebox system is state of the art and the most useful in the marketplace today because of its totally VMS (Virtual Memory System) transparency. The jukebox system was developed by Computer Upgrade Corporation of Anaheim, California. It uses Mitsubishi jukebox hardware with software from KOM, Inc. of Ottawa, Canada.

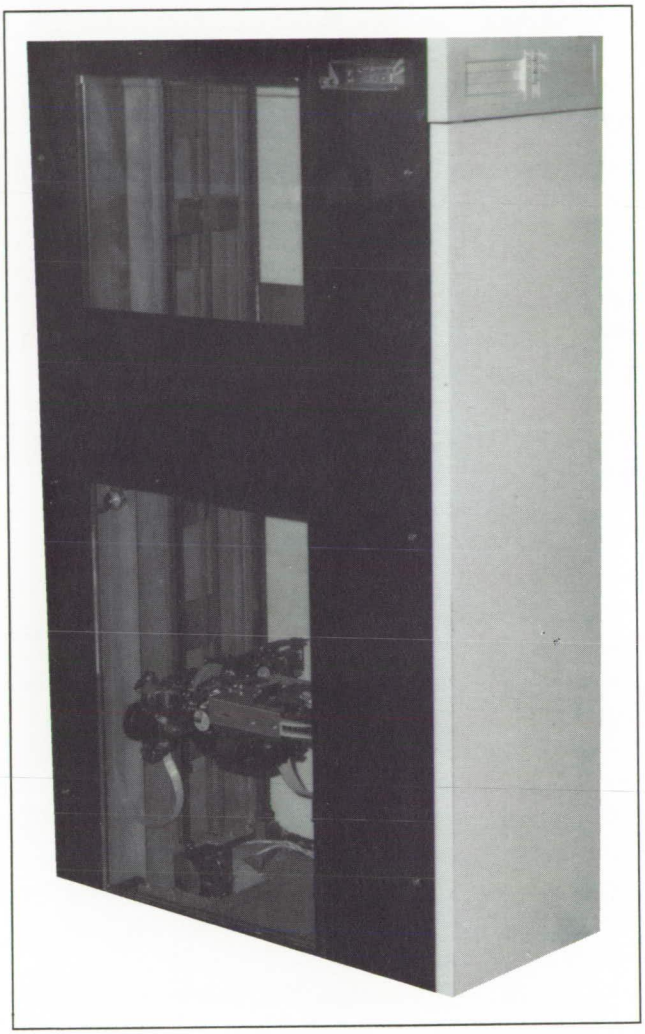


Fig. 1. Laser-based optical data base management system

Ames-Moffett contact: M. Bondi
(415) 604-6341 or FTS 464-6341
Headquarters program office: OAET

Tilt-Wing Simulation Study

L. Corliss

Renewed interest in tilt-wing configurations for V/STOL have led to a motion simulation study of an approach for tilting the wing and for aircraft longitudinal control in hover and through conversion. The geared flap or "Churchill Flap" approach was the object of this study.

The Churchill flap design mechanizes wing flap as a servo for positioning wing tilt relative to the fuselage by using the energy in the propeller slipstream (see the figure). This concept, along with advances in fly-by-wire and in analytical tools for studying flow fields, warrants a new look at this approach. The study explored control-effectiveness issues and the potential for eliminating or reducing the need for a tail-rotor or monocyclic control as on other tilt-wing designs, including the VZ-2, X-18, XC-142, and CL-84.

An initial simulation was conducted to compare the capabilities of the geared flap to the more conventional programmed-flap tilt-wing approach, focusing on the control characteristics and handling qualities. For the initial motion simulation, the Ames Vertical Motion Simulator (VMS) was used with a mathematical model of an 87,000-pound, four-propeller tilt wing having an auxiliary tail thruster for aircraft pitch control. The simulation encompassed hover through conversion and reconversion flight modes and STOL landings.

The geared flap version was implemented with both wing-on-the-beep-switch (similar to the programmed flap) and also with wing-on-the-longitudinal stick.

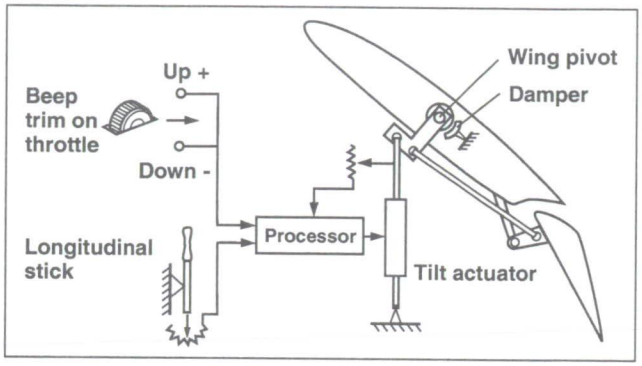


Fig. 1. Geared flap control

When operated from the beep switch, both flap versions had comparable handling-qualities ratings and both required an auxiliary pitch thruster at the tail for hover. A quick look at geared-flap-on-the-stick did appear to reduce the requirements for the auxiliary thruster, but it also resulted in certain misleading transient motion cues. A subsequent study is planned that will focus on the particulars of the geared-flap and control-law development.

Ames-Moffett contact: L. Corliss
(415) 604-6269 or FTS 464-6269
Headquarters program office: OAET

Reduced Takeoff Roll for Short Takeoff Transport Aircraft

Joseph C. Eppel

This joint Air Force/NASA program consists of the development of a nosewheel jump-strut for the Quiet Short Haul Research Aircraft (QSRA)—a STOL (short takeoff and landing) transport-size aircraft. The purpose of the jump-strut research program is to obtain data on the ability to reduce takeoff roll distance by the sudden extension of the aircraft nose wheel.

Studies of the application of this principle to the X-29A conducted by the Grumman Aircraft Company under contract to the Air Force concluded that the benefits are large and that the hardware mechanization is simple. Subsequently, ground tests of a nosegear jump-strut on a T-38 were successfully performed by the Naval Air Test Center. Follow-on simulations of nose and main gear jump takeoffs indicated a 45% reduction in takeoff ground roll.

A 1987 study by Lockheed, Burbank, investigated the jump-strut takeoff benefits for transport-size STOL aircraft and concluded that reductions of 10 to 12 percent of takeoff distances could be demonstrated on the QSRA.

The development of the jump-strut hardware and aircraft modifications were initiated in 1989 and qualification testing at the Air Force Aeronautical Laboratory, Wright Patterson Air Force Base, was completed in 1990. Flight tests to be conducted in early 1991 will investigate takeoff performance, jump-strut system operation, piloting techniques for minimum takeoff roll, and related human factors issues. The flight data will be correlated with predicted characteristics. In addition, the STOL-transport reduced-roll takeoff data base will enable validation of simulator models.

Ames-Moffett contact: J. Eppel
(415) 604-6276 or FTS 464-6276
Headquarters program office: OAET

QSRA Controls and Display Experiments

J. Franklin, Joseph C. Eppel

Flight experiments have been conducted on the Quiet Short Haul Research Aircraft (QSRA) to investigate flight-control augmentation system and head-up display design options for application to the Air Force's C-17 transport aircraft.

With Air Force support, NASA conducted a program to (1) identify a range of flight-control and display characteristics for investigation based on flight experience on NASA STOL aircraft; (2) perform a ground-based simulation program for initial assessment of these characteristics, and to establish the final configurations for flight evaluation; and (3) to conduct the flight program.

Control-response characteristics ranging from those representative of a powered-lift transport with large turbofan engines to those reflecting incorporation of direct lift control to quicken flight-path response to throttles were implemented on the QSRA's digital flight-control system. A speed-hold mode and flight-path/airspeed command system were included for evaluation as well. Head-up display presentations, whose dynamics compensate for sluggish flight-path response to throttle, and which provide speed-control guidance and wind-shear protection, were prepared in conjunction with the control system modes.

Three Air Force pilots from the C-17 Combined Test Force and a McDonnell-Douglas C-17 pilot participated in the program, along with Air Force and McDonnell-Douglas engineering staff. Over a 2 week period, 23 flight hours and 144 landings were accomplished at NASA's Crows Landing Facility. The pilots' evaluations established the variation in flying qualities associated with the control augmentation and display combinations. Approach tracking performance and landing precision associated with the various configurations were also determined.

Ames-Moffett contact: J. Franklin/J. Eppel
(415) 604-6004/6276 or FTS 464-6004/6276
Headquarters program office: OAET

Design Synthesis of High-Speed Transport Aircraft

Thomas L. Galloway, Paul Gelhausen

The Aircraft Synthesis Program (ACSYNT) is the key design synthesis tool being used in the Systems Analysis Branch for high-speed civil transport (HSCT) design studies. The design synthesis program uses the designer's specifications for an aircraft configuration to size the vehicle for specified mission requirements and to estimate performance. Modules have been added to ACSYNT for the High-Speed Research Program, which enable assessment of design parameters that affect environmental issues, such as sonic boom and takeoff noise, as well as economic feasibility.

To assess the sonic boom issue, three previously developed analysis programs have been linked together to calculate the linear approximation to the pressure field which causes a sonic boom. The basic geometry from ACSYNT is translated into a form that is used by both an arbitrary body wave-drag analysis and a supersonic lifting surface analysis. The resulting pressure field is then passed to an atmospheric propagation code to estimate the sonic boom at the ground. By integrating the three analysis programs into ACSYNT, sonic boom overpressure at the ground can be either a design optimization objective or a constraint factor. The figure compares the method's estimated sonic boom for the Concorde supersonic transport with measured cruise flight data.

The takeoff noise module utilizes previously developed programs to estimate noise levels at specified observation points in addition to noise contour areas. This module provides a method for assessing the integrated effect of engine and airframe design parameters, as well as technology advances on meeting specified airport noise goals.

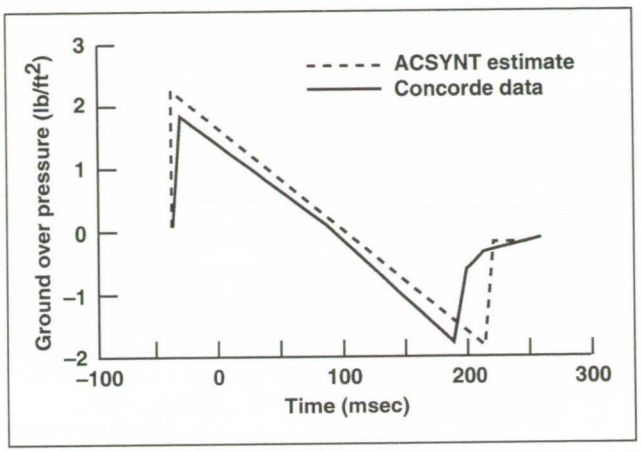


Fig. 1. ACSYNT sonic boom estimation

The economics module provides estimates of vehicle development and acquisition cost and total airline operating cost to assess the revenue requirements for a typical airline-type operation.

The analysis modules that have been added to ACSYNT provide the capability to evaluate key vehicle design parameters and technology developments, through conceptual design and trade-off studies, that can provide a more environmentally acceptable and economically practical HSCT configuration. Also, they provide a rapid means to investigate "what if?" types of technical questions, which are useful in establishing the key elements of research and technology development programs.

Ames-Moffett contact: T. Galloway/P. Gelhausen
(415) 604-6181/5701 or FTS 464-6181/5701
Headquarters program office: OAET

High-Speed Tilt-Rotor Feasibility Study

Thomas L. Galloway, David R. Schleicher

The High-Speed Rotorcraft technology research program has the objective of providing "helicopter-like" hovering performance with a forward flight speed approaching 450 knots. Several concepts are being investigated to provide that capability. A study was made by the Systems Analysis Branch assessing the feasibility and technology needs for a tilt-rotor aircraft to achieve these goals.

A baseline model of a high-speed tilt rotor (HSTR) was developed using XV-15 and V-22 parameter values and performance trends. Using the VASCOMP design synthesis code, the HSTR was sized for a civil transport mission consisting of a 450-knot, 600-nautical-mile cruise at 20,000 feet with a payload of 30 passengers. Reasonable advances in technology were projected to investigate their effect on achieving a feasible configuration.

The figure shows the individual and combined effect on the gross weight of the concept for a 20%

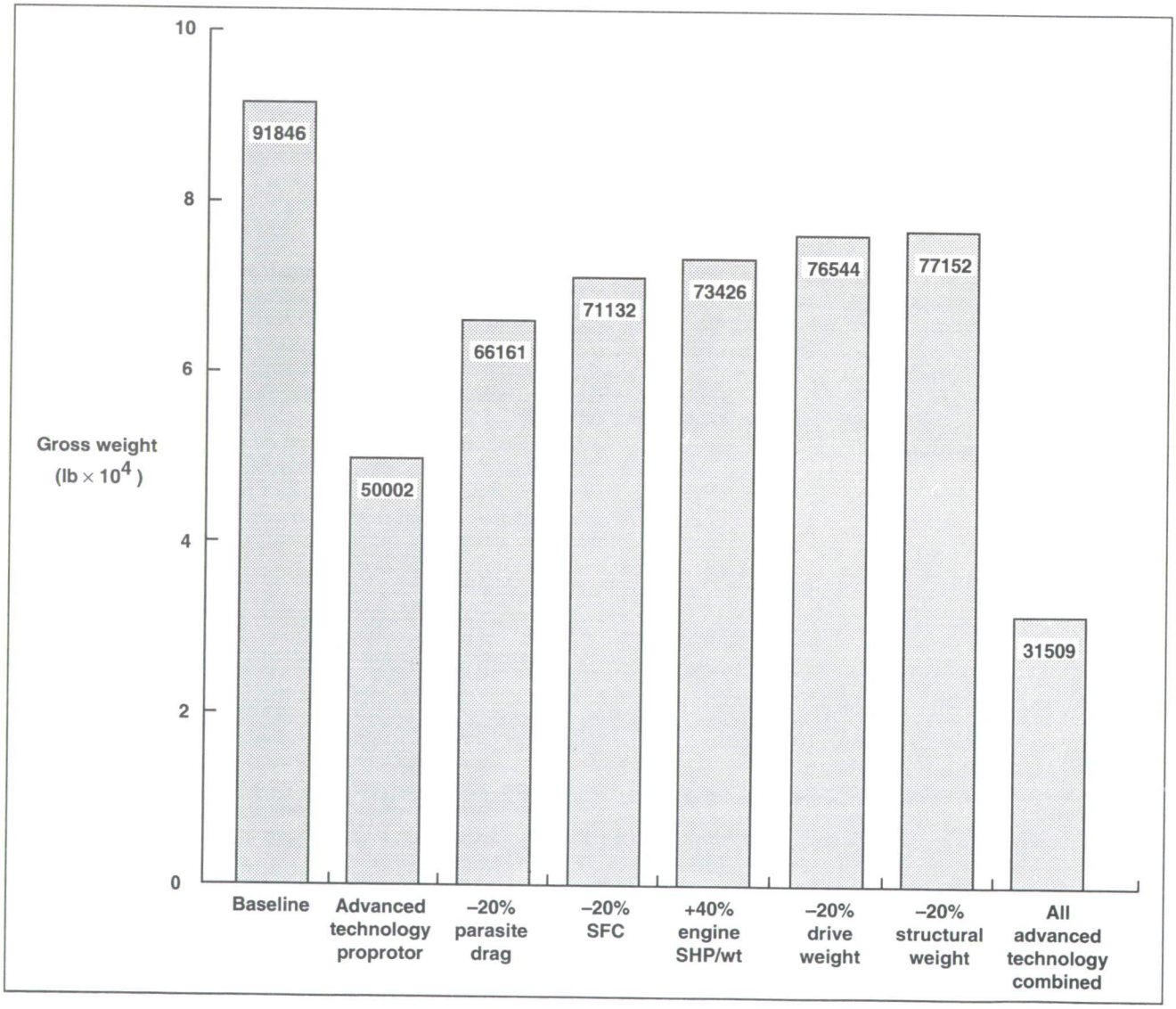


Fig. 1. HSTR advanced technology comparison

reduction in structural weight, 20% reduction in rotor drive weight, 40% increase in engine power-to-weight ratio, 20% decrease in engine specific fuel consumption, 20% decrease in vehicle parasite drag, and an increase in drag divergence Mach number from 0.63 to 0.71 for the proprotor advanced airfoil.

The advanced technology proprotor produced the largest reduction in gross weight and is the key technology in realizing a feasible size HSTR.

Although the other technologies had considerably less effect, their collective benefit enhances the promise of achieving a minimum size and cost HSTR.

Ames-Moffett contact: T. Galloway/D. Schleicher
(415) 604-6181/5789 or FTS 464-6181/5789
Headquarters program office: OAET

Aircraft Synthesis Program Institute

Paul Gelhausen

The objective of this collaborative relationship between NASA, industry, and academia is to advance U.S. capability in aircraft conceptual design by providing a standards-based interactive conceptual design code.

In 1990, the American Technology Initiative (AmTech) group arranged a jointly sponsored research project, the Aircraft Synthesis Program (ACSYNT) Institute. Project participants could gain access to ACSYNT, an Ames developed conceptual design code, and increase the scope of resources, technology and research applied to further development of ACSYNT. The Institute brings together NASA, Virginia Polytechnic Institute (VPI), airframe and engine manufacturers, and academic institutions to collaborate on the further development of ACSYNT.

Under this agreement, ACSYNT is continually updated and expanded to broaden the types of aircraft and to increase the number of technical and economic parameters addressed during the conceptual design analysis. New members are added to the Institute by paying a fee that is used to fund more research. The current members of the Institute are Boeing Helicopter, General Electric Aircraft Engines, Lockheed Aeronautical Systems, Northrop Aircraft, McDonnell Aircraft, NASA, the Naval Weapons Center, VPI, and the Air Force Academy.

This project uses the FORTRAN, PHIGS and UNIX programming standards to develop a code that is machine and graphics device-independent and thus executable on a wide range of current UNIX workstations. It provides a cooperative environment for communication with other members and enhances the utilization of resources to achieve common goals.

Current research is focused on generating three-dimensional surface models from ACSYNT's parametric data that easily can be used in higher-order design and analysis techniques. The latest version

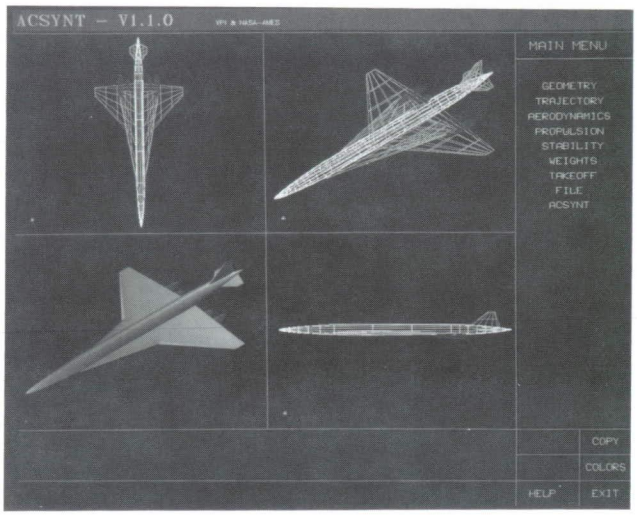


Fig. 1. ACSYNT geometry modeling interface (see color plate 2 in Appendix)

of the code includes complex-wing geometry modeling, nacelle geometry integration, calculation of surface areas, volumes, and volume distribution, B-spline surface toolkit, and carpet plotting capability (see the figure). These capabilities are combined with existing multi-disciplinary synthesis and optimization techniques into a design integration tool.

The Institute established the following near-term goals.

1. Enhance the user interface through a spreadsheet input format and upgrade to PHIGS+.
2. Expand geometry modeling through incorporation of B-spline surfaces, enhanced scaling through parametric definition of wings and fuselages, and start development of a library of aircraft components.
3. Expand the aerodynamic analysis capability through the utilization of higher-order methods.

Ames-Moffett contact: P. Gelhausen/T. Galloway
(415) 604-5701/6181 or FTS 464-5701/6181
Headquarters program office: OAET

Modal Analysis of UH-60A Instrumented Rotor Blades

Karen S. Hamade, Robert M. Kufeld

The dynamic characteristics of instrumented and production UH-60A Black Hawk main-rotor blades were measured, and the results were validated with NASTRAN finite-element models. The blades tested included production blades, as well as a pressure and a strain-gauge instrumented blade which are part of NASA's Airloads Flight Research Phase of the Modern Technology Rotor Program.

The dynamic similarity of the blades is required for accurate data collection in the flight program. This is because the UH-60 rotor consists of two instrumented and two production blades, and the blades should be in the same track. Also, most rotorcraft analysis codes assume identical blades. Blade similarity was determined by performing a shake test to measure the first 10, free-free, non-rotating blade frequencies and mode shapes. The first figure shows the shake test setup with a UH-60 blade hanging from bungee cords.

In the second figure, the instrumented blade modal frequencies are compared with the average of four noninstrumented (production) blades. The strain-gauge blade modes were within 1% of production blade frequencies. The pressure-instrumented blade frequencies were 2-3.7% lower than those of the production blades. The difference in modal frequencies between the instrumented blades and the production blades is not considered significant because the four production blades tested showed that the measurable variation between the production blades is typically as high as 2.5%.

The NASTRAN model of the production blade had excellent correlation with the test (less than 2% deviation). The model of the pressure-instrumented blade predicted the slightly lower frequencies measured in the test and were within 3% of those values.

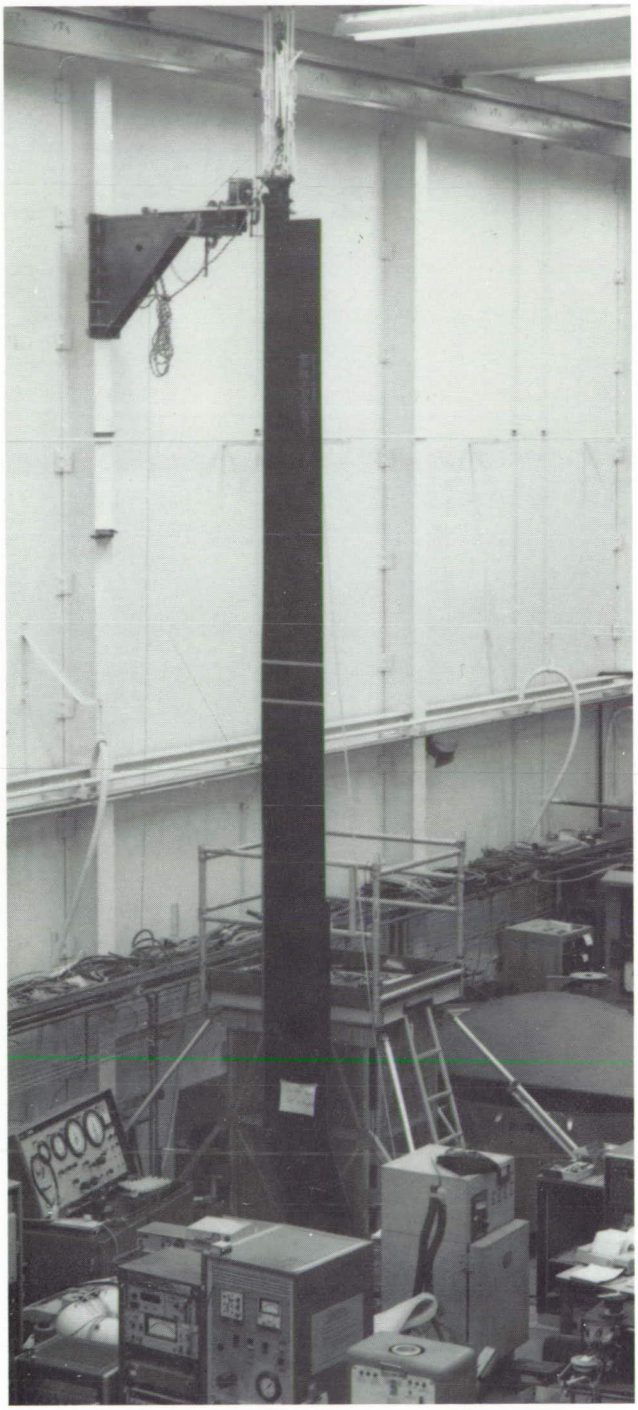


Fig. 1. Shake test setup showing a UH-60A production blade hanging from bungee cords

ORIGINAL PAGE
BLACK AND WHITE PHOTOGRAPH

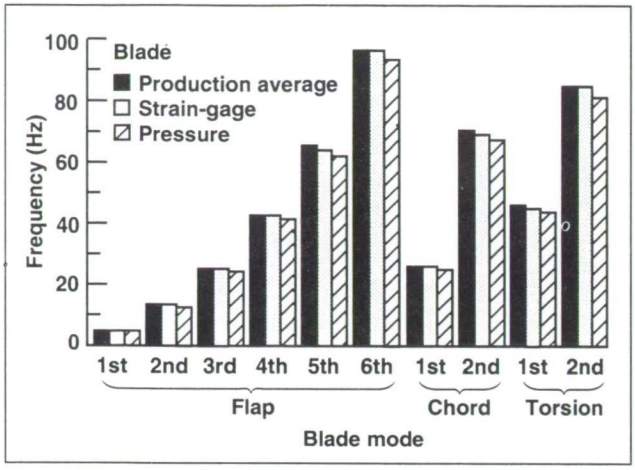


Fig. 2. Modal frequencies measured for the production (average of four blades), strain-gauge, and pressure-instrumented blades

The test verified that the instrumented blades are dynamically similar to production blades despite the large amount of instrumentation built into them. The two production blades that best matched the instrumented blades were chosen for the flight tests. Also, the correlation of the NASTRAN model with the test verified that the structural information used to create the model is a correct blade representation. These same structural data are used as input for CAMRAD and other analysis codes.

Ames-Moffett contact: K. Hamade
(415) 604-4682 or FTS 464-4682
Headquarters program office: OAET

Passive Chlorophyll Detector

Leonard Haslim, Paul McDonough

The passive chlorophyll detector (PCD) provides real-time, color-differential enhancement in the visible region. Originally investigated for military applications, the PCD may have potential for the agricultural industry. The feasibility of PCD applications for plant-growth assessment is being explored in collaboration with agricultural researchers.

The theory to be explored is that ordinary goggles, aided by an optical PCD filter, could be used to help detect the presence of stresses in plants. The agricultural community is presently conducting an investigation into whether chlorophyll levels depict stress disorders, such as dehydration. If so, the PCD might be used to aid in the assessment of plant health by providing a real-time, enhanced image of a plant's color shades, not ordinarily accessible to the naked eye.

The outcome of such a discovery would be instrumental to both the agricultural and ecological sectors in their endeavors to prevent plant, tree, and crop deterioration.

Ames-Moffett contact: L. Haslim/P. McDonough
(415) 604-6575/5673 or FTS 464-6575/5673
Headquarters program office: OAET

Biodegradable Deicing Fluids

Leonard Haslim, Paul McDonough

As a safety precaution, aircraft operated during cold weather are sprayed with fluids to remove ice (deicing) or to prevent ice and snow accretion (anti-icing). The airspace regulatory agencies (for example, FAA) and airline associations have developed standards and procedures for the use and disposal of these fluids. Currently, there are two types of fluids in use, reflecting two fundamental approaches to deicing of aircraft.

The first approach is to spray a plane with "hot" fluids which will melt ice and snow, with the aircraft departing before any further ice buildup. The second approach is to spray fluid on the plane as a "thickened gel," which deices more slowly, but provides for more time between application and takeoff. The two fluids suitable for these approaches are termed type I (unthickened) and type II (thickened) fluids, respectively. Their properties represent different compositions of the same family of chemicals, with type II compounds containing additives that cause the fluid to "cling" to the aircraft under various weather and takeoff conditions (see the figure).

The currently used toxic deicing fluids are based on glycols, primarily ethylene and propylene glycol. However, there is evidence that these fluids may produce long-term, environmental effects. In addition, type II fluids, which exhibit improved aerodynamic performance, have compounds that are nonbiodegradable. The Environmental Protection Agency (EPA) has cited one airport for water pollution for disposal of type II fluids into storm water drainage systems. Thus, there is a need to develop alternative deicers that are biodegradable.

Experimentation is under way to develop biodegradable, nontoxic, nonglycol deicer fluids, including new thickening agents. The prototype compounds appear to have the performance quality of recently developed type II deicers. Results are promising, but further research is required to develop the proper thickening characteristics.

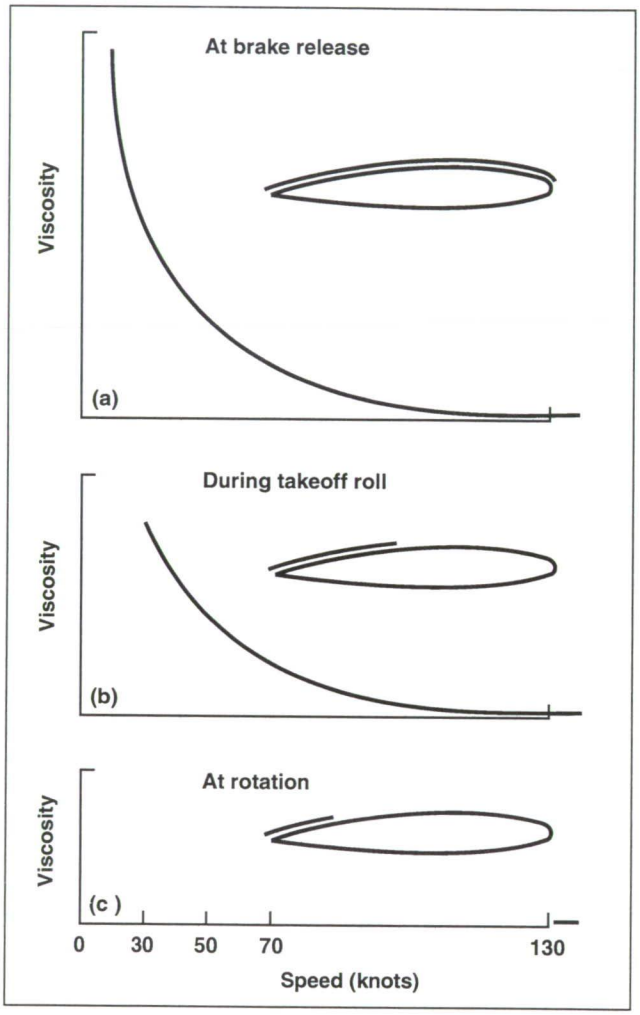


Fig. 1. Viscosity/aircraft speed graphs. (a) At brake release; (b) during takeoff roll; (c) at rotation

Ames-Moffett contact: L. Haslim/P. McDonough
(415) 604-6575/5673 or FTS 464-6575/5673
Headquarters program office: OAET

Blue Ice

Leonard Haslim, Paul McDonough

Leaking external purge service panels attached to an airplane's lavatory system have caused ice chunks weighing as much as 15 pounds to form on the fuselage's exterior. Known as blue ice (not to be confused with actual blue ice; so called only because the added disinfectant is blue), these large chunks can pose a serious safety threat and have indeed caused several airplanes to lose engines when impacted by ice that breaks free of the fuselage.

The theory is that over a period of approximately 3 to 4 hours, a steady leak causes the fluid to drip to the aircraft's exterior where it freezes at high altitudes and forms a chunk of blue ice. The chunk eventually breaks off the airframe and either flows into the airstream, presenting a potential hazard for the plane's engines, or falls to the ground.

The Air Transport Association and Aerospace Industries Association have jointly addressed the problem, and their recommendations include investigating application of a variant of the electro-expulsive deicing system (EEDS).

The EEDS ring would be a flat, circular disk that would be flush-fitted to the aircraft's skin surrounding the purge service panel (see the figure). The EEDS ring would serve as an extra safety margin to ensure that no ice would form, should the already-improved valve system still leak. The ring could be either activated by an ice sensor or pulsed continuously in an anti-ice mode. Since its power requirement is so small (less than 80 watts), it could operate from takeoff to landing without any significant drain on the aircraft's electrical system. An initial assessment has indicated the EEDS ring and power components could be easily integrated into the aircraft.

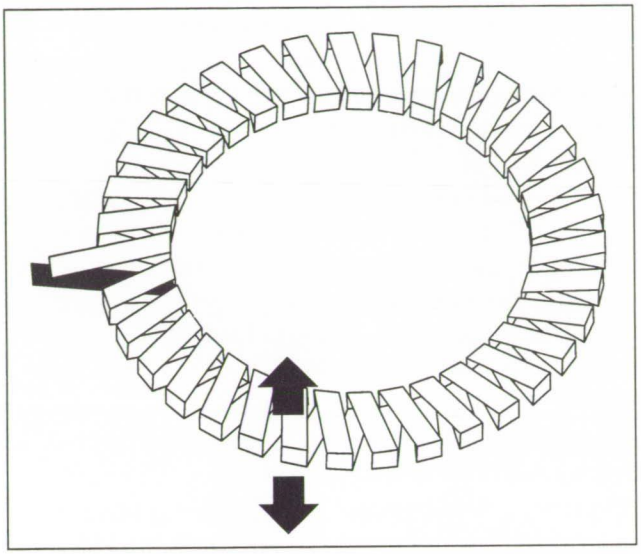


Fig. 1. Configuration of thin circular EEDS ring for prevention of "blue ice" accumulation

Ames-Moffett contact: L. Haslim/P. McDonough
(415) 604-6575/5673 or FTS 464-6575/5673
Headquarters program office: OAET

Electro-Expulsive Deicing System

ORIGINAL PAGE
BLACK AND WHITE PHOTOGRAPH

Leonard Haslim, Paul McDonough

The electro-expulsive deicing system (EEDS) has been technically advanced. In its present design, the EEDS utilizes high capacitance discharges emitted from a pulsed-energy power supply to impart a rapid and powerful current pulse into a set of conductor ribbons. These ribbons are evenly spaced in a parallel manner, folded over onto themselves, and connected in series. The conductors are embedded in a dielectric which is encased in a flexible polyurethane sheath. The entire blanket is only 0.020 inch thick, weighs a mere 4 ounces per square foot, and is easily retrofitted to any surface that requires deicing.

Successful deicing experiments were conducted at the Navy's Arctic Simulation Chamber in Point Loma, California, and several major technical advances were demonstrated (see the figure). First, the EEDS demonstrated the ability to operate effectively on any shaped substrate. The three shapes tested were a compound-curved fan shroud, a 4-inch-diameter cylinder, and a 4-square-foot flat panel.

The Navy, which funded the experiment, was particularly interested in these shapes because they represented ship superstructure components that are prone to icing. Shipboard icing can seriously impede a vessel's performance and safety. The compound-curve section was part of an LCAC (land craft air cushioned) fan shroud, the cylinder simulates a ship mast or large antenna, and the flat panel simulates personnel exit doors, which can freeze shut because of snow and ice accretion.

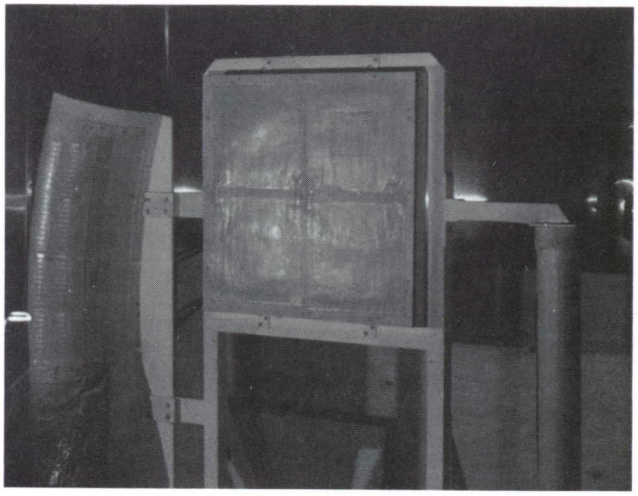


Fig. 1. Deicing experiment in Navy's Arctic Simulation Chamber in Pt. Loma, California

These successful experiments were possible as a result of advances in the pulsed-energy power supply and a unique state-of-the-art cable system. Together, these advances increased the EEDS' performance tenfold.

Ames-Moffett contact: L. Haslim/P. McDonough
(415) 604-6575/5673 or FTS 464-6575/5673
Headquarters program office: OAET

Safety Seat Cushion

Leonard Haslim, Paul McDonough

Featured at the NASA Technology 2000 Conference, the safety seat cushion (SSC) was designed for both safety and comfort. Composed of advanced fiber reinforced composites, it is lightweight, fire-retardant, and crashworthy.

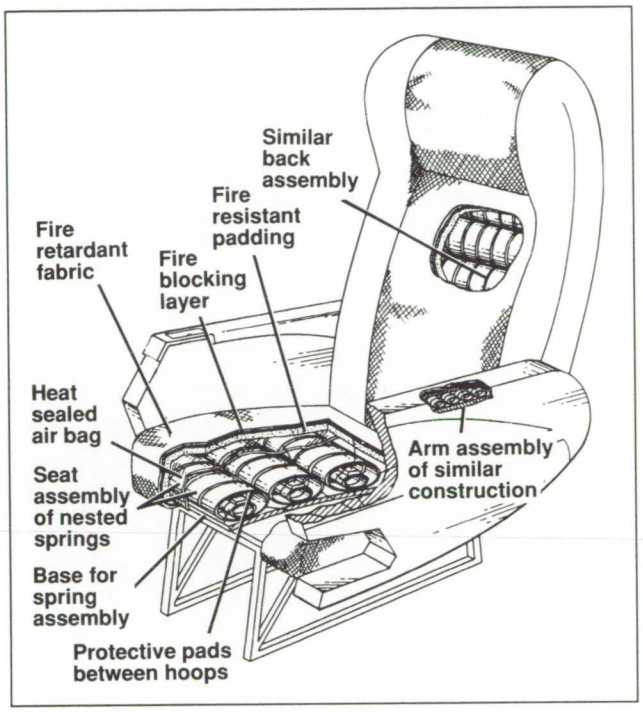


Fig. 1. Aircraft seat

The seat consists of central elliptical tubular spring supports made of fire-resistant and fatigue-durable composites surrounded by a fire-blocking sheath. The cushioning is made crashworthy by incorporating energy-absorbing, visco-elastic layers between the nested, elliptical-hoop springs, which is a highly desirable feature for helicopters. The design is intended to provide comfortable seating that meets aircraft-loading requirements without using the conventional polyurethane materials.

Current improvements incorporate interlocking hoop designs to enhance surface comfort and profiles. The new assembly, made of selected thermoplastic materials, is encased in a high-temperature-resistant sheath.

Ames-Moffett contact: L. Haslim/P. McDonough
(415) 604-6575/5673 or FTS 464-6575/5673
Headquarters program office: OAET

Puma Airloads Correlation

Francisco Hernandez

The accurate prediction of rotor airloads is currently one of the most challenging problems in the field of theoretical aerodynamics and one that is far from being solved. Computational fluid dynamics (CFD) methods are used for such predictions, but they need to be correlated with experimental data in order to assess their validity.

An international collaborative effort was undertaken by the United States, England, France, and Australia. They investigated the predicting capability of various CFD methods by comparing the calculated air loads with flight measurements obtained on a Puma helicopter at Bedford, England. A workshop was held at Ames on May 1990 to examine the results of this work.

The U.S. Army Full-Potential Rotor Code (FPR) was iteratively coupled with the CAMRAD/JA rotorcraft performance code. The coupling scheme developed by the Army uses inflow angles from CAMRAD/JA which represent the wake and blade dynamics effects. These are input as boundary conditions into FPR which computes airloads that are fed into CAMRAD/JA to obtain a new rotor wake and blade dynamic response. The process is repeated until convergence. The final solutions are the predicted air loads on the rotor system.

Aerodynamic predictions were made for several flight conditions on a Puma helicopter with four swept-tip blades using CFD methods. Results were compared with the Transonic Small Perturbation (TSP) calculations done at the Royal Aerospace Establishment (RAE) along with measured flight-test data, as shown in the figure. An evaluation of the strengths of the different CFD/lifting-line methods was made by comparing different aerodynamic parameters at different stations on the rotor disk.

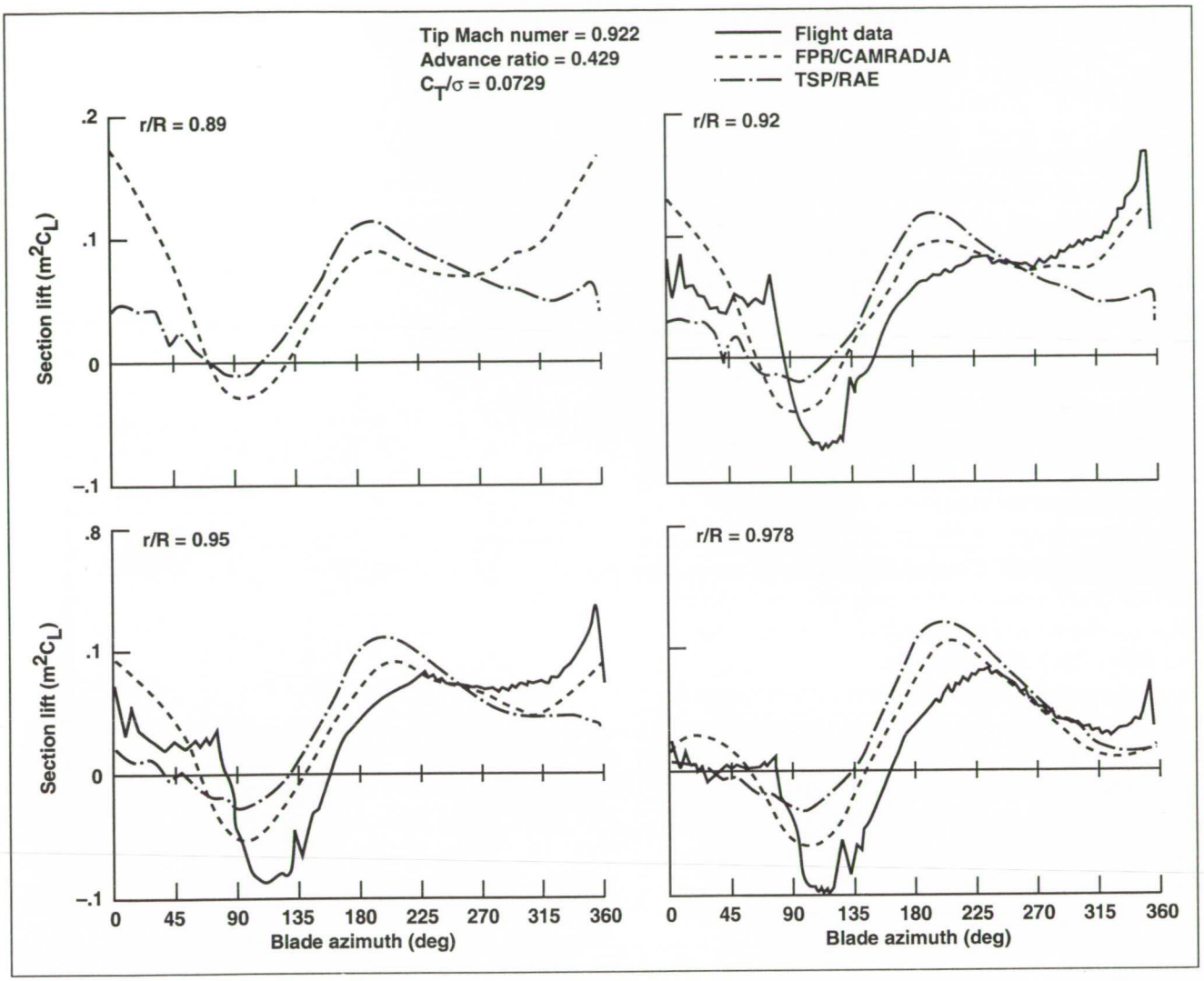


Fig. 1. Puma airloads correlation, high-speed autorotation case: section lift = 0 to 64 harmonics

Rotorcraft CFD analyses have not yet attained the level of confidence achieved in fixed-wing CFD applications, a result of the more complex aerodynamic environment present in the rotor system. The only method of determining the validity of the numerical calculations is through correlation work. This, in turn, will result in the development of better CFD codes in the near future which will be helpful in the design of improved rotor systems.

Ames-Moffett contact: F. Hernandez
(415) 604-3150 or FTS 464-3150
Headquarters program office: OAET

Multiple Instruction Multiple Data Parallel Processing

Gary Hill

Parallel (simultaneous rather than sequential) computation of program instructions offers substantial savings in machine costs and reduced computation time. Exploiting this technology for aeronautical research and engineering required developing tools for decomposing existing computer codes to determine architectures for simultaneous execution of code components.

These tools were effectively applied to single instruction multiple data (SIMD) problems such as those in computational fluid dynamics, but its momentous strength is on multiple instruction multiple data (MIMD) codes like computational electromagnetics, real-time simulation, and aircraft design synthesis and optimization. The tremendous cost advantages of the new-generation parallel processing computers and workstations can only be realized when efficient architectures for simultaneous paths through sequential codes can be found.

For example, application of parallel processing to real-time rotorcraft simulation, where accurate models are much more complex than their fixed-wing counterparts, yielded dramatic results. Improved fidelity was demonstrated by replacing the rotor-map model on the UH-60 Black Hawk training simulator at Fort Ord, California, with a more accurate blade-element representation. This was computed on a MicroVAX II with four Intel-386 based boards plugged into the backplane to be simultaneous processors instead of the usual sequential computational mode. NASA and Army pilots flew evaluations to compare the improved simulation with flight. The results persuaded the Department of Defense's Program Management for Training Devices to specify upgrading modeling for upgrades and future training simulators.

Similarly, a more powerful parallel processor was used with the Ames Crew Station Research and Development Facility (CSRDF) to replace the rotorcraft mathematical model with one that calculated the highly nonlinear rotor aeroelastics and structural dynamics in real-time. A $225,000 Silicon Graphics 4D-280GTX computer with eight nodes was interfaced with the CSRDF and was used to run the aeroelastic, blade-element rotor mathematical model at a 6-millisecond cycle time. Comparisons with rigid-body modeling showed much improved fidelity at high speeds and with high-gain-control systems. Developing the next generation of advanced rotorcraft—capable of higher speed and greater maneuverability, with precise, superaugmented control systems and hingeless rotors—will require expanded-bandwidth, real-time simulations that include aeroelastics and structural dynamics.

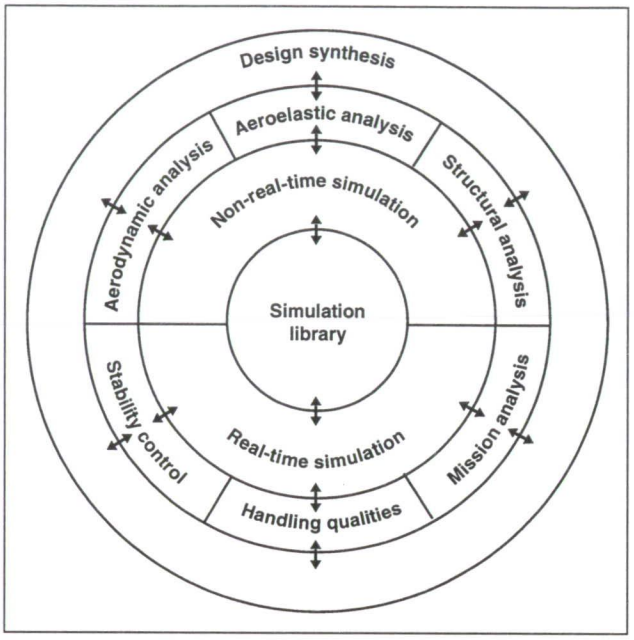


Fig. 1. Interdisciplinary design synthesis

In addition to real-time simulation, parallel processing is particularly accommodating to object-oriented and concurrent engineering. There, detailed analytic codes from the many disciplines are integrated to increased productivity, resulting in reduced design times and lower engineering costs. The schematic diagram illustrates the complete integration possible when workstation-priced parallel processors become computational engines with the power to perform both real-time and nonreal-time functions.

Ames-Moffett contact: G. Hill
(415) 604-6577 or FTS 464-6577
Headquarters program office: OAET

UH-60A Pressure Blade Calibration

ORIGINAL PAGE
BLACK AND WHITE PHOTOGRAPH

B. Kufeld

For the UH-60 Airloads Program, 242 pressure transducers have been embedded into a rotor blade for acquiring air-loads data over an extensive flight envelope that includes hover, transition, cruise and maneuvers. To assure a high degree of quality in the airloads data, calibration of the instrumentation system is vital. Calibration procedures have been developed to provide easy, accurate, and timely data for this program. Both static and dynamic calibration procedures have been demonstrated and used during the development of the UH-60 instrumentation system. A static calibration relates the output voltage of each transducer to a known constant pressure. A dynamic calibration shows the frequency response of each transducer and confirms the cutoff frequency of each transducer as installed.

The static-calibration procedure utilizes a Mylar bag to calibrate all transducers at once. A horsehair liner is placed between the blade and the bag to evenly distribute the loading pressure. The pressure inside the bag is decreased with a vacuum pump, and data points are taken with the flight data system. A static calibration can be completed in less than 1 day while the blade is installed on the aircraft.

The dynamic calibration procedure must be performed on one transducer at a time. To do the dynamic calibration, each transducer is subjected to a pressure variation from a hand-held chamber capable of outputting pressure frequency variation over a 100 to 10,000 hertz band. The hand-held chamber over a blade pressure port is shown in the first figure. A microphone is also connected to the chamber and its output is the standard for determining the frequency response function of the transducer.

The transducer system's resonance and cutoff frequencies, obtained from analysis of the signal, are also of interest. The data collected are shown in the second figure, which shows a typical resonance frequency of a transducer. The resonance frequency is a function of the transducer's tube length as installed in the rotor blade. A cutoff frequency of 2,000 hertz, which is well below the resonance frequency, has been selected for the experimental data.



Fig. 1. Pressure chamber exciting pressure transducers during dynamic calibration

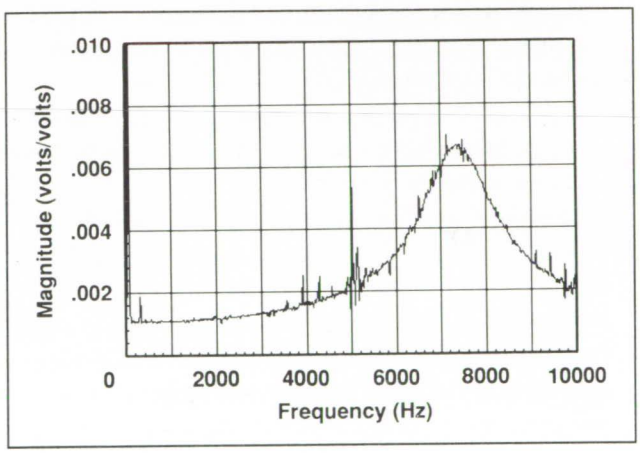


Fig. 2. Frequency-response plot of one embedded pressure transducer

Ames-Moffett contact: B. Kufeld
(415) 604-5664 or FTS 464-5664
Headquarters program office: OAET

UH-60A Flight Project Development

ORIGINAL PAGE
BLACK AND WHITE PHOTOGRAPH

Paul Loschke

The UH-60A Airloads Project is a major element of the joint NASA/U.S. Army Modern Technology Rotors (MTR) Program to provide and validate the technology and methods necessary to improve the performance, dynamics, acoustics, handling qualities, and cost of civil and military rotorcraft. Research-instrumented rotor blades have been developed to measure in-flight rotor airloads, rotor vibratory airloads and rotor dynamics on the UH-60A Black Hawk helicopter. The instrumentation/data acquisition system is attached to the rotor system hub as shown in the figure for effective measurement of rotor sensors and data transmission through the hub to the aircraft cabin for data recording.

The ultimate value of any research experiment is linked to the quality of the measured data and the calibration procedures utilized in acquiring the data. The development of calibration procedures for the instrumented rotor blades has been completed, and the results of testing the procedures are described in the article (this volume) titled UH-60A Pressure Blade Calibration.

The UH-60A airloads aircraft will support a far-field acoustics flight experiment sponsored by NASA Langley. Rotor acoustics data, measured by ground-located instruments, will be correlated with the on-board measured rotor airloads and vibratory data to acquire a high-quality data base that will help improve helicopter noise prediction computer codes. In order to acquire these flight data, the UH-60A aircraft is required to fly repeated precision trajectories over the ground-positioned acoustic instrument.



Fig. 1. UH-60A Black Hawk airloads research helicopter

A system has been developed in-house that provides real-time precision guidance; it is described in the article titled UH-60A Instrument Positioning System.

The UH-60A Airloads Project will produce the largest rotorcraft flight data base in history and requires state-of-the-art mass data base storage systems. An optical laser data storage device has been developed to interface with an existing, highly flexible data base management system. What is now available to Ames researchers is a very robust data base analysis/storage system as described in the article titled UH-60A Optical Data Base Management System.

Ames-Moffett contact: P. Loschke
(415) 604-6576 or FTS 464-6576
Headquarters program office: OAET

UH-60 Instrument Positioning System

Paul Loschke, M. Aoyagi

The UH-60 Rotor Airloads Project has a need to provide lateral and vertical guidance along a prescribed flight path in order to conduct a far-field acoustics flight program jointly with NASA Langley. An instrument positioning system (IPS) has been developed and flight tested (see the figure) that uses the conventional Instrument Landing System (ILS) receiver/indicator to display a pseudo-ILS signal generated from a ground tracking system.

Without any modification to the standard on-board ILS instruments, the IPS provides guidance data that allow flight-path control to within ± 20 feet of deviation (lateral and vertical) during helicopter flyovers of acoustic microphones at several fixed altitudes and ascent/decent paths at various angles. An error signal is generated by comparing the aircraft position measured via a ground laser tracking system with a specified trajectory in a ground computer. Lateral and vertical deviations or errors are then used to modulate the IPS frequency in the same manner as the aircraft position would in a conventional ILS configuration.

The on-board receiver processes the uplink transmission and presents deviation data on the conventional glide slope and localizer instrument display. The system will be used at the Navy's Crows Landing Facility and will utilize Navy-assigned ILS frequencies (108.95 megahertz localizer; 329.15 megahertz glide slope) during the far-field acoustic testing. The highly accurate acoustic measurements coupled with the comprehensive UH-60 airloads data will form a national data base for the noise-prediction code ROTONET.

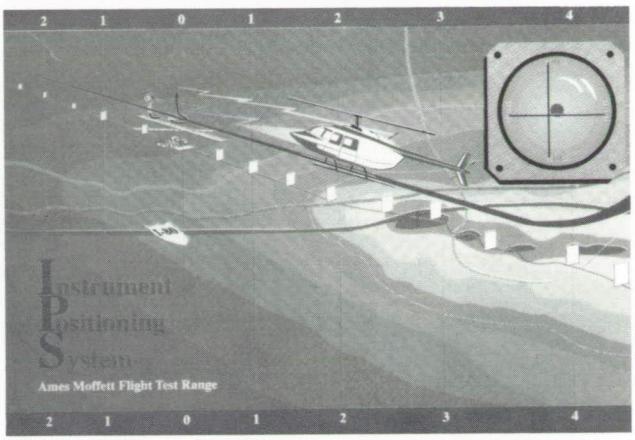


Fig. 1. Instrument positioning system at the Navy Crows Landing Facility (see color plate 3 in Appendix)

Ames-Moffett contact: P. Loschke
(415) 604-6576 or FTS 464-6576
Headquarters program office: OAET

ORIGINAL PAGE
BLACK AND WHITE PHOTOGRAPH

XV-15/Advanced-Technology Blades Flight Investigations

ORIGINAL PAGE
BLACK AND WHITE PHOTOGRAPH

Martin Maisel, J. Brent Wellman

The overall objectives of this program are to enhance the flight research capabilities of the XV-15/Tilt-Rotor Research Aircraft and extend the data base for the validation of aerodynamic, aeroacoustic, structural dynamic and aeroelastic stability analytical methods for tilt-rotor aircraft through the design and test of an advanced rotor blade.

A new rotor blade was designed using state-of-the-art airfoil sections, current performance codes, and advanced materials and structural design. The blades, called the Advanced Technology Blades (ATB), are highly twisted with a compound planform and a thin tip for reduced noise and greater hover-mode lift capability without degrading performance at high speeds in the airplane mode. The ability to change tip- and cuff-section geometry, as well as blade sweep, is also incorporated.

During 1990, flight tests of the ATB on the XV-15 Tilt-Rotor Research Aircraft addressed rotor control loads and stability. Earlier CAMRAD (Comprehensive Analytical Model of Rotorcraft Aerodynamics and Dynamics) predictions indicated that the high rotor-control loads encountered during initial XV-15/ATB flights were due to the high feathering inertia of the ATB and that they could be reduced by stiffening the rotor-control components. This year's flight-test validation of the reduced loads enabled testing in the helicopter, tilt-rotor, and airplane (see the figure) flight-modes. Further tests are planned for 1991 to investigate the effects of blade sweep and tip shape on rotor-control loads and stability.

These investigations of the XV-15/ATB rotor/control dynamics have resulted in a greatly increased understanding of the phenomena involved and have accelerated the development of improved methods

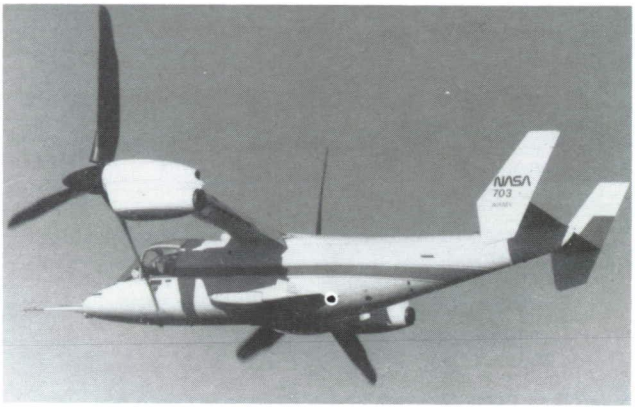


Fig. 1. Airplane-mode flight test of XV-15 Tilt-Rotor Research Aircraft with advanced technology blades

for analyzing these phenomena. The validation of this method in flight through correlation with flight data will significantly enhance our capability to predict and design for dynamic and aeroelastic phenomena for future tilt-rotor aircraft.

A series of tests to measure the hover acoustics of the XV-15/ATB was also conducted in 1990 in a joint NASA Langley/NASA Ames program. This activity examined the amplitude and directivity of the tilt-rotor hover noise for various aircraft heights above ground level (elevation angles from near in-plane to 45°). Because of the high-thrust capability of the ATB, the tip speeds tested ranged from the XV-15 design value of 771 ft/sec down to 645 ft/sec. As expected, the low tip-speed condition coupled with the thin-tip blades resulted in a low acoustic signature suitable for civil rotorcraft applications.

Ames-Moffett contact: M. Maisel/B. Wellman
(415) 604-6372/6573 or FTS 464-6372/6573
Headquarters program office: OAET

Improved Calculation of Sensitivity for Structural Parameter Identification

H. Miura, M. K. Chargin

Frequently in structural design and analysis, a deformation state is prescribed and the analysis model must be modified to reproduce the prescribed displacements. Typically, the analysis results do not agree well with the test data. Application of structural-optimization techniques has been developed to simultaneously change a large number of analysis model parameters so that calculated displacements match measured displacements; they have proven to be an effective approach for both static and harmonic loads. For this class of problems, slight modification to the displacement-sensitivity algorithm was found to be effective in improving performance of the parameter identification process.

As a simple example, imagine that we have a spring, and measure how much this spring stretches when we apply 100 pounds of force. At the same time, we will create a structural analysis model of this spring and calculate its displacement when 100 pounds of force is applied to it. If these two displacements do not agree and we know that we used accurate dimensions of the spring in the analysis model, the material constants used in the analysis model need to be adjusted. If we use the structural-optimization technique to automatically adjust material constants, first we need to calculate the displacement sensitivity, that is, how much the displacement changes as a result of unit change in each material constant in question. This sensitivity-calculation process requires displacement data. For all sensitivity analysis algorithms used in structural optimization, the displacement sensitivities are computed by using the computed displacements because no other displacement data are available.

However, for the parameter-identification problems, we have the target displacement data obtained in the tests. It was shown that the displacement sensitivities calculations based on the measured (or target) displacements have a superior quality in guiding the numerical search process. If the overall stiffness and mass characteristics are linear functions of the parameters, then the numerical search process converges in one step without requiring iteration.

For practical problems such as the shake tests of an airframe, only a fraction of the displacement degrees of freedom of a finite-element analysis model will be measured. Under such circumstances, unmeasured displacements are interpolated, then used in the sensitivity analysis.

Ames-Moffett contact: H. Miura
(415) 604-5888 or FTS 464-5888
Headquarters program office: OAET

V/STOL Aircraft Design Synthesis

Jim Phillips, Tom Galloway

The V/STOL Aircraft Sizing and Performance Computer program (VASCOMP) is one of the key design synthesis tools being used in the Systems Analysis Branch for high-speed rotorcraft design studies. A design-synthesis program uses the designer's specifications for an aircraft configuration to size the vehicle for the mission and to estimate performance. VASCOMP has been modified for the High-Speed Rotorcraft Program to (1) increase its flexibility in types of rotorcraft configurations, (2) incorporate a flight-mode conversion analysis, (3) include convertible engines, (4) enable evaluation of variable-diameter rotors, and (5) integrate a numerical optimization method.

During the process of converting from hover flight to forward cruise flight, many design parameters can affect the configuration's weight, size, and performance. A conversion method applicable to tilt-rotor and tilt-wing concepts has been developed for VASCOMP that is simple and general, requiring only the rotor-disk loading, solidity, and tip speed. It accounts for download, wing stall, the fountain effect in hover, the contraction of the rotor wake, nacelle lift and drag in the rotor wake, nonuniform lift distribution caused by the rotor wake, the flap and wing incidence profiles, and the horizontal acceleration profile.

The result is that engine and transmission sizing can now consider the power and torque required for conversion; the fuel, time, and range for conversion can be determined; and the rotor-state history during conversion can be computed. Optimized configurations now avoid unrealistic values for key design variables by factoring in penalties for marginal conversion performance. The figure shows the variation in vehicle gross weight with changes in wing loading, both when conversion is considered and when it is not for a tilt-rotor concept.

Concepts such as the trailed rotor and some variants of the folding tilt rotor, or stopped rotor, will utilize a convertible engine, having both a turboshaft and turbofan mode of operation. Modifications have been made for convertible engines that permit either turboshaft or turbofan operation in any mission segment, and that enable the engine to be sized in either mode. The engine model accounts for differences between the two modes for the power, fuel flow, gas generator speed, and power turbine speed. The addition of convertible engines is significant because high-speed rotorcraft configurations having the greatest speed potential use convertible engines. VASCOMP was also modified to handle rotors whose diameters may vary during the mission performance segments.

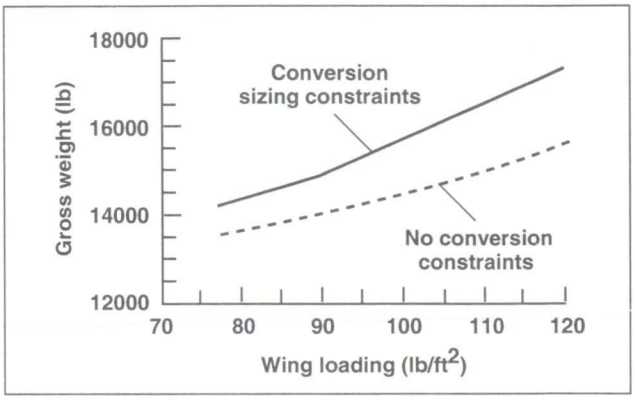


Fig. 1. Conversion effect on tilt-rotor sizing

Numerical optimization procedures can be highly useful in identifying critical design parameters during the parametric design process. An optimization procedure was coupled with VASCOMP to enhance the user's capability to study a larger number of design parameters.

Ames-Moffett contact: J. Phillips/T. Galloway
(415) 604-4126/6181 or FTS 464-4126/6181
Headquarters program office: OAET

Hypersonic Aircraft Geometry Modeling

Cathy Roberts, Jeff V. Bowles

In support of the National Aerospace Plane (NASP) program and more generic hypersonic aircraft studies, the Systems Analysis Branch of the Aircraft Technology Division has created a geometry modeling system to represent a broad range of trans-atmospheric vehicle concepts. The system models the aircraft mold-line definition, calculates input data needed to perform structural, propulsion and aerodynamic analyses, and determines internal layout of on-board components, such as fuel tanks. The overall design evaluation is then computed using a hypersonic vehicle conceptual design code called HAVOC.

The external aircraft geometry is described by four different analytical equations with 22 independent parameters. The shapes of the aircraft curves are all based on the enhanced super ellipse equation $(X/A)^M + (Y/B)^N = 1.0$. After the 22 parameters have been determined by the user, the system calculates data needed by HAVOC, such as external surface geometry and associated geometric characteristics, including vehicle volume, wetted-surface area, planform area and cross-sectional perimeter, area, and moment of inertia. It then determines the internal component layout by placing the component at a location indicated by the user and expanding or shrinking it to fit inside the vehicle external geometry.

Two components have been modeled: segmented fuel tanks and a payload or pilot compartment. The fuel tanks are represented by a three-dimensional trapezoid with a cross section consisting of a series of intersecting circles. The payload or pilot compartment is represented by a trapezoidal box. After the component layout is complete, the fuel-tank cross sectional geometric parameters (i.e., area, perimeter, and moment of inertia) are calculated for structural analysis. Then the component volumes are summed and divided by the model volume to find the packing efficiency.

The system has been used successfully to model several configurations, including the National Aerospace Plane designs, several hypersonic wave rider concepts, two SSTO (single stage to orbit) all-rocket concepts, elliptical all-bodies, wing-bodies, and the space shuttle fuselage. Data calculated by the system were then input to the HAVOC program to perform aerodynamic and structural analyses on these aircraft. The modeling system has also been used to pack the models. The figure shows the results of finding the component internal layout for the elliptical all-body model.

The geometry modeling system has provided a simple yet flexible method of modeling hypersonic aircraft concepts The calculation of packing efficiency is a particularly valuable part of the geometry-modeling system because of the dominance of hydrogen fuel tankage requirements in determining vehicle size and its effect on closure gross weight.

The hypersonic aircraft geometry modeling system will continue to be used to model trans-atmospheric vehicle concepts and provide data needed by the vehicle synthesis program. Code enhancement is ongoing. The bulk of the effort in code enhancement will focus on making the internal component models more flexible and on developing automated routines to optimize component placement in the aircraft for increased vehicle packing efficiency. The long-term plan is to merge the

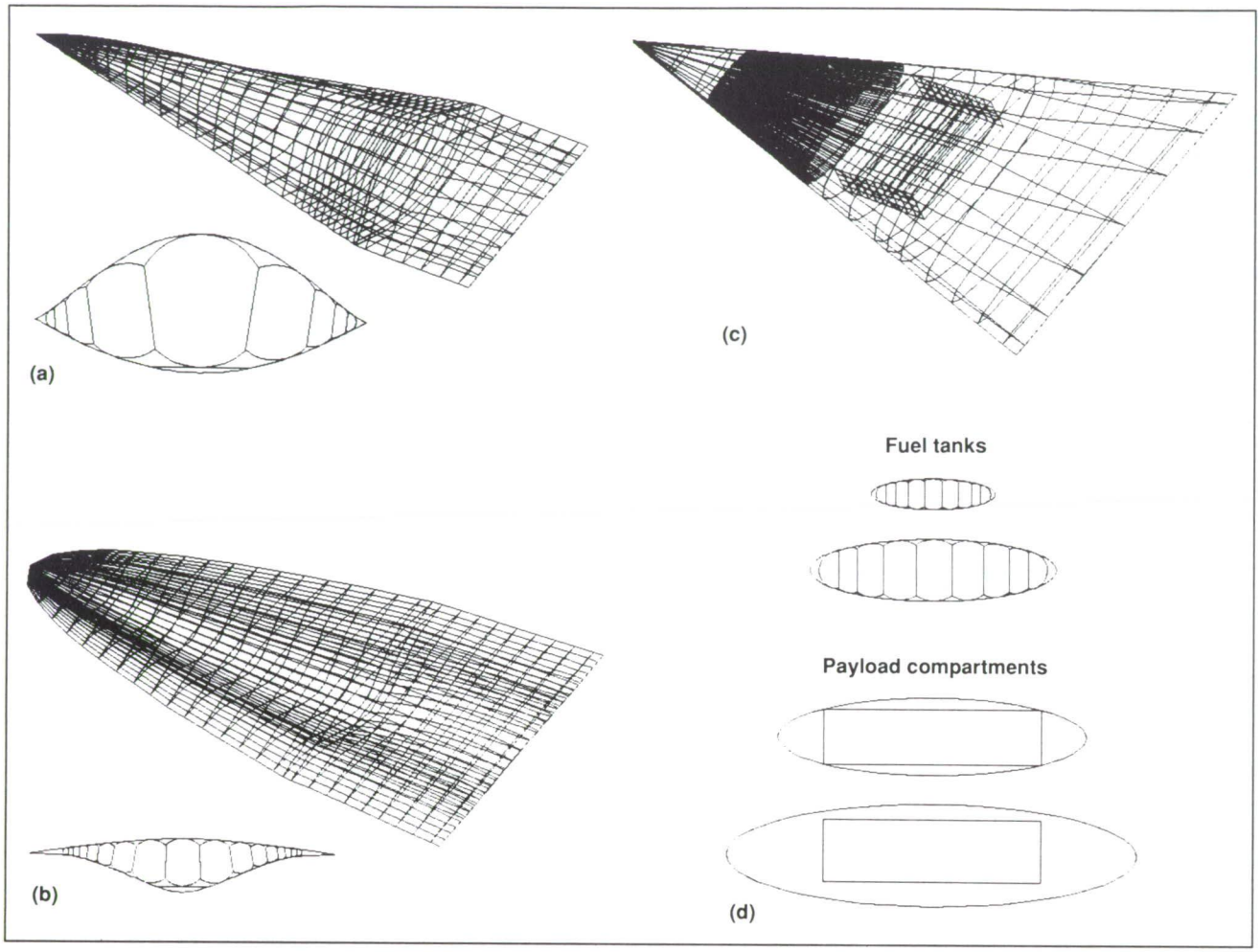


Fig. 1. Elliptical all-body fuselage with internal fuel tanks and payload compartment. (a) Lifting body model with a fuel tank packed in a typical cross section; (b) wave-rider model with a fuel tank packed in a typical cross section; (c) elliptical all-body packed with one fuel tank and a payload compartment; (d) cross-sectional fits for beginning and end of fuel tank and payload

geometry-modeling system with the HAVOC code and to use the input geometry parameters as independent design variables to find the overall optimal vehicle design.

Ames-Moffett contact: C. Roberts
(415) 604-3154 or FTS 464-3154
Headquarters program office: OAET

High-Speed Rotorcraft Technology Studies

Peter D. Talbot

Four conceptual design studies of advanced high-speed rotorcraft (HSRC) were completed in October 1990 by Boeing, Bell, Sikorsky, and McDonnell-Douglas helicopter companies. The intent of the studies was to help identify promising concepts and associated technology needs of rotorcraft having good low-speed, low-disk-loading (i.e., helicopter-like) attributes combined with high-cruise-speed capabilities (450 knots). After investigating a number of candidates, each contractor chose two advanced concepts that appeared to be most promising (e.g., tilt wing, tilt rotor with advanced high-speed proprotor, and stopped-rotor) and evaluated them in representative civil or military missions.

The figure shows concepts chosen by the contractors. Based on technology currently available, estimates of performance and weights were made to meet mission specifications. The benefits of advanced technology were then stated in terms of the potential for reduced mission gross weight and greater productivity. Based on this background, technological activities deemed to be essential to realizing these improvements were recommended.

For concepts using the rotor for propulsion in forward flight (such as the canard tilt rotor in the figure), a common result of the sizing exercises was the rapid increase in aircraft gross weight at design speeds above 400 knots. This was due to decreases in propulsive efficiency for relatively "conventional" proprotor designs and higher vehicle drag. One recommendation, therefore, was for investigations and experiments leading to a definition of highly efficient proprotors (propulsive efficiency near 0.80) that also have high figure-of-merit in hover and acceptable loads during conversion.

The high-tip-Mach-number environment for the rotor in cruise (vehicle Mach number = 0.73) suggests that highly twisted, very thin (6% thick) blades, possibly with swept tips, may be required to meet these goals. For these types of HSRC concepts, all of the "year 2000" engine performance was based on the advanced propulsion goals of the IHPTET program, and therefore no new propulsion activities

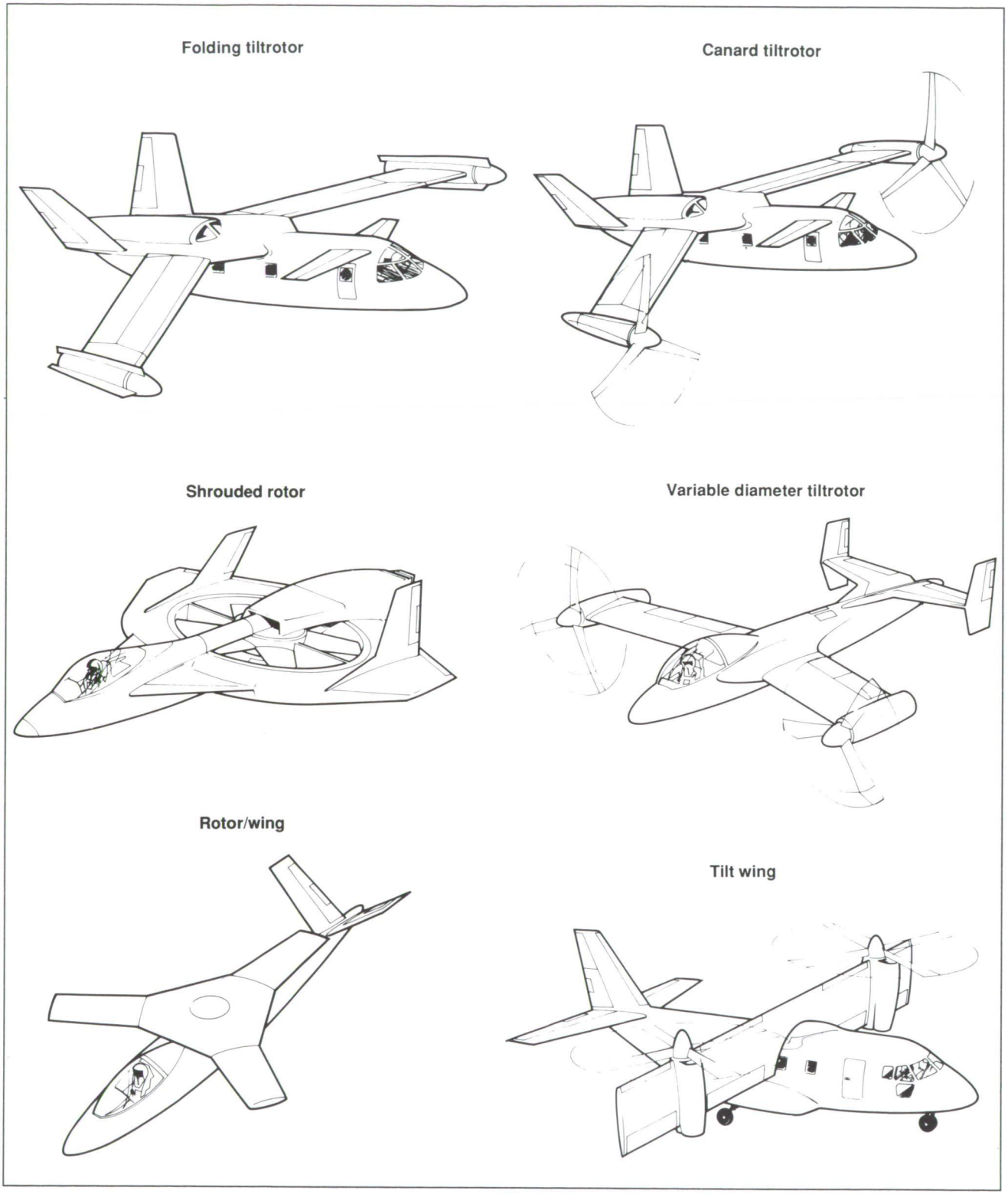


Fig. 1. High-speed rotorcraft concepts

were identified; however, the continued emphasis on IHPTET was seen to be necessary to realizing projected performance.

Ames-Moffett contact: P. Talbot/W. Snyder
(415) 604-5108/6570 or FTS 464-5108/6570
Headquarters program office: OAET

Investigation of Jet-Induced Effects in Hover

ORIGINAL PAGE
BLACK AND WHITE PHOTOGRAPH

Douglas A. Wardwell, Daniel B. Levin, Demo J. Giulianetti

A necessary ingredient to the successful design of high-speed fighter aircraft having vertical takeoff or landing capabilities or both is the identification and understanding of the complex ground-flow phenomena encountered during hover, vertical takeoff, or landing. Small-scale experiments are necessary to identify and evaluate such phenomena and to provide results that can be extrapolated with confidence to full-scale aircraft designs.

A small-scale Jet Calibration and Hover Test (JCAHT) facility became operational at Ames Research Center in August 1990 to permit the identification and assessment of jet-induced effects resulting from high-pressure air from one or more nozzles impinging on a variable-height ground plane. The JCAHT facility consists of a Jet Calibration Rig (JCR) with the capability to perform nozzle exit pressure surveys, and a Hover Test Rig (HTR) with a variable-height ground plane for model tests. The first figure shows a typical arrangement of a small-scale model mounted on the HTR above a 96- by 96-inch ground plane. Measurements include forces, moments, ground and nozzle pressures, ground-air velocities, and temperatures.

Cold air tests were performed with a 1.23-inch-diameter circular nozzle and 10- and 20-inch diameter sharp-edged circular plates. A matrix of nozzle exit pressure ratios of 1.5, 2, 3, 4, 5, and 6 were investigated at ground-plane heights of 2, 3, 4, 5, 6, 10, and 20 inches from the nozzle exit. The jet exiting from the nozzle passed through a circular hole in the center of the plate. Normal and axial forces on the plate were measured using a strain-gauge balance.

The effects of ground plane size (which ranged from 10- by 10-inches to 96- by 96-inches) were assessed and are illustrated in the second figure for 10- and 20-inch-diameter circular plates, respectively. The results show the insensitivity of lift loss to

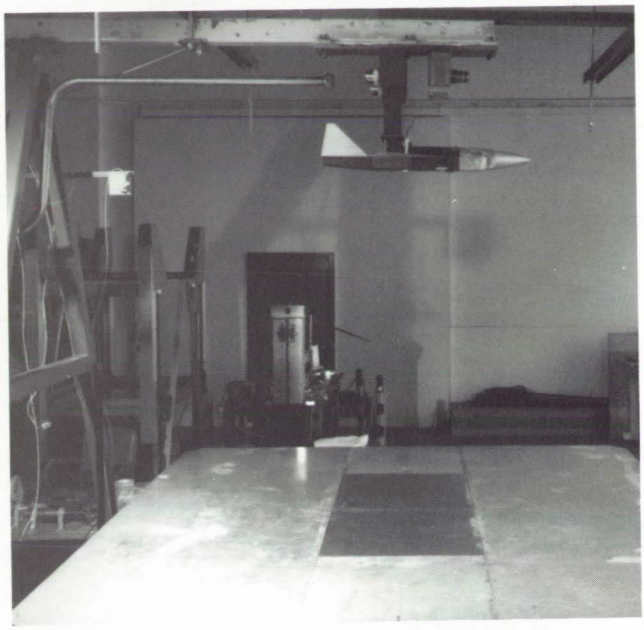


Fig. 1. Hover Test Rig showing attached model and large ground plane

ground-plane size, providing the square ground plane has equal or larger dimensions than the circular plate. This observation suggests that for obtaining jet-induced lift effects in hover for a single jet configuration, the ground plane need only be as large as the model planform being tested.

The matrices of nozzle-exit pressures and ground-plane heights were repeated for 10-inch-diameter plates to determine the influence of semiround and square circumferential edges. Also, a range of gaps (clearances) between the nozzle exit and the edge of the center hole in the plate were investigated to determine the significance of these parameters.

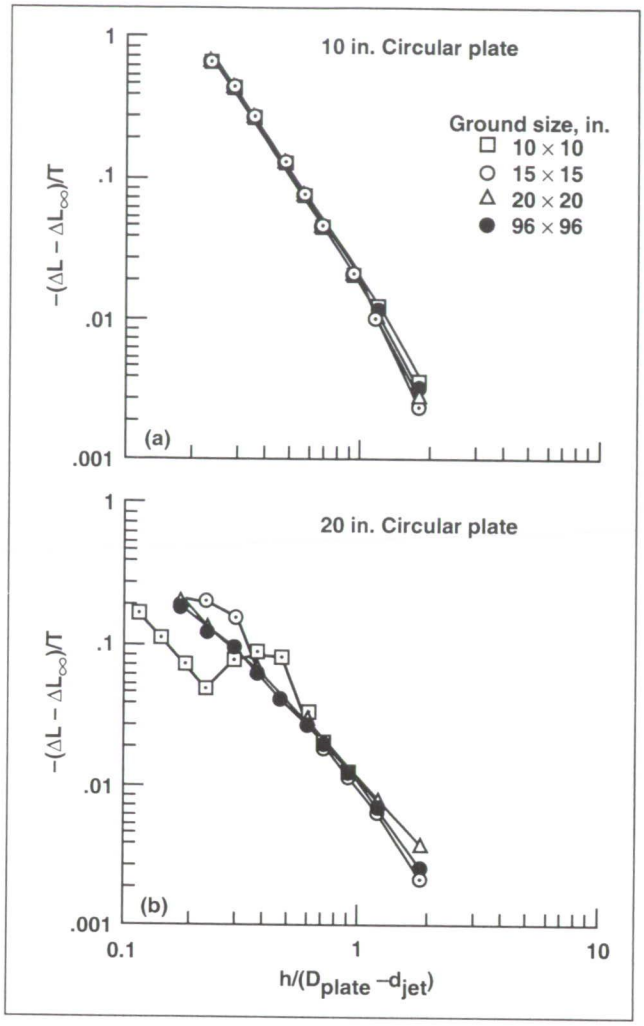


Fig. 2. Effect of ground size on lift loss on the (a) 10- and (b) 20-inch circular plates

Visualization of the flow is illustrated in the third figure, which shows a shadowgraph of the exit flow from a single circular nozzle passing through the center hole in the 10-inch circular plate at a nozzle pressure ratio of 3. Such flow is representative of the nozzle flow which could result from aircraft types such as vertical takeoff and landing (VTOL) and short takeoff and vertical landing (STOVL) aircraft during hover and vertical operations. The visualization of flow as shown in this figure will aid in evaluating the interactions between the jet, ground, and

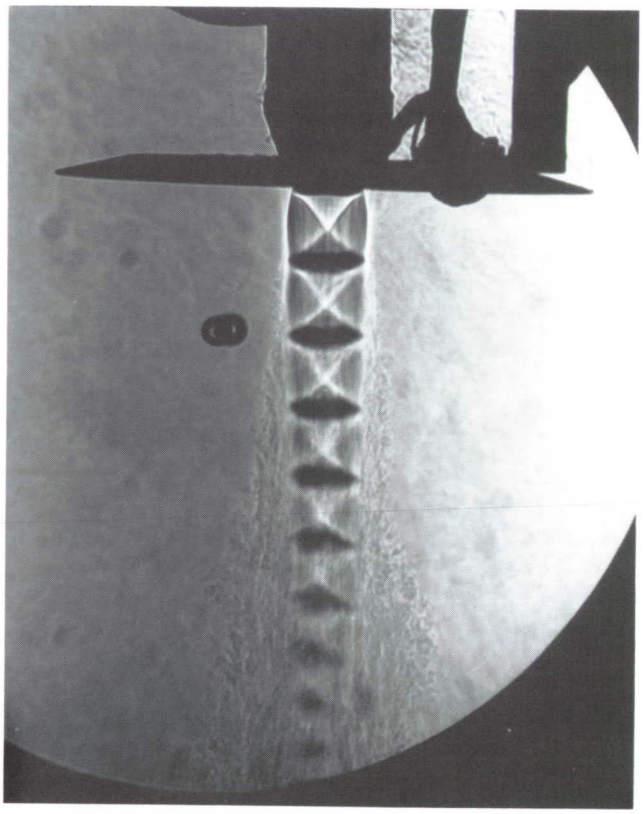


Fig. 3. Shadowgraph of jet emanating from the 10-inch circular plate at a nozzle pressure ratio of 3

airframe as well as supporting and validating computational studies used to predict these complex flows.

Future investigations will include testing of complete models of conceptual aircraft designs with various nozzle configurations. Heaters will be installed to heat the nozzle exit air up to 800°F at 1.5 lb/sec of flow at a heater inlet pressure of 450 psig. This will permit investigation of hot-gas effects which includes hot-air impingement on the ground and aircraft, as well as engine-performance degradation caused by hot-gas ingestion at the inlet.

Ames-Moffett contact: D. Wardwell
(415) 604-6566 or FTS 464-6566
Headquarters program office: OAET

ORIGINAL PAGE
BLACK AND WHITE PHOTOGRAPH

Acoustic Laboratory Data Acquisition System (ALDAS)

Michael Watts

The helicopter industry requires a more detailed analysis of acoustics data, than it did in the past, for correlation with increasingly sophisticated methods of prediction. Increasing concerns about the ability to detect helicopters, and the increased ability to predict precise spectra have generated the need for a low-cost, transportable, easy-to-use digital acquisition and analysis package.

Typically, acoustics data have been acquired on analog tape and then either analyzed directly with an analog-output narrow-band or octave-band analyzer, or digitized with a minicomputer-based system and analyzed through software. The analog-output analyzer imposes many user and operational limitations. These limitations include strictly controlled input duration and output resolution, and a restricted number of input channels–typically only one or two input channels are available at a time. Another limitation is that although most analyzers can transport the results to other types of machines, they frequently cannot transfer the exact set of analyzed data for further analysis or display.

The minicomputer-based technique overcomes many of the limitations of the analog-output devices. It is versatile, it can handle simultaneous input data channels, and the data can be saved and used by other applications or machines. However, the minicomputer-based system is not easily transportable and can be expensive.

The Acoustic Laboratory Data Acquisition System (ALDAS) was designed to exploit the advantages of the minicomputer system while overcoming its two major limitations.

ALDAS runs on the Macintosh II family computers and has the following capabilities:

1. Conforms to Apple Macintosh human interface guidelines
2. Automatic calibration of acoustic acquisition channels

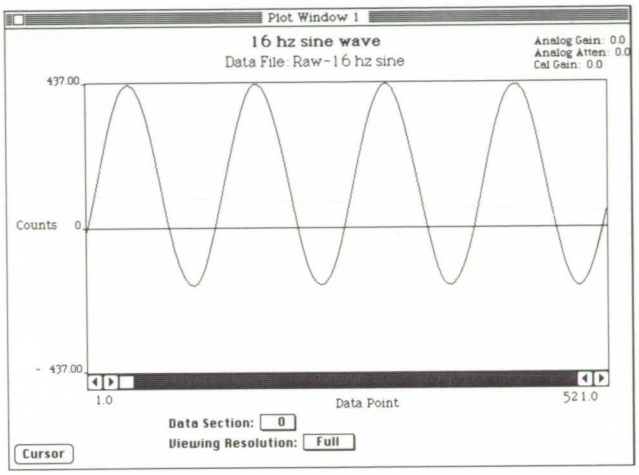


Fig. 1. Plot window showing 16-hertz time-history

3. Simultaneous acquisition of up to four channels of data at rates up to 50,000 samples per second
4. Data display in up to four scrolling windows using user-selected units
5. Amplitude spectrum and third-octave analysis with two types of spectrum averaging, nine types of windows, and four window overlaps
6. Digital filtering with three filter windows
7. Cycle averaging with user-selected cycle starting points

The figure shows the time-history of a 16-hertz sine wave in the data-plot window. The capabilities of ALDAS are continually being improved to meet the needs of users and plays an important role in rotorcraft acoustic investigations.

Ames-Moffett contact: M. Watts
(415) 604-6574 or FTS 464-6574
Headquarters program office: OAET

Civil Tilt-Rotor Study

ORIGINAL PAGE
BLACK AND WHITE PHOTOGRAPH

John Zuk

The development and validation of tilt-rotor technology by the U.S. government and industry in the past two decades has placed the United States in an international leadership position in tilt-rotor aircraft. The current military V-22 Osprey tilt-rotor aircraft is the first tilt-rotor production aircraft in the world. The implications for civil aviation are significant. A fleet of civil tilt-rotor aircraft operating in a modernized National Airspace System is expected to reduce current metropolitan air-traffic congestion and to provide a practical alternative to alleviate the short-haul air transportation demands.

A Federal Aviation Administration/NASA Civil Tilt-Rotor Missions and Applications Phase II Study, the Commercial Passenger Market, was completed. The study was conducted by the Boeing Commercial Airplane Group teamed with Bell Helicopter Textron and Boeing Helicopter. The study tasks included market-demand forecasts, economics assessments, identifications of highest pay-off technologies, an operational analysis using simulators to determine safe steep approaches to vertiports, and action to achieve a national civil tilt-rotor transportation system.

The study found that the anticipated demand for a fully market-responsive designed tilt rotor will be 2,625 vehicles by the year 2000, growing to 4,925 in the year 2010. The market value of 2,625 aircraft is $32 billion to $42 billion, with half this being a domestic market and the remainder as a potential worldwide export market. Furthermore, the manufacturer can sell it to a user at a profit. The tilt-rotor total cash operating cost was found to be only 22% higher than that for a turboprop in the same service. An analysis of the northeast corridor in the United States suggests the total trip cost would be competitive with that of fixed-wing aircraft.

The tilt rotor can significantly relieve airport congestion. A simulation of the northeast corridor airline service indicated a tilt-rotor network could open up 1,000 airport slots per day (1/3 of 1,989 daily slots) by replacing commuter aircraft. A fully market-responsive tilt rotor is different from the V-22 configuration and must meet three barrier technology

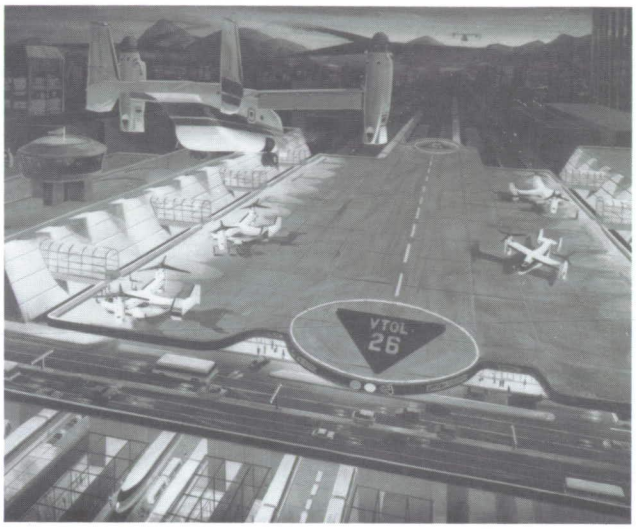


Fig. 1. Intermodal Transportation Center linking air and ground transportation

challenges: (1) low external noise, (2) human factors-based pilot controls for commercial flight, and (3) terminal-area low-speed control and navigation allowing safe, precise, steep approaches. In addition the study identifies many enhancing technologies. The preliminary piloted simulations of a civil tilt rotor indicate that steep (15°) approaches are doable.

Even though the market demand opportunity is very high, a market-responsive design is not sufficient for industry to commit to production. Additional research is required by non-industry resources. The study recommends actions for the FAA to undertake to develop timely certification and regulatory changes. These changes would allow the tilt rotors unique operating capability to be fully utilized. Also the study states the need for strategically located vertiports to be in place. The study recommends establishment of a public/private partnership to enable a national tilt-rotor transportation system.

Ames-Moffett Contact: J. Zuk
(415) 604-6568 or FTS 464-6568
Headquarters Program Office: OAET

Full-Scale Tilt-Rotor Performance

Mike Derby

A full-scale test of two different sets of XV-15 Tilt-Rotor Research Aircraft prop-rotor blades is planned for the 40- by 80-Foot Wind Tunnel in spring 1991. The test will use the Ames Prop Test Rig and its high-accuracy rotor balance system to measure isolated prop-rotor performance, oscillatory hub loads, and control system loads over the full XV-15 airplane-mode flight envelope.



Fig. 1. 1984 Ames Outdoor Aerodynamic Research Facility test with the XV-15 metal blades

The XV-15 aircraft will be tested. These three-bladed prop-rotors are both 25 feet in diameter, but utilize different airfoils and twist distribution and have significantly different solidity ratios. The two-blade sets are commonly referred to as the XV-15 metal blades and the Advanced Technology Blades (ATB).

Each blade set will be tested as an isolated prop-rotor. The test envelope will encompass the full aircraft flight envelope in airplane-mode. Airspeed will range from 100 to 250 knots with angles of attack up to 10°.

This test will provide a set of forward-flight performance data that will complement the hover performance data acquired in 1984 at the Ames Outdoor Aerodynamic Research Facility using the same prop-rotor blade sets (see figure). The test will yield the first test data acquired at tunnel speeds greater than 185 knots for the XV-15 metal-blade set. Previous development testing of the XV-15 rotor system during the 1970's was airspeed-limited in the 40- by 80-Foot Wind Tunnel. These new data will be critical to validating design analysis codes and providing information on XV-15 aircraft total performance. This will also be the first set of high-speed airplane-mode data acquired for the ATB blade set.

Ames-Moffett contact: M. Derby
(415) 604-6856 or FTS 464-6856
Headquarters program office: OAET

ORIGINAL PAGE
BLACK AND WHITE PHOTOGRAPH

Fully Coupled Structural Deformations and Computational Fluid Dynamics

Fort Felker

A method has been developed to simultaneously solve the governing equations for computational fluid dynamics (CFD) and structural deformations of the body of interest. The structural deformations of the body are determined by the pressures in the computed flow, and the computed flow depends on the configuration of the body. The CFD formulation is a finite-volume method, with arithmetic-average flux splitting. A steady-state solution is obtained directly by using Newton's method.

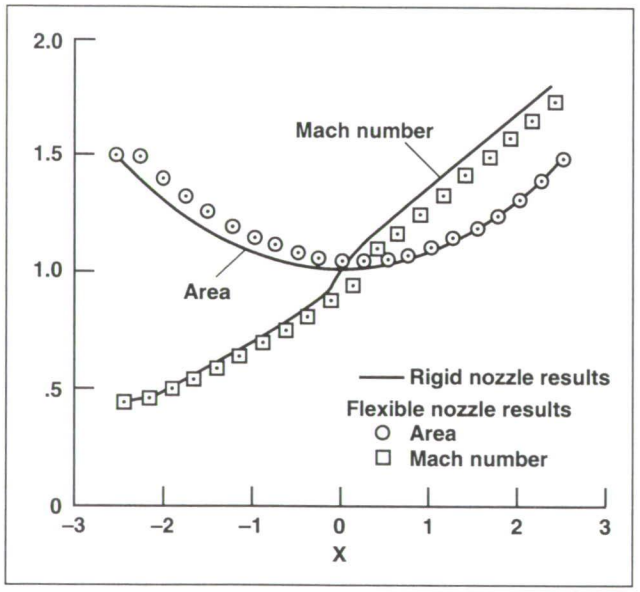


Fig. 1. Effect of nozzle flexibility on cross-section area and Mach number of transonic nozzle $k = 4 \times 10^3$

To demonstrate the method, the flow in a quasi-one-dimensional, transonic, convergent-divergent nozzle was computed. The walls of the nozzle were flexible, with their deformations from an equilibrium position determined by the local pressure and by a spring constant. The one-dimensional Euler equations were used for this model problem.

The figure shows a comparison of the results obtained with rigid and flexible nozzle walls. Significant changes in the nozzle area distribution occur upstream of the throat, whereas the most significant changes in the Mach number occur downstream of the throat.

Ames-Moffett contact: F. Felker
(415) 604-6096 or FTS 464-6096
Headquarters program office: OAET

Shadowgraph Flow Visualization of Rotor Wakes

Alexandra Frerking, Jeffrey Light

A shadowgraph test of a 7/38-scale V-22 rotor was conducted at the NASA Ames Outdoor Aerodynamic Research Facility (OARF) in 1990. The objective of the test was to investigate rotor-wake/tip-vortex interactions with a wing and image plane. Isolated rotor-wake geometry data were also acquired for three thrust conditions. The still cameras, video cameras, and strobes were set up to provide two orthogonal views for the shadowgraph rotor-wake investigations.

Preliminary reviews of the shadowgraph results are very encouraging. A representative shadowgraph picture is shown in the figure. The tip-vortex shadows are seen as dark spirals being shed from the blades, with the wake impinging upon the surface of the wing. An important shadowgraph visibility check was also conducted during the test, using large distances between the camera and screen, to demonstrate that the wide-field shadowgraph technique should work in the Ames National Full-Scale Aerodynamics Complex Wind Tunnels.

Preparations are being made to acquire shadowgraph data for a full-scale S-76 rotor in forward flight in the Ames 80- by 120-Foot Wind Tunnel. This will be the first time the wide-field shadowgraph technique will be applied to large-scale rotor flow visualization. The objectives of this test are to document the shadowgraph visibility for various operating conditions, to acquire three-dimensional wake geometry, and to validate the predicted locations of blade-vortex interactions. Current efforts are being directed toward developing an automated method for acquiring, digitizing, and reducing wake coordinates from two simultaneous images.

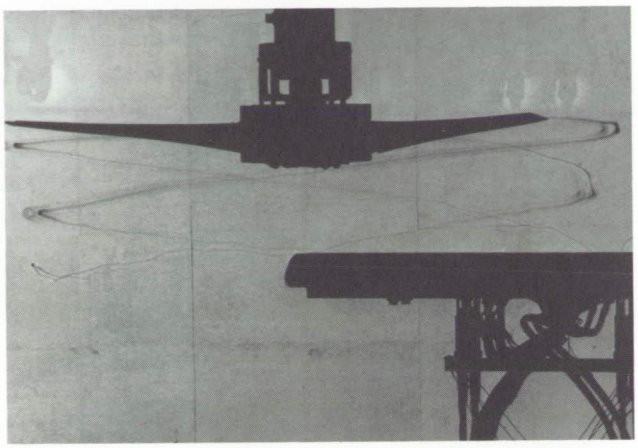


Fig. 1. Wide-field shadowgraph of a 7/38-scale V-22 rotor in a hover download configuration

Ames-Moffett contact: A. Frerking
(415) 604-6856 or FTS 464-6856
Headquarters program office: OAET

ORIGINAL PAGE
BLACK AND WHITE PHOTOGRAPH

Computation of Rotor Aerodynamic Loads in Forward Flight

Ruth Heffernan

The aerodynamic environment in which a helicopter rotor blade operates is to a large extent determined by the vortex wake of the rotor. Consequently, the analysis of rotor-wake behavior in forward flight has been of great interest for many years. Until recently, however, rotor aerodynamic analyses have been executed by using models that lack many of the important features of the actual wake structure. These analyses have typically met with indifferent success in correlating with measured aerodynamic loads in forward flight. The goal of this project was to develop and test a forward-flight aerodynamic analysis employing a novel free-wake simulation, designed to better represent the true physical rotor wake. This study was conducted by Continuum Dynamics, Inc., under a Phase II Small Business Innovation Research contract.

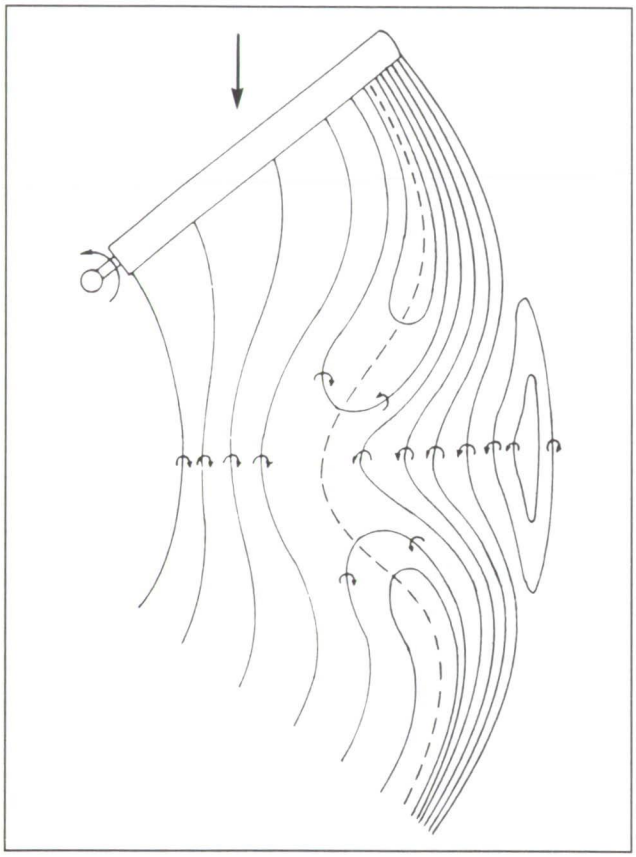


Fig. 1. Contours of constant sheet strength in the wake on the advancing side

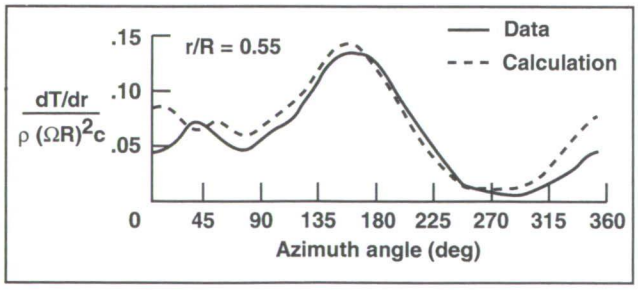


Fig. 2. Nondimensional sectional thrust versus azimuth angle for the H-34 rotor: advance ratio 0.39, –5° shaft angle of attack

The wake model developed in this program discretizes the sheet of vorticity that trails from each blade by laying out vortex filaments along contours of constant sheet strength. These filaments are composed of curved elements and distort freely in response to the local velocity field (see first figure). This approach automatically captures the full-span wake of each rotor blade and includes many features of the complex vorticity field of the rotor. These features have been coupled in a general forward-flight analysis model of isolated rotors: Computation of Rotor Aerodynamics in Forward Flight (RotorCRAFT).

Results to date indicate that this wake model, when coupled with a vortex-lattice model of the blade and a finite-element treatment of the blade structure, can successfully predict unsteady airloads. The second figure shows a typical correlation of nondimensional sectional thrust versus azimuth angle for the H-34 rotor (55% radial station, 0.39 advance ratio, –5° shaft angle). The agreement is quite close, with major discrepancies only in the region around $\Psi = 0°$. These and other correlation results, along with a complete description of the analysis development, will be published as a NASA Contractor Report.

Ames-Moffett contact: R. Heffernan
(415) 604-5043 or FTS 464-5043
Headquarters program office: OAET

Dynamic Characteristics of Bell M412 Pylon and Model 576 Test Stand

Mohammed Hoque

A shake test was conducted in the 40- by 80-Foot Wind Tunnel at Ames Research Center with the Bell M412 transmission/pylon assembly mounted on the Model 576 Test Stand. The simulated hub was excited with both broadband random and discrete excitations, and accelerometer responses were measured at various locations. The transfer functions (acceleration per unit excitation force as a function of frequency) for each of the accelerometer responses were computed, and the data were analyzed by using modal analysis to estimate the modal parameters of the configuration shown in the figure.

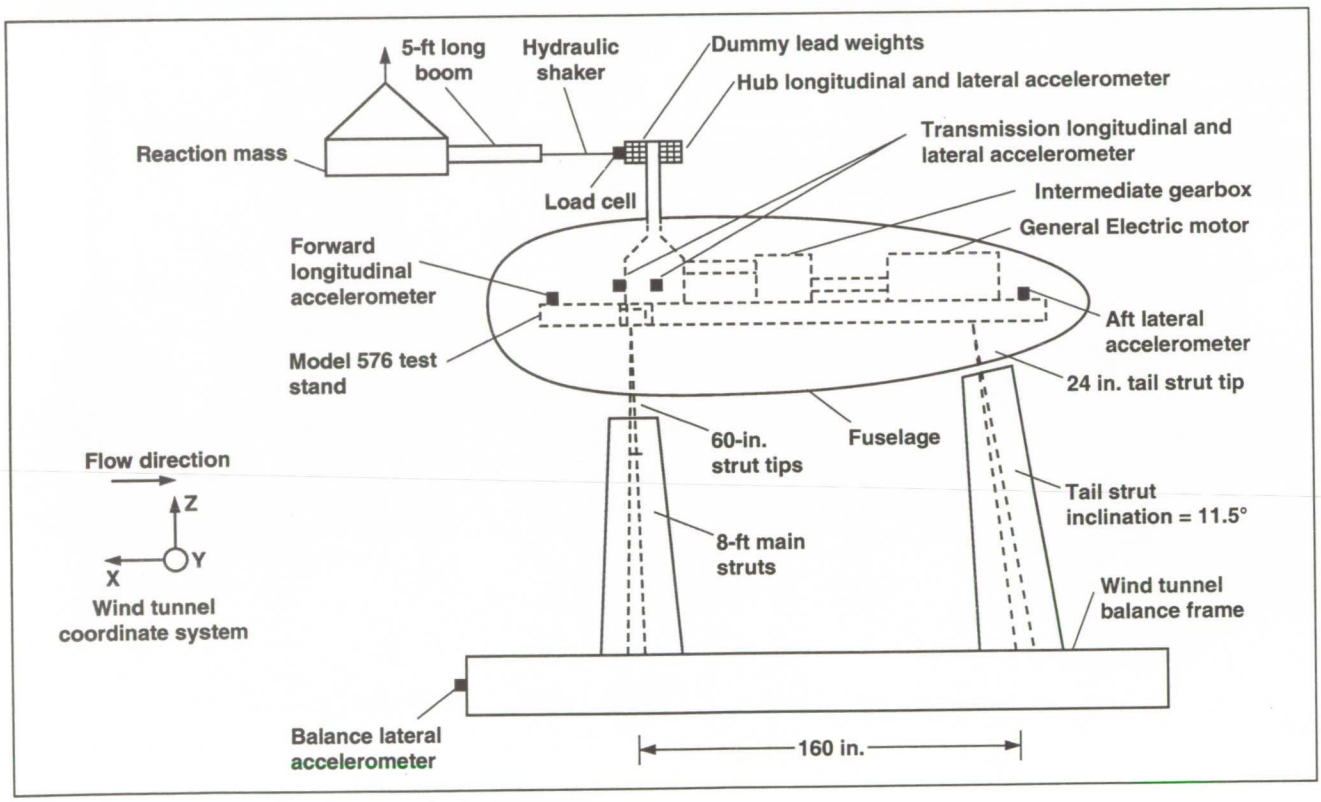


Fig. 1. Schematic of Model 576 test stand setup in the the 40- by 80-Foot Wind Tunnel

The primary objective of the shake test was to identify the non-rotating-frame/fixed-system modal damping present in the model support system (wind-tunnel balance and struts). Knowledge of the available damping in each of the shake configurations is crucial for performing a rotor test, from the standpoint of potential ground-resonance instability. The critical damping ratios, for various modes of vibration in the rotor operating range, were determined by curve-fitting the measured transfer function by using a modal analysis software package. These damping coefficients are used to analytically determine the stability of the rotor. Several combinations of wind-tunnel balance and pylon dampers were shake-tested in order to determine the test configuration that would provide sufficient damping for stable rotor operation.

The model consisted of a 1500 hp General Electric motor; a Bell M412, transmission, hub, and blades; an intermediate gearbox mounted on the Model 576 test stand structural frame; and the fuselage. The entire test setup as mounted to the wind-tunnel struts weighed 15,200 pounds. The model was mounted in the 40- by 80-Foot Wind Tunnel on 8-foot main struts with 60-inch strut tips, and on a tail strut with a 24-inch tip. The tail strut was inclined at 11.5° with respect to the z-axis. The rotor mass (including hub and blades) was simulated by attaching dummy lead weights to the hub.

From the shake-test transfer functions, the balance, strut, and pylon roll and pitch modes of vibration for the Bell M412 pylon assembly and wind-tunnel support system have been identified. Computed percent critical modal damping ratios are at least 2% for configurations consisting of eight wind tunnel balances and four or eight pylon dampers. Subsequent wind-tunnel testing up to 140 knots demonstrated the stability of the rotor/pylon/M576 test stand/wind-tunnel support dynamic system.

Ames-Moffett contact: M. Hoque
(415) 604-5043 or FTS 464-5043
Headquarters program office: OAET

Dynamic Characteristics of the Simulated Rotor Test Apparatus

Mohammed Hoque, Randy Peterson

The new 80- by 120-Foot Wind Tunnel at Ames Research Center will be used for full-scale helicopter research. A critical requirement for any rotor test in the new tunnel will be that the rotor/test-stand/support system be free of any dynamic instability. Such an instability (ground resonance) can be catastrophic if there is inadequate damping in the fixed-system modes of vibration.

Consequently, a shake test was conducted in the 80- by 120-Foot Wind Tunnel using a load frame and dummy weights to simulate the weight of the NASA Rotor Test Apparatus (RTA). The simulated hub was excited with broadband random excitation, and accelerometer responses were measured at various locations. The transfer functions (acceleration per unit excitation force as a function of frequency) for each of the accelerometer responses were computed, and the data were analyzed using modal analysis to estimate the modal parameters. The primary objective of the shake test was to determine the amount of support-system modal damping in the wind-tunnel configuration (shown in the figure) for performing a rotor test using the RTA, from the standpoint of potential ground-resonance instability.

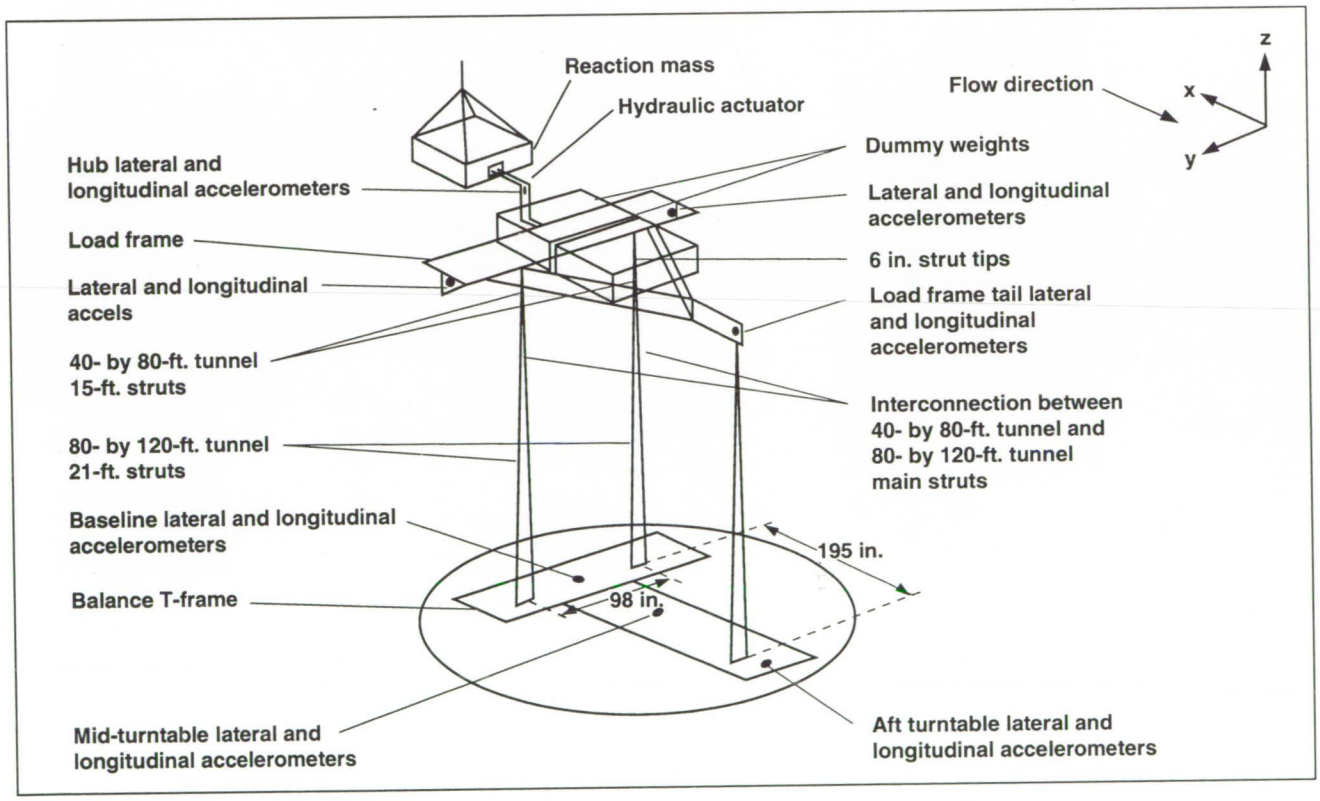


Fig. 1. Shake test setup of simulated Rotor Test Apparatus (RTA) in the 80- by 120-Foot Wind Tunnel

The model consisted of a 4,500-pound load frame, using dummy weights to simulate the RTA weight (29,200 pounds). The load frame was mounted on a combination of 40- by 80-Foot (15-foot struts and 6-inch strut tips) and 80- by 120-Foot Wind Tunnel struts (21-foot), which positioned the model strut attachment points 36.5 feet above the tunnel floor. The location of the RTA rotor hub was simulated by structural beams, without modeling the hub or the blade mass, which is considered insignificant relative to the test stand and the wind-tunnel support system.

The shake test revealed all the low-frequency modes of vibration of the wind-tunnel model support system for the simulated RTA mounted in the Ames 80- by 120-Foot Wind Tunnel. The data have been reported in a NASA Technical Memorandum. From the reduced data it was determined that there is sufficient damping in all the modes of vibration for safely performing a rotor test in this wind tunnel. However, as an added precaution, 12 wind-tunnel balance dampers have been installed between the balance system and the balance house to increase fixed-system damping to further ensure dynamic stability.

Ames-Moffett contact: M. Hoque
(415) 604-5043 or FTS 464-5043
Headquarters program office: OAET

Advanced Bearingless Rotor Research with Active Controls

Stephen Jacklin

Bearingless and hingeless rotors in modern helicopters provide increased control moment and maneuverability. However, they pose greater challenges to the dynamist and control systems engineer to accurately model the coupled rotor/fuselage system and to predict the rotor stability and loads characteristics.

In an effort to obtain better predictive capabilities, the McDonnell Douglas Helicopter Company (MDHC) and the Ames Rotorcraft Aeromechanics Branch are jointly conducting a wind-tunnel test program to study the MDHC advanced bearingless rotor design shown in the figure. Two test entries are planned. The first test will primarily study dynamics, loads, and acoustics, both with and without higher harmonic control (HHC). The second test will attempt to gain a more detailed understanding of the rotor aerodynamic loading by using a pressure-instrumented rotor built by MDHC with NASA-supplied pressure instrumentation.

The overall objective of the McDonnell Douglas Advanced Rotor Test program is to develop a high-fidelity test data base to advance the development of computer prediction codes for bearingless rotors. Most rotorcraft prediction codes cannot handle bearingless rotors because of the redundant load paths of the blade retention and control system. Nevertheless, the promise of higher maneuverability, higher agility, greater control moment capability, and improved rotor service life of bearingless rotors cannot be realized without good bearingless-rotor analytical prediction methods. Recognizing this need, NASA, MDHC, and a few others have been pursuing the development of prediction codes for bearingless rotors. Impeding this development, however, has been the lack of adequate test data for prediction-code validation.

The tests planned for the Ames 40- by 80-Foot Wind Tunnel will provide a data base for bearingless-rotor prediction-code validation and development. The testing is planned to obtain data

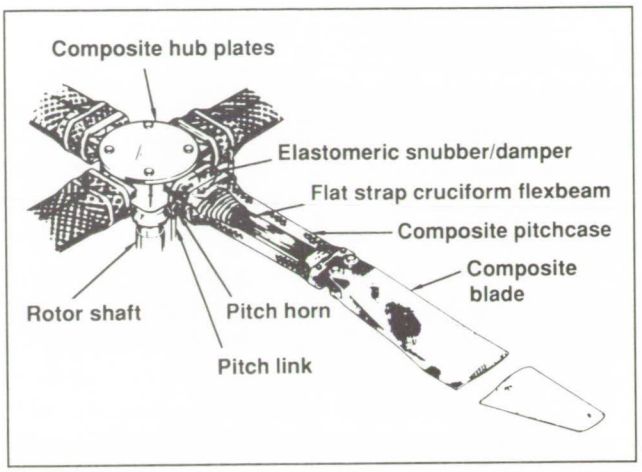


Fig. 1. MDHC advanced bearingless rotor

up to the high thrust (≈1.8 g) and high speed (≈0.5 μ) limits of the rotor. Of primary concern will be the stability characteristics and strains developed within the flexbeams attaching the rotor blades to the hub. Data will be acquired for non-zero flapping to evaluate the flight loads developed on the rotor and for later direct comparison with flight testing. A secondary goal of the testing will be to acquire a detailed acoustic data base through use of a traversing microphone mechanism. This data base will be useful in developing an understanding of blade-vortex interaction and high-speed impulsive-noise mechanisms, as well as in providing test cases for the validation of rotor acoustic prediction codes. It is also planned to evaluate the effects of open-loop higher harmonic control on the rotor loads and acoustics during the first entry to help define the baseline closed-loop controller to be studied during the second entry. Testing is expected to begin in September 1991.

Ames-Moffett contact: S. Jacklin
(415) 604-4567 or FTS 464-4567
Headquarters program office: OAET

Bell 412 Pressure/Acceleration-Instrumented Rotor

Stephen Jacklin

The Rotorcraft Aeromechanics Branch has nearly completed acquisition of a highly instrumented Bell 412 main-rotor-blade set. This rotor will have 290 pressure transducers, 46 strain gauges, and 24 accelerometers distributed among the four blades. Two aerodynamic interaction tests using a nonpressure-instrumented Bell 412 blade set have been conducted in the 40- by 80-Foot Wind Tunnel using the Model 576 test stand. Mating hardware also exists for the Bell 412 on the Ames Rotor Test Apparatus (RTA). The acquisition of this pressure-instrumented blade set will afford the opportunity to study many important aerodynamic phenomena and will provide good continuity for the in-house research program by using this previously documented and well-understood rotor system.

The manner of blade instrumentation is noteworthy. In an effort to minimize cost, it was decided to instrument an existing blade set. This required surface mounting of the pressure transducers and strain gauges. Although the strain gauges did not pose an aerodynamic problem, the many wires and 0.03-inch height of the the 290 pressure transducers had the potential for corrupting the flow. To accommodate the many wires, a 0.5-inch wide, 1-inch deep trough was cut along the upper surface of the A and C blades, just behind the spar. After laying the wires in the trough, the blade surface was restored and Fiberglas belts were placed over the pressure transducers to smooth out the airflow.

An analysis was performed at Ames to determine the optimal blade-section contours shown in the figure. The resulting belt widths accommodated spanwise flow effects for 95% of the pressure transducers up to an advance ratio of 0.40.

This rotor will be used to study a number of interesting aerodynamic phenomena. Used with the pressure-instrumented Model 576 test stand and Lynx pressure-instrumented tail rotor, a full assessment of main-rotor, body, and tail-rotor aerodynamic interactions can be performed. Information from the pressure, strain, and accelerometer gauges will be used to gain an understanding of how the aerodynamic loading changes with the application of higher harmonic control for stability augmentation or vibration reduction. The on-blade accelerometers will also provide mode-shape information and be useful in evaluating various rotor-mode control concepts. Since the dynamic range of the pressure transducers is above 40 kilohertz, it will also be possible to study various acoustic phenomena, including the influence of higher harmonic control on blade-vortex interaction noise.

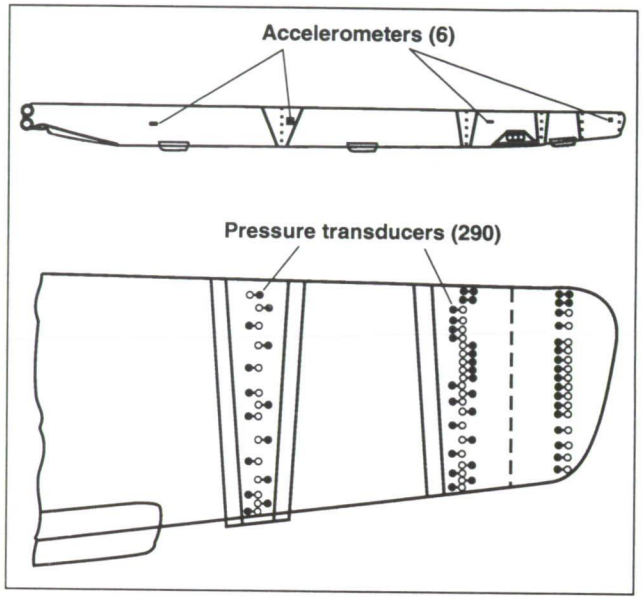


Fig. 1. Bell 412 pressure-instrumented rotor

Ames-Moffett contact: S. Jacklin
(415) 604-4567 or FTS 464-4567
Headquarters program office: OAET

Individual Blade-Control Research Program

ORIGINAL PAGE
BLACK AND WHITE PHOTOGRAPH

Stephen Jacklin

The use of rotor control for purposes other than aircraft trim has been pursued for many years. These control methods have involved blade-pitch control to improve aircraft performance (handling qualities, vibration reduction) and have relied on conventional control through the swashplate. But control through the swashplate is fundamentally limited for rotor systems with four or more blades, in that the pitch (or servo-flap) control of one blade predetermines the control for the other blades. This shortcoming of the conventional swashplate precludes the control of each blade individually, which may prove critical in reducing the high vibrations, loads, and acoustics at the limits of the flight envelope.

Recently, a German corporation (MBB and its subsidiary HFW) developed actuators for the rotating system which replace the pitch links of the rotor system (see figure). This design was flight tested at very low authority (±0.19°) on a modified BO-105 helicopter at the MBB flight test center in Munich. The use of actuators in the rotating system, one for each blade, is a breakthrough in rotor-control technology. Such individual rotor-blade control (IBC) provides for new control methods in rotor loads alleviation, vibratory hub-load reduction, fuselage vibration suppression, rotor-blade airload modification, and rotor performance improvements through blade-vortex-interaction avoidance, blade-stall suppression, and lift redistribution.

To provide greater understanding of the potential benefits of individual rotor-blade control, a joint U.S./German comprehensive wind-tunnel test program will be conducted in the Ames 40- by 80- Foot Wind Tunnel. Participants include NASA, the U.S. Army, DLR, MBB, and HFW. The approach will be to conduct a series of full-scale MBB BO-105 tests using the new German-owned IBC hardware

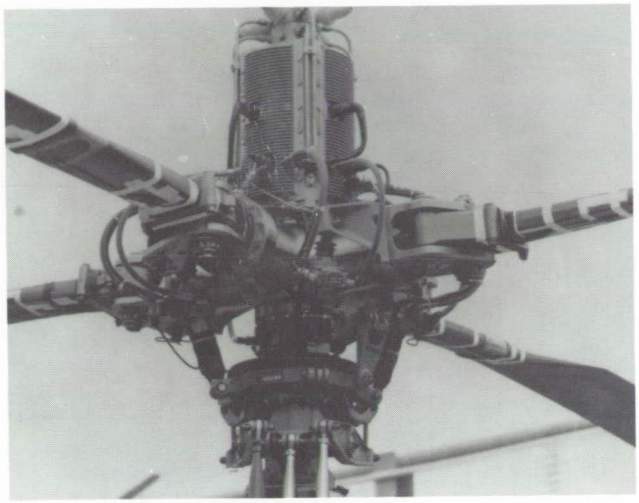


Fig. 1. Rotating individual-blade control actuators

on the Ames/Army Rotor Test Apparatus (RTA). The first tunnel entry will conduct open-loop higher harmonic control (HHC) testing to study the effects of 2/rev IBC control on rotor performance and acoustics. The testing will also compare the vibration, loads, performance, and actuator power resulting from the introduction of 3, 4, and 5 /rev HHC by using the new ±5° IBC hardware versus introduction through the conventional ±3° swashplate control hardware of the RTA. The second entry will perform closed-loop testing and will explore the full nonharmonic capability of the IBC actuators using an advanced controller developed by the research participants. The open- and closed-loop tests of the IBC system are planned for May 1992 and February 1993, respectively.

Ames-Moffett contact: S. Jacklin
(415) 604-4567 or FTS 464-4567
Headquarters program office: OAET

Real-Time Rotor Identification Methods

Stephen Jacklin

Closed-loop suppression of vibration and loads throughout the entire flight envelope of a helicopter requires accurate information about the relationship between the control inputs and the accelerations or strains to be controlled. Although off-line methods, such as the familiar least-squares technique, can be used for time-invariant systems, stochastic methods are required when the parameters change with time. Methods for obtaining such information, called on-line system-identification techniques, have been used for many years, mostly in the form of the Kalman filter method. Yet despite successful application of the Kalman filter to flight-vehicle state estimation, tracking of the helicopter vibration transfer matrix has eluded all research efforts. The general problem is that unlike the case of flight trajectory, the vibration suppression commands drive the measurement elements to zero. In this case, identification methods, having better built-in noise rejection characteristics, may avoid the instability and convergence problems encountered with the Kalman filter approach.

An on-going study is being conducted to evaluate the performance of two system-identification methods derived to have better noise-rejection capability through use of multiple measurements in the identification process. These methods, the generalized Kalman and generalized least-mean-square (GLMS) filters, are methods that are similar to the classic Kalman filter but allow for more than one measurement to be used in their formulation.

The first table illustrates that the generalization has the desirable effect of reducing the amount of user-supplied tuning information at the expense of gathering information from more measurements.

Amount of System Information Obtained from User versus Direct Measurement

Identification method	Required user supplied tuning parameters	Number of measurements in computation
Classic Kalman filter	2 matrices 1 scalar	1
Generalized Kalman filter	1 matrix 1 scalar	1 to N
Generalized least-mean-square filter	1 scalar	1 to N

This means less time need be spent adjusting the filter for successful implementation because, whereas the optimal tuning information is often unknown to the user (he must guess), past measurements are always available.

Computation Times on a 12 MIPS Machine (FPS AP-120B)

Identification method	Computation time, msec
Classic Kalman filter	0.33
Generalized 1-step Kalman filter	0.66
Generalized 4-step Kalman filter	0.67
Generalized 1-step LMS filter	0.93
Generalized 4-step LMS filter	1.53

A detailed computer simulation study is being performed to evaluate the identification performance of the two new methods against the classic Kalman filter. Preliminary results (second table) indicate improved stability and less sensitivity to tuning errors. However, in the case of the generalized Kalman filter, the improved identification performance was obtained at the expense of doubling the computation time. The generalized least-mean-square filter matched the identification accuracy of the Kalman filter method using only one measurement, but was computationally twice as fast.

By using more than one measurement, the generalize least-mean-square method improved the identification accuracy and stability at the expense of greater computation times. Nevertheless, as shown in the second table, the multistep-method computation times are still small enough, relative to the rotor rotational period (≈0.2 seconds), to permit real-time implementation.

Ames-Moffett contact: S. Jacklin
(415) 604-4567 or FTS 464-4567
Headquarters program office: OAET

Study of Aeroelastic Problems Using Active Controls

Stephen Jacklin

Although hingeless and bearingless rotor configurations are mechanically simpler and lighter, their development requires careful analysis to avoid problems induced by introducing active controls. Peretz P. Friedmann and students at the University of California, Los Angeles, investigated such problems. Previous work developed coupled rotor/fuselage mathematical models for helicopters by using computer-based symbolic manipulation methods. Those simulations considered a coupled flap-lag-torsional aeroelastic stability and response analysis, incorporating a time-domain, unsteady aerodynamic model. The blades were modeled using Galerkin-type finite elements combined with an implicit formulation, enabling a general representation of the loads.

Last year, using the previously developed model, the research was directed toward comparing helicopter vibration reduction by reducing hub forces versus reducing accelerations obtained at the pilot seat. The model consisted of a six-degree-of-freedom flexible fuselage coupled to a hingeless rotor model having three degrees of freedom per blade for rigid flap, lag, and torsional motion. It was determined that unless the fuselage was perfectly rigid, suppression of hub forces did not lead to minimized pilot seat vibration.

It was also shown (see figure) that hub shears and fuselage vibrations could be simultaneously reduced using a new higher-harmonic-control scheme, "multiple higher harmonic control" (MHHC). In this scheme, both N/rev and N+1/rev (or N-1/rev) excitations were applied in the nonrotating system. Although the blades do not "track" in the conventional sense (i.e., each blade does not have the same flap/pitch/lag trajectory around the azimuth), the N-1 excitation appeared to calm the first elastic flap blade-bending mode, thereby yielding vibration suppression. These results were presented in two papers, one at the 46th Annual National Forum of the American Helicopter Society (May 1990) and the other at the the 16th European Rotorcraft Forum.

The principal objective for next year will be to continue MHHC research using a flexible blade model. Three flap modes, two lag modes, and one torsional mode for each blade will be considered. Using this model, helicopter vibration control and multi-blade tracking using a servo-flap on the blade will also be compared with the conventional swashplate method. In doing this, an attempt will be made to find a time-history-type solution for a time-domain control of helicopter vibration and aeroelastic stability.

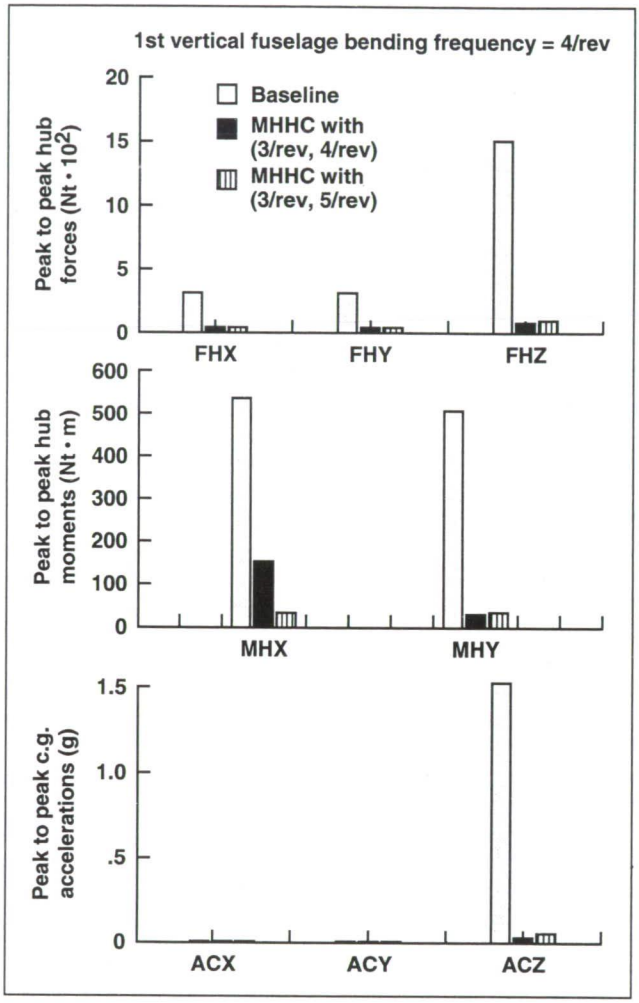


Fig. 1. Hub shears, hub moments, and C.G. acceleration without HHC and with MHHC

Ames-Moffett contact: S. Jacklin
(415) 604-4567 or FTS 464-4567
Headquarters program office: OAET

System Identification of Rotor State Dynamics

Stephen Jacklin

Theoretical research has shown that advanced flight-control, vibration-reduction, attitude-stabilization, lift-redistribution, and stall-suppression systems for the helicopter can be obtained through control of the rotor state (that is, blade position, velocity, and acceleration). As such, knowledge of the rotor state will likely become an essential part of the input data required by next-generation rotorcraft control systems. However, modern hingeless and bearingless rotor designs complicate the development of simple models for the reliable and repeatable prediction of rotor states. Therefore, obtaining rotor state information through system-identification methods is advantageous in that a predetermined knowledge of the rotor-dynamic equations is not required.

Toward this end, an approach for estimation of the complete rotor state is being studied by Robert McKillip of Princeton University. Two years ago, a 4-foot-diameter, accelerometer-instrumented rotor-blade set was constructed of urethane foam. The rotor was carefully fabricated such that its first two flapping frequencies were representative of a real rotor. Each blade incorporated six miniature accelerometers. With this approach, the blade flap and lag accelerations are obtained directly from the flap and lead-lag oriented accelerometers, and then multiplied by a sensitivity matrix to obtain the flapping acceleration and position, as shown in the figure.

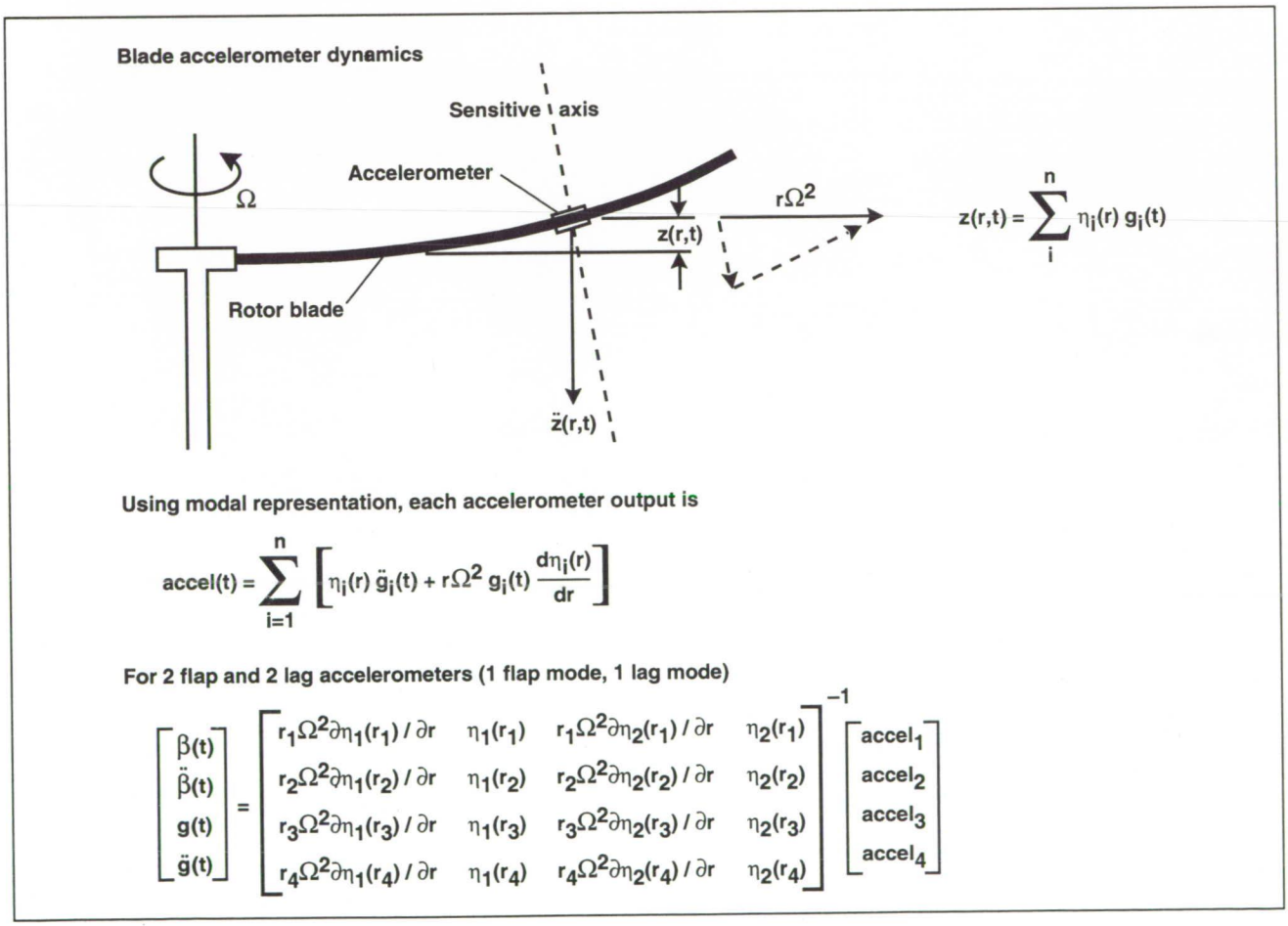


Fig. 1. Estimation of modal position and acceleration from accelerometer data

The sensitivity matrix is a function of the sensor radial location and the blade-mode shapes, both of which are assumed to be known with fairly good precision. Estimates of the flap and lead-lag rates are obtained through application of kinematic observer theory developed by McKillip.

In experiments conducted thus far at Princeton's Rotorcraft Dynamics Laboratory, some success has been achieved in reconstructing the blade state from the measured accelerations. Problems arose, in that the urethane rotor was found to be very soft in torsion. Since the observer was based on a model that neglected torsional motion, the effects of cyclic pitch and aeroelastic torsion corrupted the estimation process. Extension of the model to include torsional motion is clearly required. The data also show that low-pass filtering is required to remove the higher harmonics from the blade accelerations prior to the identification process.

Ames-Moffett contact: S. Jacklin
(415) 604-4567 or FTS 464-4567
Headquarters program office: OAET

Rotating Sensor Data for Rotor State Identification and Control

Stephen Jacklin, Ruth Heffernan, Mohammed Hoque

Next-generation high-agility and low-vibration helicopters may require the measurement and control of blade flap, lead-lag, and torsional modes. With accurate knowledge of the rotor state (that is, blade position, velocity, and acceleration), swashplate or individual blade-control commands could be generated to provide helicopter-attitude stabilization, gust alleviation, and lead-lag damping augmentation. Although direct measurement of some rotor state variables is possible using blade-angle transducers and strain gauges, the unreliability and mounting difficulty associated with these devices discourages their use.

A more feasible approach might be to measure the rotor states using blade-mounted accelerometers. In an approach proposed by Norm Ham (MIT) and Robert McKillip (Princeton), blade accelerations are obtained directly from flap and lead-lag oriented accelerometers, and flap and lead-lag positions are obtained by double integration of these signals. Then, using rotor state estimation methods based on an accurate knowledge of the mode shapes, the flap and lead-lag rates are estimated. The full-state knowledge can then be passed on to a controller as shown in the first figure.

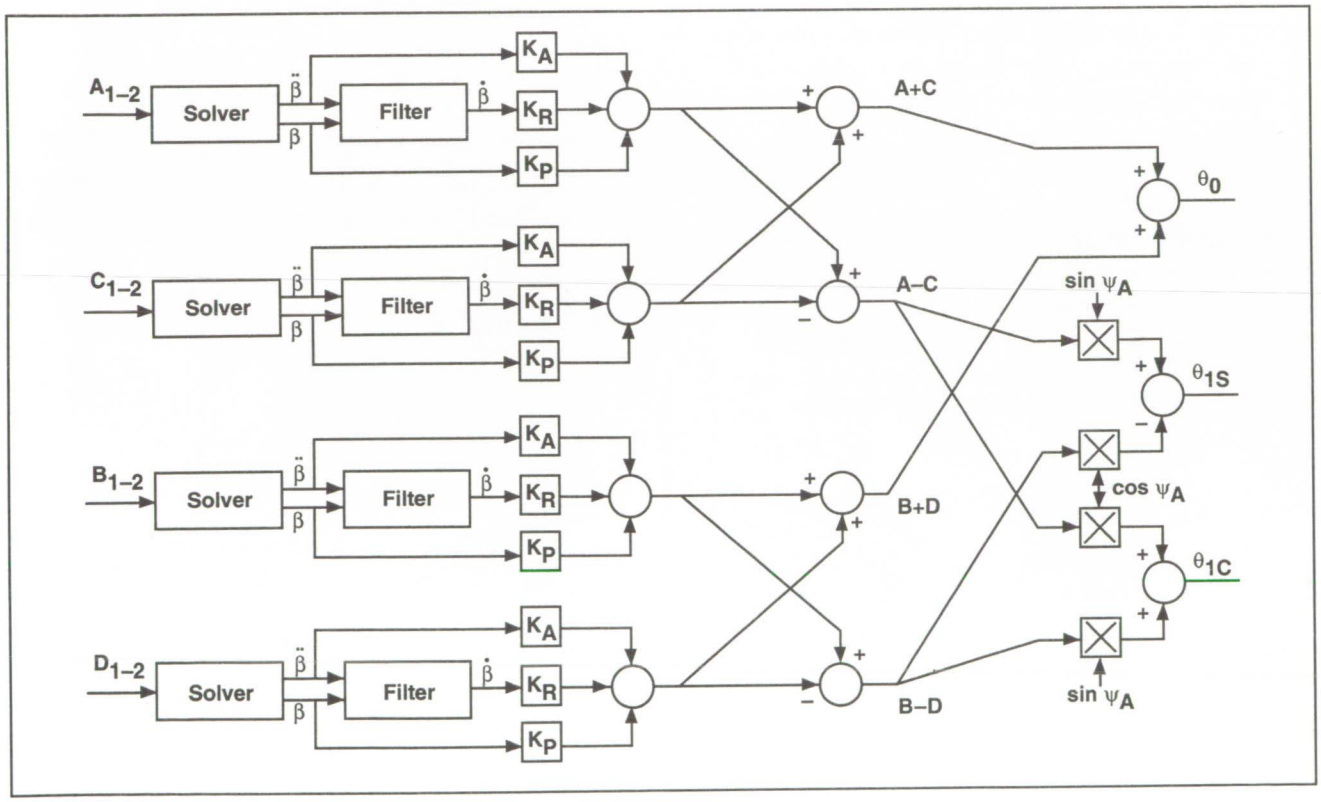


Fig. 1. Schematic of flapping control system using the conventional swashplate for a four-bladed rotor

As part of a concept validation study, accelerometers were mounted to the hub of a Bell 412 helicopter rotor being tested in the Ames 40- by 80-Foot Wind Tunnel. Although theoretical analysis supported on-blade mounting, only the hub could be conveniently instrumented during this test. Two accelerometers in both the flap and lead-lag orientation were mounted on each arm of the blade yokes, and data were taken while exciting the blade at frequencies in the expected range of controller operation. The preliminary data obtained during the wind-tunnel test indicated that filtering would be needed to eliminate the higher harmonics for lower-order mode estimation.

As shown in the second figure, for flapping acceleration, the first flapping mode was not by any means the dominant mode. Therefore, significantly more than a few modes are needed to fully reconstruct the general acceleration state. However, for any specific mode, control might be possible by filtering out accelerations at the higher frequencies. The data also show, as expected, that a separation distance of 0.05 r/R was less than ideal to characterize the flapping and lagging modes. The time-histories are nearly identical for the two stations shown.

A second test using blades with many spanwise accelerometers (four flap, two lead-lag) is planned for the first half of 1993. It is anticipated that that test will provide a more useful data set on which to base the rotor state estimation methods. This is not only because there are more sensors, but also because

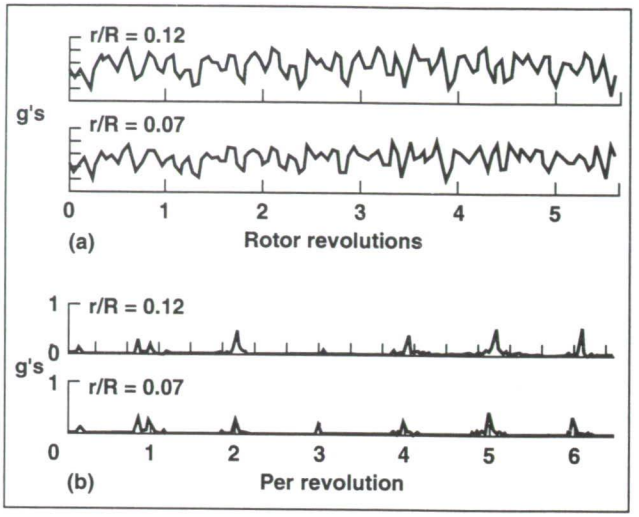


Fig. 2. Bell 412 blade yoke acceleration data with 0.8-Hz swashplate excitation at 0.5°; 316 rpm, 4° collective, –8° shaft angle, 0.2 advance ratio. (a) Blade yoke flapping acceleration; (b) harmonic analysis

the sensors are further separated radially to improve modal identification. Other methods of rotor state estimation for individual blade control are being developed to better account for multi-mode contributions in the accelerometer data.

Ames-Moffett contact: S. Jacklin
(415) 604-4567 or FTS 464-4567
Headquarters program office: OAET

The Trailed-Rotor Concept in Cruise Configuration

ORIGINAL PAGE
BLACK AND WHITE PHOTOGRAPH

Jeffrey Johnson, Stephen Swanson

In a cooperative effort between NASA, the U.S. Navy, and the McDonnell Douglas Helicopter Company, an experimental investigation was conducted in the Ames 7- by 10- Foot Wind Tunnel to determine the low-speed aerodynamic performance characteristics of the trailed rotor in its cruise configuration. The trailed rotor is a high-speed rotorcraft design in which the trailed rotor operates as a tilt rotor in hover. However, during transition, the rotors are tilted backward, rotation is stopped, and the blades are folded in a trailed configuration behind the transmission pod. Jet thrust is then relied on for forward flight. The semispan 15% scale model installed in the tunnel is shown in the figure.

The primary objectives of this test were to evaluate the aerodynamic performance of the semispan wing, quantify the interactional aerodynamics of the wing and the pod, and measure trailed-blade loads in low-speed cruise. Additional objectives of the test were to qualitatively evaluate trailed-blade vibration and make a limited comparison between the trailed rotor and the folding tilt rotor.

The test showed that wing/pod integration is crucial to the overall low-speed cruise performance. Variations in the wing-pod fillet radii significantly affected the overall aerodynamic performance and indicated that optimization of fillet geometry is critical to both wing aerodynamic performance and trailed-blade dynamics. The key to wing/pod integration is the determination of a satisfactory fillet radii. Once that was accomplished, the results from the test indicated that the trailed rotor concept does not suffer a large drag penalty by having the pod and trailed blades mounted on the wing-tip. Also, the presence of the pod and trailed blades did not reduce the lift curve of the wing, though the stall angle was reduced. The drag penalty of the trailed blades was not severe because of the pod acting as an endplate and perhaps because of favorable interaction with the wing/pod vortex. The effect of the trailed blades on the slope of the wing pitching and rolling moment curves indicates that the presence of the trailed blades will provide an increase in the longitudinal and lateral stability of the aircraft.



Fig. 1. Trailed-rotor model in the Ames 7- by 10-Foot Wind Tunnel

Finally, the qualitative observations of the trailed-blade vibrations indicated a fairly benign flow environment.

The number of rotor blades (three-, four-, and five-blade hubs were tested) did not affect the lift-curve slopes; however, the number of blades and blade twist did affect wing stall. Also, the wing drag decreased with a decrease in the number of blades. This was expected because blade area was not held constant; the three-bladed rotor had the smallest wetted surface area.

Finally, comparison of the trailed rotor and a generic folding tilt-rotor model shows that the trailed rotor has less drag than a folding tilt rotor with the same number of blades.

Ames-Moffett contact: J. Johnson
(415) 604-6976 or FTS 464-6976
Headquarters program office: OAET

Calculating Blade-Vortex-Interaction Aerodynamics and Noise by the Kirchoff Method

Cahit Kitaplioglu

Blade-vortex Interaction (BVI) noise is one of the most highly detectable and annoying helicopter noise mechanisms. Predictions of this type of noise have been the subject of intensive research but, although being improved steadily, they are still insufficiently accurate to meet the high-confidence capability needed by industry.

The acoustic field far from the helicopter is difficult to calculate using traditional methods of computational fluid dynamics because of accumulated numerical errors. The Kirchoff method was developed as an alternative approach to calculating far-field acoustics based on ideas from classic field theory, particularly electrodynamic theory. This approach extends the numerically calculated nonlinear aerodynamics close to the rotor to the acoustic far-field. This is fundamentally different from the classic aeroacoustic formulation of Lighthill, which attempts to calculate an acoustic field given that the strength of all sources (including equivalent sources accounting for propagation and nonlinear effects) is known a priori, usually an unrealistic assumption.

At the University of Minnesota, the Kirchoff technique is being applied to a detailed parametric study of transonic blade-vortex interaction noise. Airfoil shape and thickness distribution, free-stream Mach number, vortex strength and miss distance, intersection angle, and other relevant parameters as well as directivity patterns, are being studied. One specific objective of the research is to predict and compare the blade-vortex-interaction noise generated by an airfoil used on a production helicopter, as well as an advanced airfoil specifically designed to reduce BVI noise. This work is in direct support of several experimental programs being undertaken at Ames in the National Full-Scale Aerodynamics Complex.

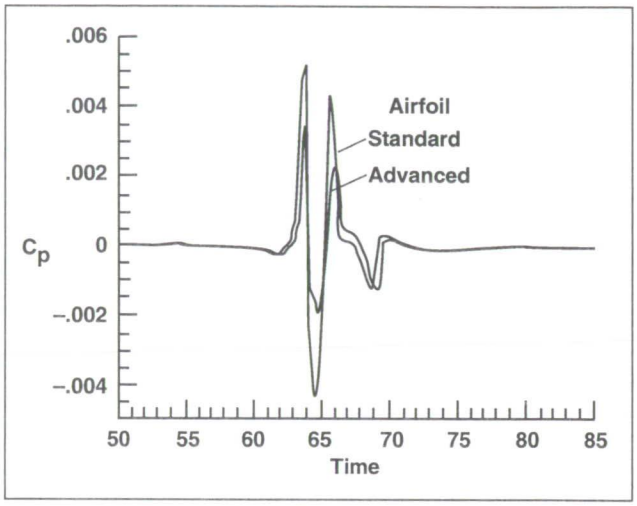


Fig. 1. Far-field acoustic characteristics during blade-vortex interaction of two airfoils

Preliminary results, an example of which is shown in the figure, indicate that the advanced airfoil may indeed exhibit lower BVI noise levels.

Ames-Moffett contact: C. Kitaplioglu
(415) 604-6679 or FTS 464-6679
Headquarters program office: OAET

Calculating Blade-Vortex Interaction by Navier-Stokes Procedures

Cahit Kitaplioglu

Blade-vortex interaction (BVI) is a well-known phenomenon that occurs in the flow field around a helicopter rotor; it is one of the primary sources of noise and vibration. BVI is a very complex, three-dimensional, unsteady phenomenon. Previous computational studies of BVI have been based on either two-dimensional unsteady models or on three-dimensional steady models. These studies have provided valuable insight into the nature and physics of the problem and laid down the ground work for further advances. Recently, Scientific Research Associates (SRA), under contract to Ames Research Center, began one of the first efforts to compute three-dimensional, unsteady BVI at arbitrary vortex-blade intersection geometries.

The proposed solution involves the use of a Navier-Stokes code with a linearized block/alternating-direction implicit-solution algorithm. The fully three-dimensional, unsteady problem is being approached in several stages, each successively more complex than the previous stage.

In the initial phase, the feasibility of using this basic approach was demonstrated by performing three-dimensional model calculations of a simple vortex interacting with an airfoil leading edge. These calculations, as well as the work of previous investigators, point to the importance of correctly modeling the vortex characteristics and the boundary and initial conditions.

During the second phase, work focused on improving the numerical scheme in order to reduce numerical errors in simulating vortex-dominated flows. The current scheme, which is second-order accurate in time and space, and which incorporates an implicit iterative procedure to reduce numerical "splitting" errors, yields a vortex as stable as the best previous models.

During the third phase, two-dimensional calculations of vortex-airfoil interactions were completed. Test cases at a Mach number of 0.8 and a Reynolds number of 10^6 were computed; they compared favorably with other results, but used fewer grid points to achieve a comparable accuracy level. Dominant processes during the interaction are the development of large pressure gradients near the upper leading edge and the development of disturbances at the root of the lower-surface shock. High-pressure pulses are emitted from the leading edge, and acoustic waves are radiated from the lower-surface region originally occupied by a supersonic pocket.

During the final phase, completed in 1990, the code was extended to the three-dimensional case, with appropriate extensions of the vortex and turbulence models (see first figure). A test case, again at Mach number 0.8 and Reynolds number 10^6, was run on the Ames National Aerodynamic Simulator.

Three-dimensional BVI is qualitatively similar to the previously obtained two-dimensional BVI. The vortex passage has a profound effect on the behavior of the shock. For the calculation parameters, the shock exhibits unsteadiness of the type first observed and classified by Tijdemann. The upper-surface shock disappears after moving forward, and the lower-surface shock also moves forward and sharpens after initially moving downstream. High-amplitude pressure disturbances appear at the leading edge and propagate upstream to the far-field, as illustrated in the second figure.

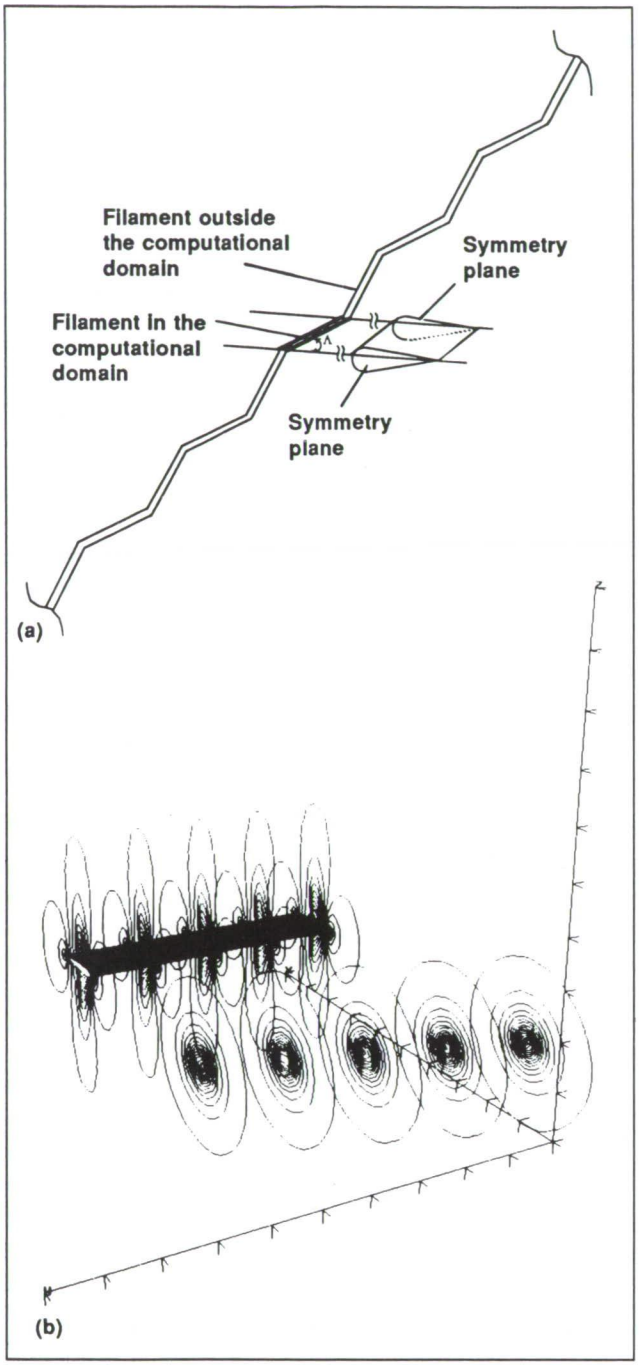


Fig. 1. Three-dimensional model. (a) Overall geometry; (b) pressure contours at initialization

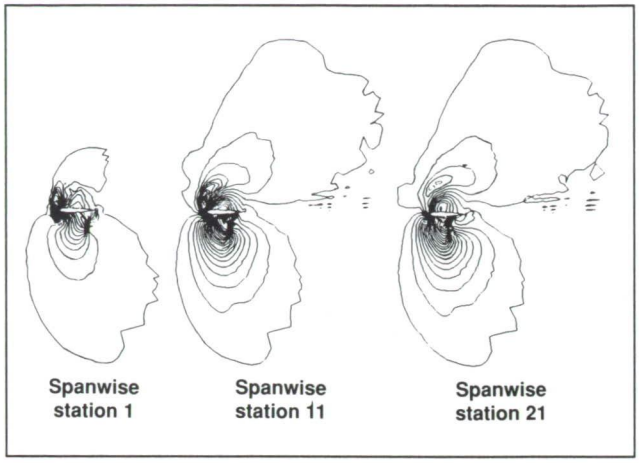


Fig. 2. Pressure fields at three spanwise stations during a three-dimensional blade-vortex interaction

This program is now complete. The project was undertaken from the start with the view to develop a tool that could be applied to the helicopter blade-vortex interaction problem. The code contains all the necessary elements (including three-dimensionality and rotationality) to do this, and is applicable at realistic Mach and Reynolds numbers and for the "strong" interaction case. Future directions for extending this research are (1) to incorporate appropriate boundary conditions for a rotating blade and (2) to couple this BVI aerodynamics code to a general rotor wake, performance, and dynamics code.

Ames-Moffett contact: C. Kitaplioglu
(415) 604-6679 or FTS 464-6679
Headquarters program office: OAET

Small-Scale Study of Rotor Blade-Vortex Interaction Acoustics

Cahit Kitaplioglu

Considerable attention has been focused during the past several years on helicopter blade-vortex interactions (BVI), particularly on their effects on externally radiated noise. Several computational codes have been developed and several tests performed to gather data on this important phenomenon.

The experiments of Caradonna stand out as being of particular interest because provision was made for independent generation and control of a vortex during its interaction with a rotating blade; whereas the rotor itself was operated in a way that minimized the influence of its own tip vortices and wake. It was possible, in this manner, to simulate important BVI geometries and to carry out sensitivity studies. Unfortunately, these experiments did not include acoustic measurements.

At Ames Research Center, a project has been initiated to perform similar experiments, but with a specific focus on acoustic measurements, as well as more detailed measurements of blade surface-pressure distributions. Such simultaneous measurements will yield a consistent data base that can be used to study both the aerodynamics and aeroacoustics of BVI in a systematic fashion.

A 7-foot-diameter, pressure-instrumented, two-bladed rotor will be mounted in the Ames 80- by 120-Foot Wind Tunnel (see figure). A separate vortex generator will be mounted upstream of the rotor at several locations to permit variation of vortex-blade encounter parameters (e.g., vortex strength, vortex age, vortex-blade miss distance, interaction angle) and to measure the sensitivity of the rotor's aerodynamics and acoustic field to small changes in these parameters. The wind-tunnel acoustic lining, as well as additional acoustic treatment, will yield a good environment for acoustic measurements. A traversing streamlined microphone stand will allow acoustic measurements at narrow angular resolutions and will yield a detailed map of acoustic-field directivity associated with various BVI geometries, as well as the sensitivity of the acoustic field to small changes in BVI parameters.

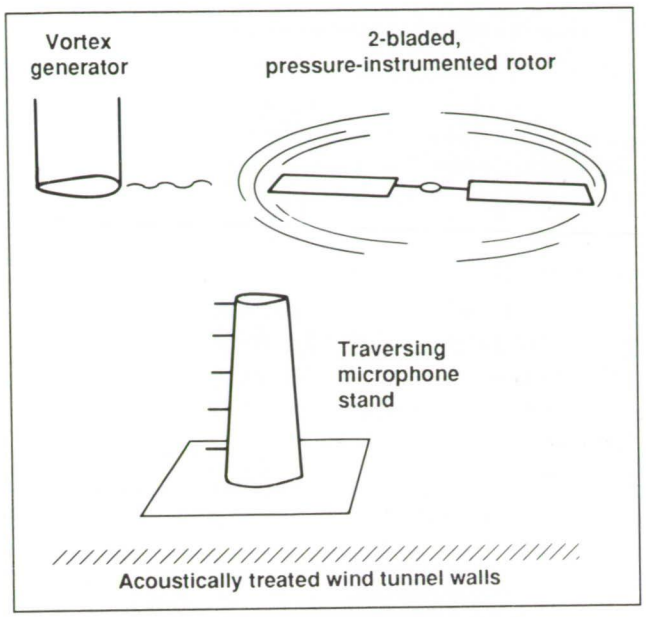


Fig. 1. Study setup in 80- by 120-Foot Wind Tunnel

During 1990 the main focus was on hardware design. Pressure transducers on the rotor have been redesigned to yield absolute pressures at the high frequencies required for acoustic correlations. A sophisticated microphone traverse system has been designed to allow a survey of the acoustic field at narrow angular resolution. Data systems for acquiring blade-pressure data and acoustic data have been extensively investigated and procurement is under way. Some data reduction and analysis software has been written. Additional hardware design and fabrication and final test preparations will be completed for tunnel entry in early FY 1992.

Ames-Moffett contact: C. Kitaplioglu
(415) 604-6679 or FTS 464-6679
Headquarters program office: OAET

General Time-Domain Unsteady Aerodynamics of Rotors

Benton Lau

The feasibility of a general theory for the time-domain unsteady aerodynamics of helicopter rotors was investigated. This investigation was conducted by Johnson Aeronautics, under contract with Ames Research Center. The wake theory gives a linearized relation between the downwash and the wing-bound circulation, in terms of the impulse response obtained directly in the time-domain.

This approach makes it possible to treat general wake configurations, including discrete wake vorticity with rolled-up and distorted geometry. The investigation establishes the approach for model order reduction; determines when a constrained identification method is needed; verifies the formulation of the theory for rolled-up, distorted trim wake geometry; and verifies the formulation of the theory for wake geometry perturbations.

The basic soundness of the approach is demonstrated by the results presented in a NASA Contractor Report. A research program to complete the development of the method is outlined. The result of this activity will be an approach for analyzing the aeroelastic stability and response of helicopter rotors, while retaining the important influence of the complicated rotor-wake configuration.

Ames-Moffett contact: B. Lau
(415) 604-6714 or FTS 464-6714
Headquarters program office: OAET

Soft Hub for Bearingless Rotors

Benton Lau

Soft-hub designs were studied that allow the direct replacement of articulated rotor systems by bearingless types without any change in controllability or need for reinforcement to the drive shaft or transmission/fuselage attachments of the helicopter. Two designs were analyzed by Advanced Technologies Inc., under a Phase I SBIR contract. Both designs were confirmed for functional and structural feasibility against design criteria and specifications established for this effort. Both systems are gymballed about a thrust-carrying universal elastomeric bearing.

One design includes a set of composite flexures to transmit drive torque from the shaft to the rotor, and another set (which is changeable) to impart hub-tilting stiffness to the rotor system as required to meet the helicopter application (see first figure).

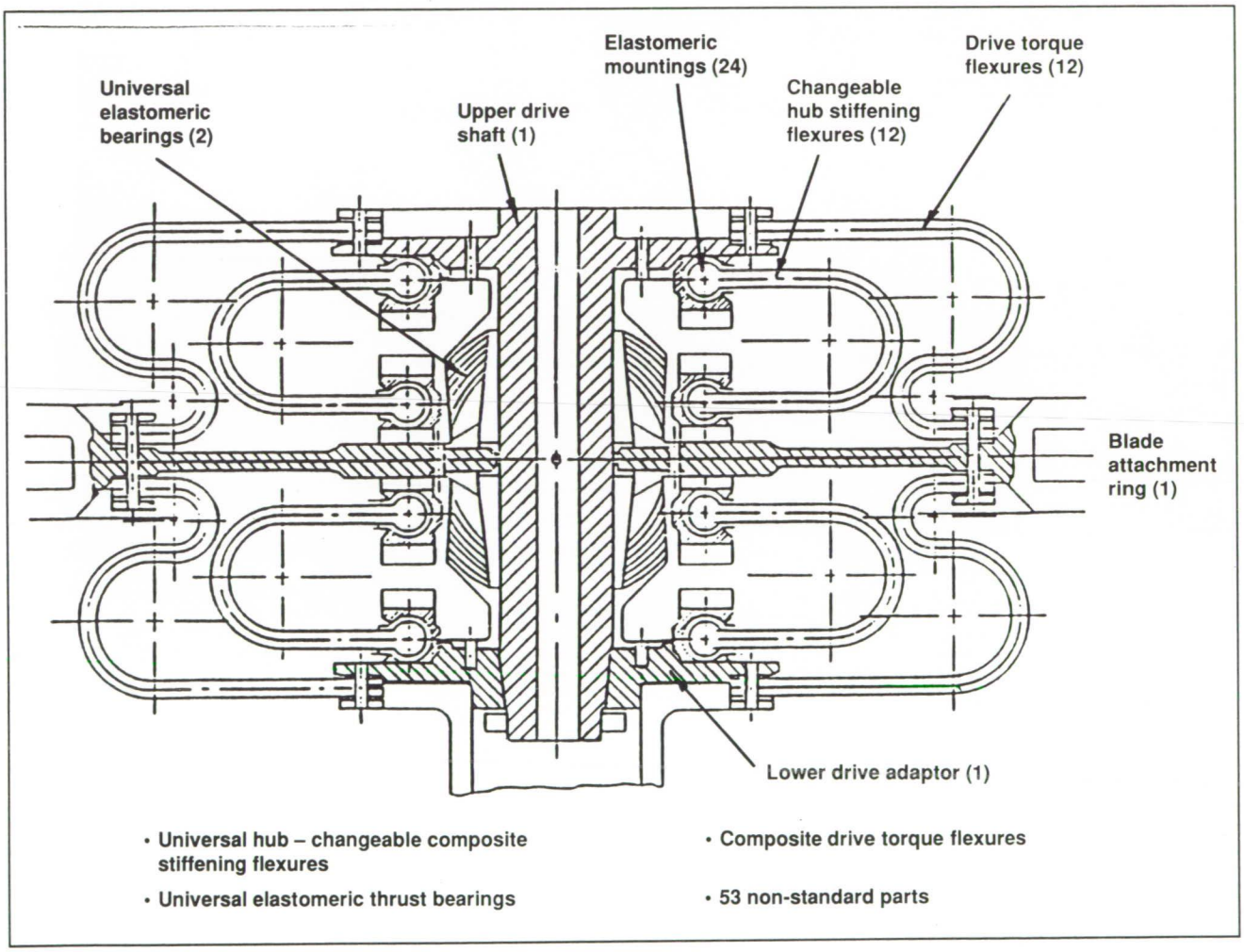


Fig. 1. Soft hub with drive torque flexures and hub-stiffening flexures

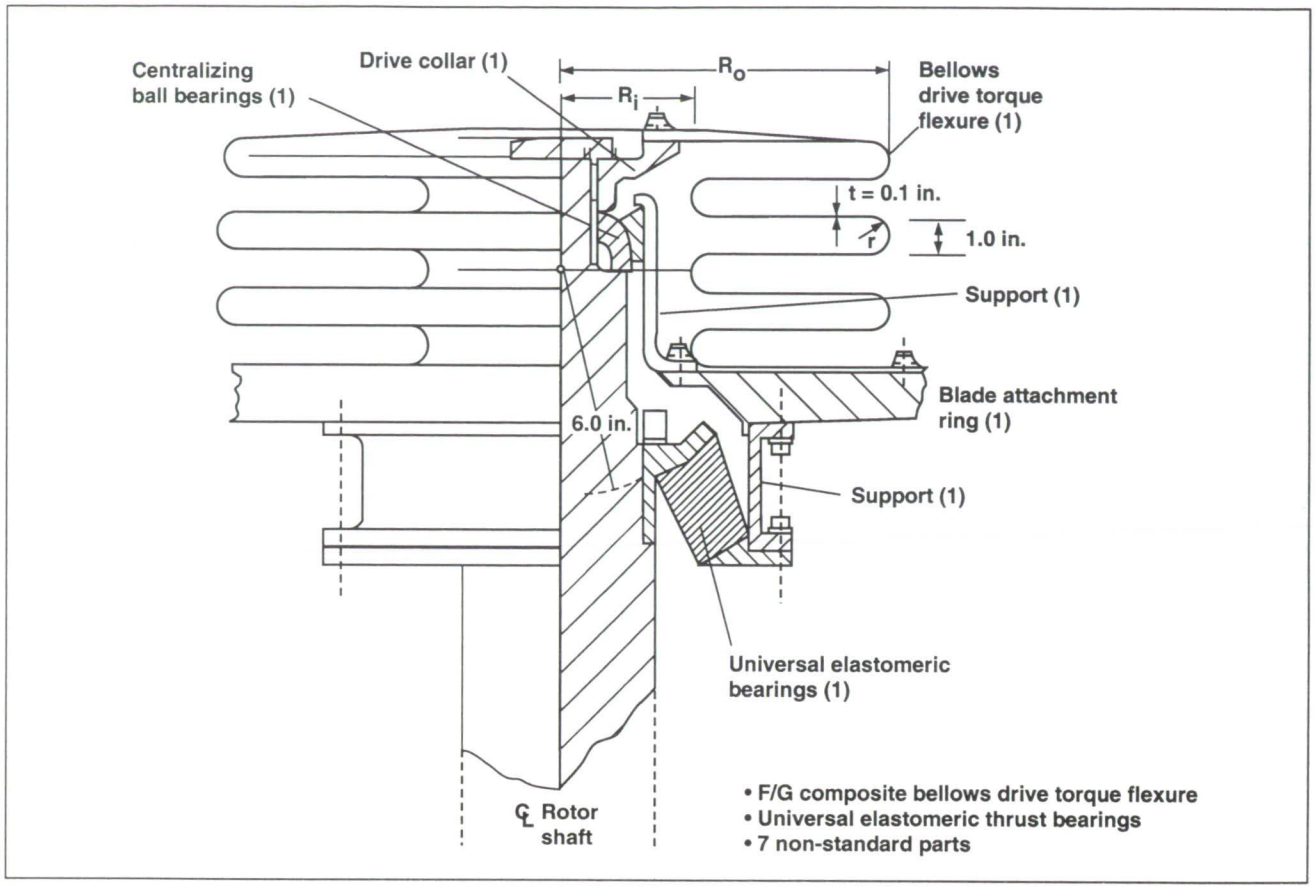


Fig. 2. Soft hub with one bellows drive torque flexure

Hub Comparisons

	Soft hub		
	With flexures	With bellows	BO-105
Weight (lb)	200.6	194	197
Drag (ft^2)	2.43	1.31	—
Cost ($)	129,750	58,050	92,460
Number of non-standard parts	53	7	162

The second design uses a composite bellows flexure to drive the rotor and to augment the hub stiffness provided by the elastomeric bearing (see second figure). Each design has been assessed for weight, drag, rough order-of-magnitude costs and number of parts, and compared with the production BO-105 hub (see table).

Ames-Moffett contact: B. Lau
(415) 604-6714 or FTS 464-6714
Headquarters program office: OAET

Lynx Helicopter Flight-Test Correlation

Benton Lau, Alex Louie

The Lynx Helicopter flight-test correlation program is a joint program with Westland Helicopter Ltd. The program objectives are (1) to increase the understanding of the modeling requirements to accurately predict aircraft performance, rotor structural loads, and retreating blade stall; (2) to validate the prediction code CAMRAD/JA at high-speed, high-load flight conditions; and (3) to compare the prediction capabilities of CAMRAD/JA with those of Westland's analytical codes and to identify shortcomings and new research directions. After selecting the flight conditions for analysis, Ames Research Center received the aircraft data set to initiate the correlation study. The harmonic content of the blade loads and the steady-flight parameters were reduced from the data set. The resulting data base was used for the correlation study.

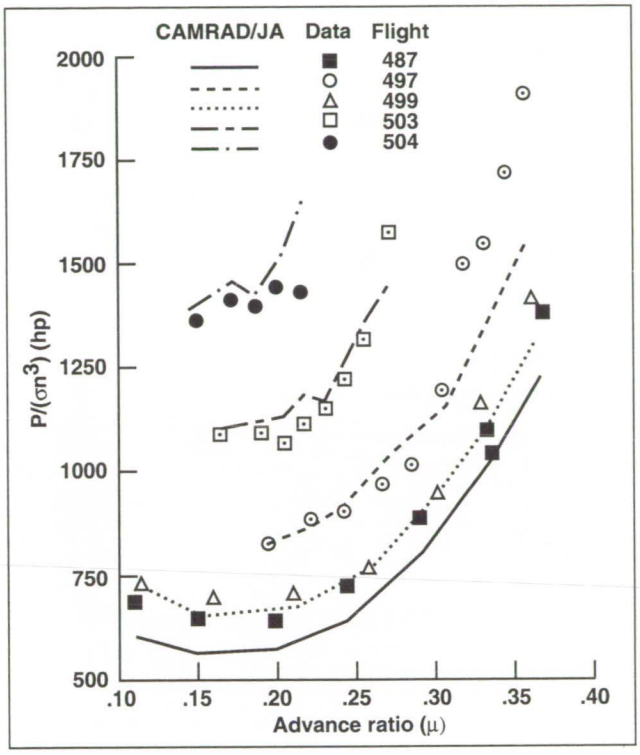


Fig. 1. Normalized aircraft power for Lynx Helicopter

Since the hingeless-rotor option in CAMRAD/JA can not properly model the lag damper, modifications were made to incorporate the damper effect in the analysis. Effects of various stall models on performance and blade-load predictions were examined. Preliminary analysis shows good correlation of the aircraft power performance (see figure). These results have been exchanged between Ames Research Center and Westland.

Ames-Moffett contact: B. Lau
(415) 604-6714 or FTS 464-6714
Headquarters program office: OAET

Panel Method Calculation of Tilt-Rotor Download

Johnson Lee

Aerodynamic interaction between the rotor and wing of a tilt-rotor aircraft in hover produces a downward force on the wing, often referred to as download. Download has a significant detrimental effect on hover performance, and a reliable computational scheme is important to attempts to reduce for download.

The flow field associated with tilt-rotor download is complex. The relative motion between the rotor and wing makes the flow unsteady, and the tip vortex shed from the rotor impinges on the wing upper surface, producing a three-dimensional vortex/boundary-layer interaction. The flow on the wing separates from the leading and trailing edges.

An algorithm based on an unsteady panel method is being developed for the flow field. The flow model combines constant strength panels for the wing and linear doublet panels for the wakes. The rotor is simulated by an actuator disk with known velocity distribution. Rotor wake is represented by curved vortex elements in order to reduce the spatial error. The Kutta condition, which equates the surface velocities on the separated line, is enforced along the leading and trailing edges on the wing. For close vortex/surface interaction, a near-field correction term is added to the induced velocity to compensate for the incompatible panel size and vortex core. Wake deflection is also implemented to avoid vortex penetration into the wing surface. Wake-merging schemes are applied to both rotor and wing wakes to reduce the computational time. The computation is able to reproduce the general flow feature observed in experiments. The calculated wing upper-surface pressure and base pressure compare favorably with experimental data.

Ames-Moffett contact: J. Lee
(415) 604-4574 or FTS 464-4574
Headquarters program office: OAET

Comparison of Helicopter Vibration Controllers

Jane Leyland

A control-optimization-method alternative to the widely used constraint-penalty methods employed by the deterministic, cautious, and dual controllers was identified, and the corresponding general equations were derived. This method seeks to minimize the actual performance index (i.e., constraint-penalty terms not adjoined to the performance index) subject to the actual constraints at specified time points. Classic max/min calculus, with the constraint vector adjoined to the performance index by means of an adjoint vector composed of Lagrangian multipliers, was used to derive necessary conditions for optimality. For this formulation, the inequality constraints were transformed to the standard equality constraint function form by defining appropriate slack variables.

Three approaches to solving this optimization problem were identified. Expression of the necessary conditions for optimality yields a nonlinear system of algebraic equations that do not appear to be easily analytically solvable. The first approach is simply to use a numerical procedure to solve the complete system of equations defining the necessary conditions for optimality. It is anticipated that there could be numerical difficulties with this approach because of the presence of switching equations in the nonlinear system to be solved. Even if a solution could be found in this manner, the question of global optimality would still have to be resolved.

The second approach should remove the numerical problems associated with the switching equations. This approach numerically solves each of the nonlinear systems of equations associated with each possible permutation of the zeros of the switching equations, and then it selects the "best" solution as the global solution. The third approach is to use a nonlinear programming method to numerically minimize the performance index subject to constraints.

It is planned to design a relatively simple stand-alone computer code to implement these approaches, and to use this code iteratively with the detailed rotor simulation program CAMRAD/JA to define the achievable performance for cases of interest. These results will then be compared with corresponding results obtained from the deterministic controller modeled in CAMRAD/JA.

Ames-Moffett contact: J. Leyland
(415) 604-4750 or FTS 464-4750
Headquarters program office: OAET

Tait-Bryan Angles Required for Diagonalizing a Real Symmetric (3 × 3) Rank-Two Tensor

Jane Leyland

Tait-Bryan angles, Euler angles, and other rotation sequences for this application refer to specific sequences of rotations of a Euclidean three-space coordinate system from an initial orientation to a new orientation. Tait-Bryan angles, which are any permutation of 1-2-3 rotations, are used to define the pitch, flap, and lead-lag angles in helicopter rotor system dynamics. The Tait-Bryan angles differ from the more familiar Euler angles, which are any permutations of 3-1-3 rotations.

The associated transformation matrices from initial to final orientation provide a simple means to express the elements of an invariant characteristic of an entity in a new coordinate system. Here it is assumed that the invariance of the characteristic is with respect to the rotations of the coordinate system under consideration and not, for example, with respect to time. The subject problem, which is a pseudo-inverse of the aforementioned procedure, is to determine the Tait-Bryan angles required to diagonalize the matrix representing the invariant characteristic in a particular coordinate system.

The process to define the Tait-Bryan angles required to diagonalize a real symmetric (3 × 3) rank-two tensor was identified. This process is applicable to commonly encountered tensors such as inertial tensors, rank-two (# × 3) covariance tensors, and the quadratic coefficient tensors.

Ames-Moffett contact: J. Leyland
(415) 604-4750 or FTS 464-4750
Headquarters program office: OAET

Scale Model (0.658) V-22 Rotor and Wing Performance

ORIGINAL PAGE
BLACK AND WHITE PHOTOGRAPH

Jeffrey Light

A comprehensive evaluation of the installed rotor performance of the V-22 tilt-rotor Osprey aircraft is being conducted in the National Full-Scale Aerodynamics Complex. The program is being conducted in two phases. The first phase is to measure rotor performance with and without the presence of the wing at speeds from 100 to 300 knots in the 40- by 80-Foot Wind Tunnel. The second phase is a tilting-rotor transi-tion test to be conducted at speeds from 0 to 100 knots in the 80- by 120-Foot Wind Tunnel.

The 40- by 80-Foot Wind Tunnel test will evaluate the rotor performance in airplane, or cruise, mode. The influence of the wing on rotor performance will be determined by measuring rotor performance with and without the wing installed in the rotor wake. Rotor performance will be measured using the five-component balance installed on the Ames Prop Test Rig (PTR). The balance will also measure dynamic hub loads owing to the presence of the wing; these loads are a significant source of airframe vibration in the V-22 aircraft.

This effort completes the testing initiated in 1988 when the rotor was tested at speeds up to 220 knots. Since the 1988 entry, the PTR control system has been upgraded, a fatigue test of the V-22 blade root has been performed, and the PTR control console has been completely revised. These extensive efforts will allow for a complete test envelope in the airplane-mode test. The data acquired in this program are important to the on-going development flight program since rotor performance measured in the wind tunnel will allow for an accurate estimate of airframe performance for the flight test vehicles.

The 80- by 120-Foot Wind Tunnel test will investigate rotor performance, loads, and acoustics in low-speed transition flight. Because of the wake interaction with the rotor, and because of the difference between helicopter and tilt-rotor tip loading, the measured performance and blade loads will provide important insights into the operating conditions of the tilt rotor during transition between helicopter mode and airplane mode. Dynamic loading both on the rotor (forces and moments) and on the wing (pressures) will be investigated. The acoustic lining in the wind tunnel will enable good quality acoustics data to be acquired on radiated noise from the rotor. Since a tilt-rotor aircraft typically transitions just after takeoff or just before landing, tilt-rotor noise generated during the aircraft transition mode is in areas near vertiports.

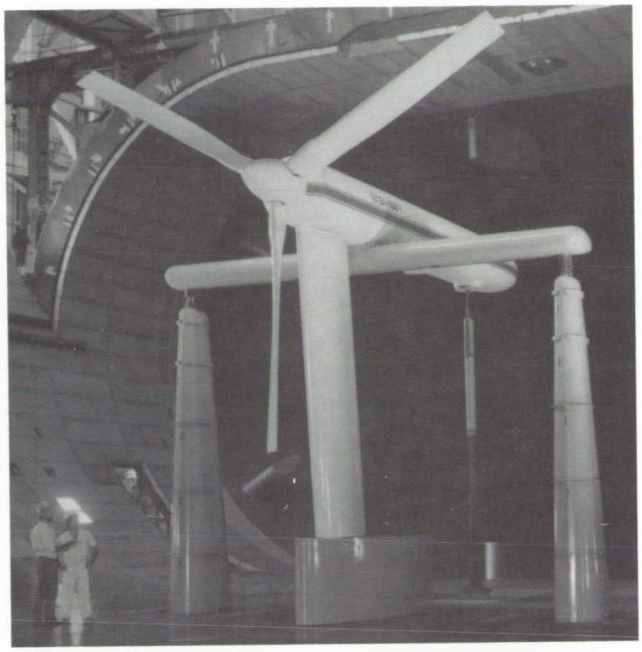


Fig. 1. First 40- by 80-Foot Wind Tunnel entry with V-22 rotor on Prop Test Rig in airplane mode

Ames-Moffett contact: J. Light
(415) 604-4881 or FTS 464-4881
Headquarters program office: OAET

Navier-Stokes Tilt-Rotor Download Research

Jeffrey Light

Computational fluid dynamics is being applied to the wing download problem of the tilt rotor. Through a grant with Stanford University, the unsteady, thin-layer compressible Navier-Stokes equations are solved using an implicit finite-difference scheme that employs lower-upper/alternating direction implicit factorization. In order to make the problem tractable, a simplified model of the rotor is used. The rotor is modeled as an actuator disk which imparts a radial and azimuthal distribution of pressure rise and swirl to the flow field. The three-dimensional grid used for the computations was generated by stacking parallel two-dimensional grids at several spanwise locations along the wing.

The Navier-Stokes analysis captures many of the complex, three-dimensional flow features of the tilt-rotor wake/wing interaction, including the fountain effect, leading- and trailing-edge separation, and the unsteady wake beneath the wing. Sample wing pressure distributions are shown in the figures for spanwise stations 0.705 and 0.891. Very good agreement is achieved at the 0.705 station, but the 0.891 station shows some discrepancies. This is believed to be caused by a higher predicted spanwise flow than found in the experiment. The time-averaged download predicted is about 20% higher than the value measured in large-scale

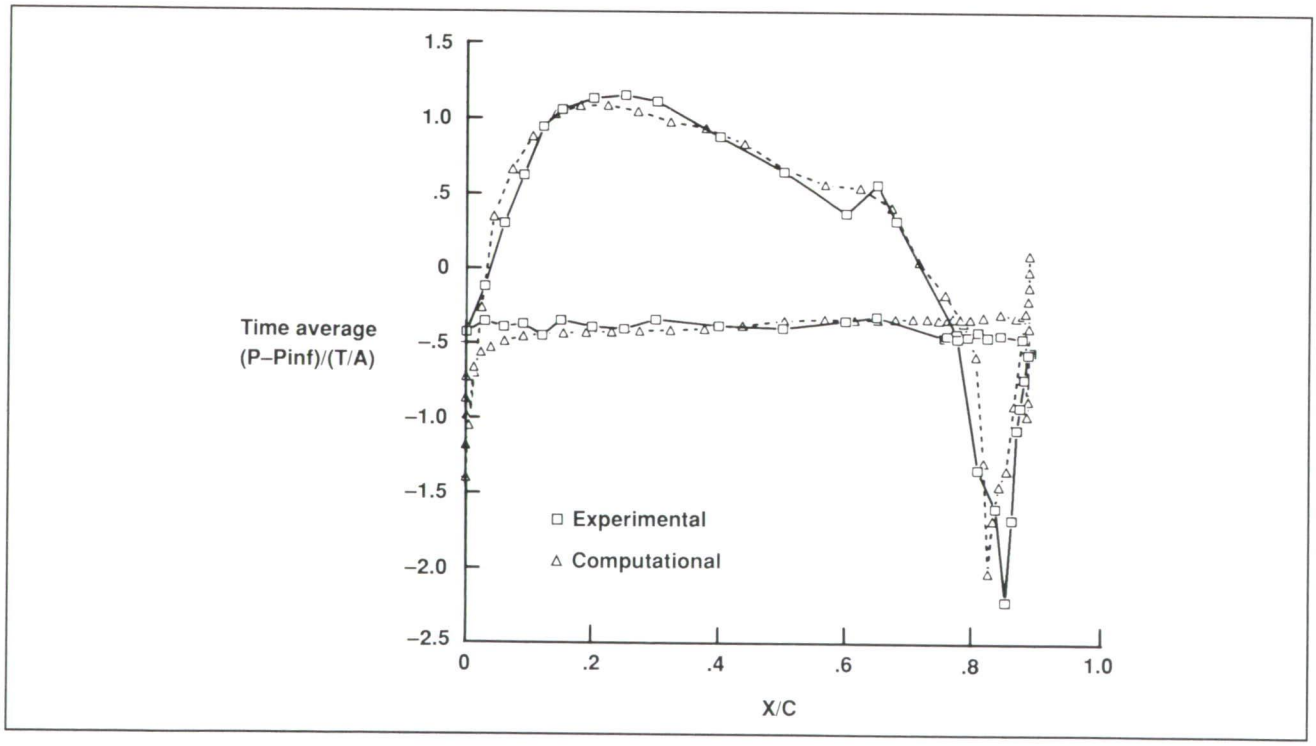


Fig. 1. Time-averaged pressure distribution (spanwise station 0.705)

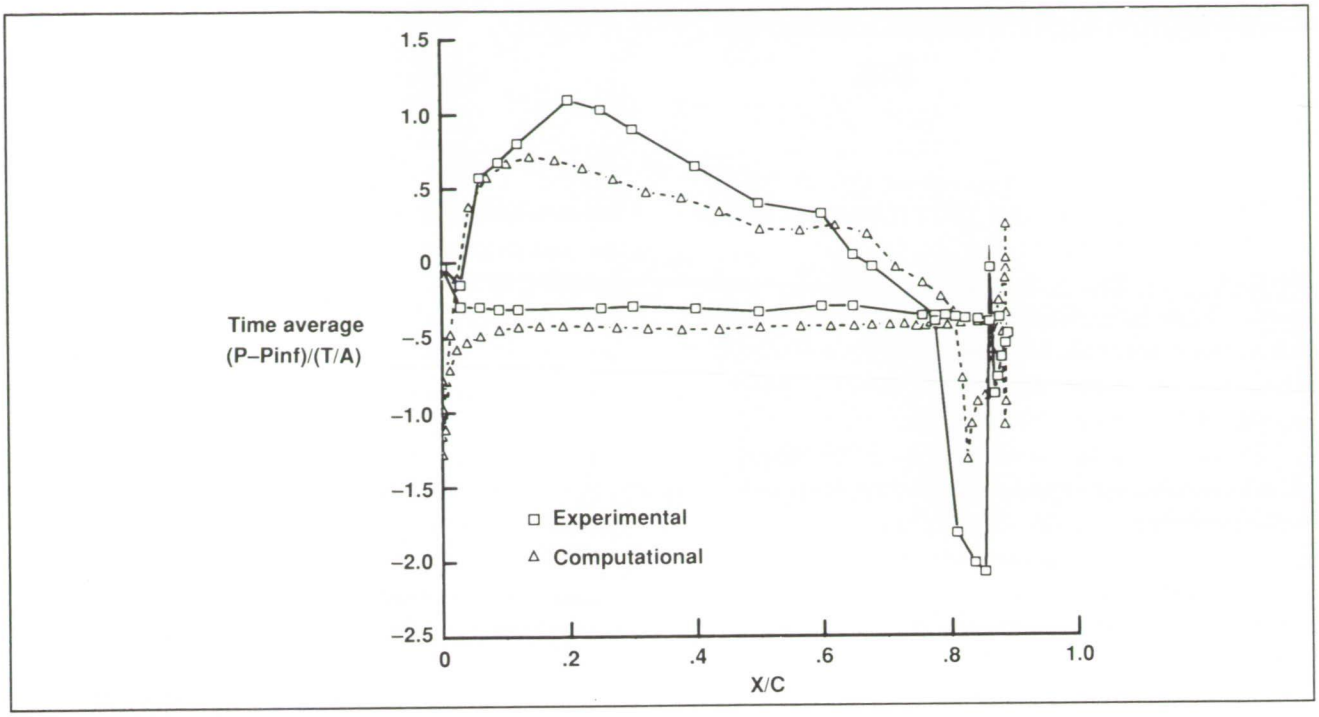


Fig. 2. Time-averaged pressure distribution (spanwise station 0.891)

testing. This can be attributed to differences between the experimental model and the computational model, as well as to limitations of the thin-layer Navier-Stokes equations for modeling the separated flow beneath the wing.

Ames-Moffett contact: J. Light
(415) 604-4881 or FTS 464-4881
Headquarters program office: OAET

Rotor Blade Optimization in Hover

Jeffrey Light

An innovative analytical method for improving the hover performance of a helicopter is being developed by Continuum Dynamics, Inc. (CDI) under contract from Ames Research Center. The objective of this Phase II Small Business Innovative Research (SBIR) contract is to minimize the hovering power required for a constant thrust value.

This work is a continuation of an SBIR Phase I effort in which it was shown that a state-of-the-art hover performance analysis could be efficiently coupled with a simple optimizing technique to produce a rotor design tool that can provide significant improvements in performance. The Phase II work has focused on two areas: improvements to the hover analysis, and improvements to the optimizing technique.

The hover analysis has been improved significantly by allowing for blade elastic deflections. This has been accomplished by coupling a finite-element blade structural analysis with the blade/wake relaxation analysis. In the process, blade structural properties have been included as design variables in the optimization procedure. The aerodynamic analysis of the blade has been further improved by including lift stall in the vortex lattice blade model. A final improvement that has been implemented is a new way of accounting for vortex filament roll-up by using an analytical/numerical matching technique.

The optimization technique has been expanded to include a sequential quadratic programming method. This technique enhances convergence to an optimal design. Also, the design parameters have been increased to include rotor collective, blade radius, and chord distribution, as well as blade twist, sweep, and anhedral. All these improvements to the analysis have been made with careful attention to improving the efficiency and convergence of the original analysis without sacrificing accuracy.

Ames-Moffett contact: J. Light
(415) 604-4881 or FTS 464-4881
Headquarters program office: OAET

Semispan Scale-Model V-22 Hover Download Test

Jeffrey Light, Alexandra Frerking

A test was recently completed at the Ames Outdoor Aerodynamic Research Facility (OARF) in which tilt-rotor performance and wing download in hover were examined. A newly developed hover test rig was used to perform this test. The rotor tested was a small V-22 blade set made from wood. The rotor performance was measured for both isolated rotor and rotor/wing configurations.

For the rotor/wing testing, a wing and image plane were placed above the downward thrusting rotor to simulate a tilt rotor in hover (see first figure). The wing was a 0.184-scale XV-15 aircraft wing with 30% trailing-edge flaps; there were three blowing slots on the upper surface. Upper-surface blowing was a new wing download reduction technique that was evaluated during this test. Two of the slots (7.5% and 22.5% of chord) blew toward the leading edge, and the third slot (60% of chord) blew toward the trailing edge.

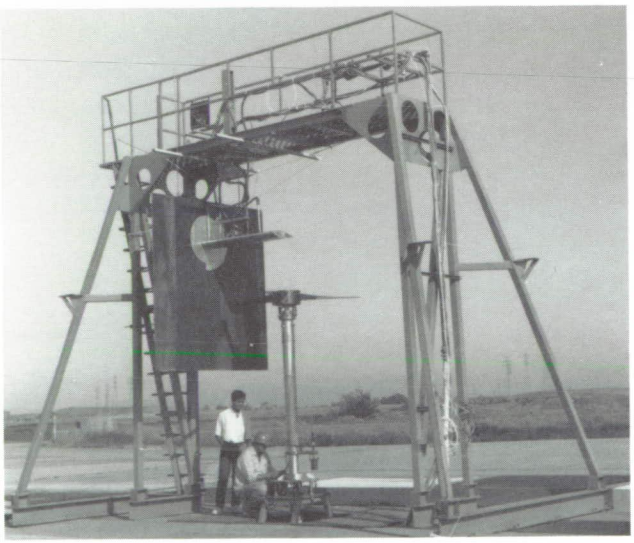


Fig. 1. Hover download test installation

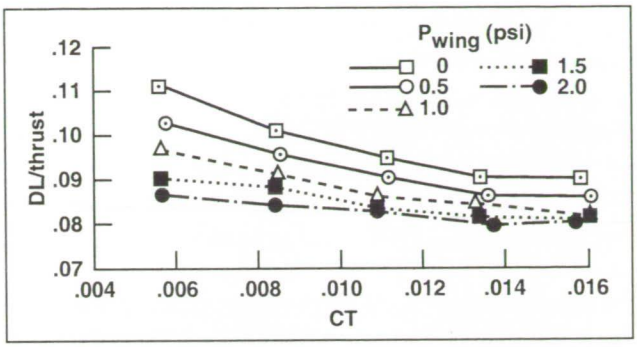


Fig. 2. Download reduction by increase in blowing slot pressure

Testing was conducted at full-scale tip Mach numbers and at thrust coefficients ranging from 0.005 to 0.017. Several wing parameters were varied to identify the configuration with the lowest download. Variables included wing flap angle (65°, 75°, and 85°), wing incidence angle (–80°, –90°, and –100°), number of blowing slots, and slot blowing pressure.

Wing forces and moments were measured using two six-component task balances, and static wing pressures were measured for several spanwise locations. The second figure shows the decrease in wing download as the slot blowing pressure increases. This demonstrates the potential of the upper-surface blowing technique.

Ames-Moffett contact: J. Light
(415) 604-4881 or FTS 464-4881
Headquarters program office: OAET

ORIGINAL PAGE
BLACK AND WHITE PHOTOGRAPH

Helicopter Drag Reduction Program

ORIGINAL PAGE
BLACK AND WHITE PHOTOGRAPH

Dan Martin

A joint test with Bell Helicopter Textron was completed in the Ames 7- by 10-Foot Wind Tunnel. The primary objective of the test was to demonstrate the feasibility of integrating helicopter hub and pylon fairings as a single unit for drag reduction, and to do so with a rotating hub. The effect of the fairings on vehicle forces and moments was also measured. A one-fifth-scale Bell Model 222 helicopter with rotating hub and blade shanks was used as the baseline model. Data were acquired for three different pylon fairing shapes, two cambered hub fairings of different diameters with flat lower surfaces, and combinations of both types of fairings. A total of 16 configurations were tested.

The first figure shows the variation of model drag with fuselage incidence angle for some typical configurations. The addition of a pylon fairing reduces the total model drag by up to 14.5% at a fuselage incidence of 2°. When a hub fairing is added to the pylon fairing, with the gap between the fairings minimized, the vehicle drag is reduced even further from the unfaired case. The results show that the combination of a pylon fairing, with an unswept rectangular planform with NACA 0034 airfoil sections, and a small cambered hub fairing yielded a total vehicle drag reduction of 20%. This low-drag configuration is shown in the second figure.

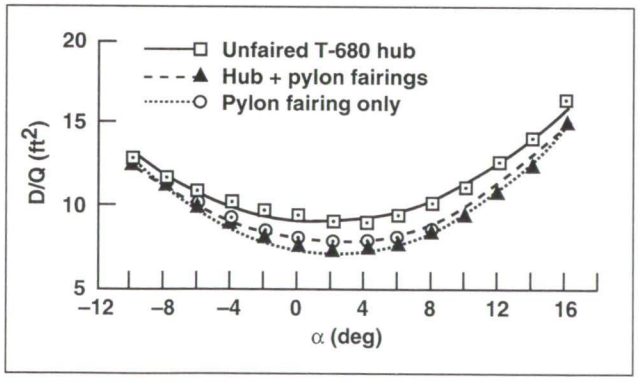


Fig. 1. Variation of full-scale vehicle drag with fuselage incidence angle



Fig. 2. Bell one-fifth-scale Model 222 with pylon fairing and 15% rotor radius hub fairing

Future efforts will concentrate on implementation issues for possible application to a flight test vehicle.

Ames-Moffett contact: D. Martin
(415) 604-4566 or FTS 464-4566
Headquarters program office: OAET

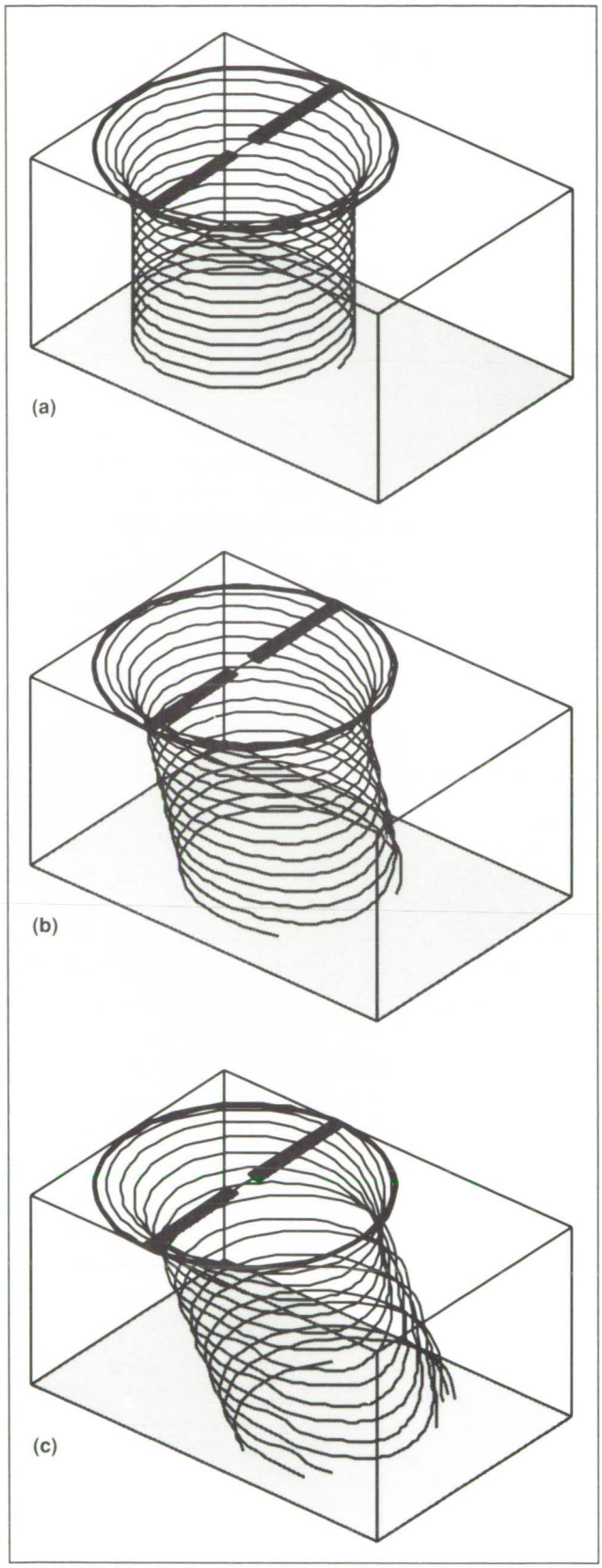


Fig. 1. Rotor wake evolution. (a) $\mu = 0.0$, (b) $\mu = 0.01$, (c) $\mu = 0.02$

The figure presents the evolution of a rotor wake for varying advance ratios. A two-bladed rotor is modeled. The efficient prediction of stable rotor-wake evolution for hover and low-advance-ratio flight demonstrates the ability of the present method for free-wake analysis.

Ames-Moffett contact: W. Miller
(415) 604-6719 or FTS 464-6719
Headquarters program office: OAET

C-2

Direct Periodic Solutions of Rotor Free-Wake Calculations

Wayne Miller

Free-wake models, which allow the wake vorticity field to evolve in free motion, represent the most accurate and physically correct approach to rotorcraft aerodynamics. The simpler but less accurate approaches such as momentum theory and prescribed wakes have proved to be inadequate for predicting complicated aerodynamic blade loading. From their inception, however, free-wake calculations have been hampered by excessive computational effort and poor convergence behavior at low advance ratios and at hover. Time-marching schemes are particularly susceptible to poor convergence and often require excessive computational time to converge the solution. Further, below a critical advance ratio, the solution will diverge depending on the specifics of the time-marching method.

To address the difficulties of convergence and the stability of predicted rotor wakes by free-wake methods, a periodic inversion method was developed. The method describes the rotor wake as a linear perturbation problem and solves for the perturbative corrections. The solution to the perturbative correction vector is obtained by inverting a linear system that describes the rotor wake over a full period. This provides for the implicit solution to the rotor wake and eliminates the solution errors and poor convergence behavior of time-marching schemes.

Evaluation of Acoustic Model of Ducts

Marianne Mosher

Making good acoustic measurements depends on isolating or separating direct signals from reflections. In wind tunnels, reflections can cause significant measurement uncertainties. This work evaluates an analytical model previously developed to study sound fields near sound sources in closed-test-section wind tunnels.

Experimental measurements and theoretical predictions of an acoustic field in a duct were made and compared. The experiment was designed to approximate a 1/10-scale model of low-frequency helicopter noise in the Ames NFAC 40- by 80-Foot Wind Tunnel. The frequency range corresponds to 27 to 84 hertz in the full-scale wind tunnel, and the wall linings approximate the acoustic sound absorption characteristics of the existing lining in the full-scale wind tunnel.

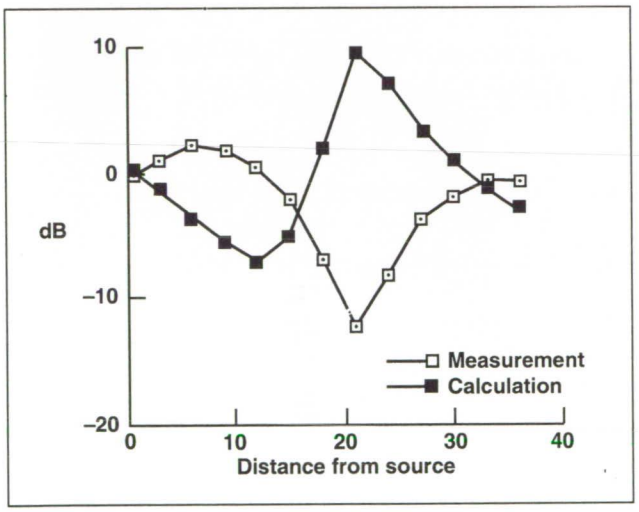


Fig. 1. Difference in sound pressure level between duct and free field for low frequency

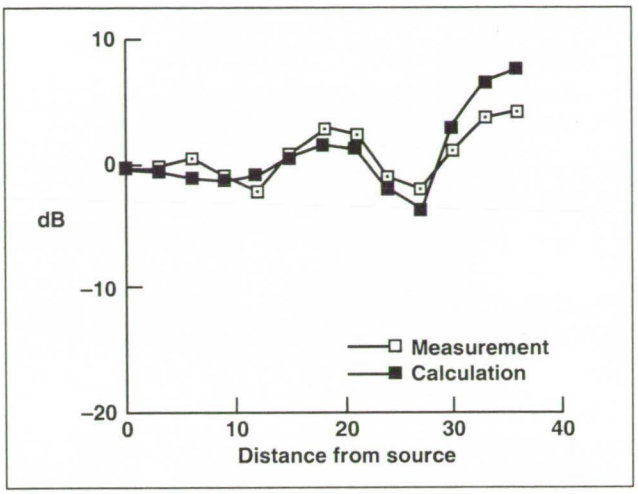


Fig. 2. Difference in sound pressure level between duct and free field for high frequency

Correlations show the theory poorly predicts reflections at the lowest frequencies with the lowest absorptions, except very close to the source (see first figure). Correlations improve with increased frequency. For the higher frequencies, correlations show very good agreement between predictions and measurements close to the source and moderate agreement far from the source (see second figure). Poor modeling of the wall boundary condition was identified as the most likely source of error in the modeling.

Ames-Moffett contact: M. Mosher
(415) 604-4560 or FTS 464-4560
Headquarters program office: OAET

Tilt-Rotor Aircraft Aeroacoustics

ORIGINAL PAGE
BLACK AND WHITE PHOTOGRAPH

Marianne Mosher

Tilt-rotor aircraft have great potential for civil and military applications because of their ability to emulate both helicopter and turboprop aircraft. However, noise can be a serious problem for tilt-rotor aircraft operations in urban areas. These aircraft produce noise from some unique mechanisms. In hover, the downwash of the rotor impinges on the wing, producing an upward fountain of air above the fuselage which passes through the rotor disk and which can even recirculate back into the rotor. The resulting flow affects both discrete frequency and broadband noise.

The effects on discrete-frequency sound of dynamic lift from the nonuniform inflow were studied with a computer model. Calculations show the directivity of the noise relates to the direction in which the blade moves through the fountain. Predicted noise levels agree reasonably well with measurements.

The effect on broadband sound of turbulence from the recirculation was studied with another computer model. Results of the calculations show that this noise radiates more strongly toward the rear of the aircraft when the blades rotate from the leading edge of the wing toward the trailing edge. Predicted noise levels are significantly less than measurements. To obtain better aerodynamic information for use in the acoustic predictions, a scale model (see figure) of the tilt-rotor aircraft was built and used for flow visualization of the fountain effect.

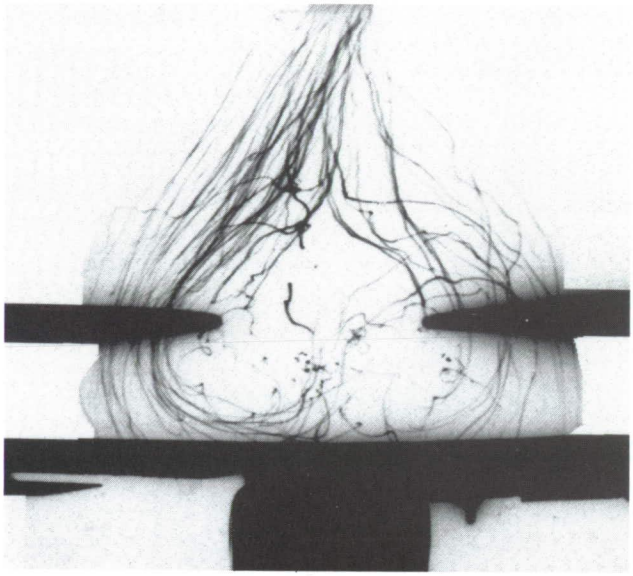


Fig. 1. Tilt-rotor aircraft model

Ames-Moffett contact: M. Mosher
(415) 604-4560 or FTS 464-4560
Headquarters program office: OAET

Active Control to Alleviate Rotor-Blade Stall

Khanh Nguyen

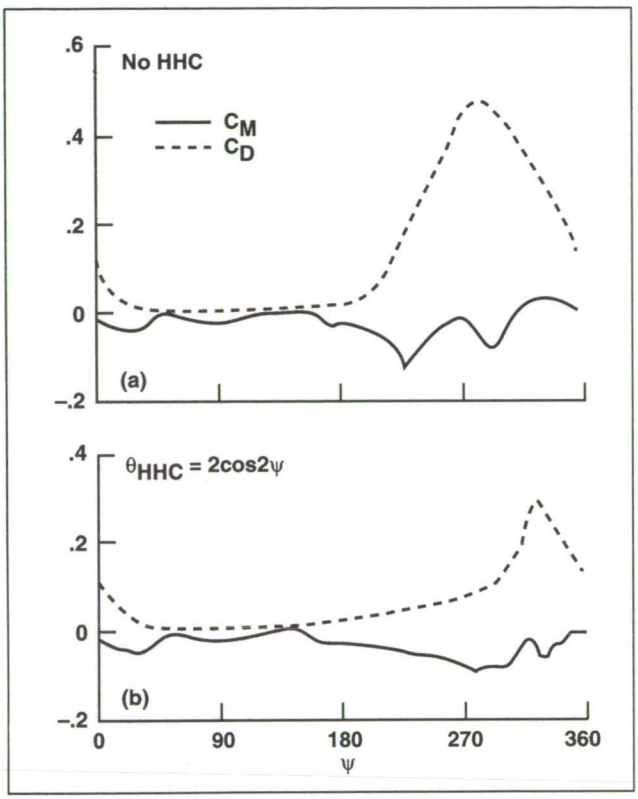


Fig. 1. Variation of drag and pitching moment coefficients at a given blade section (a) with HHC off and (b) with HHC on. Aerodynamic parameters at $r/R = 0.8$, $C_T/s = 0.08$, $\mu = 0.355$

In an effort to expand the helicopter flight envelope, it is proposed to use active control to alleviate rotor-blade stall at high-speed/high-thrust flight conditions. This study is carried out using an advanced higher-harmonic-control (HHC) analysis. This analysis employs finite-element methods in both the space and time domains, an advanced unsteady aerodynamic model, and a free-wake model. The rotor response is solved using a nonlinear aeroelastic trim procedure, including higher harmonic control effects. Preliminary results indicate that 2/rev blade-pitch control, applied at the appropriate phase angle, can significantly reduce stall on the retreating blade. Current efforts concentrate on developing an automatic stall-suppression system for general helicopter flight conditions.

Ames-Moffett contact: K. Nguyen
(415) 604-6668 or FTS 464-6668
Headquarters program office: OAET

Advanced Helicopter Rotor Analysis Code

Khanh Nguyen

An advanced code is needed that is capable of modeling a wide range of rotor configurations and that is flexible enough to accommodate a multitude of analysis options. The University of Maryland, with support from the Rotorcraft Aeromechanics Branch, has developed a comprehensive rotor-analysis code. The University of Maryland Advanced Rotor Code (UMARC) offers such capabilities within a user-friendly environment and modular structures, and incorporates state-of-the-art modeling techniques. The development of UMARC is based on the integration of several highly specialized codes which have been developed over the last decade at the University of Maryland.

The aircraft governing equations are formulated based on Hamilton's principle, and both the spatial and temporal variations are discretized using finite-element methods. The rotor blade is modeled as an elastic beam undergoing flap and lead-lag bendings, elastic twist, and radial deflections. The spatial finite-element formulation allows UMARC to model a wide range of rotor configurations, including those with complex root kinematic constraints, redundant load paths, and complex tip geometry.

The aerodynamic modelings allow several options for calculating blade airloads for both conventional and circulation control airfoils. These options range from quasi-steady aerodynamics to Leishman's dynamic stall model. Flexibility in programming development also allows computational-fluid-dynamics (CFD) interfacing capability. The steady rotor inflow can be calculated using linear inflow models, prescribed wake models, or a free-wake model. Dynamic inflow modeling is also available for the perturbation analyses.

Parallel to the modeling efforts, UMARC offers a variety of analysis options to simulate either free flight or wind-tunnel conditions for both hover and forward flight:

1. Blade natural frequencies and mode shapes
2. Coupled rotor-fuselage aeroelastic trim and performance; the flowchart for the coupled trim analysis is shown in the first figure
3. Blade and rotor-hub loads, and vibration

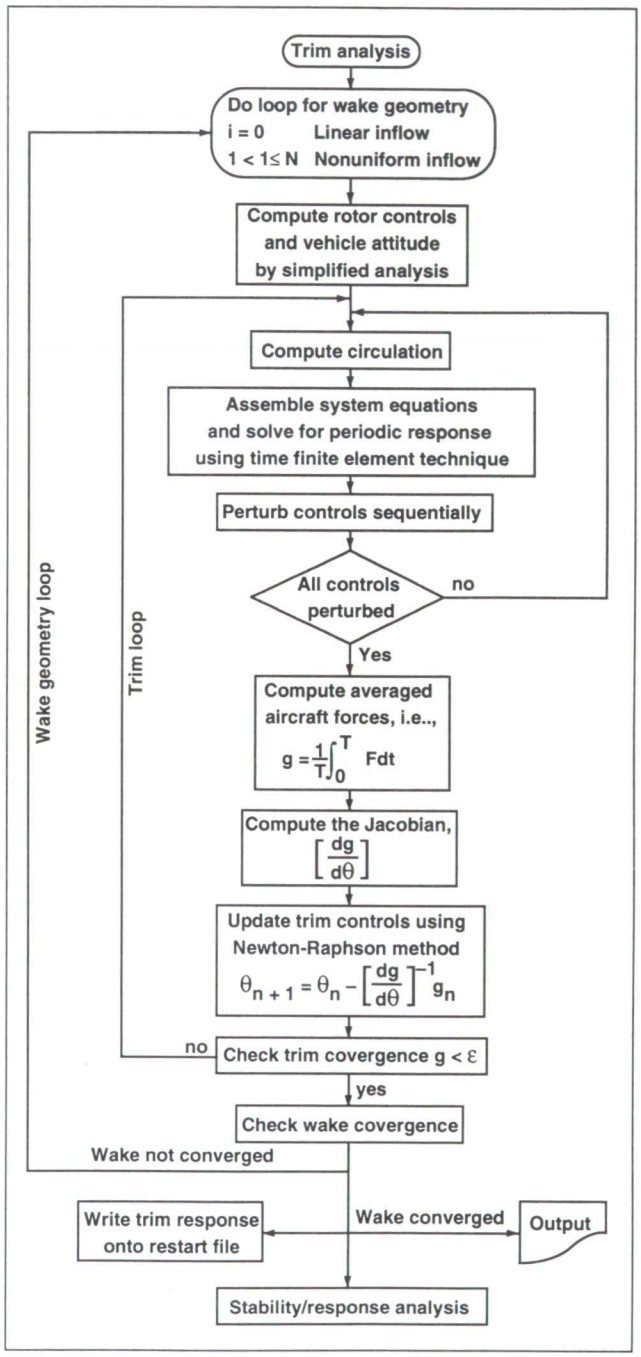


Fig. 1. Top-level flowchart for coupled rotor-fuselage aeroelastic trim analysis

4. Aeromechanical stability, including both Floquet theory and transient techniques
5. Coupled rotor-fuselage responses to a prescribed three-dimensional gust field
6. Higher harmonic control
7. Numerical optimization with aeroelastic constraints

During its development, UMARC was validated against experimental data obtained from a variety of rotor systems, including articulated, hingeless, and bearingless rotors. The results of these correlation studies with regard to rotor aeromechanical stability characteristics, blade and hub loads, trim controls, and rotor performance have generally been good. Representative results are shown in the second and third figures.

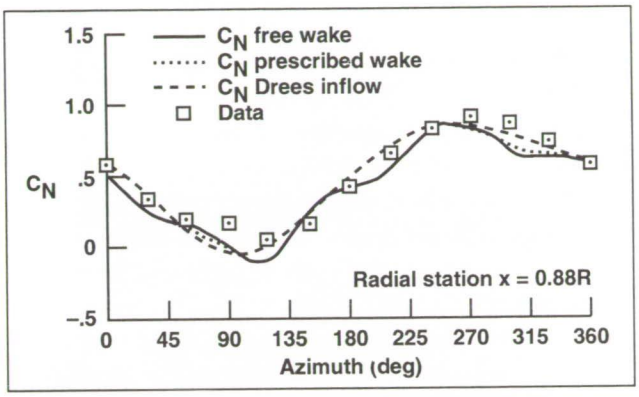


Fig. 2. Comparison of three UMARC calculated airload results with the Aerospatiale SA 349/2 flight test data ($\mu = 0.344$, $C_T/\sigma = 0.066$)

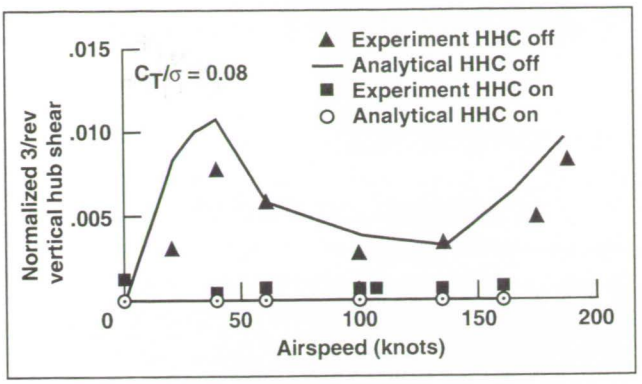


Fig. 3. Effects of higher harmonic control on the 3/rev vertical hub shear for the Boeing CH-47D scaled model rotor and UMARC calculation ($C_T/\sigma = 0.08$)

Ames-Moffett contact: K. Nguyen
(415) 604-6668 or FTS 464-6668
Headquarters program office: OAET

Bearingless Rotor Correlation Study

Khanh Nguyen

A series of wind-tunnel tests of the 1/8 Froude-scaled Boeing Integrated Technology Rotor (ITR) model have been conducted at the University of Maryland's Glenn L. Martin Wind Tunnel to investigate the aeromechanical stability of a bearingless rotor. These tests were carried out to provide the rotorcraft industry a new data base for bearingless rotor characteristics and to guarantee that sufficient stability margin is available for hub designs of this type. The data base was also used to validate the ability to predict bearingless rotor behavior using the recently developed University of Maryland Advanced Rotor Code (UMARC) .

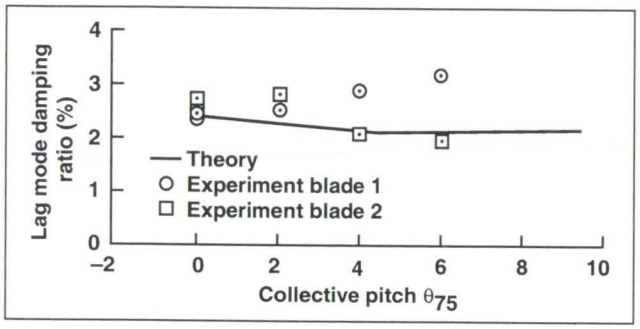


Fig. 1. Correlation of UMARC-calculated damping of the fundamental lag mode with hover test data of the Boeing ITR bearingless model rotor (817 rpm, shaft fixed)

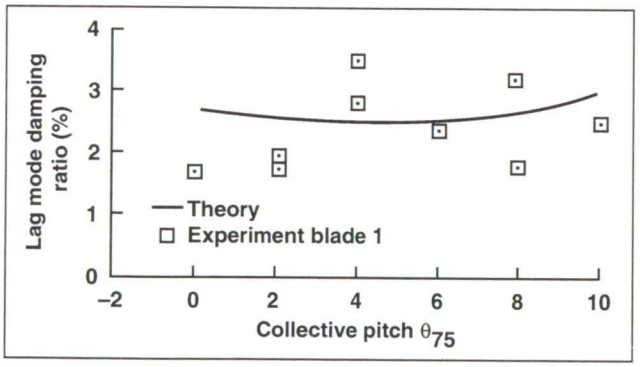


Fig. 2. Correlation of UMARC-calculated damping of the fundamental lag mode with forward flight test data of the Boeing ITR bearingless model rotor (shaft free, shaft tilt 4° forward)

The 6-foot diameter, four-bladed bearingless scaled-rotor model had been fabricated by the Boeing Helicopter Company under the NASA/U.S. Army Integrated Technology Rotor Program. In the wind-tunnel experiments, the rotor model was mounted on a two degree-of-freedom gimbal system, restrained by cantilever springs, that permitted pitch and roll motions. A refined moving block analysis was employed on-line to ensure high-quality stability measurements. The refinements include a recursive spectral analysis for improved frequency resolution and a simple frequency-domain interpretation for the Hanning's window to reduce leakage from close modes.

Two principal conclusions were drawn from this investigation: (1) both UMARC predictions and experimental results indicated that this bearingless rotor model is stable at all rpm and collective pitch settings tested, and (2) the correlation between UMARC predictions and experimental results is satisfactory. Representative results are shown for a hover condition (see first figure) and for a forward flight condition (see second figure).

Ames-Moffett contact: K. Nguyen
(415) 604-6668 or FTS 464-6668
Headquarters program office: OAET

Rotor Aeroelastic Response Analysis for Emergency Power Loss

Khanh Nguyen

A rigid flap-lag blade analysis has been developed to simulate a rotor in a wind tunnel undergoing an emergency power shutdown. These results support the safety analysis of the Sikorsky S-76 rotor to be tested in the 80- by 120-Foot Wind Tunnel.

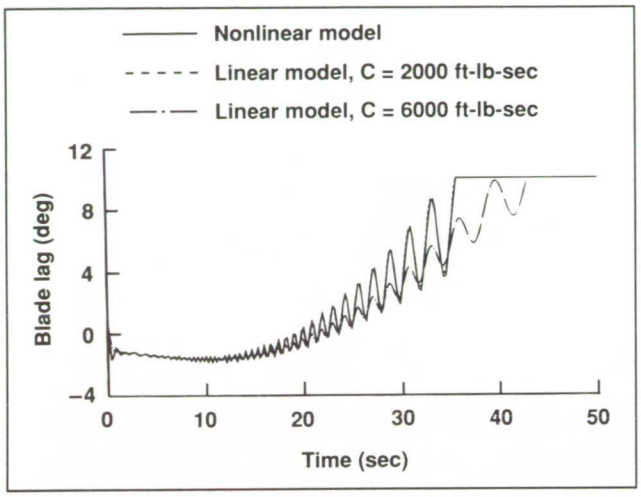


Fig. 1. Effects of lag damper model on lag response of rotor undergoing a loss of power

Simulated results show that for a rotor at a nonzero shaft tilt angle undergoing an emergency power shutdown, the oscillatory lag response is divergent. The mean lag response is large when tested at high collective pitch angles. Reducing the collective pitch during the emergency shutdown reduces the steady lag response. Increasing the rotor-shaft tilt angle increases the oscillatory lag response component. The blade lag response obtained by incorporating a nonlinear lag damper model indicates that in this case the equivalent linear viscous damping is lower than originally expected (figure).

Simulation results indicate that large oscillatory lag motions can be suppressed if the rotor shaft is returned to the fully vertical position during the emergency power shutdown.

Ames-Moffett contact: K. Nguyen
(415) 604-6668 or FTS 464-6668
Headquarters program office: OAET

Large-Rotor Test Apparatus Development

Tom Norman, Jeffrey Johnson

To enable moderate-to-large helicopter rotor system testing in the National Full-Scale Aerodynamics Complex (NFAC), NASA and the U.S. Army are jointly developing a new research test capability. The Large Rotor Test Apparatus (LRTA) is being designed and built by Dynamic Engineering, Inc., to operate helicopter rotors at up to 40,000 pounds. The LRTA will use two 3000-hp electric motors to power rotor systems (see figure). It includes a five-component balance designed for both steady and oscillatory rotor-hub load determination. An instrumented flex-coupling provides rotor torque measurement. The control system is designed to provide conventional collective and cyclic trim pitch control as well as dynamic high-frequency blade pitch control up to 40 hertz.

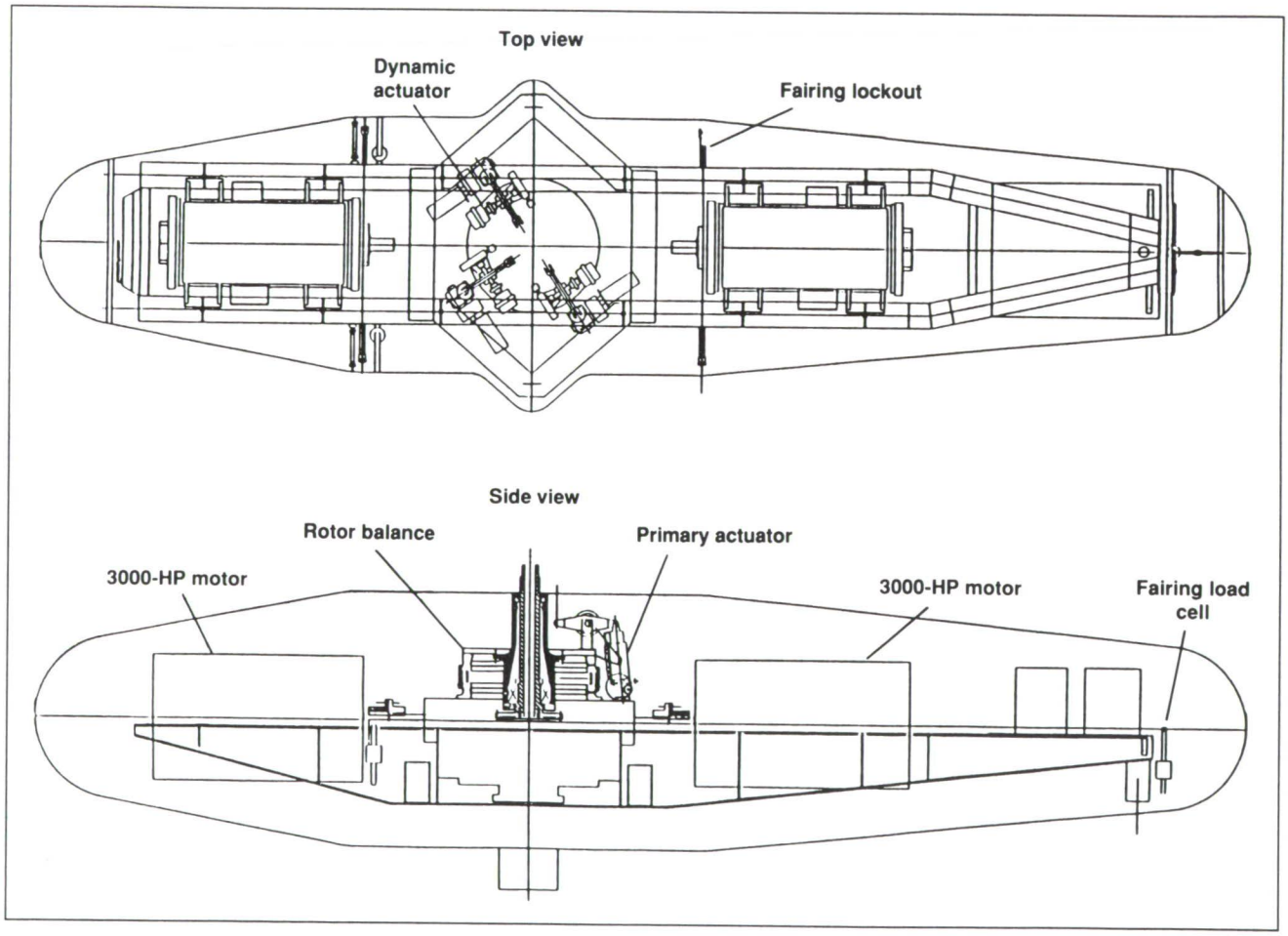


Fig. 1. Large Rotor Test Apparatus layout

The LRTA will first be used to test a pressure-instrumented UH-60 rotor system in the 40- by 80-Foot Wind Tunnel at Ames. The rotor will be operated beyond its power-limited flight envelope as a result of the greater available shaft horsepower. Detailed dynamic, aerodynamic, and acoustic measurements will be made and compared with small-scale wind-tunnel test results and flight-test results. Rotor performance and oscillatory hub loads will be acquired that will not be measured in the NASA airloads flight-test program. Hence, the wind-tunnel results will help in interpreting the flight performance measurements. Subsequent testing with the Boeing Model 360 rotor system in the NFAC is planned.

During the past year the final detailed design of the LRTA was completed and approved. A walking-beam actuation system similar to the Ames Rotor Test Apparatus (RTA) was developed for the primary and dynamic control systems. A new rotor balance design was developed which significantly reduces the influence of heat effects on balance flexure stresses. The LRTA rotor control console, designed and built by Sterling Federal Systems, was delivered to Ames. The console was built to be operational with the existing RTA and is in the process of checkout and integration with the RTA for an upcoming S-76 rotor test in the 80- by 120-Foot Wind Tunnel. In the coming year, fabrication of the LRTA fairing and chassis will begin at Ames, and Dynamic Engineering, Inc. will do further risk-reduction testing of the actuator and rotor balance designs.

Ames-Moffett contact: T. Norman
(415) 604-6653 or FTS 464-6653
Headquarters program office: OAET

Rotorcraft Aerodynamic Interaction Program

ORIGINAL PAGE
BLACK AND WHITE PHOTOGRAPH

Tom Norman, Gloria Yamauchi

The second entry of a full-scale rotor/fuselage aerodynamic interaction test was completed in the 40- by 80-Foot Wind tunnel in 1990. This second entry completed the research data acquisition initiated in the first entry in 1989. Collectively, the two entries have generated the first full-scale data base for aerodynamic interaction between a main rotor and an axisymmetric body.

The model consisted of a Bell 412 main rotor and a modified NACA 0030 body of revolution. The fuselage loads were measured independently by load cells mounted on the test stand. Combined rotor/fuselage loads were measured by the tunnel-balance system. Other data acquired were steady and unsteady fuselage pressures, blade bending moments, control system loads, mast bending moments, wind-tunnel wall pressures, and blade acceleration data.

The wall pressures will be used to develop a wall-correction method for rotors. The blade acceleration data will further the development of the individual blade control method, which ultimately aims to provide helicopter attitude stabilization, gust alleviation, and in-plane damping augmentation by using the blade-mounted accelerometers to generate inputs to the swashplate actuators.

The following configurations were tested to isolate the effects of the rotor on the fuselage:

1. Isolated fuselage: body angle of attack = 0° to –8°; tunnel speed = 20 to 140 knots



Fig. 1. Bell 412 rotor on model 576 test stand

2. Fuselage with hub: body angle of attack = 0° to –8°; tunnel speed = 20 to 140 knots; rpm = 320
3. Fuselage with hub/rotor: body angle of attack = 0° to –8°; advance ratio = 0 to 0.275; tip Mach number = 0.68

Comparison of steady and unsteady loads with the results of previous small-scale tests will determine the validity of the geometric and aerodynamic scaling used in small-scale experiments.

Ames-Moffett contact: T. Norman/G. Yamauchi
(415) 604-6653/6719 or FTS 464-6653/6719
Headquarters program office: OAET

Modern Four-Bladed Rotor Research in the 40- by 80-Foot Wind Tunnel

Tom Norman, Sesi Kottapalli, Jane Leyland

The Rotorcraft Aeromechanics Branch is planning to conduct aerodynamic, acoustic, and dynamic tests in the 40- by 80-Foot Wind Tunnel up to airspeeds of 200 knots with a modern rotor system, the four-bladed Sikorsky S-76 articulated rotor. The recently modified and enhanced Ames Rotor Test Apparatus (RTA) will provide support system functions during the test. This test is planned for the fall of 1991.

The aerodynamic portion of this test will comprehensively study the high-speed performance and noise of the S-76 rotor. Comparisons will be made with results from the 1977 S-76 test conducted in the 40- by 80-Foot Wind Tunnel prior to the recent tunnel modifications and the low-speed test results from a preceding 80- by 120-Foot Wind Tunnel test. A post-test correlation attempt will be conducted to estimate blade elastic effects on rotor performance at high airspeeds. This correlation effort will involve comparing the wind-tunnel rotor lift-to-drag ratio (L/D) with an analytical estimate of the L/D, with and without blade elasticity. Because of the difficulties involved in such comparisons, it is hoped that reliable conclusions can be drawn based on semi-empirical (perhaps normalized) comparisons such that the test and analytical L/D's trend in a roughly similar manner. The next step would be to bring in the analytical "rigid blade" L/D and then finally attempt to estimate the effect of blade elasticity on rotor performance.

Acoustic tests will be conducted with a view to study external noise reduction with respect to blade-vortex interactions (BVI). The effects of blade leading-edge modifications on the external noise level (determined by the blade-tip aerodynamic loading, vortex strength, and blade-vortex distance) will be studied. The tunnel testing will also involve a second rotor system with a modified leading-edge airfoil to evaluate the influence of this change on radiated BVI noise.

This test will also evaluate the potential of a conventional swashplate control system to generate effective higher harmonic control (HHC) pitch inputs to the blade in an open-loop fashion for noise, loads, and vibration reduction. This planned test will be a first for a full-scale rotor with HHC under high-speed conditions (up to 200 knots) and moderate thrust (10,000 pounds).

All HHC pre-test activities have been specified. Test objectives and approach, run conditions, data-acquisition, and post-test data processing requirements have been largely defined and documented. A series of checkout tests intended to verify the proper and safe functioning of the HHC system down to the individual actuator level has been defined and documented.

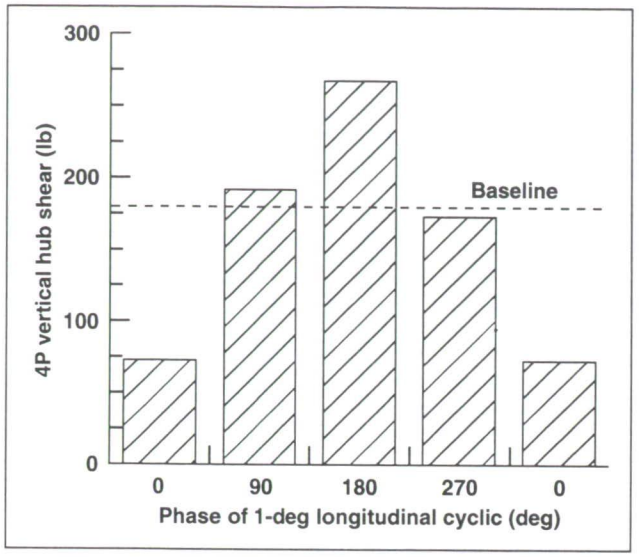


Fig. 1. Open-loop longitudinal cyclic suppresses vertical hub shears

Analytical results from the present HHC pre-test aeroelastic analysis qualitatively confirm what was observed in the 1985 Sikorsky flight test involving the S-76 aircraft. A longitudinal cyclic (composed of rotating system 3P and 5P inputs) is predicted to be more effective than a collective input (4P input) or in general even a lateral cyclic input. These inputs were analytically simulated with the analysis program CAMRAD/JA. The figure shows the 4P vertical hub shear (10,000 pounds rotor thrust at 80 knots) obtained as a variation of the phase of a 1° HHC longitudinal cyclic input. A longitudinal cyclic at 0° phase is quite effective in suppressing the vertical shear. Further analytical studies are continuing.

Ames-Moffett contact: T. Norman
(415) 604-6653 or FTS 464-6653
Headquarters program office: OAET

Rotorcraft Aeroelastic Stability Program

Randy Peterson, Benton Lau

Current-generation helicopter rotor systems are sophisticated mechanical systems that operate with very high loads in an adverse aerodynamic environment. To relieve the high rotor-blade-root moments and maintain dynamic stability, helicopter rotor blades typically have several hinges, bearings, or dampers at the blade root. These mechanical devices operate in the rotating system and experience large oscillatory loads. They require frequent maintenance and can drastically reduce the reliability of the rotor systems. With the recent advances in high-strength composites, advanced rotor systems have been designed with a minimum of hinges and bearings. These systems have reduced maintenance and improved reliability without degrading the aerodynamic performance or aeroelastic stability.

Both full-scale and small-scale wind-tunnel test programs, in addition to some flight tests, have verified these designs, as well as the structural and operational integrity of the rotor systems. However, several very important areas of hingeless and bearingless rotor technology have not been adequately investigated. For example, the dynamic characteristics of these rotors in forward flight have not been adequately predicted using conventional analysis methods. One reason these rotors present a challenge is their aeroelastic coupling, which changes with flight condition. Also, analytical modeling techniques are just beginning to predict the aeroelastic stability of these rotors at moderate and high forward flight speeds.

To address these and other problems, a full-scale BO-105 rotor system will be tested on the National Full-Scale Aerodynamics Complex Rotor Test Apparatus (RTA). This program will investigate the aeroelastic behavior of full-scale hingeless rotor systems. This program also involves correlation of rotor-system performance and loads between a 40% scale model of the BO-105, flight tests of a BO-105 helicopter, and the full-scale wind-tunnel results. The flight-test program is scheduled for spring 1991. The first model-scale test is scheduled for fall 1991 with the full-scale test to follow. To accurately measure both steady and dynamic rotor forces and moments, a rotor balance has been designed, fabricated, and calibrated for the RTA.

To expand the analytic capability of rotorcraft aeroelastic analyses, a research project is being conducted by Syracuse University. The university has recently completed the validation of a transfer-matrix approach for predicting the aeroelastic stability of redundant-load-path bearingless rotor systems in hover. The forward-flight formulations using the same transfer-matrix approach have been completed and are currently being implemented in a computer code.

Ames-Moffett contact: R. Peterson
(415) 604-5044 or FTS 464-5044
Headquarters program office: OAET

Light Helicopter Risk Reduction and Demonstration/Validation Program

Randy Peterson, Larry Young

In support of the U.S. Army Light Helicopter (LH) program, the National Full-Scale Aerodynamics Complex (NFAC) has provided test facilities and personnel to the two contractor teams for the development of a next-generation helicopter design. The first test program with the McDonnell Douglas Helicopter Company and Bell Helicopter Company (SuperTeam) under the Risk Reduction effort in the 40- by 80-Foot Wind Tunnel was completed in November 1989. A second test program with the SuperTeam under the Demonstration/Validation (Dem/Val) contract was completed in July 1990.



Fig. 1. Bell/MDHC isolated rotor hover performance test prior to testing in the 40- by 80-Foot Wind Tunnel

Both test programs with the SuperTeam were conducted in two phases. The first phase of each program was conducted at the McDonnell Douglas Helicopter Company Remote Test Facility (RTF) with the objectives of acquiring isolated rotor hover performance and providing a complete checkout of their new test stand prior to entry in the 40- by 80-Foot Wind Tunnel. The figure shows the test stand at the RTF.

The second phase of each test program acquired both hover and forward-flight rotor and airframe performance and anti-torque data, rotor dynamics and loads data, and rotor aeroelastic stability data.

Ames-Moffett contact: R. Peterson
(415) 604-5044 or FTS 464-5044
Headquarters program office: OAET

ORIGINAL PAGE
BLACK AND WHITE PHOTOGRAPH

Testing of Large Ram-Air-Inflated Wings

James C. Ross

Paratroopers, civilian sport parachutists, and paraglider pilots all use ram-air inflated wings (parafoils) to slow and guide their descent. These wings are made of nylon or similar fabrics assembled to produce upper and lower wing surfaces. Fabric ribs are sewn between the surfaces at several spanwise locations to control the airfoil shape. The leading edge is left open to admit ram air that inflates the wing. A parafoil can be packed and deployed like a parachute but can be glided to a soft landing over a relatively large area.

Parafoils are currently under consideration for use in recovering space payloads for two NASA projects: the Advanced Launch System and the Assured Crew Recovery Vehicle. The advantage of parafoils over standard canopy parachutes is their ability to glide to a predetermined recovery site with a soft landing on solid ground rather than in water. This saves on transportation costs to return the payload to a refurbishment site and reduces damage to the payload caused by the corrosive effects of salt water. The latter is particularly important for the Advanced Launch System since the propulsion and avionics modules that will be recovered are extremely sensitive to corrosion.

Most parafoils have been developed using "cut-and-try" experimentation that depends strongly on the experience of the designer. A series of tests of the Advanced Recovery System was performed in the 80- by 120-Foot Wind Tunnel at Ames Research Center during 1989 and 1990. The tests were a cooperative research effort involving NASA (Ames Research Center and Marshall Space Flight Center) and Pioneer Aerospace Corporation. The amount of aerodynamic force data available for parafoil design was greatly increased by these tests.

Nine parafoil configurations were tested during the program. One of the wings flying in the wind tunnel is shown in the first figure. The wing sizes ranged from about 25 to 60 feet in span and from 10 to 20 feet in chord. Full-scale parafoils proposed for the flight recovery system would have spans of 180 feet and would be capable of delivering payloads of up to 60,000 pounds.

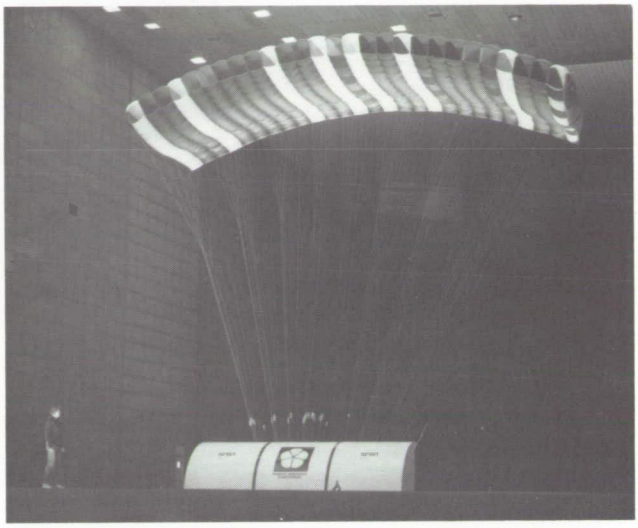


Fig. 1. Model of 60- by 20-foot parafoil flying in the test section of the 80- by 120-Foot Wind Tunnel

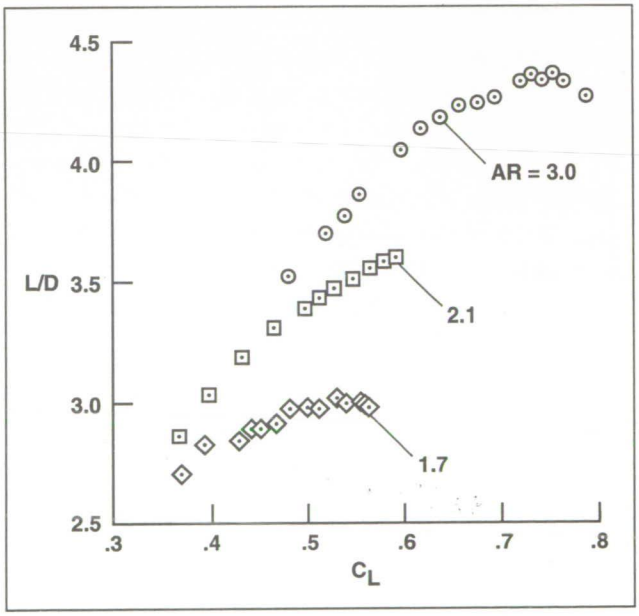


Fig. 2. Effect of aspect ratio on wing performance. Dynamic pressure = 6 pounds per square foot, 20-foot chord wing

ORIGINAL PAGE
BLACK AND WHITE PHOTOGRAPH

The effects of various wing parameters were determined during the tests. These include the effect of aspect ratio, anhedral ratio (a measure of the spanwise radius of curvature of the wing), and airfoil section shape. Some typical data are shown in the second figure, demonstrating the effect of the wing aspect ratio on the lift-to-drag ratio (L/D). The aspect ratio was varied by changing the span while holding the wing chord constant (20 feet here). The Reynolds number for these data is 5×10^6 based on the chord. As expected, the L/D and the maximum lift coefficient (C_{Lmax}) both decrease with decreasing aspect ratio.

During the two phases of testing, improvements were made in both wing design and testing techniques. The performance of the first wings tested was very sensitive to dynamic pressure. As the dynamic pressure increased from 4 to 12 pounds per square foot, the maximum L/D decreased by 25%. This was traced to increased wing deformation under the increased load. By tailoring the support lines, subsequent wings did not demonstrate load-sensitive performance. In addition, during the tests, improvements in wing design increased the maximum L/D from approximately 3.0 to 4.4. Several additional design improvements, including airfoil shape and inlet geometry, have been identified that may increase the performance even further.

A novel application of three-dimensional stereo ranging was used during the tests to determine the wing angle of attack. The ranging system, shown schematically in the third figure, has two video cameras in the test section, both of which are aimed at the lower surface of the wing. The signals from these cameras are sent to a personal computer equipped with two video frame-grabber cards and two monitors. Simultaneous images from the two cameras are captured and stored on the computer. By selecting the same point in the two images, the three-dimensional location of that point can be determined. If the locations of the leading and trailing edges of the wing are determined, the angle of attack can be easily computed. The squares on the lower surface of the wing (shown in the first figure) were used for convenient reference points. This ranging technology gave an accurate measure of the wing angle of attack and twist distribution and will become an important tool in wind-tunnel testing in the future.

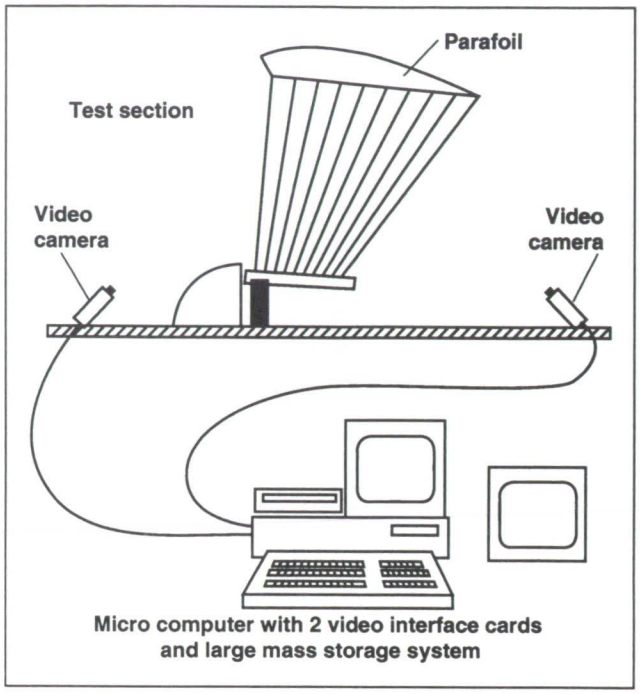


Fig. 3. Schematic of three-dimensional stereo ranging system used to measure parafoil angle of attack and deformation

Ames-Moffett contact: J. Ross
(415) 604-6722 or FTS 464-6722
Headquarters program office: OAET

Short Takeoff and Vertical Landing CFD Validation Studies

ORIGINAL PAGE
BLACK AND WHITE PHOTOGRAPH

Karlin R. Roth

Traditionally, the development of short takeoff and vertical landing (STOVL) aircraft has been guided primarily by experimental investigations. Because of the cost of full-scale powered testing and the lack of adequate prediction methods for powered-lift systems, STOVL design is currently one of the most lengthy and costly aerospace design problems. Since various STOVL concepts have the unique ability to satisfy critical national needs, NASA and industry are interested in developing computational methods that could reduce the cost of the powered-lift design cycle.

Computations and experiments directed toward evaluating the flow about STOVL aircraft have usually been performed independently with differing goals. As a result of this lack of coordination, existing data generally are not detailed enough or are of the wrong type to provide meaningful comparisons between theory and experiment. To address this issue, a combined experimental/computational-fluid-dynamics (CFD) research program was initiated to validate computational methods for STOVL-type flows. Because of the synergistic coupling of Ames' strong base in the experimental and flight study of STOVL concepts with Ames' excellence in CFD, it is expected that a significant advance in state-of-the-art STOVL concepts and design can be made by this program. The results of this research program are expected to affect both the U.S. STOVL and the U.S./U.K. Common Technology Development programs and to support the Ames "Computation through Flight" Vision.

The primary objective of the experimental program is to provide data of sufficient detail and quality for evaluating the capability of CFD to predict the important flow parameters and to provide a data base for improving the modeling capability of CFD algorithms. To meet this objective, a simplified STOVL configuration model was fabricated. The

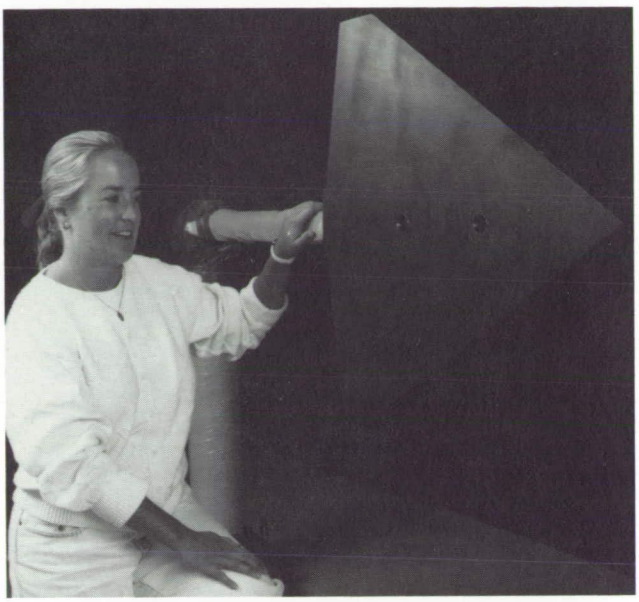


Fig. 1. STOVL model installed in the 7- by 10-Foot Wind Tunnel

model geometry, a Delta wing (E-7) planform with two circular, high-pressure air jets located in a simplified fuselage, was designed to minimize the geometric complexity while retaining the critical aero/propulsive/ground interaction flow physics. Collaboration between experimental aerodynamicists and CFD practitioners was emphasized in the design phase to ensure that the data will be adequate for code validation.

The transitional flight characteristics of this representative STOVL aircraft configuration were measured in the 7- by 10-Foot Wind Tunnel during the period August to November 1990.

The model installation is shown in the figure. The measured flows had a maximum free-stream Mach number of 0.2 and a maximum nozzle pressure ratio of 3. Ambient temperature was maintained at the jet exits.

The experimental results include forces and moments measured with an internal balance, steady and dynamic pressures measured at 281 surface-pressure ports, and jet pressures and temperatures. Flow-field surveys were made upstream and downstream of the model and near the tunnel walls to verify boundary conditions for the planned computations. Total-pressure surveys of the jet exits were also made. Flow visualization, including Schlieren and laser light sheet, was used to provide a description of the three-dimensional flow field.

A second test entry to study ground effects is planned for fall 1991. During this test, flow-field laser velocimetry and hot-wire measurements will also be made.

The development and validation of powered-lift CFD technology utilizing the National Aerodynamic Simulation (NAS) computer facility has been an ongoing research effort. Some significant achievements include the validation of the F3D code for propulsion-induced flow fields, such as jets in a crossflow both in and out of ground effects; incorporation of multiple-grid schemes; and implementation of a jet turbulence model. The computational approach is based on these technologies which have reached the application level. Three-dimensional Navier-Stokes computations of the STOVL CFD configuration have been initiated.

Ames-Moffett contact: K. Roth
(415) 604-6678 or FTS 464-6678
Headquarters program office: OAET

Modern Four-Bladed Rotor Research in the 80- by 120-Foot Wind Tunnel

Patrick Shinoda

The Rotorcraft Aeromechanics Branch will be conducting its first rotor test in the Ames 80- by 120-Foot Wind Tunnel with a newly acquired Sikorsky S-76 rotor hub/blades system mounted to the recently modified Ames Rotor Test Apparatus (RTA). This rotor system was acquired to provide an opportunity to study important aerodynamic, dynamic, and acoustic phenomena of a modern four-bladed rotor system.

The purposes of this test are (1) to learn the capabilities of this national facility for testing full-scale rotors (rotor performance and acoustics in hover and in low-speed forward flight, and documenting any facility effects on the rotor system); (2) to acquire a rotor performance data base in the 0- to 60-knot velocity range for refinement of theoretical predictions; (3) to acquire a rotor performance data base for the rotor system under high-load/low-airspeed/high-angle-of-attack conditions; (4) and to determine the effectiveness of the Ames-developed wide-field shadowgraph technique with a full-scale rotor system.

To accurately measure the rotor performance and loads both statically and dynamically for this and upcoming tests, the RTA was recently modified to accommodate a rotor balance built by Dynamic Engineering, Inc. The balance is installed between the transmission and control-system/upper-pylon. The balance has a load capability of 22,000 pounds thrust, 4,400 pounds side force, and 428,000 inch-pounds of hub moment. A flex-torque coupling built by Bendix will provide rotor torque measurement capability to 432,000 inch-pounds. Because of the height change of the control system, a fairing was added this year to the upper portion of the RTA (see figure).

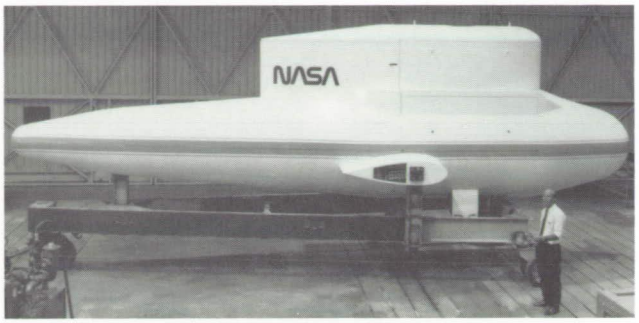


Fig. 1. Newly modified Rotor Test Apparatus fairing for rotor balance installation

There are number of current activities in progress for this test. The rotor balance has been calibrated by Modern Machine and Tool, shipped to Ames, and installed on the RTA. The first integration phase of the newly acquired rotor control console (built by Sterling Software) for this test is near completion. The rewiring of the RTA for the new rotor-control console is near completion, and hardware to check-load the rotor balance installed in the RTA has been completed.

Planned activities in preparation for this test include installed check-load of the rotor balance, S-76 rotor-system installation, RTA rotor-controls-to-rotor-console integration/calibration, and drive-system checkout operations. The wind-tunnel entry is scheduled for May 1991.

Ames-Moffett contact: P. Shinoda
(415) 604-6732 or FTS 464-6732
Headquarters program office: OAET

ORIGINAL PAGE
BLACK AND WHITE PHOTOGRAPH

Correlation of Measured Tail-Rotor Acoustics with ROTONET Predictions

David Signor, Martin Hagen

Acoustic data from an outdoor hover test of a Lynx tail rotor were correlated with ROTONET, a program developed at NASA Langley Research Center. The objective of the test was to increase understanding of the effect of ingested atmospheric turbulence on rotor acoustics. The rotor performance, blade loads, acoustics, and turbulent inflow were measured. The Lynx tail rotor and microphone array are shown in the first figure. The hot-wire anemometers used to measure the inflow and the ambient atmospheric turbulence are not shown in the figure.

ROTONET was chosen for correlating the measured acoustics because it has the capability of including measured atmospheric turbulence. Although ROTONET is designed for predicting the acoustics of an entire aircraft in flight, the inputs to the various modules can be adjusted to accommodate a tail rotor in hover. The Lynx tail-rotor blade geometry was modeled directly in ROTONET. Airfoil coefficient tables (C_l, C_m, C_d) were available for the Lynx tail-rotor airfoil (modified NACA 0012) and were substituted for the values calculated by ROTONET.

Three noise sources were calculated with ROTONET. Module LRN calculated the rotor tone noise. Module RBN calculated the 1/3-octave broadband noise. Modules ABL, STL, and TIN were used to calculate the turbulence ingestion noise. Measured inflow turbulence properties were substituted for the properties calculated within ROTONET. The calculated acoustic spectrum from each source was summed and compared with the measured spectrum.

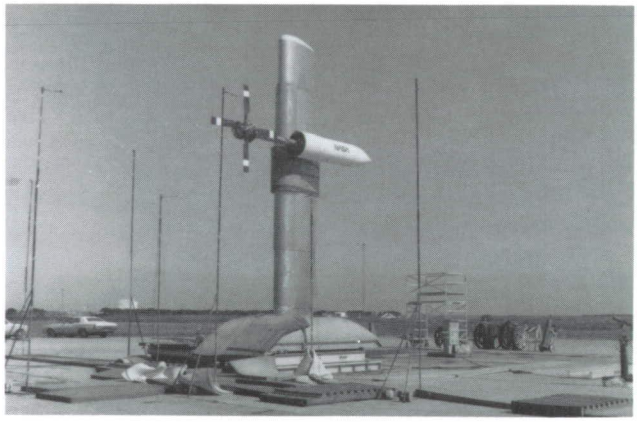


Fig. 1. Lynx tail rotor and microphone array

ORIGINAL PAGE
BLACK AND WHITE PHOTOGRAPH

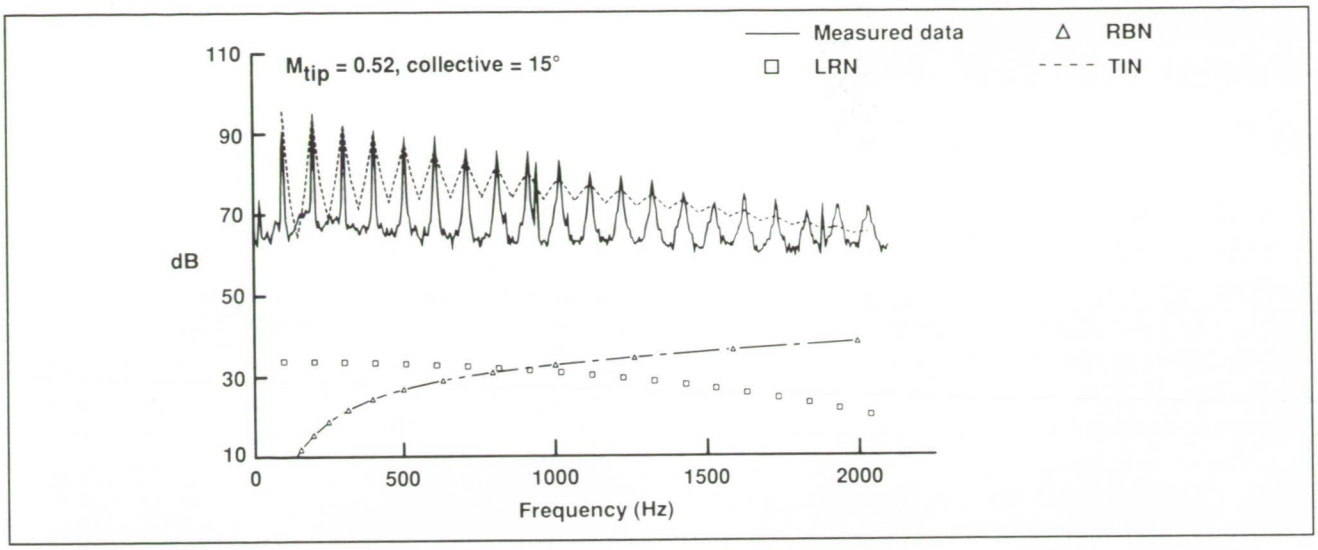


Fig. 2. Measured tail-rotor acoustics compared with ROTONET

A representative acoustic spectrum is shown in the second figure. The data were acquired 4.5 rotor radii from the rotor on the inflow side, on the rotor axis. The spectra for each of the three individual sources are shown for reference. Since the broadband and tonal noise make little contribution along the rotor axis, the summed spectrum lies on top of the turbulence ingestion noise output from ROTONET. The second through fifth rotor harmonics correlate well with ROTONET.

Ames-Moffett contact: D. Signor
(415) 604-4562 or FTS 464-4562
Headquarters program office: OAET

Steady/Dynamic Rotor Balance for the Ames Rotor Test Apparatus

ORIGINAL PAGE
BLACK AND WHITE PHOTOGRAPH

David Signor, Johannes M. van Aken

A five-component rotor balance with steady and dynamic load-measuring capability has been designed, fabricated, and calibrated by Dynamic Engineering, Inc. (DEI) and Modern Machine and Tool Co. (MMT) under contract to Ames Research Center. The steady/dynamic rotor balance (S/DRB) consists of two 36-inch-diameter rings, connected to each other by four rectangular, instrumented flexures. The balance is 22 inches high and weighs 1,900 pounds. The balance gauge capacities (static loads) are 22,000 pounds of thrust, 4,400 pounds in the axial and side force directions, and 430,000 inch-pounds of pitch and roll moment. The balance, installed inverted in the calibration stand at MMT, is shown in the figure. The balance shares a common centerline with the rotor shaft. The rotor shaft has an in-line flex-coupling, which has been instrumented to measure rotor torque up to a maximum of 430,000 inch-pounds.

The S/DRB will be installed in the Ames Rotor Test Apparatus (RTA) for testing with the Sikorsky S-76 rotor, the MBB BO-105 rotor, and the Bell 412 rotor for all future NFAC test programs.

The wind-tunnel scale system is presently used in the National Full-Scale Aerodynamics Complex to measure steady rotor performance. The data from the tunnel scales are contaminated by the airloads on the model-support strut tips and the RTA fairing. Tare runs are made to correct the scale data to obtain the actual rotor hub loads. The S/DRB will provide a new capability for measuring rotor loads directly and accurately. Accurate knowledge of the rotor forces and moments will allow for a better simulation of trim flight-test conditions in the wind tunnel and should improve the correlation between wind-tunnel and flight-test results.

Oscillatory rotor loads are directly coupled to aircraft vibration levels. The S/DRB will be used to measure directly the rotor oscillatory forces and moments and will therefore aid in predicting in-aircraft vibration levels resulting from rotor forcing. The S/DRB will also be a valuable tool in the active control studies planned for the NFAC tunnels, in that the S/DRB-measured oscillatory loads can be used as input to the active controls to reduce helicopter vibration levels.

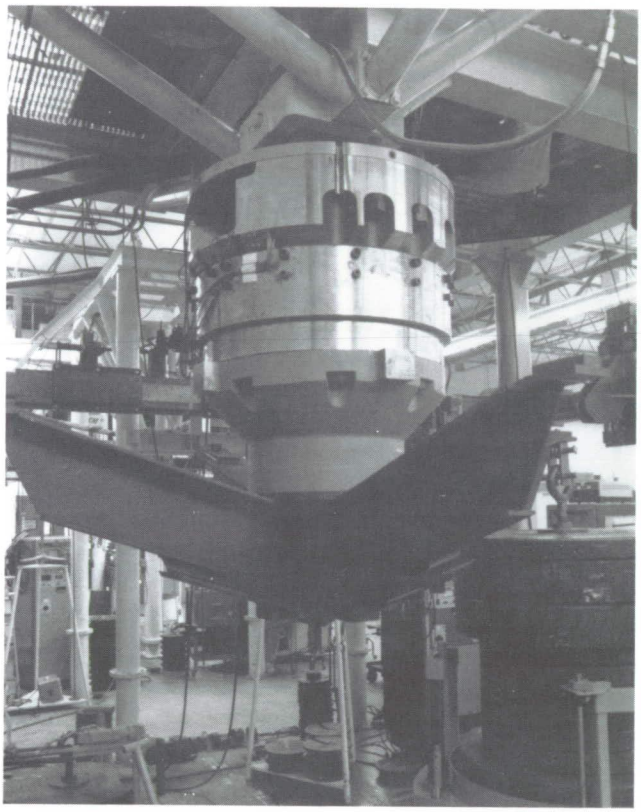


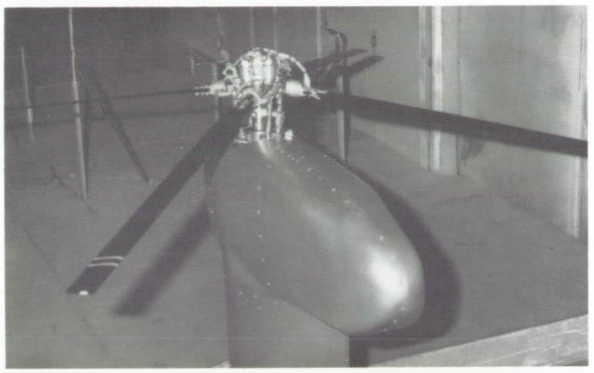
Fig. 1. RTA steady/dynamic rotor balance in the calibration stand

Ames-Moffett contact: D. Signor
(415) 604-4055 or FTS 464-4055
Headquarters program office: OAET

In-Flight Rotorcraft Acoustics Program

David Signor, Gloria Yamauchi,
Marianne Mosher

A flight-test program has been established to acquire in-flight acoustic data which will be critical to understanding and reducing helicopter noise. The acoustic energy of a single main-rotor helicopter while generating blade-vortex interaction noise will be measured. This condition occurs when a helicopter is in a gradual descent. Blade-vortex interaction (BVI) noise is typically experienced with the helicopter on approach to landing and can be annoying to the surrounding community.



1/16th-scale model



Full-scale rotor



S-76 Aircraft

Fig. 1. In-flight Rotorcraft Acoustics Program correlation from model to flight

The BVI data from each of these helicopters will be compared with similar data acquired with identical rotor systems in the 40- by 80- Foot Wind Tunnel. This will allow the acoustic properties of the 40- by 80- test section to be validated. In-flight full-scale BVI data will also be correlated with small-scale data to improve the understanding of scaling effects.

The technical approach will be to fly the Ames YO-3A airplane in formation with various civilian helicopters. The three rotor systems of primary interest are the MBB BO-105, Sikorsky S-76, and Bell 412. A commercially available infrared distance-measuring device and line-of-sight markings on the YO-3A will be used to determine the relative positions of the aircraft and the helicopter. Each helicopter will have an N/rev signal, obtained from a phototach, sent to the data-acquisition system on board the YO-3A. The YO-3A has two wing-tip microphones and a single tail-mounted microphone.

The BO-105 and S-76 helicopters will be flight tested first, for these rotor systems are scheduled to be tested in the 40- by 80- Foot Wind Tunnel in 1991. The flight test of the Bell 412 will include measurements of tail-rotor noise, as well as main rotor BVI.

Ames-Moffett contact: D. Signor
(415) 604-4055 or FTS 464-4055
Headquarters program office: OAET

ORIGINAL PAGE
BLACK AND WHITE PHOTOGRAPH

Results of Full-Scale Testing of E-7A Ejector-Lift, Vectored-Thrust Aircraft

Brian Smith

Short takeoff and vertical landing (STOVL) fighter aircraft offer the advantages of increased basing flexibility and enhanced up-and-away maneuverability. Recent advances in propulsion technology, innovative designs, and a better understanding of powered-lift aerodynamics have made possible the development of aircraft designs that combine the high performance required of the next generation of fighter aircraft with the advantages of STOVL capability. Tests of a full-scale, powered model designated the E-7A in Ames' 40- by 80 and 80- by 120-foot wind tunnels have demonstrated the practicality of a STOVL concept employing an ejector-lift, vectored-thrust propulsion concept.

During the full-scale wind-tunnel tests, an installed ejector thrust augmentation ratio (defined as total ejector thrust divided by the thrust of the primary nozzles) of 1.58 was demonstrated. This is the highest performance level that has been achieved to date in a realistic full-scale aircraft, and it provides sufficient thrust-to-weight ratio for controlled hover. The lifting-ejector system has the additional benefit of reducing jet temperatures and pressures at ground level under the forward portion of the aircraft while in hover. The E-7A configuration was also shown to have satisfactory acceleration and trim characteristics throughout the transition regime from hover to wingborne flight and vice versa.

The E-7A wind-tunnel model shown in the first figure was funded by NASA, the Canadian government's Department of Industry, Science, and Technology, and the U.S. Defense Advanced Research Projects Agency.

The large body of data obtained during the two tests in the wind tunnels at Ames has made possible detailed analyses of the significant propulsion system/airframe interactions which characterize the generic class of STOVL aircraft. Entrainment of ambient flow into the lifting jets and downstream jet wakes, as well as engine and propulsor inlet flows, can drastically alter the pressure distribution on the wing and fuselage in hover and during transition to wingborne flight.

Typical interaction effects include interference with the lifting capability of the wing and changes in the drag and stability of the vehicle. For example, the second figure shows the interference effect that the propulsion system (ejector and vectored ventral nozzle) has on the aerodynamic lift (total measured lift minus lift provided by the propulsion system) of the E-7A model in the vertical-lift configuration. If no interference effects were caused by the propulsion system, the aerodynamic lift for the vertical-lift configuration would be identical to the aerodynamic lift for the cruise configuration, where propulsion-induced interference effects on lift are negligible. The loss in aerodynamic lift caused by the interference effect of the propulsion system when the model is in the vertical-lift configuration must be compensated for by increasing the propulsive lift in order to achieve the desired total lift.



Fig. 1. E-7A wind-tunnel model

ORIGINAL PAGE
BLACK AND WHITE PHOTOGRAPH

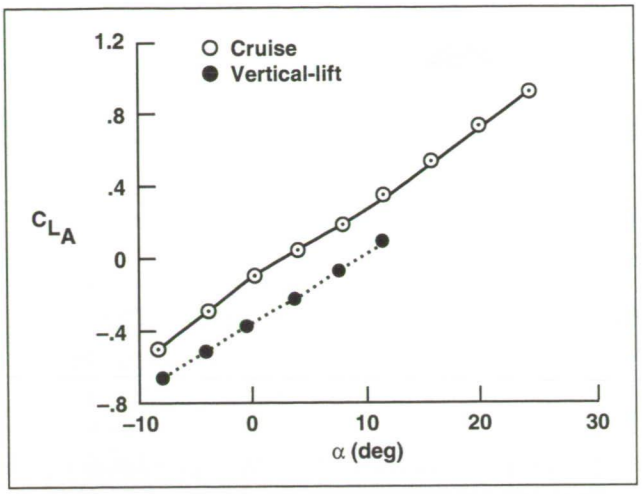


Fig. 2. Uncorrected lift coefficients for different operating modes of the E-7A

In order to make proper use of the data obtained during wind-tunnel testing, it is necessary to correct the measured forces and moments on the model for the effects of the surrounding wind-tunnel walls. When a model is tested in a wind-tunnel environment, the walls of the test section constrain the flow around the model in a way that is different from what the model would experience in free air. Typically, greater lift is measured in the wind tunnel than would be measured in free air. Other effects include changes in the model drag and pitching-moment characteristics. Application of the advanced panel method, PMARC (Panel Method Ames Research Center), to this problem has yielded promising results.

The third figure presents a comparison of uncorrected and corrected lift coefficients for the E-7A cruise configuration as tested in the two large wind-tunnel test sections at Ames. The corrections were made using results from panel-method

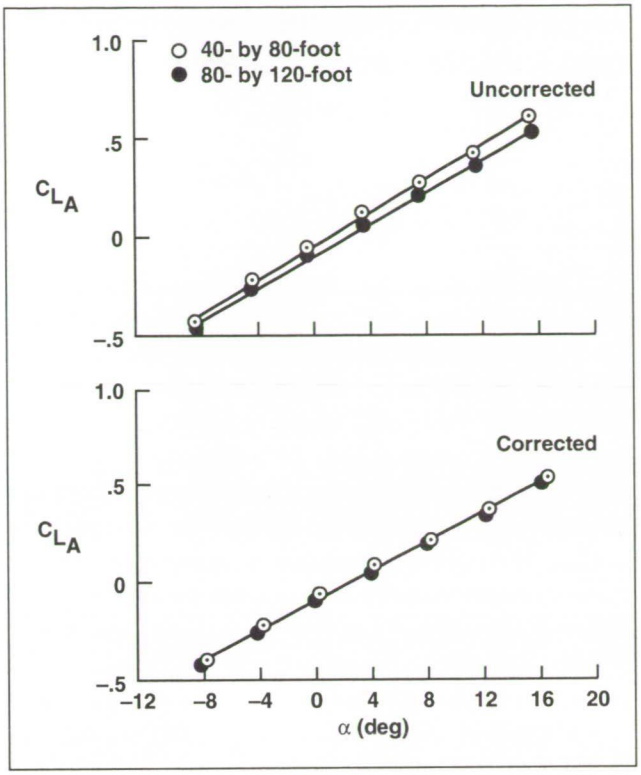


Fig. 3. Comparison of uncorrected and corrected lift data for the E-7A in cruise mode

calculations run with and without the presence of the wind-tunnel walls. It can be seen that the PMARC corrections effectively collapse the data from the two wind-tunnel tests. Ongoing work in this area includes extension of this correction technique to the powered lift configuration.

Ames-Moffett contact: B. Smith
(415) 604-6669 or FTS 464-6669
Headquarters program office: OAET

Aerodynamic Interaction between Vortical Wakes and Lifting Two-Dimensional Bodies

Paul Stremel

The numerical prediction of the strong interaction between vortical wakes and the viscous flow field about bodies is of considerable importance in the design analysis of rotorcraft. The flow field surrounding a helicopter is highly complex owing to the lack of symmetry and the unsteady aspects of the flow. This unsteady, asymmetric flow field is complicated further in that the wake shed from the rotor blades interacts with other components of the aircraft (e.g., rotor blades, forward fuselage, tail boom). These interactions are, in general, strong ones in which the rotor wake collides with the fuselage components. A precise understanding of strong vortex interactions is needed in order to optimize the aerodynamic capabilities of rotorcraft.

A computational fluid dynamic (CFD) method for computing the aerodynamic interaction between an interacting vortex wake and the viscous flow about arbitrary two-dimensional bodies has been developed to address this helicopter problem. The interaction of a periodic vortex wake with the flow about an elliptic cylinder at angle of attack of 45° and a Reynolds number of 3,000 has been calculated. The interacting vortex wake is represented by an array of clockwise rotating finite-core vortices which are introduced into the flow upstream of the elliptic cylinder.

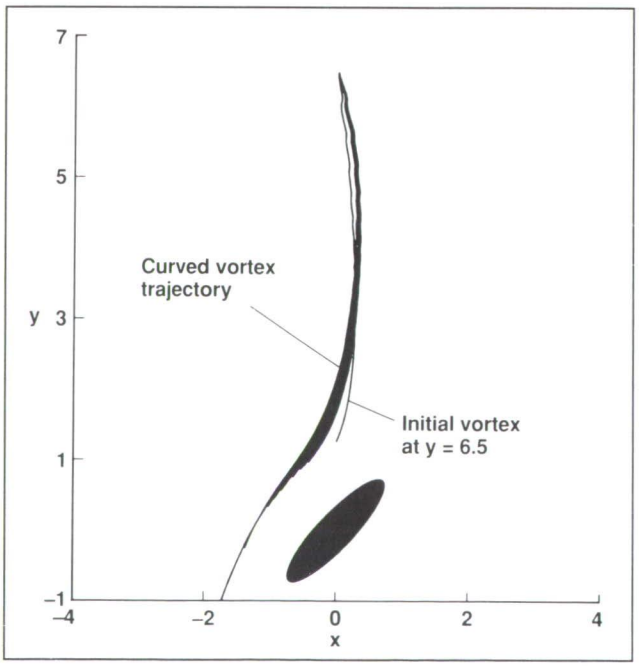


Fig. 1. Vortex trajectories

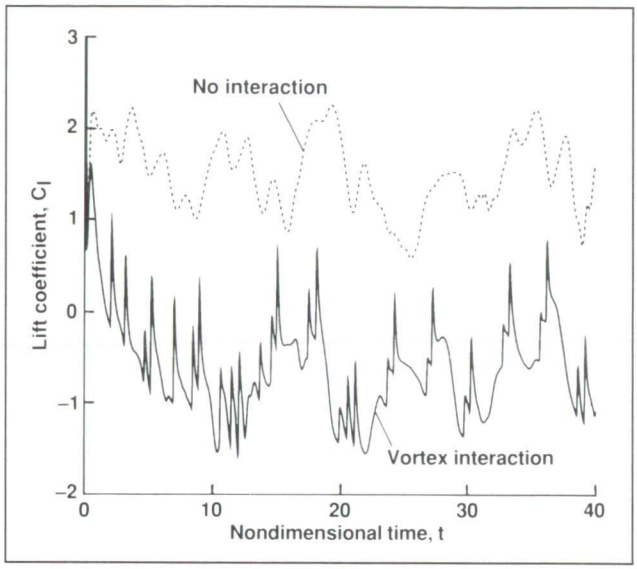


Fig. 2. Lift coefficient for vortex interaction

This is shown in the vortex trajectories of the first figure. This figure represents the vortex trajectories during the entire interaction. The lift coefficient during the vortex interaction is shown in the second figure and demonstrates the significant reduction in the mean lift resulting from the vortex interaction.

The method is currently being extended for the prediction of aerodynamic interaction between vortical wakes and aircraft components in three dimensions.

Ames-Moffett contact: P. Stremel
(415) 604-4563 or FTS 464-4563
Headquarters program office: OAET

Direct Solution of the Velocity-Vorticity Formulation

Paul Stremel

A method previously has been developed for the prediction of vortex/bluff-body interaction in two dimensions. The method solves the velocity/vorticity form of the incompressible Navier-Stokes equations for the flow-field velocity and vorticity and a finite-core representation of the interacting vortex wake. The predicted results using this method demonstrate the significant variation in the lift and drag on two-dimensional bodies during a vortex interaction. The method, however, does not directly satisfy the conservation of mass and, therefore, requires computational iteration at each time-step in order to converge the solution.

These iterations can become excessive and constitute a limitation to this method. An alternative method for the solution of the flow-field velocity and vorticity has been developed. In this method, the flow field velocity and vorticity are solved by the velocity-vorticity formulation using a staggered-grid approach in a fully coupled manner. In the staggered-grid method, the vorticity is defined at the mesh nodes, and the velocity components are defined at the midpoint of the mesh cell sides. This arrangement allows for the accurate representation of the definition of vorticity at the node points and the conservation of mass at the cell centers. Additionally, the fully coupled method provides for the implicit solution of the flow field and requires only a single iteration to obtain the solution at each time-step. The solution is obtained by utilizing an ADI (alternating direction implicit) method for the solution of the block-tridiagonal matrix resulting from the finite-difference representation of the governing equations. The solutions to both the scalar and periodic block-tridiagonal systems are incorporated into the implicit solution. The method provides for the direct solution of the flow field and satisfies the conservation of mass to machine zero at each time-step.

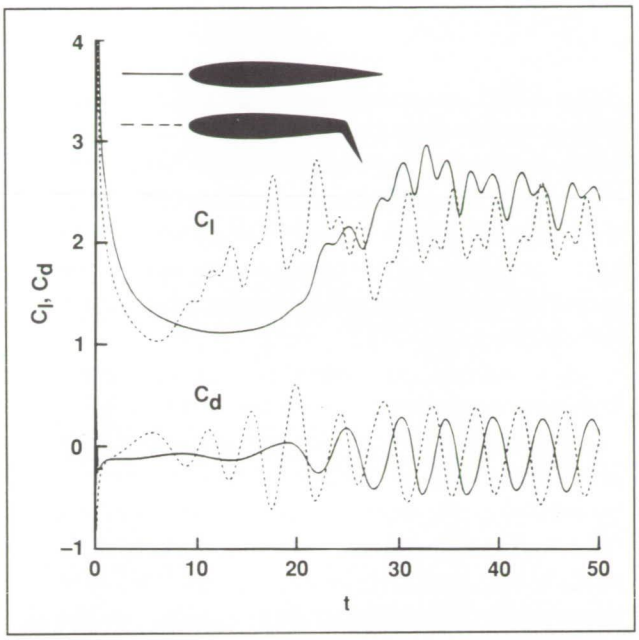


Fig. 1. Lift and drag for a NACA 0012 airfoil at an angle of attack of –90° with and without a deflected flap

The predicted flow about circular and elliptic cylinders using the current method is in excellent agreement with the results of other numerical analyses and with results obtained from experiment. The calculated lift and drag on a NACA 0012 airfoil at angle of attack of –90° with and without a deflected flap is shown in the figure. A 20% reduction in the drag on the airfoil is predicted for the deflected flap configuration with respect to that for the undeflected flap. The method is currently being extended to general three-dimensional flow analysis.

Ames-Moffett contact: P. Stremel
(415) 604-4563 or FTS 464-4563
Headquarters program office: OAET

Zonal Flow Analysis Method

Paul Stremel

The flow field surrounding a rotorcraft is very complex and difficult to model. As a result, a three-dimensional analysis is required to provide sufficiently accurate results for predicting rotorcraft performance. This places enormous demands on computer memory and computational effort and is a limiting factor with current computers. A method that would lessen the computational requirements would be of great benefit to the design analysis of rotorcraft.

A zonal method is being developed to provide a computationally efficient procedure for the analysis of rotorcraft by reducing the computational mesh size without loss of accuracy. This is accomplished by providing an accurate representation of the far-field boundary condition very near the rotorcraft just outside the viscous region of the flow. This is beneficial in several ways. First, a reduction in the number of computational mesh points outside of the viscous region would result in a more computationally efficient model. Second, a more effective use of the computational mesh can be made to model the viscous region surrounding the rotorcraft. Third, the iterative convergence rate of the method will be accelerated owing to the reduce mesh size.

At present, the method has been developed for two-dimensional flow analysis. A comparison of the Mach contours predicted by the present method and those predicted by ARC2D are presented in the figure. The results are computed for a NACA 0012 airfoil at Mach number 0.3 and at an angle of attack of 5°. Results are shown for ARC2D with a far-field boundary at 25 chord lengths and for the zonal method with the far-field boundary represented at 0.14 chord lengths.

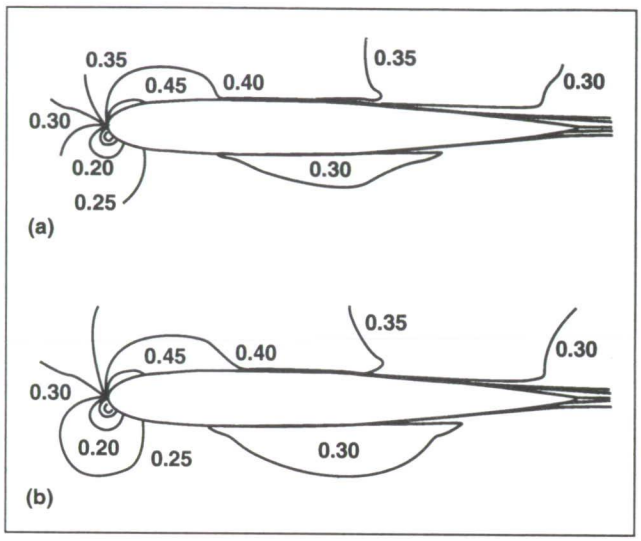


Fig. 1. Comparison of computed Mach number contours. (a) Zonal method, far-field boundary at 0.14 airfoil chords; (b) ARC2D, far-field boundary at 25 airfoil chords

Excellent agreement is shown between the results of the methods, thus verifying the accuracy of the present method. The present method reduced computer time by a factor of 10 and reduced the total number of iterations from 1,000 to 200-300 for a given accuracy when compared with other numerical methods. The method is currently being extended to three-dimensional analysis and to the prediction of a rotor in forward flight.

Ames-Moffett contact: P. Stremel
(415) 604-4563 or FTS 464-4563
Headquarters program office: OAET

Stopped Rotor/Disk High-Speed Rotorcraft Research

Stephen Swanson, Robert Stroub

Conventional helicopters, which have excellent hover and low-speed performance characteristics, are limited to speeds below 220 knots. At higher speeds, power requirements, rotor loads, and vibration become excessive. Airplanes have excellent high-speed flight performance, but are inefficient for hovering and short takeoff and landing (STOL) flight.

In the Stopped Rotor/Disk concept, the vertical flight attributes of a helicopter and the efficient forward flight characteristics of an airplane are combined.

The Stopped Rotor/Disk is a stop/stow high-speed rotorcraft design. However, the rotor is not stopped and then stowed in or near the fuselage, as in other stop/stow designs. Rather, the rotor blades are retracted into a large circular hub fairing (60% of the rotor diameter). The hub fairing, or disk, doubles as a lifting surface during conversion and high-speed flight.

For hover, the Stopped Rotor/Disk uses a high-hinge-offset rotor, with the hinge at approximately 55% of the rotor diameter; the large-diameter disk is aerodynamically equivalent to a large root-cutout (50% to 60% of the diameter). For low-speed flight up to rotor conversion, the Stopped Rotor/Disk acts as a compound helicopter, with turbojet engines providing forward thrust and with lift being generated by the rotor, the disk, or an auxiliary wing. Since the rotor is required to generate only lift and trim moments, the rotor's planform, twist distribution, and airfoils can be optimized for hover and low-speed flight. Methods being investigated for generating rotor torque include reaction-drive rotor tip-jets and disk-rim jets, or shaft-drive using convertible engines. Anti-torque and yaw control would be provided by NOTAR-type technology to reduce high-speed drag penalties.

As with any stop/stow high-speed rotorcraft design, the most difficult challenge is to develop a rotor conversion method by which to stop and stow the rotor without generating severe rotor loads or adverse flight dynamics. In the Stopped Rotor/Disk, this is solved by transferring the lift load from the rotor to the disk, or auxiliary wing, thereby reducing the rotor thrust to a minimum. Conversion is achieved by retracting the rotor blades into the disk while increasing the rpm so as to maintain a constant rotor advance ratio. When the rotor blades are entirely enclosed in the disk, the rotor and the disk are stopped. The low-thrust and constant advance ratio condition of the rotor will minimize rotor-blade loads. One area that requires considerable research is the effect of variable hinge-offset, a result of the rotor retraction, on rotor dynamics and loads.

For high-speed forward-flight, the Stopped Rotor/Disk flies as a fixed-wing aircraft, utilizing the disk as a circular wing. Since the low-aspect-ratio disk with its elliptical/circular-arc airfoil is not an efficient lifting surface, two possible approaches are being reviewed as ways of improving the cruise lift-to-drag ratio. The first approach is to use a conventional wing as the primary lifting surface for transition and high-speed flight, relegating the disk to a nonlifting, low-drag fairing. The second approach is to mechanically design the rotor blades such that during cruise they can be re-extended from the disk into the airstream as fixed wings, thereby increasing the aerodynamic efficiency of the disk.

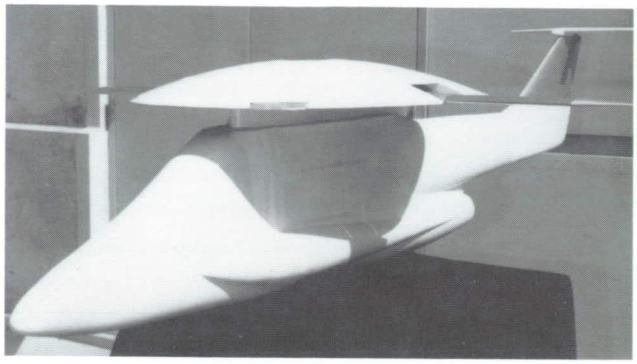


Fig. 1. Small-scale Stopped Rotor/Disk wind-tunnel model

As a first step in establishing the feasibility of the Stopped Rotor/Disk, small-scale, low-speed wind-tunnel testing will be conducted to evaluate its cruise aerodynamics. A joint Ames and U.S. Navy wind-tunnel test is scheduled for early 1991 utilizing the Ames 7- by 10- Foot Wind Tunnel. The fuselage and nonrotating disk to be used in the test are shown in the figure. The primary objectives of the test are to examine the aerodynamics of the disk and its interactions with the rotor blades, fuselage, tail surfaces, and an auxiliary, conventional wing.

In addition to the experimental work, preliminary analytical work is being conducted using the rotor performance code CAMRAD/JA. The code will be used to study the rotor-blade loads and dynamics generated during conversion.

Ames-Moffett contact: S. Swanson
(415) 604-4565 or FTS 464-4565
Headquarters program office: OAET

ORIGINAL PAGE
BLACK AND WHITE PHOTOGRAPH

Tilt-Rotor Whirl-Flutter Alleviation

Jan van Aken

The development of the next-generation tilt-rotor aircraft will be accompanied by an increase in maximum flight speed. The potential for the occurrence of whirl-flutter aeroelastic instability therefore is also increased and could limit the maximum speed. This research effort demonstrates the use of active controls to alleviate tilt-rotor whirl flutter.

A NASA-developed program, CAMRAD (Comprehensive Analytical Model for Rotorcraft Aerodynamics and Dynamics), is used to obtain a set of linear differential equations, which describe the motion of the tilt-rotor aircraft at various flight speeds. The hub motions due to wing/body vibration are standard input to CAMRAD. This hub motion resulting from free-vibration wing motion is calculated using a separate structural analysis program.

The CAMRAD output consists of the open-loop system matrices which describe the aircraft motion in the state-variable domain. These matrices form an input to a separate program, called MORDUAC (Modification Of Rotorcraft Dynamics Using Active Controls), which performs the closed-loop, active-controls calculations. Additional input to the MORDUAC program consists of the sensor model and the active controls feedback gain factors. An eigen analysis is performed in MORDUAC to determine the flutter stability for both the open- and closed-loop systems. Time-response calculations can be performed to estimate the magnitude of the required active control settings for closed-loop stability.

The option of superimposing signal noise onto the closed-loop sensors exists. By appropriately selecting the sensor model input, the effect on aircraft stability owing to feedback of pure state-variables to the active controls can be analyzed with MORDUAC. A separate utility is used to combine aircraft trim information from the CAMRAD code with wing vibration data from the structural analysis program to define a sensor model input to MORDUAC, which is based on physically measurable signals.

A sensor model, based on the feedback of pure state variables, was studied for a baseline, cantilevered-wing tilt-rotor aircraft, and it was shown that the onset of whirl flutter could be delayed by feeding back the wing accelerations in the vertical and horizontal directions to the longitudinal cyclic. The analysis is being extended to a sensor model, which uses physically measurable signals. The number of sensors and their locations on the aircraft are varied to study the performance of various feedback control schemes on the whirl-flutter speed limit of this baseline tilt-rotor aircraft.

An advanced tilt-rotor aircraft configuration, which uses the joined-wing concept, is also being studied. This aircraft has forward and aft swept wings, which are structurally joined at the wing tip, where the engine pylon and rotor are located. The baseline joined-wing tilt-rotor configuration without active controls shows improved wing aerodynamics, but results in a lower whirl-flutter speed than the cantilevered wing tilt-rotor aircraft. Initial results of closed-loop analyses in the state-variable domain show that whirl-flutter alleviation for the joined wing aircraft is again possible by feeding back vertical and horizontal wing motion to the longitudinal cyclic.

Ames-Moffett contact: J. van Aken
(415) 604-6668 or FTS 464-6668
Headquarters program office: OAET

Stability Analysis of Tilt Rotors in the National Full-Scale Aerodynamics Complex

Jan van Aken, Ruth Heffernan

A critical factor in determining the flight envelope of any tilt-rotor aircraft is a thorough understanding of rotor stability. Similarly, the operational envelope of a model tilt-rotor in a wind tunnel must take into consideration the overall stability. With this in mind, an extensive analysis of tilt-rotor stability is being conducted using the CAMRAD/JA analysis. This analysis is in preparation for tilt-rotor forward flight performance tests scheduled for NASA's 40- by 80-Foot Wind Tunnel. Two rotor configurations are being examined: a 0.658-scale V-22 rotor, and a full-scale XV-15 rotor with advanced technology blades (ATB). In both analyses, the rotors are mounted on the Prop Test Rig (PTR), a test bed for operating tilt-rotor models in the National Full-Scale Aerodynamics Complex.

Features of the CAMRAD/JA tilt-rotor stability analysis include a modified control-system stiffness model to account for stiffness coupling between the cyclic and collective controls, a drive-train model, and 32 degrees of freedom (including nine PTR body modes) in the flutter analysis. CAMRAD/JA was run with a uniform inflow wake model, since the more sophisticated wake models were seen to have a negligible effect on the stability.

Using this basic model, plus properties of the appropriate rotor blades, analyses were performed to determine the stability boundary, and the sensitivity to various parameters including rotor rpm (502 to 546 rpm for the V-22 model, 421 to 589 rpm for the ATB model) , rotor torque (6,000 to 21,000 foot-pounds), control-system stiffness (±20% of the baseline values), rotor-blade structural damping (0.5% to 2%), shaft angle (0° to 12°), and the presence of the wing. For both rotor models, the shaft angle and the presence of the wing had almost no effect on the stability. The other parameters, however, caused significant changes in stability.

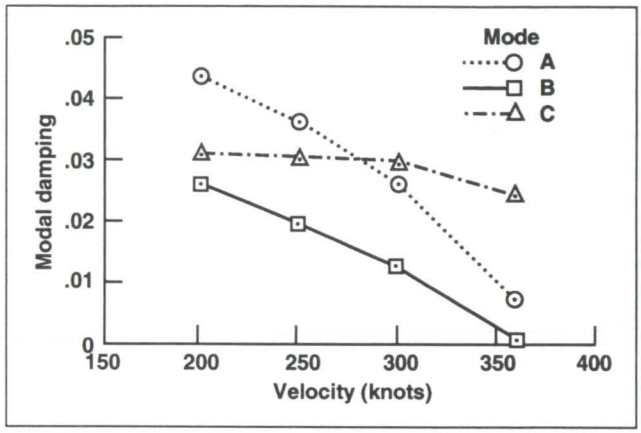


Fig. 1. Effect of forward velocity on the stability of three rotor modes for the V-22 0.658-scale model; 0.5% blade structural damping and 80% of baseline control-system stiffness

The V-22 stability analysis was performed for a velocity sweep from 0 to 360 knots in airplane mode at fixed shaft angle. The figure shows a plot of damping as a function of speed for the most critical rotor modes. At 300 knots, the maximum speed obtainable in the 40- by 80-Foot Wind Tunnel, no instabilities were found for the V-22 scale model. For the least stable condition (421 rpm, 21,000 foot-pounds torque, 80% control system stiffness, 0.5% blade structural damping) at 360 knots, one mode, a rotor speed mode (not shown in the figure), was slightly unstable. This slight instability was eliminated by increasing the blade structural damping to 1.5%. Moreover, this degree of freedom does not exist on the wind-tunnel model since the electric motors in general maintain constant rotor rpm.

Ames-Moffett contact: J. van Aken
(415) 604-6668 or FTS 464-6668
Headquarters program office: OAET

Particle Image Velocimetry Applied to Rotor Aerodynamics

Alan J. Wadcock

Conventional laser velocimetry is non-intrusive but inherently slow because the technique involves single-point measurements. Particle image velocimetry (PIV) is also a non-intrusive measurement technique yet offers simultaneous whole flow-field measurement capability. In addition, PIV simplifies interpretation and understanding of complex flow fields because of its flow-visualization character. The goal is to apply PIV to the study of time-dependent rotor flows and to thereby acquire global velocity data for validation of computer codes.

The first step is to illuminate the plane of interest in a flow seeded with small tracer particles and to obtain a multiply exposed photograph of the instantaneous positions. Conventional fine-grain film is used for this purpose, for it provides the spatial resolution not available from video images. The local fluid velocity is then derived from the measured spacing between images of the same particle and the time between exposures.

The second step is to interrogate the transparency with a low-power laser beam. Interference of light scattered by a given particle pair generates a set of Young's fringes having an orientation which is perpendicular to the direction of the local velocity vector and a spacing which is inversely proportional to the magnitude of the velocity. The measurement of the local velocity in both magnitude and direction is therefore transformed into a determination of the corresponding fringe spacing and orientation.

For efficient processing of the data it is necessary to automate the image analysis. Commercial image recognition systems provide acceptable evaluation times but are expensive because of the hardware needed. Interactive systems do not depend on expensive hardware but need the help of an operator and are therefore much slower.

A low-cost image processing system has been assembled for the automatic analysis of PIV fringe patterns. The system is based on a Macintosh IIfx with 8 MB of memory and a 13-inch color display. A Scion frame grabber is used to capture video images of the fringe patterns to be analyzed and an I/O Tech IEEE488 controller board is used to interface with the stepper motor controllers used to position the transparency. The heart of the computational machine is a MacDSP board by Spectral Innovations, an array processor which is used to analyze the fringe patterns. Captured images are 552 pixels wide by 436 pixels tall. Only the central 256 x 256 pixels are analyzed. Each interrogation point takes 1 second to analyze; a complete transparency can be interrogated at 1,000 points in a little over 15 minutes.

Present efforts are being devoted to small-scale experimental studies in water. The goal is to extend this technique to rotor flows in air.

Ames-Moffett contact: A. Wadcock
(415) 604-4573 or FTS 464-4573
Headquarters program office: OAET

Tilt-Rotor Aeroacoustic Model Research Program

Larry Young

Predicting and improving the aeroacoustic characteristics of civilian and military tilt-rotor aircraft is critical to their success. To accomplish this, moderate-to-large scale wind-tunnel testing of current generation tilt-rotor technology is required. This testing provides the data necessary to verify the aeroacoustic prediction methods, and to demonstrate advanced civil tilt-rotor and high-speed rotorcraft technologies.

Currently, NASA does not have the capability to test a complete (full-span, dual-rotor, with scaled airframe) tilt-rotor aircraft model in its wind-tunnel test facilities. Industry does have a limited number of full-span tilt-rotor models, but these are currently inactive and would require considerable refurbishing to make them operational. Additionally, most of the industry test models are Froude-scaled and not tip-Mach-number scaled and are, therefore, not suitable for either acoustic or aerodynamic research.

Ames and Langley and the U.S. Army are jointly defining a new tilt-rotor aeroacoustic research program. The cornerstone of this research program is the development of an approximately 1/4-scale Tilt-Rotor Aeroacoustic Model (TRAM). The TRAM is to be used as a test bed for wind-tunnel testing at several research facilities, including the Duits-Nederlandse Windtunnel in The Netherlands, the National Full-Scale Aerodynamic Complex at Ames Research Center, and the 14- by 22-Foot Subsonic Tunnel and the Transonic Dynamics Tunnel at Langley Research Center.

The TRAM will have the capability of being configured as three different test installations: an isolated rotor test stand; a semispan installation; and the full-span, dual-rotor installation. The current planning for the joint research program calls for isolated rotor and semispan testing in the Duits-Nederlandse Windtunnel, isolated rotor and full-span testing in the National Full-Scale Aerodynamic Complex at Ames, and isolated rotor and semispan testing in the 14- by 22-Foot Subsonic Tunnel at Langley. The first wind-tunnel test of the Tilt Rotor Aeroacoustic Model is scheduled for 1994.

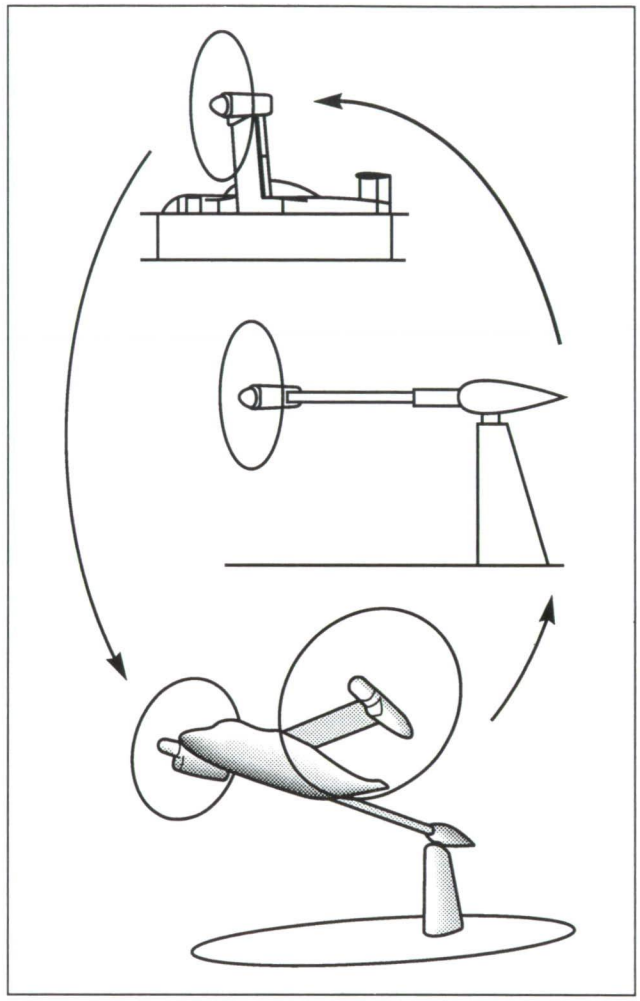


Fig. 1. Tilt-Rotor Aeroacoustic Model: unparalleled research capability with three test configurations

Ames-Moffett contact: L. Young
(415) 604-4022 or FTS 464-4022
Headquarters program office: OAET

Approximate Reasoning-Based Intelligent Control

Hamid Berenji

This research is focused on the development of techniques based on approximate reasoning and fuzzy-logic control and provides a set of tools for reasoning with fuzzy and imprecise control knowledge. We extend the conventional approaches of the control theory by using the knowledge of a skilled human operator in the development of an intelligent controller.

A major focus of our research has been to provide learning capabilities for these controllers to automatically improve their performance by learning from experience. We have developed techniques for integrating approximate reasoning with reinforcement learning in the design of intelligent controllers. The approach selected here is to test these techniques on a set of small but challenging control problems (e.g., cart-pole balancing, trajectory generation for a three-joint robotic arm) and extend these methods to larger size, more challenging control problems (e.g., the rendezvous and docking operation of the space shuttle with a satellite in space).

In 1990, we extended our previous integrated approach for fuzzy-logic control and reinforcement learning. The new approach is simpler for application in real control problems. We completed an interface program to this technique which allows the user to observe the progress of the learning in the model by noticing the number of successful trials and rule modifications before any failure; the program can also demonstrate the rule modifications based on the learning after a failure.

After the learning process is complete, the system will be able to avoid future failures. Also, the

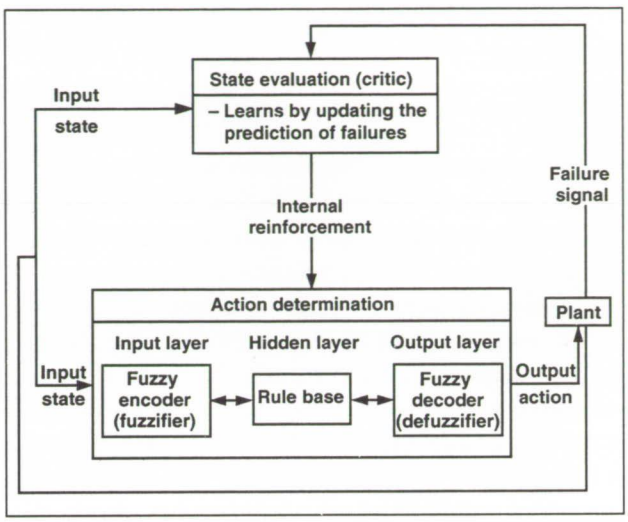


Fig. 1. The architecture for the learning fuzzy-logic controller

software provides the facility for the user to influence the direction of the learning in terms of rule modifications. This interface has been developed for the cart-pole balancing system. The system learns to balance the cart and the pole significantly faster than with the other algorithms published in the literature. We expect that with minor modifications, the algorithm will be applicable to larger problems such as the systems mentioned above. The figure illustrates the architecture of the new approach.

Ames-Moffett contact: H. Berenji/P. Friedland
(415) 604-6070/4277 or FTS 464-6070/4277
Headquarters program office: OAET

Principal Investigator in a Box

Silvano Colombano, Irving Statler, Mike Compton

The goal of the Principal Investigator (PI) in a project called PI in a Box is to help improve the quality of the scientific results of experiments conducted in space. Our approach is to use expert-systems technology to develop an "intelligent assistant" for astronauts performing space-borne science.

The system is designed to assist in collecting and analyzing experimental data, recognizing "interesting" data, managing the experiment protocol, and diagnosing and troubleshooting the experiment apparatus. The project team's efforts this year focused primarily on bringing together the various components into a functioning system and using the system to help collect actual data from the "Rotating Dome" (an experiment in vestibular physiology devised by Laurence Young of MIT) in preparation for the first Spacelab Life Sciences Mission (SLS-1) currently scheduled for May 1991.

Integration of the Two-Computer System

A "Data Computer," which supports the data collection and quality-monitoring modules, has been successfully integrated with an "AI Computer" that supports the data analysis, protocol management, and diagnostic modules. Together, these computers enable the modules to efficiently process real data while they are collected from astronaut subjects. An Executive Module, also completed this year, mediates communications between the various modules. The first figure provides a module-level diagram of the system architecture.

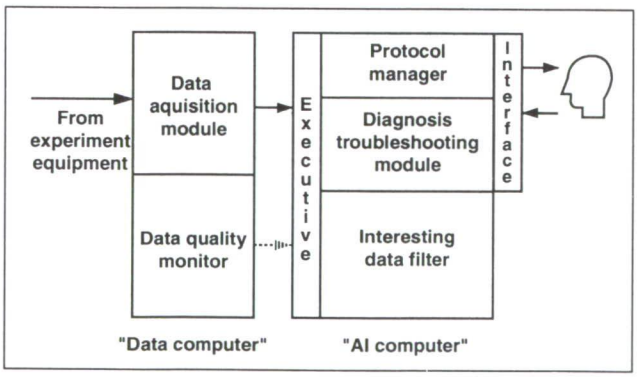


Fig. 1. PI-in-a-box system architecture

Use of the System during Baseline Data Collection for SLS-1

This year, the system was used on the ground to help collect "baseline data" for the dome experiment in preparation for SLS-1. Ground baseline data are typically collected at various times before a mission (launch-minus-150 days, launch-minus-75 days, launch-minus-45 days, and launch-minus-15 days), and immediately after the mission. The PI-in-a-box system was used to collect preflight data at the first SLS-1 baseline data-collection session this past summer, and will also be used during the subsequent baseline data-collection sessions in early 1991. PI-in-a-box will also be used on the ground during the SLS-1 mission in May 1991, and permission is being sought for its intended use by astronauts in flight during the SLS-2 mission in 1993.

Integration of the New User Interface

The success of PI-in-a-box depends on its acceptance by the astronauts. Therefore, attention is being given to understanding the expected human-machine interactions and to designing the appropriate "user-friendly" interface (see the second figure). Code FL has the major responsibility in this area. Code FL's goal is to develop anecdotal scenarios of interactions, particularly in the off-nominal situations, to stimulate discussions of these scenarios among members of the PI team, and to establish consensus on expected interactions. After interactions are agreed upon, they will proceed with the interface design.

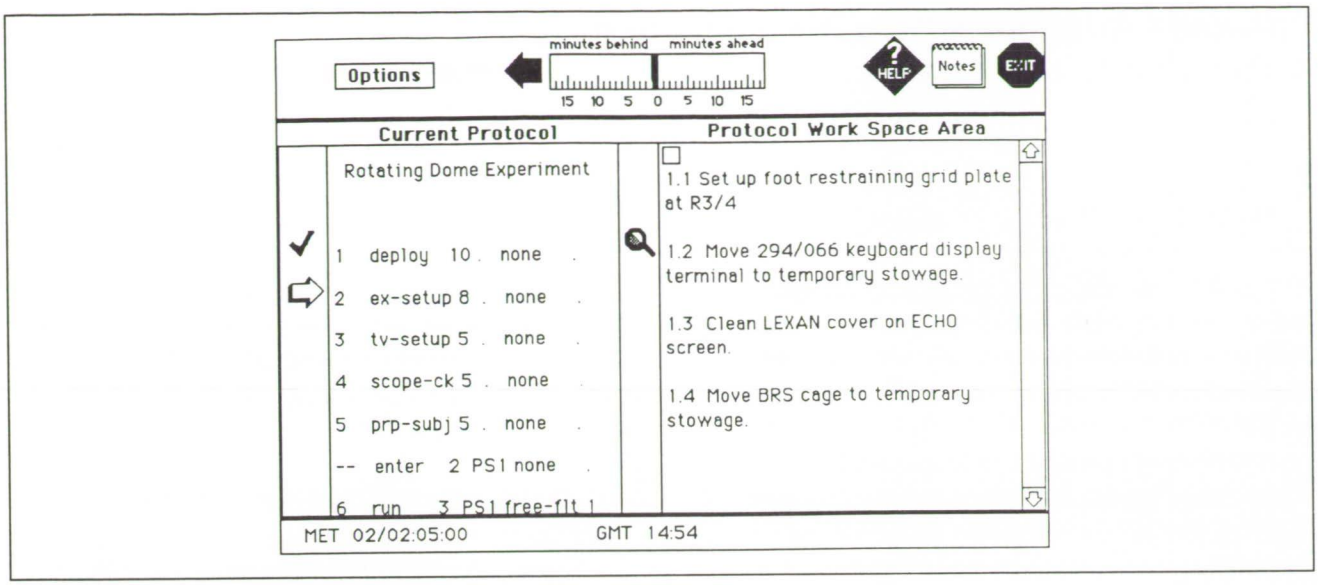


Fig. 2. New user interface prototype

Researchers have developed the anecdotal scenarios for the interactions during the experiment setup phase and the interesting-data phase, and are currently assisting with the diagnosis/troubleshooting phase.

On the basis of these scenarios, Johnson Space Center's (JSC) Human-Computer Laboratory is designing the corresponding interfaces which will be evaluated by astronauts in simulated scenarios. Code FL researchers are continuing with the development of the interaction scenarios and are assisting JSC on the interface design. Code FL researchers will participate in the interface evaluations which will take place at JSC.

The PI-in-a-box team consists of individuals from the Ames Artificial Intelligence Research Branch, the Ames Aerospace Human Factors Research Division, the Human-Computer Interaction Laboratory at Johnson Space Center, and the Man-Vehicle Laboratory and Computer Science Department at MIT.

Ames-Moffett contact: S. Colombano/
P. Friedland
(415) 604-4380/4277 or FTS 464-4380/4277
Headquarters program office: OAET

Advanced Automation: An Assessment of Processing Requirements

Gloria Davis

NASA's operational use of advanced processor technology in space systems lags behind its commercial development by an average of 15 years. One of the reasons for this is that mission computing requirements are frequently unknown, unstated, misrepresented, or simply not available in a timely manner.

An effort was undertaken to assess NASA's requirements for space-borne processing technology. This was accomplished by collecting the computational requirements from missions through three media:

1. A questionnaire that quantifies hardware and software requirements, capabilities, and limitations of space automation systems
2. Interviews at each of the NASA centers with representatives of various advanced automation and robotic projects
3. A workshop dedicated to identification of computational processing requirements, capabilities and limitations in which NASA, industry, and academia could exchange requirements, identify problem areas, and recommend solution approaches. This was held July 9 -11, 1990.

The assessment was designed to identify the computational requirements for NASA missions. In doing so, a baseline forum was established in which both hardware and software developers communicated their requirements and capabilities. The results of this assessment will be integrated into the Ames Advanced Architecture Testbed and be used to:

1. Identify, in a timely manner, current and future computational system requirements
2. Enable (leverage) common technology in describing the requirements
3. Establish guidelines for mapping optimal software applications onto optimal hardware systems
4. Establish evaluation criteria of system architectures
5. Create a library of benchmarks based on NASA's real applications which enhance the credibility of new architectures.

Ames-Moffett contact: G. Davis
(415) 604-4388 or FTS 464-4388
Headquarters program office: OAET

Integrated Planning, Scheduling, and Control

Mark Drummond

A long-standing problem in the field of artificial intelligence (AI) is that of designing systems that can synthesize a plan, the execution of which can be expected to satisfy a given goal. Ideally, the automatically produced plan is then passed on to a robot, a manufacturing system, a group of people, or some other form of effector that can follow the plan and produce the desired result. The design of these automatic planners has been addressed in AI since its earliest days, and a large number of techniques have been introduced in progressively more ambitious systems over a long period. In the AI Research Branch at Ames, the Entropy Reduction Engine (ERE) project is extending these classical techniques in a variety of ways.

The ERE project is a focus for research on planning and scheduling in the context of actual plan execution. The eventual goal of the ERE project is a set of software tools for designing and deploying integrated planning and scheduling systems that are able to effectively control their environments. To produce such software tools, we are working toward a better theoretical understanding of planning and scheduling in terms of closed-loop plan execution.

There are two main subgoals for our research. First, we are integrating the representations and methods of traditional AI planning with those of classical scheduling. Our second research subgoal is to make sense of planning and scheduling in terms of modern-discrete-event control theory. The next paragraphs consider these two complementary goals in slightly more detail.

Traditional AI planning deals with the selection of actions that are relevant to achieving given goals. Various disciplines, principally operations research, and more recently AI, have been concerned with the scheduling of actions; that is, with sequencing actions in terms of metric time and metric resource constraints. Unfortunately, most of this work in scheduling remains theoretically and pragmatically disconnected from planning.

A scheduling system must be given a set of actions to sequence: if the scheduler cannot find a satisfactory sequence of the given actions, the scheduler will simply fail. In contrast, a planning system is able to suggest alternative actions, such that if the suggested actions are added to the initial set, a feasible schedule will result. We are working toward a single coherent theory of reasoning about actions that can be directly implemented as useful planning and scheduling tools.

Most planning and scheduling work assumes that the job of the automatic system is done when a plan or schedule has been generated. This view is hopelessly optimistic since actions, once planned and scheduled, often fail during subsequent execution. In the ERE project, we view the business of planning and scheduling as that of controlling the behavior of an environment in order to actually achieve user-specified goals. A planning or scheduling system cannot simply produce a plan or schedule and then vanish; instead, the system must persist in its attempt to actually achieve the specified goals in the user's environment.

Most of our effort over the past year has been focused on integrating plan formation and plan execution. We have implemented a simulator to test our ideas and to enable rigorous empirical validation of our developing theory. Using this simulator, we have designed and tested a planning system that is able to reason about the probability of goal satisfaction, given only prior knowledge of actions that can be taken and a statement of the goal to be satisfied.

Using this planning system, we have undertaken the study of how plans can be used to increase the probability of goal satisfaction. We have discovered that for some problems, little or no plan is needed; the background probability of success is sufficiently high that no explicit "plan" is required. For other problems, plans are required to avoid what would otherwise be almost certain failure. We have begun to classify problems, based on the role that a plan plays in helping to increase the probability of goal satisfaction.

The primary result of this work has been the design and implementation of an algorithm to incrementally form plans that attempt to maximize the probability of goal attainment. After finding an initial plan, the algorithm improves the probability of that plan being "correct" by finding high-probability plan failures and then fixing them, before they actually occur. This algorithm has been presented to AI and control theory audiences, and has helped establish critical connections between the techniques of traditional control and those of AI planning. We will explore and strengthen these connections in future work.

Ames-Moffett contact: J. Bresina/P. Friedland
(415) 604-3365/4277 or FTS 464-3365/4277
Headquarters program office: OAET

Control Systems Group Summary

Brian Glass

The Control Systems Group pursues applied research in hybrid (mixed symbolic and numerical) control techniques for improving mission safety and efficiency in aerospace systems. In 1990, group activities were focused on four tasks.

1. Developing a coordinating system for planning and scheduling spacecraft and planetary habitat resources, including crew activities; the Habitat Executive prototype software was developed during 1990 in coordination with the Artificial Intelligence Research Branch
2. Performing ongoing AI research in two areas: representing multiple levels of abstraction in a model-based reasoning system (i.e., model granularity), and temporal reasoning
3. Acting as a consultant to contractors (given recent experience with fielding the only thermal automation expert system); these likely "clients" are developing the Space Station Freedom thermal flight systems, and include thermal fault diagnosis software designers, verification and validation personnel, operator interface developers, and thermal flight control software developers
4. Writing and presenting the thermal automation test results from the Systems Autonomy Demonstration Project, concluded during the previous year; a half-dozen papers and reports were generated during 1990.

Ongoing work is expected to continue in these and in other areas of advanced autonomous control.

Ames-Moffett contact: B. Glass
(415) 604-3379 or FTS 464-3379
Headquarters program office: OSF

Optical Image Processing and Control

Charles Jorgensen

Digital image processing is computationally very intensive. The identification of critical image features has traditionally been performed by means of computations such as the Fourier transform, which involves large matrices of data. Such computations severely limit the throughput of conventional digital image processing techniques.

Digital methods for recognizing objects regardless of their position, scale, and angular orientation (which are even more computationally intensive) do not run in real time and are not readily adapted to new objects. The analog parallelism of optics provides an inherent advantage over electronics for space-borne applications that require (1) rapid evaluation of large amounts of data and (2) compact, low-weight processors with low power requirements. A powerful tool for such processing is an optical correlator. An input wave form does not need to be measured as a matrix of discrete values. Instead, transforms occur optically in parallel over the entire input field and lead to a potential for much faster processing speeds for real-time image recognition and feedback control.

The Photonics Group has utilized the principle of the optical Fourier transform to develop a new type of optical filter designed to recognize objects over a range of views. When a scene is input to the laboratory optical correlator, the presence of a target such as a tool or a Shuttle Orbiter can now be recognized even when the object is located in any translational position and is rotated at any angle within a 60° range. Using just one optical filter, the correlator has been shown to dynamically track an object moved in a curved path over the input field.

The same technique, when combined with the use of more than one optical filter and a robotic arm, has been demonstrated to resist object occlusion, to recognize objects in the presence of multiple alternatives, to track, and to rapidly learn new targets. In one experiment, a target's position and in-plane rotational orientation were determined after sequencing through only 15 filters. Previous techniques for determining in-plane rotation and orientation required the use of 180 filters to provide the same 1° resolution, and over an order of magnitude more processing time. This new approach was shown to be extendable to include out-of-plane rotation and scale distortions, which previous pattern recognition systems have not been able to handle. A unique characteristic was the incorporation of neural network processing concepts.

Previously, successful attempts to teach neural networks to perform distortion-invariant pattern recognition have been limited to hybrid systems where a feature set is extracted either electronically or optically. A neural network was then trained to identify objects based on the feature set. Since the data-reduction step is the most computationally complex and time consuming, these hybrids were best seen as primarily optical or digital processing devices, not as integrated neural systems. The photonics work in higher-order neural networks (HONNs) has demonstrated a neural architecture which performs the complete *feature extraction–pattern classification* paradigm. Using a third-order neural network, 100% accurate invariance to distortions of scale, position, and in-plane rotation has been demonstrated.

The Photonics Group has also developed a new algorithm for performing spectral analysis suitable for optical implementation. A breadboard optical matrix processor, which is part of a program to detect small amounts of materials in the plume of shuttle engines rapidly enough to shut down the engine before major damage occurs, has been built.

Finally, recent work on electro-optic analysis of materials has demonstrated the ability to detect extremely small cracks in riveted, metal aircraft panels. A pattern recognition algorithm was developed which demonstrated performance levels equivalent to those of human analysts but at much greater speed, offering the potential for increased aircraft safety and more cost efficient inspection procedures.

Ames-Moffett contact: C. Jorgensen/M. Reid
(415) 604-6725/4378 or FTS 464-6725/4378
Headquarters program office: OAET

Optimization of Multiprocessor Computing

Charles Jorgensen

In order to increase processing speed, modern computer designs have moved from single processors toward coordinated clusters of asychronous or parallel devices. Although such hardware designs promise to provide orders-of-magnitude faster responses, their effective use still depends on the ability of resource management software to (1) properly trade off the time lost in interprocessor communications against the gain of concurrency, (2) exploit unique behavioral characteristics of software programs, and (3) take advantage of differing multiprocessor hardware features. Unfortunately, the actual performance gains of many proposed resource management strategies can only be evaluated indirectly by simple objective functions, such as the number of processors used and the time cost of running a code segment. As a result, they can fall far short of their potential.

The multiprocessing group has conducted research to determine how software can be mapped onto alternative multiprocessor designs so as to minimize actual execution time. An analytical procedure called Post Game Analysis has been developed in which program-to-processor code assignments are improved *between* program executions. The method uses real-world timing-data gathered during program execution. It incrementally reduces computation time by applying heuristics (or rules of thumb) to resolve conflicting processing goals such as the detection of bottlenecks, the sharing of computation loads, the capturing and recognition of code references to nearby processors, and the avoidance of processor competition for the same tasks.

In order to determine which heuristics are most effective for particular architectures, a processing simulation environment called AXE (see the figure) was developed. It is composed of a model of software captured in a behavioral description language (BDL), a generic multiprocessor model, and a visualization environment to study the execution of different processor-software mixes.

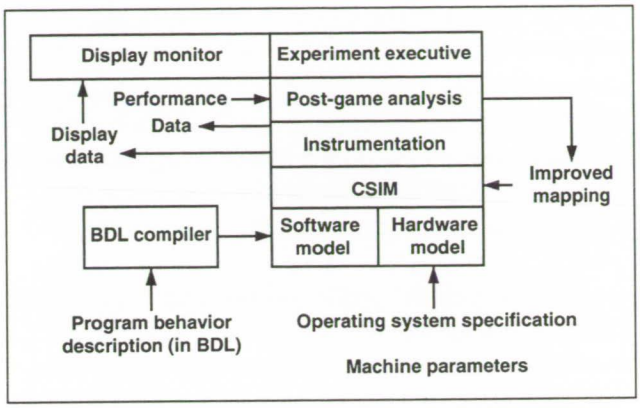


Fig. 1. Components of the AXE experimentation environment

BDL models can be specified at many levels of abstraction and can be made to behave very closely to actual code in terms of message patterns, functional block allocations, and central processor unit (CPU) use. When actual code is unavailable or unrealistically large, BDL permits simplified analysis of existing or potential new processor designs using generic code behaviors. The multiprocessor model includes capabilities for the easy description of processor hardware including memory, site-specific operating system, CPU interconnection topology, communication speed, scheduling, and routing algorithms.

Taken together, AXE provides an integrated environment for computation model specification, processor architecture specification, simulation test (CSIM), data collection, and experimentation. It enables prediction of alternative mapping effects on execution time and resource contention. Recently, the AXE environment was enhanced by the addition of new visualization tools, and it is being used to evaluate aeronautic airflow models.

Ames-Moffett contact: C. Jorgensen/J. Yan
(415) 604-6725/4381 or FTS 464-6725/4381
Headquarters program office: OAET

Scientific Modeling Assistant Project

Richard M. Keller, Michael H. Sims

The goal of the Scientific Modeling Assistant Project is to study modeling as a human problem-solving activity, and to provide computational support for scientists engaged in this activity. In particular, we are building software that functions as a scientific modeling assistant to aid scientists in building, using, sharing, and modifying scientific models.

Although model-building is an integral part of the scientific enterprise, there is little computational support available to the scientist performing this task. Without such support, scientific model-building can be a time-intensive and painstaking process, often involving the development of very large, complex computer programs. Unfortunately, these programs cannot easily be distributed and shared with other scientists because the implemented code is very detailed, idiosyncratic, and difficult for anyone but the original scientist/programmer to understand.

To facilitate model-building, the current software prototype includes an interactive, intelligent graphical interface; a high-level domain-specific modeling language; a library of physics equations and experimental data sets; and a suite of data-display facilities. Rather than construct models using a conventional programming language, scientists will use our graphical interface to "program" visually by using a more natural high-level data-flow modeling language.

The terms in this language involve concepts (e.g., quantities, equations, and data sets) that are familiar to the scientist. In constructing this tool, we are using a variety of advanced software techniques, including artificial intelligence (AI) knowledge representation, automatic programming, and truth-maintenance techniques, as well as techniques from object-oriented programming, graphical interfaces, and visualization.

During 1990, the concept of a scientific modeling assistant was conceived and software was implemented to test its practicality. As a test-bed for this research, we developed a prototype in the domain of planetary atmospheric modeling. This prototype—known as the "McTitan" system—is being used to reconstruct a model of the thermal and radiative structure of Titan's atmosphere that was originally developed in Fortran by Christopher P. McKay in the Ames Theoretical Studies Branch.

Our initial research has focused on a small portion of the overall Titan model—gas composition. The purpose of the gas-composition portion is to develop a profile of Titan's atmosphere that describes the pressure, temperature, and density of gases at various altitudes above its surface.

This problem is underconstrained because of the shortage of empirical data on Titan. The major source of relevant experimental data is the Voyager I flyby of Titan in November 1980. As Voyager I passed by the far side of Titan, it sent back radio waves that passed through Titan's atmosphere and then on to receiving stations on Earth. Because of the density of gases in the atmosphere, the radio waves were refracted slightly as they passed through it. The amount of refraction was measured at different altitudes above the surface. These refractivity data serve as a starting point for inducing the desired atmospheric profile in the Titan gas composition model.

In brief, the atmospheric profile is determined as follows (see the figure). First, for each atmospheric point profiled, the Voyager I refractivity data are used to compute the number-density (ND) of the gases at that altitude. The number-density of a mixture of gases is defined as the number of molecules per volume of the mixture. Assuming that the identity and relative percentages of gases in a mixture are known, the number-density can be computed as a function of refractivity.

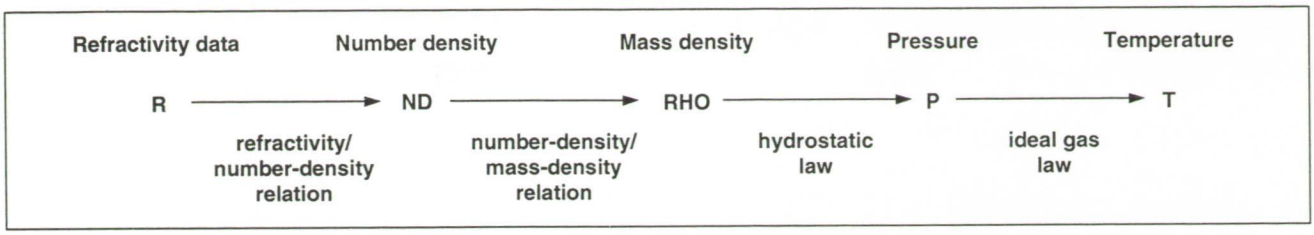


Fig. 1. Determining the atmospheric profile

Next, using the molecular weight of the various gases in that mixture, the mass-density (RHO: mass per volume of mixture) can be computed from the number-density. The hydrostatic law can then be used to determine the pressure (P) from the mass-density by essentially summing the weight of the atmosphere above each profile point.

Finally, the temperature (T) can be determined from the mass-density and the pressure by applying an equation of state, such as the ideal gas equation. The figure illustrates a level of abstraction at which a physicist might describe the problem, and is far more comprehensible than the corresponding Fortran code. Our system's graphical interface and modeling facilities permit a physicist to construct and manipulate models at this level of abstraction.

Once we have refined our system, Dr. McKay and his colleagues intend to use the software assistant to support their future planetary atmospheric modeling activities, including those related to the upcoming Cassini mission to the Saturn system. Although the current prototype is tied to the planetary atmospheres domain, we are also investigating the applicability of these ideas to ecological modeling, where we are studying a model of the carbon, water, and nitrogen cycles in a forest ecosystem.

This particular model was developed by Steven W. Running (U. of Montana), and is in use by our collaborators in the Ames Ecosystem Science and Technology Branch. More broadly, one of our long-term goals is to develop a general-purpose scientific modeling "shell" that can be instantiated for a particular modeling task by adding domain-specific knowledge.

Ames-Moffett contact: R. Keller/M. Sims
(415) 604-3388/4757 or FTS 464-3388/4757
Headquarters program office: OAET

GEMPLAN/COLLAGE Multi-Agent Planning Systems

Amy Lansky, Andrew Philpot

This work addresses the problem of generating coordinated plans of action for multiple agents in domains with complex coordination requirements. It deals with both action-generating and action-ordering, as well as resource allocating and timing (and thus, in principle, it covers both planning and scheduling issues). The GEMPLAN system (and its successor, COLLAGE) is unique in that it (1) provides a broader range of plan construction techniques than most artificial intelligence (AI) planning systems, (2) uses localized (partitioned) search to control the inherently explosive cost of planning, and (3) integrates planning operations both before and during plan execution.

Over the past year, we have focused on both technical development of the GEMPLAN and COLLAGE systems, as well as on investigation of suitable applications for this technology. We have narrowed our focus to two application areas: construction planning and data-analysis planning. We plan on focusing the continued development of the existing GEMPLAN system and guiding the design and implementation of the newer COLLAGE system in order to meet the needs of these and similar domains.

In the area of facility construction planning, GEMPLAN/COLLAGE takes the role of a building or facility general contractor, constructing a plan of action that actually results in a finished structure and that considers all the requirements and constraints of the building, subcontractors, resources, etc. After an initial plan is constructed, and plan execution (the construction process itself) begins, GEMPLAN/COLLAGE would continue to monitor plan execution and environmental changes, and then would replan as necessary. GEMPLAN has already been applied to a house-building domain, and we are currently working on a larger office building domain. We anticipate that the construction application area will have potential in assisting with some of NASA's infrastructural requirements, as well as with any other kind of complex construction task.

The second application area is aiding EOS scientists to help formulate plans for data analysis. Along with Rich Keller and Ames ecologists Jennifer Dungan and David Peterson, we are formulating the concept of a Data Analysis Workbench that provides both scientific modeling and data analysis planning assistance. Whereas the goal of much ecological science is to build and verify models of Earth processes and to use those models to project behavior, much of the day-to-day work done by these scientists (50% to 90%) is spent planning HOW to do analysis; for example, deciding the best way to register data sets, which algorithms to use (e.g., for projection), which codes to use, and on which platforms to run them.

Problems arise because many of the data analysis planning decisions are affected by multiple (sometimes conflicting) aspects of the projected data analysis task—for example, the possible data input sources, the area of study, the type of data being studied and its properties, and the underlying assumptions made by the various models that will be used.

Much of this decision making could be done completely (and certainly assisted) by automated tools. This kind of aid will be even more necessary given the anticipated quantity of data that will be made available by the EOS instruments, the wide spectrum of scientists that will be accessing that data, and the public's expectations of the results to be gained by Mission to Planet Earth. Tools that will assist the data-analysis process and foster transfer and sharing of information and techniques between scientists will be quite important.

Effective planning and scheduling are inherently extremely complex and expensive tasks. Such complex problems expand immensely as one attempts to scale such systems up to very large domains. During FY1990, one of our primary technical focuses was on the use of "locality," or domain structure, to partition domain information, as well as planning search. Localized reasoning provides a way of alleviating the costly nature of planning (especially multi-agent planning) by partitioning the planning search space into smaller, cheaper, localized search spaces and by providing heuristic guidance in the search of these trees.

Over the past year, we have completed the implementation, formal complexity analysis, and empirical testing of localized search. We have found the technique to have nearly universal benefit, with this benefit growing exponentially as the problem size itself grows. In addition, our localized search technique was developed to be applicable to any kind of reasoning system that utilizes search, not just planners. For example, NASA scientist Monte Zweben has begun integration of localized search into his scheduling system. Techniques such as localized search will become critical as AI systems are scaled up to large, complex domains.

Learning from our experience with GEMPLAN, we have begun the design and implementation of the new COLLAGE system. COLLAGE (Coordinated Localized algorithms for Action Generation and Execution) may be viewed as a generalization and improvement of the GEMPLAN architecture. It will be a combined planning/dynamic-planning system for multi-agent coordinative reasoning, with flexible methods for control of planning search. It will generalize GEMPLAN's localized search mechanism to include much more flexible control over both internal and external regional search.

Ames-Moffett contact: A. Lansky/P. Friedland
(415) 604-4431/4277 or FTS 464-4431/4277
Headquarters program office: OAET

Comparison of Microprocessors for Space Station Freedom

Yuan-Kwei Liu

The objective of this task is to analyze the feasibility of replacing the Intel 386, which has been proposed as the baseline processor for the Space Station Freedom (SSF) Data Management System (DMS), with the more advanced i486. The hardware configuration for this analysis includes an IBM PS/2 Model 70-A21 computer, which has a 25-MHz Intel 386 processor, with an added Intel 387 floating-point coprocessor. An IBM 486/25 Power Platform, which has a 25-MHz i486 processor, was used to swap with the 386 board for the comparison. The software configuration includes a Lynx real-time operating system kernel, which has been proposed for use on the DMS, along with the GNU C compiler, and the C version of the Dhrystone and Whetstone Benchmarks.

The i486 instruction set architecture (ISA) has six more instructions than the 386 ISA, and is 100% upward binary compatible with the 386. All of the software running on the i486, including operating systems, can be executed on the 386 without compilation or linkage. This is the most significant advantage of the i486 compared with other processors. As for the power consumption, the i486, which has an on-chip floating-point processing unit, actually consumes less power than the 386 and 387 combined. The availability of a space-qualified i486 processor that meets the MIL-STD-883C Class S requirements is scheduled in 1993, before the first launch, which is scheduled in 1995.

The i486 has 8-Kbyte on-chip cache; but it has no error-detection and correction (EDAC) code, and is thus not suitable for space applications. The cache can be disabled by software when the computer is running, but the software has to be incorporated into the operating system kernel owing to the protection in the processor. Therefore, a device driver program, which is the interface between the kernel and a physical device, was written to disable and enable the cache in order to evaluate the performance difference.

When implementing the device driver, a crucial error was found in the Lynx Assembler, which has been proposed for use on the DMS. The error has been reported to Lynx Real-Time Systems, Inc., and to IBM, which is the DMS contractor. The i486, with the on-chip cache disabled, has about the same performance level as the 386. However, some external caches with error correction code may increase the performance of the i486; this is currently under evaluation.

Ames-Moffett contact: Y. Liu
(415) 604-4832 or FTS 464-4832
Headquarters program office: OSF

Fault-Tolerant Systems

F. Ann Patterson-Hine, David L. Iverson

Future NASA missions will increasingly depend on the development of techniques for intelligent fault management in systems that must continue to operate regardless of problems. Fault-tolerant systems require not only high reliability but must also detect faults, assess and confine damage, recover from errors, and provide fault treatment and continued service.

Hardware systems were the early focus of fault-tolerance practices; however, in today's distributed environment, it is the ability of software to perform fault management that assures continuous operation. The investigation of innovative fault-tolerance strategies is necessary because of high performance demands and constraints on hardware availability in space applications. Constraints on weight, power, and volume in on-board systems makes it imperative that systems be designed using minimal redundancy. The system must perform dependably for extended periods of autonomous operation, even when faced with unanticipated situations, including hardware failures or software faults.

Traditional reliability analysis tools such as fault trees and other system models, implemented in an object-oriented environment, provide the basis for the development of new techniques for software analysis, instrumentation, and run-time control. Hybrid modeling techniques are being developed to extend the representational capabilities of the standard reliability models. Strategies for fault detection, diagnosis, and system reconfiguration are being developed and applied to avionics and space systems.

A fault-tree diagnosis system has been developed which enables fast and flexible diagnoses in the dynamic distributed computing environments planned for future space missions. The algorithm uses a knowledge base that is easily changed and updated to reflect current system status. Augmented fault trees represented in an object-oriented form provide deep system knowledge that is easy to access and revise as a system changes.

Given such a fault tree, a set of failure events that have occurred, and a set of failure events that have not occurred, this diagnosis system uses forward and backward chaining to propagate causal and temporal information about other failure events in the system being diagnosed. Once the system has established temporal and causal constraints, it reasons backward from heuristically selected failures to find a set of basic events that are a likely cause of the occurrence of the top failure event in the fault tree.

The diagnosis system has been implemented in Common LISP using Flavors. It has been tested and demonstrated on examples of the Space Station Freedom Data Management System, and on commercial and military aircraft elements. It is being made available through COSMIC.

Ames-Moffett contact: A. Patterson-Hine
(415) 604-4178 or FTS 464-4178
Headquarters program office: OSF

Photonics and Optical Processing

Max Reid

Analog optical processing utilizes free-space propagation between components, allowing natural implementations of algorithms requiring large degrees of parallel computation. The parallelism of optics provides an inherent advantage over electronics in space-borne applications that require rapid evaluation of large amounts of image data or other sensor data using compact, low-weight processors with low power requirements.

Optical processors capable of performing 100 billion operations per second with a volume of only 200 cubic centimeters, a mass of less than one kilogram, and power requirements of only 30 watts are feasible within 5 years. Suitable applications for analog optical processors are problems whose solutions involve either vector-matrix operations, as in control problems, or Fourier transform operations, as in correlation-based pattern recognition.

Optical pattern recognition techniques are being applied to robotic vision for manipulating objects. The use of an optical processor has been demonstrated in the loop of a robotic system to recognize objects (such as a particular tool among a set of tools) and to determine their orientation in three-dimensional space, allowing the robot to perform grappling maneuvers.

Optical pattern recognition is being applied to autonomous planetary landing. An input image sequence from a planetary lander camera can be rapidly processed with an optical correlator to guide the lander to a target landing site. This active closed-loop control results in a much smaller landing area footprint, and would allow a lander to safely set down closer to interesting terrain features than could be done with an open-loop system.

A laboratory demonstration has been performed showing the control of a robot-tip trajectory following a flight-path trajectory down to a simulated terrain board by real-time image processing and control. Work is continuing with Dryden Flight Research Center, initially to obtain sample landing sequences using potential flight profiles, and subsequently to flight test the resultant hardware and algorithms.

Optical matrix-vector processors are being applied to the analysis of high-bandwidth multispectral imagery. An example of such imagery is that of the engine plume of the space shuttle main engines (SSME). Real-time analysis of the SSME plume for anomaly detection could prevent catastrophic engine failure, for the engine could be shut down once elemental traces which precede failure are detected. Algorithms suitable for implementation of this spectral analysis on optical matrix processors have been implemented and demonstrated in the laboratory. Work is continuing with Marshall Space Flight Center and Stennis Space Center to apply these techniques to real SSME data, and to do real-time analysis of an instrumented SSME test stand.

Ames-Moffett contact: M. Reid/N. Sliwa
(415) 604-4378/4668 or FTS 464-4378/4668
Headquarters program office: OAET

Parallel Systems Research

Nancy Sliwa

Future NASA missions will increasingly utilize distributed and parallel computer systems. However, the difficulty in writing and monitoring the execution of software on such systems has made the development of validatable programs for such systems an intractable problem.

There are three major problem areas:

1. Static and dynamic automated mapping strategies for parallel computations on multicomputers
2. Software tools and methods for the data collection, abstraction, and visualization for multiprocessing systems; these tools will be used for performance tuning as well as debugging—to help reconstruct the schedule that caused an error after the error has occurred
3. Performance prediction tools applicable to very large applications on multicomputers.

One of the most difficult issues to be addressed while developing resource management strategies involves choosing an appropriate level of abstraction for modeling concurrent program execution without resorting to lengthy instruction-set level simulations or general stochastic models. The AXE experimentation environment was designed to facilitate such investigations at the operating system level using discrete-time simulation. It provides an integrated environment for computation modeling, simulation, data collection, experimentation, and multicomputer architecture specification.

Hardware and software monitoring facilities in AXE can record and display the performance of the simulated multicomputer. The current implementation uses five panels displayed on a color screen to represent the instantaneous load of each processing site and intersite message transmission, the overall system load *value* and *distribution*, overall utilization of communication channels, the number of unprocessed messages per user-process, and the state of individual computing processes (whether it is computing, idle or blocked).

The researcher can observe the dynamic variation of system parameters, as well as the state of the computation — thus obtaining immediate feedback about whether the resource management strategy currently tested is working or not.

The AXE program is being combined with capabilities from other institutions to provide an integrated suite of analysis and visualization tools. One such example involves an instrumentation and visualization package developed at Oak Ridge National Laboratory. The package includes a library (PICL) and a visualization tool (Paragraph). PICL provides a set of basic calls for parallel programming (e.g., communication and synchronization primitives) with built-in instrumentation. Paragraph takes event files generated by PICL and allows the user to view a variety of representations of the execution of the application (e.g., Gant diagrams, processor utilization graphs).

Another example involves the transfer of the PIE system developed at Carnegie-Mellon University. PIE is an integrated programming, instrumentation, and visualization tool. At the user level, PIE provides an editor as well as a graphical representation of the program structure. One can also view graphical execution profiles of the application. The user may point to certain displayed events in one window and navigate back to portions of code (displayed in the editor) directly associated with that event. PIE instrumentation is automated and invisible to the user. Furthermore, program code does not need to be rewritten since annotation is done automatically. Enough flexibility was designed into PIE to make it easy to be implemented on many computer systems and languages.

These programs are being used for performance analysis and optimization for the Space Station Freedom Data Management Systems, and for computational fluid dynamics codes on multiprocessors.

Ames-Moffett contact: N. Sliwa/J. Yan
(415) 604-4668/4381 or FTS 464-4668/4381
Headquarters program office: OAET

Differential Thermal Analyzer: Gas Chromatograph Autonomous Controller

David E. Thompson, Deepak Kulkarni, Richard Levinson

This project is developing artificial-intelligence (AI)-based software that autonomously controls a new geochemistry laboratory instrument and that provides assistance in data analysis of planetary soils. This instrument combines two well-known materials analysis methods: differential thermal analysis (DTA) and gas chromatography (GC). The proposed software will enable autonomous operation of a DTA-GC, relieving the laboratory staff of the need to constantly attend to the system, and permitting eventual use of this system in remote or hostile environments such as Death Valley, Antarctic dry valleys, or Mars.

A differential thermal analyzer is a programmable oven—it heats soil samples at a controlled rate. The heating causes the soil to undergo thermal events such as phase changes in the mineral structure (or even melting or crystal reorganization) and release of gases that are physically adsorbed or are bonded in the lattice structure of the particular minerals. The character of such an event (that is, its duration, strength, and onset temperature) is indicative of the mineral structure, proportion, and content in the soil.

A gas chromatograph contains a column of material through which evolved gas mixtures flow for purposes of constituent identification. When a mixture flows through the column, the individual gas compounds separate and can be identified chemically according to their relative flow rates. By coupling a GC to a DTA, the scientist can determine both structural and evolved gas chemistry of a single sample, and both sources of information are combined for a more complete and unambiguous characterization. Such a system can perform analysis either for target minerals, for unknowns, or for toxics.

This project began in early fiscal year 1990, and significant work has been accomplished in both the geochemical and software development aspects. The geochemists have performed about 140 sample runs on various mineral mixtures and on standards, forming the basis of the library. A full conceptual software model for the control architecture has been created and implemented. This system allows copy-and-edit of experiment profiles and plan-monitoring of new hypotheses and control protocol as these are suggested from the interpretation component of the software.

The interpretation component includes modules for feature identification from sensor signals, classification and matching (or partial matching) of these features against library curves, and explanation of the matches based on geochemical knowledge and environmental constraints. The explanations justify the hypotheses for particular mineral family assemblages which are inferred to be constituents in the unknown soil sample, and the inference predicts control software scenarios that must be assumed and implemented by the controller for unambiguous identification of the sample.

Although not all of the interpretation components have been completed, the basic architecture is in place, and the feature recognizer and classifier are currently operative on actual data. The geochemical explanation model, which fuses environmental information with the current experiment's data, is still in development. The plan-monitor system is in place, and options for control decisions for real-time changes in experiment profiles are completed.

Future work includes folding in a fault-diagnosis system, a user systems interface for the data analysis mode of operation, and actual physical replacement of the DTA and GC software systems with our developed software.

Ames-Moffett contact: R. Mancinelli/P. Friedland
(415) 604-6165/4277 or FTS 464-6165/4277
Headquarters program office: OAET

Space Shuttle Ground Processing Scheduling

Monte Zweben

Scheduling is a ubiquitous problem for NASA. Those responsible for space shuttle ground processing, space shuttle crew operations, deep-space probe operations, and space telescope operations are a small subset of the people confronted by complex scheduling problems. The constraint-based scheduling project of the Ames Artificial Intelligence Research Branch is developing automated scheduling tools to assist in the development, monitoring, and control of schedules in dynamic operations environments. We will highlight the research accomplishments of the past year as well as describe an experiment under way, the eventual goal of which is to deliver this Ames-developed technology to the Kennedy Space Center's Space Shuttle ground processing management team.

Typically, a scheduling problem is posed as a set of interrelated activities, each with a set of resource requirements. Activities are related to each other by different types of precedence relations. Each resource requirement is designated by a type of a resource and a quantity. For example, consider an inspection activity and a repair activity for a subsystem of the space shuttle. The inspection is required to precede the repair and each activity requires three technicians, one engineer, and a quality-control expert. A solution to a scheduling problem is the placement of each activity on a timeline with an assignment of resources such that each activity satisfies its precedence requirements and no resource is over-subscribed.

Once a schedule is developed for any particular problem, it is rarely executed precisely as scheduled. Uncertainty caused by broken machinery and instrumentation, sick personnel, delayed deliveries, and other unplanned events greatly complicates operations scheduling. Therefore, rescheduling in light of these exigencies is essential to maintain productive operations. Rescheduling decisions are often made by management without the aid of intelligent software. Thus, decisions are made reactively without adequate concern for optimality.

In cooperation with the Lockheed Artificial Intelligence Center and the Lockheed Space Operations Company, we are developing a scheduling tool that will assist the Kennedy Space Center ground processing team. Our tool will allow managers to track schedules, realize resource contention, and identify conflicting Space Shuttle configuration requirements. As problems are identified by our tool, the managers can resolve them manually through a graphical interface or automatically with the system's search component. This automatic component will provide suggestions to managers about how problems can be resolved in a quick but efficient manner. It is expected that our tool will help streamline the complicated and dynamic process of preparing the space shuttle for launch. We are currently shadowing the scheduling of the STS-37 mission of the shuttle Atlantis. This experiment will provide us with the data, knowledge, and user requirements necessary to build an effective scheduling tool to be used for future missions.

This year has also resulted in significant research results. The first result is the development of a new scheduling technique called constraint-based simulated annealing. This technique iteratively improves a complete, but possibly flawed schedule, until the schedule is of acceptable quality or until the user interrupts the scheduling process. This technique differs from most others in its "anytime" characteristics; that is, it can be interrupted at any time and the best solution it derived in the time allotted is supplied. Most other search techniques do not provide solutions when interrupted.

Another research result is the application of machine learning to our scheduling system. Machine learning techniques allow systems to review their performance and modify decision making to enhance performance. We developed a learning technique that could recognize resource bottlenecks after solving multiple scheduling problems. Decisions were then automatically modified according to this acquired knowledge, enabling performance improvements of 30-40%.

Ames-Moffett contact: P. Friedland
(415) 604-4277 or FTS 464-4277
Headquarters program office: OAET

Learning Receptor Positions

Albert J. Ahumada, Jr.

The human retinal cones are not arrayed in regular rows and columns like the elements of current solid-state video sensors. The cone density drops surprisingly steeply as one moves away from the center of the fovea. Even in the fovea, where the cone array is most regular, there is significant variation in density and packing orientation. Psychophysics and visual experience suggest that somehow this array of sensors leads to an extremely accurately reconstructed image in terms of geometrical position. Theories explaining the ability to make fine geometric judgments typically assume knowledge of cone position, either implicitly or explicitly. The goal here is to introduce some computational theories that provide plausible solutions to the problem of how the brain knows the positions of the photoreceptors.

Three separate models have been developed and tested. In models 1 and 2, spontaneous activity generates calibration signals inside the visual system. These can be thought of as pre-experiential models. Model 1 copies the configuration of receptor positions from the retinal level to a higher level. Model 2 interpolates the image between these positions, allowing other visual processes to sample the reconstructed image at arbitrary positions. Model 3 refines the image reconstruction on the basis of experience, allowing compensation for optical distortions, imperfections in the prior mechanisms, and new errors which may develop as the retina continues to develop after birth.

Although each model performs a useful task on its own and need not be associated with the others, the second two use the results of their predecessors. All three models are self-organizing, in that they do not depend on feedback from external systems. Mathematically, however, they have the character of feedback processes rather than competitive processes. They use locally derived error signals to guide the calibration process.

Ames-Moffett contact: A. Ahumada, Jr.
(415) 604-6257 or FTS 464-6257
Headquarters program office: OAET

Networks for Image Acquisition, Processing, and Display

Albert J. Ahumada, Jr., Andrew B. Watson

The human visual system consists of networks that sample, process, and code images. Understanding these networks is a valuable means of understanding human vision and of designing autonomous vision systems based on network processing. The Human Interface Research Branch at Ames has an ongoing program to develop computational models of such networks.

The models predict human performance in detection of targets and in discrimination of displayed information. In addition, the models are artificial vision systems that share properties with biological vision which has been tuned by evolution for high performance in complex, dynamic environments. The shared properties include variable-density sampling, noise suppression, multi-resolution coding, and fault-tolerance. The research stresses analysis of noise in visual networks, including sampling, photon, and processing unit noises.

Specific accomplishments include the following:

1. Models of sampling-array growth with variable density and irregularity comparable to that of the retinal cone mosaic
2. Noise models of networks with signal-dependent and independent noise
3. Models of network connection development for preserving spatial registration and interpolation
4. Multi-resolution encoding models based on hexagonal arrays (HOP transform)
5. Mathematical procedures for simplifying analysis of larger networks.

Ames-Moffett contact: A. Ahumada, Jr.
(415) 604-6257 or FTS 464-6257
Headquarters program office: OAET

Geographical Orientation

Vernol Battiste

The environments in which helicopters operate extend from the closely monitored Air Traffic Control (ATC) system to remote and hazardous areas where little flight guidance is available. Before flight, pilots plot their courses on maps and select specific features to use as geographical checkpoints. In flight, they compare visible features in the external scenes with those on the maps.

However, loss of geographical orientation remains a significant cause of helicopter incidents and accidents. Currently, helicopter pilots rely on paper maps that contain symbolic, graphic, and alphanumeric information about terrain contours and significant natural and cultural landmarks. Although electronic map displays are under development, human factors guidelines for display formats and interface designs do not yet exist.

Ames researchers evaluated the features pilots use to maintain geographical orientation in a familiar environment. Emergency Medical Service pilots generated from memory maps of their service area and for each of the 38 missions flown, and completed a questionnaire rating the utility of different features for geographical orientation. Each flight was also video taped. Results suggest that pilots flying in a familiar area rely on named cultural and natural features for geographical orientation. In contrast, pilots flying in unfamiliar areas rely on terrain contours, bodies of water, changes in vegetation, and latitude and longitude coordinates.

Laboratory and simulation research conducted at the University of Illinois compared performance with forward and downward projections of symbolic maps presented sequentially or simultaneously. The results suggest a benefit for maps that present information in the same orientation and simultaneously with the view out the window. Increased map complexity significantly extended the time required to encode its information. However, once encoded, mental rotation of the map was a holistic process unaffected by complexity. Way-finding, distance estimation, and localization benefited from a fixed north-up map, whereas reorienting to the flight path after a detour benefited from a rotating track-up map.

This work was extended in a field study conducted at the U.S. Army Aviation Center. The goal was to compare the features selected as geographical way points before and during a flight and to quantify the benefits of presenting map information oriented north-up or in the direction of flight in a realistically complex environment.

Ames has initiated a joint development effort with two local companies to develop a prototype electronic map display for simulation and flight research and for commercial use by helicopter, general aviation, and commuter operators. Preliminary flight tests demonstrated the feasibility of using a low-cost global positioning satellite receiver to determine helicopter location; the system achieved accuracies within ±25 feet.

The data from these flights and interface software were successfully integrated with a low-cost, electronic chart display. In parallel, researchers at Ames, Stanford University, and the University of Illinois are conducting research to develop human factors principles for design of displays and pilot interfaces. The prototype system will be tested in flight research at Ames and in the Stanford University Hospital Life Flight in FY91.

Ames-Moffett contact: V. Battiste
(415) 604-3666 or FTS 464-3666
Headquarters program office: OAET/U.S. Army

Human-Centered Aircraft Automation Philosophy

Charles E. Billings, E. James Hartzell

The Air Transport Association's National Plan for the Enhancement of Safety through Human Factors, and all subsequent deliberations, have identified the lack of a scientifically based philosophy of aircraft automation as an important shortcoming in planning for the future aviation system.

In an attempt to redress that shortcoming, researchers at Ames Research Center, in consultation with colleagues at Langley Research Center, Boeing, and Douglas, have been preparing a document on human-centered aircraft automation philosophy, containing a rationale, concepts, and guidelines for automation. It makes extensive use of examples from previous and current aircraft automation, and addresses, in particular, conceptual and philosophical issues posed by aircraft automation as it has evolved over the past 60 years.

The document is now undergoing review within NASA and the aviation industry, prior to revision and final issuance. As developed, its primary intent is to stimulate a more effective dialogue between cockpit designers and aircraft operators with regard to the attributes required of automation in a rapidly changing air transport environment.

Ames-Moffett contact: C. Billings
(415) 604-5718 or FTS 464-5718
Headquarters program office: OAET

Traffic-Alert Collision Avoidance System

Sheryl L. Chappell, Charles E. Billings

The Traffic-Alert and Collision Avoidance System (TCAS II) is a stand-alone system that can detect the presence of any nearby transponder-equipped aircraft. TCAS provides the pilot with a display of traffic in the immediate vicinity, an advisory of traffic approaching too close within 40 seconds, and an advisory of how to avoid traffic approaching within 25 seconds. TCAS II is mandated by the FAA for all large commercial transport aircraft by 1993.

Ames researchers conducted a high-fidelity simulation flown by current airline pilots to answer the following questions. Can a pilot detect a change in the maneuver advisory? Can a pilot respond quickly enough to avoid an intruder just seconds away? The results of this study provided performance parameters, pilot reaction times, and aircraft accelerations for the TCAS logic. This logic dynamically determines the appropriate pilot maneuver.

Ames researchers also improved the maneuver displays, resulting in both speed and accuracy increases for the pilots' responses. The industry standard was changed to reflect NASA's contribution. The TCAS II resolution advisory displays now include a green target area designating a safe range of vertical speeds to be achieved in addition to the red area depicting vertical speeds to be avoided.

Through industry interaction, NASA established airline/manufacturer consensus for TCAS in the "glass cockpits." The results can be found in NASA Technical Memorandum 101036.

Ames researchers continue to provide human factors expertise to the FAA and airlines on an as-needed basis. An Ames principal investigator served as panelist for the TCAS Installation and Federal Deadlines Workshop conducted by the Office of Technology Assessment of the U.S. Congress. Addressed were the human factors concerns as TCAS becomes a part of the U.S. aviation system.

Ames-Moffett contact: S. Chappell
(415) 604-6909 or FTS 464-6909
Headquarters program office: OAET

Space Habitability Research Program

Yvonne A. Clearwater, E. James Hartzell

Habitability in the context of space facilities is defined as the extent to which an environment promotes the productivity, performance, and well-being of its occupants. The earliest applications of habitability research are to the design and operation of the Space Station Freedom.

Since the station will be a confined setting situated in a hazardous environment and dominated by machine functions, its human occupants will experience high levels of environmental stress. Habitability on the station, both for work and non-work functions, must be optimized to meet NASA's 90% productivity goal and to ensure that all other mission objectives can be met.

Current habitability research focuses on developing behaviorally based architectural and interior design guidelines. Ames researchers are also studying analogous environments such as long-duration space flights, Antarctic research stations, and undersea laboratories to better understand how humans respond to isolated and confined settings similar to the space station. This work will eventually expand to test the stress countermeasure value of various interior design treatments.

Guidelines are being developed to assist in interior design and decor by assessing human performance requirements and applying principles of environmental psychology. The guidelines will assist planners in ensuring a comfortable and nonmonotonous environment. These guidelines will also help scientists to select appropriate graphics, color, and lighting schemes.

Long-range human habitability research will be applied to the planning and design of future habitats and vehicles that will enable permanent residency in space and on other planetary surfaces.

Ames-Moffett contact: Y. Clearwater
(415) 604-5937 or FTS 464-5937
Headquarters program office: OAET

Circadian Rhythms and Performance of Flight Crews

Linda J. Connell, E. James Hartzell

This program examines the effects of sleep loss, circadian-rhythm disruption, operational parameters, individual characteristics, and crew behavior on flight crew physiology, subjective well-being, and performance. Specifically, the effect of these variables associated with flight duty are under investigation in the areas of flight-deck alertness, sleep strategies and environment, adaptation to schedules, physiological consequences, and crew performance. The overall goal is to develop strategy recommendations, operational guidelines, and countermeasure techniques to mitigate the effects of fatigue. The studies combine simulator and laboratory research with field studies on aircrews operating in various flight environments.

Previous field research has produced the world's largest data base on fatigue and circadian factors in aircrews. We extensively analyzed the archival data to better understand the nature of the relationship between sleep and circadian rhythms in long-haul transport pilots. Statistical analyses revealed strong similarities to the relationship seen in time-isolation studies, thereby suggesting that the biological clock uncouples from the environmental time-cues in crews who fly multisegment transmeridian trips. A technical report is being completed and will be available by fall 1991. We are also continuing our interactions with various air carriers and pilot associations to provide advice on scheduling and crew-sleep strategies for long-haul operations.

Further analysis of our overnight cargo flight data has resulted in proposed recommendations to the industry along with suggested individual strategies for pilots. Additional analysis is under way to gain a better understanding of the wide variations among crew members in coping with such duty patterns. Although some individuals experience little or no sleep loss, others become severely sleep-deprived across a week of duty. Technical reports on this research and studies of overwater helicopter crews are in preparation.

A recent study on flight-deck alertness has been completed on long-haul transport aircrews. The opportunity for a 40-minute scheduled rest period was rotated among the three B-747 crew members during the cruise portion of four trans-Pacific flights. Compared with a no-rest group of pilots, this planned rest opportunity proved to be a very effective fatigue countermeasure. The rest-group pilots had increased levels of alertness on the flight deck, especially during the critical landing phase.

A flight crew survey has been completed on the acceptability and potential design of an "alertness manager" to be incorporated into long-haul "glass cockpits." This device will provide feedback to crew members on their levels of alertness, as well as activities to minimize boredom. The prototyping of such a device represents an effort to capitalize on cockpit automation to enhance alertness rather than reduce it through lessened pilot activity.

In order to better understand the performance implications of long-haul fatigue and circadian desynchronization, we have initiated a full-mission study of B-747 crews returning from a week of Pacific duty as compared with rested crews who have been off duty for several days. In collaboration with researchers from Ohio State University and the University of Pennsylvania, we will examine the kinds of errors committed, communication patterns, crew coordination, and overall crew performance differences between the two groups. This will be the first simulator study to examine the effect of long-haul fatigue.

Ames-Moffett contact: L. Connell
(415) 604-3229 or FTS 464-3229
Headquarters program office: OAET/FAA

Perspective Displays to Aid in Low-Visibility Curved Approaches

Nancy S. Dorighi, Stephen R. Ellis

The purpose of this research is to determine whether computer-generated perspective displays represent a significant improvement over conventional flight-deck displays when flying low-visibility microwave-landing-system (MLS) curved approaches. Research has shown that pathway displays can improve pilot situational awareness and tracking accuracy. This research will evaluate whether the improvements are significant enough (1) to increase safety in low-visibility approaches and especially complex curved approaches, and (2) to increase airport capacity by more closely spacing airplanes.

As the number of commercial aircraft in flight continues to increase, there is a growing need to develop more sophisticated cockpit information displays to enable pilots to handle the increased traffic, especially during approach to landing. In order to more closely space airplanes, pilots will need to track more easily and accurately their positions and be able to react more quickly to deviations from those positions. This research will study whether position information provided by conventional instruments and displays could be assimilated more quickly and easily when presented in a perspective display with look-ahead capability, such as a three-dimensional tunnel.

Poor visibility or no out-the-window view (as in the planned high-speed transport aircraft) requires sophisticated displays on which the pilot can rely with confidence. A pathway leading him through a curved approach, which includes terrain features that cannot be seen because of fog or other adverse weather, would provide more information and in a more natural format than the conventional alternating-direction implicit and map displays. Furthermore, continuous guidance through a curved path without the back-and-forth communication required today for vectoring would reduce controller and pilot workload and provide more efficient and safe use of the air ways.

A collaborative technical exchange program is under way with Boeing Commercial Airplanes to evaluate perspective pathway displays for the Boeing High Speed Civil Transport. Boeing's expertise in flight-deck systems and operational knowledge of air-traffic-control implications will complement the research at Ames Research Center in cockpit vision systems.

This 3-year program is in the early planning stages. A full-scale simulation is planned in the Ames Man-Vehicle Systems Research Facility, which will evaluate the displays in a realistic multi-aircraft, air-traffic-controlled environment.

Ames-Moffett contact: N. Dorighi
(415) 604-6018 or FTS 464-6018
Headquarters program office: OAET

Integrated Rendezvous and Proximity-Operations Displays

Stephen R. Ellis

This program's objective is to provide and evaluate display concepts for Space Station proximity-operations displays or other generic displays of relative orbital position. The display concepts will emphasize the use of metrical computer graphics to present spatial information to astronauts or other occupants of a space station.

An interactive proximity-operations planning system has been developed which allows on-site design of fuel-efficient, multiburn maneuvers in a multispacecraft environment, such as that about a space station. Maneuvering takes place in, as well as out of, the orbital plane. The difficulty in informal planning of such missions arises from higher-order control dynamics resulting from the unusual and counter-intuitive character of relative orbital motion trajectories and complex operational constraints. This difficulty may be overcome by visualizing the relative trajectories and the relevant constraints in an easily interpretable graphic format to provide the operator with immediate feedback on his design actions.

The new display uses inverse dynamics to remove control nonlinearities associated with orbital maneuvering and provides a graphic tool for visualizing structural, plume-impingement, and velocity constraints on orbital maneuvering. Two experiments evaluating performance of untrained users have been completed and have shown that only very brief training periods are needed to learn to plan orbital maneuvers with this system.

The visualization providing this feedback shows a perspective "bird's-eye" view of a space station and co-orbiting spacecraft referenced to the Station's orbital plane. The operator has control over two modes of operation: (1) a viewing system mode, which enables exploration of the spatial situation about the space station; and (2) a trajectory design mode, which allows the interactive "editing" of way points and maneuvering burns to obtain a trajectory complying with all operational constraints. Thus, through a graphically aided interactive process, the operator may continue to improve his design until all constraints are met.

An experimental program in which operators design a series of missions varying in complexity and constraints has been implemented. Operator actions (that is, viewing system or trajectory design) have been recorded. Review of the trajectory design characteristics is used to identify the heuristic design rules which may be utilized in an automated design system.

Experimentation with the improved display has uncovered a new visual illusion associated with three-dimensional interpretation of multi-orbital trajectories. Careful selection of the display's viewing direction may control this problem, but continued research into required geometric, symbolic, and computational enhancements is required to further optimize presentation of three-dimensional orbital information.

This work is being conducted jointly by Ames Research Center, the Israel Institute of Technology (Technion), and the University of California, Berkeley.

Ames-Moffett contact: S. Ellis
(415) 604-6147 or FTS 464-6147
Headquarters program office: OAET

Virtual Interactive Environment Workstation

Stephen R. Ellis, Michael W. McGreevy

The application of human capabilities outside vehicles and shelters will be a vital element of Space Station, Lunar base, and Mars exploration missions. Because extravehicular activity (EVA) will account for much of the human presence and robots will assist in many chores, telepresence and interactive visualization systems will provide essential crew-performance-enhancement capabilities.

To support NASA's mission requirements for augmented human capability, the Human Interface Research Branch is continuing to develop the Virtual Interactive Environment Workstation (VIEW). This device is a multisensory personal simulator and telepresence device. It consists of a custom-built, wide field-of-view, stereo head-mounted display; a custom video processor; magnetic head tracker; fiber-optic gloves; magnetic gesture trackers; voice input/output; and an audio symbol generator. The Virtual Workstation is being developed to enable greatly improved situation awareness in complex spatial environments; to enable high-fidelity telepresence for control of telerobots; to simulate workstations, cockpits, and module interiors; and to enable improved scientific visualization interfaces for exploration of planetary surface data.

The third-generation monochrome viewer and video processor electronics have been completed. Ad hoc demonstration software has been replaced by a system software library for programming the viewer, tracker, and glove. A directional acoustic signal processor, the "Convolvotron," has been designed and is being fabricated. Initial operational capability (IOC) of the prototype system will be achieved by the end of the year. Upon reaching IOC, the hardware and software will be integrated into a stable configuration for user interface research, and generic development will end. Recently, a major documentation activity has been completed, and technology transfer activities are increasing.

Application software is under development for a joint effort between Ames and NASA's Jet Propulsion Laboratory (JPL) in which the Virtual Workstation will be used to provide an alternative operator interface in telerobotics supervisory control. In another project, a highly dextrous anthropomorphic end-effector under development at JPL and the Ames Virtual Workstation will demonstrate high-fidelity dextrous telepresence between Ames and JPL.

Ames-Moffett contact: S. Ellis
(415) 604-6147 or FTS 464-6147
Headquarters program office: OAET

Human Performance Issues with Sensor Imagery

David C. Foyle, Mary K. Kaiser

Electro-optical imaging systems are being introduced into military and civilian operation, allowing pilots to fly at very low levels and avoid obstacles in reduced visibility. These systems transduce energy that is normally not perceptible to the human visual system into a viewable image on a display. Such systems include infrared imagery (thermal energy) and night-vision goggles (intensified visible light). However, pilots are generally not able to achieve the same performance with these systems that they can with direct vision in daylight conditions. The goal of this research is to contribute to improved system specifications and training requirements by identifying and studying the most significant limitations that are likely to be improved, but not solved, in the foreseeable future.

The offset location of infrared sensors and changes in relative contrasts and shadowing create one class of problems. A microprocessor-based training system will be developed, integrating the results of laboratory and simulation research. This system should provide a more efficient and cost-effective method of improving pilots' performance with night-vision systems than the current practice of flight training. Research is under way to identify attentional problems and distortions in motion perception and range estimation caused by an offset eye point.

Although the monocular display format used in the infrared systems leaves the unaided eye "free" to view peripheral motion cues and cockpit instruments, and to verify the identity of objects directly, differences in information available to the two eyes may create binocular rivalry. Pilots must selectively focus their attention on one visual field or simultaneously process different visual images. Laboratory and simulation research is being conducted at the Technion (Israel Institute of Technology) to identify the perceptual and cognitive costs and benefits of monocular and binocular display formats.

Laboratory research suggests that people can use their eyes as separate information channels, selectively focusing their attention on information presented to either eye. However, they have difficulty dividing their attention between two (different) visual fields. Simulation research evaluating pilots' abilities to fly using a monocular helmet display, while monitoring panel displays or a projected visual scene with the other eye, suggests that binocular rivalry occurs when there is motion in the irrelevant visual field and when information displayed independently to the two eyes must be integrated to perform a dynamic control task.

Visual representations of thermal and intensified light environments may differ substantially from pilots' expectations of the appearance of objects. A series of studies has been conducted to identify the characteristics of thermal images that contribute most to the problems pilots are encountering. Simulation research will compare performance with simulated out-the-window and infrared imagery to further investigate the relative importance of display parameters.

Ames-Moffett contact: D. Foyle
(415) 604-3053 or FTS 464-3053
Headquarters program office: OAET/FAA

Innovative Flight Training Methods

Sandra G. Hart

As the complexity of civil and military rotorcraft and their range of operational environments increases, traditional training methods are increasingly inappropriate, and training time and cost continue to escalate. Although it is clear that not all skills require the same level of physical fidelity for acquisition and transfer, nor the same training philosophy, decisions about which methods are most appropriate are based on tradition rather than scientific principle. The goal of this research is to identify or develop more efficient and effective methods of improving flight-related skills and to bridge the gap between theoretically motivated academic research and the operational training environment.

One approach, that of using low-cost, intrinsically motivating, computer "games" to develop more efficient attention-management skills and effective strategies for coping with very high workload, was evaluated in the Israeli Air Force Flight School, funded by a NASA grant to the Technion (Israel Institute of Technology). The rationale was that some of the skills normally acquired during flight training could be developed through exposure to a carefully constructed "game" that is structurally, rather than physically, similar to the task of flying.

Trainees who received 10 hours of training on the game performed significantly better in flight school than did the control group, which received no game training. The differences between experimental and control groups increased as the complexity and difficulty of the flights increased. Not only did playing the game improve by 50% the likelihood that trainees would complete flight school, but performance on the game predicted success in flight school better than did selection test scores and initial flight performance.

At the request of the Commander of the U.S. Army Aviation Center, Ames researchers are conducting a field study to determine the effectiveness of special-purpose, as well as commercial, video games in improving the performance of Army aviators during initial entry rotary-wing training. Video-game training was completed in July 1990. The flight school performance of the 72 participants in the study will be monitored for the next 18 months and analyzed to determine the influence of 10 hours of structured video-game practice.

In addition, Ames researchers conducted a survey at the Aviation Center to determine the relationship between casual video game experience and performance in flight school. The preliminary results demonstrated a significant correlation, suggesting that information about video-game experience and expertise might provide useful information to aid in pilot selection.

Ames-Moffett contact: S. Hart
(415) 604-6072 or FTS 464-6072
Headquarters program office: OAET/FAA

Pilot Behavior and Workload Management Program

Sandra G. Hart

Ames researchers have conducted extensive research to define the relationship between the demands imposed on pilots and measures of workload and performance. Although considerable progress has been made in developing measures that provide useful information in the design, evaluation, and operation of complex systems, the relationships among measures of workload and performance and objective task demands remain complex and even contradictory. It is still not clear how much workload is "too much," "too little," or "just right." Consequences of suboptimal workload on system performance and pilots' mental, physical, and emotional well-being are also not known.

To resolve these issues, we need to understand how pilots dynamically manage their time, priorities, attention, resources, and efforts to achieve acceptable performance while maintaining a comfortable level of workload. People do not passively translate task demands into performance. Their behavior reflects their perceptions of how well they are doing; current and projected workload; time available; and the priorities, difficulty, and durations of remaining tasks. Although these adaptive and creative behaviors continue to make human participation in advanced systems essential, they have received little research attention. Thus, little information is available about how pilots manage their time and resources or about the effects of different strategies.

Researchers at Ames, in cooperation with NASA Langley and the U.S. Air Force Armstrong Aerospace Medical Research Laboratory, have established a joint program, with funding from the FAA. The objectives of the program follow.

1. Determine how changes in strategies affect pilot workload and system performance. In FY90, laboratory and simulation research performed at the University of Illinois established some of the factors that allow operators to schedule the performance of task components and to manage their time and resources effectively. Software was developed to assess the subjective and objective effects of different task-performance strategies.
2. Develop figures of merit that reflect the overall quality of performance. A candidate method was developed in 1990 by NASA and USAF researchers and is being tested in laboratory and simulation research.
3. Identify optimal and suboptimal workload regions. Research conducted in FY90 at the University of Minnesota, the University of Cincinnati, and Catholic University explored the "underload" region characteristic of transport operations.
4. Quantify the performance, subjective, and physiological symptoms of suboptimal levels of workload. A series of complex laboratory tasks was used at Ames and at the University of Illinois to catalog some of the relevant task parameters and classes of measures.
5. Evaluate methods of improving operators' abilities to manage workload extremes. A field study is under way at the U.S. Army Aviation Center to evaluate the effectiveness of computer-game trainers in developing pilots' workload-management skills.

Ames-Moffett contact: S. Hart
(415) 604-6072 or FTS 464-6072
Headquarters program office: OAET/FAA/ U.S. Air Force

Knowledge Organization and Information Transfer Research

E. James Hartzell

This research looks at relief procedures (RPs) in air-traffic-control (ATC) room settings and also addresses the broader issues of sequential position responsibility found in all continuous operation aviation environments.

Switching from one human operator to the next when shift changes occur is seen as a critical time period when opportunities for system failure abound. Recent accidents have also demonstrated that many issues involving information organization and transfer of information arise when one aircraft is handled in succession by a number of different controllers at different facilities. Whether in the ATC room or on the flight deck, critical information needs to be passed from one person to the next in order to insure a smooth and safe operation.

This research addresses a variety of specific operational questions, including the amount of overlap needed between shifts, the design of automated controller stations to support shift-change activities, training requirements, and the organization of information to be passed along.

The research activities involve analysis of National Transportation Safety Board accident reports and Aviation Safety Reporting System incident reports, as well as analysis of digitized and video-taped data collected with the Portable Air Traffic Control Simulation System (PASS) developed at Ames. This enabled us to manipulate relief briefing situations, which will also be analyzed. Future work includes analysis of operational error data.

Ames-Moffett contact: J. Hartzell
(415) 604-5792 or FTS 464-5792
Headquarters program office: OAET

Visual Flight-Path Control Research

Walter W. Johnson, C. T. Bennett

Helicopter pilots must remain continuously aware of the location and orientation of their vehicles, relationships with the immediate environment, and the current and projected risks of natural and man-made threats. They obtain much of the information necessary for vehicle control and obstacle avoidance by monitoring the environment, with only occasional reference to flight instruments. At night and in low visibility, the limited visual cues available must be augmented by computer-generated displays, night-vision goggles, or sensor imagery. However, little is known about how human beings orient themselves to the immediate environment and extract dynamic information from direct visual cues, light-intensification systems, thermal imagery combined with computer-generated flight symbols, or cockpit displays.

The Ames Rotorcraft Human Factors Research Branch is conducting research to identify the visual cues pilots use to regulate speed, heading, altitude, and attitude in order to specify the minimum visual cues necessary for these tasks. Experiments are conducted in part-task and high-fidelity simulators to determine how pilots extract and use information in computer-generated visual scenes for vehicle control in the presence of translational (lateral, longitudinal, and vertical) and rotational (pitch, roll, yaw) disturbances. Data from these studies will be incorporated into a formal computational model that describes how pilots use optical cues to regulate vehicle orientation, altitude, speed, and heading. This model, formulated in the time-domain (rather than the more typical frequency-domain) will provide detailed information about pilots' control strategies. Research is also directed at establishing the way pilots utilize visual information to determine the structure of the terrain. Theoretical models of structural specification from relative motion, motion parallax, contour deformation, as well as static cues (shading, occlusion, familiar size), are validated against performance data.

Theoretical models of structural specification and movement regulation will be formulated and modified to better reflect operator performance. Few formal models currently reflect the critical role that frame of reference has been shown to play in perception. For example, there are frames of reference associated with the vehicle (e.g., window frames) and those associated with the outside world (e.g., the horizon and gravitational force) in flight. The frame of reference a pilot adopts may strongly influence the way he perceives movement of the aircraft and objects in the environment, as well as the way he controls the vehicle. The long-term goal of this research is to develop guidelines for the design and use of augmented displays based on human perceptual and performance capabilities.

FY90 research examined the acquisition and control of glide slope during descents to hoverpads. These studies suggested that initial acquisition was governed largely by the optical height-to-width ratio of the landing pad, while subsequent glide path corrections appeared to depend on keeping the pad in the center of the field of vision. Other research examined the details of manual-control corrections during a simulated hover task. These analyses have been used to generate computational models of how changes in optical variables lead to discrete manual-control adjustments.

Ames-Moffett contact: W. Johnson
(415) 604-3667 or FTS 464-3667
Headquarters program office: OAET

Crew Factors beyond the Flight Deck

Barbara G. Kanki, E. James Hartzell

Team Performance and Information Flow in Aircraft and Shuttle Maintenance Operations

The goal of this research is to identify group communication patterns that facilitate effective information exchange both within teams and between interfacing teams in aircraft maintenance operations. Because of similarities between aircraft and shuttle maintenance, the initial phases of this in-house project have focused on two work environments: (1) the cargo operations facility at Kennedy Space Center (KSC), and (2) maintenance facilities in airline maintenance operations.

The current phase of research consists of developing a method and collecting preliminary data at KSC as a test bed for understanding the information management process and validating the method itself. Following analysis of the communication interface among operations teams in this testbed situation, we hope to identify both formal and informal means of effective information exchange. The next phase will consist of an assessment of how the test bed results can be transferred and generalized to aircraft maintenance operations.

NASA/NOAA Undersea Habitat Project

In conjunction with the National Oceanic and Atmospheric Administration (NOAA) and the National Undersea Research Center, Ames researchers have been studying the Aquarius undersea habitat as a space station analog environment. The undersea setting provides a natural field situation for systematically observing teamwork and various issues of habitability under relatively isolated and confined conditions.

Before Hurricane Hugo stopped operations in September 1989, data collection had been completed for 11 teams of oceanographic researchers living and working on the ocean floor 7 to 14 days in the Aquarius saturated habitat. Each team member completed a battery of measurements before the dive and also completed daily and post-dive surveys. Combined with systematic ratings made by topside personnel and the on-site Ames investigator, an integrated performance measure of task productivity, crew satisfaction, and operational safety has been formulated.

The analysis of videotaped observations of habitat activities and the investigation of habitability issues pertaining to food and sleep were also initiated. Upon relocation of the habitat to another Caribbean location and once dive operations are re-instated, two new projects are being considered: (1) to design a computer workstation network to enhance communication and team coordination between aquanaut teams and surface support teams (which will also provide a practical technological means for conducting telecommunications studies of information flow and management); and (2) to investigate issues of crew composition and crew resource management training with respect to aquanaut dive teams, as well as the topside support teams with whom they interface.

Ames-Moffett contact: B. Kanki
(415) 604-5785 or FTS 464-5785
Headquarters program office: OSSA/FAA

Crew Factors in Aircrew Performance

Barbara G. Kanki, E. James Hartzell

Automation and Crew Coordination

The University of Miami and Ames collaborators have recently completed a full-mission simulation to compare crew coordination and information transfer within crews in a traditional cockpit setting and in an automated cockpit. The objective is to identify critical performance issues of automated cockpits. Reflecting an integrated approach of controlled experimentation in real work settings, direct comparison of two contrasting cockpit environments (standard versus automated) was possible through utilization of simulation facilities provided by an airline's training center.

Twelve crews of active line pilots from each aircraft type were selected; each flew the same route and experienced the same problems and environmental conditions while an in-flight observer evaluated crew performance. Thus far, data analysis has focused on performance issues as defined by analysis of errors and expert ratings and their relationship to subjective workload assessment.

Crew Communication Process Research

The fundamental interactive and sequential organization of communication processes between individuals underlies the crew processes that are critical to understanding crew performance. They are the mechanisms by which crew members coordinate their activities, transmit and receive information, and solve problems.

Ames researchers have produced new techniques for analyzing sequential and interactive speech patterns that are now being applied in both natural and high-fidelity simulated environments. Communication patterns linked to performance differences have been identified, including (1) the degree of homogeneity characterizing the speech patterns of low-error crews versus higher-error crew performances, and (2) the distinctive differences in the use of question-answer and command-acknowledgment sequences, as well as differences in the relative rates of overall communication and nonresponse.

We are currently implementing a communication-based program for analyzing group processes from a number of different perspectives representing different levels of analysis. The following projects are based on transcribed and coded videotape data from full-mission flight simulations:

1. Leadership/management styles
2. Team decision-making strategies
3. Distribution of task-related attention across crews
4. Shared mental models and crew problem-solving
5. The effects of more highly automated aircraft systems.

A project has also been initiated using actual recordings of aircrews in radio contact with air traffic controllers. Further development of this line of research into a program of communication research is anticipated.

Ames-Moffett contact: B. Kanki
(415) 604-5785 or FTS 464-5785
Headquarters program office: OSSA/FAA

Crew Resource Management Research

Barbara G. Kanki, E. James Hartzell

The Ames and University of Texas Cockpit Resource Management (CRM) evaluation project is designed to assess the effect of CRM training programs in various commercial and military air transport settings. Longitudinal data are being collected using standardized research instruments developed as part of the project, including a survey of crew-member attitudes regarding flight-deck management, a CRM seminar evaluation form, the Line Loft Worksheet (a form for expert ratings of crew performance in simulator and line settings), and the Line Oriented Flight Training (LOFT) Survey (crew-member attitudes regarding LOFT).

The research involves repeated use of these instruments to isolate changes as a result of formal CRM training. A data base being created has grown dramatically during the past few years and contains more than 17,000 records from 12 organizations. The data base, with participant identities removed, will provide a national resource that can be used by a number of researchers to investigate specific theoretical and applied problems.

Crews with formal training in CRM were contrasted with crews having no such training. Initial findings indicate that a higher proportion of crews who have received formal CRM training are rated above average in crew performance during both line operations and LOFT. The number of crews showing below average performance is halved. Additionally, the data indicate that CRM training produces highly significant, positive change in attitudes regarding personal capabilities and appropriate flight-deck behavior. These findings are the first positive indications that crew coordination training is accomplishing its intended goals.

However, this must be qualified by three highly unexpected findings: (1) A "boomerang" effect: a subgroup of individuals given CRM training shows less favorable attitudes following training; (2) large differences are found in attitudes and performance within organizations among crew members flying different aircraft and also between organizations; and (3) variations in participant reactions to various CRM training seminars presented by the same instructor appear to relate to both the personalities of participants and to processes that develop within groups.

CRM evaluation issues include more than the overall effect of training on crew members. They are concerned with the evaluation of specific training techniques and materials, as well as aspects of the CRM implementation (e.g., scenario design, LOFT evaluator, and check-airman training). Future directions of CRM research will include its transfer to other operational settings, including aquanaut/topside operations, the air traffic control system, aircraft maintenance, and the astronaut corps.

Ames-Moffett contact: B. Kanki
(415) 604-5785 or FTS 464-5785
Headquarters program office: OSSA/FAA

Socio-Organizational Influences on Team Performance

Barbara G. Kanki, E. James Hartzell

This research is being conducted in a collaborative effort by Ames researchers and Harvard University and is directed toward empirically identifying major social and organizational influences on aeronautical and space crew performance. Such influences include leadership, crew formation, and role structure within crews, as well as the effective partitioning of authority and autonomy between flight crews and ground-based crews. Groups under investigation represent actual intact social systems performing their tasks within the normal operational context, thus requiring a large-scale cross-organizational field investigation.

Currently, the method for this observational study has been developed, pretested, and documented in several papers and has been successfully applied in observing three U.S. air carriers, three international air carriers, and two military transport units. Although an additional overseas carrier is due to participate, results indicate that (1) theoretical concepts empirically distinguish between crews led by captains with relatively good versus poor leadership histories, and (2) the behavior of captains in the early stages of their crew's formation is significantly associated with subsequent crew behavior and performance.

A controlled simulator experiment will be designed in order to confirm and extend the findings obtained from the multi-organization field study. A goal will be the direct test of the effect of explicit cockpit resource management (CRM) training on aircrew performance; however, the favorableness of the performance situation will also be manipulated. Thus, social/organizational factors found to be critical variables in the field study can be experimentally tested in a controlled research setting. The experimental portion of the study will be designed and conducted jointly with Ames researchers and researchers from the University of Texas. A final report will be produced which will integrate the findings of the large-scale field study described above and the extensive data base generated from multiple data sources.

Although aeronautical teams have been the subjects of this project, the method and generalized findings can provide guidelines for the design, management, and training of effective work teams in many operational settings.

Ames-Moffett contact: B. Kanki
(415) 604-5785 or FTS 464-5785
Headquarters program office: OSSA/FAA

Image Fusion

James O. Larimer

Remote-sensing systems that form geometric images (e.g., television imagery) are an enabling technology for space exploration. This technology is used to control remote robots, to remotely explore planets, and to aid communications in the emerging field of telescience. Current television-based technology presents a monocular view that is band-limited temporally, spatially, and chromatically.

TV technology standards are a compromise between producing a reasonable "illusion" for the viewer and using the available channel capacity of the broadcast media. Channel capacity is an important driver in developing remote-sensing systems, but the realism of the visual illusion is not. For example, TV technology is designed to match the spectral band-sampling characteristics of the human visual system, but remote-sensing systems can employ multiband nonvisual spectral filters. Microwave spectra and infrared emission spectra have become important electromagnetic bands for remote sensing systems to sample and create geometric images. Combining these multiband images into a single "interpretable" image (i.e., image fusion) remains a largely unsolved problem.

The image fusion of multiband images can be done using "reverse engineering" principles derived from the study of the image-fusion properties of the human visual system. The human visual system fuses three different spatially correlated, spectrally limited contrast records sampled independently by each eye. The images of the two eyes, each with a different eye point, are fused to form a single "perceptual" image. A single picture element (pixel) in the human visual system can be represented as a three-dimensional vector in the space created by three band-limited spectral filters that encode the image into three contrast records.

These records are spatially correlated and the eye decorrelates them by creating an edge record and two orthogonal chromatic surface quality records. These re-coded dimensions are sampled at different spatial and temporal resolutions. The goal of this element is to use the multiresolution re-coding strategy of the human visual system to re-code and display multiband contrast records captured by remote sensing systems.

A multiband variant of the hexagonal-oriented, orthogonal quadrature pyramid (HOP) model of the human visual system is being applied to the multiband image fusion problem where the spectral bands are outside of the *visual* spectral region and include both imaging radar and infrared images.

Ames-Moffett contact: J. Larimer
(415) 604-5185 or FTS 464-5185
Headquarters program office: OAET

Modeling of Cockpit Display Visibility

James O. Larimer

The goal of this project is to develop mathematical models of the visibility of cockpit objects imaged on the retina in terms of a visual system footprint. This footprint represents the projection onto the cockpit model of the sensory capabilities of the human visual system when considered as a detector/filter system.

As another example of the human performance models developed as part of the Army-NASA Aircrew/Aircraft Integration (A^3I) program, the computational methods produced by this contract with the Stanford Research Institute/David Sarnoff Research Center will enable crew-station design engineers to perform basic visibility assessments of potential cockpit designs while they are still in prototype form. This type of model will aid in selecting the appropriate locations for and visual characteristics of instruments, controls, windows, visors, sun shields, etc., during the conceptual design phase, thereby reducing design costs and enhancing the quality of the final product.

The existing three-dimensional computer-aided design tools and anthropometric modeling capabilities of A^3I will be used to describe the physical specification of potential designs and to define the instantaneous volume field of view. Based on such information, this effort will develop methods to project the retinal photoreceptor apertures onto the cockpit model and support empirically based predictions about the legibility of characters and symbols. Because the human retina is highly inhomogeneous, the retinal footprint produced will also be highly inhomogeneous.

With this approach, the rendered cockpit model will be projected (using a technique such as pseudocoloring) where the image resolution is correlated with an abstraction of actual human observer resolution. Because factors (such as ambient illumination in the cockpit, the adaptive state of the pilot, and the reflective/emissive properties of displays) are critical to consider in such contexts, this project will incrementally develop modeling techniques to address these aspects.

Rendering of the visibility information will be possible for regions of constant acuity (spatial resolution) or may be concentrated on a single instrument with a high-fidelity representation of its image. In the latter case, the designer can visualize the effects of illumination, pilot adaptation, afterimages, head position and point of regard on the appearance of the instrument as seen by the pilot. Such outputs will aid the crewstation designer in understanding the consequences of his choices for the location, size, and characteristics of cockpit instruments and controls from a human engineering standpoint.

Begun in October of 1988, the first prototype of this visibility model is currently undergoing integration with the A^3I Man-Machine Integration Design and Analysis System (MIDAS) workstation in preparation for demonstrations during the summer of 1990.

Ames-Moffett contact: J. Larimer
(415) 604-5185 or FTS 464-5185
Headquarters program office: OAET/U.S. Army

Filling in the Retinal Image

James O. Larimer, Jennifer Gille

The optics of the eye form an image on a surface at the back of the eyeball, which is called the retina. The retina contains the photoreceptors that sample the image and convert it into a neural signal. The spacing of the photoreceptors in the retina is not uniform and varies with retinal locus. The central retinal field, called the macula, is densely packed with photoreceptors. The packing density falls off rapidly as a function of retinal eccentricity with respect to the macular region, and there are regions in which there are no photoreceptors at all. The retinal regions without photoreceptors are called blind spots or scotomas.

The neural transformations that convert retinal image signals into percepts fill in the gaps and regularize the inhomogeneities of the retinal photoreceptor sampling mosaic. The filling-in mechanism is so powerful that generally we are not aware of our physiological blind spot, where the nerve head exits the eyeball, or other naturally occurring scotomas (such as the central-field loss that occurs during night vision). Individuals with pathological scotomas are also unaware generally of the field losses that result from the pathology.

The filling-in mechanism plays an important role in understanding visual performance. For example, people with peripheral field loss are usually unaware of the loss and subjectively believe that their vision is as good as ever, yet their performance in tasks such as driving can be severely impaired.

The filling-in mechanism is not well understood. A systematic collaborative research program under way at Ames and at the Stanford Research Institute has been designed to explore this mechanism. It has been known for some time that when an image boundary is stabilized on the retina, the boundary is not perceived. Using image-stabilization techniques, we have been able to show that retinally local adaptation (the control of sensitivity) can be separated from more central neural effects which control the appearance of fields. In particular, we have shown that the perceived fields, which are in fact different from the image on the retina as a result of filling-in, control some aspects of performance and not others. We have linked these mechanisms to putative mechanisms of color coding and color constancy.

Ames-Moffett contact: J. Larimer
(415) 604-5185 or FTS 464-5185
Headquarters program office: OAET

Information Management and Transfer

Sandra C. Lozito, Sheryl L. Chappell

The effective management and transfer of information within the National Aviation System (NAS) is critical to a safe and efficient air transportation system. The Flight Human Factors Branch has an ongoing research program to develop design principles for advanced flight-deck information management systems and computer-aided design technology to facilitate the integration of new information. Since air-to-ground as well as airborne information transfer is a part of this research, aircraft/air traffic control (ATC) integration into the future NAS will benefit from this effort.

A multi-faceted approach has been undertaken to attain the program goals. This approach includes (1) the development of methods for quantifying aircrew information requirements and information processing capacity, (2) the identification of current operational problems that could be eliminated by improved system design, (3) the development and evaluation of prototypical information management systems, (4) the development of part-system simulation technology as a low-cost design and evaluation tool, and (5) the development of computer-aided design technology based on information management principles.

Analyses of Aviation Safety Reporting System (ASRS) incidents of information-transfer factors contributing to in-flight weather encounters were completed as was a comprehensive survey of air carrier, aircrew weather information requirements. In addition, an analysis of party-line data from ASRS incident reports was conducted to examine the effect of frequency monitoring on information transfer and management. A line-oriented flight simulation study was conducted to evaluate the effectiveness of ground-air transmission of microburst/wind-shear information. The study revealed that significant improvements in aircrew planning and decision-making could be realized with the use of data-link transmitted weather information.

In support of advanced communications-management system development, prototype data entry and retrieval systems were developed to support digital air-ground communication. One phase of a grant to develop and evaluate flight-deck interfaces for automating ATC clearance delivery was also completed. Study results indicate significant enhancements in flight-management-systems operations with graphical interfaces using clearance information transmitted by data link. Additional efforts are also ongoing to develop a part-task simulation that would provide a realistic means of exploring issues relevant to the evaluation of different methods of information transfer and management within the cockpit.

Ames-Moffett contact: S. Lozito
(415) 604-0008 or FTS 464-0008
Headquarters program office: OAET/FAA

Visualization for Planetary Exploration

Michael W. McGreevy

The objective of the Visualization for Planetary Exploration program is to conduct research and develop crew interfaces for in-space terrain exploration systems. The approach is to (1) review mission operational experiences, mission constraints and opportunities, and the state of the art in exploration technology; (2) investigate user behaviors and requirements; and (3) enlist interdisciplinary expertise to develop, implement, demonstrate, and evaluate advanced crew interfaces.

Field studies have been conducted in desert terrain to understand operations central to planetary surface exploration. In addition, a planetary terrain-visualization test-bed is under development to support focused user interface research. This powerful computer system provides dynamic interaction with planetary terrain data.

The Virtual Workstation is a powerful user interface device for NASA's mission-oriented applications including computational fluid dynamics, planetary data visualization, in-space telepresence, and Space Station telerobotics. Beyond these applications the Virtual Workstation is also a uniquely useful user-interface research device. Using head-tracked head-mounted displays, the Virtual Workstation provides the user with a vivid experience of three-dimensional space. It can be used with computer graphics systems as a personal simulator, surrounding the user with a virtual interactive environment. Alternatively, it can utilize head-slaved cameras and other sensors to provide telepresence. In either case, an instrumented glove may be used to detect hand shape and position to enable the user to manipulate objects in computer generated or remote environments.

Preliminary discussions with planetary geoscientists indicate a strong scientific interest in the development of Virtual Workstation technology for planetary surface telepresence. A leading concept is to extend the reach of human exploration beyond the perimeter of manned extravehicular activity by use of telepresence from centrally manned bases to numerous unmanned rovers. Geoscientists with decades of experience in field work believe that human presence contributes a tightly coupled and essential interplay of cognitive, perceptual, manipulative, and locomotor skills that can complement automated rover operations. By using telepresence, these unique human skills may be applied over a greater area at an earlier date.

Ames-Moffett contact: M. McGreevy
(415) 604-5784 or FTS 464-5784
Headquarters program office: OAET

Optimal Image Combination Rules for Heads-Up Display

Jeffrey B. Mulligan

Heads-up displays are often constructed by simply placing a half-silvered mirror in front of the observer without considering whether image combination by reflection (image addition) is the best that can be done. This research investigates the perceptual consequences of image combination by a variety of rules, including a multiplicative rule which might be implemented in a heads-up display by means of a programmable filter (liquid crystal display, or LCD).

Before it can be determined which method of image combination is "best," it is necessary to first specify what task must be performed. A number of different criteria may be specified, but one which seems sensible is that the two images should be separable by the observer; that is, to selectively attend to one or the other with minimal interference from the unattended image.

This problem has been approached experimentally using oppositely moving random-dot patterns. The coloring of the composite patterns can be set to correspond to a variety of combination rules. For some of these rules, subjects report "twinkling" or noise in addition to the two motions depicted. It has been found experimentally that this noise is minimized when the patterns are combined additively; however, other researchers using a different type of stimulus have results at odds with this. The results have implications for theories of motion processing in the brain in addition to their applications to engineering design of heads-up displays.

Ames-Moffett contact: J. Mulligan
(415) 604-3745 or FTS 464-3745
Headquarters program office: OAET

Flight Management System Human Factors

Everett A. Palmer, Sheryl L. Chappell

A number of activities have been initiated to support the development of more effective interfaces to on-board flight management systems. In collaboration with an airline training department, researchers at Ohio State University will collect data on the problems pilots have when initially learning and operating current flight management systems (FMS) with the control display unit (CDU).

In another collaborative study, in-flight observations are scheduled to be made of FMS use by pilots during terminal-area operations on approximately 100 airline flights. The data will help us determine the situations in which pilots have problems editing their flight plan with the FMS and the situations in which FMS tasks interfere with other cockpit tasks. These data will also be used to assess the feasibility of using the CDU for data link communications.

A part-task simulator has been developed by other researchers at Ohio State University to evaluate interface concepts for an in-flight planning decision aid. This project is focused on identifying the factors that influence the failure of a pilot to consider an alternative flight plan that is superior to the pilot's current flight plan. The part-task simulator allows a pilot to explore options for flight planning while en route. A goal of the system is to reduce cognitive fixation by allowing the pilot to easily explore the implications of alternative flight plans.

In addition to the above research studies, a major effort has been initiated this year in the Man-Vehicle Systems Research Facility to develop an experimental flight management system in the Advanced Concepts Flight Simulator that can be used to support future phases of the Aviation Safety/Automation Program. By involving industry early in the design phase, the final system should be a unique tool for joint NASA/industry research on FMS design and use.

Ames-Moffett contact: E. Palmer
(415) 604-6073 or FTS 464-6073
Headquarters program office: OAET

Error-Tolerant Cockpit Systems

Everett A. Palmer, Asaf Degani

The objective of this research is to develop the technology necessary for the design of error-tolerant cockpits. A key feature of error-tolerant systems is that they incorporate a model of expected pilot behavior. The system uses this model to track pilot actions, infer pilot intent, detect unexpected actions, and alert the crew to potential errors. In some sense, the goal is to develop an "electronic check pilot" that can intelligently monitor pilot activities.

We are pursuing a number of alternative ways to track pilot activity. We have investigated techniques based on (1) a rule-based script of flight phases and procedural actions, (2) operator function models, and (3) Bayesian temporal reasoning. Under a grant to the Georgia Institute of Technology an intent inferencing system (OFMspert), originally developed for a satellite communications operator, was modified this year to track the action of crews flying the B-727 simulator in the Man-Vehicle Systems Research Facility (MVSRF) at Ames.

The technology developed for the rule-based cockpit procedures monitor has been used this year to develop an interactive electronic checklist display for the Advanced Concepts Flight Simulator (ACFS), also located in the MVSRF. The electronic checklist has been designed to provide a graphic display of the status of checklists and checklist items (pending, skipped, or completed). The checklist program also can sense the state of many aircraft controls and systems and can thereby provide a redundant check that procedural steps have in fact been completed.

Full-mission scenarios have also been developed to test the effectiveness of different electronic checklist designs in reducing procedural errors. Preliminary testing is now under way with airline crews.

Ames-Moffett contact: E. Palmer
(415) 604-6073 or FTS 464-6073
Headquarters program office: OAET

Development of a Touch-Panel Operated Electronic Checklist

Everett A. Palmer, Asaf Degani

Recent field studies and research in the area of cockpit procedures has shown that one of the disadvantages of a paper checklist is the lack of an explicit display of pending and completed procedural steps, as well as the inability to switch reliably between multiple active procedures.

Two levels of electronic checklists are currently running on a touch-screen display in the Advanced Concepts Flight Simulator (ACFS) cab at NASA Ames Research Center:

1. A pointer checklist: This system aids the pilot in conducting normal or emergency procedures by providing a feedback for accomplished items, as well as for intentionally and inadvertently skipped items. The checklist display automatically calls up the appropriate subsystem display. The system is designed to allow the pilot to branch from checklist to checklist without losing track of uncompleted checklists and without getting lost in the electronic procedure manual.
2. A sensed checklist: This system has all the capability of the pointer checklist, but goes one step further. The sensed-checklist system can sense the state of configuration items such as flap position, gear position, and wing/engine anti-ice, thereby providing redundant monitoring and feedback to the flight crew on the state of the system.

A full-mission simulation scenario to evaluate these levels of checklists and their effects on human error has been designed for the ACFS.

Ames-Moffett contact: E. Palmer
(415) 604-6073 or FTS 464-6073
Headquarters program office: OAET

Human Factors of Flight-Deck Checklists: The Normal Checklist

Everett A. Palmer, Asaf Degani

The improper use, or the non-use, of the normal checklist by flight crews is often cited as the probable cause of, or at least a contributing factor to, many aircraft accidents. During this field study, researchers analyzed the normal checklist, its functions, format, design, length, use, and limitations of the persons who must interact with it. A list of design guidelines for normal checklists was developed as a result.

The currently used paper checklist has several design weaknesses: the lack of a pointer system, the inability to store skipped items, space limitations, and a limited branching and tracking capability. However, the study results indicate that this is only the outer shell of the checklist problem. The real problems that emerged were the design concepts and social issues surrounding checklist use.

Checklist designs that do not "run parallel" with activities of external agents (such as gate agents, cargo loaders, refueling agents, and flight attendants) have an inherent disadvantage. Omission of checklist items sometimes occurs when an item that could not be completed in sequence is deferred by the crew to be accomplished later on. In addition, checklists should not be tightly coupled with other critical tasks such as takeoff, taxiing, and landing. Every effort should be made to provide buffers to help recover from a checklist error.

Several checklist philosophies currently used in the industry do not accommodate the limitations of the operators, leading some pilots either to misuse them or to not use them at all.

The checklist is highly susceptible to production pressures ("making schedules"). These pressures encourage substandard performance when the crew is rushing to complete the checklist. Furthermore, under production pressures, checklists are sometimes relegated to second-place status in order to save time, thereby leading some pilots to shortcut part, or even the entire, procedure.

It was also found that the socio-technical environment in which the pilot operates has a substantial effect on checklist performance. If the individual captain chooses not to use the checklist for any reason, no one can force its use.

As a result of this field study, researchers have produced 16 guidelines for checklist design and checklist management/use.

Ames-Moffett contact: E. Palmer
(415) 604-6073 or FTS 464-6073
Headquarters program office: OAET

Human Factors of Advanced Technology Transport Aircraft

Everett A. Palmer, E. James Hartzell

The purpose of this 3-year field study was to determine by direct contact with airline pilots, instructors, and supervisors what problems are being encountered in line operations of Advanced Technology Transport aircraft.

Many problems and benefits of new technology in the cockpit emerge only after extensive pilot experience in actual operations. Field studies provide a way of systematically tapping and documenting the lessons learned on the line by these experienced pilots. Two airlines participated in the study, and over 200 pilots volunteered to participate. The principal investigator, Earl Wiener (University of Miami), attended ground school and made many observation flights from the jump seat.

The results of the study show that pilots are generally very positive about the aircraft and its automatic features, but they have some reservations about safety. Pilots feel that automation reduces workload in routine operations but increases it if the Flight Management System must be reprogrammed. Pilots are concerned that there is too much head-in-the-cockpit time, and they are concerned about degradation of their manual flying skills and take active measures to avoid this. Pilots also feel that crew coordination is especially important in this aircraft, and they are concerned that the air traffic control system does not take advantage of the advanced navigation and guidance capabilities of this aircraft.

Some additional effects of cockpit automation on crew coordination concern the traditional role definitions (such as pilot-flying versus pilot-not-flying). Even though these roles are spelled out by the airlines' operations manual, they often break down. Numerous pilots complained of a lack of clarity about "who does what," a problem usually not present in well-standardized traditional cockpits. Supervision by the captain of the first officer may be more difficult, and at the very least it may be considerably different than that in traditional two-pilot cockpits.

There may be a de facto transfer of authority from the captain to the first officer because many of the first officers are more proficient than the captains on the cockpit display units which the pilots use to enter information into the flight management computers. One pilot will often do tasks assigned to the other pilot, usually with that pilot's consent and awareness, for a variety of reasons. Although this may at times be effective cockpit resource management, it can undercut standardization, which is the foundation of safe piloting.

A full-mission simulator study is being conducted to further investigate the interaction of cockpit automation and crew coordination. The main variables in this follow-on study will be the level of cockpit automation and whether the captain is the pilot-flying or the pilot-not-flying.

The final report, *Human Factors of Advanced Technology ("Glass Cockpit") Transport Aircraft*, was published in June 1989 as NASA Contractor Report 177528.

Ames-Moffett contact: E. Palmer
(415) 604-6073 or FTS 464-6073
Headquarters program office: OAET

Process Measures of Pilot Behavior: Methods and Tools

Everett A. Palmer, E. James Hartzell

A number of activities have been initiated to develop methods for describing and analyzing the process by which pilots and crews perform normal flight tasks and cope with malfunctions. In collaboration with Klein Associates, a full-mission scenario was flown by three airline crews on the Man-Vehicle Systems Research Facility's B727 simulator. The scenario included flight legs with malfunctions (1) that could be dealt with by following written procedures, or (2) that required the crew to devise their own way of coping with the problem. An adaption of Newell and Simon's Problem-Behavior-Graphs was developed to document how each crew assessed and coped with the abnormal situations.

These full-mission data have also been used by researchers at the University of California, San Diego, to adapt cognitive anthropology methods to the aviation environment. These techniques are enabling us to produce a detailed account of the flow of information between the various users and machines operating in a limited portion of the aviation system. To support this type of analysis, a software program named JUMPSEAT has been developed to allow an analyst to view the video recording of a flight in synchrony with the on-line computer data generated during the flight. This system has been used to support the transcription of pilot communications and the coding of the time of observable events on cockpit video tapes.

In a separate grant project, researchers at the University of Illinois are developing a software tool called MacSHAPA to support summary descriptions, statistical analyses, and modeling of "raw" protocol data.

Ames-Moffett contact: E. Palmer
(415) 604-6073 or FTS 464-6073
Headquarters program office: OAET

Computational Models of Human Cognition: Modeling the NASA Test Director

Roger W. Remington

The objective of this research is to advance the use of operator aiding systems based on artificial intelligence (AI) through the in-depth analysis and modeling of a demanding NASA human-system interface. AI-based computational models of human cognition and information processing will be used to analyze the cognitive demands of the NASA Test Director station in the launch control center at Kennedy Space Center (KSC). This project has been tied to a real application problem from its inception and has the objective of recommending ways to improve system performance in that setting. A second objective is to bring together psychologists and computer scientists working in concert to recommend improved operator interfaces that employ artificial intelligence in this NASA operating domain.

The specific goals are to (1) evaluate the utility of existing cognitive models for understanding complex tasks, (2) develop better models, (3) address both information acquisition and symbolic levels of cognition, (4) provide improved graphical interfaces for model development and information presentation, and (5) provide functional specifications for improved human-system interfaces based on computational models that capture important limitations in human cognition. The long-term scientific goal is a set of cognitive models and model-building tools that will allow human-factors engineers to better analyze the cognitive demands imposed by specific system designs. An improved analysis of cognitive demands will provide a basis for identifying which aspects of a complex task should be automated.

Model development will be supported by empirical validation. The validated models will be used to provide KSC with functional specifications and techniques for assessing advanced launch concepts. Future launch concepts will include intelligent systems used to aid operators. Computational models that approximate aspects of human cognition can be used to assess the effect on the operator of proposed automation or other restructuring of operations of the launch control center. By working together, psychologists and computer scientists can enhance the utility of intelligent systems by ensuring that the division of labor and the human interface to the intelligent aid are compatible with human perceptual and cognitive abilities.

Analysis and modeling efforts will lead to guidelines that address information presentation requirements and will identify functions whose automation would significantly reduce operator workload. Where possible, the work will be integrated with on-going technology development projects at KSC, especially those dealing with the introduction of artificial intelligence into the control room.

Ames-Moffett contact: R. Remington
(415) 604-6243 or FTS 464-6243
Headquarters program office: OAET

Aviation Safety Reporting System

William D. Reynard, E. James Hartzell

The Aviation Safety Reporting System (ASRS), managed by NASA at the request of and with funding from the FAA, was established in 1976. The ASRS has received, processed, and analyzed over 167,000 voluntarily submitted aviation incident reports from pilots, air-traffic controllers, and others.

These reports describe both unsafe occurrences and hazardous situations. ASRS offers incident reporters confidentiality, and the FAA provides limited immunity for unintentional aviation safety transgressions the reporters may have committed. In exchange, the program receives safety information which can be used to remedy reported hazards, to provide data for planning and improving the National Airspace System, and to conduct research on pressing safety problems. The ASRS's particular concern is the quality of human performance in the aviation system.

The ASRS program is unique among aviation reporting systems. Its special capabilities include the following:

1. Proof of the concept to acquire, analyze, and utilize incident data
2. Unique methods to capture otherwise inaccessible human performance data
3. One-of-a-kind data base of actual incident information as reported by the event's participants
4. World's largest repository of human performance information
5. Consistent support and utilization of the program by government and industry
6. Proven capability for diverse application to both research and operations
7. Ability to actively monitor the aviation system
8. Capability of effective technology transfer as evidenced by ASRS-type systems in other countries and disciplines.

In addition to screening and processing report receipts for entry to a data base, the ASRS maintains that data base and supporting computer hardware and software, and interrogates the data base to satisfy the information requirements of government and industry organizations. Report receipts can be statistically analyzed for trends and problem concentrations, although there are important theoretical limitations on the use of ASRS data for this purpose.

Since its inception, ASRS has published more than 40 research reports based on its data, covering

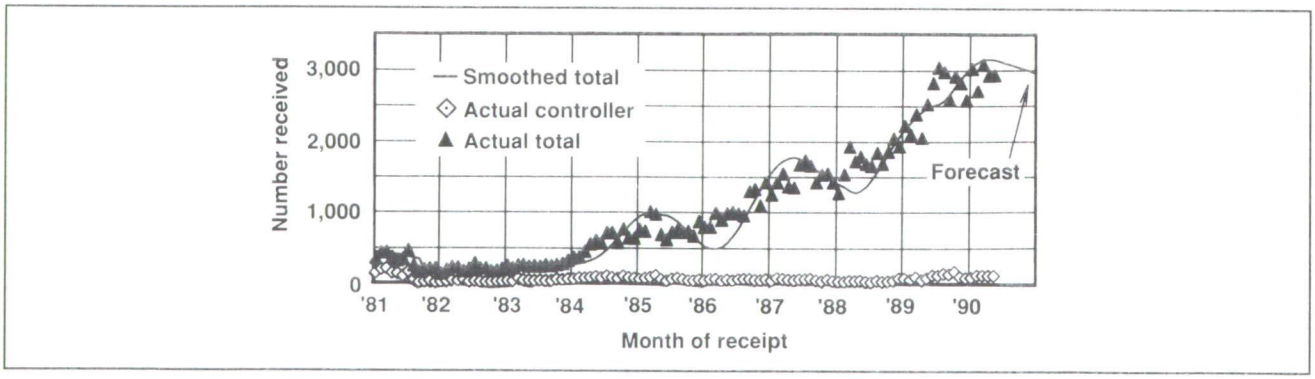


Fig. 1. ASRS report intake

the full spectrum of aviation activity. In addition, the program has issued over 1,100 alerting messages and responded to more than 2,000 special data requests from elements of the aviation community and the public. The ASRS also publishes a monthly safety bulletin, *Callback,* and a quarterly safety and training publication, *Direct Line.*

The ASRS currently operates under an Interagency Agreement with the FAA that is effective until September 1992, The program has achieved a productive and active rapport with FAA operational and research organizations, and is consistently used by NASA, the National Transportation Safety Board, the Department of Defense, and the aviation community. A large and growing report volume continues to challenge ASRS resources; however, with increased FAA and NASA support, the program has the potential to significantly increase its operational and research activities.

Ames-Moffett contact: W. Reynard
(415) 604-6467 or FTS 464-6467
Headquarters program office: FAA

Individual Crew Factors in Flight Operations: In-Flight Sleep

Mark R. Rosekind

This research is part of a program that focuses on individual variables that determine overall crew performance. The main emphasis is on fatigue and circadian rhythmicity and how they are affected by operational parameters, individual characteristics, and crew behavior. The overall goal is to develop personal strategies, operational guidelines, and countermeasure techniques to mitigate the effect of fatigue, especially among transport aircrews. Field studies, designed to document sleep loss and its causes in long-haul operations, comprise a major part of this effort.

Research activities in FY90 have concentrated on completing field studies of planned cockpit rest in non-augmented trans-Pacific B-747 operations. This work is being carried out in collaboration with Stanford University and the University of Pennsylvania. A total of five experimental crews and four control crews underwent continuous EEG monitoring while flying four trans-Pacific flights over 6 days. Volunteers also completed a vigilance performance task several times during flight and maintained daily logbooks of all layover sleep.

The experimental crews were allowed a 40-minute sleep period in their cockpit seats, one at a time, during cruise. Both the physiological and performance data revealed a striking and consistent improvement in alertness for the experimental "rest" crews as the trip progressed, especially during the night flights. A final report will be available in fall 1990.

A second effort being initiated is an examination of how well long-haul crews sleep in on-board sleep facilities (bunks). This project extends our previous international cooperative research on layover sleep and will involve collaboration with foreign researchers and airlines. Using polysomnographic recordings of sleep, combined with environmental monitoring of noise, the field research will assist the industry in determining the adequacy of various bunk designs to meet the needs of augmented crews during extended overwater flights. An effort is also being made to determine the most effective way to rotate sleep times among the various crew members.

Related laboratory work is examining the potential role of timed bright light for resetting the biological clock and sleep cycles to meet operational demands. Collaborative research conducted last year with Japanese researchers demonstrated a beneficial effect in a small number of subjects flown from Tokyo to San Francisco. Data collection has been completed on a 12-hour phase shift in the Ames Bedrest Facility and these more controlled results will be available in a technical report early in FY91.

Ames-Moffett contact: M. Rosekind
(415) 604-3921 or FTS 464-3921
Headquarters program office: OAET/FAA

Pilot Decision-Making

Robert J. Shively

Civil and military pilots must make critical decisions under time-pressure and in stressful situations, yet little is known about decision-making behavior under these circumstances. Pilots may have to acquire and integrate an enormous amount of information to make timely and appropriate decisions, but they may ignore relevant information and thus adopt suboptimal strategies under stress.

By maintaining situational awareness, adverse trends may be detected. By constructing alternative responses and formulating contingency plans, pilots can prepare for unexpected events and "stay ahead of the aircraft." However, relatively few studies have quantified the relationship between contingency planning, decision efficiency, and flight safety. Such information is needed to improve the design of decision aids, evaluate new systems, and develop relevant training procedures.

Research is under way at Ames and at the Georgia Institute of Technology (1) to evaluate how pilots make decisions under stress, (2) to model this behavior, and (3) to develop methods to improve pilots' abilities for making timely and appropriate decisions with currently available resources or computerized decision aids.

Existing decision models are being evaluated under well-controlled conditions and in more realistically complex and dynamic environments. Simulation research at Ames evaluates the effects of crew planning on subsequent decisions and flight safety. In-flight research is conducted to analyze decision-making in helicopter law-enforcement operations.

Many civil emergency medical service (EMS) incidents and accidents have been attributed to poor pilot judgment. Pilots accept or continue flights when they are tired, with deteriorating weather, or when other risk factors are present. Although helicopters play a critical, life-saving role, they have an unacceptable safety record.

Ames sponsored two government/industry workshops to provide an opportunity for representatives from organizations responsible for medical evacuation to share common experiences, problems, and solutions. The EMS Safety Network was established within the Aviation Safety Reporting System (ASRS) to develop a data base of civil, public service, and military EMS incidents which can be analyzed to assess the effects of crew size, duty hours, procedures, missions, and other factors on pilot workload, fatigue, judgment, and performance.

An expert system was developed to aid pilots in assessing the potential risk associated with a particular mission and to reduce the emotional aspects of the decision process. A field study was conducted by Ames researchers with the cooperation of a hospital-based operator to evaluate this system and develop a data base of information on (1) crew workload and fatigue, (2) in-flight procedures and communications, (3) the cues pilots use to maintain geographical orientation, and (4) decision-making behaviors in EMS operations.

Ames-Moffett contact: R. Shively
(415) 604-6249 or FTS 464-6249
Headquarters program office: OAET/FAA

Army-NASA Aircrew/Aircraft Integration Program

Barry R. Smith

The Army-NASA aircrew/aircraft integration (A^3I) program is a joint Army and NASA exploratory development effort to advance the capabilities and use of computational representations of human performance and behavior in the design, synthesis, and analysis of manned systems. A^3I is managed and executed by the Computational Human Engineering Research Office, an organization under the U.S. Army Aeroflightdynamics Directorate, and by the NASA Aerospace Human Factors Research Division. Both are at Ames Research Center.

The program's goal is to conduct and integrate the applied research necessary to develop an engineering environment containing the tools and models needed to assist crew-station developers in the conceptual design phase. A major product of this goal is the development of a prototype Human Factors/Computer-Aided Engineering (HF/CAE) system called MIDAS (Man-Machine Integration Design and Analysis System) (see the figure). This system provides design engineers/analysts with interactive symbolic, analytic, and graphical components which permit the early integration and visualization of human engineering principles.

MIDAS is currently hosted on a number of networked Symbolics and Silicon Graphics workstations. It serves as the framework into which research findings and models (developed by or sponsored through the Computational Human Engineering Research Office) are incorporated.

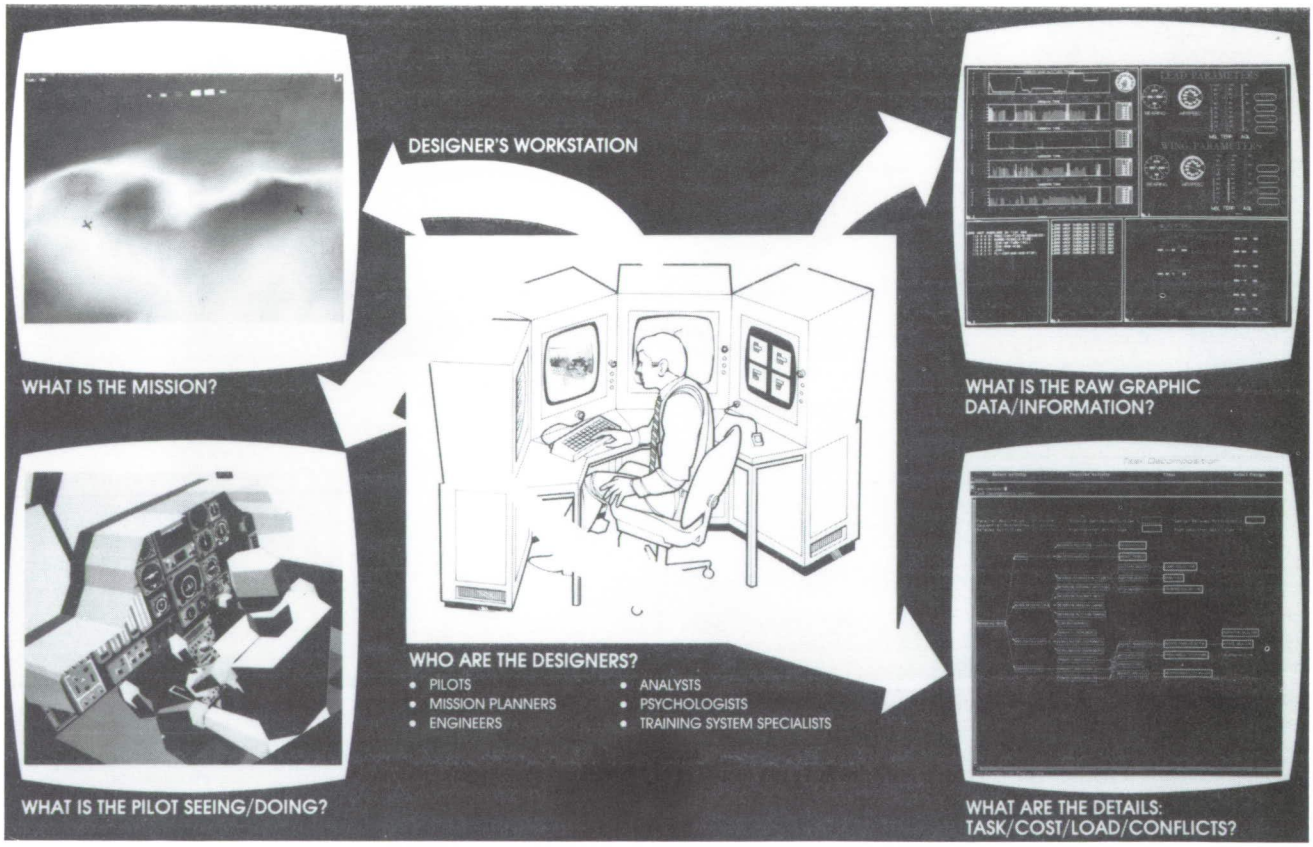


Fig. 1. Man-Machine Integration Design and Analysis System (MIDAS)

Seventy to eighty percent of the life-cycle cost of an aircraft is determined in the conceptual design phase. After hardware is built, mistakes are hard to correct and concepts are difficult to modify. Engineers responsible for developing crew training simulators and instructional systems currently begin work after the cockpit is built, when it is too late to affect its design. MIDAS gives designers an opportunity to "see it before they build it"; to ask "what if" questions about all aspects of crew performance, including training; and to correct problems early. The system is currently focused on helicopters; however, its model and principal basis permits generalization to other vehicles.

MIDAS contains tools to describe the operating environment, equipment, and mission of manned systems with models of human performance/behavior used in static and dynamic modes to evaluate aspects of the crew-station design and operator task performance. The results are presented graphically and visually to the design engineers, often as a computer simulation of "manned flight." In this sense, MIDAS is similar in concept to computational tools such as finite-element analysis and computational fluid dynamics, which are used to improve designs and reduce costs.

The program began in the fall of 1984 and four major phases of development have been completed toward a 1994 target date for a full prototype system. The most recent phase of development, demonstrated during June 1990, focused on the expansion of several elements of the system along with the integration of a dynamic, opportunistic scheduling model and two new applied vision models. In addition, during 1990 an A^3I sponsored book, *Human Performance Models for Computer-Aided Engineering*, was published by Academic Press.

Based on a 1989 National Research Council report of the Panel on Pilot Performance Models, Committee on Human Factors, this important work provides A^3I an assessment of the vision and cognition models relevant to human engineering in aerospace systems. The result is a clearer view of the possibilities for computer-aided human engineering as undertaken by NASA.

Ames-Moffett contact: B. Smith
(415) 604-4264 or FTS 464-4264
Headquarters program office: U.S. Army

Aviation Display Design

Barry R. Smith

The goal of this research effort with Chris Wickens, University of Illinois, is to establish how principles of display formatting and organization are modified by context effects, and how they can be provided within a computational basis in experimental scenarios that better approximate real-world complexity.

Previous research examined a number of specific display design principles related to information integration, color, space, and display modalities. Work under this grant will take these known principles, supplement them, and explore their generality and continued validity in the context of multi-element displays and environments with increased task complexity. In the process, there is a goal to establish the foundations of quantitative computational modeling that account for the higher-level cognitive processes involved in translating displayed information into task requirements. This is necessary to allow some measure of display efficiency to be predicted in the context of the Army-NASA aircrew/aircraft integration (A^3I) MIDAS workstation.

These experimental objectives will be carried out using two general simulation environments: (1) the TASKILLAN simulation on an IRIS 2400, which provides much of the visual characterization of low-level helicopter flight with reference to head-up-device (HUD) instruments, and (2) a "generic display environment" created on an IBM AT to portray the graphical presentation of instrument outputs. Investigations will be centered on theories of display proximity (referring to physical display variables that allow two or more channels of information to be perceived as similar) and task proximity (referring to the degree of relevance of two or more information processing channels to each other or to the unified goal of one task). The dimensions of display quantification used include the number of display "objects," spatial separation, consistency/compatibility in stimulus-response or stimulus-comprehension mappings, and resource competition.

Started in late 1989, the research findings and quantitative models arising from this grant have formed the core of several models used within the A^3I program to predict operator performance and workload by clearly describing the complex interactions between mission demands, cockpit configuration, and pilot information processing characteristics. One example is the prototypical Display Layout Analysis component of MIDAS which was extremely well received by visitors to our 1990 demonstrations.

Ames-Moffett contact: B. Smith
(415) 604-4264 or FTS 464-4264
Headquarters program office: OAET/U.S. Army

Dynamic Anthropometric Modeling

Barry R. Smith

One of the most fundamental requirements for model-based human engineering and analysis in a wide array of applications is a representation of human anthropometry and motion. A grant with Norman Badler, University of Pennsylvania, has been established to meet this need with easily created, realistic, and physically quantifiable human figure motion via an interactive computer graphics system for human modeling in a three-dimensional space environment.

Major research topics within this project include (1) task-simulation mechanisms that facilitate human task animation by developing an interface between artificial intelligence and graphical motion control; (2) task-simulation-result reporting with graphical animations and various workload performance measures including reach and view assessments, collision and interference detection, strength or reaction force assessment, and psychomotor task load; and (3) the use of human agent models such as hand preference or fatigue within the task simulation.

The resulting computer program, JACK, allows the user to select different-sized human figures or graphic mannequins that include the 5th, 50th, and 95th percentile male and female based on NASA astronaut demographics. These mannequins can then be placed within a three-dimensional object environment created and stored by using a number of modeling packages. Articulation is achieved using a goal-solving technique based on specifying body-joint orientations or end-effector (limb) goals. Joint limitations have been installed to eliminate unreasonable movements. Kinematic and inverse kinematic controls are applied so that goals and constraints may be used to position and orient the figure, with external/internal forces and torques applied to produce motion. A movement-time concept based on Fitt's law has been incorporated based on reach site distance and width.

Supporting graphic output in wire-frame, solid-filled, or smooth-shaded modes, key poses can be stored and interpolated for animation, which allows environmental limitations to be detected as a function of human size and movement characteristics. In addition, by attaching the "view" of the environment to the mannequin's eye, JACK displays a perspective corresponding to what the mannequin would "see" while moving in the environment. This provides the first step toward further analysis and conclusions about object occlusion and visibility.

Begun in the fall of 1987, JACK is being further enhanced, both in-house and by the developer, as an integral part of the Army-NASA aircrew/aircraft integration (A^3I) program's MIDAS workstation. The most recent version has a flexible 17-segment vertebral column which adds an important new dimension of realism to torso movement. In addition, through an agreement with the developer, during 1990 the A^3I team was able to place JACK into NASA's Computer Software Management Information Center (COSMIC) repository and distribute the software to five major defense contractors for their internal use.

Ames-Moffett contact: B. Smith
(415) 604-4264 or FTS 464-4264
Headquarters program office: U.S. Army

Symbolic Operator Model

Barry R. Smith

The symbolic operator model of the Man-Machine Integration Design and Analysis System (MIDAS) is complex and continually evolving. It currently contains two major subcomponents: the scheduling model and the loading model. During a simulation, this model attempts to execute assigned mission activities subject to specified constraints, state variables, and other simulation object requirements.

It does this by (1) updating the simulated operator's goal list to delete terminated or inappropriate goals; (2) examining equipment and world-state variables to determine if event-response activities are required; (3) tracing the decomposition of mission goals to their lowest level; finding matching equipment operation patterns or activities that will satisfy them; (4) sorting these matched goal-activity patterns by priority; (5) interacting with the scheduling and loading operator model components as appropriate; and (6) executing these activities subject to physical resource (hand, eye, etc.) requirements, visual, auditory, cognitive, and psychomotor load limits, and temporal/logical constraints.

This constraint-based, opportunistic model of operator scheduling behavior was developed using the blackboard architecture provided as part of the Generic Expert System Tool. The scheduler contains modular components or knowledge sources that represent individual stages in the scheduling process, with an extended task-based decomposition (a "divide-and-conquer" technique) used to partition the overall scheduling problem. It closely interacts with the MIDAS task-loading model for reasoning about resource interactions between plausible concurrent tasks.

The task-loading model is based on current research in multiple-resource theory, scaling, workload, and perception. Based on attributes of the mission tasks, world state, operator, and crew station equipment, a resource classification taxonomy is used to classify individual tasks in terms of their demands on the visual, auditory, cognitive, and motor-processing dimensions. In addition, conflict matrices are used to describe the interactions of these resource demands across different processing dimensions and tasks. An initial version of the task-loading model has been coded in Symbolics Common Lisp, and technical exchange efforts are currently under way with Boeing's Helicopter Division to demonstrate its use during 1991 on actual aircrew tasks.

Ames-Moffett contact: B. Smith
(415) 604-4264 or FTS 464-4264
Headquarters program office: U.S. Army

Visibility Modeling Tool

Barry R. Smith

Computer-aided engineering (CAE) has revolutionized the way engineers create designs. It is now possible to use mathematical models of objects or processes to evaluate the performance of a design before the object is actually built. Classic examples include the finite-element analysis of strength used to evaluate the forces acting on structures such as bridges and the computational fluid dynamics (CFD) analysis of models used to evaluate the lift properties of wings.

The visibility modeling tool is a human factors (HF) CAE tool designed to help the crew station design engineer obtain answers to questions about the visibility of information in potential avionic displays. The primary goal of this HF/CAE visibility tool is to evaluate potential designs before they are built; thereby reducing design costs, enhancing the quality of the design engineer's product, and shortening the design time. For this tool to be maximally useful, the evaluation that it provides to the engineer must be in an easily understood format. Thus, user friendliness through graphics is another goal of the project. The visibility modeling tool is being developed as an integrated component of the Army-NASA aircrew/aircraft integration (A^3I) program's MIDAS system.

To model visibility, it is necessary to consider (1) the three-dimensional geometry of the crew station or cockpit; (2) the reflective and emissive properties of surfaces and objects in that space; (3) ambient lighting; (4) the pilot or astronaut eye points; (5) what the crew member is looking at; (6) how this affects convergence and accommodation; (7) far, near, and retinal obstructions such as window posts, helmet margins, and retinal insensitivities; and (8) the current adaptation state of the pilot's visual system. All of these factors are being incorporated into the visibility modeling tool at a level of realism that is adequate to generate reasonably valid estimates of visibility.

The program contains two major components—a binocular volume field of view model and a visibility assessment portion which models the sensory capabilities of the human visual system as a detector/filter system. Through a unique mixture of in-house effort and grants and contracts with scientists at universities and research institutions, this effort spans problems from basic vision science, to the application of three-dimensional models, to problems in computer-aided design (CAD).

Currently in place are a grant with The Lighthouse (A. Arditi, principal investigator) and a contract with Stanford Research Institute/David Sarnorff Research Center (J. Bergen, principal investigator). In addition, there are collaborative agreements and a university consortium agreement on closely related topics in human vision. Much of the basic computer system architecture for the visibility modeling tool has been previously developed and tested as part of the A^3I program (i.e., communication protocols and system integration). In addition, the A^3I/MIDAS three-dimensional CAD system is used to rapidly prototype the geometry of various cockpits and avionics of interest, and the dynamic anthropometric model "JACK" is used to visualize the operator's head/body position within the selected environment.

During the most recent phase (demonstrated in June of 1990), computational models were completed which allow assessing the pilot's binocular visual-field volume and the legibility of letters and symbols on typical cathode ray tubes. Analytical results from this visibility modeling effort were provided to McDonnell Douglas Helicopter Company and used as part of their critical design review for AH-64 Apache cockpit modifications under the Longbow program. During 1991, basic developmental work will proceed by modeling accommodation; that is, human optical blur, surface quality, visual-motion detection, and color discrimination.

Ames-Moffett contact: B. Smith
(415) 604-4264 or FTS 464-4264
Headquarters program office: U.S. Army

Motion Processing in Man and Machine

Andrew B. Watson

People navigate almost effortlessly through complex environments, relying on a sophisticated visual capacity for estimating motion of self and objects. The Human Interface Research Branch (Code FLM) has an ongoing program of research to understand and model the human motion-sensing mechanism, and to develop algorithms for motion sensing in autonomous vision systems. This research will have important applications in the areas of robotics, obstacle avoidance, autonomous vehicles, and nap-of-the-Earth flight, and will also provide insights into the motion information required by pilots for flight control.

Recent accomplishments include new algorithms for estimation of two-dimensional image-velocity fields from image sequences, and algorithms for estimating three-dimensional motion parameters from the two-dimensional velocities. Also completed was a study on the dependence of human direction-of-motion judgments on the contrast of picture elements. The results show strong contrast-dependent biases, which are a powerful means of distinguishing between alternative models and which may have practical consequences in themselves.

Ames-Moffett contact: A. Watson
(415) 604-5419 or FTS 464-5419
Headquarters program office: OAET

Perceptual Components Architecture

Andrew B. Watson

There is great interest in new and extended standards and architectures for electronic transmission of visual information. These include extensions of conventional analog broadcast TV (high-definition TV), digital packet-switched video, and so-called open architecture TV.

Packet video is a scheme in which the video signal is digitized and broken down into small (100 - 1,000-bit) packets over an asynchronous packet-switched network. The principal virtues of packet video are (1) it allows integration of diverse information sources (video, speech, and data); (2) it exploits the variable-bit-rate network to provide constant quality, despite the bursty nature of video signals; and (3) it allows simple multiplexing of multiple video sources, which in turn yields improved channel utilization and transmission efficiency.

Whatever the details of its implementation, packet video will require that the image stream be coded efficiently and robustly. The code should be designed to match the perceptual apparatus of the human viewer.

A perceptual components architecture (PCA) for digital video partitions the image stream into signal components in a manner analogous to the human visual system. These components consist of achromatic and opponent color channels, divided into static and motion channels, and further divided into bands of particular spatial frequency and orientation. Bits are allocated to individual bands in accordance with human visual sensitivity to that band, as well as in accordance with the properties of visual masking. PCA has desirable features such as efficiency, error tolerance, scalability, device independence, and extensibility.

During the past year we have defined the basic structure of a prototype PCA and studied the spectra of natural image sequences. We have also implemented and demonstrated the first prototype of three-dimensional (space-time) PCA coding of motion sequences.

Ames-Moffett contact: A. Watson
(415) 604-5419 or FTS 464-5419
Headquarters program office: OAET

Q-3

Pyramid Image Codes

Andrew B. Watson

All vision systems, both human and machine, transform the spatial image into a coded representation. Particular codes may be optimized for efficiency or to extract useful image features. We have explored image codes based on the primary visual cortex in man and other primates. Understanding these codes will advance the art in image coding, autonomous vision, and computational human factors.

In the cortex, imagery is coded by features that vary in size, orientation, and position. We have devised a mathematical model of this transformation, called the hexagonal oriented orthogonal quadrature pyramid (HOP). In a pyramid, code features are segregated by size into layers, with fewer features in the layers devoted to large features. Pyramid schemes provide scale invariance and are useful for coarse-to-fine searching and for progressive transmission of images.

The HOP is novel in three respects: (1) it uses a hexagonal pixel lattice; (2) it uses oriented features; and (3) it accurately models most of the prominent aspects of the primary visual cortex. The transform uses seven basic features (kernels) which may be regarded as three oriented edges, three oriented bars, and one non-oriented "blob." Application of these kernels to non-overlapping 7-pixel neighborhoods yields six oriented, high-pass pyramid layers, and one low-pass (blob) layer. Subsequent high-pass layers are produced by recursive application of the seven kernels to each low-pass layer.

Preliminary results from use of the HOP transform for image compression show that 24-bit color images can be coded at about 1 bit/pixel with reasonable fidelity. Future work will explore related codes and more detailed comparisons with biological coding, as well as applications to motion processing and shape perception.

Ames-Moffett contact: A. Watson
(415) 604-5419 or FTS 464-5419
Headquarters program office: OAET

Three-Dimensional Auditory Display Systems

Elizabeth M. Wenzel

Auditory cues can provide a critical channel of information in complex spatial environments during periods of high visual workload and when visual cues are limited, degraded, or absent. Some or all of these conditions will be present in space station operations, such as monitoring and control of autonomous and semiautonomous telerobots, conducting extravehicular activity, using visor displays, and managing complex on-board space station systems. Auditory information can also enhance the utility of virtual environment displays, such as Ames' Virtual Workstation.

Spatial auditory displays require the ability to generate localized sound cues in a flexible and dynamic manner. Ames is currently investigating the underlying perceptual principles of auditory displays and is also developing a prototype signal processor based on these principles. Rather than use a spherical array of speakers, the prototype maximizes portability by synthetically generating three-dimensional sound cues in real-time for delivery through earphones. Unlike conventional stereo, sources will be perceived outside the head at discrete distances and directions from the listener. This is made possible by numerically modeling the effects of the outer ears on the sounds perceived at various spatial locations (see the figure). These "head-related transfer functions" (HRTFs) can then be applied to arbitrary sounds in order to cause them to seem spatially located.

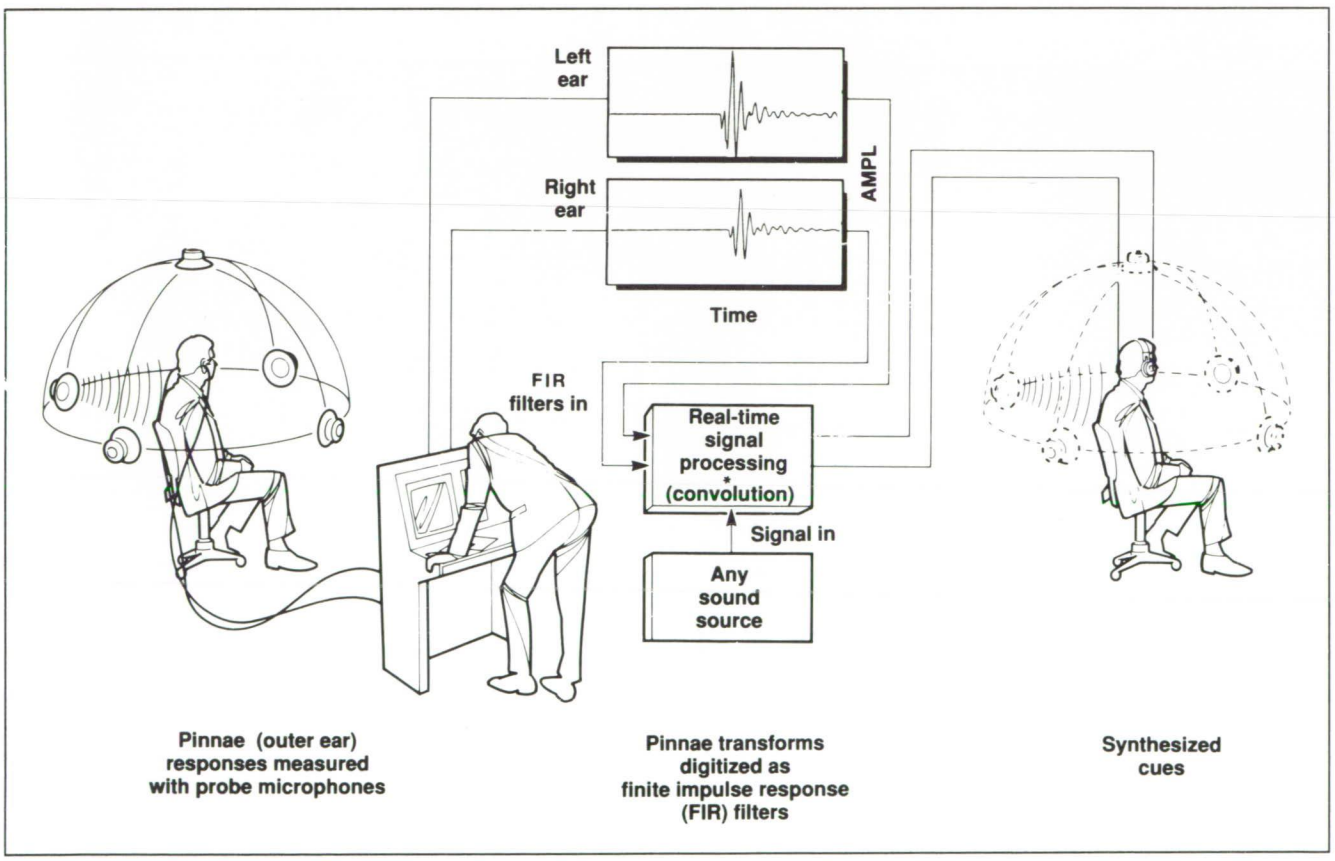


Fig. 1. Synthesis technique for simulating three-dimensional sounds over headphones

In 1990, the "Convolvotron," a prototype version of a signal processor for synthesizing the HRTFs in real time, was converted to a printed circuit board (PCB) for greater reliability and ease of replication. The PCB, capable of synthesizing up to four independent and simultaneous localized sources, is currently available and is being used in a variety of research and industrial laboratories in addition to the Ames auditory laboratory.

A nondirectional audio display, based on well-established electronic sound-synthesis standards, is also under development. An initial version of an auditory symbol editor was completed in 1990. This system will enable researchers to investigate auditory symbols for communication of meaning apart from verbal content. In addition, experience in the integration of this system with the virtual workstation will benefit the later incorporation of the spatial audio display system.

Research at Ames and in cooperation with the University of Wisconsin, Madison, is under way. This research includes perceptual validation of the synthesis technique in both practical and more basic areas. Practical issues include required computational resolution and signal bandwidth and the degree to which the general population of listeners can obtain adequate cues from non-individualized HRTFs. Basic issues include acoustic determinants of individual differences in localization behavior and factors that enhance externalization and reduce front/back confusions such as head movements and environmental reflections.

Ames-Moffett contact: E. Wenzel
(415) 604-6290 or FTS 464-6290
Headquarters program office: OAET/FAA

An Exact Linear-Error Attitude Control Law

Ralph Bach, Jr., Russell Paielli

A new attitude-control law has been derived that realizes exact linear-error rotational dynamics. The control law can be implemented with either a direction-cosine or quaternion formulation, although its derivation depends on certain interesting and previously unknown properties of the "error" quaternion.

The figure shows a simple quaternion implementation for spacecraft attitude control. The quaternion e* represents the commanded attitude, and the quaternion e represents the actual attitude of the spacecraft. In the conventional configuration, the control law is a linear combination of the attitude error and angular rate. The resulting control system, although stable, exhibits nonlinear dynamics. The "linear-error" configuration utilizes a nonlinear control law, but the system exhibits linear error dynamics. For small errors, the two configurations operate similarly, but for large errors, as shown in the figure, the linear-error system exhibits a predictably linear response.

The control of rotational dynamics is essential to all aircraft and spacecraft flight. The kinematic relations for attitude formulations are nonlinear; the most practical formulations (direction-cosine and quaternion) are non-minimal; that is, there are equality constraints to be maintained. The usual techniques for control-system design are based on linear theory. One approach is to divide the nonlinear system into locally linear segments, which leads to gain scheduling and the possibility of "switching" transients. The exact linear-error control law described here realizes linear-error dynamics even in the presence of large attitude tracking errors. This property is desirable because the selection of design parameters and the analysis of stability are simplified, and the resulting dynamic performance is very robust.

The exact linear-error control law has been derived for use in a model-reference application. The use of both feed-forward and feedback provides the potential for tracking command signals of a higher bandwidth than by using feedback alone. A discussion of the theory and a presentation of simulation studies for a typical spacecraft attitude-control system will be included in a forthcoming report.

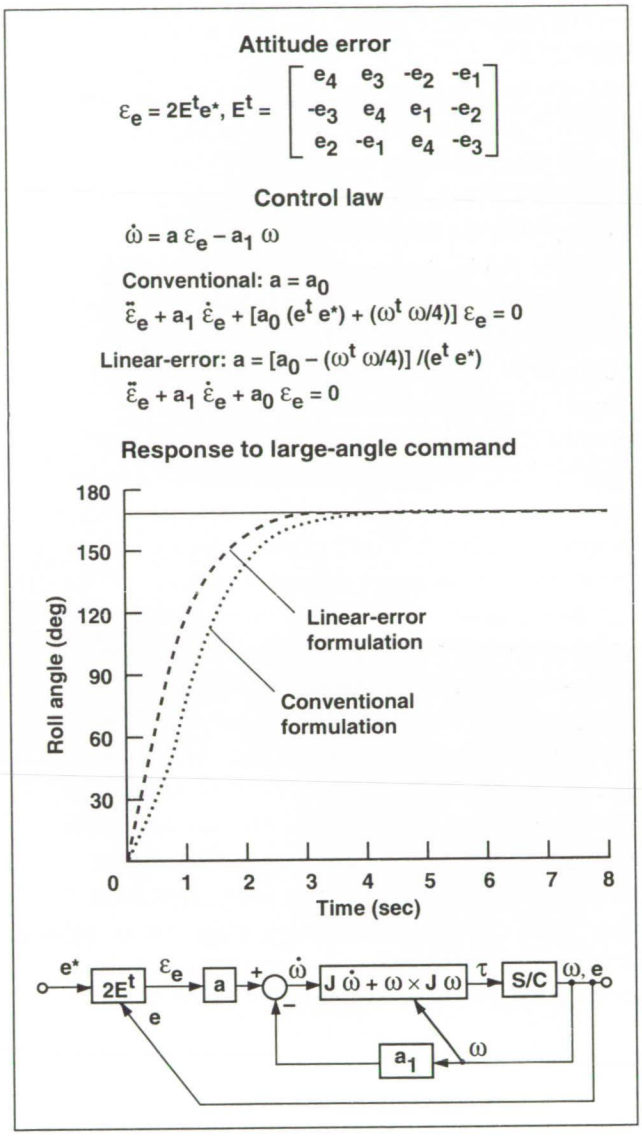


Fig. 1. Quaternion attitude-control systems

Ames-Moffett contact: R. Bach
(415) 604-5429 or FTS 464-5429
Headquarters program office: OAET

Field-Based Passive Ranging Using Matched Velocity Filters

Yair Barniv

Helicopters in covert nap-of-the-Earth operations require passive ranging for obstacle avoidance. A single or a stereo pair of visual or infrared forward-looking cameras can be used to produce a stream of images (per camera) which is called optical flow. The three-dimensional location, and in particular the range, of some chosen objects or of all discernible points in the field of view can be recovered from the optical-flow imagery. Feature-based localization suffers from the need to identify objects between successive frames; whereas field-based methods operate on all pixels, which are identified by their gray-level rather than by their shape. Velocity filtering (VF) is a particular field-based method which has been used as a track-before-detect method for target detection. It is very efficient computationally because of its inherent parallelizability.

Accomplishments to date include doing the theoretical and performance analysis work for the VF method and developing the VF algorithm, which has produced very encouraging results on real laboratory data. The algorithm was interfaced with the SUN workstation environment as opposed to being a stand-alone program. This enables us to share the image data base—especially that obtained recently from a helicopter test flight. This environment also enables us to display data and results in a variety of ways by using perspective views, false color, and animation methods.

It has been experimentally found that the VG algorithm, like most other algorithms, has its own advantages and shortcomings. Our goal is to incorporate ideas and methods from fundamentally different types of algorithms so as to complement the weaknesses of one by the strengths of another. Work was done toward that end in a pixel region growth in order to average the algorithm's results over more than one pixel at a time and thus increase its robustness.

Currently, the VF algorithm is being modified in many ways to improve and extend its performance and robustness. One of the important issues is extending the existing algorithm to operate on data from a maneuvering vehicle. In addition, theoretical work is in progress to determine the range accuracies obtainable from a combined stereo/optical-flow passive ranging. A special emphasis is given to range-accuracy degradation caused by non-perfect sensor/platform alignment.

Ames-Moffett contact: Y. Barniv
(415) 604-5451 or FTS 464-5451
Headquarters program office: OAET

Obstacle-Avoidance Guidance and Control

Victor Cheng

The functions for obstacle-avoidance guidance and control have progressed from the concept development stage to the detail development stage. In a parallel effort, a helicopter simulation with three-dimensional graphics has been developed on a Silicon Graphics, Inc. IRIS 4D/240GTX computer workstation to provide a readily available platform for evaluation of the guidance and control software.

Obstacle-avoidance guidance and control constitute one of the critical components for automated nap-of-the-Earth rotorcraft flight. It is the only guidance function in the overall guidance structure that uses on-line information of the outside world furnished by the obstacle-detection system. The helicopter simulation provides a valuable in-house capability for evaluating the performance of the guidance and control software, thus improving on the efficiency of the research and development effort by providing timely feedback of the algorithms' performance.

The helicopter simulation uses the TMAN model developed at Ames to model the helicopter dynamics. The graphics model is that of a UH-60 helicopter. The terrain model is based on Defense Mapping Agency data, and it uses the smooth shading capability of the IRIS system to render realistic images. The obstacle data base consists of simple tree forms randomly distributed on the terrain surface. The manual-control interface involves the use of a joystick and a mouse to provide the pitch and roll cyclic, rudder, and collective inputs.

In the automatic guidance mode, simulation of the sensor and obstacle-detection system is accomplished through the use of IRIS graphics hardware capabilities to speed up range-map calculations over those possible with software implementations. The range data are converted into an inertial data base, which is necessary in anticipation of future sensor-fusion models. The obstacle-avoidance guidance examines the inertial data base to discern the obstacles and the terrain profile. It performs two-dimensional path selection for obstacle avoidance and uses the altitude profile to perform three-dimensional ground-hugging guidance.

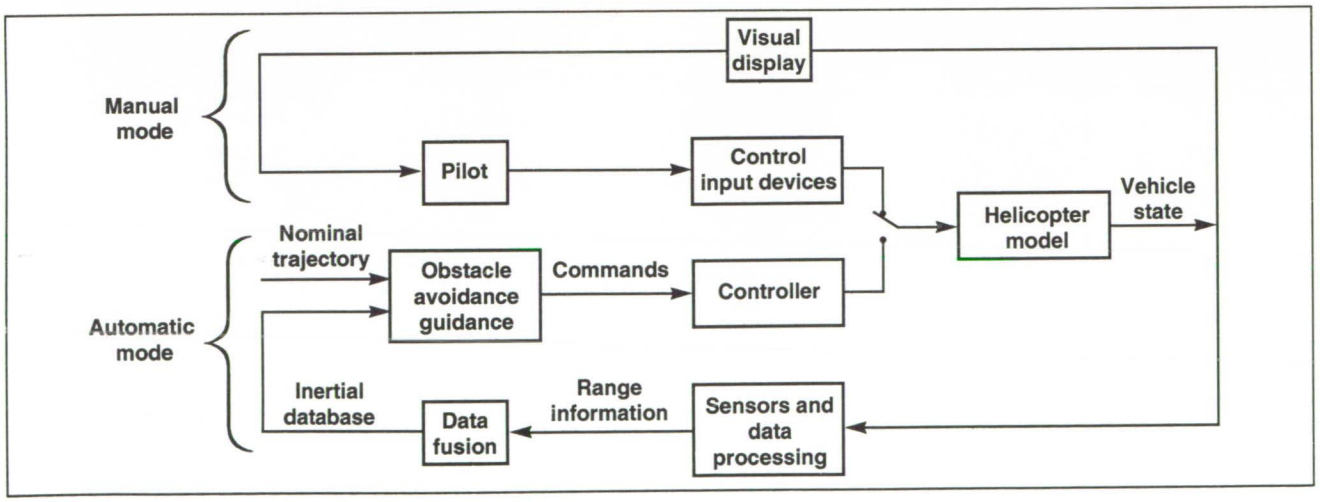


Fig. 1. Implementation of guidance and control system

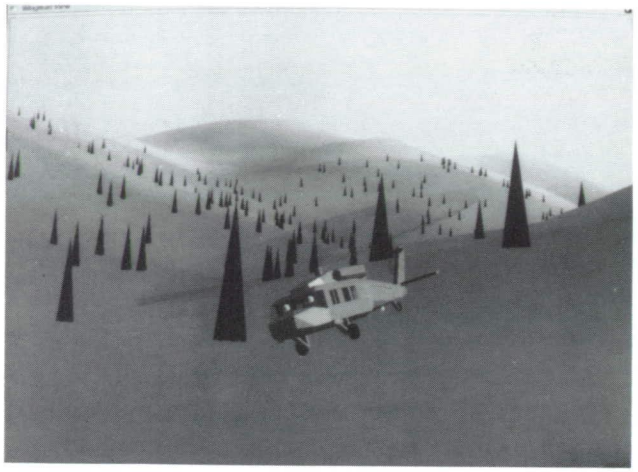


Fig. 2. Simulation display

The guidance command will drive an autopilot designed by researchers at Georgia Institute of Technology for the TMAN vehicle model. The simple feedback control at the front end of the autopilot is being replaced by a more sophisticated trajectory coupler that will observe the performance limitations of the vehicle model. Full operational capability of the guidance and control law for the helicopter simulation is expected soon.

Ames-Moffett contact: V. Cheng
(415) 604-5424 or FTS 464-5424
Headquarters program office: OAET

ORIGINAL PAGE
BLACK AND WHITE PHOTOGRAPH

Automatic Nap-of-the Earth Flight Simulation

Richard A. Coppenbarger

To determine pilot acceptability of fully automatic nap-of-the-Earth (NOE) flight, a motion-based flight simulation involving five evaluation pilots was conducted on the Ames Research Center's VMS facility in December 1989. The guidance and control system was developed by Systems Technology Incorporated (STI) under a NASA Small Business Innovation Research contract. The rotorcraft mathematical model and the automatic flight-control system were integrated with obstacle-detection and avoidance logic to allow simulation through a planned NOE course. Each course consisted of approximately 40 way-points at which either a simple heading change or an aggressive vertical maneuver was commanded.

A head-down "moving map" display was provided in the cockpit for monitoring course progress. Simulated flights were conducted at a constant ground speed of 15 knots and a constant terrain clearance of 20 feet. Terrain attributes for guidance purposes were obtained by preflight parameter identification using Fourier analyses. Unmapped terrain features, such as small hills and power lines, were placed along the courses as obstacles to be detected by modeled sensors. Vertical, lateral, and speed-change maneuvers were executed time-optimally for obstacle avoidance. Strong emphasis was placed on the development and utilization of head-up display (HUD) symbology for a pilot to

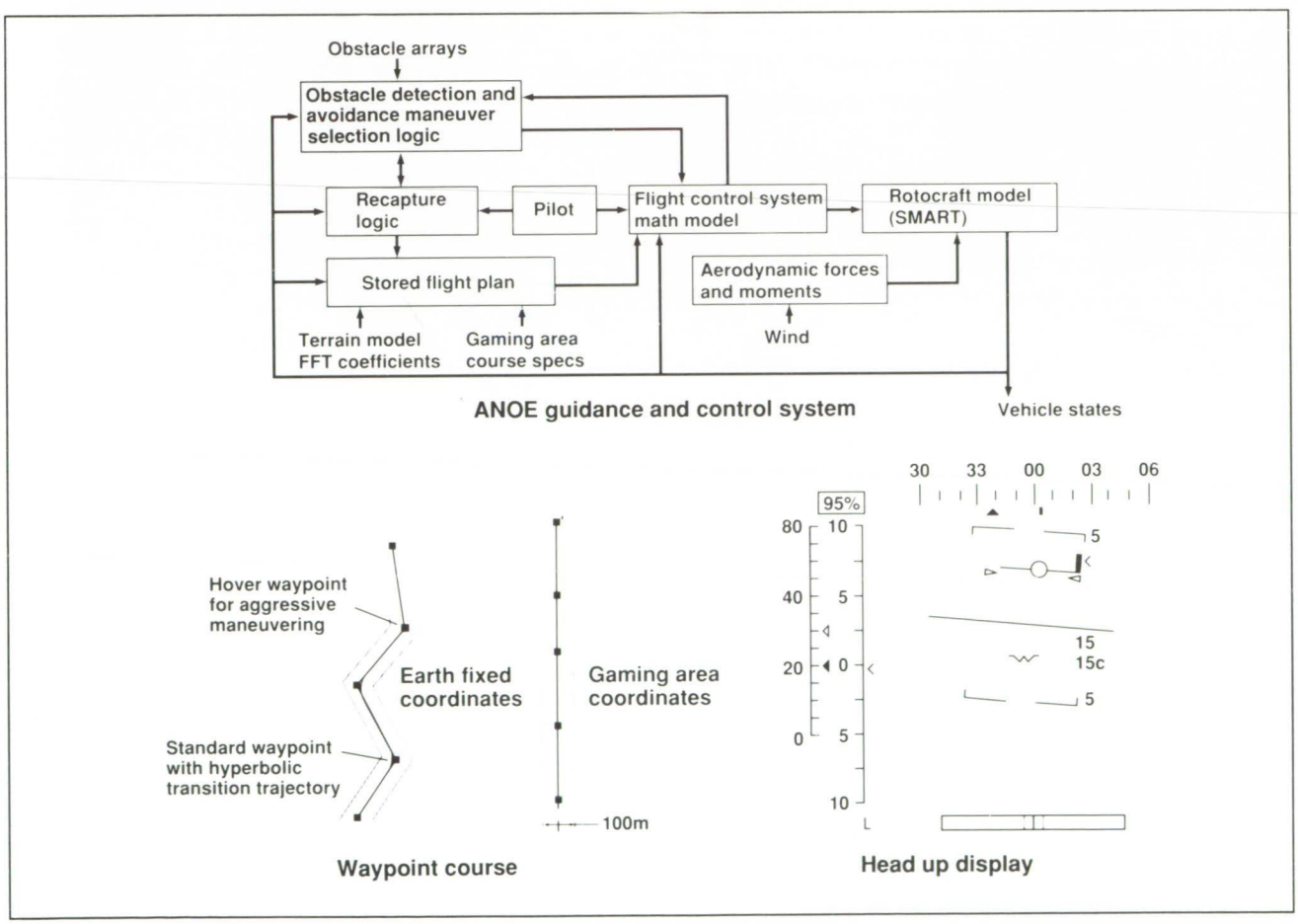


Fig. 1. Automatic nap-of-the-Earth flight simulation

monitor flight status and, if necessary, override the automatic system and assume manual control.

To serve as surrogates for actual mission tasks, several side tasks were included to be performed by pilots during automatic flights. The side tasks were incorporated to provide a cockpit workload similar to that expected in a single-pilot, light-helicopter environment. Data were taken for three different course profiles at two visibility conditions (500 and 1,000 feet) with both automatic and manual control. Recorded data included (1) numerical time-histories of aircraft states, strip-charts, pilot comments and evaluation forms (including a Cooper-Harper evaluation of the model under manual control), and (2) videos of numerous runs showing the computer generated imagery together with the HUD and moving-map display. Additional pilot commentary regarding all aspects of the system was obtained during a post-simulation debriefing.

A real-time, fully automatic NOE flight simulation with a pilot in the loop has been developed and tested on a motion simulator. This simulation is considered a preliminary step toward developing an on-board system to aid a pilot in conducting NOE flight through hostile terrain under poor visibility conditions. The many elements of automated NOE flight have been integrated and tested to obtain pilot opinion of the emerging technology. Insight gained from early pilot evaluations is extremely valuable in helping to direct current research efforts in this field.

The results of the simulation have been consolidated in a paper to be presented at the AIAA Guidance, Navigation, and Control conference in August 1990. A final report from STI describing, in detail, the flight-control system and piloted simulation will be completed by July 1990. To carry out further development in response to pilot suggestions, the flight-control system has been integrated with a graphical data base on an IRIS power series workstation. Efforts will be directed toward improving the manual-automatic control interface through a "control wheel steering" approach in which manual stick commands can be superimposed upon automatic commands without disengaging the automatic system. Improvements in HUD symbology will also be implemented.

Ames-Moffett contact: R. Coppenbarger
(415) 604-5433 or FTS 464-5433
Headquarters program office: OAET

Final Approach Spacing Tool

Tom Davis, Heinz Erzberger, Chris Brinton

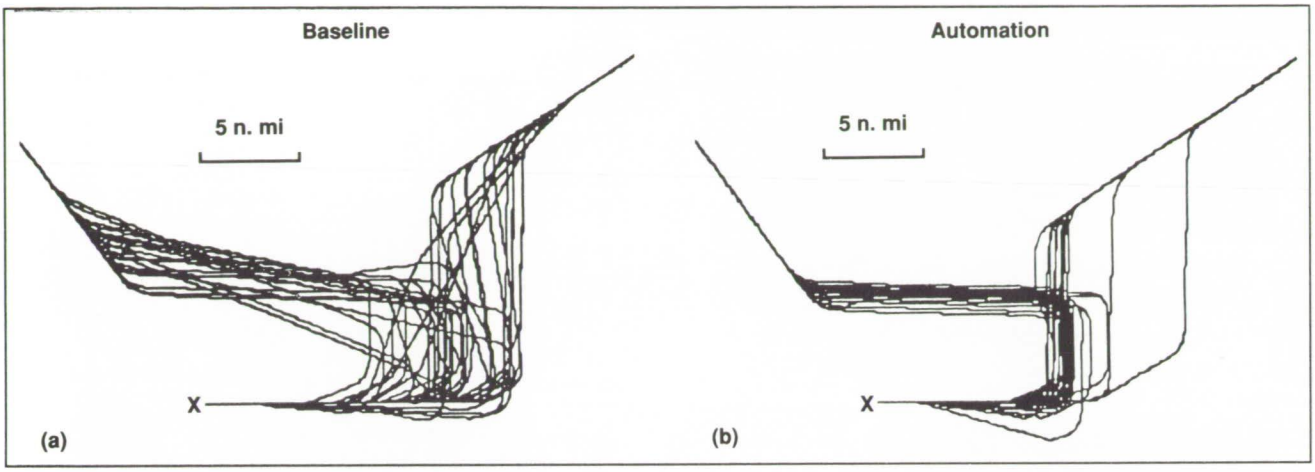


Fig. 1. Simulator evaluation of the Final Approach Spacing Tool. (a) Landing rate 38.8 aircraft per hour; (b) landing rate 43.4 aircraft per hour

The Final Approach Spacing Tool (FAST), an element of the integrated Center/TRACON Automation System (CTAS) designed at Ames, was evaluated by operational air-traffic controllers in a real-time simulation. The simulation addressed the issues of interarrival spacing at the runway, airspace utilization, and controller acceptance.

The FAST system monitors each aircraft's current state (position, airspeed, and heading) and predicts arrival time based on the local TRACON's standard arrival operations, the controller's inputs, the aircraft's performance characteristics, and current weather conditions. Based on a conflict-free scheduled arrival time at the runway, an efficient path to the runway is synthesized using speed control, path stretching, and path modification. The suggested path and speed commands are displayed to the controller automatically or by utilizing mouse-based functions through a color graphics interface.

All major components of FAST have been completed. These include (1) a trajectory synthesis algorithm which makes predictions of aircraft arrival times based on aircraft performance and weather conditions; (2) an off-route vectoring advisory capability; (3) a rescheduling capability for arrival position shifts within the TRACON; (4) a missed approach and tower en route advisory capability; (5) an interactive controller graphical interface; and (6) communications links and protocols to the Traffic Management Advisor (TMA) and Center Descent Advisor (DA) controller displays.

A real-time simulation evaluation was conducted in January 1990. Operational controllers were fed runway capacity-limited arrival rates for instrument-flight-rules (IFR) conditions with a mix of heavy and large aircraft. The evaluation demonstrated that the automation achieved a decrease of 9 seconds in interarrival spacing at the runway. This translates to an increase in landing rate of 4.6 aircraft per hour. In addition, controllers used up to 10 n.mi. in additional airspace along the final approach course when no automation advisories were available. The evaluation questionnaire showed strong controller acceptance of the FAST system and the Denver TRACON chief expressed interest in evaluating this concept.

A follow-on simulation is scheduled for July. This simulation will determine the benefits of FAST without automation in the Center (DA), and will evaluate the effects of varying wind conditions. Live traffic evaluations could be conducted as early as 1991 if the FAA chooses to approve the installation of a demonstration system.

Ames-Moffett contact: T. Davis
(415) 604-5452 or FTS 464-5452
Headquarters program office: OAET

Civil Tilt-Rotor Airworthiness Criteria

ORIGINAL PAGE
BLACK AND WHITE PHOTOGRAPH

W. Decker

Continued development of the V-22, Osprey, tilt-rotor (see the figure) for the military prompts the need to introduce a new aircraft class into the National Airspace System. Recognizing that civil operators will seek to exploit the unique capabilities of the tilt-rotor, new airworthiness criteria must be developed for this aircraft class. A series of experiments has been initiated on the Ames Research Center Vertical Motion Simulator (VMS) by a joint team of NASA, the Federal Aviation Administration (FAA), and the British Civil Aviation Authority (CAA) to address operational and airworthiness issues for tilt-rotor class aircraft.

Building upon experience gained from a series of experiments dating back to 1983 with the 13,000 pound XV-15 aircraft, a new series of experiments commenced in October 1989, with a 40,000-pound transport-category simulation model. In the first experiment, terminal-area operations were examined with a focus on the question of where to perform the reconversion from airplane mode to rotor-borne flight during approaches in instrument meteorological conditions (IMC). The well-augmented transport-category aircraft provided a less distinct preference for conversion before glide-slope intercept (versus complete conversion on glide slope) than previous studies with the less-augmented XV-15 model.

A second experiment with the transport-category simulation model was conducted on the VMS in March 1990 to examine steep approaches using raw guidance data. This operational mode could represent a backup for more augmented or automated approach aids and served to expose fundamental issues that must be resolved by those higher levels of augmentation or automation.

In this experiment it was found that raw guidance data could provide acceptable glide-slope tracking and pilot workload for IMC approaches on a 6° glide slope, but that steeper approaches produced at least some unacceptable performance. Handling-qualities issues contributing to poor performance on steeper approaches included difficulties inherent in "backside of the power curve" control and low-speed lateral-directional control in the presence of crosswinds and turbulence. In addition, the inability to see the landing spot over the nose of the aircraft on the steepest approaches (20° and 25°) was judged most disturbing to pilots.

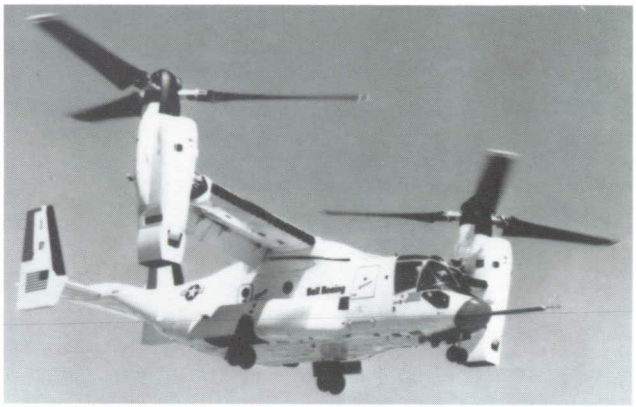


Fig. 1. V-22 Osprey

A third experiment was begun in November 1990 to examine potential task-performance and workload improvements for the IMC steep-approach task provided by a flight director or a flight-path vector display. The flight-path vector display represents application to the tilt-rotor of display technology previously developed at Ames Research Center for conventional and other vertical flight aircraft.

Ames-Moffett contact: W. Decker
(415) 604-5362 or FTS 464-5362
Headquarters program office: OAET

Design of Automation System for Terminal-Area Air Traffic Control

Heinz Erzberger

NASA has designed a set of automation tools to assist air traffic controllers in the efficient management of arrival traffic. Extensive tests of these tools in real-time simulation have demonstrated the potential for substantial increases in capacity and reductions in controller workload. The complete set of tools, referred to as the Center/TRACON Automation System (CTAS), consists of the Traffic Management Advisor (TMA), Descent Advisor (DA), and Final Approach Spacing Tool (FAST) (see the figure). The FAA has recently selected CTAS as the basis for future terminal automation and is considering field evaluations and operational implementation of this concept.

The TMA aids the flow controller in coordinating flights from multiple sectors by generating efficient landing schedules. The TMA includes algorithms, a graphical interface, and interactive tools for use by the Center traffic manager or TRACON controllers. The primary algorithm is a real-time scheduler which generates efficient landing sequences and landing times for arrivals within about 200 n.mi. from touchdown. Its graphical interface and interactive tools are designed to assist the traffic manager in monitoring the automatically generated landing schedules, to override the automatic scheduler with manual inputs, and to change scheduling parameters in real-time.

The descent advisor is a set of computer tools designed to assist the center controller in controlling descent traffic. These tools build upon the Ames-developed collection of algorithms for accurately predicting and controlling aircraft trajectories. The DA can be used whether the aircraft is on or off a standard route, and whether ATC requires an in-trail spacing or a metering mode. The DA uses a wide variety of interactive graphic features to provide a clear visual context for understanding the computed information. It provides fuel-efficient and conflict-free descent clearances, adapted to aircraft type, to meet TMA-generated landing times.

FAST assists TRACON controllers in sequencing and spacing aircraft for maximum runway throughput. It predicts time to the runway by using each aircraft's performance characteristics, current winds, and expert controller rules for choosing the most desirable approach path. Based on the landing time specified by the TMA, FAST synthesizes a speed profile and horizontal path. Aircraft heading and speed advisories are displayed utilizing color graphics symbols.

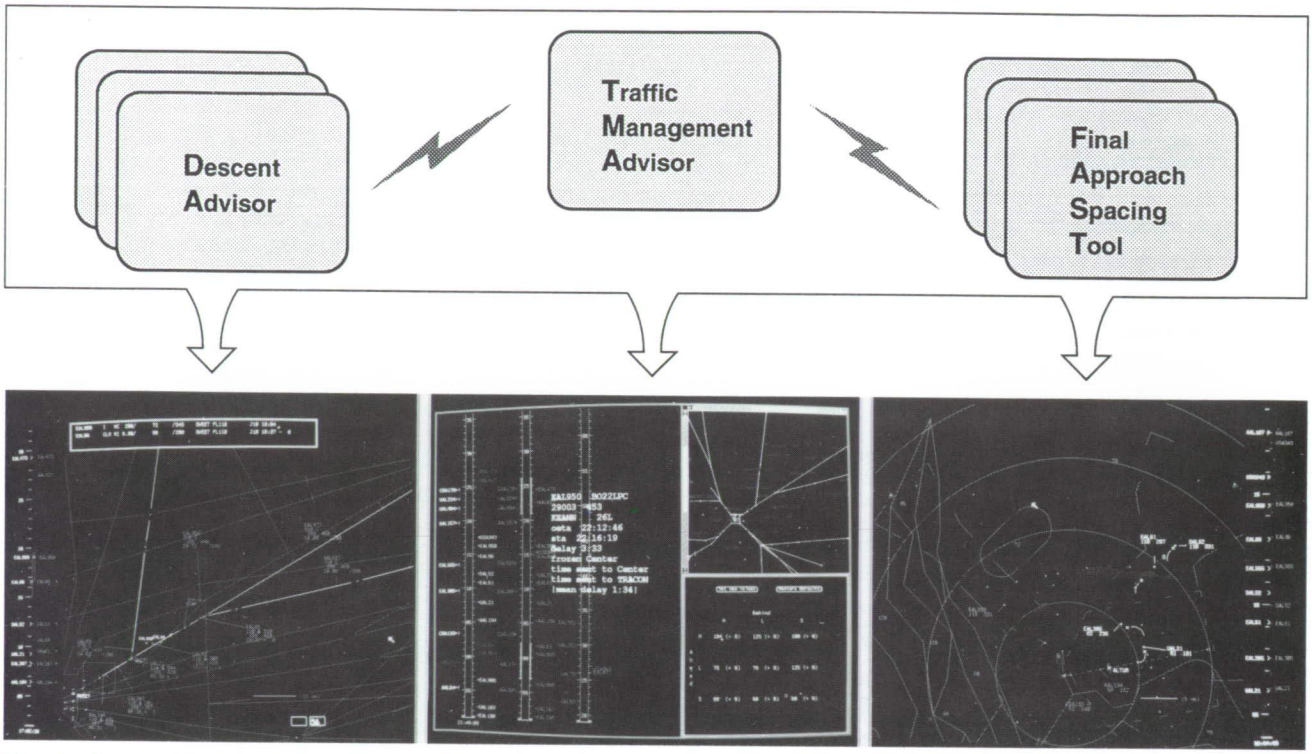


Fig. 1. Center/TRACON Automation System

A multisector Center/TRACON implementation of this system is operational in the ATC Simulation Laboratory at Ames. The Laboratory is a facility for real-time simulation of advanced ATC systems which can have controllers and airline pilots as evaluation subjects. In addition, the facility is capable of receiving live traffic data from a Center/TRACON so that current operations can be observed and integrated with simulated traffic.

Ames-Moffett contact: H. Erzberger
(415) 604-5425 or FTS 464-5425
Headquarters program office: OAET

RASCAL In-Flight Simulator

ORIGINAL PAGE
BLACK AND WHITE PHOTOGRAPH

M. Eshow, J. V. Lebacqz, D. C. Watson, W. Hindson

The Rotorcraft Aircrew Systems Concepts Airborne Laboratory (RASCAL) is being built up from a UH-60 Black Hawk helicopter at the Ames Research Center (see the figure). It will have a variable-stability capability to allow in-flight validation of integrated controls research and automated nap-of-the Earth guidance concepts for enhanced maneuverability, agility, and operational effectiveness. Progress toward the development of the RASCAL research systems continued in 1990 with further concept definition and preliminary design of key system components.

The concept-definition phase focused on the requirements for control-system failure detection and recovery, control-system performance, on-board computation, sensors, and displays. The preliminary design then provided candidate near- and far-term system architectures to link the various components for the fulfillment of safety and performance requirements. The major components considered for the preliminary design were the computers, sensors, failure monitors, and busing architecture. Implementation of the preliminary design began in 1990 with the procurement of an inertial navigation sensor and a laboratory version of the candidate flight-control computer.

The detection of failures in the fly-by-wire variable-stability system is crucial to the safety, airworthiness, and research flight envelope of the vehicle. During research operations, an evaluation pilot will fly the aircraft through the computers to the fly-by-wire research actuators, while the safety pilot monitors the corresponding movement of his mechanical controls. In the event of a failure in the research system or an unsafe flight condition, the safety pilot disengages the fly-by-wire system and resumes control of the aircraft through the mechanical control system. The role of the failure monitors is to detect failures before the safety pilot senses them and to return control to the safety pilot with minimal aircraft transients.



Fig. 1. RASCAL UH-60A helicopter

In order to define the specific performance requirements of the failure monitors, a piloted simulation was conducted on the Ames Vertical Motion Simulator. Failures were inserted into a model of the variable-stability system and notional failure monitors of varying performance capability were implemented to return control to the safety pilot. A subjective rating scale was developed to allow the pilot to express his perception of the severity of the failure and his ability to recover from it. Several hundred evaluations were conducted documenting acceptable monitor performance as a function of fly-by-wire actuator performance, task, and flight condition. A paper describing the results and the use of the failure rating scale was published this year.

Analysis of the simulation results has provided design goals for the RASCAL failure-monitoring system. Bench tests using actuator and monitor hardware are being conducted at Ames to determine how to achieve those goals. In addition, a second simulation will be conducted in 1991 to include more detailed design features of RASCAL and to further validate the monitoring concepts resulting from the bench tests.

Ames-Moffett contact: M. Eshow/V. Lebacqz
(415) 604-5272/5009 or FTS 464-5272/5009
Headquarters program office: OAET

Control Research on the V/STOL Research Aircraft

John D. Foster

Major technological barriers to routine vertical landing operations of vertical and short takeoff and landing (V/STOL) fighter-class aircraft occur in adverse weather and low-visibility conditions. These barriers are (1) the complex interaction of kinematics, aerodynamics, and propulsive forces and moments during the conversion from airborne to jetborne flight; and (2) the resulting poor handling qualities and limited control authorities that these interactions create. Ames Research Center is conducting a flight research program to integrate the propulsive and aerodynamic controls in ways that provide enhanced flight-path precision and mission capability but that minimize the design requirements for "extra" propulsive capability (e.g., bleed-air requirements).

The Flight Systems and Simulation Research Division is developing an integrated attitude and thrust-vector control system to be flown on the YAV-8B V/STOL Research Aircraft (VSRA) Harrier. The system, outlined in the figure, will be fly-by-wire with mechanical backup and will use two flight computers to provide fail-safe operations. It will provide (1) new display capabilities, which would assist a pilot in guiding his aircraft from forward flight to hover and vertical landing on small ships or

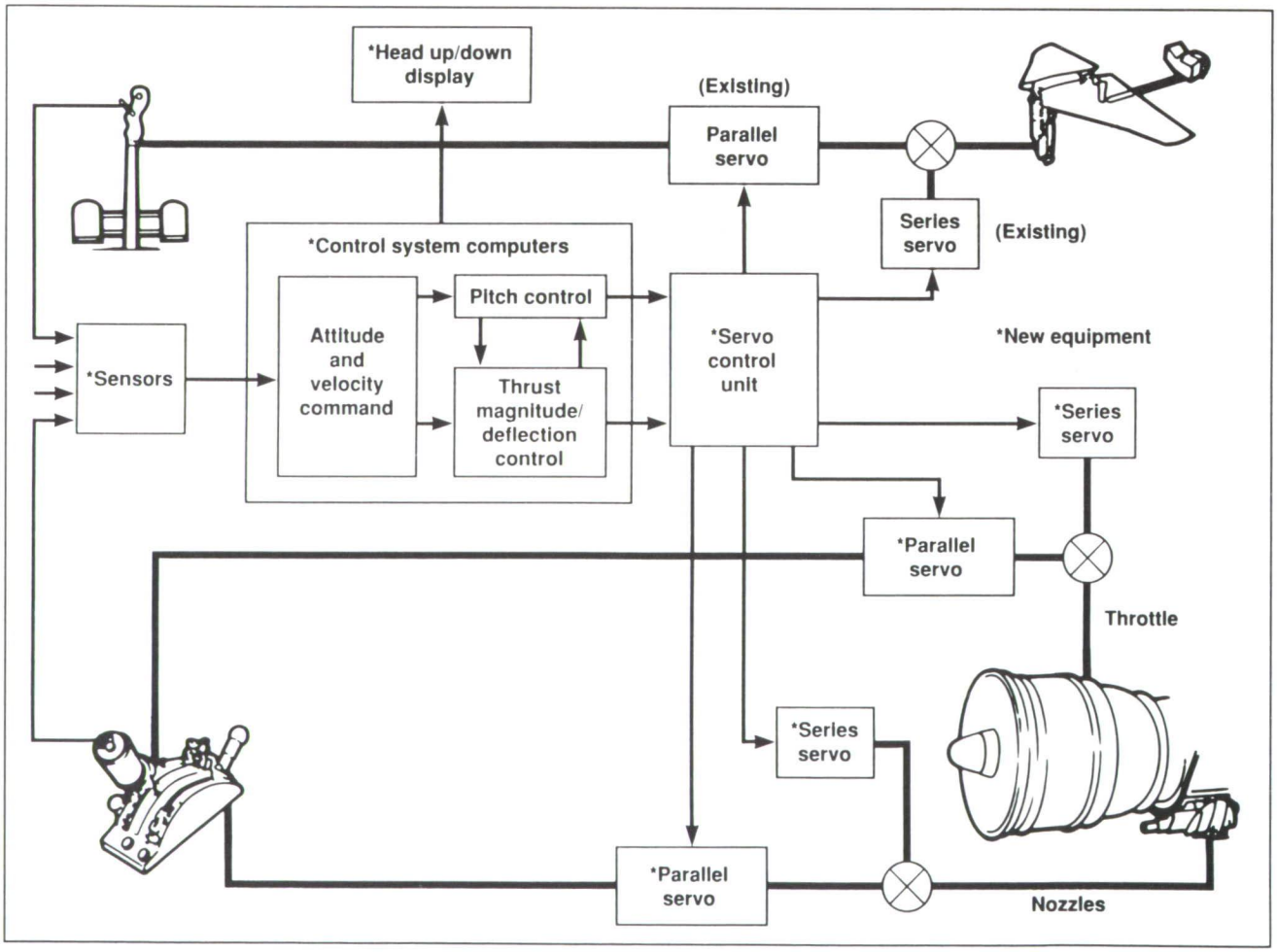


Fig. 1. V/STOL Research Aircraft integrated flight/propulsion control system (longitudinal/vertical channel)

confined sites; and (2) automatic integration and management of the thrust of the jet engine and its movable nozzles, which would enable the pilot to successfully land at these sites.

This year several significant development milestones were reached.

1. A major hardware goal was achieved with the installation and checkout of the new research system, including heads-up and panel-mounted displays driven by a programmable symbol generator, dual flight computers to control the displays and the engine and airframe controls, dual sensors to include ring-laser-gyro inertial navigation units to drive the flight computers, and a data telemetry system to send data to a ground station for on-line monitoring and later analysis. The installation effort, which included extensive electrical wiring as well as design and fabrication of electronic equipment racks to fit the limited space available, was accomplished by the in-house Ames staff.
2. A major software goal was achieved with the completion and checkout of flight software for the flight guidance/display experiment and flight evaluation of the redundant sensors and state estimator for the integrated controls phase of the program. This task included all software interfaces to the various sensors (Mil-1553B data buses, Arinc 429 and 568/582 buses and analog sensors), as well as a parallel processing capability which allows separation of the research software (controls, displays, state estimation) from the system input/output functions into separate processors. The flight software was developed by an in-house staff using structured software design methods.
3. A successful post-maintenance check flight was completed in November of 1990. The objectives of the flight were to verify proper operation of the basic Harrier aircraft after the major disassembly and modifications that were required to install the research system, and to establish the basic operation of the research system. The aircraft was flown throughout its complete flight envelope, from hover to 400 knots and from inverted flight to positive 4 g's, with all system checks successfully completed. The research system was operated during the complete flight. The system was shut off in flight and successfully restarted, and the heads-up display modes for transition and hover functioned successfully.

The VSRA will now undergo a series of flight checkouts to calibrate the system operation. An approach and hover guidance display flight experiment will be conducted after the checkout is complete. When the display experiment is completed, new servo actuators will be added next year to allow control of the jet engine's thrust and vectoring nozzles by the flight computers.

Ames-Moffett contact: E. Moralez
(415) 604-6002 or FTS 464-6002
Headquarters program office: OAET

Control-System Concepts and Design Criteria for STOVL Aircraft

J. Franklin

Following previous fixed-base simulation experiments on supersonic short takeoff and vertical landing (STOVL) aircraft reported in 1988 and 1989, the Vertical Motion Simulator was used to (1) evaluate flying qualities for integrated flight/propulsion controls for transition, hover, and landing, (2) develop transition acceleration criteria, (3) establish the influence of ground effect and hot-gas ingestion on thrust/weight required for vertical landing, and (4) document control power use and system-dynamics characteristics for powered-lift operation.

The influence of integrated flight/propulsion control modes on handling qualities during transition, hover, and landing was substantiated for land-based and shipboard operations. Effects of forward speed and control modes on flying qualities for rolling vertical and slow landings were established. Transition acceleration requirements were defined, including the effects of jet-induced aerodynamics, thrust-vectoring efficiency, and excess thrust. Thrust margins were defined for vertical landing as a function of ground effect and hot-gas ingestion, including requirements for sink-rate control and landing abort, and for manual and velocity command control modes. Pitch, roll, and yaw control-power utilization, including reaction control bleed, the influence of thrust transfer rates and engine dynamic response, and the interface of side-stick control inceptors with control modes were established for powered-lift operations. Contributions of simulator motion cues were identified for the various control tasks.

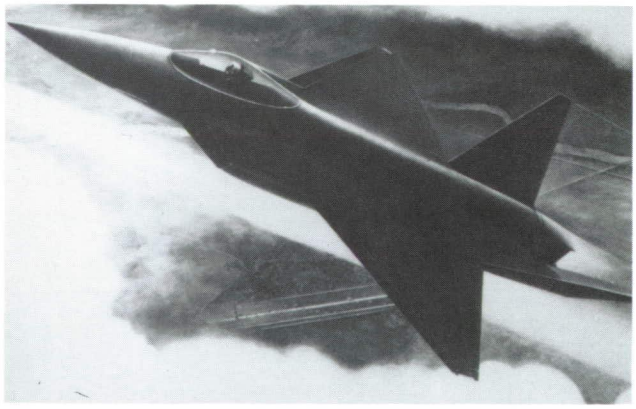


Fig. 1. Mixed flow remote lift STOVL aircraft

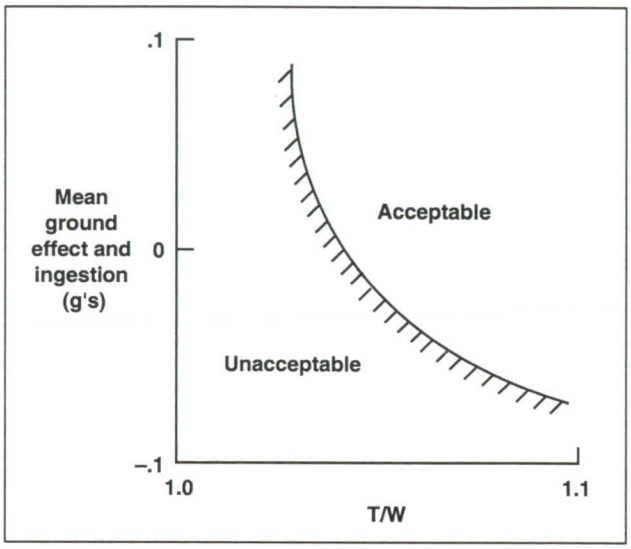


Fig. 2. Influence of ground effect and hot gas ingestion on thrust margin for vertical landing

Ames-Moffett contact: J. Franklin
(415) 604-6004 or FTS 464-6004
Headquarters program office: OAET

Four-Dimensional Aircraft/Air Traffic Control Operations Study

Steven Green

A real-time simulation was conducted to evaluate the effectiveness of the Ames-developed Center/TRACON Automation System (CTAS) in assisting controllers with the management of mixed traffic (four-dimensional equipped and unequipped aircraft), and the effect of CTAS on piloted four-dimensional equipped aircraft operations. This air traffic control (ATC) experiment is unique in that it was the first joint simulation involving both the Ames and Langley research centers.

The focus of the experiment was to study the operational issues concerning the handling of four-dimensional equipped aircraft in the arrival flow. The real-time ATC simulation facility at Ames was used to create the ATC environment and traffic scenarios for the controller test subjects (see the figure). The major components of the ATC simulation included (1) the pseudo-pilot simulation, which generated and controlled the air traffic; (2) the traffic management advisor (TMA), which scheduled all traffic for coordinated flow between the Center sectors and TRACON; and (3) the descent advisor (DA), which provided the Center controllers with a variety of automation tools for the sequencing of traffic.

The final approach spacing tool (FAST), which assists in TRACON operations, was employed in an auxiliary capacity to study the TRACON flows generated by the Center arrival activity. The Langley TSRV 737 piloted simulator was used to introduce four-dimensional traffic into the arrival flow. The Ames and Langley facilities were connected via transcontinental voice and data links. This experiment employed six active Center controllers as test subjects, working in teams of two. The pilot subjects, used by Langley for the TSRV, were current B-737 captains from several major air carriers.

It was determined that the accommodation of a four-dimensional aircraft in the arrival flow requires careful coordination of procedures between the pilot and the controller. Otherwise, conflicts may develop that add to the controller's workload. Special emphasis was placed on the development of efficient, yet effective, procedures and phraseology for four-dimensional operations. However, the experience of the simulation leads to the broad conclusion that a ground-to-air data link may be required for proper integration.

Overall, the response from the controller subjects was favorable: they strongly encouraged the development and operational implementation of the ground-based automation tools. The controllers were quite enthusiastic about the four-dimensional capabilities demonstrated by the TSRV and they appreciated how airborne four-dimensional capabilities could improve the efficiency of air traffic control.

The simulation demonstrated the capability of the ATC Automation Laboratory to examine complex issues in the design of future ATC concepts. Results from this study have been presented at several technical meetings and seminars.

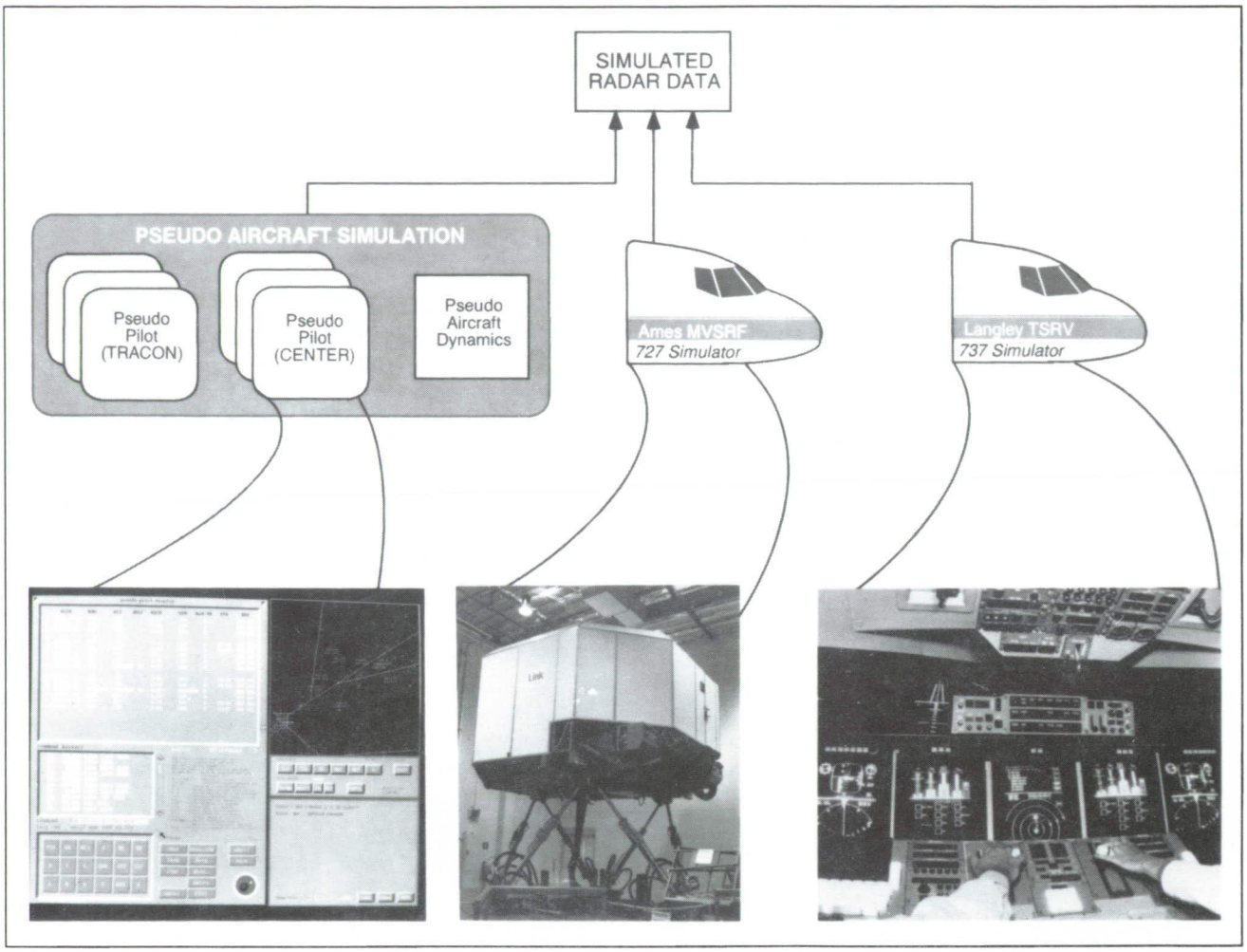


Fig. 1. Air traffic simulation

Additional simulations are planned to further refine the automation tools and procedures, as well as to develop new capabilities such as a simulation of an air-to-ground data link and advanced four-dimensional pseudo-aircraft. The long-term goal, however, is to prepare the automation tools for evaluation in live traffic.

Ames-Moffett contact: S. Green
(415) 604-5431 or FTS 464-5431
Headquarters program office: OAET

ORIGINAL PAGE
BLACK AND WHITE PHOTOGRAPH

Terminal-Area Operations with the NAVSTAR Global Positioning System

B. David McNally, Thomas Schultz

The NAVSTAR Global Positioning System (GPS) is a constellation of 24 satellites that provides 16-meter Precision Military Code (P-code) navigation accuracy, and 100-meter Clear Acquisition Code (C/A-code) accuracy. Local corrections to satellite range measurements uplinked to the aircraft are the basis of differential GPS (DGPS) navigation, which provides an even more precise position solution. Three-meter-or-better accuracy is expected with the current P-code receivers navigating in the differential mode.

The C/A code has been shown to achieve 10-meter accuracy in a differential configuration. Even greater accuracies are achievable by tracking the carrier frequency. Because of the significant improvement in accuracy attainable with DGPS, NASA has entered into a joint program with the Department of Defense (DOD) and the Federal Aviation Administration (FAA) to determine the actual improvement based on flight evaluations and to develop operational procedures for making effective use of the DGPS capability.

The project is divided into two distinct phases. Phase 1 will evaluate the differential capability of the NAVSTAR GPS to provide precise three-dimensional positioning information using the P-code of the NAVSTAR GPS in terminal approach and control operations (see the figure). Phase 2 will

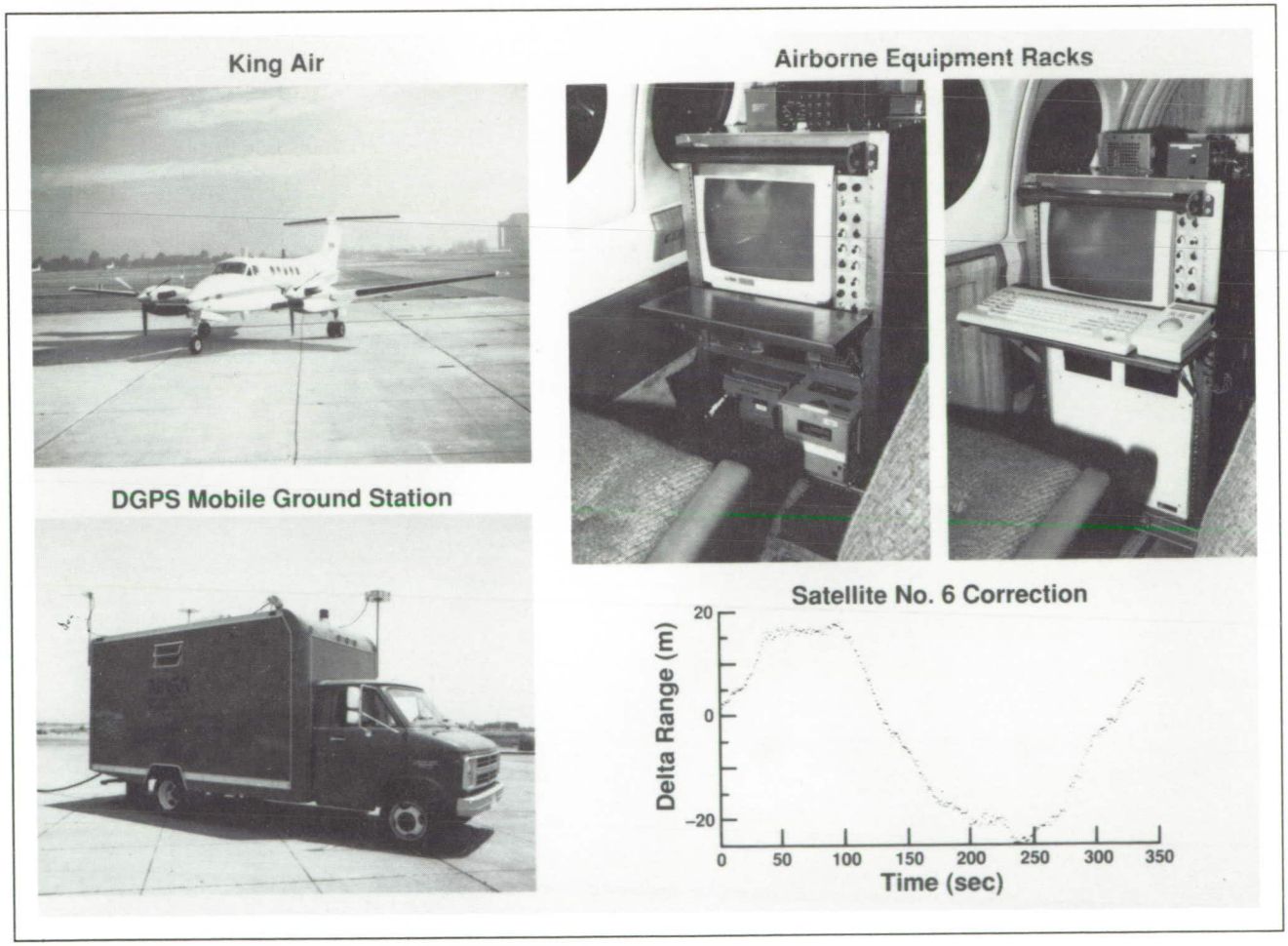


Fig. 1. Terminal approach operations for Global Positioning System

ORIGINAL PAGE
BLACK AND WHITE PHOTOGRAPH

evaluate operational uses of differential GPS in the civil environment, including approach and landing, and procedures to support more efficient air traffic control (ATC) operations. A major research activity will be aimed at developing techniques for tracking the carrier frequency in flight in order to achieve even greater navigational accuracy in support of precision approach and landing guidance.

Hardware components including three P-code GPS receivers, two inertial navigation units, and three VME-based research computers have been installed and tested in the laboratory, airborne, and ground systems. Key software modules including sensor interface, real-time data display and collection, and truth-data collection have been developed and tested. Primary components of the airborne and ground reference systems were installed in a NASA twin turbo-prop aircraft (NASA 701), and a mobile ground reference station. Initial flight tests were completed at the Crows Landing facility. Nineteen approaches in three flights were flown during the period from April 20 to May 8, 1990. The test aircraft was tracked by laser and radar during testing to provide the true position solution.

During the next several months more of the DGPS system software will be developed. Particular emphasis is being placed on development of a navigation filter which integrates information from the GPS receiver and the inertial navigation unit. Initial flight tests of the fully integrated DGPS system were conducted in December 1990. Real-time navigation and guidance system evaluation flight tests are scheduled for April 1991.

Ames-Moffett contact: D. McNally
(415) 604-5440 or FTS 464-5440
Headquarters program office: OAET

ORIGINAL PAGE
BLACK AND WHITE PHOTOGRAPH

Display and Guidance Improvements for AV-8B Harrier

Vernon Merrick, Ernesto Moralez

Current AV-8B Harrier vertical landing operations at land-based sites and ship decks are performed using a combination of one-step engine nozzle movement, engine-thrust modulation, and aircraft attitude changes to modulate aircraft deceleration and bring the aircraft to a hover. The specific point in the approach at which the engine nozzle is moved to the vertical position is left to pilot judgment. This judgment depends largely on the airspeed, wind speed, and visual cues, with the added restriction of performing the decelerating approach below the cloud ceiling.

The weather minima used for AV-8B landing operations are currently 1/2-nautical-mile visibility and 200-foot cloud ceiling for shipboard landings, and 1-nautical-mile visibility and 300-foot ceiling for land-based sites. In these poor weather conditions and at night, the pilot's visual cues are correspondingly degraded, and the resulting approach is less precise; with nighttime shipboard operations, there is the added difficulty of determining the range rate relative to the ship.

As part of the first phase of the NASA V/STOL Research Aircraft (VSRA) program, an exponential speed guidance law was formulated which mimics the approach technique currently used by Harrier pilots. A simulation evaluation of this law, flown by Ames research pilots with Harrier experience, was conducted using 1/4-nautical-mile visibility and 100-foot cloud ceiling weather conditions. The law will be tested in flight using the VSRA, which is a YAV-8B Harrier that has been modified for V/STOL controls and display research.



Fig. 1. AV-8B Harrier

The favorable results of the simulation have generated sufficient U. S. Marine Corps interest to warrant additional planned evaluation of the guidance law in both a TAV-8B (two-seat trainer) and an AV-8B (see the first figure). Two of the key VSRA Head-Up Display (HUD) symbol elements will be added to the existing AV-8B HUD. The first element is a ghost aircraft with which the pilot flies in formation. This ghost aircraft flies a perfect approach ahead of the pilot's aircraft. The second element is an acceleration error ribbon that indicates to the pilot (1) when to rotate the thrust-producing nozzles to the vertical position, and (2) the subsequent pitch attitude necessary to track the speed of the ghost aircraft for smooth, precise deceleration to a hover (see the second figure). In addition, the symbol drive-law logic for the existing AV-8B flight-path symbol will be modified to incorporate improvements developed for the VSRA.

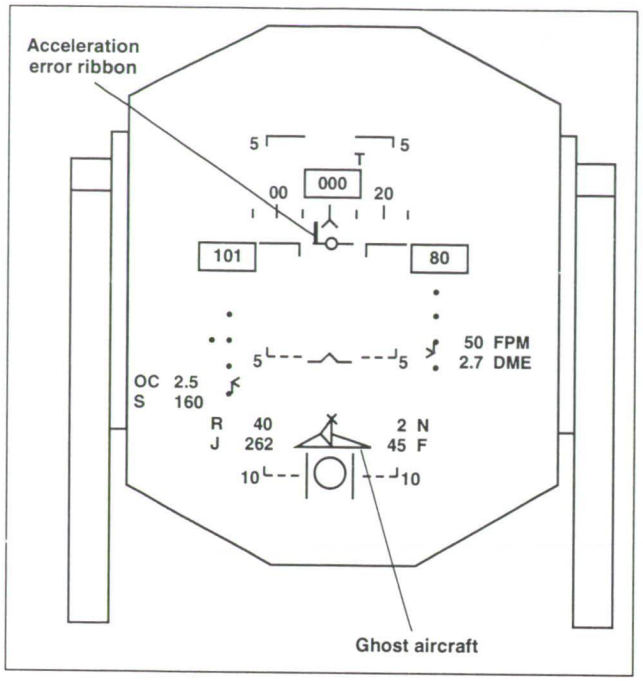


Fig. 2. Ames modifications to AV-8B head-up display

A recent meeting of representatives from the Marine Corps, the Naval Weapons Center, NAVAIR, the Naval Air Test Center, McDonnell Aircraft, and NASA developed the approach, responsibilities, and preliminary hardware and software modifications required for flight testing. The symbol and drive-law descriptions have been delivered to McDonnell Aircraft and to the Naval Air Test Center for incorporation in their AV-8B simulation facilities. After acceptance by the contractor, the necessary aircraft modifications will be made at China Lake Naval Weapons Center for flight testing.

Ames-Moffett contact: E. Moralez
(415) 604-6002 or FTS 464-6002
Headquarters program office: OAET

Optimal Scheduling/Sequencing of Aircraft Traffic

Frank Neuman

The function of the aircraft-traffic scheduling algorithms is to plan automatically the most efficient landing order and to assign optimally spaced landing times to all arrivals. Several scheduling algorithms were initially implemented in a fast-time simulation, and the statistical performance of the scheduling algorithms was determined.

The most straightforward scheduling method assigns the landing order on a first-come first-served basis (FCFS). In this method, after aircraft enter the Center, they are scheduled in the order they are predicted to land, using a nominal path, flight plan, preferred descent speeds, and altitude profiles. The FCFS scheduler adds appropriate delay times to insure proper spacing, which depends on the weight classes of the aircraft.

An effective method of reducing the average delay time without changing the order of the aircraft is "time advance" (TA). This method recognizes the beneficial effect of occasionally speeding up an aircraft during periods of heavy traffic in order to reduce gaps that naturally occur in FCFS schedules (see the first figure).

Separation requirements differ for different types of aircraft trailing each other. Advantage is taken of this fact through mild reordering of the traffic, to shorten the groups, thereby improving on the FCFS and TA methods by minimizing the average delay per aircraft. A sequencing and scheduling optimizing method called constrained position shifting (CPS), which considers switching the FCFS order of landing for adjacent aircraft, was developed several years ago (see the second figure).

The CPS method makes several assumptions that cannot be fulfilled in an operational system. However, analysis of the results for an optimal

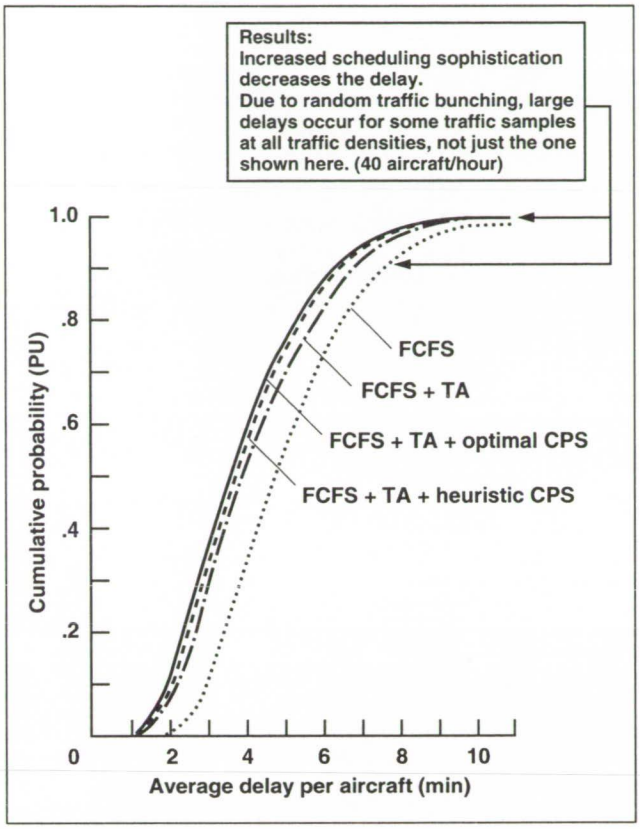


Fig. 1. Cumulative distributions of average delay/ aircraft in a traffic sample; 40 aircraft/hour, sample size 1.5 hours

single-position-shift CPS permitted the design of a heuristic CPS.

These methods of scheduling, FCFS, TA, and heuristic CPS, have been implemented in a Traffic Management Advisor (TMA) Station, which is part of an automated system for management of arrival traffic. The scheduler in this system permits the selective use of any of these scheduling schemes.

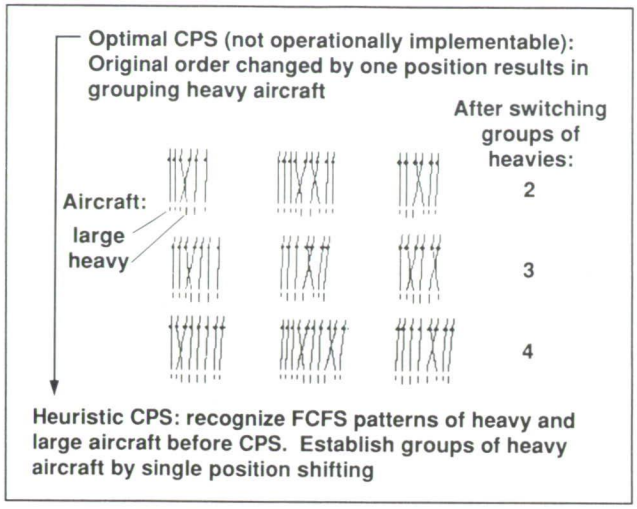


Fig. 2. Constrained position-shift examples

Fast-time simulation was used to statistically evaluate the scheduling methods which are implemented in the TMA by using a large number of realistic traffic samples to determine their overall effect on aircraft delays. Additionally, the fast-time simulation is used to show the effects of other variables on delays such as traffic distributions, lengths of traffic samples, and winds. Actual delays for different samples with the same statistical parameters vary widely, especially for heavy traffic.

Ames-Moffett contact: F. Neuman
(415) 604-5437 or FTS 464-5437
Headquarters program office: OAET

In-Flight Display Research for Hovering and Landing

Jeffery A. Schroeder, Vernon K. Merrick

A flight evaluation of a previously simulated display concept was conducted on the NASA/Army CH-47 Variable Stability Research Aircraft. The display concept applies to flight vehicles that hover. Hovering vehicles, depending on the type of control system utilized, can be difficult to fly even in conditions with good outside-the-window visibility. This display concept, however, extends the operational envelope of these aircraft by allowing the pilot to fly the aircraft using only the essential flight information presented on the display. Thus, the pilot does not have to look outside the aircraft, and can land in zero visibility.

The display, shown in the figure, combines status and command information in two viewing perspectives to the pilot: horizontal and vertical. In the horizontal perspective, aircraft status information is provided in a plan view of the aircraft that shows the horizontal vehicle position and velocity relative to a desired landing pad. The velocity is shown as a line from the center of the display which represents its magnitude and direction.

In the same plan view perspective, command information is provided to the pilot in the form of a velocity-predictor symbol (shown as the largest circle at the end of the velocity vector in the figure). The pilot positions this predictor symbol in order to control the vehicle velocity. At constant velocity, the predictor symbol and the velocity vector coincide. Thus, the pilot can control the vehicle velocity by using his stick to cause the velocity predictor symbol to remain in a pilot-chosen place on the display.

The vertical perspective shows the aircraft height above the ground in addition to a command diamond that blends aircraft vertical velocity with vertical command lever (collective or throttle) information. Proper blending eases the pilot workload in the vertical control of the aircraft. This vertical perspective is superimposed on the horizontal perspective, and has previously raised concerns over its potential success.

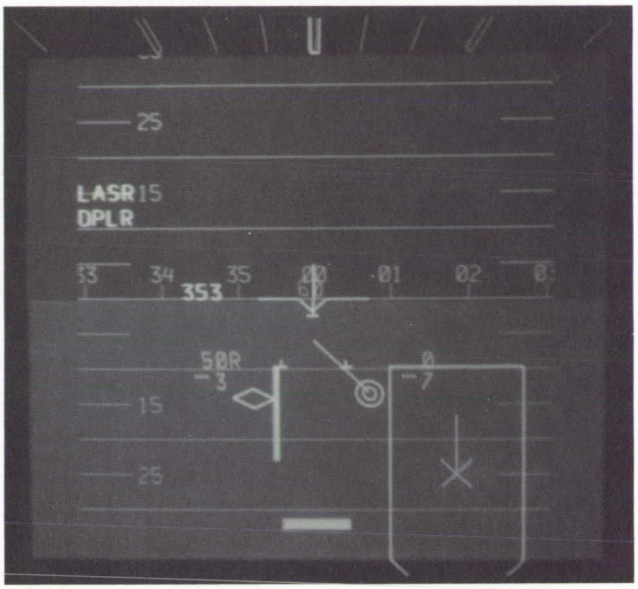


Fig. 1. Hover and landing display

The horizontal perspective concept is used in the AH-64 Apache helicopter, and NASA and the Army are improving this method by changing the logic that drives the velocity-predictor symbol. By carefully considering the vehicle-plus-control-system response to pilot inputs with known models of pilot behavior, a velocity predictor can be designed that is both easy to fly and that results in a good aircraft response as a result of the pilot controlling the predictor.

As part of the development of this new design philosophy, an analysis procedure was developed that incorporates the four important elements to be considered in display design: the control system dynamics, the display dynamics, the guidance strategy, and the pilot. With this analysis procedure, controls and displays can be easily compared with each other prior to either simulation or flight.

Flight evaluations of this new predictor design were made by three NASA test pilots. Three different control systems were evaluated with the predictor design accounting for each control system. The display was presented on a color cathode-ray tube on the instrument panel. The evaluation pilot's windows in the CH-47 were obstructed, and the pilot wore an instrument hood to block his vision of the outside world. Thus, the helicopter was flown using only information presented on the display and none from the outside world.

Landings to touchdown were flown from 40-foot offsets horizontally and vertically. Landings to within 2 feet of the desired touchdown point were made for over half of the attempts for two of the three control systems. This landing accuracy in instrument conditions has not been achieved prior to this experiment.

In addition to validating the new predictor design, this flight experiment also showed that existing sensors will allow the landing accuracies described. The flight experiment also demonstrated that the superposition of the horizontal and vertical perspectives is feasible.

Ames-Moffett contact: J. Schroeder/V. Merrick
(415) 604-4037/6194 or FTS 464-4037/6194
Headquarters program office: OAET

Validation of Vision-Based Obstacle-Detection Algorithms Using Flight Data

Phillip Smith, Banavar Sridhar

The objective of this project is to develop a data base from flight test measurements that will allow verification of computer vision-based obstacle-detection and passive range-estimation algorithms for use in pilot-aiding during rotorcraft nap-of-the-Earth (NOE) flight.

Research in image-based obstacle detection and passive range estimation has led to the development of several candidate algorithms. A real-world data set based on actual flight data is necessary for further developing and evaluating these algorithms for use in NOE applications. In the absence of available real-world rotorcraft data which integrate the required data components, the NOE Image and Truth (NOE-IT) Data Acquisition Test Flight Project has been undertaken to develop data necessary for implementation and validation of a computer vision-based obstacle-detection system.

Implementation of the system will require three major data components: (1) video imagery data, (2) motion states of the video camera, and (3) camera calibration parameters. Validation requires direct measurements of the obstacle range relative to the rotorcraft for comparison with the results of the vision-based passive ranging algorithms. In addition, the video imagery, motion state measurements, and true range information must be correlated with respect to time (see the figure).

NOE-IT employed an instrumented Boeing CH-47B Chinook (NASA 737) as a test-bed on which a video camera and recording equipment were installed to provide the imagery data. Rotorcraft motion was obtained from the inertial navigation unit and other on-board instruments whose output was transmitted to a ground station. With the results of

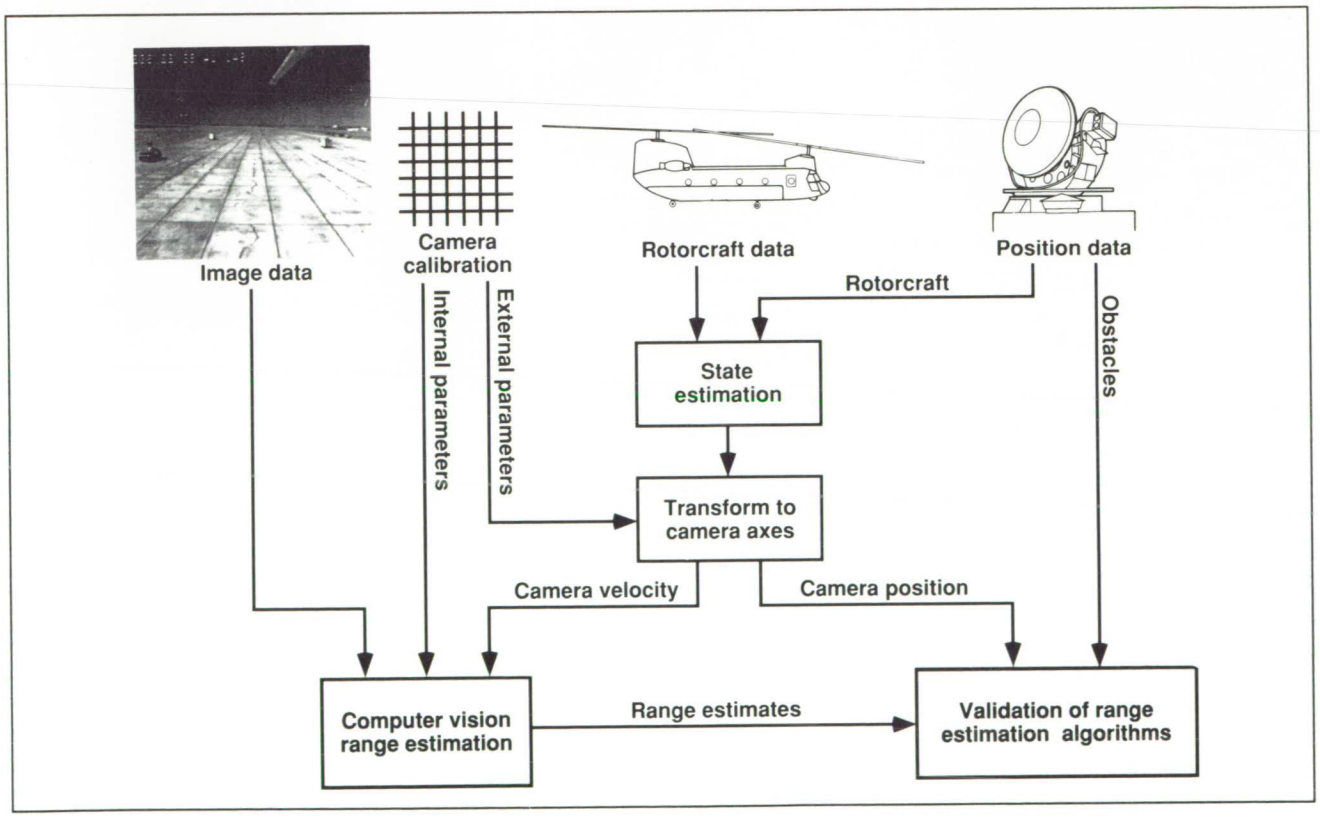


Fig. 1. Validation of vision-based obstacle-detection algorithms using flight data

the camera calibration analysis, the camera motion states can be derived from the directly measured rotorcraft motion. Laser tracking provides ground-truth measurement of the rotorcraft's location while both laser tracking and surveying provide the obstacle locations to complete the data set.

Significant post-flight processing is required to transform the raw measurements collected during test flight into a form suitable for the validation of passive range-estimation algorithms. Calibration of the camera is necessary to accurately determine its position and orientation with respect to the helicopter body axes so that rotorcraft-state measurements may be transformed into the camera's axes system. Camera calibration is also used to determine the camera's internal properties, such as the focal length, which are used directly by the vision algorithms. State-estimation techniques are required during post-flight processing to ensure internal consistency among rotorcraft-state measurements before algorithm validation can be undertaken.

Since completion of the NOE-IT test flights in August 1989, a full camera calibration analysis has been performed leading to the development of a new calibration method, and state-estimation techniques have been employed to ensure internal consistency among rotorcraft state measurements. Current efforts focus on the completion of consistency checking between the video imagery, camera motion, and true range measurements to demonstrate integrity of the data set before its use in research and validation activities.

Ames-Moffett contact: P. Smith
(415) 604-5469 or FTS 464-5469
Headquarters program office: OAET

Integrated Stereo/Motion Vision for Obstacle Detection

Banavar Sridhar, Ray Suorsa

The objective of this program is to develop obstacle-detection algorithms for the autonomous guidance of vehicles and, in particular, for rotorcraft nap-of-the-Earth (NOE) flights. The reliable detection of obstacles is a key element in advancing the automation of rotorcraft. The obstacle-detection approach is based on the maximal use of passive sensors, such as low-light-level television (LLLTV) cameras, forward-looking infrared (FLIR), and others.

Range information about the objects can be computed by taking a sequence of images from a single sensor and combining the optical flow resulting from the sensor motion with vehicle states from an inertial navigation system. However, the range information provided by a single passive sensor is sensitive in the direction of flight, which is referred to as the focus of expansion. This problem can be overcome by the use of more than one sensor, which is referred to as a stereo method.

Research in this area has focused on quantifying the errors in motion and stereo methods and on ways to combine stereo and motion information in a complementary manner. Assuming off-the-shelf cameras a meter apart on a helicopter, stereo performs better than motion for all objects within 3° of the direction of flight. Motion performs better than stereo whenever the camera moves 10 to 20 meters between images.

The figure shows how the ratio of motion-to-stereo-error varies as the ratio of the distance

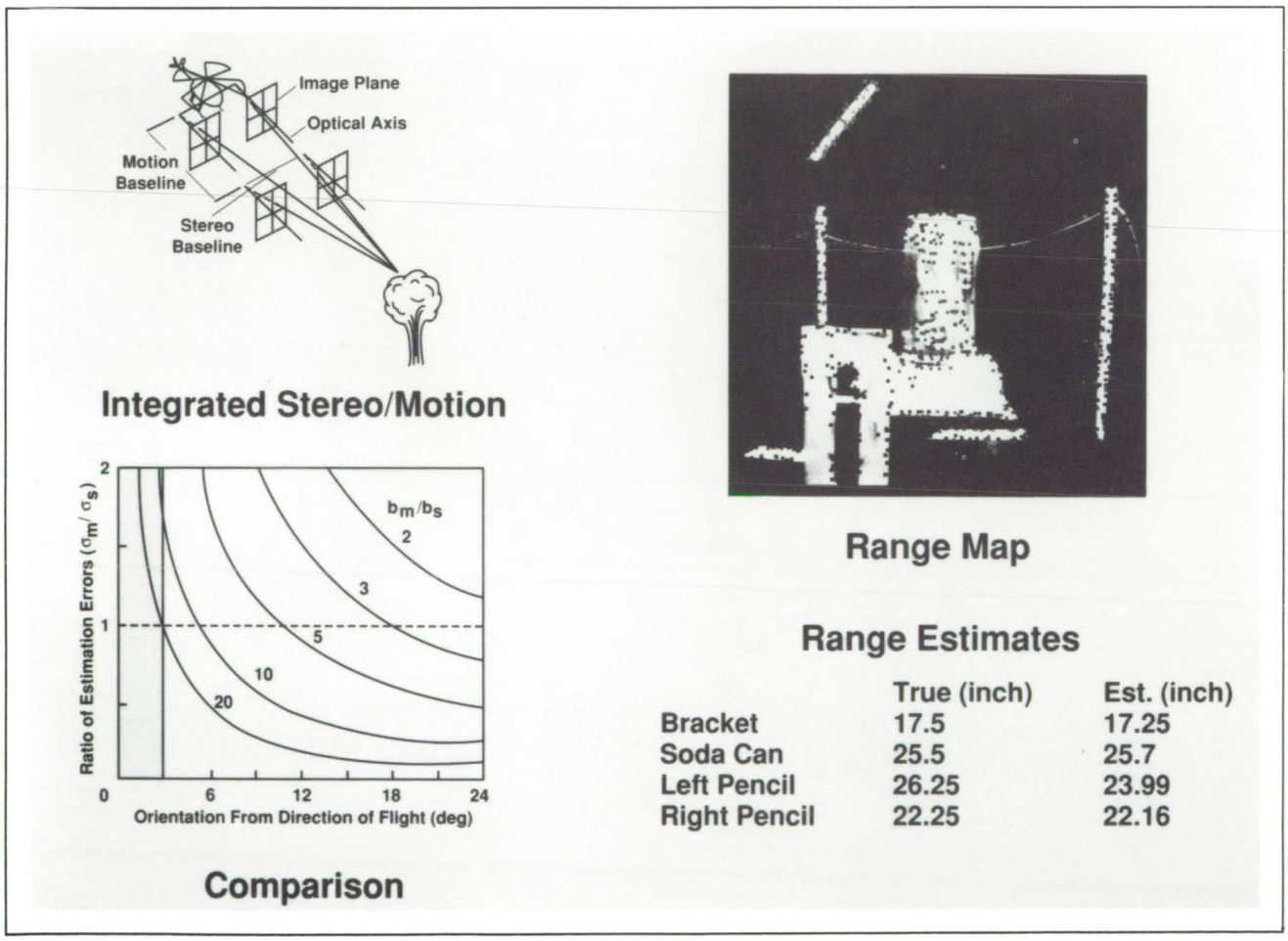


Fig. 1. Integrated stereo/motion vision for obstacle detection

between the camera positions in motion to the distance between the cameras in stereo. The combination of motion and stereo methods will provide better range estimates over a field of view of interest in helicopter flight.

Significant accomplishments during this year include (1) quantitative comparison of stereo and motion methods for a low-altitude helicopter flight scenario; (2) development of a recursive stereo algorithm; and (3) an integrated stereo and motion method based on an extended Kalman filter. The Kalman filter provides a natural setting to combine the information from the two sensors. The results of this research were presented at the 1990 American Control Conference.

The obstacle information provided by the integrated approach needs to be augmented by other techniques, such as scene analysis, to provide more complete obstacle information.The plan for next year includes integration of stereo, motion, and scene analysis to provide more complete obstacle information and the validation of these algorithms by using both laboratory and flight data.

The obstacle detection resulting from this effort will provide an initial range map for use by rotorcraft obstacle-avoidance algorithms and can be considered as a candidate for detecting hazards during the terminal descent phase of a Mars landing.

Ames-Moffett contact: B. Sridhar
(415) 604-5450 or FTS 464-5450
Headquarters program office: OAET

Laboratory for Vision-Based Detection Research

Raymond Suorsa, Banavar Sridhar

The objective of this project is to design and integrate the necessary components for a network-based image processing environment to develop and validate obstacle-detection algorithms useful for pilot-aiding during rotorcraft nap-of-the-Earth (NOE) flight.

The goal of the NOE vision group is to demonstrate the feasibility of machine-vision-based obstacle detection and avoidance for fully instrumented rotorcraft. To perform the necessary research, an image processing environment was needed that could generate, store, and retrieve large sequences of multicamera images with complete motion information of the camera stored with each image. Additionally, routine low-level image processing, image display, and data-visualization software were needed to support image-processing research.

The hardware in the laboratory consists of Sun workstations and a Silicon Graphics workstation, all running UNIX and the Network File System (see the figure). One of the Suns serves as host for a Megavision image processor, X-Y-ø motion table, a Sony 9600 VTR , an optical disk drive and a dedicated image buffer disk. The software includes low-level interface routines provided with the image processor, and HIPS, a UNIX-based image processing package useful for routine low-level image processing. Most of our software follows the HIPS idea of UNIX pipeline prototyping with our own extensions for feature lists, range maps, etc., that are not supported by HIPS alone.

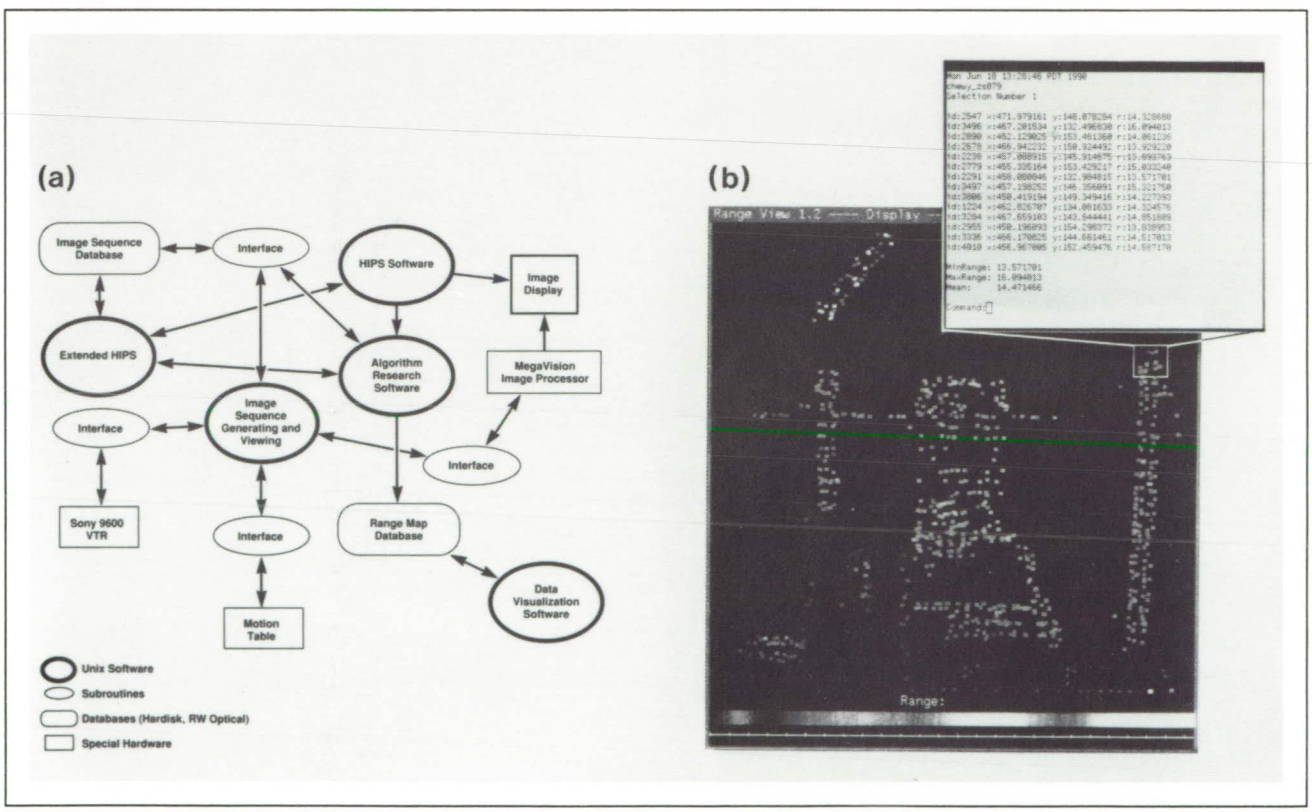


Fig. 1. Nap-of-the-Earth image processing laboratory. (a) Software environment, (b) visualization software

An important result of the laboratory has been the creation of data-visualization software designed to work with feature-based obstacle-detection algorithms. These data-visualization programs have proven to be the most used and relied upon programs yet written for the laboratory. It is clear that algorithm research can advance only as the tools to display the results advance.

The current system allows researchers to create image sequences with precisely controlled camera motion from easy to use window-base software. The resulting images can be preprocessed using HIPS or the Image Processor with simple command line functions.

Ames-Moffett contact: R. Suorsa
(415) 604-5451 or FTS 464-5451
Headquarters program office: OAET

Computer Aiding for Low-Altitude Helicopter Flight Project

Harry N. Swenson

Helicopters that operate in threat areas have a need for low-level, maneuvering penetration capability for operations at nighttime and under adverse weather conditions. Currently, low-level penetration is accomplished through the use of terrain following (TF) radars, forward-looking infrared (FLIR) systems, and night-vision goggles (NVG). This combination is in place in the USAF Special Operations Forces (SOF) CH-53 Pave Low III aircraft and is proposed for the U.S. Army's SOF aircraft. Though these systems provide a low-level penetration capability, the development of digital terrain maps, advanced navigation systems, and high-speed on-board computer systems enable more effective terrain-masking performance.

As an element of the Automated nap-of-the-Earth (ANOE) Program, a low-altitude guidance concept has been developed that takes advantage of knowledge of terrain to define a valley-seeking trajectory for improved low-level penetration performance. The basic algorithm, and control/display designs have been developed and successfully tested in piloted simulations over the past few years. The last simulation, completed in January 1989, included Army, NASA, and Air Force pilots, and has led to a memorandum of agreement (MOA) between NASA-Ames and the U.S. Army Avionics Research and Development Activity (AVRADA) for a joint flight experiment in the AVRADA UH-60 Star helicopter (see the figure).

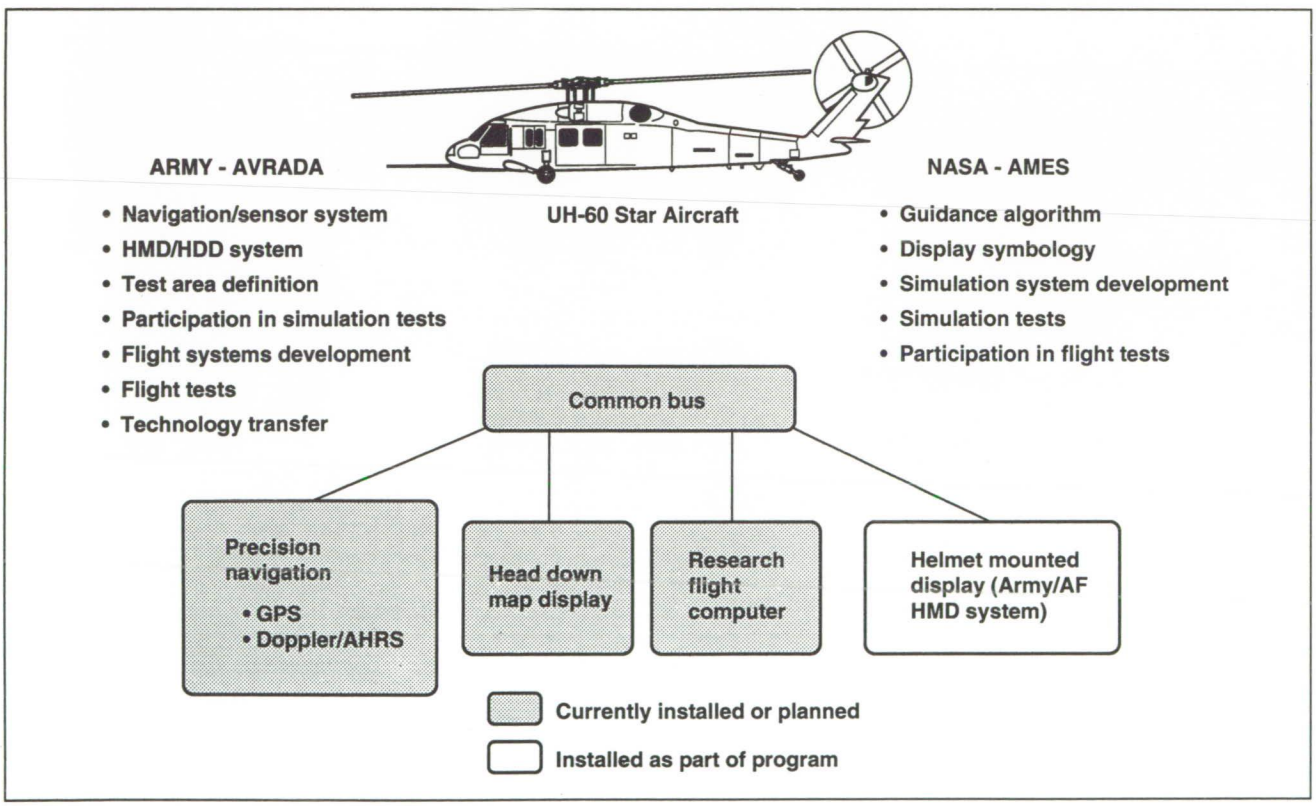


Fig. 1. Computer-aided low-altitude helicopter flight

In support of the flight evaluation, two simulations have been scheduled on the Ames Vertical Motion Simulator. The first was initiated in June 1990 and will be a detailed operational evaluation of the algorithm using a UH-60 aircraft model, a helmet-mounted display, and a terrain model of the Carlisle Pennsylvania area, which is the test area for actual flight test. Major research issues will include conversion of the display symbology from the head-up-display format to the helmet-mounted display and an evaluation of the effect of navigation errors on operational performance. The second simulation will include an interface with a replication of the flight computer and will be used to validate the flight software and develop the detailed flight-test plan. The flight test is scheduled for August of 1991.

Ames-Moffett contact: H. Swenson
(415) 604-5469 or FTS 464-5469
Headquarters program office: OSSA

Rotorcraft Flight-Control Design Methods

Marc D. Takahashi

Analytical work was conducted as part of the SCAMP (Superaugmented Control for Agile Maneuvering Performance) program, one purpose of which is to investigate the use of new control design methods to design high-bandwidth flight-control systems for rotorcraft. These flight-control systems will improve future helicopter designs by enhancing agility and allowing more precise maneuvering.

Rate-command and attitude-command four-axes flight-control laws were developed for a UH-60 helicopter mathematical model in hover. Rate-command and attitude-command refer to the response type of the flight-control law; rate-command gives constant angular rate for a constant input in the pilot controls, and attitude-command gives constant angular change for a constant input to the pilot controls. The type of response of the design depends on the task the helicopter is expected to perform and the visual conditions.

The design method is a linear multi-input/multi-output method that uses frequency-dependent weighting of the sensitivity, complementary-sensitivity, and control-input transfer-function matrices. These transfer-function matrices are directly related to the control-system performance, and their weighting allows the designer to adjust these functions to give acceptable feedback properties. Examples of these properties include system stability over a large operating envelope, and helicopter insensitivity to upsetting wind gusts.

The mathematical model of the helicopter includes rotor-blade flapping and lagging dynamics and was validated by correlation with flight-test data from a UH-60. Time delays are included in the analysis to represent computational, zero-order-hold, sensor, and actuator delays, which would be present if the control designs were implemented on a real helicopter.

The designs were checked for compliance with the Aeronautical Design Standard (ADS-33C) and met most of the requirements in theory. This design standard is a new set of requirements for combat helicopter flying qualities. Ongoing work is being conducted to further evaluate the flight-control designs, which includes pilot evaluations in the Vertical Motion Simulator.

Ames-Moffett contact: M. Takahashi
(415) 604-5271 or FTS 464-5271
Headquarters program office: OAET

Rotorcraft System Identification

Mark B. Tischler

Rotorcraft system identification is a procedure by which a mathematical description of a vehicle's dynamic behavior is extracted from flight-test data. System identification can be thought of as an inverse of simulation. Simulation requires the adoption of (a priori) engineering assumptions to allow the formulation of model equations. These simulation models allow the prediction of aircraft motion. In contrast, system identification begins with measured aircraft motion and "inverts" the responses to extract a model which accurately reflects the measured aircraft motion, without making a priori assumptions. Applications of system-identification results include (1) comparison of wind-tunnel and flight characteristics; (2) validation and update of simulation models; (3) demonstration of handling-qualities specification compliance; and (4) optimization of automatic flight control systems.

A comprehensive frequency-response method for rotorcraft system identification has been developed. The overall concept is to (1) extract a complete set of nonparametric input-to-output frequency responses that fully characterizes the coupled helicopter dynamics, and (2) conduct a nonlinear search for a state-space model that matches the frequency-response data set. An integrated user-oriented software package for the frequency-response method (comprehensive identification from frequency responses: CIFER) has been developed in-house, and was completed in 1990. A User's Manual was prepared and a 5-day workshop was planned for January 1991.

In 1990, CIFER was extensively used in the Flight Dynamics Branch to identify dynamic models of a variety of aircraft: the BO-105 helicopter, AH-64 helicopter, UH-60 helicopter, AVSTOVL aircraft, and civil tilt-rotor. Part (a) of the figure shows, for example, the excellent prediction of pedal response obtained using a model of the BO-105 helicopter extracted using CIFER from flight data at 80 knots. This work was completed as part of U.S. participation in AGARD group 18 "Rotorcraft System Identification." Current efforts are focused on preparing for the January 1991 industry workshop on CIFER, at which time the software is to be released to U.S. industry and laboratories.

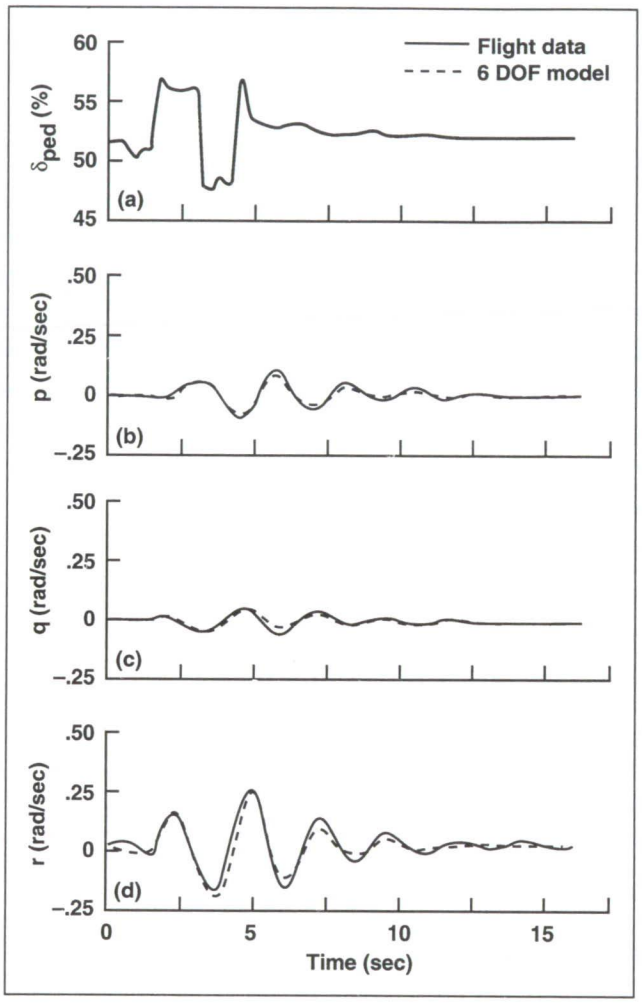


Fig. 1. Comparison of flight response to pedal input with prediction of six-degree-of-freedom (DOF) model obtained from CIFER. (a) Pedal input, (b) roll rate, (c) pitch rate, (d) yaw rate

Ames-Moffett contact: M. Tischler
(415) 604-5563 or FTS 464-5563
Headquarters program office: OAET

Helicopter Stick Dynamics Investigations

D. Watson, J. Schroeder

The objective of this work was to determine how variations in cyclic-center-stick dynamic characteristics affect helicopter flying qualities.

Irreversible hydraulic flight controls isolate the pilot from all aerodynamic flight loads. Helicopter cyclic-center sticks typically have artificial force-feel characteristics designed for positive centering around trim. Spring gradient and preload, damping, and friction are chosen to provide the pilot with desirable control feel. The effective inertia of the stick is a function of the stick itself plus the mechanical flight-control linkages.

Because the pilot must move the stick in order to control the aircraft, the physical stick characteristics can have a dramatic effect on the pilot's perception of the overall aircraft's flying qualities. Design guidelines currently exist for static spring gradients and preloads. There has not been a consensus, however, on how the dynamics of the stick affect handling qualities or how they should be accounted for in measuring aircraft responses for handling-qualities-specification compliance. Relative to fixed-wing aircraft, helicopters typically have lower spring gradients and correspondingly lower natural frequencies, suggesting a negative effect on handling qualities.

An experiment was conducted in concurrent ground and in-flight simulations to investigate the influence of typical helicopter force-feel system dynamics on roll-axis handling qualities. The static characteristics of the helicopter sticks, namely spring gradient and preload, were held constant while inertia was used to vary the natural frequency. Two damping ratios were used and held constant.

The results indicated that the stick does not act simply as a dynamic filter appended to the aircraft response. Once the pilot grips the stick, it becomes an integral part of the pilot's limb, and the stick's dynamics are no longer independent of the pilot's neuromuscular system. Therefore, it is the stick's physical characteristics, rather than its natural frequency and damping ratio alone, which are important to the pilot.

An effective stick inertia of 5 to 7 pounds-mass at the grip established an upper limit for desirable stick characteristics and is recommended as a design guideline. Comparison with published fixed-wing data using higher spring gradients and with several operational helicopters supports this boundary.

Ames-Moffett contact: D. Watson
(415) 604-4037 or FTS 464-4037
Headquarters program office: OAET

Helicopter Yaw Response Requirements

Matthew S. Whalley

A piloted simulation investigation was performed on the Ames Research Center's Vertical Motion Simulator (VMS) to investigate helicopter yaw response requirements as specified in the U.S. Army Aeronautical Design Standard 33C, "Handling Qualities Requirements for Military Rotorcraft." Examined during the test were the small-amplitude and moderate-amplitude requirements.

ADS-33C specifies the small-amplitude yaw response requirement in terms of bandwidth. For target acquisition and tracking, a bandwidth of 2 radians/second is required for Level 2 handling qualities and a bandwidth of 3.5 radians/second is required for Level 1 handling qualities.

ADS-33C also specifies the moderate-amplitude yaw response requirement in terms of attitude quickness. Attitude quickness is defined as the ratio of the peak heading rate to heading change achieved during a rapid heading change. This requirement applies to heading changes between 10° and 60°.

The main reason for conducting this experiment derived from the realization that the tail-rotor thrust and thrust-rate-of-change needed to perform a 180° turn in 5 seconds, as required in ADS-33C, was substantially less than the implied thrust and thrust-rate-of-change required by the attitude-quickness requirement. Achieving consistency between the two sections of the specification would require a modification of the existing moderate-amplitude requirement boundaries. Therefore, the primary objective of this experiment was to provide precise hover and low-speed yaw control handling-qualities data on which new boundaries could be based.

Configuration bandwidth and attitude quickness were varied during this experiment by varying the yaw damping derivative N_r, and the tail-rotor collective-pitch actuator-rate limit. Yaw damping was varied between –1.0 1/rad and –4.0 1/rad. Actuator-rate limit was varied from unlimited down to 50% of full throw per second. The maximum achievable yaw rate was held constant at 60°/sec (Level 1 as specified by ADS-33C).

Four tasks were examined. Two tasks were performed in hover: an aggressive target-acquisition task which required heading changes between 10° and 60°, and an aggressive 180° heading change. In forward flight, a target-acquisition task, and a sum-of-sines target tracking task were performed.

Data were collected using both a conventional control arrangement with pedals and with a three-axis side-stick (pitch,roll, and yaw). Six engineering test pilots participated in the experiment. Data were collected from over 1,000 runs in the form of time-histories, Cooper-Harper ratings, and pilot commentary.

The results from the sum-of-sines tracking task shown in the first figure clearly support the current yaw bandwidth requirement of 3.5 rad/sec for Level 1, and 2 rad/sec for Level 2.

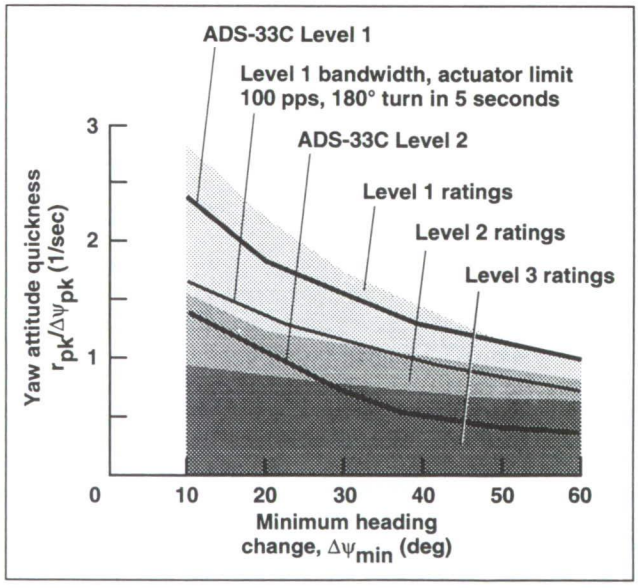


Fig. 1. Preliminary results: Attitude quickness, Cooper-Harper ratings for the hover turn task

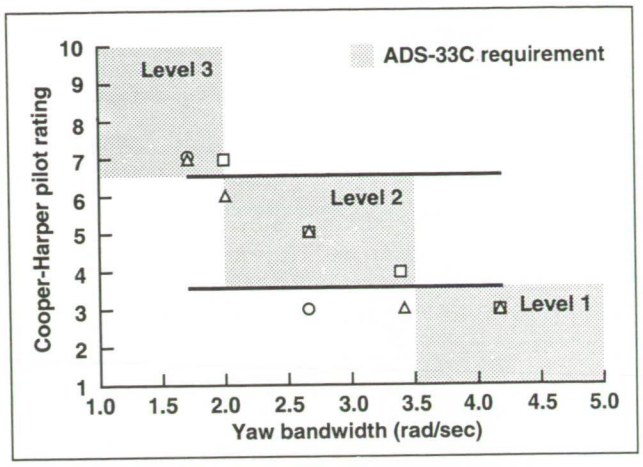


Fig. 2. Preliminary results: Bandwidth, Cooper-Harper ratings for the sum-of-sines tracking task

The results from the target-acquisition tasks shown in the second figure indicate that a relaxation of the attitude-quickness requirement could be made without sacrificing Level 1 handling qualities. Also, given the Level 1 attitude-quickness performance indicated by the results of this study, the 180° turn in hover could still be performed satisfactorily in 5 seconds.

Ames-Moffett contact: M. Whalley
(415) 604-3505 or FTS 464-3505
Headquarters program office: OAET

Separation of Turbulence and Maneuver Loads from Airline Flight Records

R. C. Wingrove, R. E. Bach, Jr.

Flight incidents at cruise altitudes involving large g-loads are a continuing problem that must be better understood to improve safety. The large changes in g-loads can cause injuries and aircraft damage. Especially, the large changing g-loads might cause major structural failures with the aging airline fleet. These incidents have been attributed to clear-air turbulence; however, based on Ames' analysis of the flight records, a portion of the g-loading in some of the cases may have come from ensuing aircraft maneuvers that are triggered by less severe winds.

One way to investigate the nature and effects of atmospheric disturbances and to separate the maneuvering effects is through analysis of airline flight records obtained during severe encounters. Past analysis was hindered by insufficient data. Recent encounters have involved modern airliners equipped with multichannel digital flight data recorders (DFDRs). These digital records provide a means to determine and analyze the turbulent wind environment. Also, the DFDR provides a means to determine the aircraft maneuvers and their contribution to the measured g-loads.

In conjunction with the National Transportation Safety Board, researchers from Ames have analyzed a series of 13 cases, listed in the table, that were initially reported as clear-air turbulence accidents. All of the encounters involved airliners equipped with DFDRs. Ten cases show significant changes in g-loads due to variations in the vertical winds. Results from these 10 cases indicate positive loads to +1.7 ΔG and negative loads to –2.0 ΔG. Three other cases show large changes in g-loads due to aircraft pitch maneuvers instigated by atmospheric disturbances (see the figure).

Results for these three cases indicate that at the time the g-load initially rose into the Mach buffet region, there were sharp push-downs with pitch angle changes to –8°, resulting in negative loads to –1.9 ΔG. In the maneuvering there are oscillations in the g-load with a time period of 5 seconds, which is the same as the aircraft longitudinal short-period motion.

Digital Flight Records from Airliners Encountering Large g-Load

Case	Date	Aircraft	Location	Altitude, ft	G load
1	11/3/75	DC-10	Calgary, Canada	33,000	+1.6 –0.2
2	4/4/81	DC-10	Hannibal, MO	37,000	+1.7 –1.0
3	7/16/82	DC-10	Morton, WY	39,000	+1.6 –0.6
4	10/12/83	DC-10	Near Bermuda	37,000	+1.6 –0.6
5	11/25/83	L-1011	Offshore SC	37,000	+2.1 –1.0
6	1/22/85	B-747	Over Greenland	33,000	+2.7 –0.0
7*	4/7/86	DC-10	Jamestown, NY	40,000	+1.8 –0.4
8	9/27/87	L-1011	Near Bermuda	31,000	+2.2 –0.5
9*	11/12/87	A-310	Near Bermuda	33,000	+2.0 –0.6
10	1/20/88	B-767	Chicago, IL	25,000	+1.4 –0.2
11	3/24/88	B-767	Cimarron, NM	33,000	+1.7 –0.2
12*	6/6/89	DC-10	Garden City, KA	37,000	+1.9 –0.9
13	6/16/89	L-1011	Jacks Creek, TN	24,000	+2.2 –1.0

*Significant maneuvering

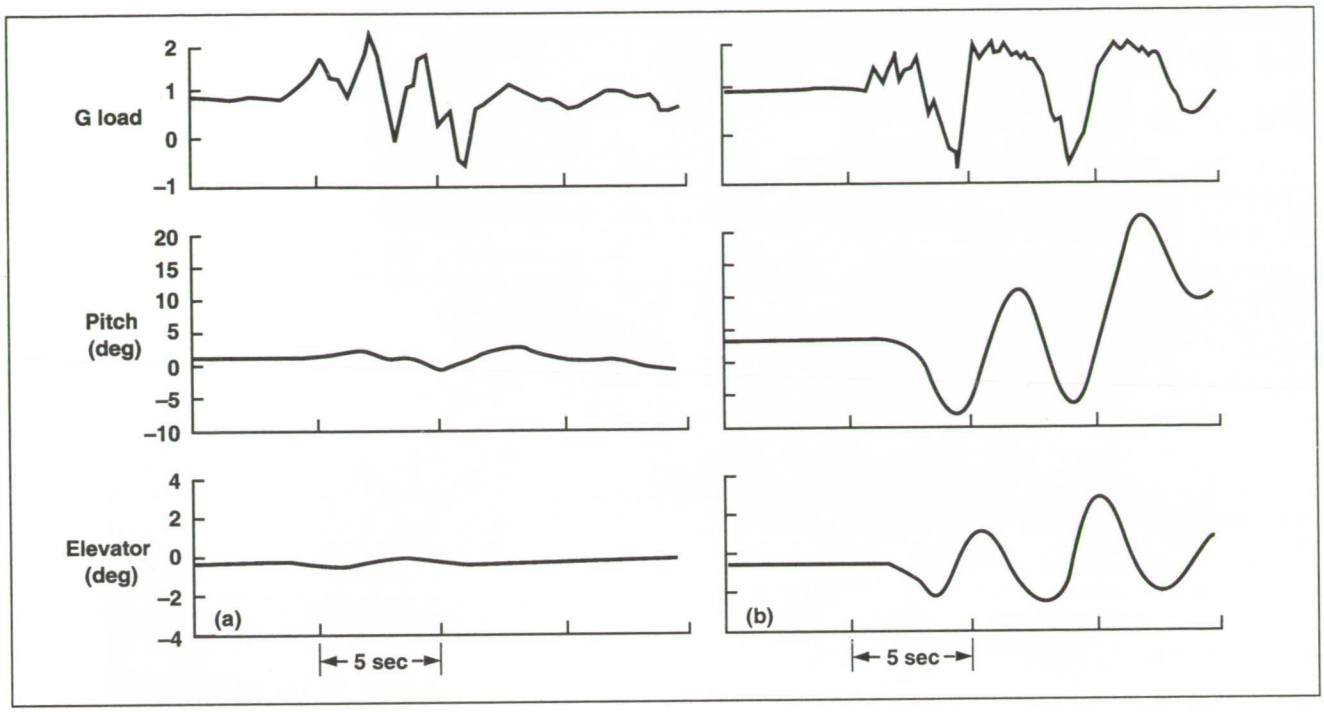


Fig. 1. Two cases with large loads; (a) severe turbulence, L-1011 near Bermuda; (b) significant maneuvering, A-300 near Bermuda

For the first time, with the modern DFDR, sufficient data are available to permit separating atmospheric disturbances and maneuver-induced g-loads. New analytical methods are being developed to quantify the g-load magnitudes attributed to either the winds or the maneuvers.

Ames-Moffett contact: R. Wingrove
(415) 604-5429 or FTS 464-5429
Headquarters program office: OAET

F-16XL Supersonic Laminar Flow Control Research

Bianca T. Anderson

NASA is conducting flight research to determine the feasibility of maintaining laminar flow on a highly swept wing configuration at supersonic speeds. This is a joint program between Ames-Dryden Flight Research Facility and Rockwell International/North American Aviation which uses the F-16XL as the test vehicle. Computational analysis and support is also being provided by Ames Research Center and Langley Research Center. Rockwell International designed the wing glove shape and suction system using existing computational tools. The computational predictions of pressure distributions and extent of laminar flow will be compared and validated with the flight test results.

For this flight research, a porous (active) glove with a perforated titanium surface manufactured by Rockwell International was installed on the left wing. During flight, a suction system, mounted in the fuselage, draws the low-energy boundary layer through the surface of the porous glove to maintain a laminar boundary layer. Fiberglass or passive glove fairings were installed just inboard and outboard of the active glove where the state of the boundary layer without suction is monitored and the chordwise pressure distributions are measured.

The first figure is a diagram of the suction system and instrumentation on the aircraft and glove. The two rows of flush static pressure orifices installed on the passive glove are used to obtain detailed measurements of the design airfoil pressure distribution, especially near the leading edge. Both the active and passive gloves are instrumented with hot-film gages to determine the boundary-layer transition location and the state of the leading-edge attachment line boundary layer. The suction system is instrumented with pressure transducers and temperature sensors to determine the mass flow rate of the air flowing through the system.

Flight pressure distribution data obtained for the design condition of Mach 1.6, 44,000 feet, and an angle of attack of approximately 1° for the two rows of pressure orifices are plotted in the second figure. The computational predictions for the design condition and an angle of attack of 2° are also plotted for comparison. The computational data shows reasonable agreement with the flight data. There are differences between the two sets of data in the aft shape of the outboard pressure distribution. These differences are being analyzed and may be due to differences between the design airfoil shape and the actual airfoil shape on the aircraft.

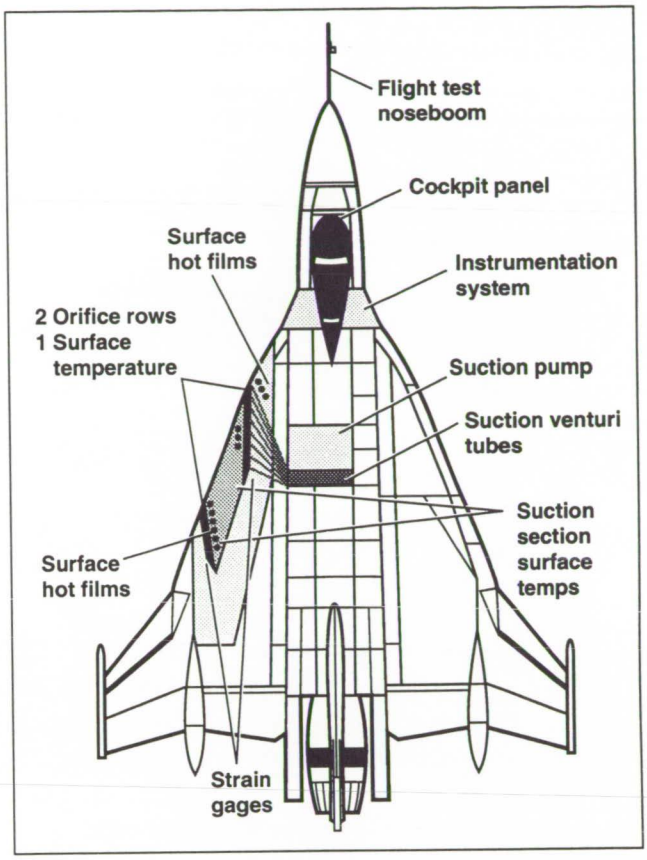


Fig. 1. Layout of suction system and instrumentation on the aircraft and glove

214 INTENTIONALLY BLANK PRECEDING PAGE BLANK NOT FILMED

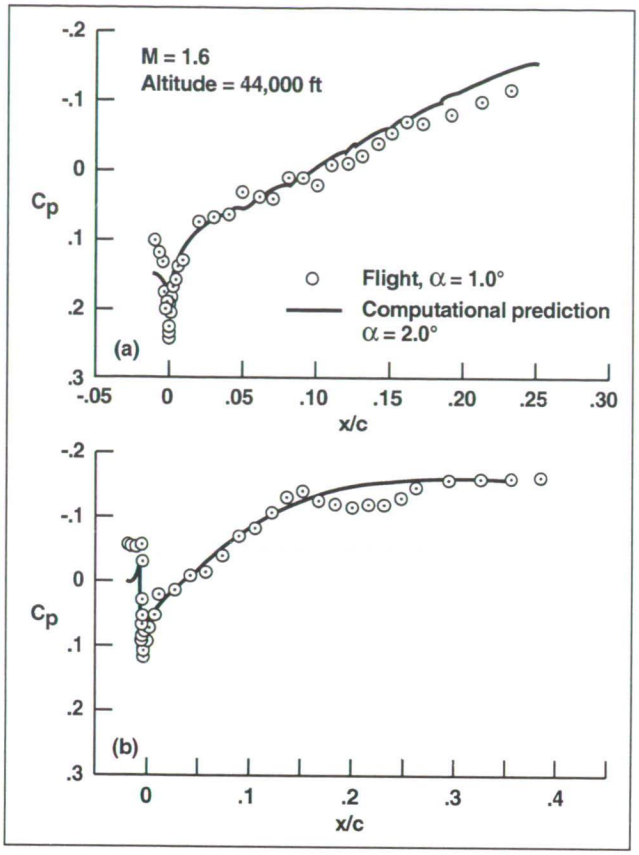


Fig. 2. Flight and computational pressure distributions on inboard and outboard glove orifice rows. (a) Inboard orifice row; (b) outboard orifice row

The attachment line is being evaluated to determine the Reynolds number and angle-of-attack envelope which results in laminar flow on the attachment line with and without the suction system operational. Preliminary transition data obtained for the leading-edge region of the active and passive gloves without the suction system operational are plotted in the third figure. These data indicate a

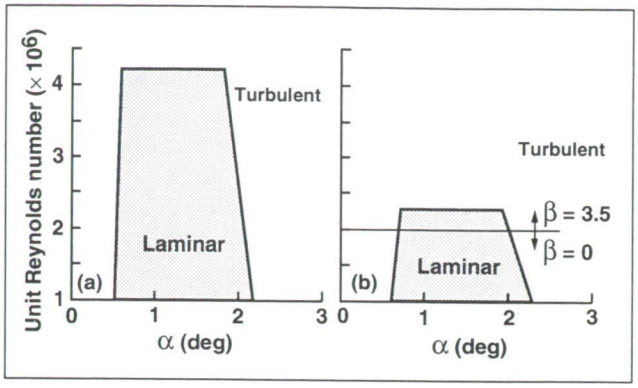


Fig. 3. Preliminary flight data at glove leading-edge region showing laminar attachment line envelope without suction. (a) Passive glove; (b) active glove

laminar attachment line boundary layer on the passive glove for unit Reynolds numbers slightly above 4 million per foot, which is the highest unit Reynolds condition flown to date. The preliminary data indicate a laminar attachment line boundary layer on the active glove for unit Reynolds numbers up to 2.3 million per foot with –3.5° of sideslip.

This study will also include placing micro-thin hot-film sheets on the glove leading edge to evaluate the attachment line flow and to accurately locate the stagnation point. Additionally the laminar regions of the active glove will be documented with the suction system operational which will conclude the first phase of the experiment. The flight test envelope will include Mach numbers from 1.2 to 1.7 and altitudes from 35,000 to 55,000 feet.

Ames-Dryden contact: B. Anderson/D. Fischer
(805) 258-3701/3705 or FTS 961-3701/3705
Headquarters program office: OAET

Propulsive Techniques for Emergency Control

Frank W. Burcham, Glenn B. Gilyard

In an emergency, consider using throttles to augment or replace aircraft flight control systems. Throttles may be able to control some aircraft with multiple engines to a rudimentary degree. Airplanes with total hydraulic system failures, such as the B-747 and DC-10, have been flown for substantial periods with only engines for control.

To study the use of the propulsion system for control, Ames-Dryden Flight Research Facility has conducted preliminary flight, ground simulator, and analytical studies. These preliminary studies set out to determine the degree of control power available for various classes of airplanes, and to investigate possible control modes that could be developed for future airplanes.

Airplanes studied included: (in flight tests) the Lear 24, PA-30, and F-15; (in simulators) the B-720, F-15, MD-11, and B-727. All demonstrated some degree of controllability, and that up-and-away flying is possible, although with a very high workload.

Landing airplanes using only the throttles is much more difficult than up-and-away flying. Simulations of the B-720 and the F-15 have been evaluated for the landing task. It was found that manual throttle control for landing is, at best, extremely difficult. The pilot has to contend with low response rates in pitch and roll, a 1-second delay before any response occurs, and a poorly damped longitudinal phugoid in pitch. The first figure shows the results of several manual landings of the B-720. Touchdown location is shown along with a vertical bar that is the sum of sink rate in feet/second and bank angle in degrees. Pilot ratings were mostly 9s and 10s. Many of these landings were not survivable; however occasional successful landings did demonstrate that sufficient control power was available.

Therefore, a system was designed to control the throttles through a conventional control stick, and provide appropriate feedback parameters to stabilize the phugoid and improve the roll characteristics. With this augmented system, landings were easier.

The second figure shows the touchdown data with the augmented system operating. All landings were on the runway with combined sink rate and bank angle of less than 12. Pilot ratings were in the 3-4 range. This same control mode was also evaluated on the F-15, and similar results were obtained.

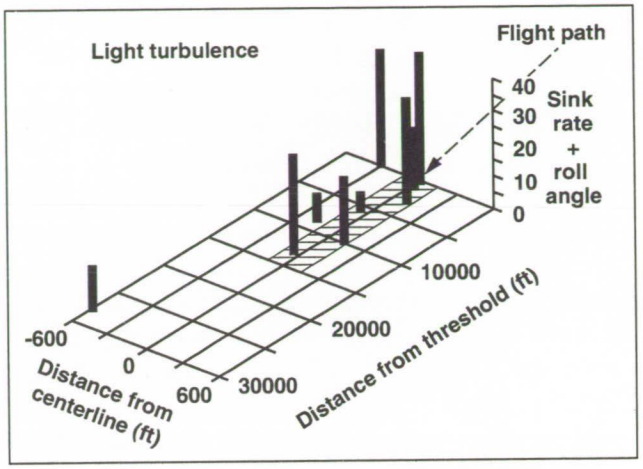


Fig. 1. Manual throttles-only control landings, B-720, 160 knots

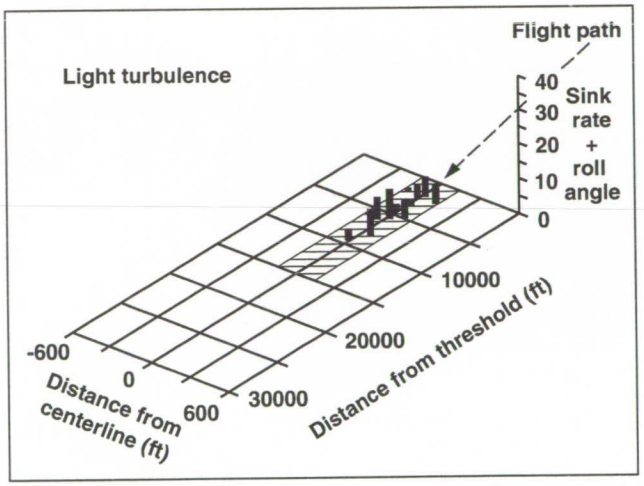


Fig. 2. Augmented throttles-only control landings, B-720, 160 knots

On future airplanes with digital engine and flight controls and data bases, such a control mode could be implemented in software and serve as an additional and independent level of flight control system redundancy.

Ames-Dryden contact: F. Burcham/G. Gilyard
(805) 258-3126/3724 or FTS 961-3126/3724
Headquarters program office: OAET

Flight-Test Results of the X-29A at High Angle of Attack

Robert Clarke

The X-29A airplane has completed the first stage of a high angle-of-attack (α) flight-test program. This first block of testing included flight envelope expansion to 66° α at 1 g and maneuvering clearance up to 35° α at airspeeds up to 200 knots.

In general, the airplane was found to have excellent high α flight characteristics. The airplane develops light to moderate buffet starting about 13° α and remains at this level for the entire high α envelope. The wing rock free envelope extends up to 35° α. Minor wing rock develops at higher α, but this wing rock has a much smaller amplitude than preflight predictions. The 1-g high α characteristics slowly deteriorate at higher angles due to the development of asymmetric yawing moments. X-29A test pilots have characterized this degradation in control as "gradual and predictable." Pitch authority has been excellent up to 40° α with gradual degradation due to the development of inertial coupling as the yaw asymmetries develop. The maneuvering characteristics are excellent and generally are near the preflight predictions, except that wing rock does not dominate the airplane response at high α.

Designers of modern fighters are in an ever-widening search for new capabilities that can be

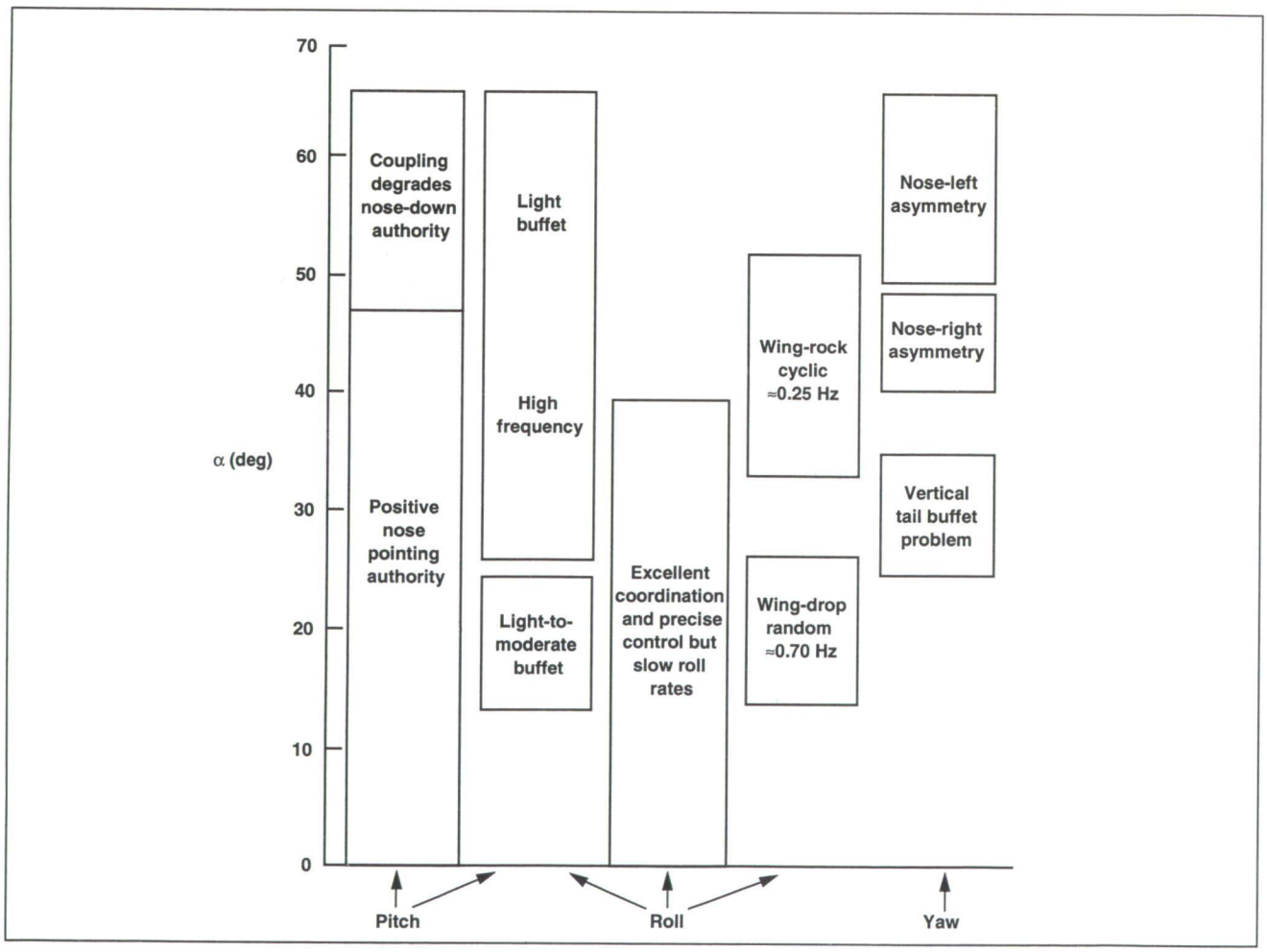


Fig. 1. General flight characteristics, X-29 forward-swept wing (ship 2), high angle-of-attack envelope expansion

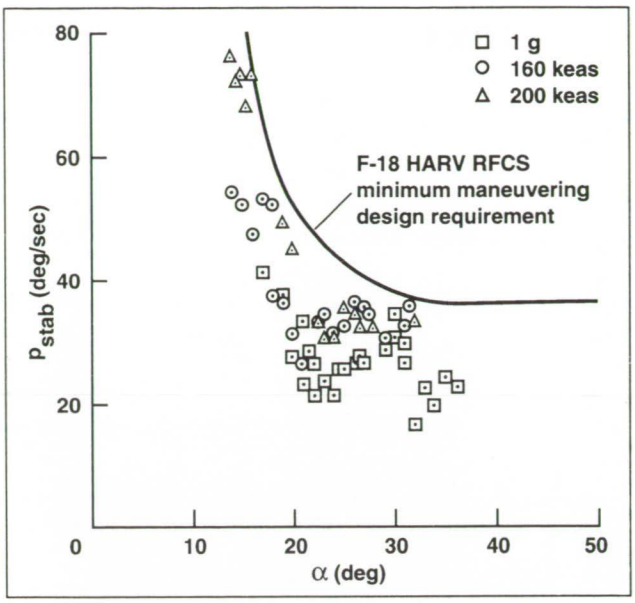


Fig. 2. Roll Capability (lateral stick alone), X-29 forward-swept wing (ship 2), high angle-of-attack envelope expansion

exploited in air combat situations. Increased high α maneuvering capabilities can provide advantages over a potential adversary in a one-on-one air combat scenario. The flight control system (FCS) can be designed to enhance high α maneuverability and reduce the chance of departures and spins. Comparisons of simulated air combat of the X-29A with an F-16A, F-15A, or F-15C showed that approximately 70% of the firing opportunities for the X-29A occurred at angles of attack above 30° α. These simple point mass simulation studies showed a significant advantage in generating firing solutions to the airplane which maneuvered better at high α. The X-29A has the unique characteristic of the forward-swept wing which has been predicted to provide aerodynamic advantages at high α.

The X-29A No. 2 airplane is the first airplane to fly at high α conditions with a forward-swept wing, the first manned airplane to fly at high α with a 35% statically unstable pitch axis, and the first airplane to fly at high α with a large lateral instability controlled by the FCS.

The airplane had no observed problems due to the forward-swept wing technology at high α. In fact, the forward-swept wing may have contributed to many of the good characteristics that were found. The first figure shows some of the general characteristics of the airplane at high α. The longitudinal instability did not seem to go away at high α as predicted and this caused some trim differences which created a problem in trying to define pitch pointing capabilities. Lateral instability was slightly less unstable overall and lateral-directional control power was higher which led to excellent control of wing rock. Stability axis roll rates for the X-29A are shown in the second figure. The airplane continues to demonstrate many of the predicted high α advantages of the technologies used in its design.

In addition, the engine and subsystems worked well at high α even under severe conditions. The initial high α control laws worked well and proved very robust to the high α aerodynamic differences. The aileron-to-rudder interact and wing rock suppression systems allowed excellent control of the airplane with lateral stick. Inertial and kinematic coupling did not prove to be a problem below 40° α, but above 50° α inertial coupling prevented complete testing of the pitch pointing capability.

Flight-test data showed the following:

1. Roll rate to aileron gain could be reduced 10% across the board and up to 20% in most areas, which resulted in increased roll performance without wing rock problems.
2. A filter is required on the roll rate signal to prevent nuisance actuator failure indications.
3. Dial-a-Gain concept was valuable for research flexibility before full FCS changes are made.
4. Predictions about the air data system made during the FCS design were pessimistic and the system worked better than expected. In hindsight the flight data show that the sideprobes performed adequately for FCS gain scheduling purposes and the system did not need to be made single string on the noseboom probe.

A second control law modification was made and will be tested in FY 91 to examine potential improvements in roll control authority at high α.

Ames-Dryden contact: R. Clarke
(805) 258-3799 or FTS 961-3799
Headquarters program office: OAET

Thermoelastic Vibration Testing

ORIGINAL PAGE
BLACK AND WHITE PHOTOGRAPH

Michael W. Kehoe

Proposed high-speed aircraft will encounter flight regimes that differ significantly from those of previous flight vehicles. These vehicles will be subjected to extremely hot surface temperatures and large temperature gradients throughout the structure. The resulting temperature conditions can seriously affect the structural integrity of the vehicle. Variations in the structure's elastic characteristics due to thermal effects can be observed by changes in either its global stiffness or vibration frequencies and mode shapes. Parameters which are likely to affect these characteristics are thermal stresses and changes in elastic modulus. Changes in elastic modulus as a function of temperature and internal stresses due to temperature effects can be determined through experiments to provide a data base for analysis code validation. The objectives of this research are to develop instrumentation and modal test techniques, and to conduct high-temperature vibration tests on metal and composite structures to create an experimental data base for analysis code validation.

Experiments have been designed to measure the modal characteristics of structures at elevated temperatures. The initial test articles are simple aluminum and composite flat plates suspended by bungee chord to simulate free-free boundary conditions. These test articles are placed in an oven, heated with infrared quartz heaters, and then vibrated to determine their modal parameters.

Each plate tested is instrumented with thermocouples to measure the temperature distribution on the plate during heating. The plate modal response to impact excitation is measured by accelerometers to temperatures of 500°F and by a laser vibrometer at temperatures above 500°F. The use of the laser vibrometer during a typical test is shown in the first figure.

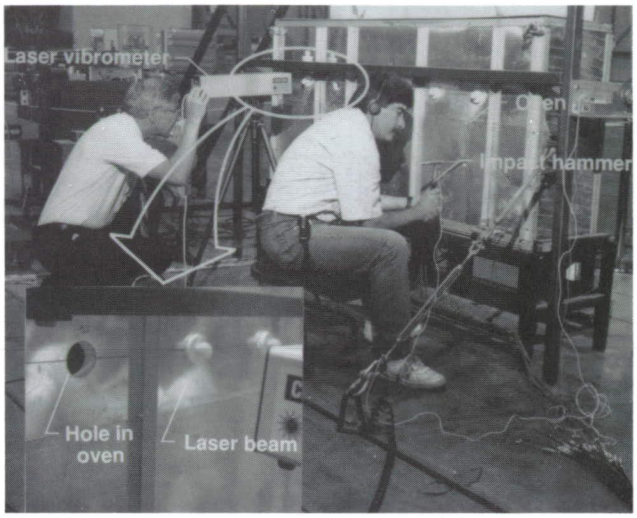


Fig. 1. Thermoelastic vibration testing with a laser vibrometer

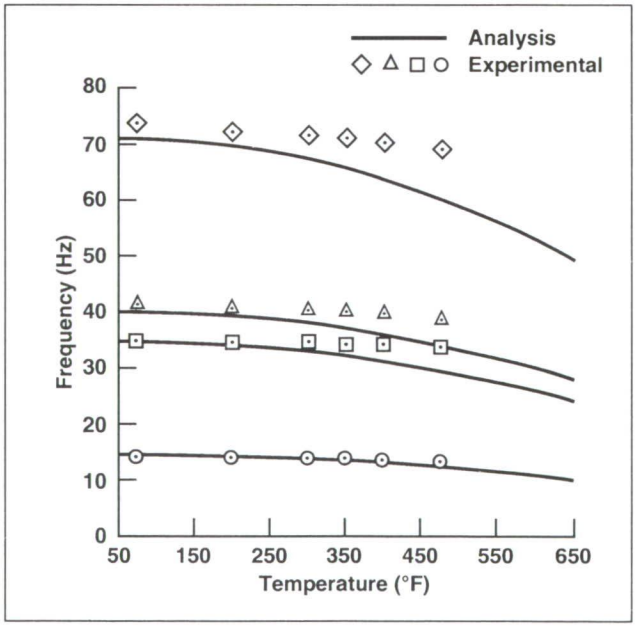


Fig. 2. Comparison of predicted and measured modal data

Aluminum plate data have been acquired at temperatures of 200, 300, 350, 400, 475, and 600°F. In addition, data have been acquired at nonuniform and transient heating conditions. Similar data have been acquired for a composite plate.

Analyses were performed using the Structural Analysis Routines (STARS) program to predict the change in frequency as temperature increased. A comparison of the predicted and experimental frequency for the first four aluminum plate vibration modes is shown in the second figure. The data indicate that analyses predicted greater frequency changes than those measured, particularly at the elevated temperatures. Similar data comparisons were made for nonuniform and transient heating.

Future plans include testing more complicated structures with uniform, nonuniform, and transient heating patterns. These include built-up composite and aluminum structures and a titanium honeycomb, Rene 41 panel.

Ames-Dryden contact: M. Kehoe
(805) 258-3708 or FTS 961-3708
Headquarters program office: OAET

Pegasus "Add-On" Hypersonic Flight Experiments

Greg Noffz, Robert Curry

NASA is conducting an ongoing generic hypersonic research program aimed at helping develop technologies for future hypersonic aircraft. A portion of this overall program consists of the Pegasus "add-on" flight experiments. These experiments are conducted on the Pegasus boosters during their normal missions using add-on or secondary payloads consisting of various instruments. The specific objectives include the development of measurement techniques, evaluation of analytic prediction tools used in the development of Pegasus, and augmentation of the empirical aerothermal data base. The add-on flight experiments are a joint effort between Ames Research Center's Dryden Flight Research Facility and Moffett Field.

A research instrumentation system, developed by NASA, was installed in the first stage of the vehicle. This system was constrained to have minimal impact on either the primary payload mission or the flight operation. Data obtained from the research system were correlated with flight conditions, determined through an extensive post-flight trajectory analysis conducted using radar, balloon, and inertial data.

The research system on Flight 1, which occurred in April 1990, included 86 temperature sensors distributed on the wing surfaces, leading edge, and the wing-fuselage fairing (or fillet). The majority of sensors were embedded in the ablating thermal protection system (TPS), thereby causing minimal perturbation of the local structure and thermal boundary layers. These sensors can provide direct measurements for comparison with analytic predictions. In addition, some thermocouples were mounted on plugs fabricated from high-temperature reusable shuttle insulation (HRSI). The plugs are nonablating and can be easily modeled, thus the temperature measurement at the surface allowed for

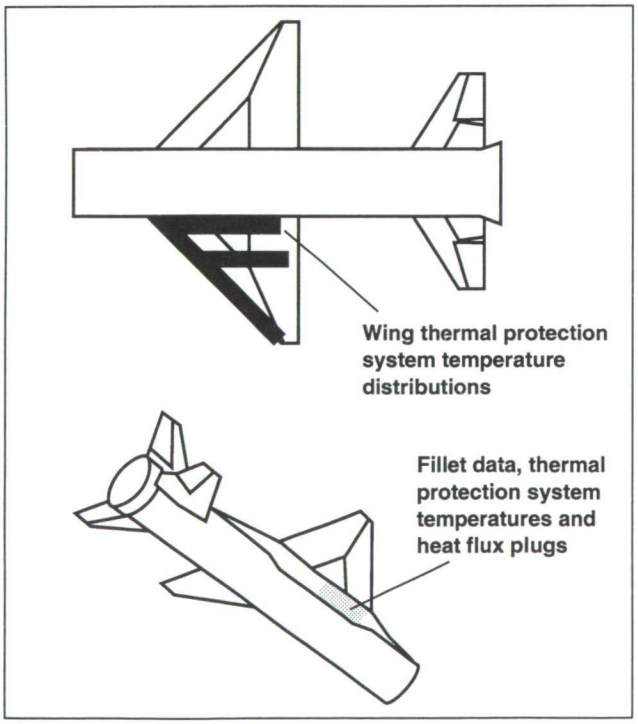


Fig. 1. Schematic of Pegasus instrumentation configuration

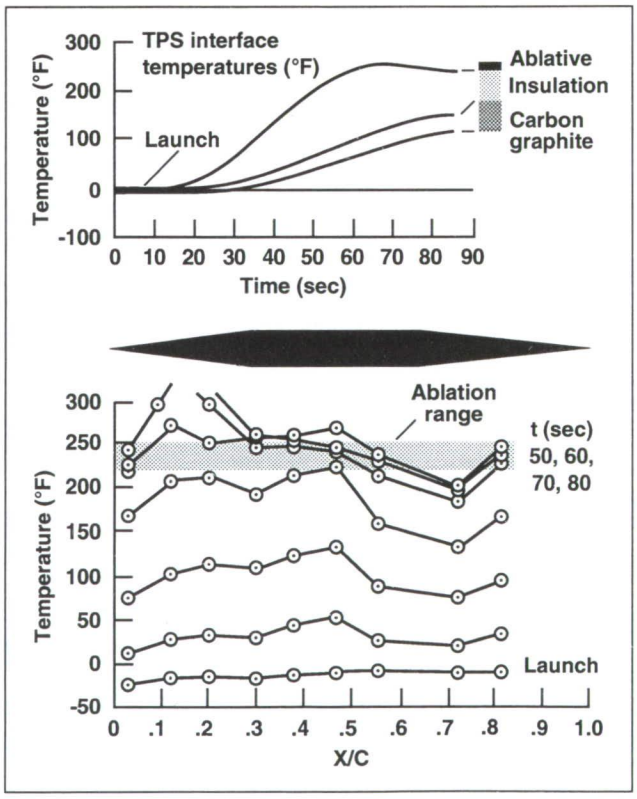


Fig. 2. Temperature profiles versus time and chord location

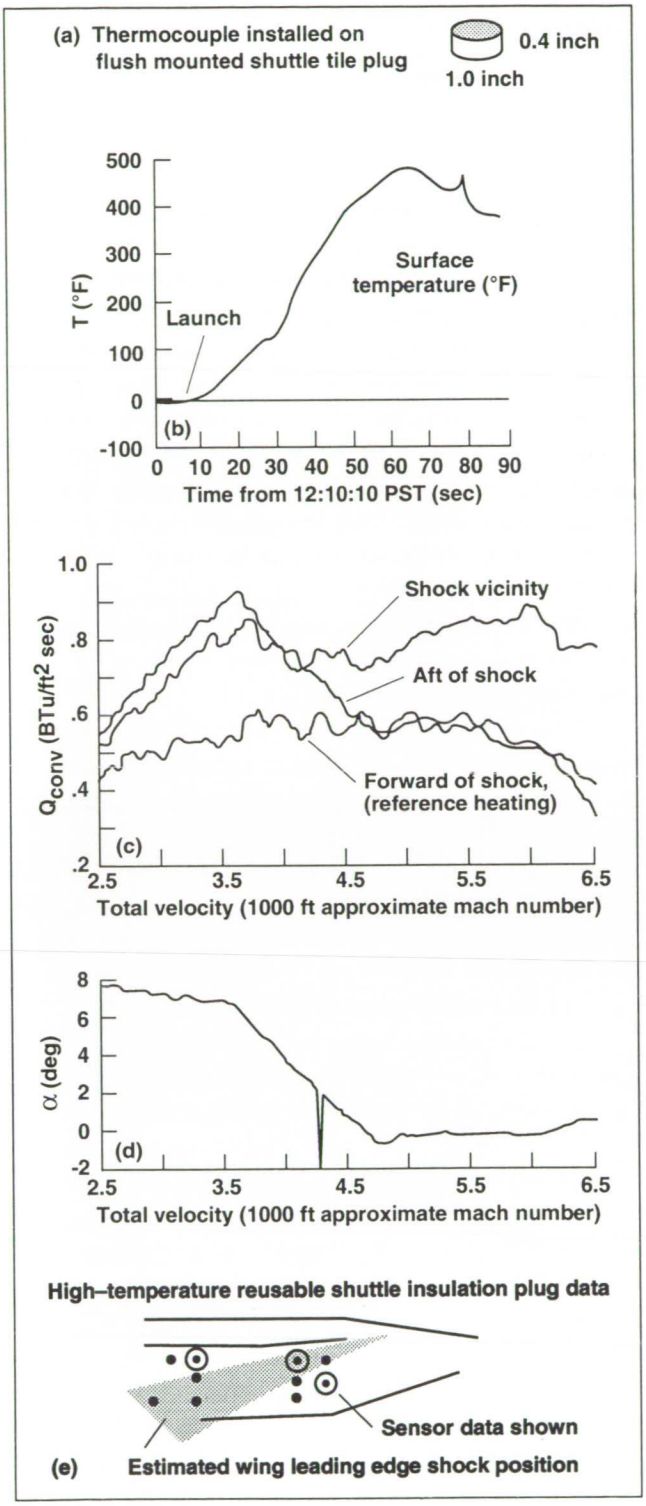


Fig. 3. Heating rates and plug schematics. (a) Schematic of high-temperature reusable shuttle insulation (HRSI) plug; (b) typical HRSI plug temperature profile; (c) derived heat versus time for three HRSI plugs; (d) angle of attack (alpha) versus time for the Pegasus; (e) schematic of plug locations on the wing-body fillet with the three sensors whose data are indicated

derivation of surface heat flux. All data were incorporated into the baseline Pegasus telemetry stream with minimal impact (see the first figure).

The second figure shows typical temperature profiles measured by a "stack" of thermocouples within the TPS. The temperature measured just under the ablative usually levels out between 200 and 230° F, while the carbon-graphite structure remains between 100 and 140° F.

This is not always the case, however. The second figure also shows temperature versus X/C at different times for the inboard row of foil thermocouples (only those thermocouples on the inboard row located just under the ablative). About halfway back on the windward panel, the temperatures just below the ablative exceeded the ablation temperature (approximately 250° F) and in one case the upper range limit of 320° F. This behavior was also observed on the outboard row.

The third figure shows a typical surface temperature profile for an HRSI plug mounted in the wing-body fillet. The temperatures measured on the surface of the nonablating plug are much higher than those measured within the TPS and are more responsive to changes in flight condition. The figure also shows derived heat flux for three such sensors: one is always ahead of the wing shock during times of aerodynamic heating, one is usually within the wing shock region, and one is usually behind it. During the higher alpha portion of the plot (2,500 < velocity < 4,000 feet/second), the plugs in and behind the shock region see the effect of the wing compression field. As the alpha drops off (velocity > 4,000 feet/second), only the plug within the shock region continues to measure an elevated heating rate.

Similar instrumentation is being installed on the second launch vehicle at this time. Data from this flight are expected to substantiate the aerodynamic conclusions from Flight 1 as well as evaluate new instrumentation techniques. A flush air-data system, a nonablating flight test fixture suitable for transition experiments, and a stand-alone research data acquisition system are being developed for follow-on flights.

Ames-Dryden contact: G. Noffz/R. Curry
(805) 258-2417/3715 or FTS 961-2417/3715
Headquarters program office: OAET

Advanced Multidisciplinary Analysis

Kevin L. Petersen, Kajal K. Gupta

Efforts to develop and improve integrated systems analysis techniques have resulted in significant technical achievements this past year. A summary of two specific developments follows.

An advanced integrated systems analysis technique has been developed and used to model and analyze the key cross-discipline interactions so dominant in modern high performance aircraft. The general purpose, finite-element program STARS (Structural Analysis Routines) is combined with unsteady aerodynamic codes and hybrid flight controls analysis methods to provide an integrated multidisciplinary analysis capability. This linear analysis tool is capable of predicting aeroelastic and aeroservoelastic dynamic stability of highly integrated aircraft, such as the X-29 and F-18 High Angle-of-Attack Research Vehicle (HARV) (see the first figure).

This year, a comprehensive finite-element structural dynamics model of the F-18 HARV was developed, including the turning vane control system (TVCS) structural components. A corresponding unsteady aerodynamics model was then generated using the constant pressure and doublet lattice techniques for supersonic and subsonic flows, respectively. Models of the F-18 HARV flight control systems are coupled with the aerodynamic and structural models to provide an integrated aeroservoelastic analysis capability. Open- and closed-loop frequency responses are computed to assess the dynamic stability characteristics of the total vehicle. These aeroservoelastic stability predictions are a vital part of overall flight safety assurance and have already been used to steer the flight envelope expansion efforts on the F-18 HARV program. This analysis capability will continue to be exercised throughout the flight program whenever modifications to the vehicle's flight control systems are made.

Hypersonic vehicles will be characterized by unprecedented levels of aerodynamic, structural, propulsion, thermal, and control interactions that will likely impose severe constraints on the dynamic stability and controls performance margins required for safe flight. This research is aimed at developing a predictive analysis capability which enables effective prediction of flight-critical, dynamic stability and controls performance parameters and characteristics. An integrated, nonlinear, multidisciplinary simulation analysis approach is required to accommodate these requirements. This year's research efforts have led to the development of a comprehensive methodology and approach addressing these most difficult requirements.

The methodology builds on fundamental technology approaches within each critical discipline area and integrates each discipline in a consistent manner to provide a comprehensive analysis framework (see the second figure). A critical factor in the success of the methodology requires continuous attention to software computational improvements and advances in hardware computing technology. Key elements of the approach include: three-dimensional (3-D) unstructured tetrahedral grid generation with adaptive mesh capability, external aerodynamic flow solvers using 3-D Navier-Stokes or Euler equations with boundary-layer interface codes and a finite-element formulation, 3-D internal flow propulsion codes, an advanced finite-element structural code with heat transfer and advanced materials characterization capabilities, and a nonlinear simulation of a hypersonic vehicle. The code integration approach has been defined and various component developments are under way.

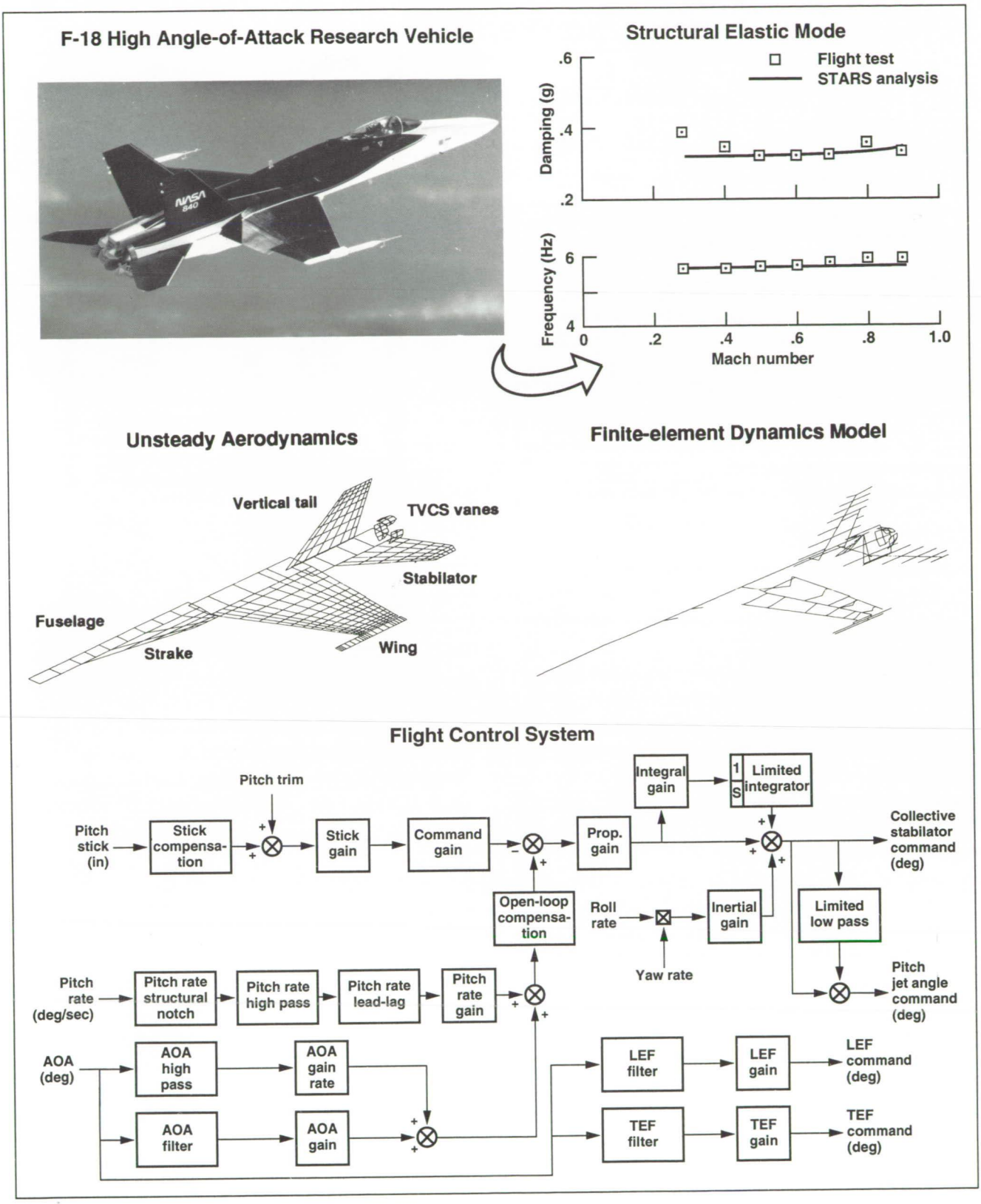


Fig. 1. Integrated systems analysis

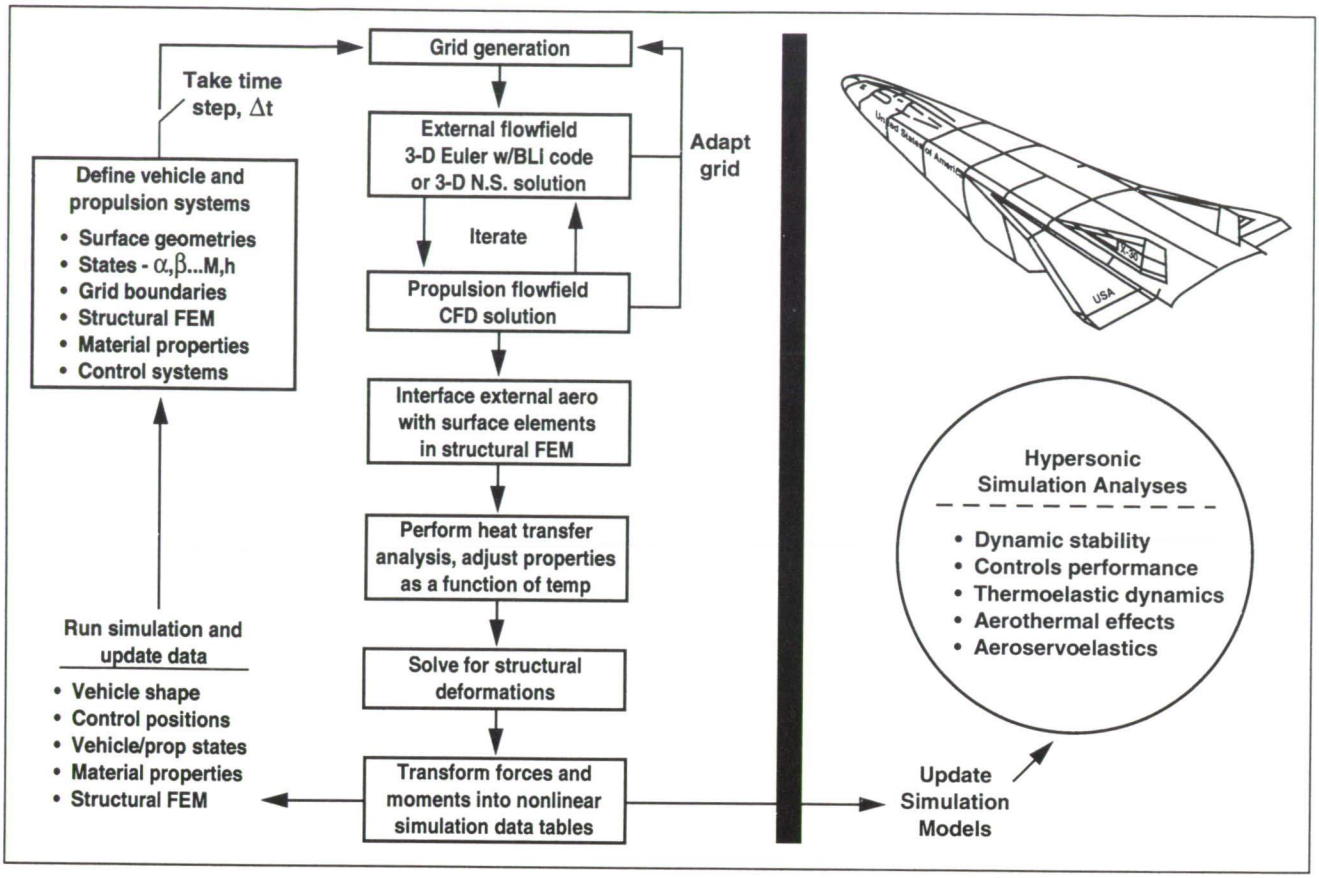


Fig. 2. Nonlinear multidisciplinary simulation, approach

Successful development of this nonlinear methodology will provide the first truly integrated and comprehensive analysis capability which can account for key multidiscipline (aerothermal, thermo-structural, aeroservoelastic, etc.) effects inherent in hypersonic vehicle designs.

Ames-Dryden contact: K. Petersen
(805) 258-3189 or FTS 961-3189
Headquarters program office: OAET

F-18 High Angle-of-Attack Research Vehicle Vortex Flow Field Results

David M. Richwine, David F. Fisher

A strong vortical flow field exists on the upper surface of the leading-edge extensions (LEX) of the F-18 High Angle-of-Attack Research Vehicle (HARV) at high angles of attack. This flow field has been extensively documented for pressure, velocity, and flow direction using a 16-probe flow direction rake at a location near the canopy on the right LEX (see the first figure). Each hemispherical-tipped five-hole probe measured the local total and static pressures and was also used to determine the local flow direction while the rake was traversed through the LEX vortical flow field.



Fig. 1. Leading-edge extension (LEX) surface rake located on the upper surface of the right LEX of F-18 HARV

Results from this rake are shown in the second figure for an aircraft angle of attack of 30°. In this figure, the local flow direction for the area swept by the rake is shown. A vortex core can clearly be identified above the LEX. The local static pressure coefficients as measured by the rake are shown in

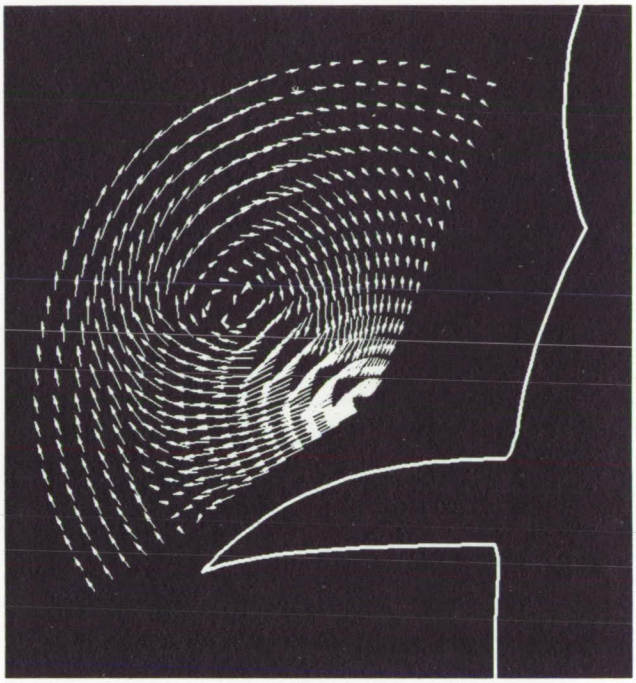


Fig. 2. Local flow direction through LEX vortex as determined from LEX rake, a = 30°

ORIGINAL PAGE
BLACK AND WHITE PHOTOGRAPH



Fig. 3. Local static pressure measured through LEX vortex with LEX vortex survey rake (see color plate 4 in Appendix)

the third figure. A region of low static pressure can be seen at the vortex core. Static pressure coefficients from orifices on the LEX surfaces have been combined with the static pressure coefficients from the rake in the fourth figure. Also shown in this figure are the primary, secondary, and tertiary separation line locations previously obtained from surface flow visualization results. The surface pressure results show good correlation with the rake results. The surface flow visualization results have previously

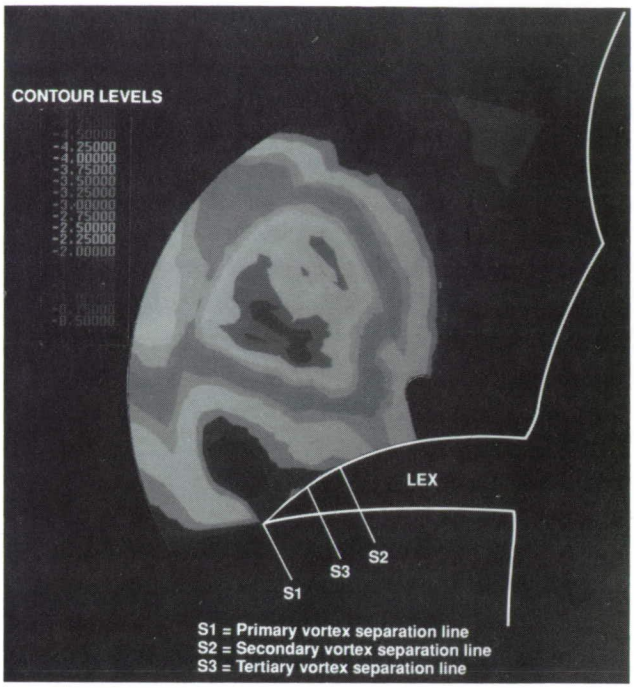


Fig. 4. Correlation of off-surface and surface LEX static pressure coefficients with surface flow visualization results (see color plate 5 in Appendix)

been shown to have good agreement with the surface pressures.

Analysis of these rake data and comparison to computational solutions are progressing.

Ames-Dryden contact: D. Richwine/D. Fisher
(805) 258-2170/3705 or FTS 961-2170/3705
Headquarters program office: OAET

Computer-Aided Systems Testing

Joel R. Sitz

Improved techniques to flight-qualify human-rated control systems are being developed at the Ames-Dryden Flight Research Facility. Automated verification and validation testing techniques have successfully been applied to the X-29 Forward Swept Wing (FSW) and the F-18 High Angle-of-Attack Vehicle (HARV) flight research projects. The new techniques have reduced the time required to perform closed-loop software validation tasks by a factor of three. These validation tasks include aircraft systems testing using several levels of flight hardware in-the-loop including aircraft in-the-loop.

The computer-aided systems testing (CAST) system is a distributed processing environment. The architecture of the CAST system is based on a new, real-time communications interface network called the Universal Memory Network (UMN). The UMN is able to connect dissimilar computer platforms at very high bandwidths (40 megabytes/second) over distances of up to 2 kilometers with no special computer protocols necessary. The UMN was developed under contract to the Dryden Flight Research Facility for use in the Integrated Test

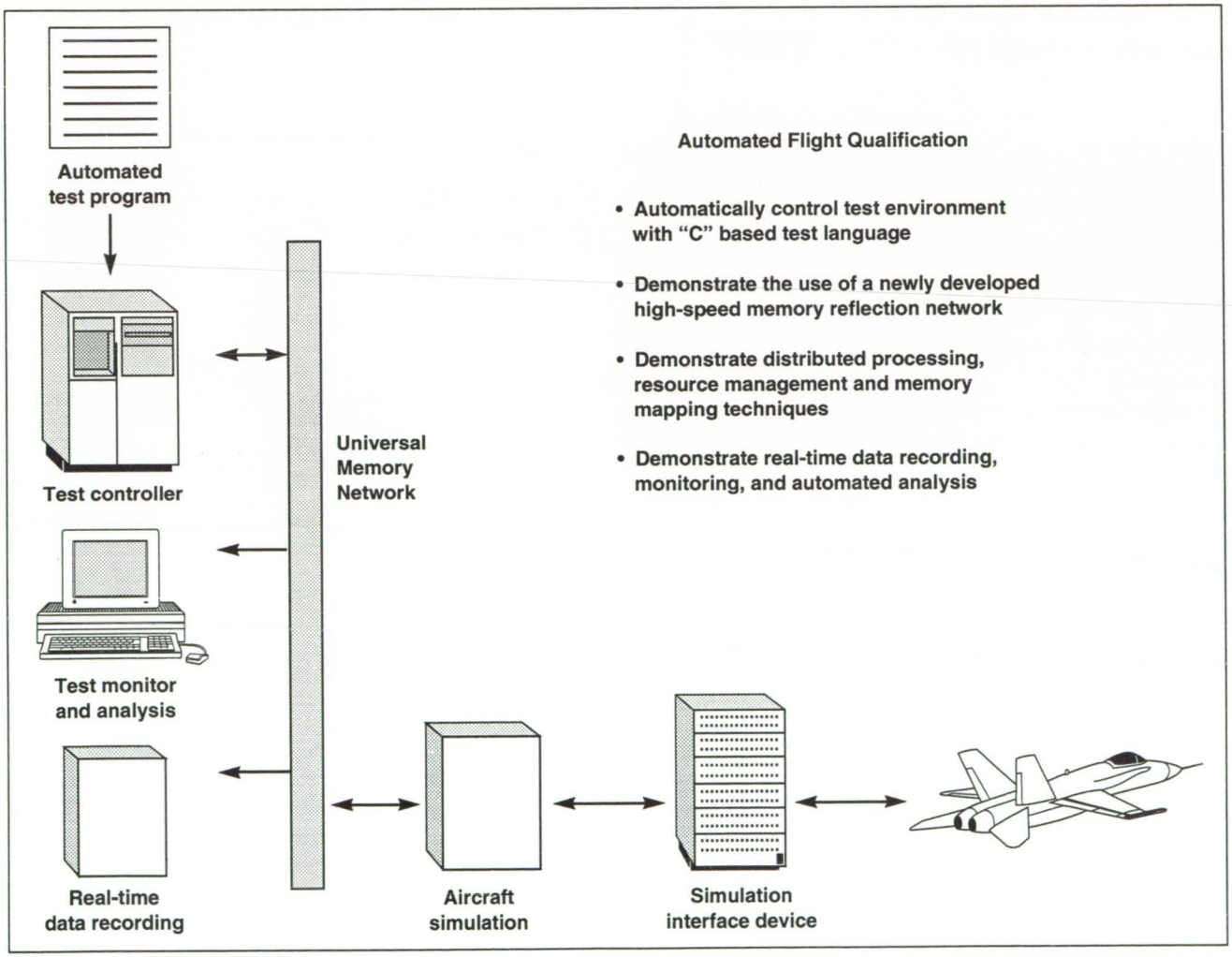


Fig. 1. Automated flight qualification

Facility. The UMN allows the nonlinear real-time simulation, the test engine (controller), the test monitor, and the high-speed data recorder to share memory over long distances.

The high-speed data recorder is being used on the F-18 HARV project. The recorder records simulation and aircraft data at rates up to 500,000 32-bit words/second. This information significantly reduces the time required to troubleshoot hard-to-repeat problems that may occur during testing.

The user can interactively control the major elements of the CAST environment through a graphical user interface running on a high-speed Unix workstation. Automated control is accomplished by writing a test procedure in "C" which is executed by the test engine (controller). Application-to-application communication and movement of data are accomplished with the UMN.

The CAST system is being used by the F-18 HARV project at Dryden to flight-qualify the Research Flight Control System used on the F-18 HARV. Dryden has also adopted the CAST approach for future flight research projects.

Ames-Dryden contact: J. Sitz
(805) 258-3666 or FTS 961-3666
Headquarters program office: OAET

Western Aeronautical Test Range Color-Alphanumeric Panel Display Processing System

James Skultety

Modern flight research requirements at the Ames-Dryden Flight Research Facility have necessitated the upgrade of existing Mission Control Center display hardware and software. The Western Aeronautical Test Range (WATR), using low-cost, off-the-shelf and custom components, has engineered an advanced workstation system to meet the majority of flight research data display requirements.

The Color-Alphanumeric Panel is an Intel 80386-based display processing workstation that replaces the existing Alphanumeric CRT and color panel systems currently used in Dryden's WATR Mission Control Center. Previous display processing programs ran on the Telemetry Radar Acquisition Processing System with data being distributed to displays in each mission control room. These programs are replaced by a single program running on 12 workstations located in each mission control room, thus offloading the primary real-time telemetry processor of its display generation responsibility.

Centralized control for the workstations is provided by the CAP Master Processor (CAMP). CAMP is used to distribute system control information to each workstation during mission setup. This eliminates the need for support personnel to manually configure individual workstations.

The system could run a real-time display generation and processing program called VENTANA.

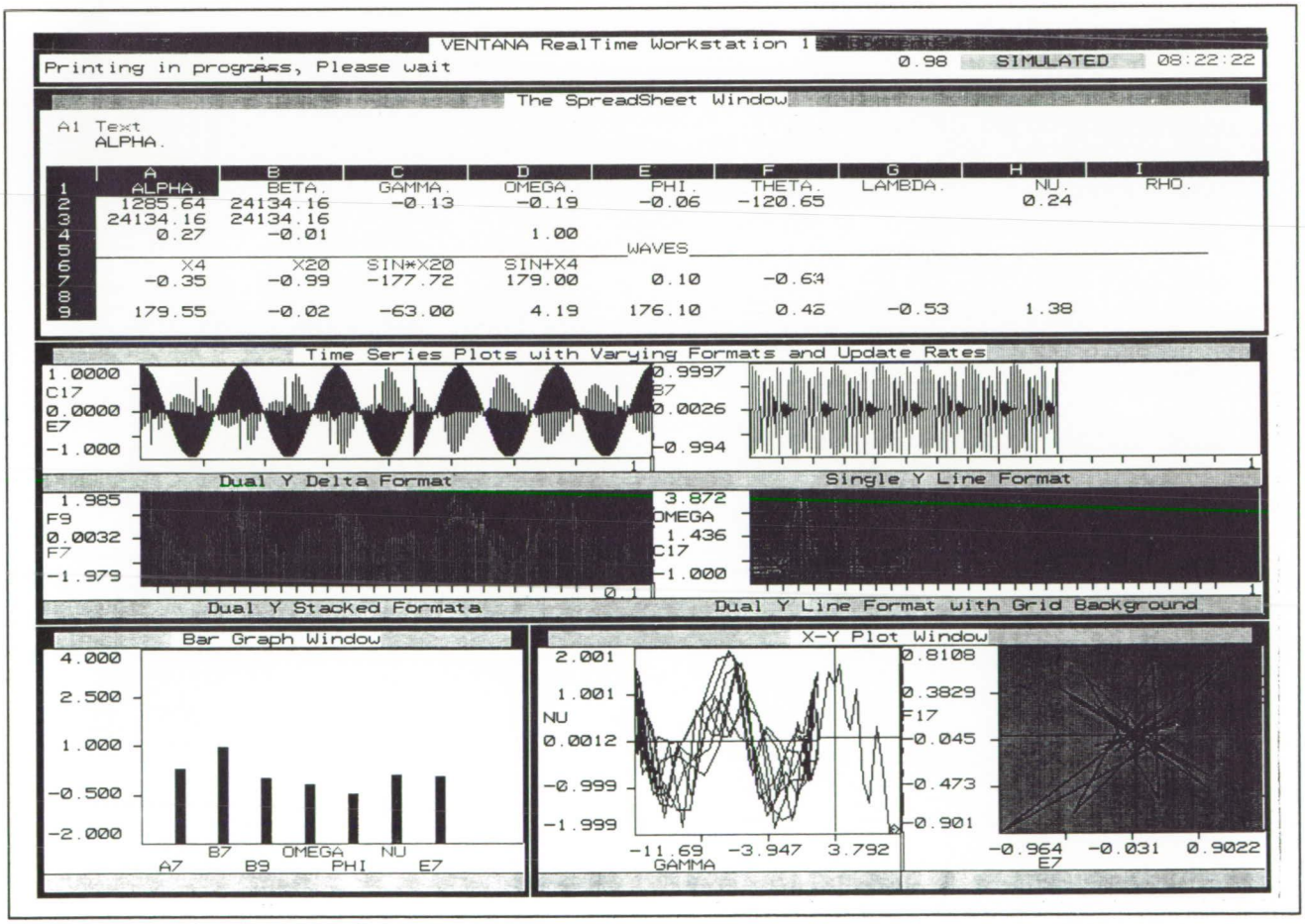


Fig. 1. VENTANA software graphics display

VENTANA provides a user friendly interactive spreadsheet interface that connects real-time data from the telemetry processor to multiple pages of high-resolution color graphics displays. The user spreadsheet allows the interactive manipulation of data so that user-defined equations, time series charts, bar graphs, and X/Y plots may be configured in real time. The majority of Mission Control Center displays will be configured, validated, and stored before flight for use during missions.

The Color-Alphanumeric Panel Display Processing System provides (1) quick access to all telemetered pulse code modulation data in real time, (2) user friendly and user configurable software, (3) real-time modifiable windowed displays, and (4) low-cost local processor platforms which meet the majority of flight research data display requirements.

Refer to "Western Aeronautical Test Range Shared Memory System" by D. Wheaton in this publication for additional information.

Ames-Dryden contact: J. Skultety
(805) 258-3242 or FTS 961-3242
Headquarters program office: OSO

Scientific and Technical Electronic Publishing System

Gene Waltman

The Scientific and Technical Electronic Publishing System (STEPS) is Ames Research Center's innovative automated system used to improve the quality, production, management, and tracking of technical reports, documents, and presentation materials. STEPS is a networked electronic platform for the entire publishing operation, and includes a disparate group of hardware, software, peripherals, and networks. Tracking and document work flow are managed by a subsystem, the STEPS Tracking and Retrieval System (STARS).

STEPS has been designed to improve the quality, timeliness, and quantity of publications produced. In addition, managing these documents has also been improved. The STARS data base not only allows for storing, retrieving, and archiving the many components (text, illustrations, plots, etc.) of each publication, but it also includes other data needed to track the progress of the production of these components. Work assignments and progress, editorial changes, and due dates are examples of other information stored in STARS, which is available to the managers, authors, editors, graphic artists, and other personnel involved in producing these complex documents.

Most of STEPS has been built using off-the-shelf components, such as Macintosh personal computers, standard graphics and text processing packages, and easily obtained peripherals—printers, scanners, and network components. Even the STARS data base has been developed using a commonly available data base management system. This design goal will allow for ongoing, low-cost improvements and enhancements in future features and capabilities.

Funded by Ames Research Center, the initial development of STARS was centered at the Dryden Flight Research Facility because the facility is a smaller organization than the Moffett site. The two sites will have compatible although not necessarily identical systems.

The figure shows how STEPS is configured at Dryden. All workstations are Macintosh personal computers.

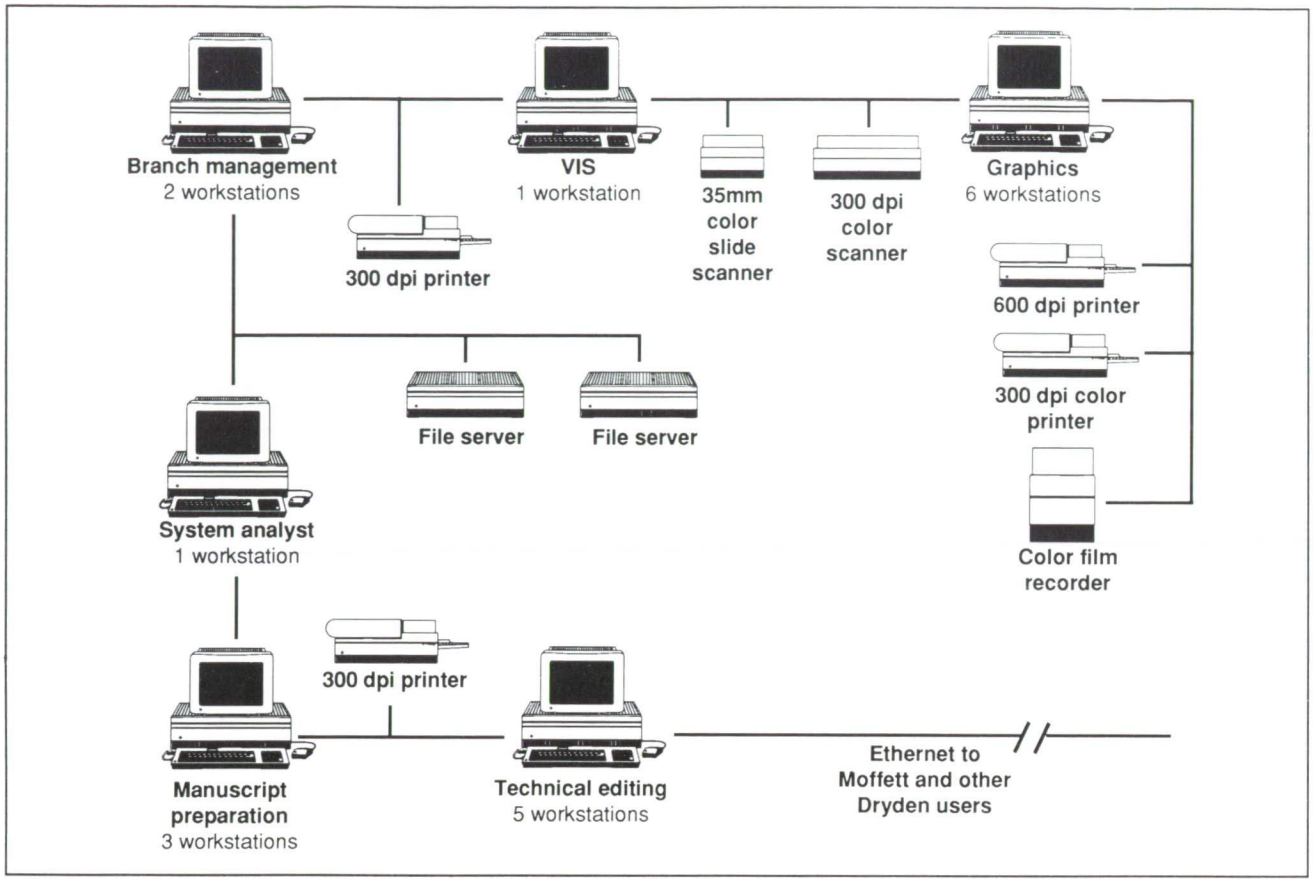


Fig. 1. Dryden system configuration

So far, STEPS has improved transferability—nearly all text and about 50% of the artwork is now submitted in electronic form—from a wide variety of workstations and computer platforms. STARS has allowed better tracking and reporting capability along with greater accessibility and networking capabilities. Authors, editors, and others now have network access to archives and statistical information about the publishing process. As the system continues to grow, it will provide even greater flexibility.

Ames-Dryden contact: G. Waltman
(805) 258-3761 or FTS 961-3761
Ames-Moffett contact: S. Parkhurst
(415) 604-6948 or FTS 464-6948
Headquarters program office: OAET

Western Aeronautical Test Range Shared Memory System

Duane Wheaton

A high-performance distributed shared memory (DSM) system has been designed, tested, and soon will be installed in the real-time processing and display computers of NASA's Western Aeronautical Test Range (WATR). This system will provide the foundation for the processing improvements necessary to support future flight research programs.

The DSM uses unidirectional point-to-point links to transfer information between WATR computers and mission control room displays. Information transfer to other computers is accomplished by storing to local memory. This simple topology allows multiple concurrent transfers while eliminating the

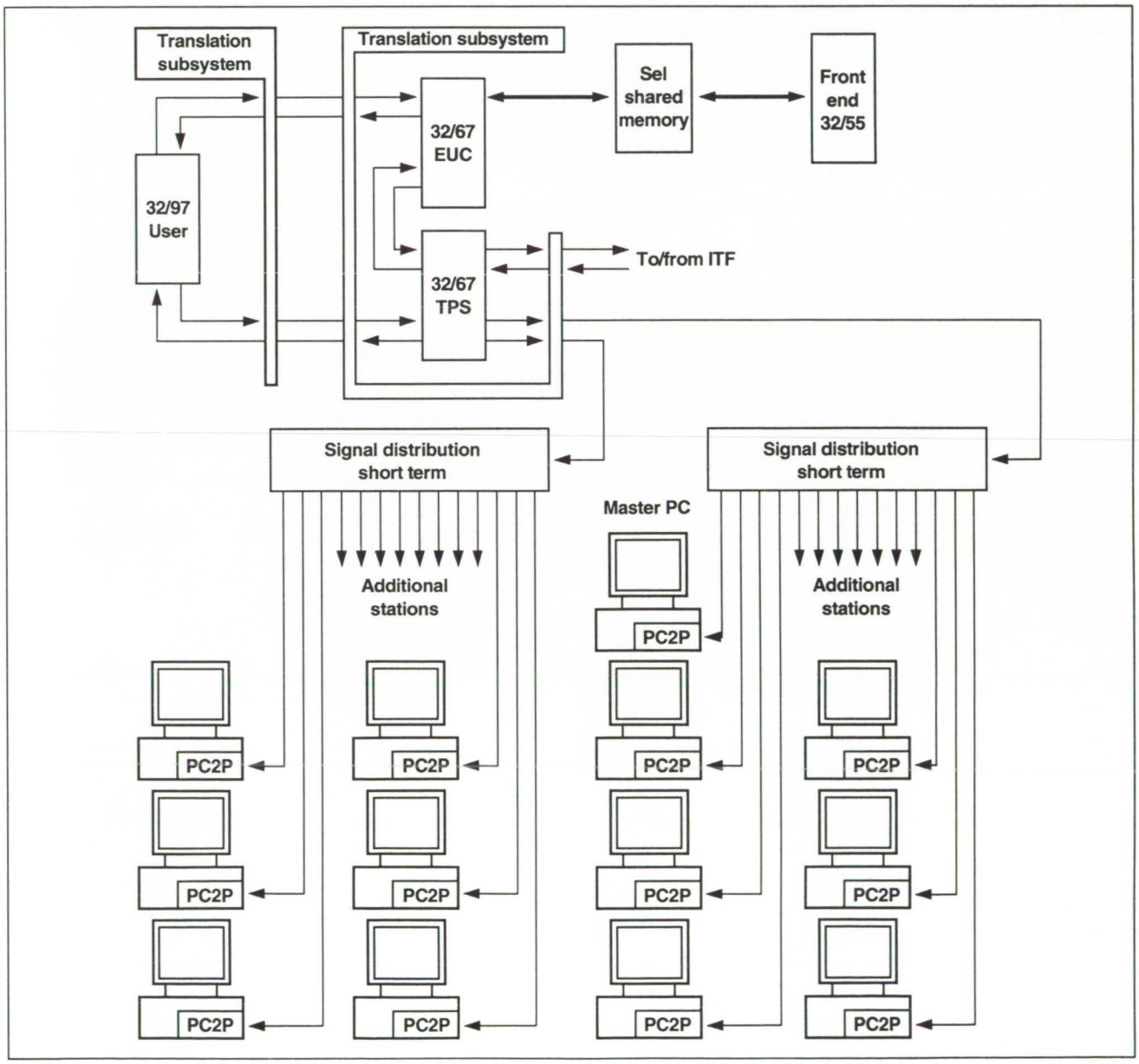


Fig. 1. WATR shared memory system

arbitration bottlenecks associated with more conventional shared memories. Because information is delivered to each destination through the external port of an asynchronous two-port memory, latency and overhead are minimized while fault tolerance is maximized. Finally, because of its point-to-point nature, each new connection to the DSM adds bandwidth to the system.

Each DSM port is implemented on two redundant and independent serial data links. The data links are compatible with fiber optic media, allowing processors and displays to be kilometers apart. The data transfer rate for each link is 6.7 megabytes per second. Each port supports a peak data transfer rate of 26.7 megabytes per second, and a sustained transfer rate of 13.3 megabytes per second.

The DSM supports 8-, 16-, and 32-bit transfers with "on-the-fly" source-to-destination memory address translation, as well as floating-point format conversion. These features allow a very loosely coupled connection to non-WATR ("stranger") computers for real-time flight support.

The current implementation of the DSM is for Encore computers and IBM PC-AT compatibles, with a planned 1991 expansion to support Silicon Graphics IRIS workstations. Since the DSM architecture is compatible with a wide variety of computers, it is anticipated that other devices will be integrated into the DSM system as necessary.

Refer to "Western Aeronautical Test Range Color-Alphanumeric Panel Display Processing System" by James Skultety in this publication for additional information.

Ames-Dryden contact: D. Wheaton
(805) 258-3782 or FTS 961-3782
Headquarters program office: OAET

Navier-Stokes Simulation of Flow Through a Highly Contoured Diffuser Inlet

Wei J. Chyu, Daniel P. Bencze

A numerical technique is being developed for the analysis of inlet flow associated with highly maneuverable aircraft. Toward this end, an offset, super-elliptic, subsonic diffuser inlet (cross sections varying from rectangular to circular as shown in the first figure) was chosen because of its realistic inlet geometry and the availability of the experimental data for code verification. To treat the complexity of the inlet geometry and the flow simulation, a multizonal approach combined with a two-grid topology was used to represent both the internal and external flow fields, and an implicit, approximately factored, partially flux-split finite-difference code, called F3D, was used to solve the three-dimensional thin-layer Navier-Stokes equations.

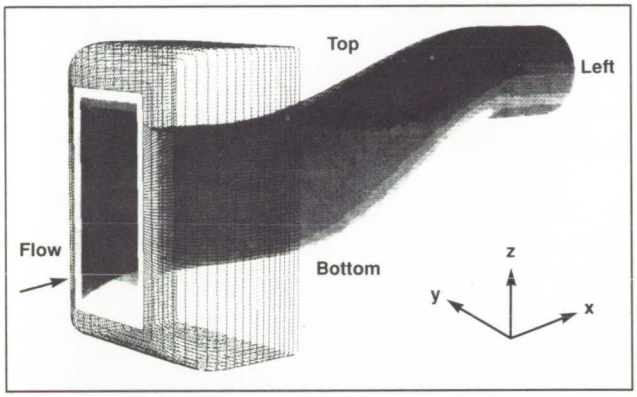


Fig. 1. Inlet geometry

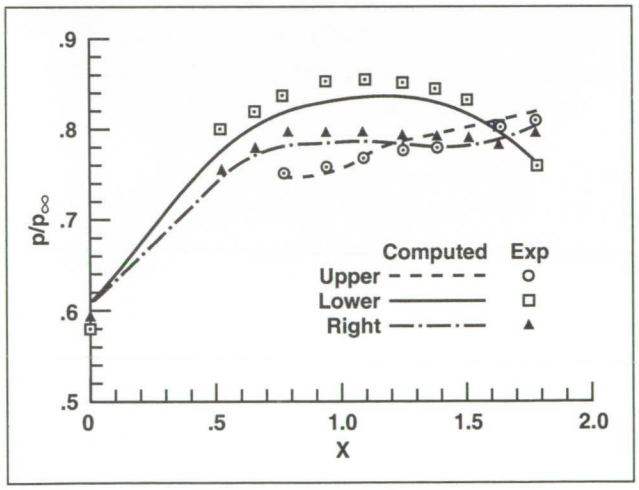


Fig. 2. Static pressure, $p_{exit}/p_\infty = 0.8$

The second figure shows both the computed and the experimental pressures along the duct walls at a mass flow condition corresponding to the exit pressure ratio, $p_{exit}/p_\infty = 0.8$. The Mach contours (see the third figure) and the velocity vectors (not shown here) at this mass flow rate show the patterns of flow separation and secondary flow (counter-rotating vortices) inherent with a highly offset diffuser inlet.

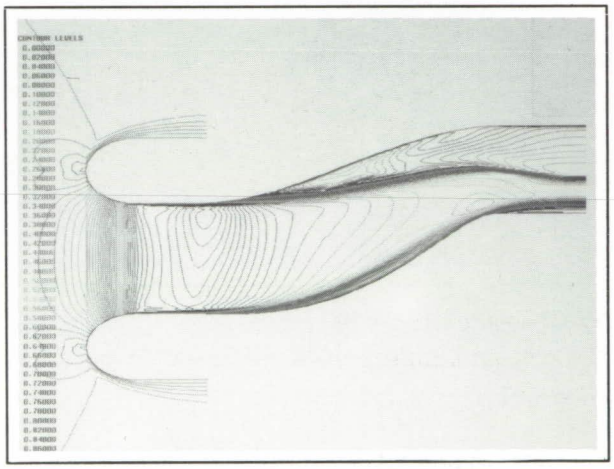


Fig. 3. Computed Mach contours, $p_{exit}/p_\infty = 0.8$ (see color plate 6 in Appendix)

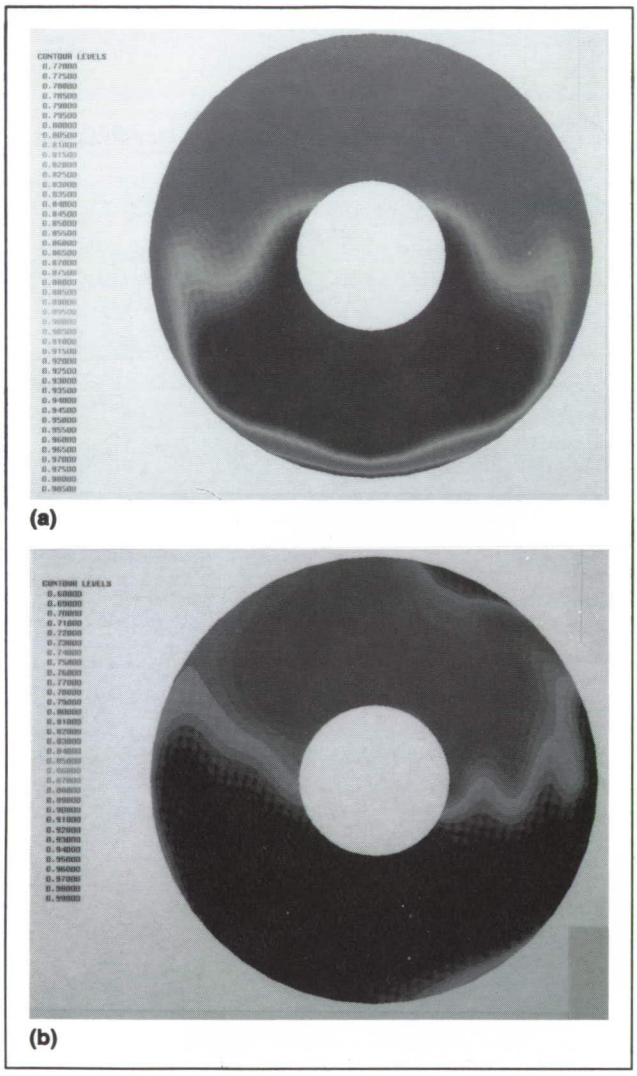


Fig. 4. Total pressure on engine face, $p_{exit}/p_\infty = 0.8$. (a) Computed, (b) experimental (see color plate 7 in Appendix)

Parts (a) and (b) of the fourth figure show the computed and experimental total pressure distributions at the engine face for $p_{exit}/p_\infty = 0.8$. The instrumentation hub in the model (circular hole in the center of the figures) was not modeled in the computations. Both the computed and the measured total pressures show highly nonuniform pressure distributions and a large total-pressure loss in the upper wall region of the engine face where the vortical flow is present.

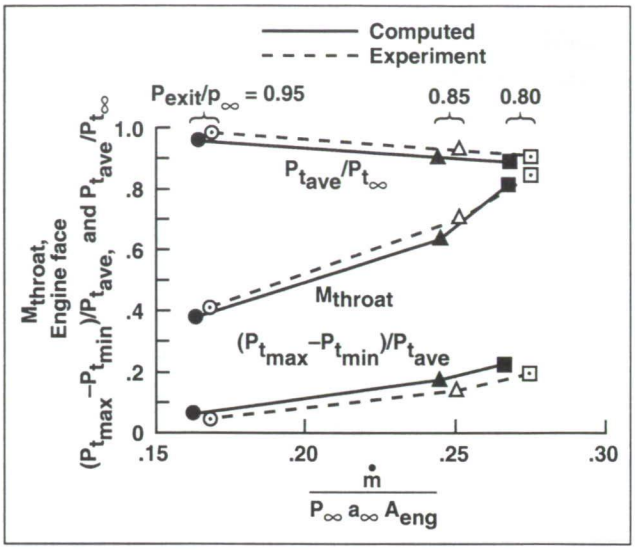


Fig. 5. Diffuser performance

The overall performance of the inlet is shown in the fifth figure where the average throat Mach number, M_{throat}, and the engine face total pressure, Pt_{ave}/Pt_∞, and pressure distortion $(Pt_{max} - Pt_{min})/ Pt_{ave}$, are plotted against the total mass flow rate, $m/\rho_\infty a_\infty A_{engine}$.

Although additional numerical studies are required to investigate these complex internal flow fields with large separated regions, the present study indicates that the current level of computational techniques permits analysis of these more complex inlets. This makes possible the investigation of design variables associated with integration of the forebody/inlet system.

Ames-Moffett contact: D. Bencze
(415) 604-6618 or FTS 464-6618
Headquarters program office: OAET

Sonic Boom Pressure Signature Computations Using Euler Codes

Susan E. Cliff-Hovey

Comparisons of experimental pressure signatures with extrapolated near-field pressure signatures obtained with Euler computational fluid dynamics (CFD) codes for three different configurations are presented. The Euler signatures were obtained at distances less than a body length below the configuration and used as input to an extrapolation code. The extrapolation code is a waveform parameter method based on geometric acoustics and the isentropic relations. The configurations used in this study consist of a cone-cylinder with a 6.48° included angle, a rectangular wing with parabolic sections and an aspect ratio of 0.50, and a Delta wing-body with 69° leading-edge sweep (see the first figure).

The Euler CFD codes used were two three-dimensional finite volume schemes, TEAM (Three-dimensional Euler/Navier-Stokes Aerodynamic Method) and FLO60. The TEAM code is a modified version of Jameson's FLO57 with Navier-Stokes capability. TEAM uses multiple-zoned structured grids and was used on all three configurations. FLO60 is an isolated-wing code which uses a single block H-H grid and computes the flow variables at each cell vertex. FLO60 was used on the low-aspect ratio rectangular wing only.

The grid for the cone-cylinder consists of four zones and was swept at an angle approximating the Mach angle with nearly 500,000 grid points. The flow conditions were Mach 1.68 and alpha 0.0. The computational data were taken at H/L = 1.1 and extrapolated to an H/L = 10.0. The solutions obtained using TEAM indicate that the rise time and maximum overpressure agree well with experiment (see part (a) of the second figure).

Computations for the low-aspect ratio wing were obtained by TEAM and FLO60 (see part (b) of the second figure). The computations agreed fairly well with the experimental data. The FLO60 signatures were obtained on a 192 × 128 × 64 grid and were extrapolated from an H/L of 0.75 to 1.0 using the waveform parameter method. The TEAM codes used a 10-zone grid and gave results comparable to FLO60. However the bow shock strength is more accurately predicted by TEAM than by FLO60. The rear shock strength is accurately predicted by both codes, but the correlation of FLO60 with the experiment is slightly better aft of the bow shock than for TEAM.

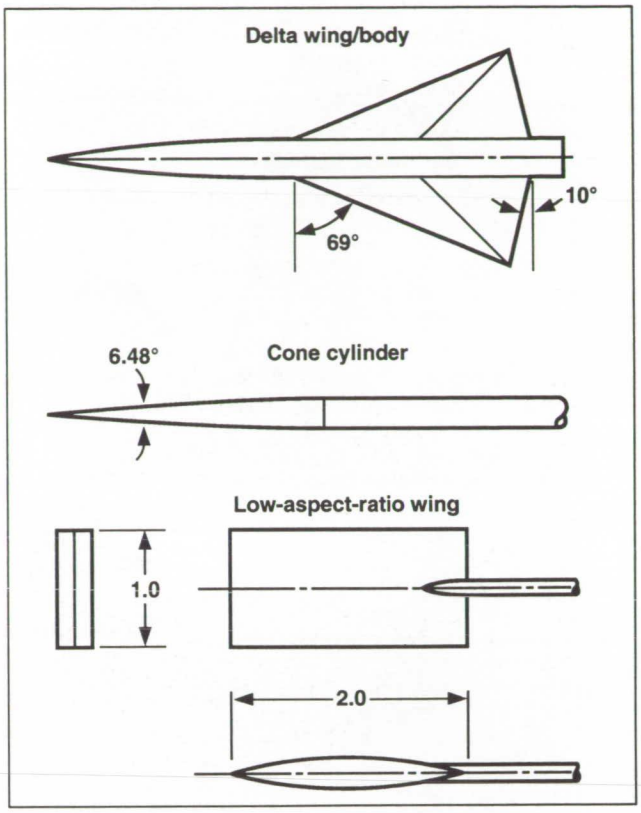


Fig. 1. Computational fluid dynamics validation models

Solutions for the delta wing/body were obtained with TEAM. The flow conditions include Mach 1.68 and 2.70 at lift coefficients of 0.0, 0.08, and 0.15. The grid used for these computations consisted of 34 blocks, and had approximately 1.5 million grid points. The rear-facing step at the base of the model was not modeled. The sting was modeled with a constant cross-sectional area and with a short ramp connecting the base of the model to the sting.

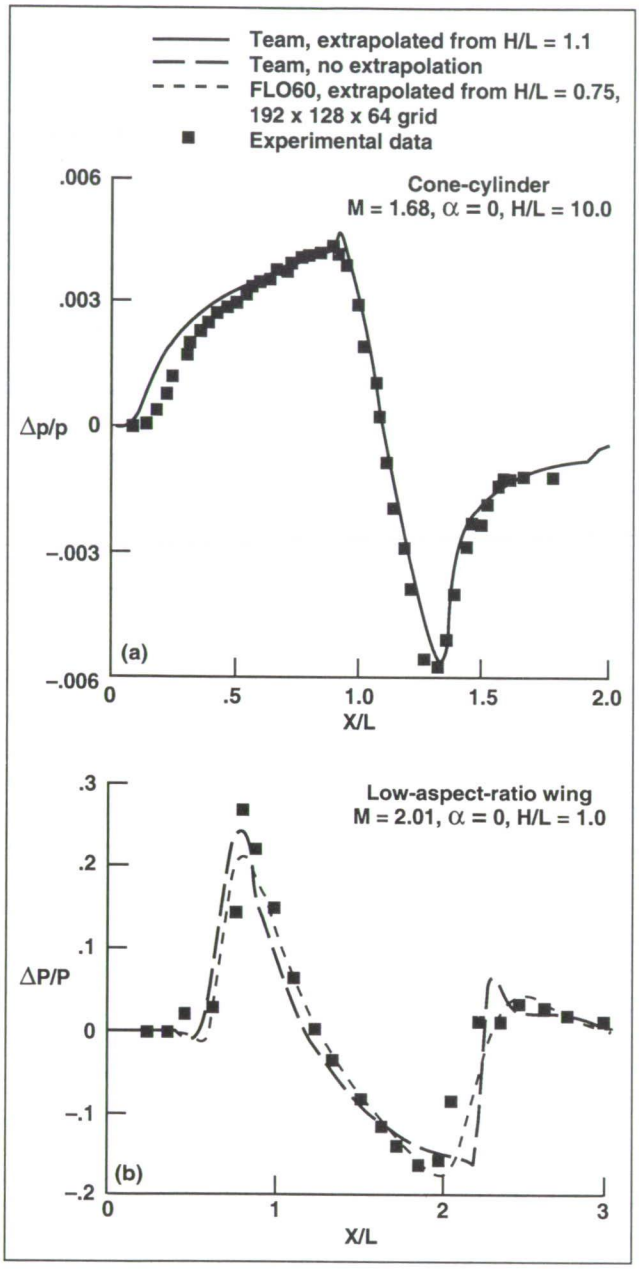


Fig. 2. Comparison between computational and experimental data. (a) Cone-cylinder, (b) low-aspect ratio wing

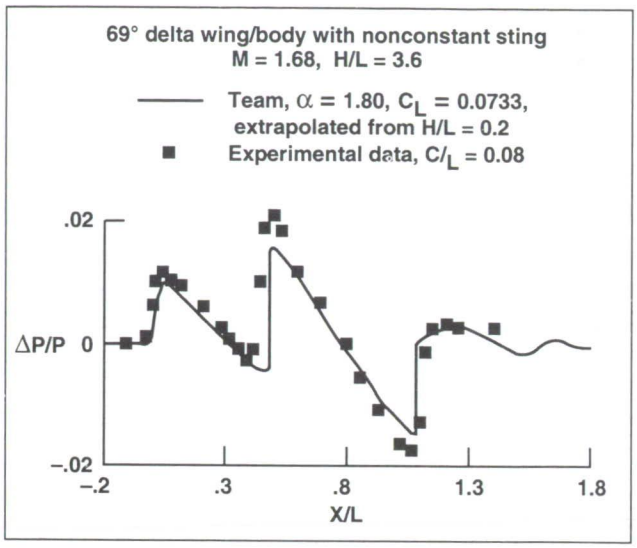


Fig. 3. Comparison between computational and experimental data

The comparison of experimental and computational pressure signatures at Mach 1.68 and Cl = 0.08 are shown in the third figure using the nonconstant area sting. The overall comparison is good; however, the wing and tail shock are slightly weaker than in the experiment. This may be due to the computational lift coefficient being slightly less than the experimental value. The computations at Cl = 0.15 (not shown) show a weaker tail shock than the experiment. This may be due to inaccurate modeling of the model base-sting intersection.

Ames-Moffett contact: S. Cliff-Hovey or R. Hicks
(415) 604-5656 or FTS 464-5656
Headquarters program office: OAET

Aircraft Aerodynamics Using Solution-Adaptive Unstructured Grids

Jahed Djomehri, Larry Erickson

Shock formation and flow separation from sharp edges are essentially inviscid, rotational physical processes. Thus, the physics of both can be simulated with the Euler equations. However, a primary obstacle to computing complex flows about realistic aircraft is the difficulty in generating an appropriate grid. The grid must accurately represent the geometric details of the aircraft, and must also be clustered densely enough in regions of concentrated shocks and vorticity to capture the large flow-field gradients there without unrealistic numerical dispersion and dissipation of the physical process. Unstructured grids are inherently appropriate for conforming to complex surface shapes typical of realistic aircraft, and are the key to generating a solution-adaptive grid that can concentrate itself in the regions of large flow gradients.

We are investigating a solution-adaptive, unstructured-grid code developed through grants with the University of Wales and Imperial Valley College, Imperial, Calif. This code includes a grid generator which discretizes arbitrary surfaces into triangular-shaped elements. From this surface triangulation the code then forms a flow-field set of grid points, by the advancing-front method, that are connected by tetrahedra. These tetrahedra are used to form linear shape function finite elements, which discretize the spatial derivatives in the Euler equations. The time derivatives are discretized with a two-term Taylor-Galerkin approximation that resembles a Lax-Wendroff approach. After a solution is obtained on the initial grid, error estimates based on a measure of the solution gradient are used to generate a new grid on the aircraft surface and in the flow field. The new grid gets densely clustered in regions of high flow gradients, and becomes less densely clustered in regions of small flow gradients.

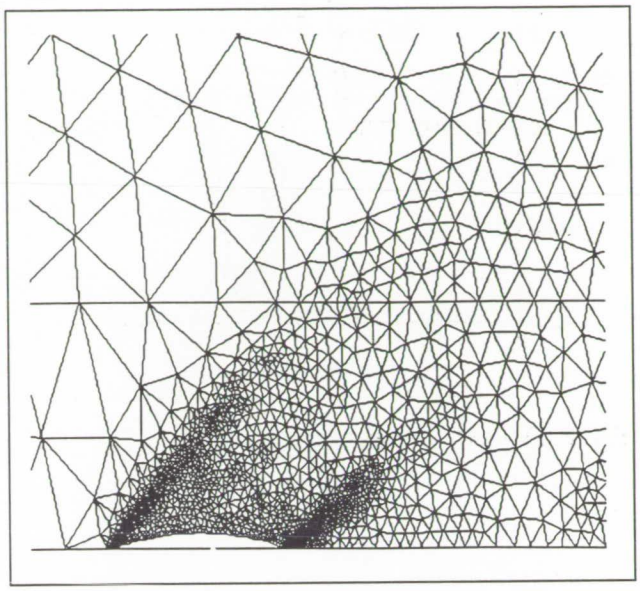


Fig. 1. Solution-adaptive grid at wing plane-of-symmetry

An example is shown in the two figures for a low-aspect ratio rectangular wing having a parabolic-arc airfoil. The first figure shows a portion of the flow-field grid. This view is at the wing's plane-of-symmetry and we see the triangular bases of the flow-field tetrahedra. The airfoil section is at the bottom of the grid, enmeshed in a very dense cluster of points that have been generated as part of the solution-adaptive process; for this case the angle-of-attack was 0°, and the free-stream Mach number was 2.01. The flow-field grid was constructed in two pieces, separated by a horizontal line one chord length above the wing section. (The horizontal and vertical dimensions are not quite at the same scale.) Pressures could then easily be computed along this

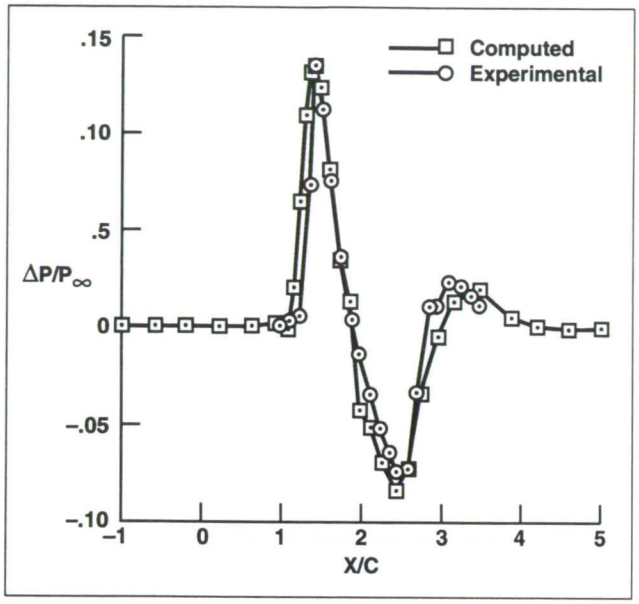


Fig. 2. Off-body pressure distribution

line for comparison with wind tunnel results. (Such near-field results can be used for predicting sonic-boom signatures at ground level.)

The comparison of pressures is shown in the second figure, where the horizontal position of the wing is between x/c of 0.0 and 1.0. At the one-chord-length height above the wing, the pressure field is about three chord-lengths long. The agreement between the computed and experimental data is quite good over the first half of this length and then it begins to deteriorate. Examining the first figure suggests that the grid is still not quite dense enough in this aft region.

Ames-Moffett contact: L. Erickson
(415) 604-6217 or FTS 464-6217
Headquarters program office: OAET

Euler Computations of a Generic Fighter

Aga M. Goodsell

Computational fluid dynamics (CFD) is becoming increasingly important in the analysis and understanding of flows about complex configurations. The validation of CFD codes for a wide range of flight conditions is essential if they are to become useful tools in aerodynamic design and analysis. The objective of this research is to evaluate the solutions of flow fields about a generic fighter with delta wings obtained from an Euler code to determine their validity over a wide range of angles of attack.

Flow fields about a generic fighter model have been computed using FLO57, a three-dimensional, finite-volume Euler code. The Euler equations provide the correct Rankine-Hugoniot shock jump conditions and allow for the transport of vorticity, but cannot model the viscous effects present in the flow field. Computed pressure coefficients, forces, and moments at Mach numbers 1.2, 1.4, and 1.6 and angles of attack between 0 and 20° are compared to wind tunnel data to determine the applicability of the code for the analysis of fighter configurations.

Two configurations of the generic fighter were studied, a wing/body alone and a wing/body with a displaced chine on the forebody. Experimental results on the generic fighter were obtained by Gary Erickson at Langley Research Center and John Schreiner at Ames Research Center in the Ames 6- by 6-Foot Supersonic Wind Tunnel.

The model, shown in the first figure, has a 55° swept cropped delta wing of aspect ratio 1.8 and taper ratio 0.2. The airfoils used in the wing were modified NACA 65A005 sections with sharp leading edges. The chine had wedge cross sections and was mounted on the forebody 0.5 inches above the wing.

At Mach 1.2, computational results were obtained on both the wing/body and wing/body/chine configurations. At low to moderate angles of attack (4° and 8°), the pressure correlation between computational and experimental data shows good agreement. At higher angles of attack, the pressure comparison shows some disagreement near the leading edge. This may be due to a lack of grid refinement near the leading edge and to the modeling of the leading edge itself. The results on the wing/body/ chine configuration show a slight improvement in the pressure computations over the wing/body configuration.

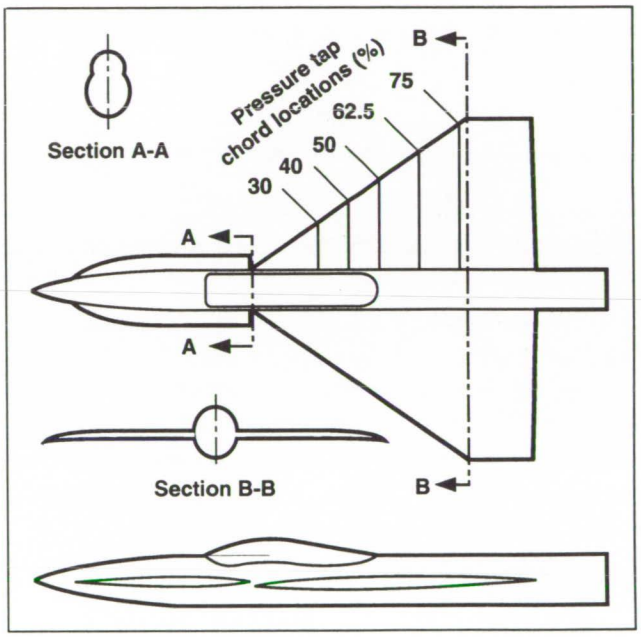


Fig. 1. Generic fighter

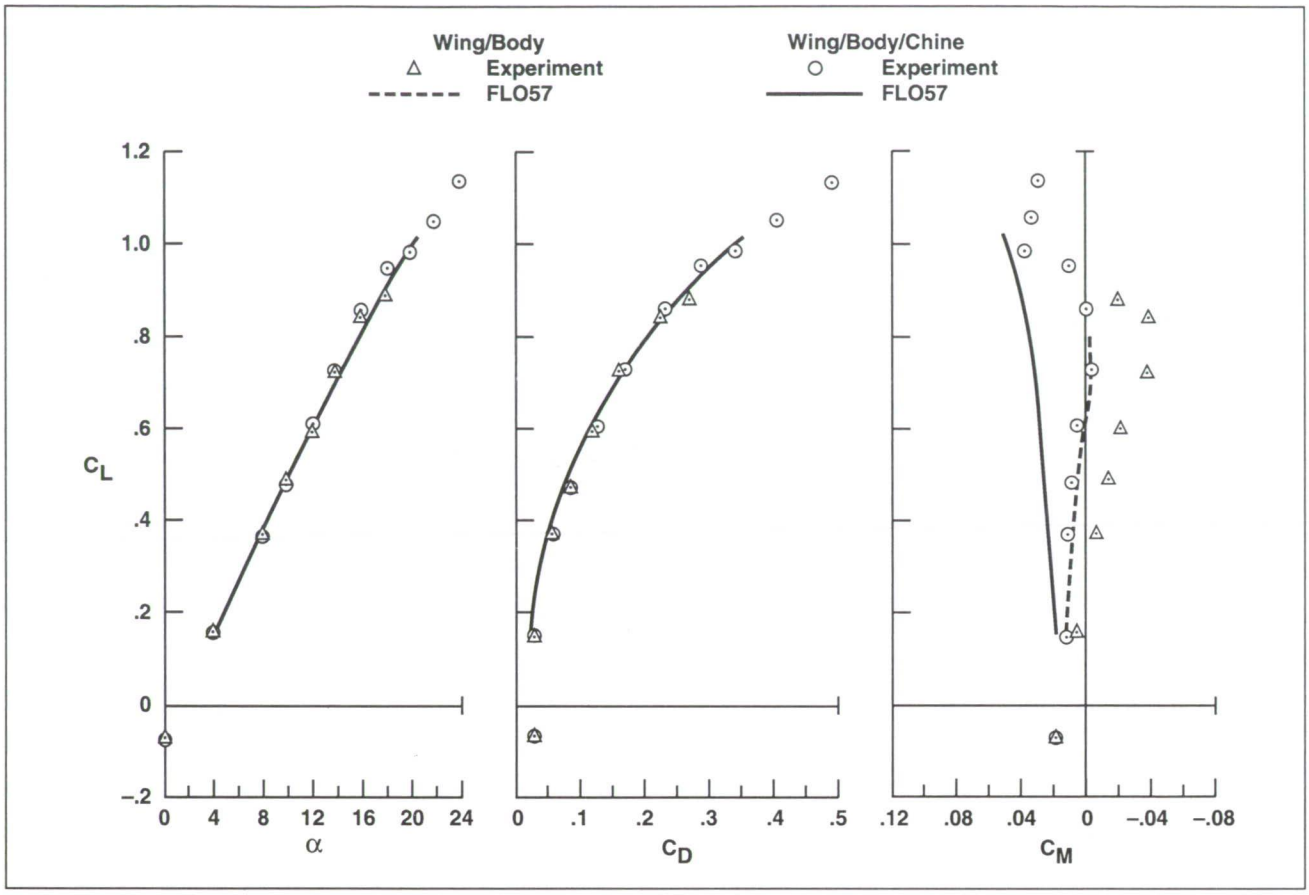


Fig. 2. Lift, drag, and moment comparisons at M = 1.2

The second figure shows the lift, drag, and moment curves for both configurations. The force comparisons show good agreement in lift and drag through 12° for both configurations. Although the moment comparisons are not as accurate, the increment between the wing/body and wing/body/chine configurations is well predicted by the Euler code. Accurate moment predictions are difficult to obtain since both the pressure magnitudes and distribution must be correct. The addition of the chine does not seem to affect the lift and drag of the model, but has the largest effect on the moment curve.

Ames-Moffett contact: A. Goodsell
(415) 604-3621 or FTS 464-3621
Headquarters program office: OAET

Sonic Boom Prediction Using TranAir

Michael D. Madson

The end of the 1980s brought back a renewed interest in the development of a new, efficient supersonic aircraft for use in the commercial airline industry. The High-Speed Research Program (HSRP) has been established so that research using modern design and manufacturing techniques may be performed in an effort to design and build a high-speed civil transport that can compete with existing subsonic transports in terms of cost to the passenger. Several challenges await this effort, one of which is trying to reduce sonic boom levels to a level low enough to make overland supersonic flight possible. The prediction of sonic booms at large distances away from the aircraft requires an accurate prediction of the near-field pressure signature, and an accurate extrapolation technique in predicting the pressure signature at large distances from the aircraft.

The TranAir code solves the nonlinear full-potential equation for subsonic, transonic, and supersonic flow about arbitrary configurations. The code was applied to several supersonic configurations, both generic and realistic, in an effort to establish its ability to accurately predict pressure fields away from the models. This near-field prediction was then input into a well-established extrapolation routine for predicting mid- and far-field signatures. TranAir embeds a surface-paneled geometry in a rectangular array of flow-field grid points. The initially uniform grid is locally refined using a solution-adaptive refinement technique. This adaptive capability allows the grid to be refined into the flow-field, accurately capturing shocks emanating from the model.

The first figure shows the paneled definition of a wing/body geometry and the final refined grid along the two planes of symmetry. The second figure shows the Mach Number contours along the centerline of the geometry for a free-stream Mach number of 1.68, and an angle-of-attack of 0°. The ability of the code to capture shock regions well into the flow field is evident in the figure.

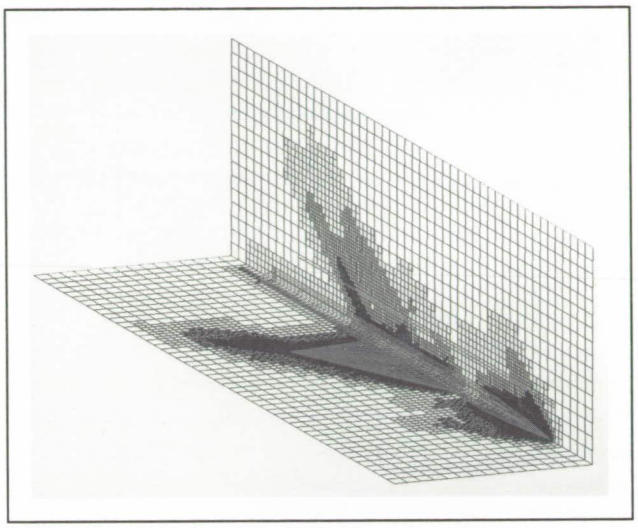


Fig. 1. Refined grid for wing/body geometry from TranAir (see color plate 8 in Appendix)

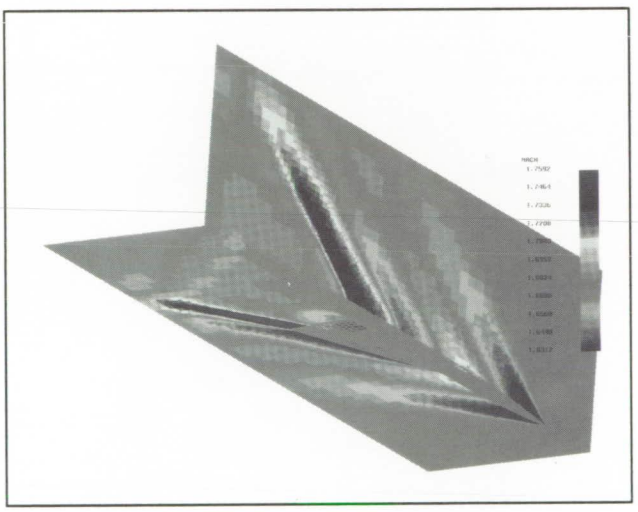


Fig. 2. Centerline Mach Number contours for wing/body geometry at M = 1.68 and α = 0 (see color plate 9 in Appendix)

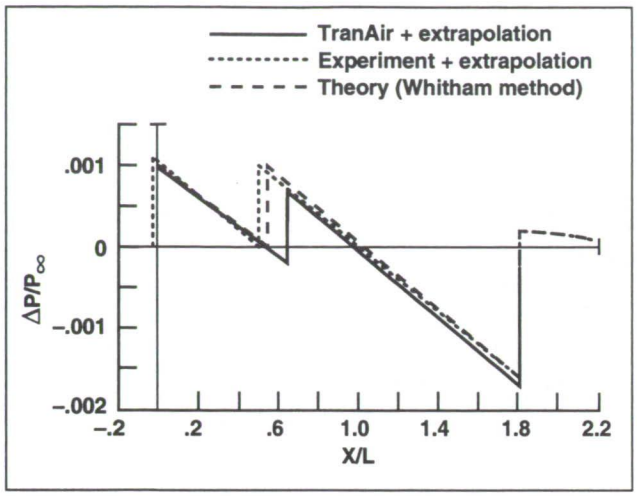


Fig. 3. Extrapolated sonic boom signatures for wing/ body geometry

The third figure shows a plot of $\Delta p/p_\infty$ (where p is pressure) at a distance of 130 body lengths away from the geometry along its centerline. The TranAir result, extrapolated from 0.2 body lengths away from the geometry, is plotted along with a theoretical prediction based on the Whitham method, and an extrapolation of wind tunnel data. It is seen that the magnitudes of the shocks were well predicted by TranAir, but the location of the TranAir-predicted wing shock was slightly downstream relative to the other predictions. The cause for this difference is being investigated.

Initial results obtained for the various models analyzed to date have shown that TranAir is a useful tool in the prediction of sonic booms generated by realistic configurations.

Ames-Moffett contact: M. Madson
(415) 604-3621 or FTS 464-3621
Headquarters program office: OAET

Unstructured Euler Flow Solutions Using Hexahedral Cell Refinement

John E. Melton, Scott D. Thomas, Gelsomina Cappuccio

A well-established, structured Euler code (FLO57) was used to develop a topologically independent, unstructured, hexahedral-based Euler code (TIGER). The TIGER program uses a modified version of the Jameson four-stage, finite-volume Runge-Kutta algorithm to integrate Euler equations. The unstructured nature of the program allows for user-specified local grid refinement in areas of large flow gradients. Cells may be repeatedly split into eight smaller cells to provide increased resolution where large flow-field variations exist. Because this refinement is done locally, specific regions of the flow field can be analyzed with higher grid resolution, while unnecessary refinement in other regions of the flow field is avoided.

The use of hexahedral-based grids also allows the use of current conventional grid-generation techniques to generate the starting grid and eliminates many of the difficulties associated with generating unstructured tetrahedral grids and visualizing tetrahedral-based flow-field data. An efficient program structure is critical in avoiding large CPU-time and memory penalties. The resulting code runs at a rate equivalent to conventionally structured Euler and Navier-Stokes solvers and uses simple, straightforward programming techniques to take advantage of the vector-processing capabilities of the CRAY Y-MP.

An interactive graphical analysis tool (GIRAFFE) was developed with the flow solver to visualize the unstructured flow data, check the boundary condition specifications, and perform the grid refinement. The GIRAFFE program can display data using color mapping and contour lines on user-specified, unstructured flow-field planes. Additional analysis capabilities include the display of refined cells, surface data, and the ability to refine local regions of the flow field using various refinement criteria.

The TIGER program has been used to successfully compute solutions with refinement for a variety of configurations over a wide range of Mach numbers and angles of attack, including the Generic Fighter, the ONERA M6 wing, and a variety of two-dimensional airfoils.

The enhanced resolution of the wing vortices on the Generic Fighter is shown in the first figure. Both

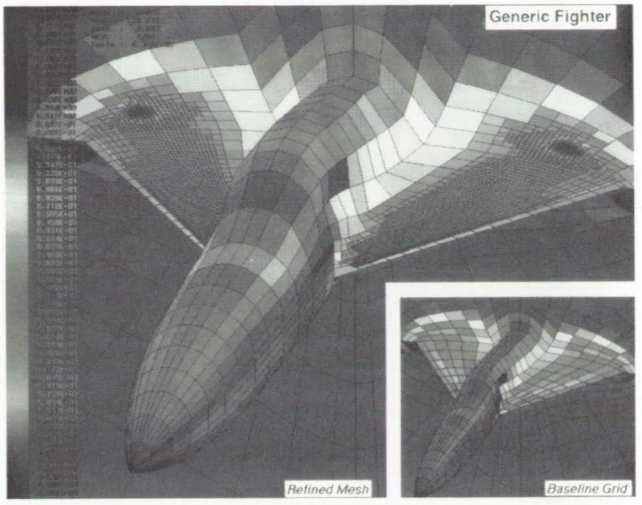


Fig. 1. Generic fighter (see color plate 10 in Appendix)

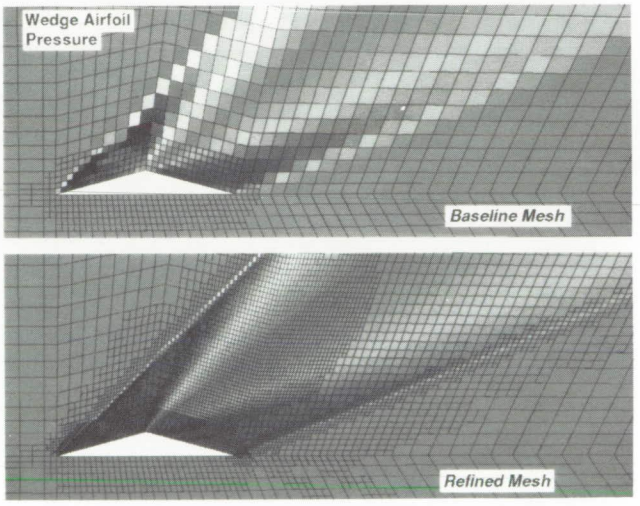


Fig. 2. Wedge airfoil pressure (see color plate 11 in Appendix)

the body surface and crossflow grids were refined using a criterion chosen for the enhancement of vortices. The second figure shows a supersonic two-dimensional wedge airfoil, and demonstrates the increase in shock-wave resolution provided by an appropriately refined grid.

Ames-Moffett contact: G. Cappuccio
(415) 604-6463 or FTS 464-6463
Headquarters program office: OAET

Computation of Induced Drag for Elliptical and Crescent-Shaped Wings

Stephen C. Smith

Recent interest in the induced drag characteristics of crescent-shaped wings has led to a closer look at the methods used for determining induced drag from computational aerodynamic methods. Induced drag may be computed by integration of surface pressure, or by evaluation of a contour integral in the Trefftz plane. Recent studies by other researchers have indicated significant drag savings for crescent wings compared with traditional elliptical wings, but these studies relied on surface pressure integration of a rather sparse panel model using a low-order panel method.

Induced drag is often computed as a span efficiency by dividing the theoretical minimum induced drag of an elliptically loaded, planar wing by the induced drag of an existing wing with the same lift, span, and area. Although nonplanar wings (e.g., with winglets) often have less drag than the theoretical minimum, span efficiencies greater than 1.0 are not expected for planar wings, so results showing span efficiencies of 1.05 or more for crescent wings have attracted considerable interest.

A high-order panel method was used to study the induced drag of crescent and elliptical wings using both surface pressure and Trefftz-plane integration. Induced drag computations for a crescent wing using surface pressure integration were strongly affected by panel density. Accurate results were obtained only when the spanwise as well as chordwise panel density was sufficient to resolve the highly three-dimensional flow field near the tip of the crescent wing. Trefftz-plane results for the two-wing planforms do not show this sensitivity to panel density or angle of attack.

For this study, the crescent wing had an elliptical leading edge and a straight trailing edge, whereas the elliptical wing had a straight quarter-chord line. These two wing shapes are shown in the first figure. Span efficiencies of 0.994 for the crescent wing and 0.987 for the elliptical wing were computed by the Trefftz-plane technique.

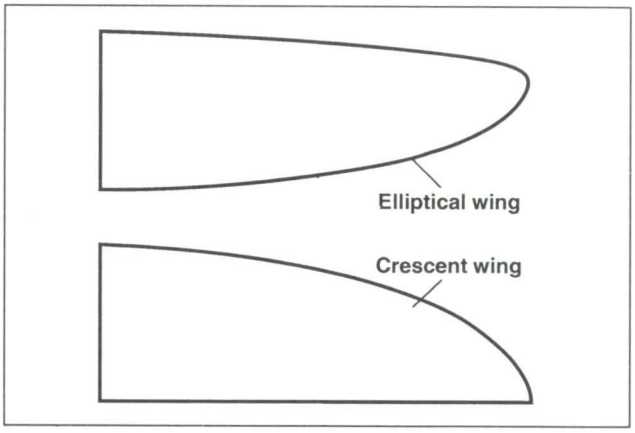


Fig. 1. Comparison of elliptical and crescent-shaped wings

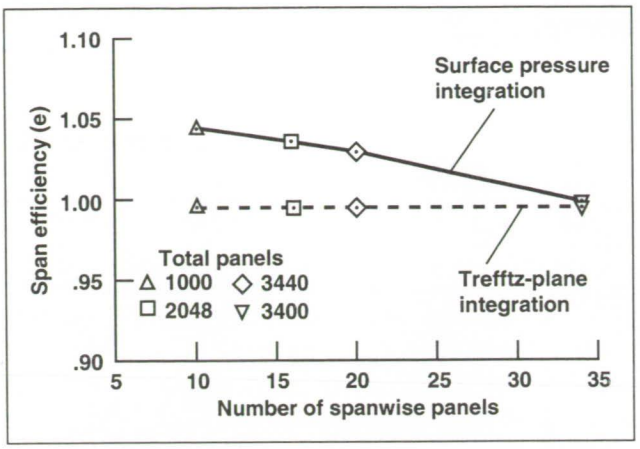


Fig. 2. Span efficiency of crescent wing computed by surface pressure integration and Trefftz-plane integration, for various panel densities

When panel density was increased to the limit allowed by the panel code, surface pressure integration gave the same results, as shown in the second figure. The slightly higher span efficiency of the crescent wing is attributed to a more nearly elliptical spanwise lift distribution, as well as nonlinear interactions between the vortex wake and the highly swept wingtip. Previous results showing unusually high span efficiencies for crescent wings seem to be an artifact of inaccurate surface pressure integration.

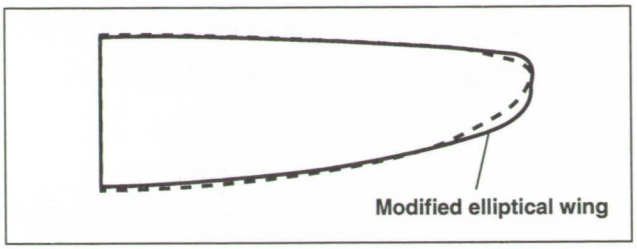


Fig. 3. Elliptical wing modified to produce elliptical lift distribution

The chord distribution of the elliptical wing was modified to produce an elliptical span loading on a wing with a straight quarter-chord line. The resulting wing shape is shown in the third figure. This wing demonstrated a span efficiency equal to that of the crescent wing.

Ames-Moffett contact: S. Smith
(415) 604-5856 or FTS 464-5856
Headquarters program office: OAET

Three-Dimensional Laser Doppler Velocimeter for Supersonic Turbulent Flows

James L. Brown

Measurements of all three velocity components using a three-dimensional laser Doppler velocimeter (3D LDV) are being performed in Ames Research Center's High Reynolds Channel I for turbulent flow at Mach 3. Previous difficulties associated with obtaining the third component of velocity have been overcome—this is making it possible to obtain highly accurate measurements of the turbulent Reynolds stresses, which are so important to turbulence modeling.

Errors associated with 3D LDV measurements of the turbulent Reynolds stresses (⟨u'2⟩, ⟨v'2⟩, ⟨w'2⟩, ⟨v'w'⟩, ⟨u'v⟩, ⟨u'w'⟩) can be quite large. A novel computer simulation of the 3D LDV turbulent flow helped reveal two primary sources of error associated with a lack of coincidence. The computer study also suggested a new coincidence scheme for determining whether all three signals had been received at the same time (U.S. Patent 4,925,297).

The figure shows measurements of the turbulent Reynolds stresses obtained in an axisymmetric Mach 3 turbulent boundary layer. Measurements with the 3D LDV compare well with previous measurements by a two-dimensional laser Doppler velocimeter. The additional terms measured by the 3D LDV include ⟨v'w'⟩ and ⟨w'2⟩. Transverse stress ⟨v'w'⟩ is expected to be zero everywhere (which it is), while ⟨w'2⟩ is expected to be approximately equal to (⟨u'2⟩ + ⟨v'2⟩)/2 as is the case for the new coincidence scheme. Note that measurements of ⟨w'2⟩ using the old 3D LDV coincidence scheme were also acquired, resulting in ⟨w'2⟩ = ⟨u'2⟩, which is clearly in error. The ⟨v'w'⟩ term was measured using the old

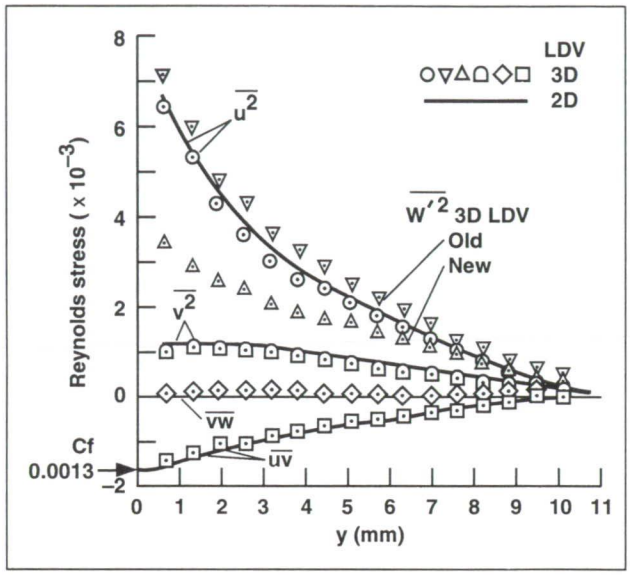


Fig. 1. Three-dimensional Reynolds stress measurements for a supersonic boundary layer, M = 3, $Re_x = 15 \times 10^6$.

coincidence scheme (not shown) and also deviates significantly from the new measurements and the expected value of zero.

Tests are proceeding on a fully three-dimensional asymmetric flare flow at Mach 3, in which all six Reynolds stresses are being measured for turbulence modeling purposes.

Ames-Moffett contact: J. Brown
(415) 604-6192 or FTS 464-6192
Headquarters program office: OAET

Finite-Difference Algorithms for Computational Acoustics

Sanford Davis

Numerical simulation of acoustic wave motion remains a challenging computational problem. The main requirement for accurate simulation is to maintain phase coherence over many time steps. Since numerical dissipation ("artificial viscosity") will cause all propagating waves to eventually decay, a neutrally stable algorithm is almost mandatory. With currently available computer resources, the main issue is that of prescribing an algorithm with sufficient phase and amplitude fidelity to track signals over long distances. In the past year, a new compact finite-difference algorithm was developed and applied to acoustic wave motion. A novel aspect of the technique is that the finite-difference molecules are defined directly from the governing matrix partial differential equations without separate consideration of space- and time-discretization.

The importance of phase coherence is shown in the first figure, which depicts the phase error per time step for a commonly used second-order scheme compared with the new algorithm. A phase ratio of one over the complete spectrum of wavelengths indicates perfect resolution. (The amplitude ratio is assumed unity.) In common with all finite-difference algorithms, the phase ratio depends on both the nondimensional wavelength and the Courant number, $Cn = U\tau/h$.

From the first figure significant phase errors appear for $\lambda > 5h$, while the new algorithm shows almost no phase distortion in this range. Both algorithms use the same 3-point spatial mesh, but severe restrictions on the mesh size are apparent using the second-order method for simulating short waves. Curves for Cn of 0.25, 0.50, and 0.75 are shown in the figure.

An example of algorithmic-induced phase distortion is shown in the second figure. The computation is for a half-sine pulse generated at the left

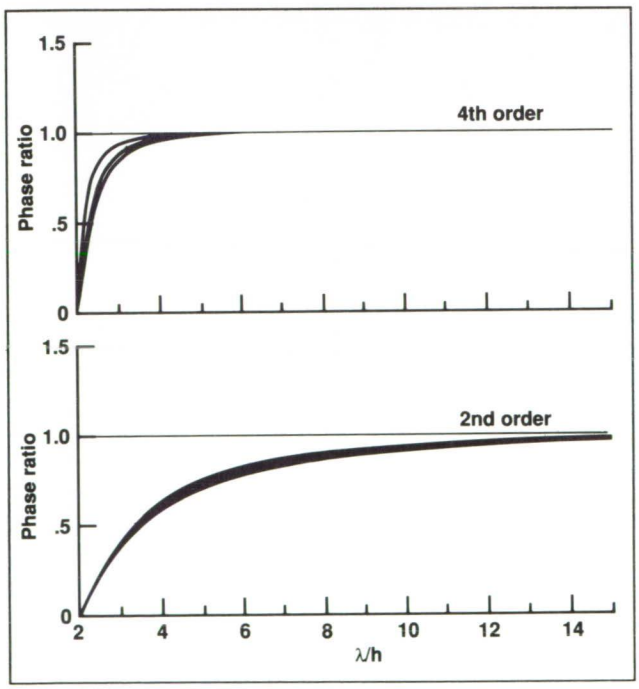


Fig. 1. Phase distortion per time step using two neutrally stable implicit algorithms

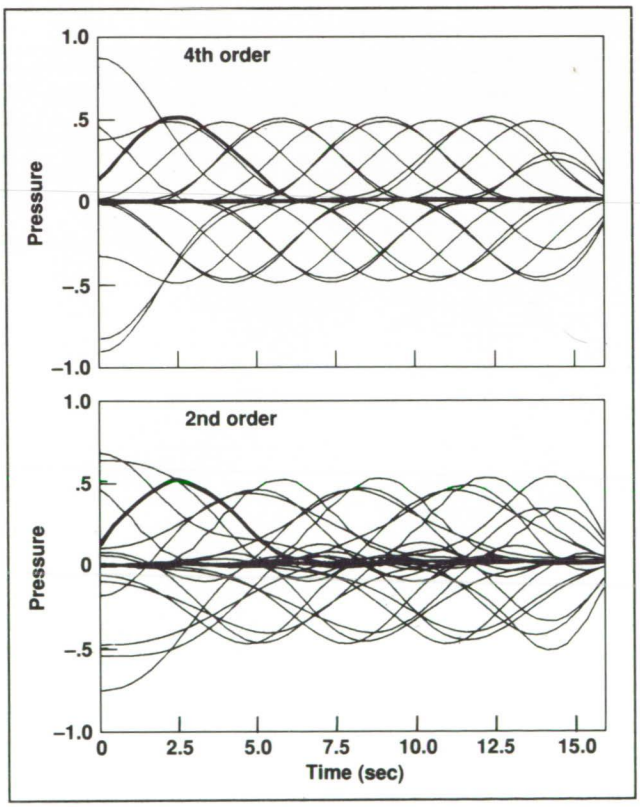


Fig. 2. Acoustic velocity waves in a pipe. Comparison between second- and fourth-order numerical methods. Initial wave shown in bold

end of a 16-meter-long pipe. The impedance condition at the right end of the pipe is a time-domain version of the classical low-frequency, open-end impedance relation. Acoustic velocity waves are shown at equidistant times after about six reflections from the left and right ends of the pipe. Both curves were computed on a 50-point mesh with a time step based on a Courant number of 0.75 using a 3-spatial-point computational molecule. The top curve was computed with the new fourth-order algorithm and the lower curve with a commonly used second-order Crank-Nicolson type scheme. Neither algorithm possesses any dissipation, either natural or artificial, so the waves will never decay.

After a number of reflections, the second-order algorithm is essentially useless since small phase errors accumulate to such an extent that the original signal is scrambled beyond recognition. In contrast, the top curve retains its phase accuracy over the entire computation. This increase in accuracy is obtained without increasing the size of the computational molecule or additional algorithmic complexity.

A second example is the diffraction of a two-dimensional plane wave by a flat plate. A plane wave with wave numbers $(k_x, k_y) = (0, 1.45/\text{meter})$ interacts with a 3.26-meter-wide flat plate. The computation is shown on a uniform 50×60 grid on a field 16×16 meters with a time step determined by a Courant number of 0.80.

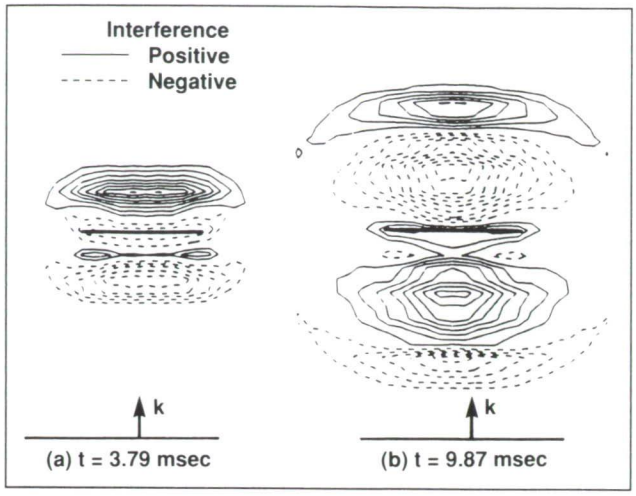


Fig. 3. Scattering of a harmonic plane wave by a flat plate. Contours of interference pressure shown at two instants of time

The pressure interference field (difference between incident plane wave and total diffracted field) is shown for two time steps in the third figure. The instantaneous interference pattern, in both the incident and shadow regions, is clearly delineated.

Ames-Moffett contact: S. Davis
(415) 604-4197 or FTS 464-4197
Headquarters program office: OAET

Separating Flow Study

Dave Driver

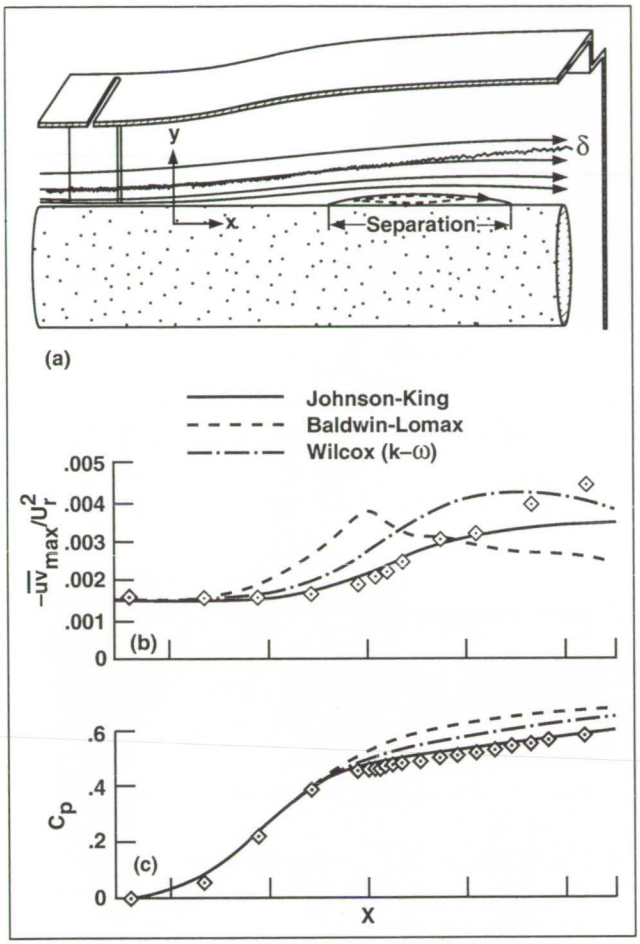


Fig. 1. Separating flow experiment, (a) streamlines; (b) axial distribution of peak Reynolds shear stress—measured and computed; (c) axial distribution of measured and computed surface pressure

Separation limits the lift that an airfoil can generate, increases drag, and often leads to flow unsteadiness. Predicting whether a given flow will separate and, if so, to what extent, remains one of the greatest challenges to computational fluid dynamics, primarily due to inadequate turbulence models. Consequently, a coordinated experimental and computational effort was undertaken to study the role of turbulence in separation.

Flow along a straight circular cylinder was made to separate by virtue of an adverse pressure gradient (see the figure). The separation bubble was short and thin relative to the boundary layer thickness, and the bubble size was very sensitive to the turbulent mixing. Measurements of mean velocity and turbulent Reynolds stresses were performed with a three-component laser Doppler velocimeter developed at Ames Research Center. Skin friction was measured with an oil-flow laser-interferometer.

Measured Reynolds shear stress ($\overline{uv}$), seen in the figure, provides the glue (so to speak) that prevents flow separation. The steady growth in shear stress is well predicted by the Johnson-King turbulence model, also shown in the figure. Other turbulence models tend to overpredict the initial growth rate of the maximum shear stress. Accurate prediction of the Reynolds stress is critical to the prediction of surface pressure as can be seen in the figure. The Johnson-King model which most accurately predicts the initial evolution of the stresses also most accurately predicts the pressure.

These data are providing new physical insight into flows with separation and are being used as a test case for developing new turbulence models. It is one of the few separating flow experiments that offers a complete set of Reynolds stress measurements.

Ames-Moffett contact: D. Driver/F. Menter/ D. Johnson
(415) 604-5396/6229/5399 or FTS 464-5396/ 6229/ 5399
Headquarters program office: OAET

Turbulence Modeling Near Solid Boundaries

Paul Durbin

In high-speed flow over a solid surface, the fluid immediately next to the surface is in a state of turbulent motion. This turbulence increases the frictional drag on the surface, and promotes transfer of heat from hot surfaces. It is necessary to account for these properties in engineering calculations. The great complexity of turbulent motion makes a literal representation of turbulence impractical, so simple, statistical models have been developed to represent some of its averaged effects. By necessity these models involve a certain amount of empiricism; because of this, the models are not universal, but rather have a limited range of applicability.

In the present research, we have developed a new model for the near wall region. Previous attempts in this area have resorted to so-called damping functions to make the models agree with experimental data. This practice seems quite unattractive because it amounts to drawing a curve through a particular set of data. Our effort has been to develop a more predictive model that will be useful in a wider range of flows.

Our work originated with the observation that the component of turbulent velocity perpendicular to the boundary controls the rate of transport of momentum, or heat, toward the wall. By developing an equation that describes the behavior of this component, we were able to compute the averaged flow and the turbulence intensity without resorting to damping functions.

The figure shows a prediction by the model compared to data. The curve marked v^2 is the component of turbulent intensity normal to the wall and the curve marked k is the total turbulent kinetic energy. The figure shows how the normal component is suppressed as the wall at $y = 0$ is approached; by contrast, the total energy k

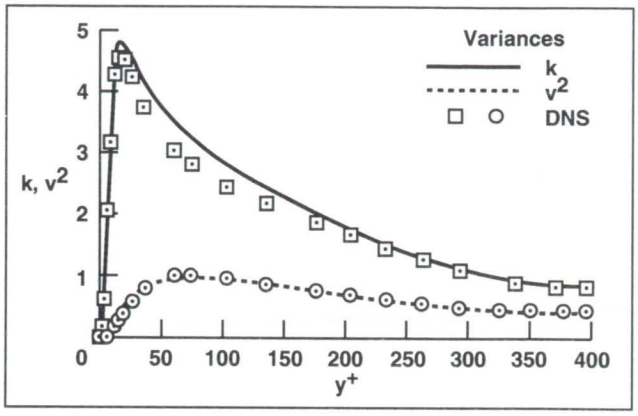


Fig. 1. Total turbulent kinetic energy and turbulent intensity component normal to the wali from the model compared to direct numerical simulation data

increases as the wall is approached, before decreasing sharply at the wall.

These behaviors represent different physical effects, which had to be suitably modeled. The normal component is blocked by the wall—that is, because the flow cannot go through the wall, it turns away from the normal, into the tangential direction. The total kinetic energy increases as the turbulence extracts energy from the forces driving the flow. This causes the energy peak. Nearer to the wall the energy is reduced by viscous friction, which dissipates the energy. Viscous dissipation is greatest near boundaries; the laws of fluid dynamics require that the kinetic energy be reduced to zero at the wall.

Ames-Moffett contact: P. Durbin
(415) 604-4726 or FTS 464-4726
Headquarters program office: OAET

Nonlinear Sonic Boom Prediction Method

Thomas A. Edwards

Conceptual studies are under way for a new supersonic commercial transport. One of the key obstacles to its economic viability is the international ban on supersonic flight over land. Therefore, considerable effort is being committed to developing an aircraft that generates an acceptably quiet sonic boom for overland operations. To accomplish this, an accurate sonic boom prediction method is needed.

Existing sonic boom prediction methods are based on linearized supersonic flow and acoustic wave propagation theories. The accuracy of this approach has been demonstrated for many simple shapes and for flight vehicles at low angles of attack. However, the accuracy of the prediction deteriorates as the Mach number or the flight attitude of the vehicle increases. The loss of accuracy is mainly due to the emergence of significant nonlinear effects as shock waves become stronger. Also, complex aircraft configurations are difficult to model with simplified theories. Therefore, a more complete aerodynamic model is needed to accurately predict the sonic boom generated by new supersonic transport concepts.

An investigation using computational fluid dynamics (CFD) to predict the nonlinear flow field near supersonic aircraft has been completed. In this study, a CFD code was applied to several test cases for which experimentally measured sonic boom data were available.

Sonic boom measurements are made at large distances from the vehicle—in the case of an aircraft in flight, ground-level measurements are at least several hundred body lengths from the airplane. Using CFD for the entire distance would be prohibitively expensive, so the CFD solution is carried out far enough to resolve the nonlinear effects, usually about one or two body lengths. This solution is then used by a linear wave propagation method to determine the far-field sonic boom.

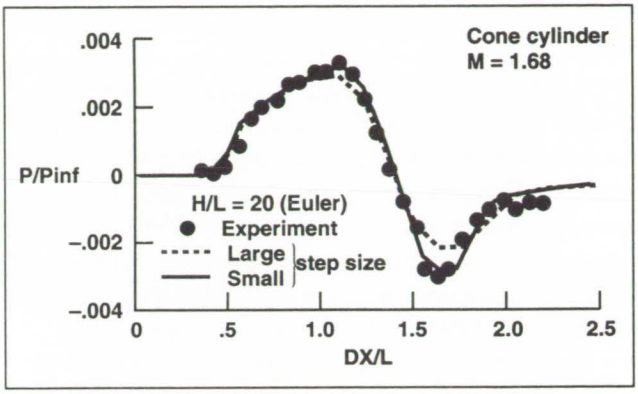


Fig. 1. Comparison of the sonic boom overpressure measured experimentally and predicted by the present computational method

A comparison between an experimentally measured sonic boom and the predicted result is shown in the accompanying figure. As can be seen, the correlation is very good. The current method has been applied to several test problems of varying geometry and flight conditions to demonstrate its accuracy and reliability. To obtain accurate results, it was found that the flow field must be resolved in great detail; therefore, an adaptive-grid procedure was implemented to achieve the necessary resolution with reasonable computational cost. This capability will now be applied to minimize the sonic boom generated by candidate supersonic transport designs.

Ames-Moffett contact: T. Edwards
(415) 604-4465 or FTS 464-4465
Headquarters program office: OAET

Aeroelastic Responses Associated with Vortical Flows

Guru P. Guruswamy

Flows with vortices play an important role in aircraft design and development. In general, strong vortices form on aircraft at large angles of attack. For aircraft with highly swept wings, strong vortices can even form on the wings at moderate angles of attack. Formation of vortices changes the aerodynamic load distribution on a wing. Vortices formed on aircraft have been known to cause several types of instabilities such as aeroelastic oscillations for highly swept flexible wings. Such instabilities can severely impair the performance of an aircraft.

For accurate computation of flows and their interactions with structures, it is necessary to solve the Navier-Stokes equations and couple them with the structural equations. Such efforts have already begun at Ames Research Center. During FY 90, methods were developed to accurately couple the Navier-Stokes solutions with the structural equations and they are incorporated in the wing version of the aeroelastic code, ENSAERO. The capability of ENSAERO has been extended to model the blended wing-body configurations.

ENSAERO computes aeroelastic responses by simultaneously integrating the Navier-Stokes equations and the modal structural equations of motion by using aeroelastically adaptive dynamic grids. The flow is solved by time-accurate, finite-difference schemes based on the Beam-Warming algorithm. Using ENSAERO, computations were made for a typical flexible blended wing-body configuration to demonstrate the effects of vortical flows.

The figures demonstrate the effects of vortical flows on flexible wings. The first figure shows the vortex-dominated unsteady pressures on the deformed wing. The second figure shows the time responses of the sectional lift. For this case, flow separations associated with the presence of vortices have led to sustained aeroelastic oscillations. This phenomenon has been observed in both wind tunnel and flight tests.

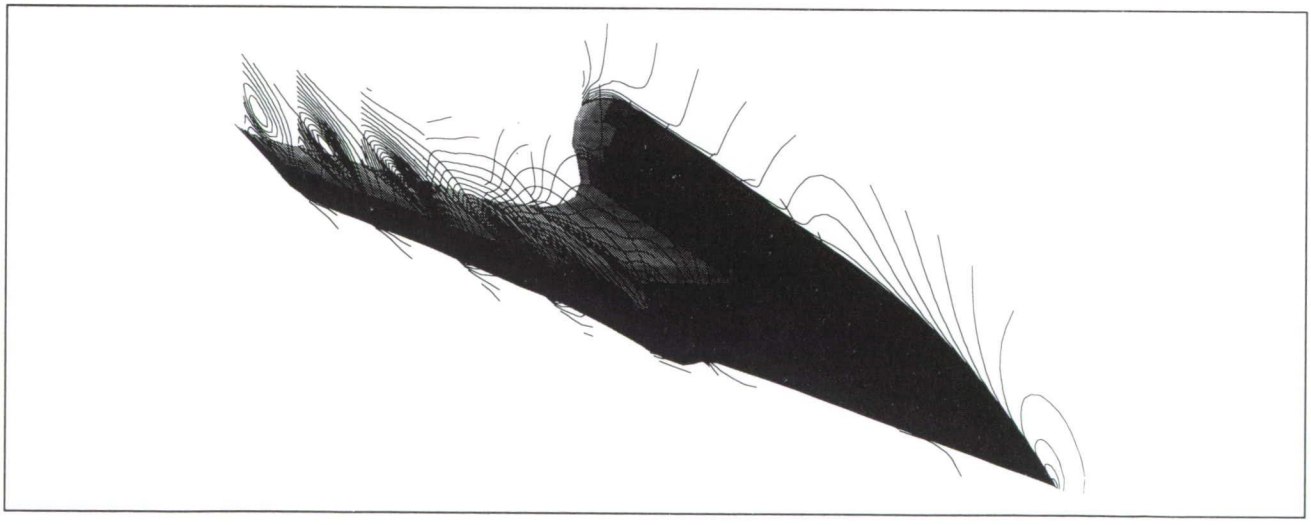


Fig. 1. Vortex-dominated density contours at M = 0.98, Alpha = 7.0°

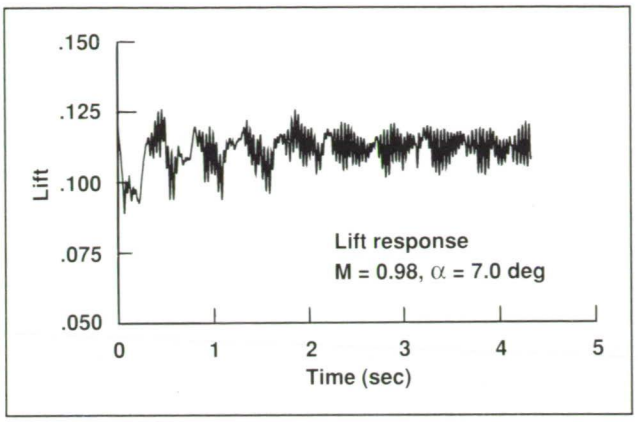


Fig. 2. Unsteady lift responses associated with sustained aeroelastic oscillations

In this project, Navier-Stokes equations are successfully coupled with structural equations of motion for advanced aeroelastic applications. With this new computational tool, practically important aeroelastic phenomena such as vortex-induced wing oscillations can be studied. This work has advanced the state of the art of computational fluid dynamics (CFD) applications to aeroelasticity. ENSAERO will be further extended to model full aircraft, and complex aeroelastic phenomena associated with vortical and separated flows will be studied.

Ames-Moffett contact: G. Guruswamy
(415) 604-6329 or FTS 464-6329
Headquarters program office: OAET

Laser Doppler Velocimeter for Three-Dimensional Near-Surface Measurements

Dennis Johnson

Studies are being performed on a laser Doppler velocimeter (LDV) approach, which shows excellent potential as a measurement technique for three-dimensional (3-D) near-surface applications. As a result of the advances in computational fluid dynamics, there is an increasing need for measurements of fluid velocities (mean and fluctuating) and their correlations in the region very near the surface of wind tunnel models of aircraft components. These data are needed to aid in the development and validation of theoretical turbulence models for Reynolds-averaged, Navier-Stokes computational methods. Measurements are especially needed for cases where the flow is highly 3-D and separated.

Fundamental to the LDV approach is a laser beam-turning probe that is inserted into the flow as shown in part (a) of the figure. This probe, since it only needs to turn the incident laser beams, can be made sufficiently small (6 millimeters in diameter or smaller) so as to have a minimal influence on the flow being investigated. The beam-turning probe permits the direct measurement of the elusive crossflow velocity component with the incident beams at a grazing incidence to the surface. Also, it allows the laser beam focusing lens and the scattered-light-collecting lens to be placed close to the measurement region of interest. This results in both improved spatial resolution and increases sensitivity to particle light scattering. (It is the velocity of submicron particles that is actually measured by the LDV technique.)

Other key elements are the use of an optically smooth measurement port (surface roughness much less than the wavelength of light) and the collection of particle-scattered light at 90° with respect to the propagation direction of the incident laser beams. Both have the effect of reducing the amount of noise-producing stray light reaching the photodetector. To further eliminate measurement errors due to noise-in-signal caused by surface light scattering, discrete Fourier transform signal processing is incorporated.

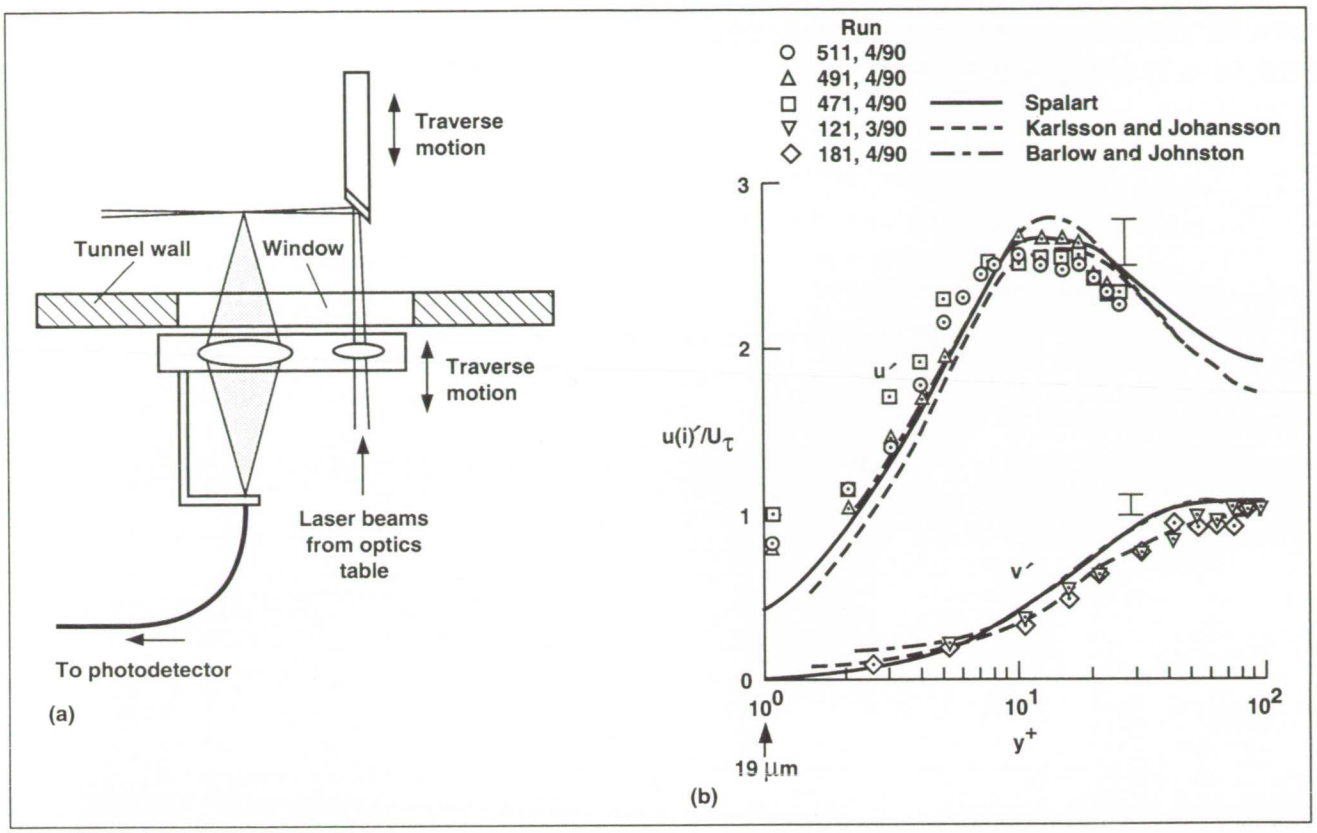


Fig. 1. Laser Doppler velocimeter for three-dimensional near-surface measurements. (a) Schematic of optical layout, (b) near-surface turbulence intensities

Shown in part (b) of the figure as symbols are demonstration results obtained in a two-dimensional air flow turbulent boundary layer. The velocity fluctuations in the streamwise direction, u', and those normal to the surface, v', are plotted versus distance from the wall. The results are in nondimensional wall coordinates. Displayed as lines are results of other researchers. The solid lines represent computer simulation results. The other results were obtained in water flow experiments by conventional LDV techniques. The viscous sublayers were substantially thicker in those experiments. In terms of actual physical distance, data have been obtained much closer to the surface with the present LDV approach than was possible in the water flow studies.

Ames-Moffett contact: D. Johnson
(415) 604-5399 or FTS 464-5399
Headquarters program office: OAET

Structure of the Turbulent Separated Flow Behind a Backward-Facing Step

Srba Jovic

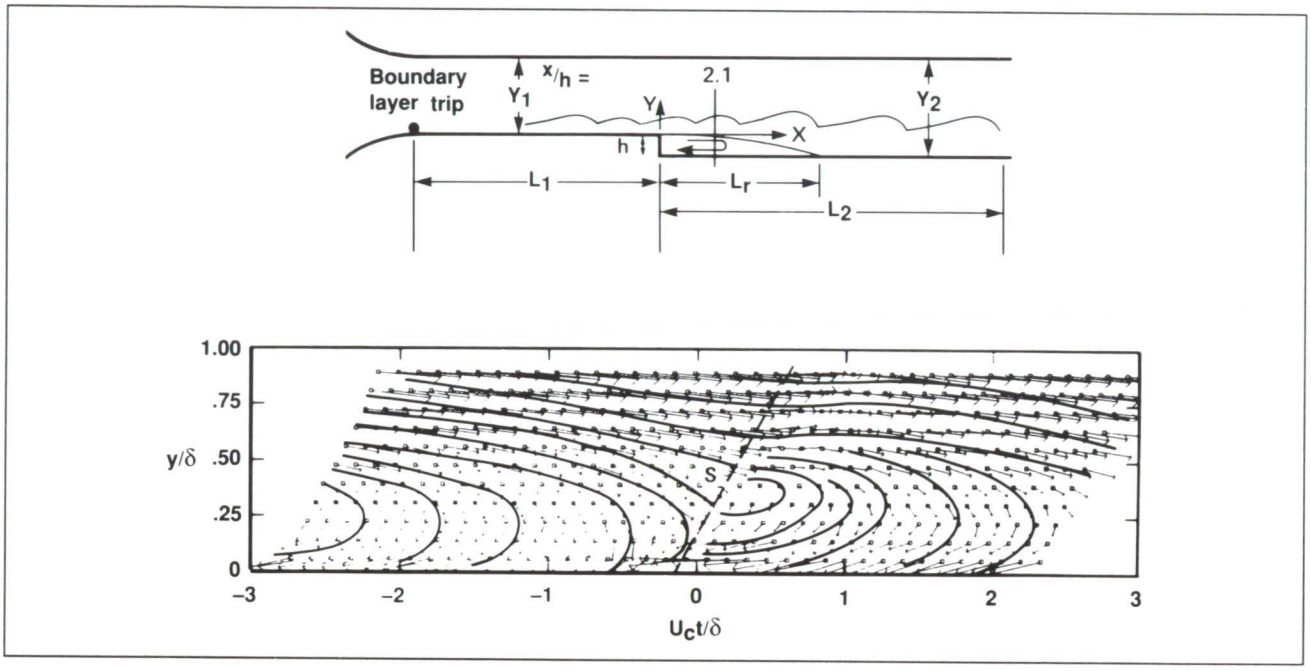


Fig. 1. Phase-averaged velocity vector field at x/h = 2.1

Turbulence plays an important role in aerodynamics—the effect of decreasing or enhancing the turbulent mixing can be dramatic. Prediction and control of turbulence will play a big role in optimizing the performance of future aerodynamic designs.

While turbulence (at first glance) appears to be a random stochastic motion of fluid, it is becoming evident that some coherent large scales of fluid motion (structure) recur periodically. A major effort has begun at Ames Research Center to study these large-scale structures for boundary layers, with and without separation. The current study is being performed using a rearward-facing step geometry, in which the flow is separated downstream of the step. The main purpose of the study is to assess the role of large-scale coherent motions on the transport of heat and momentum.

The large-scale coherent motion, seen in the figure, was detected by an array of hot-wire probes 2.1 h downstream of the step. This ensemble average of conditionally sampled data shows that a large scale of motion exists which is as large as the width of the boundary layer. Additional measurements downstream indicate that these large-scale motions persist far downstream, possibly as far as 60 to 100 step heights. The spanwise extent of these structures was also investigated, which indicated that the fluid motion is relatively coherent over a span of about one boundary layer thickness.

Learning about the fundamental mechanisms that govern heat and momentum transfer will help predict, control, and optimize the performance of various aerodynamic designs.

Ames-Moffett contact: S. Jovic
(415) 604-6211 or FTS 464-6211
Headquarters program office: OAET

Three-Dimensional Instability of Rotating Flows with Oscillating Axial Strain

N. Mansour

Many internal combustion engines use swirl to enhance the "turbulence" levels at the end of the compression cycle. Engine designers argue that high turbulence levels at top dead center enhance fuel/air mixing and increase flame speeds. Swirl is induced in an engine by proper design of the inlet port and sometimes by shrouding the valve. The tangential flow becomes solid-body rotation by the time the piston reaches bottom dead center. However, solid-body rotation will not produce turbulent kinetic energy. The observed turbulent kinetic energy enhancement must come from the interaction between the rotating flow and the oscillating axial strain. We consider flows subjected to uniform rotation and spatially uniform, time-oscillating strain along the axis of rotation. The fluid is assumed to be compressible but at low Mach number with negligible density fluctuations. It is being compressed and expanded periodically along the axis of rotation.

The equations of motion for perturbed, uniformly rotating flows with uniform axial-time periodic strain are desired from the Navier-Stokes equations in the low Mach number limit. It is found that the perturbation equations admit exponentially growing three-dimensional solutions. The type of instability is broadband in that the stability of the flow is independent of the wave number (k), but dependent on the angle of the wave (α) with respect to the axis of rotation. We find that for a given compression ratio (c = volume at the end of the compression/ volume at the end of the expansion), bands of unstable regions exist. We find that for swirl ratios (s = swirl frequency/engine frequency), less than 0.25 of the flow stays in the stable region.

For swirl ratios between 0.25 and 0.5 one band of α values becomes unstable. As the swirl is increased more bands of α values become unstable. For swirl ratios greater than two, three bands are unstable, and the rest of the bands are close to being neutrally stable.

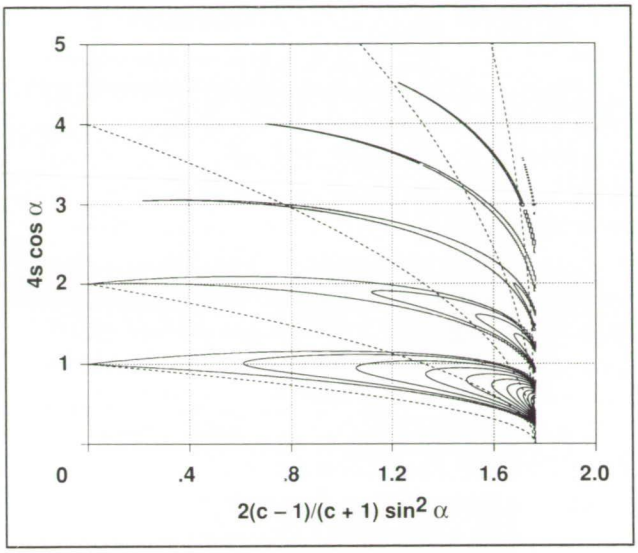


Fig. 1. Isolevels of the amplification factor ($A \geq 1$). Levels start at 1 (neutral curve) and are at 0.5 increments; the dashed lines are parabolas for s = 0.25, 0.5, 1, 2, and 4. Compression ratio c = 16

Finally, we point out that for high swirl ratios the angles in the first band are close to $\pi/2$ and the range in the angle of unstable waves narrows. The waves in the first band in this case are becoming two-dimensional. This means that there is a range of swirl ratios (s between 1 and 4) that is effective in producing three-dimensional instabilities. It is interesting to note that engines using swirl are designed to operate in this range of swirl ratios by empirical determination.

Ames-Moffett contact: N. Mansour
(415) 604-6420 or FTS 464-6420
Headquarters program office: OAET

Simultaneous Temperature and Density Measurements in Air Using Laser-Induced Fluorescence

Robert McKenzie

A new capability has been demonstrated for simultaneously measuring temperature and density in air flows using a single laser pulse. Ultraviolet light from a tunable, argon-fluoride excimer laser (193 nanometer wavelength) is both absorbed and scattered by the oxygen molecules resident in air. The subsequent broad-band fluorescence and simultaneous Raman scattering, from the oxygen, provides two independent, radiometric signals which are sensitive to the temperature and density. Measurements obtained at a point in the flow (1 millimeter diameter) can be acquired at a rate of 30/second.

The figure shows the pulse-averaged temperature and density measurements obtained in a cell containing a low-speed air flow, the pressure of which was held constant while the temperature was varied. The measured values agree well with the ideal gas law for the two values of constant pressure selected. The lowest temperature and density measured correspond to the free-stream conditions in Ames Research Center's 3.5-Foot Hypersonic Wind Tunnel under stagnation pressure and temperature of 100 atmospheres and 1000 Kelvin, respectively.

Results show that both temperature and density can be measured from a single laser pulse with accuracies better than ±2%. Mathematical models of the process (developed at Ames) indicate that this high accuracy can be maintained at temperatures as low as 60 Kelvin and densities as low as 0.01 amagat, which correspond to conditions at Mach 10 in the Ames 3.5-foot wind tunnel.

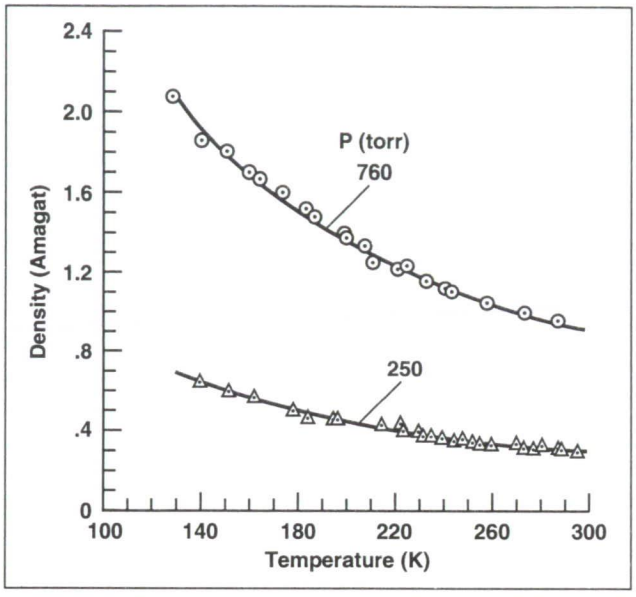


Fig. 1. Temperature and density measurements in a low-speed air flow with variable temperature at constant pressure. The solid lines are isobars

The results demonstrate the viability of this nonintrusive technique for measuring temperature and density, both of which are useful to the modeling of compressible turbulence and the validation of numerical codes for complex, hypersonic flow.

Ames-Moffett contact: R. McKenzie
(415) 604-6158 or FTS 464-6158
Headquarters program office: OAET

Transition to Turbulence in a Mixing Layer

Robert D. Moser, Michael M. Rogers

The three-dimensional (3-D) plane mixing layer is an important problem for the study of mixing and chemical reaction in fluid systems. Of particular importance is the transition to turbulence, since turbulence can be very efficient in its ability to mix scalar quantities. Both laboratory and computational experiments have revealed that the early development of a plane mixing layer is dominated by Kelvin-Helmholtz rollers and organized 3-D structures. However, the mechanisms by which this ordered 3-D flow can become turbulent had not been determined. By studying the development of a computed 3-D time-developing mixing layer, such a mechanism was discovered. A low-heat-release, fast diffusion-limited reaction was also simulated to address the question of mixing efficiency.

The computer simulations were performed with very simple initial conditions, which were known from previous work to lead to the organized structures commonly observed in both simulations and experiments. These are the Kelvin-Helmholtz rollers and the 3-D rib vortices. In addition disturbances were added which cause neighboring spanwise rollers to "pair" or amalgamate. Such pairing is a common feature of experimental and simulated mixing layers.

It was found that if the 3-D rib vortices were sufficiently strong, a pairing would trigger a transition to turbulence, which would be complete by the time of the next pairing. Before the pairing, the strong rib vortices (which extend from one Kelvin-Helmholtz roller to the next) result in rollers with a highly 3-D internal structure. When two such highly 3-D structures are brought together by a pairing, they disturb and distort each other, which leads to the breakup of the structures.

As the roller continues to evolve, the spanwise vorticity tends to organize into thin sheets as shown in the first figure. These vortex sheets are many times longer and wider than they are thick. They are therefore subject to the same two-dimensional Kelvin-Helmholtz instability as the original mixing layer. Such a secondary Kelvin-Helmholtz rollup is shown in the boxed region of the first figure.

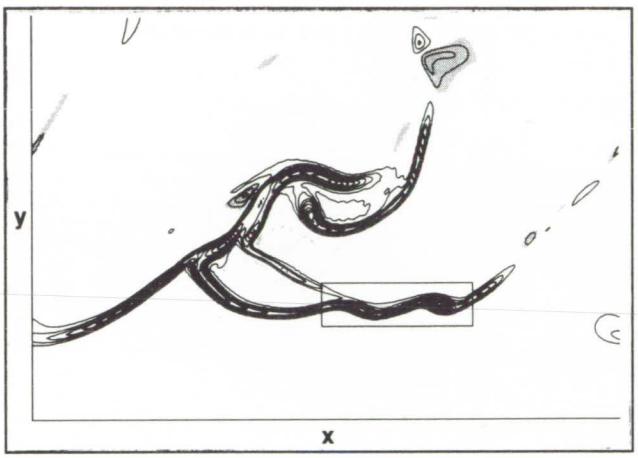


Fig. 1. Contours of constant spanwise vorticity in the mixing layer between the first and second pairings

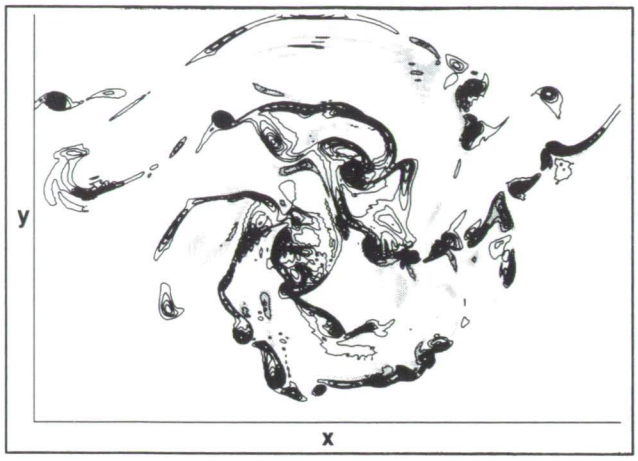


Fig. 2. Contours of constant spanwise vorticity in the mixing layer at the time of the second pairing

The instability of the secondary shear layer (vortex sheet) is one of perhaps several mechanisms which produce small-scale turbulent eddies starting from the organized structures in the pre-transitional mixing layer. Thin vortex sheet formation and subsequent breakdown occurs repeatedly, thereby producing more small-scale eddies until, by the time of the second pairing, the flow is completely turbulent. The spanwise vorticity in this fully turbulent state continues to be organized into thin sheets which undergo the Kelvin-Helmholtz instability. Thin sheets of spanwise vorticity at various stages of development can be seen clearly in the second figure.

The major question remaining regarding this transition is why the spanwise vorticity continually reorganizes into thin sheets. Also, there may be other transition mechanisms that do not rely on pairing as a trigger. Continued study of this interesting problem will contribute to our understanding and, eventually, our ability to control mixing and chemical reaction in practical devices.

Ames-Moffett contact: R. Moser
(415) 604-4733 or FTS 464-4733
Headquarters program office: OAET

Computational Fluid Dynamics Impact on Turbomachinery Design

A. A. Rangwalla

The objective of this analysis was to perform a computational fluid dynamics (CFD) analysis for a new-generation turbine design to be used in rocket propulsion systems; in particular to study the effect on stage efficiency of the axial gap between the stator and rotor airfoils in the first stage of the generic gas generator turbine. The approach used was to solve the unsteady, two-dimensional, thin-layer, Navier-Stokes equations in a time-accurate manner with an implicit, upwind-biased, finite-difference scheme. A system of patched and over-laid grids that move relative to each other were used for the computations to permit the relative motion between the stator and rotor airfoils in the stage.

A study of the effect of the axial gap (between the stator and rotor rows) on stage efficiency was performed. The flow through the stage for three different axial gaps was computed. Post processing of the computed data showed that the axial gap chosen for the preliminary design resulted in a fairly strong shock in the stage, thus increasing total pressure losses by 30% (over expected losses). Increasing the axial gap to 0.35 inches (from 0.2 inches) resulted in shock-free flow in the stage.

The modified design (with an axial gap of 0.35 inches) is expected to have lower total pressure losses and lower fatigue stresses (increased structural integrity). The increase in weight and length due to the increased axial gap is expected to be minimal.

Ames-Moffett contact: A. Rangwalla
(415) 604-3782 or FTS 464-3782
Headquarters program office: OSSA and OAET

ORIGINAL PAGE
BLACK AND WHITE PHOTOGRAPH

Computational High-Alpha F-18 Aerodynamics

Yehia Rizk, Ken Gee, Lewis B. Schiff

The objectives of the NASA High Alpha Technology Program include the development of flight-validated computational methodology adequate to predict the aerodynamics of aircraft maneuvering at large angles of attack. High-alpha flows are characterized by large regions of three-dimensional separation, and roll-up of the separated flows to form concentrated vortex structures on the leeward side of the aircraft.

In a continuing effort to understand these complex flows, a zonal, implicit, three-dimensional, flux-split Navier-Stokes code (F3D) has been used to study flow surrounding the NASA F-18 High Alpha Research Vehicle (HARV) at high-alpha flight-test conditions. The code uses a combined overset/patched zonal grid methodology, and includes an algebraic eddy-viscosity turbulence model, which accounts for the vortical flows generated above the aircraft at large incidence.

The F3D code, previously used to compute high-alpha flows surrounding the isolated F-18 fuselage and wing leading-edge extension (LEX), was extended toward computing flow about the complete F-18 aircraft geometry. The computational geometry includes the full F-18 fuselage and LEX geometry (with faired-over engine inlets), the wing with deflected leading-edge flap, and the horizontal and vertical tails.

The computational predictions are in excellent agreement with HARV flight-test measurements. In the figure, the computed surface flow and separation patterns on the fuselage and wing are indicated by the red particle traces. The off-surface LEX vortex structure is indicated by the magenta traces and helicity density contours. The computation indicates that the LEX vortex breaks down, or bursts, above the wing. The computed vortex breakdown position is in close agreement with flight-test visualizations.

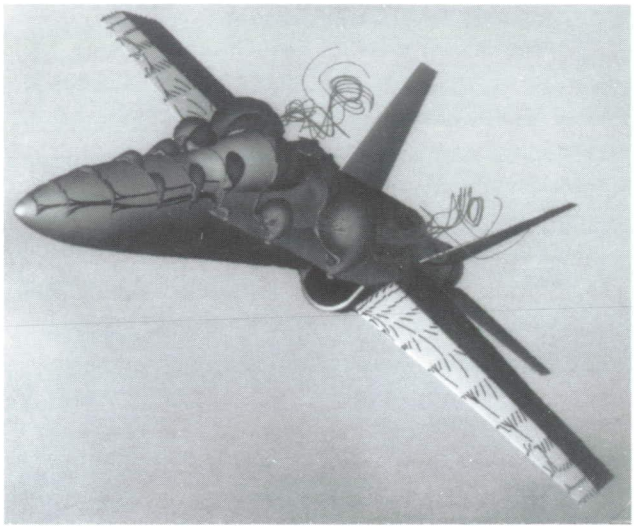


Fig. 1. Computed flow structures about F-18 wing and body, $M_\infty = 0.243$, $\alpha = 30.3°$, $Re_{\bar{c}} = 11.0 \times 10^6$ (see color plate 12 in Appendix)

The computational predictions, validated by comparison with F-18 HARV flight-test measurements, demonstrate the capability to reliably predict the highly complex three-dimensional separated and vortical flows characteristic of the high-alpha regime.

Ames-Moffett contact: Y. Rizk
(415) 604-4466 or FTS 464-4466
Headquarters program office: OAET

Pre-Processor for Three-Dimensional Elliptic Grid Generation

Reese L. Sorenson

Computational fluid dynamics (CFD) has become an accepted component in the aerodynamicist's kit of tools. But a consensus is emerging that generating computational grids (the networks of points at which the numerical solutions are actually found) is the major bottleneck in the application of CFD to realistic problems. A recent Ames Research Center workshop on the subject concluded that 50 to 80% of the CFD practitioner's time is spent on grid generation.

Much of that grid-generation time is spent collecting and formatting input for the grid-generator program. A grid consisting of multiple blocks fitted together is found necessary in applying CFD to most realistic aerodynamic problems, and even relatively simple multiple-block grids require that hundreds (if not thousands) of lines of input data be collected and formatted. Obviously, any computational tool that facilitates this process is of great value.

The new computer program 3DPREP is such a tool. It is a highly interactive graphical program, running on a powerful scientific workstation. It is a pre-processor which assists the scientist or engineer in collecting and formatting input data for the proven Ames grid-generator program 3DGRAPE. Thus it stands by itself as a productive and functioning system, and it serves as a proof-of-concept for other such tools.

The program offers the user attractive and functional screen layouts with a dialogue-entry facility for the novice; a random-access facility for experts to use in entering new data cases or modifying existing cases; a collection of useful computational utilities; a means of plotting surfaces with rotation and translation; and context-sensitive on-line help. The ultimate products of the new program are data files that are formatted for use as input to the grid generator. Thus the user can create or modify grid-generation data quickly and easily.

Tests have shown that the use of this new program can reduce the time required to generate a grid by a factor of 10. This new program, 3DPREP, consists of approximately 45,000 lines of "C" language, complementing 3DGRAPE's 15,000 lines of FORTRAN. The new program is in the alpha-test phase (in use by a small collection of local users). Plans are to release it shortly in beta-test (for use by others, at remote locations, but with close communication between developer and user), and later to transfer it to the Computer Software Management and Information Center (COSMIC) for general release.

The next step in this research into reducing the burden of grid generation is to combine the new input pre-processor with the grid generator in a more complete grid-generation system. This is an ambitious project because the pre-processor must run on a workstation to have the graphical capabilities it requires, but the grid generator must run concurrently on a supercomputer to have the required computing power. Linking the two programs, running concurrently on two different computers, is a non-trivial task. Future plans also include adding other grid-generation software, such as grid-quality measurement tools.

Ames-Moffett contact: R. Sorenson
(415) 604-4471 or FTS 464-4471
Headquarters program office: OAET

Computational Study of Pneumatic Forebody Flow Control

Domingo Tavella, Ken Gee, Lewis B. Schiff

The objectives of the NASA High Alpha Technology Program include the development of flight-validated computational methods adequate to predict the aerodynamics of aircraft maneuvering at large angles of attack, and the use of these tools to develop novel aerodynamic control concepts for increased aircraft maneuverability at high-alpha conditions.

Currently, at large angles of attack, fighter aircraft maneuverability is limited by a drop-off of yaw control power developed by the conventional rudders. Control of the fuselage forebody flow is being examined as a means of providing additional yaw control. Both mechanical devices (actuated strakes) and pneumatic concepts are being examined.

A promising pneumatic forebody flow control concept uses thin sheets of air, injected tangentially along the aircraft surface from slots located along the sides of the fuselage. Interaction of the external aircraft flow and the jet flow amplifies the effects of the jets to generate large yawing moments.

In a continuing effort to understand these complex flow interactions, an implicit, three-dimensional, flux-split Navier-Stokes code (F3D), has been used to study application of pneumatic forebody flow control to the NASA F-18 High Alpha Research Vehicle (HARV). The code uses a multi-block zonal methodology, and includes an algebraic eddy-viscosity turbulence model, which accounts for the vortical flows generated above the aircraft at large incidence.

The F3D code was previously used to compute high-alpha separated and vortical flows surrounding the isolated F-18 HARV fuselage forebody and wing leading-edge extension (LEX) at full-scale flight conditions. The computational predictions are in excellent agreement with HARV flight-test measurements.

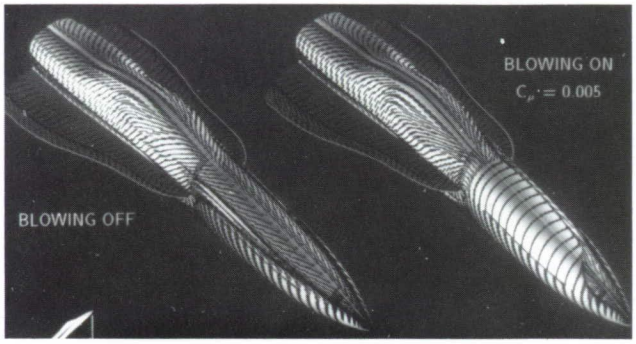


Fig. 1. Effect of asymmetric tangential blowing on the F-18 surface flow pattern, $M_\infty = 0.2$, $\alpha = 30°$, $Re_{\bar{c}} = 11.52 \times 10^6$ (see color plate 13 in Appendix)

To study slot blowing, the code was extended to include the slot configuration in the computation. Computational solutions, shown in the figure, extended wind tunnel test results to full-scale flight conditions. In the figure, the computed surface flow and separation patterns on the fuselage and LEX are indicated by the red particle traces. The skewing of the separation across the leeward symmetry line (shown in yellow) is clearly visible when blowing is turned on. The resulting yawing moments are comparable to those generated by the actuated strake concept. Further computations were used to design an improved slot configuration, which yielded comparable yawing moments with reduced slot momentum flux, resulting in a twofold increase in slot efficiency.

Ames-Moffett contact: D. Tavella
(415) 604-3996 or FTS 464-3996
Headquarters program office: OAET

An Efficient Supersonic Wind Tunnel Drive System for Mach 2.5 Flows

Stephen W. D. Wolf, James A. Laub, Lyndell S. King

The drive system of a supersonic wind tunnel must provide sufficiently large pressure ratios across the test section of the wind tunnel to produce and sustain the desired test velocity. We refer to these pressure ratios as the start and run compression ratios, respectively. In general, the start compression ratio is greater than the run compression ratio due to hysteresis in the aerodynamic behavior of supersonic flow. In a typical Mach 2.5 wind tunnel (where the air speed is 2.5 times the local speed of sound), the start compression ratio is of order 3 to 4 and the run compression ratio is of order 2. The variation from wind tunnel to wind tunnel is mainly attributed to the use of different diffuser geometries and model supports.

It is interesting to note that the majority of supersonic wind tunnels operating today were built in the 1940s and 1950s, when the main goal was simply to manufacture a supersonic testing capability. Consequently, these original supersonic tunnels tended to be very inefficient and required special expensive compressors to drive them. This situation can no longer be tolerated in new supersonic wind tunnel designs.

This work, to find a more efficient drive system, is part of the development of a new Mach 2.5 Laminar Flow Supersonic Wind Tunnel (LFSWT) for boundary-layer transition research in the Fluid Mechanics Laboratory (FML). To minimize costs, it was decided to drive the LFSWT by using an existing nonspecialist indraft compressor. Consequently, to achieve the desired test envelope, we must operate the tunnel at very low compression ratios, down to 0.62, using a unique drive system.

A one-eighth-scale model of the LFSWT, called the Proof-of-Concept (POC) supersonic wind tunnel (with a 1- × 2-inch test section), was built to evaluate a novel injector drive system based on the work of Spiegel (reported in 1953). This drive system concept uses the massive mass flow capability of the indraft compressor (up to 240,000 cubic feet per minute) to drive large ambient injectors which in turn can pump the flow through the test section.

A schematic of the POC layout is shown in the first figure. The two ambient injectors and the test section are connected to the mixing region. We designed the POC to allow the ratio between the injector and test section mass flows to be varied up to about 15. This range of mass flow ratio is an order of magnitude greater than previously investigated. Also, the POC design allows the Mach number of the injectors to be varied independently of mass flow up to about Mach 2, which is the maximum supported by the compression ratio across the injectors.

The experimental work with POC is carried out in association with computational fluid dynamic (CFD) studies using Navier-Stokes codes. In the second figure, we compare steady-state flow-field wave patterns, in the POC test section exit, found from flow visualization (using a focusing schlieren technique) and CFD predictions. In this test case, we have installed a supersonic diffuser just downstream of the test section (as indicated in the first figure). Air is entering the diffuser from the left at about Mach 2.5.

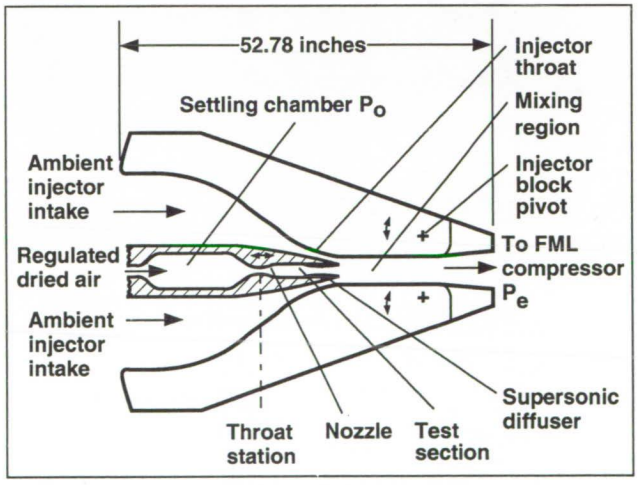


Fig. 1. Schematic of the Fluid Mechanics Laboratory Proof-of-Concept supersonic wind tunnel

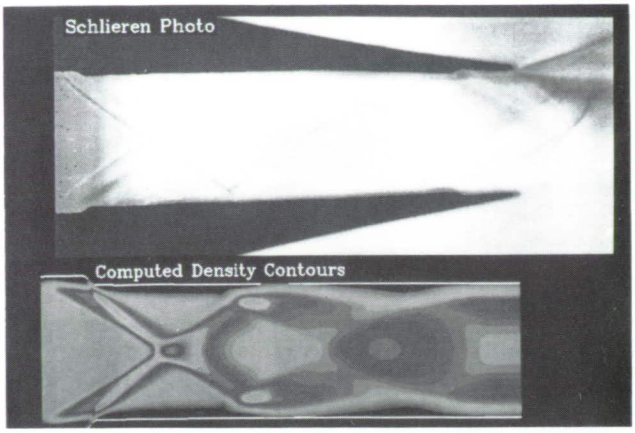


Fig. 2. Comparison of observed and predicted wave patterns in a Proof-of-Concept supersonic diffuser (see color plate 14 in Appendix)

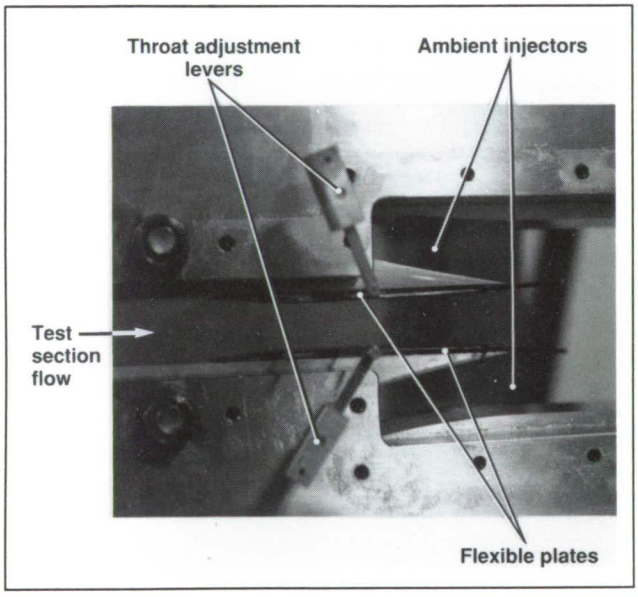


Fig. 3. Proof-of-Concept variable-throat supersonic diffuser

Our POC studies have shown that we can operate a Mach 2.5 supersonic wind tunnel with a start and run compression ratio of approximately unity. That is to say that the total pressure upstream of the test section is the same as the total pressure in the compressor inlet manifold (i.e., 8 pounds per square inch absolute). The test Reynolds number is 1.75 million per foot in this case. Prior to this work, the minimum run compression ratio achieved at Mach 2.5 was 1.41.

This significant improvement in drive system efficiency was achieved by using a variable-throat supersonic diffuser (as shown in the third figure) combined with two relatively large Mach 2 injectors (where the ratio of injector to test section mass flows was a high 7.2) and a mixing region followed by a subsonic diffuser. The low run/start compression ratio developed in POC should be achievable in large-scale supersonic wind tunnels by scaling up the drive system as appropriate. This drive system, which requires only a nonspecialist indraft compressor, offers a significant cost saving over conventional drive systems. This may in turn allow more wind tunnels like the LFSWT to be built.

Ames-Moffett contact: S. Wolf
(415) 604-4140 or FTS 464-4140
Headquarters program office: OAET

ORIGINAL PAGE
BLACK AND WHITE PHOTOGRAPH

Efficient Algorithm for Viscous Incompressible Flows

Seokkwan Yoon, Dochan Kwak

Numerical solutions of the Navier-Stokes equations using explicit schemes can be obtained at the expense of efficiency. Conventional implicit methods, which often achieve fast convergence rates, suffer high cost per iteration. A new implicit scheme based on lower-upper symmetric-Gauss-Seidel (LU-SGS) relaxation offers a very low cost per operation as well as fast convergence. An efficient numerical method based on this LU-SGS scheme is developed for solving three-dimensional viscous incompressible flow using the concept of pseudocompressibility. The present algorithm offers additional advantages when solving the flow equations with source terms, such as the centrifugal force or Coriolis force term.

A new computer code, INS3D-LU, has been developed based on this algorithm. This code is completely vectorized on oblique planes of sweep in three dimensions. The computational efficiency is very high, achieving 150 million floating point operations per second on the Cray Y-MP, requiring only 7 microseconds per gird point, per time step.

The INS3D-LU code has been used to solve real-world problems such as the High-Pressure Oxidizer Turbopump (HPOTP) of the Space Shuttle main engine (SSME). The convergence speed is excellent, achieving 9 orders of magnitude residual drop in 1000 steps for solving the inducer portion of the SSME HPOTP rotating at a constant speed. This means that flow solutions for an inducer with 0.25 million grid points with constant rotational speed can be obtained within 25 minutes of Cray Y-MP time. This computer code is being applied to liquid rocket propulsion systems design.

Despite its fast convergence, the LU-SGS scheme requires less computational work per iteration than most explicit schemes. In addition, the LU-SGS algorithm is amenable to massively parallel processing. The INS3D-LU code has been parallelized, and a speedup of over 7 gigaflops and a processing rate of over 1 gigaflop were achieved on the 8-processor Cray Y-MP using 1 million grid points. Therefore, the present method combined with massively parallel computer architecture will result in turn-around that is fast enough for routine three-dimensional aerodynamic design.

Ames-Moffett contact: S. Yoon
(415) 604-4482 or FTS 464-4482
Headquarters program office: OAET

A Three-Dimensional Self-Adaptive Grid Code

Carol Davies, Ethiraj Venkatapathy

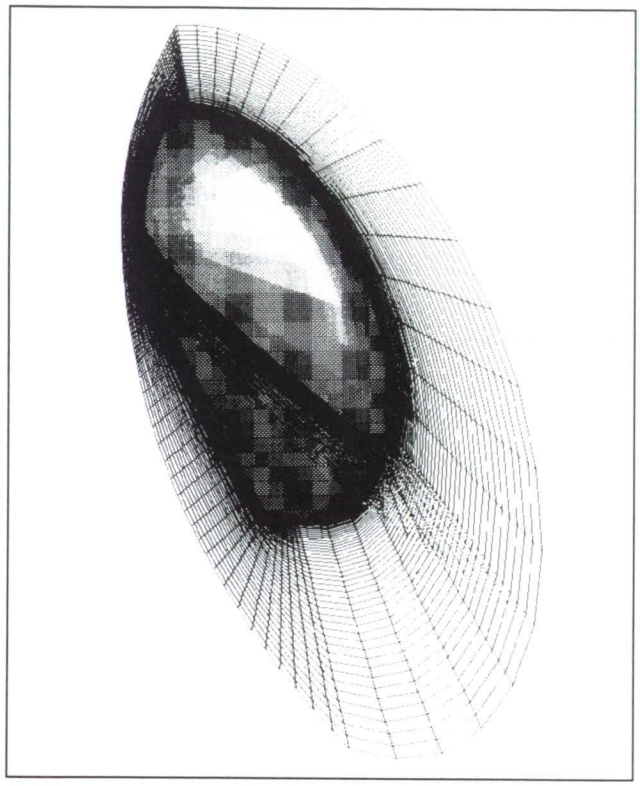


Fig. 1. Original grid

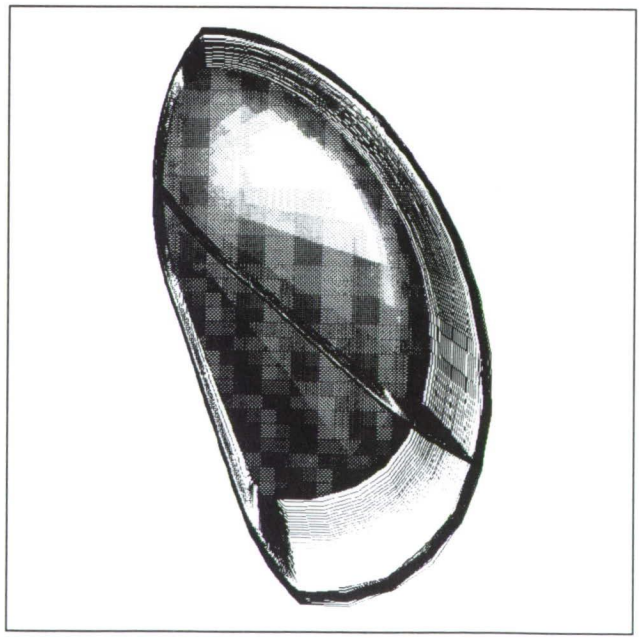


Fig. 2. Pressure contours

Solution-adaptive grid methods have become useful tools in computational fluid dynamics problems for efficient and accurate flow predictions. A three-dimensional (3-D) self-adaptive grid code (SAGE) has been developed that is robust, user friendly, efficient, and well-documented. It is an extension of the previously reported and extensively used two-dimensional version of the code, SAGE2D.

The 3-D adaption takes place as a sequence of two-dimensional adaptions of the computational surfaces, with smoothness and orthogonality maintained between surfaces. The methodology is based on Nakahashi and Deiwert's scheme, posed in an algebraic, unidirectional manner.

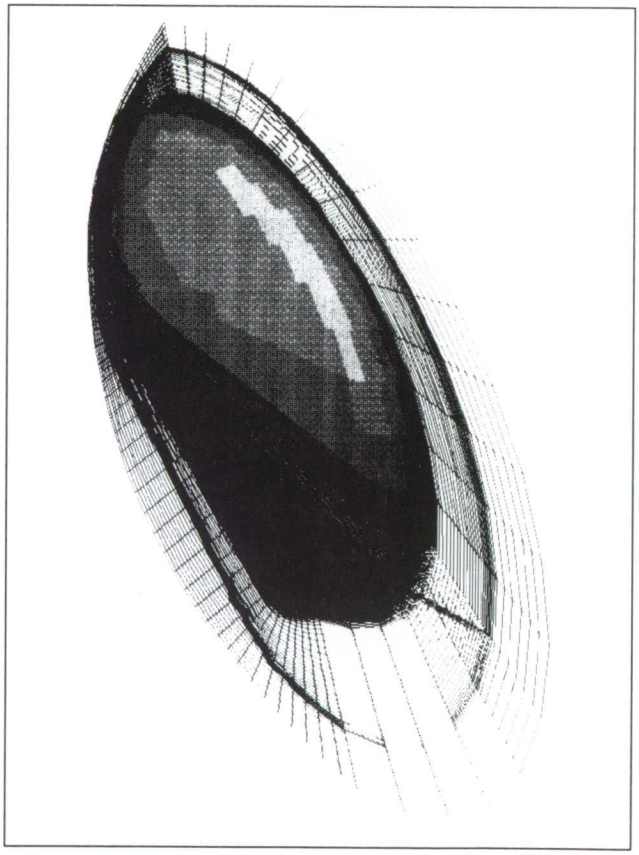


Fig. 3. Adapted grid

The procedure is analogous to applying tension and torsion spring forces proportional to any flow gradient at every grid point and finding the equilibrium position of the resulting system of grid points. In this manner, points will be redistributed into regions of high-flow gradients while maintaining smoothness and orthogonality of the grid. Input options provide a variety of both mathematical-control and adaption-descriptive parameters. To maintain simplicity, internally generated parameters are also available.

The figures show an example of grid adaption for the forebody of the Aeroassist Flight Experiment vehicle. The first figure is the initial grid used to generate the intermediary flow solution. The computed pressure contours are shown in the second figure, where the blunt body shock is clearly outlined. The grid points were redistributed based on the pressure contours, and the adapted grid, showing the points clustered in the shock region, is seen in the third figure.

Ames-Moffett contact: G. Deiwert
(415) 604-6198 or FTS 464-6198
Headquarters program office: OAET

Direct Particle Simulation of Coupled Vibration-Dissociation

Brian L. Haas, Iain D. Boyd, Donald Baganoff, William J. Feiereisen

The finite rates of chemical reactions and thermal excitation processes in gases result in thermochemical nonequilibrium in the hypersonic rarefied flow field associated with vehicles during entry. Appropriate thermochemical models are necessary to adequately simulate this flow.

The low-density nature of this flow is such that traditional computational simulation methods based upon the familiar Navier-Stokes equations are not applicable. Direct particle simulation methods offer an alternative for studying this highly rarefied flow in which the gas is modeled as a collection of moving and colliding particles in accordance with the principles of kinetic theory and statistical mechanics. Unfortunately, the chemistry models employed in previous particle simulations fail to capture the important nonequilibrium behavior that is characteristic of coupled vibration-dissociation (CVD).

It is understood that energetic collisions occurring in high-temperature flows will gradually excite the vibrational mode of stable molecules to higher energy levels. As depicted in the first figure, CVD theory dictates that a molecule AB will eventually break apart if it experiences a collision with partner X, which causes its vibrational energy to exceed its dissociation threshold. Consequently, dissociation behind a shock wave should be delayed while awaiting this gradual vibrational excitation. This behavior significantly affects temperatures and densities in the flow as well as the heat transfer experienced by the vehicle.

Consistent with the CVD theory above, a new chemistry model has been developed which favors dissociation among vibrationally excited particles. Particle simulation methods have traditionally modeled the vibrational energy mode as a simple harmonic oscillator with uniformly spaced quantum energy levels. The new chemistry model, while applicable to the simple harmonic oscillator, has also been modified for application to the anharmonic oscillator based upon the Morse interatomic potential. The anharmonic oscillator is a more realistic description of the vibrational mode and has nonuniformly spaced quantum levels as shown in the first figure.

The new chemistry model was used in simulating thermochemical relaxation behind strong shock waves in nitrogen over a range of conditions as distinguished by the free-stream degree of dissociation. Delayed dissociation downstream of the shock, characteristic of CVD behavior, is observed as an incubation distance between the simulated nonequilibrium density profile and that associated with chemically equilibrated flow.

Comparison of simulated incubation distances to those from experimental investigations are made in the second figure. Favorable agreement with experimental results indicates that the new chemistry model appropriately captures dissociation incubation behavior.

Unlike the previous model, the new chemistry model was also successful in coupling the effects of dissociation upon the vibrational excitation process.

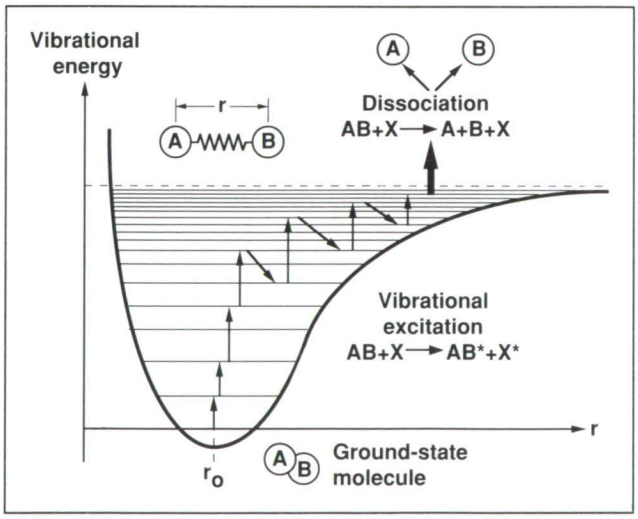


Fig. 1. Coupled vibration-dissociation theory dictates that dissociation occurs from the highest energy levels after excessive vibrational excitation of anharmonic molecules

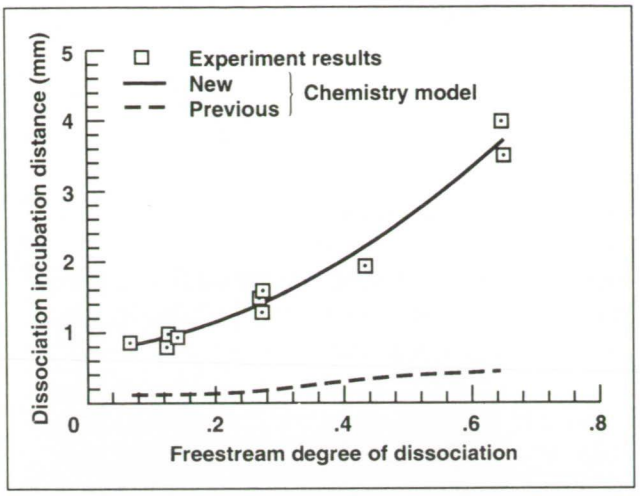


Fig. 2. Dissociation incubation distances in strong shocks demonstrate improvement of the chemistry model used in particle simulation methods for capturing coupled vibration-dissociation behavior

Since dissociation occurred preferentially from the upper quantum levels, these levels remained nearly depleted in this dissociation-dominated flow while the lowest vibrational quantum levels equilibrated with the translational temperature. The resultant bimodal transient vibrational energy distributions obtained by these particle simulations agreed qualitatively with published theoretical results obtained from detailed solutions of differential rate equations governing vibrational energy level populations. The new chemistry model represents a significant improvement over the previous model in capturing CVD behavior with particle simulations of hypersonic rarefied flows.

Ames-Moffett contact: B. Haas
(415) 604-4228 or FTS 464-4228
Headquarters program office: OAET

Low-Density Silica Fiber Ablators

William D. Henline

Recent tests and analyses have shown that Space Shuttle rigid tile heat shield materials can be used as efficient, lightweight ablators, similar to the Apollo heat shield material. Preliminary re-entry heating simulation tests on the Space Shuttle materials were conducted in the arc-jet facilities at Ames Research Center, and the theoretical analyses were conducted as part of the work being performed in support of the Space Exploration Initiative (SEI).

To date, the lowest density ablators have initial densities in the range of 25-35 pounds per cubic foot. These include silicone rubber and the Apollo ablator heat shield. Most materials of this type are charring (black) ablators and perform best at higher atmospheric pressures. Future planetary entry missions included in the SEI will most likely use a high-altitude (low-pressure) aeropass (aerobraking) maneuver to planetary orbit as part of the mission instead of a direct (one-step) planetary entry or return. Under these conditions, operating pressures will be quite low (0.01 to 0.2 atmospheres). This results in reduced mechanical loading on vehicle heat shield materials. For this application it was thought that materials with densities lower than the traditional ablators, such as Space Shuttle rigid tile materials, could be used.

The rigid tiles are made of silica fibers (SiO_2) and are called reusable surface insulation (RSI). One variety is designated LI-2200 and weighs 22 pounds per cubic foot. Arc-jet tests of the LI-2200 RSI material together with a solid silica reference sample (which weighs 140 pounds per cubic foot) were performed in Ames' 60-MW Interaction Heating Facility. Runs were made over pressures ranging from 0.08 to 0.44 atmospheres and recession data were recorded and analyzed.

The second figure shows an example of an ablating LI-2200 RSI sample in the heating facility. The first and third figures show pre and post tests,

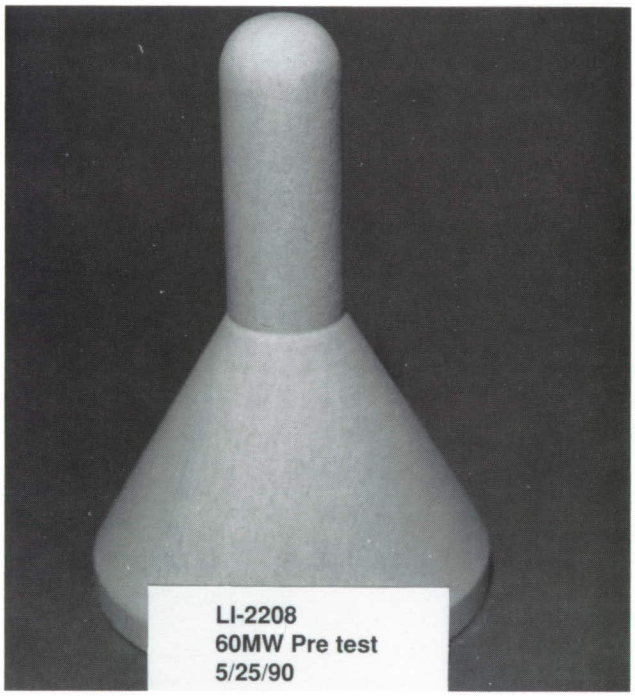


Fig. 1. Pre-test sample

ORIGINAL PAGE
BLACK AND WHITE PHOTOGRAPH

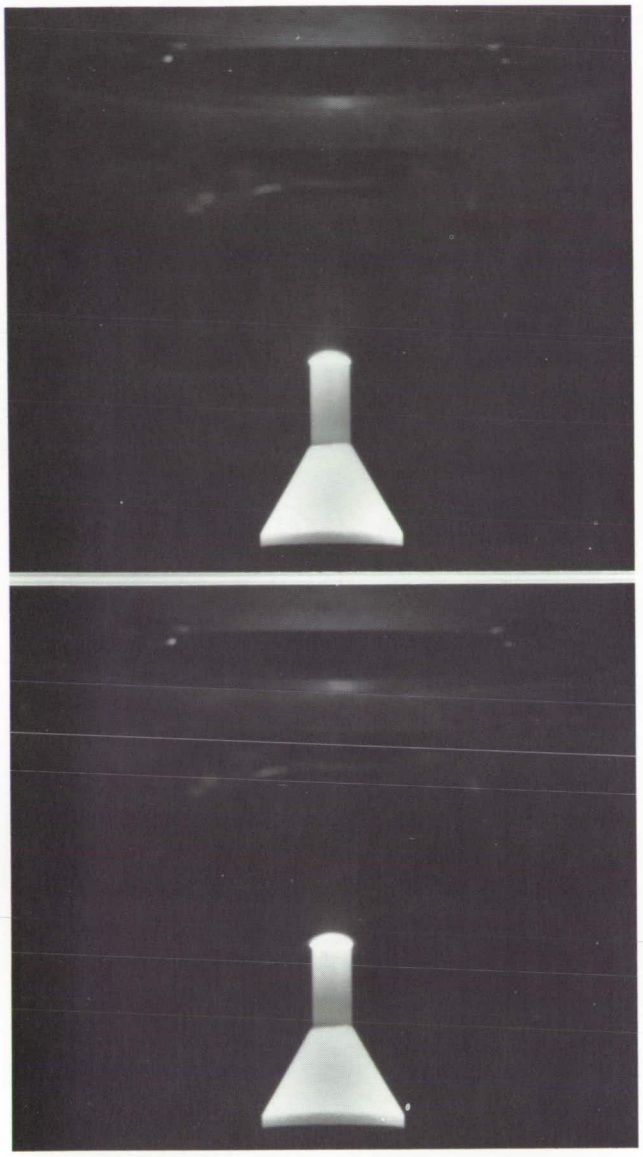


Fig. 2. Ablating LI-2000 reusable surface insulation sample

respectively. The testing confirmed that LI-2200 can work well as an ablator at these lower pressures. Further testing and analysis showed that LI-2200 is actually a more efficient ablator than the solid silica material.

ORIGINAL PAGE
BLACK AND WHITE PHOTOGRAPH



Fig. 3. Post-test sample

For vehicles using high-energy aerobraking aeropass maneuvers where operating pressures are quite low, these results show that low-density Shuttle RSI materials can be used as ablators, resulting in better weight efficiency than traditional Apollo heat shield materials. Improvement of the RSI tile ablation performance may be possible by using polymer fillers to minimize both the density and specific recession in very high energy environments. These materials would most likely be used in the very high velocity entry environments such as those that would occur on return to Earth from Mars or other outer planets.

Ames-Moffett contact: W. Henline
(415) 604-6623 or FTS 464-6623
Headquarters program office: OAET

Nonequilibrium Hydrogen-Air Reaction in Nozzle Recombination

Seung-Ho Lee, John Cavolowsky

A problem associated with the National Aerospace Plane (NASP) scramjet engine involves chemical nonequilibrium in the expanding nozzle. In the combustion chamber, combustion of hydrogen is incomplete due to high-temperature dissociation of water vapor. The unburned hydrogen-bearing species must be converted into water vapor in the expanding nozzle. Failure to do so results in a reduction in exhaust velocity and engine thrust. For this reason it became desirable to study the chemical reactions in a nozzle in an environment similar to that expected with such a vehicle.

Ames Research Center's 16-inch shock tunnel has been studied for simulating high-speed propulsion nozzle kinetics. Facility run time has been established and spectroscopically clean flow has been obtained for OH absorption measurement. The OH concentration in the nozzle flow field of the shock tunnel is measured using a laser-absorption technique. The laser is operated at a wavelength of 306.687 nanometers, which is the centerline wavelength of j = 5 rotational line of R1 band of OH. For the case of nozzle expansion from high temperature and high pressures, results of the one-temperature model do not agree with experimental data, the number density of OH at the j = 5 rotational level ($N_{j=5}$), as seen in the first figure.

The one-temperature model gives substantially higher values than the experimental data, even when the rate coefficients are multiplied by a factor of 10. The factor 10 increase in the rate coefficients have virtually no impact on the calculated $N_{j=5}$.

Existing experimental data on the relaxation times of H_2 and D_2 suggest the possibility that the observed disagreement between the theory (one-temperature model) and the experiment may be due to the development of a two-temperature nonequilibrium phenomenon. At the temperature prevailing in the nozzle, the rotational mode of the hydrogen-bearing molecules contains much more energy than the vibrational modes. Therefore, the two-temperature phenomenon is attributable mainly to the rotational nonequilibrium. Two different models have been developed for calculating rotational relaxation time. In the 2-T(slow) model, the rates of excitation of all three hydrogen-bearing molecules (H_2, OH, and H_2O) are the same as that of hydrogen. In 2-T(fast) model, only H_2 molecules are assumed to be excited vibrationally and rotationally by the collisions with H_2.

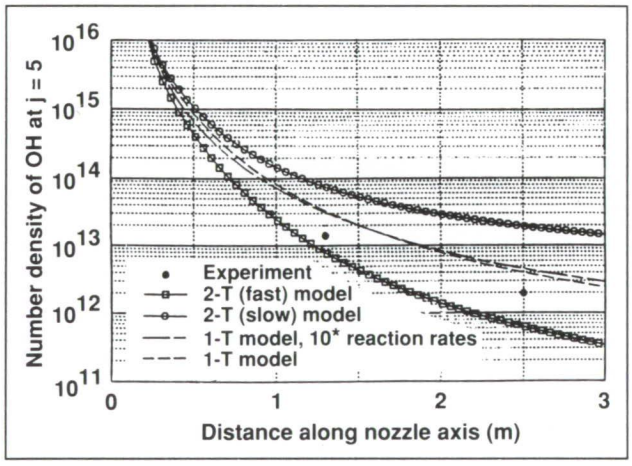


Fig. 1. Number density of OH at the j = 5 level along the nozzle axis for the wet case using one- and two-temperature models

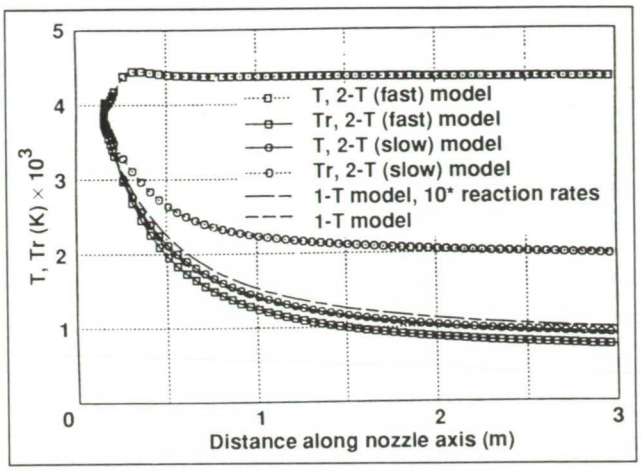


Fig. 2. Translational and rotational temperature distributions along the nozzle axis for the wet case using one- and two-temperature models

In the second figure, translational and vibrational-rotational temperatures (T and T_r) are compared for the wet case. As the figure shows, T varies little among the different models. However, T_r differs greatly between the two two-temperature models, 2-T(slow) and 2-T(fast): the 2-T(fast) model shows much greater deviation of T_r from T. With the 2-T(slow) model, T_r is about two times larger than T; while with 2-T(fast) model, T_r is about four times larger than T at the nozzle exit. In the first figure, the two two-temperature models give the values that bound the experimental values.

The two-temperature nonequilibrium phenomenon would be of concern to the NASP project because the phenomenon affects the engine thrust. For instance, for the wet case shown in the first and second figures, the nozzle exit velocities at x = 3 meters calculated by the one-temperature (standard NASP rates), 2-T(slow), and 2-T(fast) models are 3.809, 3.683, 3.621 kilometers/second, respectively. Engine thrusts are proportional to these velocities. Refinement of the model with more experimental data will yield the phenomenon accurately.

Ames-Moffett contact: G. Deiwert
(415) 604-6198 or FTS 464-6198
Headquarters program office: OAET

Very-High-Temperature Heat Shield Material Development

Daniel J. Rasky

Recent tests have shown new very-high-temperature ceramic composite materials to outperform Space Shuttle reinforced carbon-carbon (RCC) heat shield material, sustaining more than twice the heat flux loading, and able to operate at temperatures over 4000°F. The new ceramics, based on zirconium (Zr) and hafnium (Hf), were tested as part of the Advanced Refractory Composite Program being conducted at Ames Research Center. The objective of the program is to develop reusable heat shield materials with operating temperatures from 4000 to 5000°F. By contrast, existing reusable heat shield materials, such as the Shuttle rigid tiles or RCC heat shield (which is used in the highest temperature areas on the Shuttle), have maximum operating temperatures near 3000°F. Future programs such as the National Aerospace Plane and the Space Exploration Initiative would benefit greatly from the development of new heat shield materials with considerably higher temperature and heat flux capabilities.

Studies performed in the 1960s and early 1970s have shown that Zr- and Hf-based ceramics are good candidates for making heat shields that can operate in the temperature range from 4000 to 5000°F. The most promising materials were found to be diboride composites (ZrB_2 and HfB_2) with a 20 volume percent (v/o) loading of silicon carbide (SiC).

In connection with the Advanced Refractory Composites Program, samples of 19 different zirconium- and hafnium-based ceramic composites materials were obtained from four industrial sources: Manlabs Incorporated, Cerac Incorporated, Science Applications International Corporation, and Lanxide Corporation. Materials obtained from Manlabs included new carbon fiber and SiC platelet-reinforced diboride composites developed specifically for NASA. In addition, samples of RCC were obtained from LTV Missiles Division. These materials were then tested in the Ames 60-MW Interaction Heating Facility, which provides re-entry heating simulation, generating surface temperatures on the samples from 2700 to 5200°F.

An example of results obtained from the arc-jet testing is illustrated in the figure, which shows post-test photographs for two samples mounted in their graphite holders. A Cerac-supplied ZrB_2 + 20v/o SiC particulate composite is shown in part (a) of the figure, and a Shuttle RCC sample is shown in part (b) of the figure. These two samples were tested at the same conditions of 3 minutes at a heat flux more than twice the maximum reusable allowable for RCC.

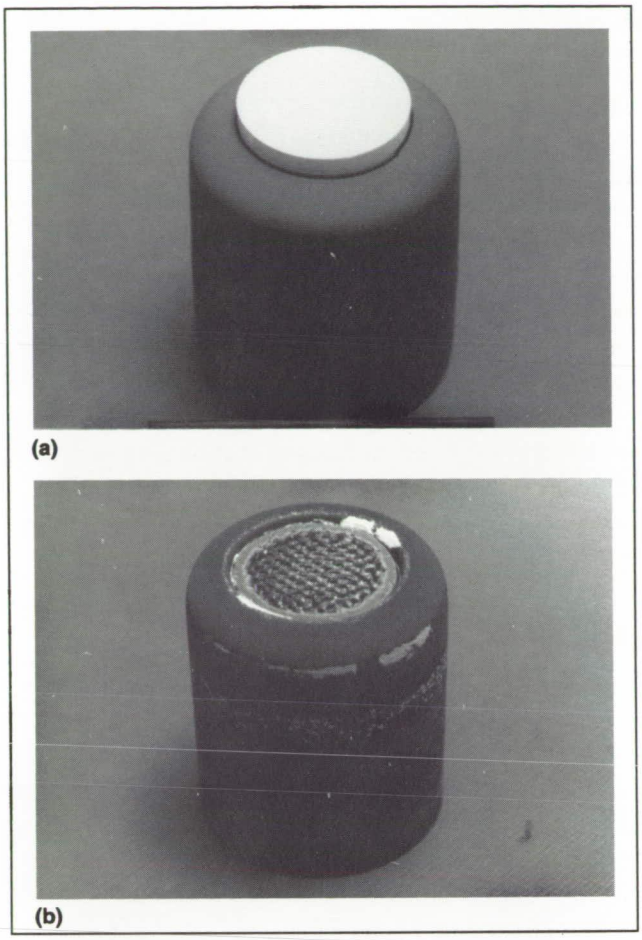


Fig. 1. Post-test photographs of two samples in their graphite mounts. Both samples were tested at the same conditions. (a) ZrB_2 + 20v/o SiC particulate composite from Cerac Incorporated; (b) Shuttle RCC heat shield sample (SiC coated carbon-carbon) from LTV Missiles Division

The ZrB_2 + 20v/o SiC composite sample formed a thin, adherent, glassy oxide coating on its exposed surfaces, and reached a temperature of 3300°F. No rounding occurred at the sample edges, and the graphite holder (which originally had been flush with the sample) recessed approximately 2.5 millimeters during the exposure. The sample lost only 0.01 gram of weight and actually grew 0.03 millimeter during the exposure due to the formation of the oxide layer.

The RCC sample, by contrast, underwent significant recession of 1.98 millimeters with a weight loss of 1.31 grams and (as shown by the figure) actually recessed inside the graphite mount. The SiC coating on the sample was lost after approximately 100 seconds of testing, and the exposed carbon-carbon substrate material can be seen in the figure.

Additional testing showed that the diborides could operate at temperatures over 4000°F with very minimal weight loss, and that the new carbon fiber and SiC platelet-reinforced materials performed as well as, and even better than, the particulate materials. Further testing and evaluation is planned to confirm and more fully explore the behavior and operating limits of these materials. The results obtained to date clearly show the potential of zirconium- and hafnium-based composite ceramics for significantly increasing the temperature and heat flux capabilities of reusable heat shield materials.

Ames-Moffett contact: D. Rasky
(415) 604-1098 or FTS 464-1098
Headquarters program office: OAET

ORIGINAL PAGE
BLACK AND WHITE PHOTOGRAPH

Prediction of Hydrogen Recombination Rates

David Schwenke

To accurately model properties of engines, it is necessary to have reliable estimates of the rates of various chemical reactions that are taking place. For hypersonic vehicles, much of the chemical phenomena takes place under very harsh and complex conditions which makes reliable experimental measurements difficult or impossible. Thus, to obtain useful design parameters, it is very valuable to use computational chemistry methods. Because of the complexity of the calculations, to make this procedure feasible, it is necessary to identify the subset of reactions for which the combustion process is most sensitive. In our present studies, we have focused on the hydrogen recombination process $H + H + M \rightarrow H_2 + M$ for various third bodies M. We will consider M = H, H_2, H_2O, and Ar. For hydrogen-burning engines, the rates for hydrogen recombination are thought to be very important in determining engine thrust.

Several computational steps are involved in the determination of the recombination rate parameters. The ultimate goal is to determine the rate coefficients k^M in the rate expression

$$-dC_{H_2}/dt = \left(C_H^2 - C_{H_2}K_{eq}\right)\sum_M C_M k^M$$

where C_A is the concentration of species A, t is time, and K_{eq} is the equilibrium constant for $H + H \rightarrow H_2$. The k^M are functions of temperature but not of any concentrations.

The first step is the determination of the potential energy surface (PES) for the H + H + M system. This can be further broken down into the solution of the electron motion problem for fixed nuclear position to yield a potential energy and then the construction of an interpolating function to give the potential energy at arbitrary nuclear positions. This is required because the solution of the electron motion problem is very expensive, even though highly optimized state-of-the-art electronic structure methods are used. During FY 90, the PES for $M = H_2O$ has been determined. Because of the dimensionality of this system (the $H + H + H_2O$ PES is a function of nine coordinates specifying the nuclear positions), it was necessary to develop new techniques to reduce the number of geometries for which electronic structure calculations were carried out while retaining the accuracy of the final result.

Once the PES is shown, it is next necessary to determine the effect of nuclear motion. In this step, cross sections are calculated for the microscopic processes

$$H_2(v,j) + M \rightarrow H_2(v',j') + M$$

and

$$H_2(v,j) + M \rightarrow H_2(v',j') + M$$

where v,v' are vibrational quantum numbers and j,j' are rotational quantum numbers. The computational approach used in the present work is to estimate the cross section by means of the quasiclassical trajectory method. The trajectories are computed from the forces generated by the PES for each M separately. So far extensive calculations have been carried out for M = H and H_2, while some calculations have been performed for $M = H_2O$ and Ar. The cross sections are Boltzmann averaged over internal energies to yield temperature-dependent state-to-state rate coefficients which are input to the next step.

Although we use the quasiclassical trajectory method to determine the nuclear dynamics, this is not the most reliable procedure. The nuclear motion is controlled by quantum mechanics, and only a fraction of all the quantum mechanical effects are included in the quasiclassical trajectory method. However, quantum mechanical calculations using current algorithms are very expensive, so calculations of the scope required for the study of recombination are not feasible using quantum mechanics for nuclear motion. Nonetheless benchmark quantum mechanical calculations are required to quantify the errors in the quasiclassical trajectory method, and thus algorithmic improvements for quantum mechanical calculations have been an area of study.

The final step in the calculations is the simulation of a macroscopic system to determine the rate coefficients k^M. This simulation includes all internal state nonequilibrium effects and requires the state-to-state rate coefficients for all M and the solution of the master equation to give the time-dependent concentrations of all the internal H_2 v,j states. Once the time-dependent concentrations are known, it is necessary to analyze the results to give the phenomenological rate coefficients, the k^M. This final step has been completed for the H and H_2 mixture at high temperature, and preliminary calculations have been carried out for systems including Ar or H_2O as well.

These nonequilibrium calculations are feasible because of the relatively small number of internal states of H_2. This molecule has only 348 internal states whereas other candidates for recombination studies (e.g., $H + OH \rightarrow H_2O$ or $N + N \rightarrow N_2$) have many more internal states. Thus it is necessary to develop approximate methods to extend these calculations to other systems. Several methods are under consideration and we are optimistic that in the future it will be possible to make reliable estimates of recombination rate parameters for most systems of interest to various NASA projects.

Ames-Moffett contact: D. Schwenke
(415) 604-6634 or FTS 464-6634
Headquarters program office: OAET

Measurements of Relaxation Rate Parameters in a Shock Tube

Surendra Sharma

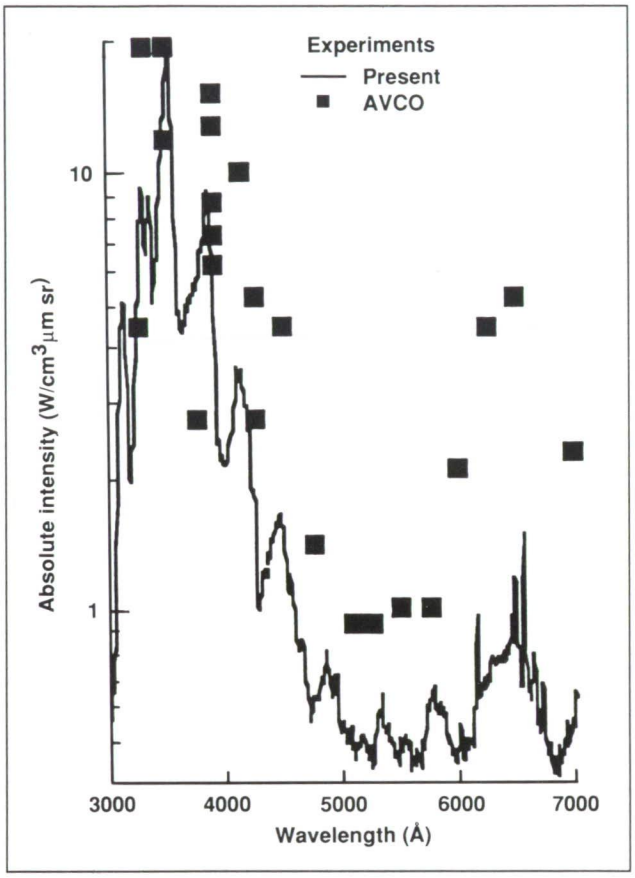


Fig. 1. Nonequilibrium spectrum of air at a shock velocity of 10.2 kilometers/second at 0.1 Torr of pressure

Considerable efforts have expanded in recent years to model the effects of high-temperature real gas phenomena occurring in the flow around hypersonic vehicles. Experiments can provide the needed physical constants and verify the validity of such thermophysical models. Series of tests are planned at Ames Research Center's Electric Arc Shock Tube Facility.

In this series of experiments, the intensities of the radiation emitted behind a normal shock wave in air were measured at a shock velocity of 10.2 kilometers/second. Both a time-resolved broad-band radiation intensity measurement and a time-frozen spectral measurement were conducted. The nonequilibrium spectrum recorded at the point of peak radiation in the spectral range of 3000-7000 angstrom is compared with the AVCO data (1960s) in the first figure. The measured data are much more detailed (4200 data points), recorded with 700 points per shot, and can be used to validate computational fluid dynamics (CFD) radiation codes.

By analyzing the measured data, the rotational and vibrational temperatures are measured (1) at the point of peak radiation: $T_R = 4195 \pm 115$ K and $T_V = 9540 \pm 220$ K and (2) in the equilibrium region T = 9620 K. The fact that the rotational temperature is different from the equilibrium temperature suggests that the CFD community should not only model the vibrational nonequilibrium but also the rotational nonequilibrium in the flow computations.

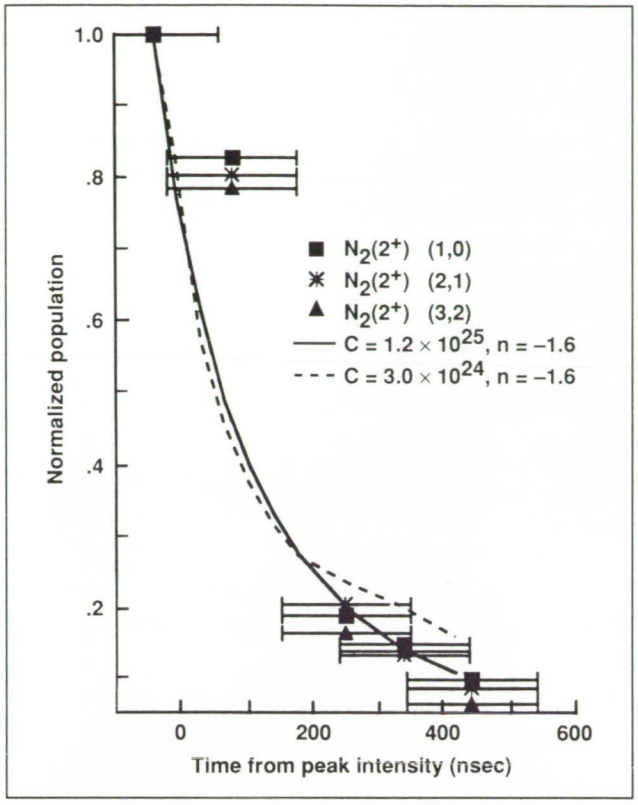


Fig. 2. Normalized population density of $C^3\Pi_u$, the upper state of the $N_2(2^+)$ band system, as a function of time

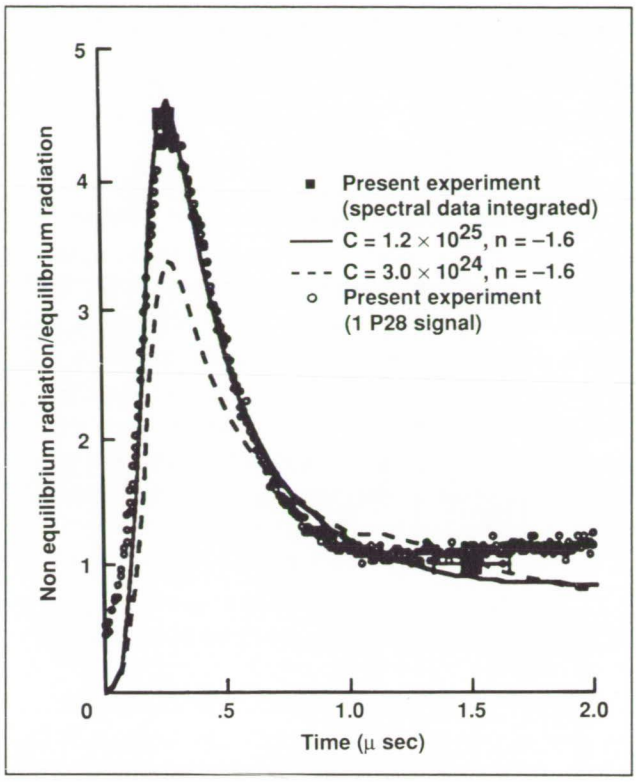


Fig. 3. Normalized total radiation as a function of time

High energy experiments indicate that the electrons show a greater affinity for nitrogen molecules and may play a larger role in their dissociation. However no experimental data for the temperatures of our interests (4,000-50,000 Kelvin) are available.

In this experiment we have monitored the N_2 population during relaxation (see the second figure) and by comparing the measured data (in the second and third figures) with the theoretical predictions, it is established that the N_2 dissociation rate by electron impact is given by $K = 1.2 \times 10^{25} (TT_v)^{0.8} \exp(-113200/(TT_v)^{0.5})$ $cm^3\ mol^{-1}\ s,^{-1}$ where T and T_v are the translational and vibrational temperatures respectively.

Ames-Moffett contact: G. Deiwert/C. Park
(415) 604-6198/5394 or FTS 464-6198/5394
Headquarters program office: OAET

Computational Analysis of Plume-Induced Separation

Ethiraj Venkatapathy

The Malemute rocket that carried the boost-phase signature experiments was predicted to be unstable due to plume-induced separation. Design modifications to the tail section were suggested to improve the stability. The objective of this study was to perform computational experiments of the propulsive-plume flow, including the Malemute hardbody; analyze the numerical solutions for the plume-induced separation phenomenon; and evaluate the modified geometry for improved stability.

An ideal gas, upwind, full Navier-Stokes code was used to predict the complete supersonic flow around the original and the modified axisymmetric version of the Malemute rocket at four different flight trajectory points. The numerical simulations clearly showed plume-induced separation at higher altitudes and the resulting instability due to fin ineffectiveness. The extent of separation and the peak heating due to separation were also predicted.

Computed velocity direction near the tail section for the original boattailed afterbody configuration for free-stream conditions corresponding to 40 kilometers altitude is shown in the figure. Large separation due to the jet plume effects can be clearly seen. A tail cone assembly was added to the aft body to limit flow separation, and numerical simulations were performed for the modified design. Analysis of the numerical solutions allowed a thorough evaluation of the aft body modifications with respect to the plume-induced separation. The modified aft body was able to limit the plume-induced separation to a very small region and, thus, increased stability was predicted. Special heat-shield and nonablative coatings to prevent ablation were determined from heat transfer predictions. Numerical simulations performed provided a clear insight into the plume-induced separation phenomenon.

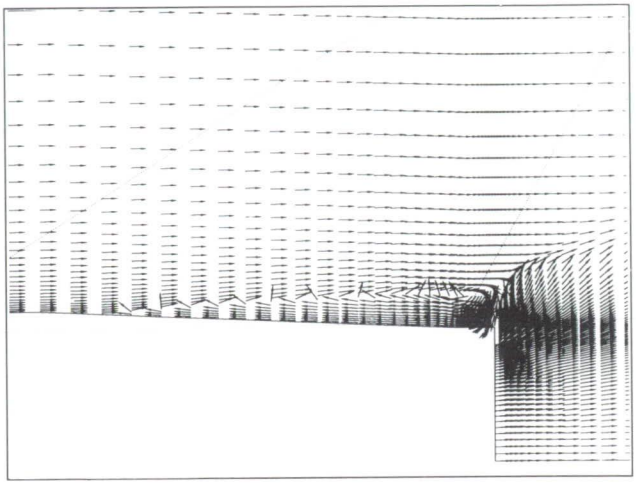


Fig. 1. Computed velocity directions for the boattailed afterbody at 40-kilometer altitude

The vehicle was launched successfully with the modified tail section. The increased understanding gained from the numerical simulations of the modified design and the application of heat-shield and nonablative coatings at appropriate regions are believed to be major reasons for the success.

Ames-Moffett contact: G. Deiwert
(415) 604-6198 or FTS 464-6198
Headquarters program office: OAET

Characterizing Crop Plan Performance for Regenerative Life Support Technology

David Bubenheim

The goal of the Controlled Ecological Life Support System (CELSS) program is to combine biological, physical, and chemical processes capable of recycling food, air, and water to support long-term missions with humans in space. CELSS research and development has concentrated on characterizing operation of the potential component technologies. For the plant system, the approach has been to identify the flexibility and response time for food, water, and oxygen production, as well as carbon dioxide consumption processes. Work during the past year has emphasized three specific areas of crop physiology research: (1) maximizing and characterizing food production potential, (2) maximizing and characterizing water production potential, and (3) reducing the production of inedible biomass.

Food Production

Wheat yields in controlled environments are 16 times greater per unit area, per unit of time, than high field yields, 6 times greater than the world record field yields, and 3 times greater than that reported by the Soviets during their BIOS experiments testing biological life support approaches (see table). Only 9 square meters of wheat were required to provide 100% of the food energy necessary per person. If all of the food requirements are satisfied with adequate crop area, all of the water and air revitalization needs are met at the same time and additional equipment to regenerate water and air is not necessary.

Wheat Yields in Controlled Environments

High Yields in CELSS Crops				
Wheat	Days to harvest	Edible $g\ m^{-2}$	Harvest index	Yield $g\ m^{-2}\ d^{-1}$
High field avg	120	500	45	4.2
World record	140	1456	45	10.4
Soviet BIOS	60	1314	?	21.9
Utah St Univ 1988	79	4760	44	60.3
Ames 1990	58	3799	48	65.5

Water Production

When wheat is grown to maximize food production, environmental conditions around the plant actually minimize water production. In a maximum food production environment, 3.8 square meters of crop provide all of the water required for potable and hygiene needs while 0.25 square meters of crop supply the potable water required per person. Taking advantage of the dynamic nature of the plant, water production via transpiration can be increased by modifying the environment, analogous to the changing of the feed streams in a chemical processing plant. By favoring water production, enough water has been transpired to account for potable needs using only 0.07 square meters (of crops) per person. It is expected that further reductions to about 0.02 or 0.01 square meters per person will result in improved controlled environment facilities.

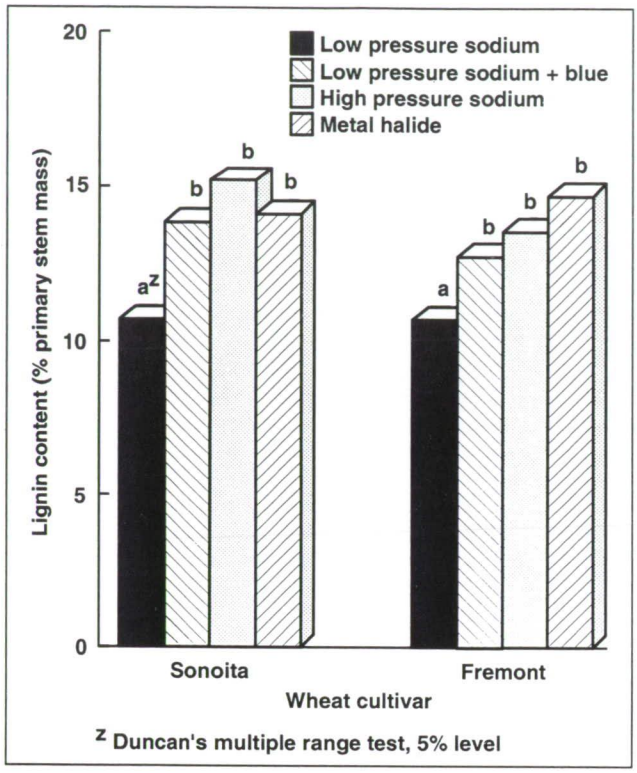


Fig. 1. Lignin synthesis as a function of lamp type

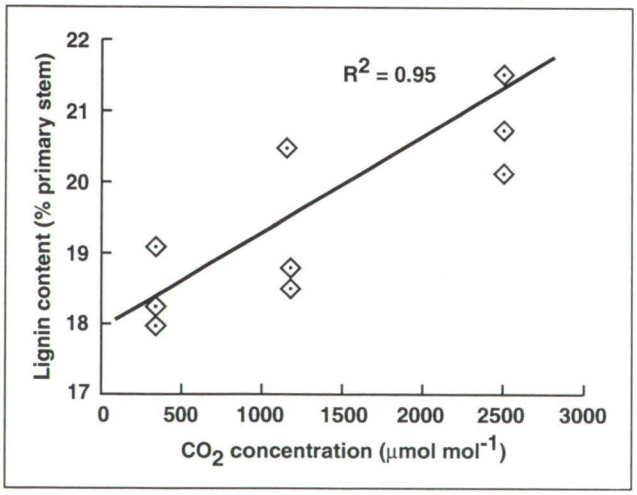


Fig. 2. Effect of CO_2 concentration on lignin synthesis

Inedible Biomass Reduction

When plants grow, a certain amount of inedible biomass is necessary to successfully complete a life cycle. Leaves provide the site for photosynthesis, and stems physically support the leaves and edible products. The mass of this inedible portion can be considered as "overhead" in the production system. Experimentation has focused on the reduction of lignin; it is nondigestible, and its association in the cell wall with cellulose reduces the effectiveness of biological breakdown of cellulose to the component sugars. Using wheat as a model system, lignin content has been reduced by 30%. This has been achieved by growing the plants under monochromatic yellow light, provided by highly efficient low-pressure sodium lamps. Lignin synthesis appears to be controlled by the blue-absorbing photoreceptor and not the photochrome system (see first figure). Determination of the control mechanism will allow development of a photoreactor control model (for minimizing lignin production) to apply to other crops which cannot be grown under monochromatic yellow light.

It has also been determined that increased CO_2 concentration causes elevated lignin synthesis (as shown in second figure). The high yields attained in the production research rely on elevated CO_2 concentrations; as CO_2 increases, so does photosynthesis and consequently plant productivity. Efforts to determine the potential for spectral control of CO_2 induced lignin synthesis are planned for 1991.

Results of the inedible biomass reduction research are being used to better determine the amount of composition of inedible biomass to be processed by waste management systems for regenerative life support.

Ames-Moffett contact: D. Bubenheim
(415) 604-3209 or FTS 464-3209
Headquarters program office: OSSA

Hydrocarbon Contamination on Polytetrafluoroethylene Exposed to Oxygen Atoms

Morton Golub, Ted Wydeven

A study of the surfaces of fluorocarbon polymers exposed to atomic oxygen [$O(^3P)$]—either in low earth orbit (LEO) on the Space Shuttle or within or downstream from a radio-frequency (RF) oxygen plasma—was summarized in the Research and Technology Annual Report for 1989. That study, which involved the use of electron spectroscopy for chemical analysis (ESCA) to characterize the surface oxidation experienced by various fluorine-containing polymers, was an outgrowth of the realization that polytetrafluoroethylene (PTFE or Teflon) is one of the most stable plastics in the LEO environment, where oxygen atoms are the principal constituent.

During the former ESCA study, it became evident that unless the PTFE surface is free of hydrocarbon contamination, anomalous changes in the oxygen content, and hence the surface properties, may be improperly ascribed to the $O(^3P)$-exposed film. Thus, for a PTFE film whose ESCA spectrum was reported by Morra et al., in 1989, to have "a weak structure due to hydrocarbon contamination," the oxygen-carbon (O/C) ratio increased sharply (from 0.014 to 0.129). Correspondingly, the fluorine-carbon (F/C) ratio decreased sharply (from 1.73 to 1.26), at very short times of exposure to an oxygen plasma. However, for longer duration exposures, such changes in the O/C and F/C ratios reversed direction, and these ratios assumed values similar to those of the unexposed PTFE.

These ESCA results conflicted with prior observations that PTFE experienced a very small but monotonic increase of surface oxidation with time of exposure to $O(^3P)$ in an RF O_2 discharge, while the F/C ratios were virtually unchanged. Therefore, it is concluded that the "spikes" observed in the plots of O/C or F/C versus exposure time are not characteristic of PTFE, but are instead a result of the hydrocarbon contamination.

The above conclusions are illustrated in both figures. They are composite plots of ESCA-derived O/C and F/C ratios, respectively, as a function of exposure time for the following sets of data: (1) data

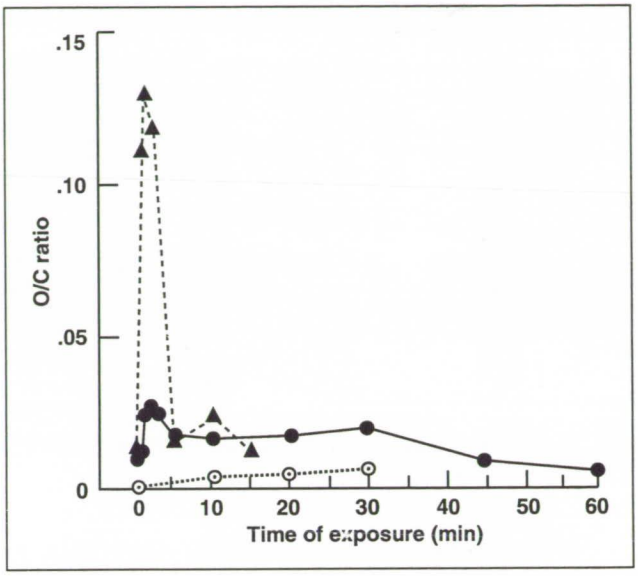


Fig. 1. Effect of time exposure of O_2 plasma on the O/C ratio of polytetrafluoroethylene

from Morra et al., for a PTFE with an initial F/C ratio (1.73), well below the theoretical value of 2.0; (2) the author's prior data for clean PTFE, showing no hydrocarbon contamination (initial F/C = 2.0), and exposed for 10, 20, and 30 minutes "in the glow" of an O_2 plasma; and (3) "new" (as-yet unpublished) data for a PTFE film (initial F/C = 1.96, O/C = 0.0098), similar to that used in the author's prior work but with a small amount of hydrocarbon contamination, though much less than in the PTFE sample used by Morra et al. From an analysis of the ESCA spectra obtained by Morra and the present authors, the hydrocarbon content in Morra's PTFE was estimated at 12.1 times that of the "new" PTFE.

As seen in the first figure, the former polymer exhibits a spike in the O/C-exposure time plot whose amplitude (or Δ(O/C)) is approximately 0.115/0.017, or 6.7, times the amplitude of the spike for the latter polymer. For the clean PTFE (data which were published previously), which had no detectable hydrocarbon contamination, there is no spike at all.

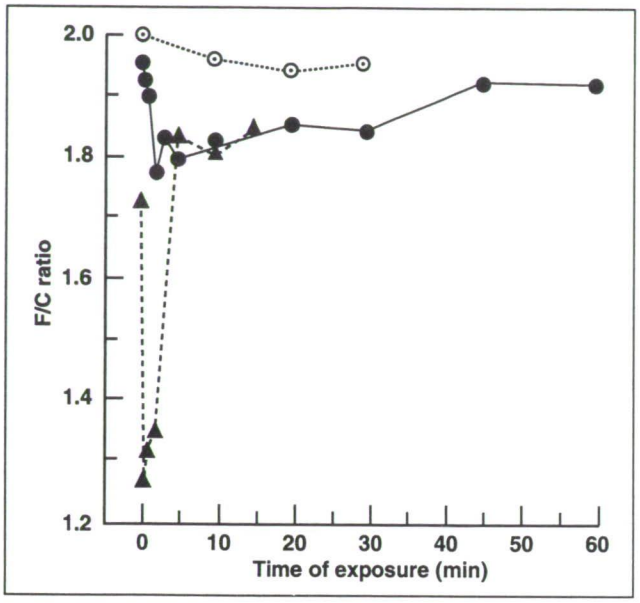


Fig. 2. Effect of time exposure to O_2 plasma on the F/C ratio of polytetrafluoroethylene

To the extent that there is oxygen uptake by the O_2 plasma-exposed PTFE, the F/C ratio necessarily decreases, whether or not F detachment occurs. This is reflected in the second figure, which shows changes in the F/C ratios accompanying the changes in the O/C ratios of the first figure. As in the second figure, the amplitude of the spike in the F/C-exposure time plot for Morra's PTFE (Δ(F/C) = –0.47) is greater than that (–0.19) for the new PTFE, while the clean PTFE again shows no such spike.

It was noted that two samples of PTFE retrieved from exposure in LEO showed a correlation between oxygen uptake and the level of hydrocarbon contamination; thus, the sample with 1.3 atom % C had an oxygen uptake of 0.58 atom % O, while the sample with 2.8 atom % C had an oxygen uptake of 0.90 atom % O. In fact, it is suggested that the $-CF_2CF_2-$ structure per se (characteristic of an ideally pure PTFE) undergoes negligible oxygen uptake in LEO.

Finally, the two figures show that a steady-state surface composition is approached on prolonged exposure to the O_2 plasma. Once the hydrocarbon contamination is oxidized away, the surface of an initially "unclean" PTFE film acquires the same level of oxygen uptake as that acquired by a pristine PTFE film.

Ames-Moffett contact: R. Lamparter
(415) 604-1159 or FTS 464-1159
Headquarters program office: OSSA

Benefits of Recycling (Loop Closure) in a Space Habitat

Mark Hightower

Current space missions use open-loop life support systems, where all supplies needed are taken up, and all waste streams generated are discarded for return to Earth. Future long-duration space habitats will have closed-loop life support systems, where some of the waste streams generated will be continually processed to recover usable supplies for recycling. This will decrease both the amount of input supplies needed from Earth and the amount of unusable waste generated. For long-duration space missions, the incentive for recycling is accentuated by the high cost of placing each additional kilogram of supplies into space. To understand quantitatively how recycling would increase the efficiency of a space habitat, some simple mathematical relationships have been established.

A simple derivation based on material balance considerations reveals that the supply savings factor (SSF) can be expressed in the following formula: $SSF = 1 - r$, where r is the recycle ratio, the fraction of the total waste stream that can be continually recycled and reused. The SSF is the ratio of "the quantity of input supplies needed for recycle ratio r" to "the supplies needed without recycling." The life support extension factor (LSEF) can be expressed as follows, $LSEF = 1/SSF = 1/(1 - r)$, and is the other side of the equation. With greater recycling, life can be supported for a longer time in space on the same quantity of input supplies from Earth. A simple case can easily illustrate these concepts. If $r = 0.80$, then $SSF = 0.20$, and $LSEF = 1/0.20 = 5$. $SSF = 0.20$ indicates that only 20% of the quantity of supplies required without recycling are needed with recycling (for the same period of time). $LSEF = 5$ indicates that life could be sustained 5 times longer on the same quantity of supplies as the open-loop case. The above equations are a simple case of a more rigorous treatment which is beyond the scope of this brief note. This simple case assumes that the amount of maintenance supplies (spare parts, etc.) required for the closed-loop system are the same as for the open-loop system.

A "material balance analysis" was performed, using spreadsheets, based on space waste composition data to determine the level of recycling attainable from a strictly physical/chemical life support system with air revitalization and water reclamation only. The amount of maintenance supplies required is an assumed value estimated to be the same for the closed- and open-loop cases.

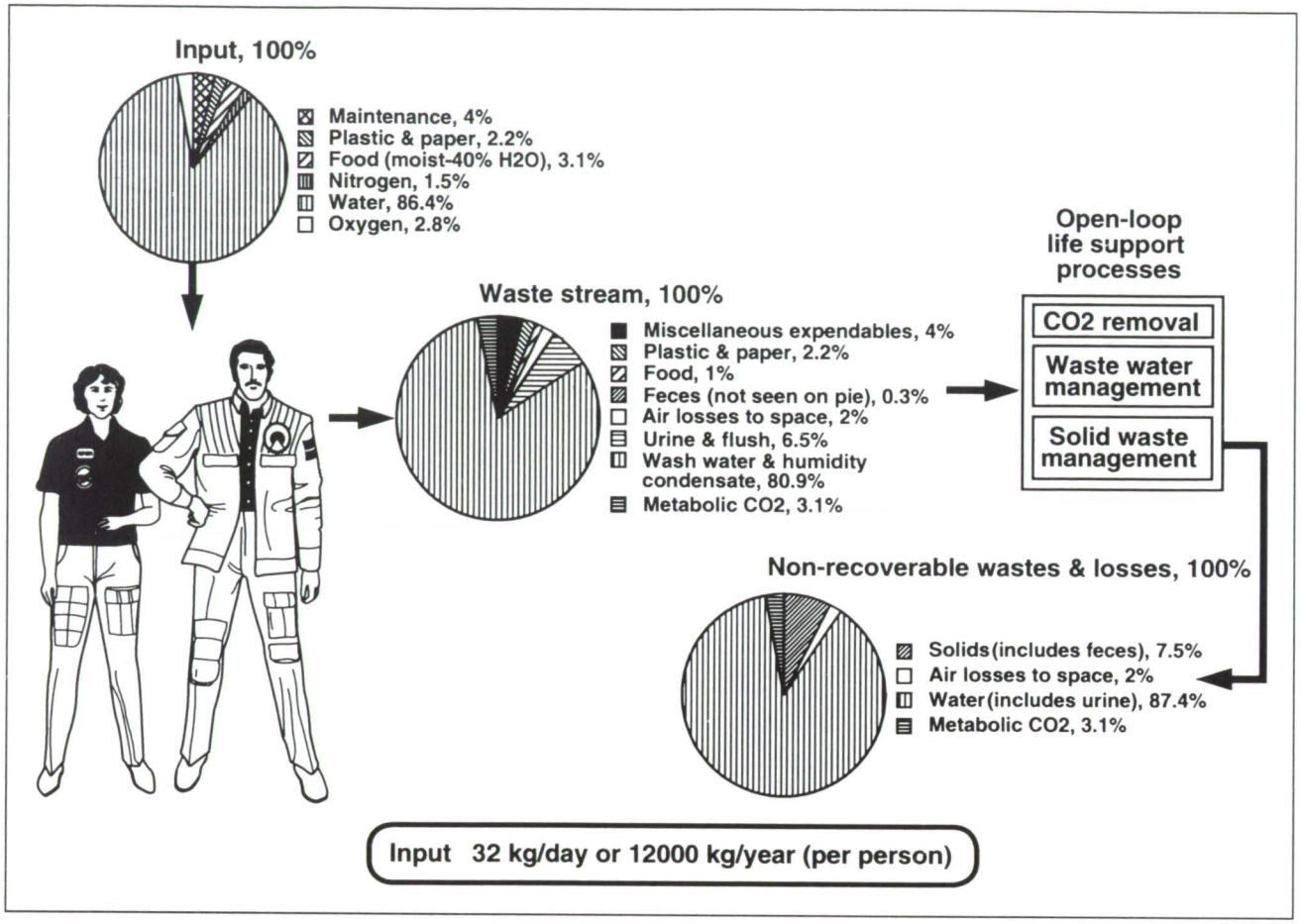


Fig. 1. Open-loop life support—system throughput

The first figure shows that 32 kilograms/person-day of input supplies are required to sustain an open-loop habitat. The second figure shows that with a closed-loop life support system, 89% (i.e., r = 0.89) of the waste stream can be recycled and reused, which lowers the input supplies required to 3.5 kilograms/person-day.

It is significant to compare the resupply launch cost of open-loop versus closed-loop systems. Assume that a crew of eight is supported for one year, and that it costs $11,000 per kilogram launched into space. The resupply launch costs would be $1,028 million per year for the open-loop case versus $112 million per year for the closed-loop case. The closed-loop case saves $916 million per year in launch-related costs over the open-loop case.

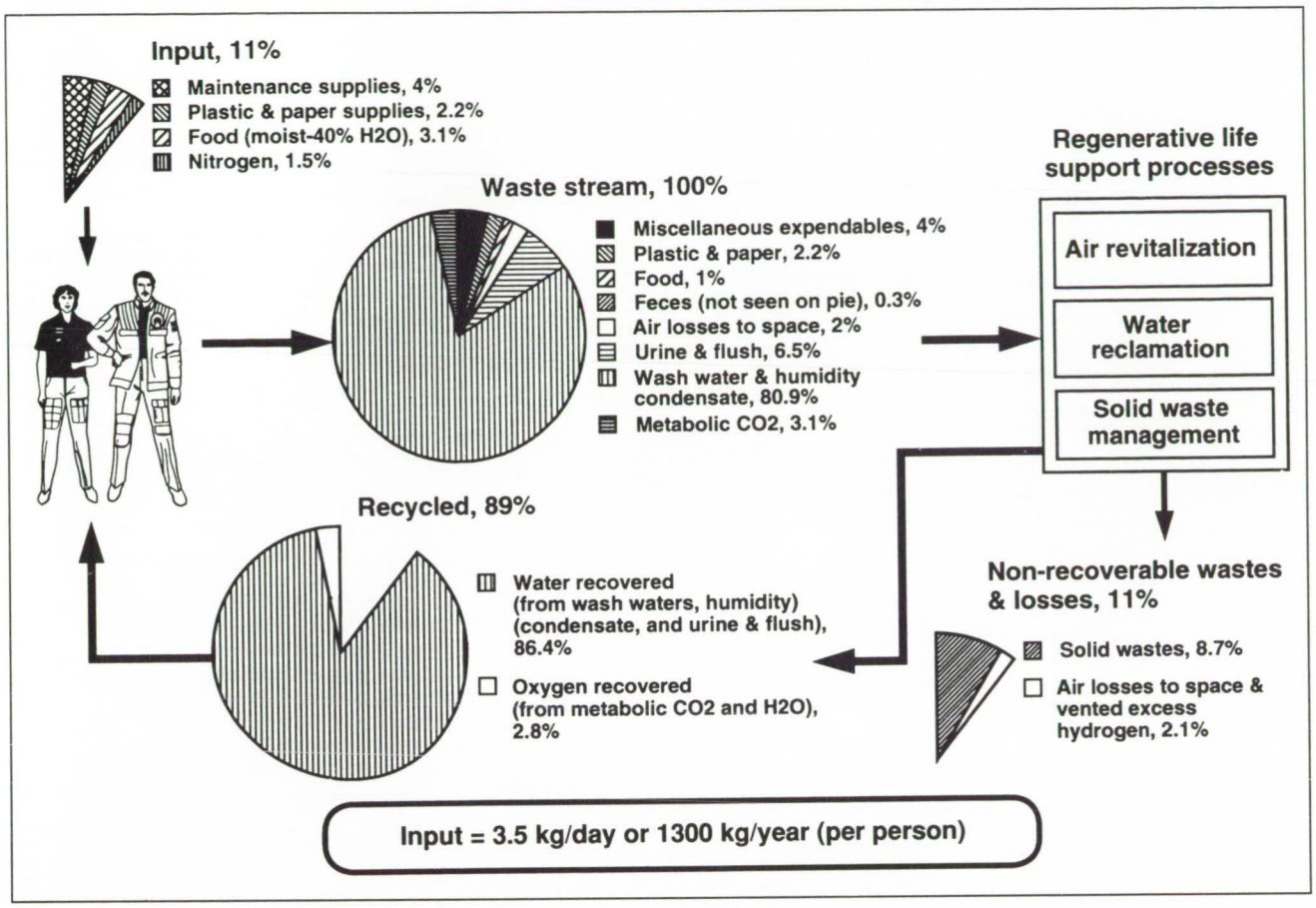


Fig. 2. Effect of recycling in a closed-loop physical/chemical system

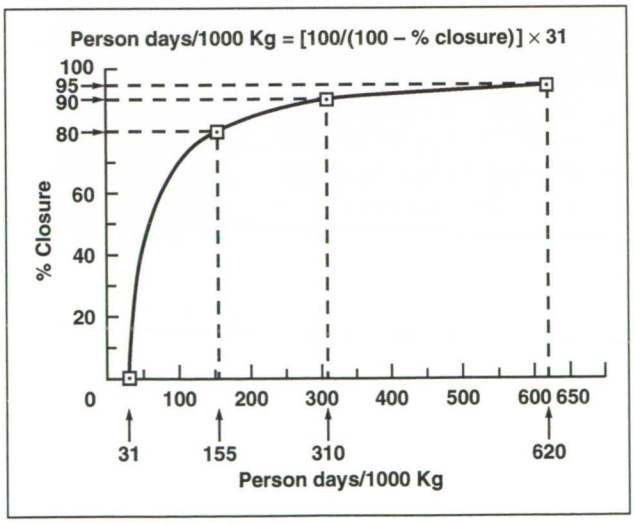


Fig. 3. Effect of percent closure on person-days of life support provided per 1000 kilograms of supply input

The third figure illustrates the mathematical relationship between recycle ratio and life support extension. Recycle ratio is expressed as a percentage and is called percent closure, and life support extension on the abscissa is actually the product of LSEF and 31 person-days/1000 kilograms of supplies, the amount of life support provided for the open-loop case. The three points highlighted on the diagram are for illustration purposes only. Going from a percent closure of 80% to 90% doubles the life support provided. Going from a percent closure of 90% to 95% doubles the life support again. It is not the intention of the diagram to imply that 90% or 95% closure is possible, but to show the potential benefits of these increases in percent closure if they can be achieved.

Ames-Moffett contact: J. Fisher
(415) 604-4440 or FTS 464-4440
Headquarters program office: OSSA

A Fiber-Optic-Based Total Organic Carbon Sensor

John W. Hines, Jeff Roe, Christopher Miles

The development of a fiber-optic-based total organic carbon (TOC) sensor is under way in a collaborative effort among the Advanced Life Support Division and the Sensors 2000! Program at NASA Ames Research Center and Teknekron Sensor Development Corporation, Inc. Presently, no reliable sensor system exists for real or near-real time monitoring of TOC in aqueous solutions in the parts-per-billion range. The development of such a sensor would provide accurate control data in the partially and totally closed-loop water reclamation systems required for long-duration space flight missions.

The TOC sensor is predicated on monitoring changes in the refractive index of an unclad fiber optic cable which has been coated with organic carbon sensitive receptors. The actual sensor is a fiber optic cable that has had a section of its cladding removed. This unclad portion is treated, and compounds with hydrophobic and hydrophilic affinities are bound to its surface.

The first figure shows the actual fiber configuration. Measurements are made by monitoring the change in the index of refraction of this special section of fiber as hydrophobic and hydrophilic compounds are absorbed by it.

A monitoring system using this sensor, shown in the second figure, basically consists of a light source (in this case a helium-neon laser), the special fiber, a photodetector, and its associated signal conditioning hardware. Preliminary studies have shown that, with the current fiber and experimental configuration, the system has a detection limit of approximately 7 parts per million for such organics as hexane and benzene. Preliminary studies have been initiated with simple detergent compounds; however, no conclusive data have yet been obtained.

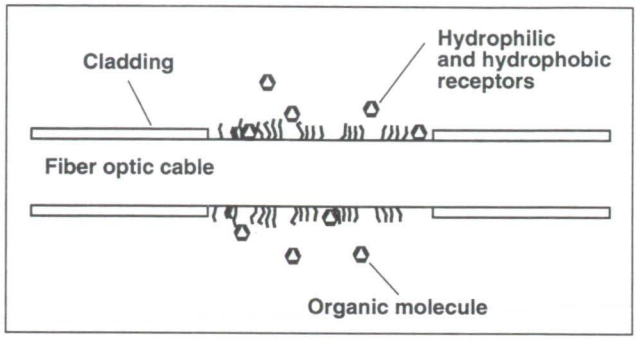


Fig. 1. Fiber-optic-based total organic carbon sensor configuration

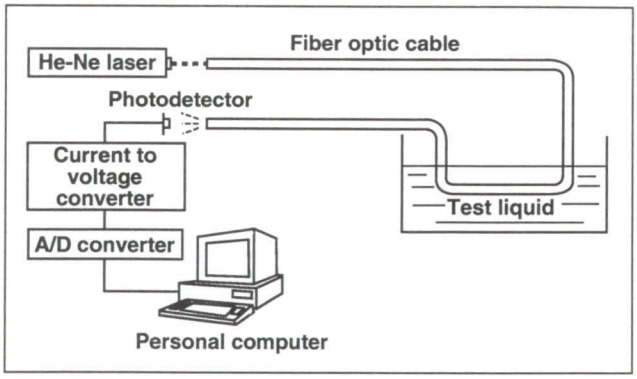


Fig. 2. Sensor system test configuration

Development of this sensor technology is still in its early stages, but results to date clearly demonstrate that this approach can be used to monitor total organic carbon. Further refinement of the experimental set-up and the fiber optic receptor coatings should show an increase in sensor resolution and accuracy. Further technological enhancements in this area are crucial to NASA's attempts to develop monitoring systems for partially and totally closed-loop water reclamation systems.

Ames-Moffett contact: J. Hines
(415) 604-5538 or FTS 464-5538
Headquarters program office: OAET

Salad Machine: A Vegetable Production Unit for Long-Duration Space Missions

Mark Kliss, Bob MacElroy

The design and construction of a salad vegetable production unit to be installed on Space Station Freedom is being conducted at NASA Ames Research Center in collaboration with personnel at Kennedy Space Center, Johnson Space Center, and university scientists and engineers. This unit (or derivatives of it) will also be applicable to other extended duration missions, such as those involving establishment of Lunar bases or use of a Mars Transfer Vehicle. The primary function of the vegetable production unit or "Salad Machine" will be to provide a variety of fresh salad vegetables to crew members for consumption. The first two figures illustrate current design concepts.

As a dietary supplement, the percentage of total caloric food intake per person derived from the Salad Machine is expected to be quite modest (approximately 5%). It is anticipated, however, that the activity of growing plant species by crew members, and the introduction of "space grown" food into their diet, will provide an intrinsically beneficial effect on the morale and psychological well-being of the crew during long-duration missions. It is difficult to assign a dollar value or quantify increases in human

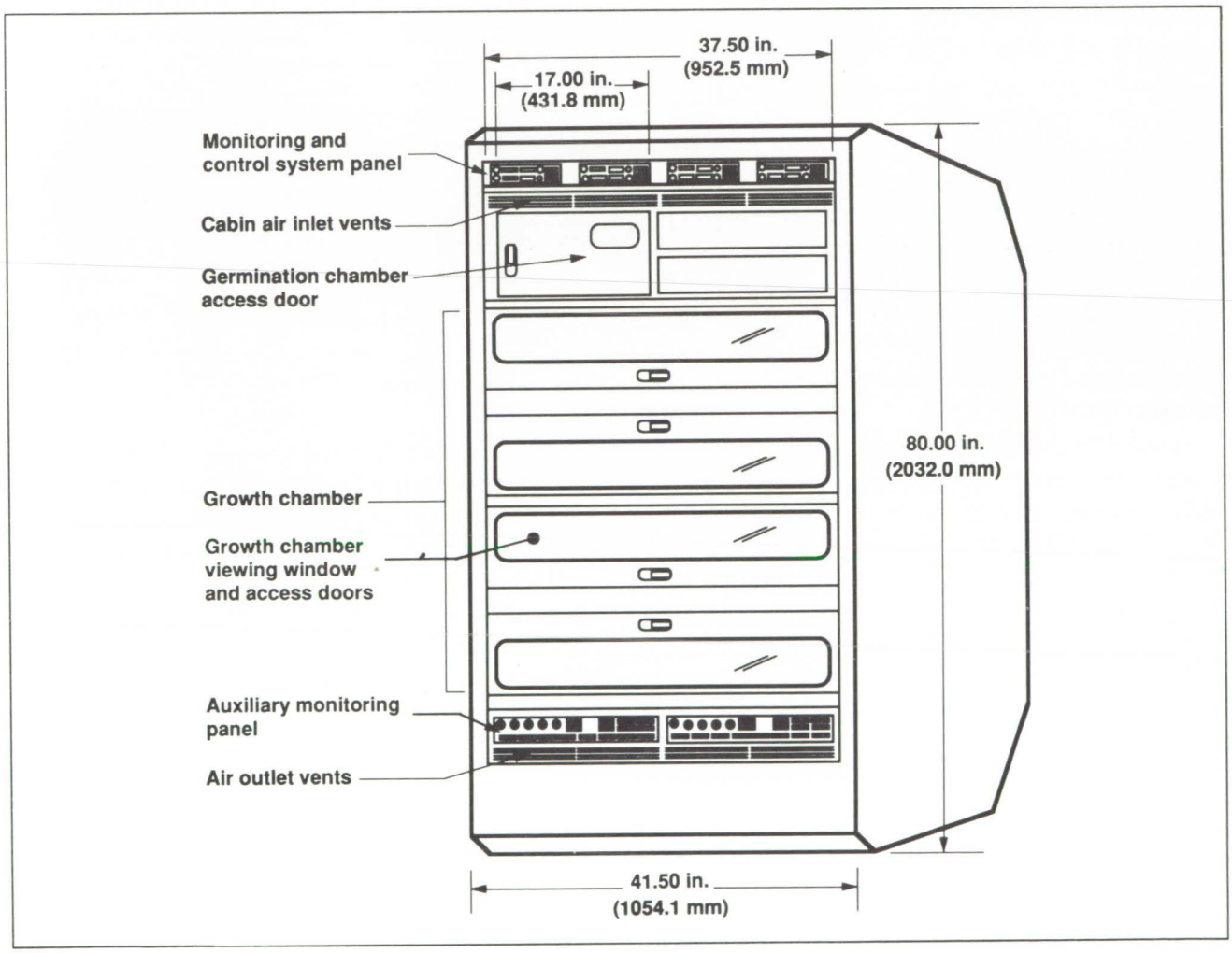


Fig. 1. Salad machine preprototype in Space Station Freedom standard rack configuration

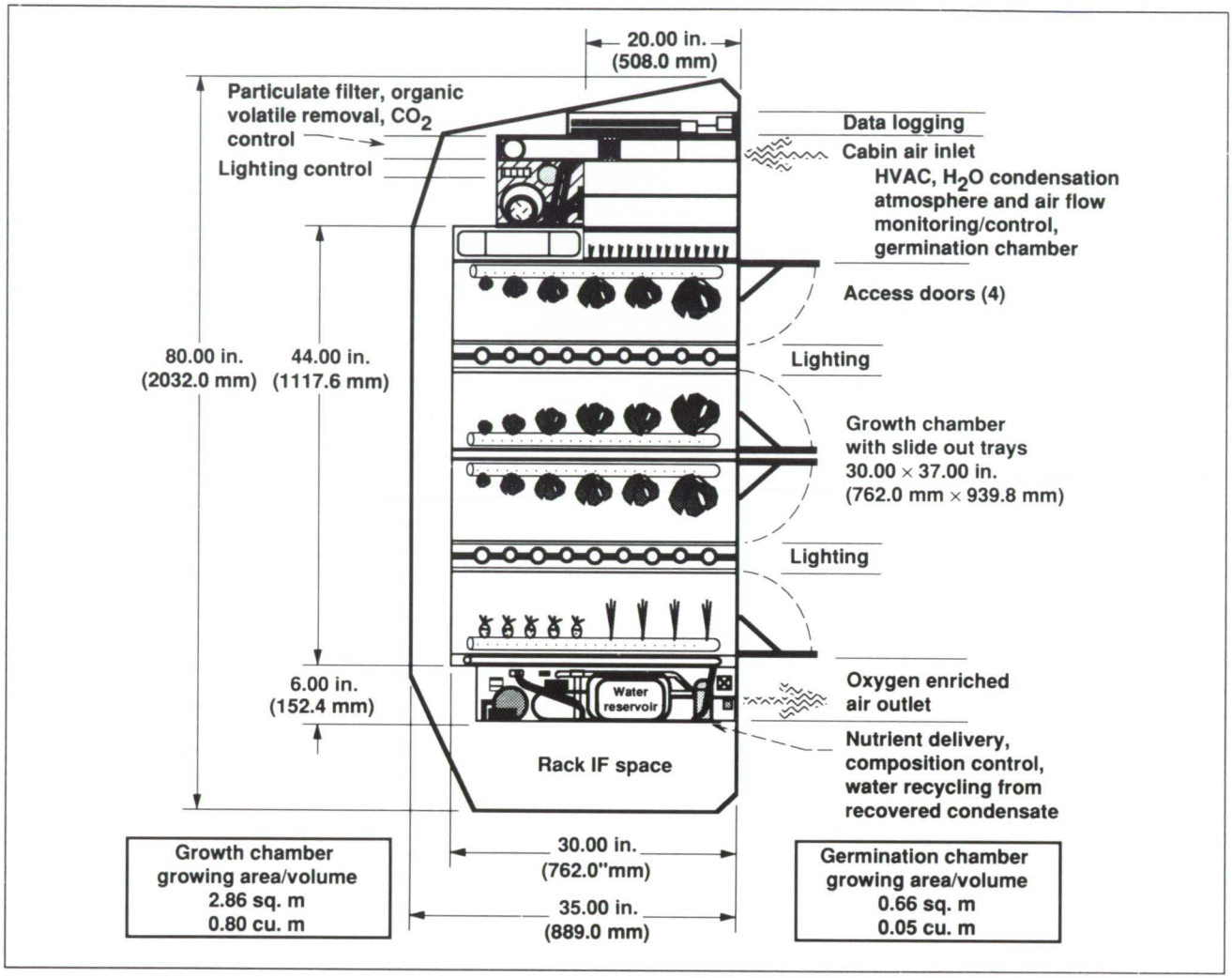


Fig. 2. Section view of the salad machine integrated systems design concept

productivity resulting from improved morale, but Soviet data from the BIOS program suggest that horticultural activities and the presence of plants produce psychological benefits for humans kept in isolated environments for extended periods.

A secondary objective of the Salad Machine will be to recover the water that is transpired by plants during the growth cycle. This function is necessary to minimize the water requirements of the vegetable production unit, but will also allow an evaluation of the water purification capabilities inherent to higher plants. It is conceivable that the Salad Machine could evolve to use "gray water" for producing potable water through plant transpiration. Finally, the near-term operation of the Salad Machine on Space Station Freedom will provide limited flight experiment capabilities to augment the Controlled Ecological Life Support System flight program, and should provide answers to certain technical questions associated with the implementation of future bioregenerative life support modules.

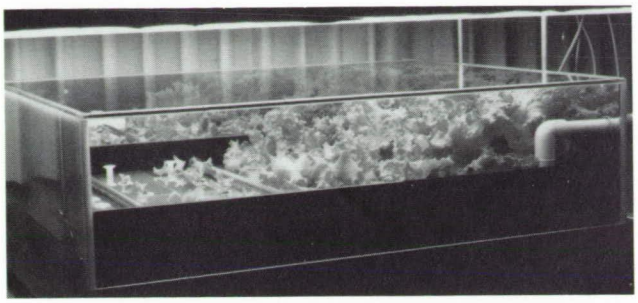


Fig. 3. Laboratory version of one of the four proposed rectangular plant growth shelves



Fig. 4. In one concept being evaluated in the laboratory research unit, seeds are germinated in seed "cassettes" and then inserted into the plant growth chamber, where nutrients are delivered via a hydroponic method

General system constraints associated with the operation of the Salad Machine on Space Station Freedom have been identified. The vegetable production unit will be contained within the payloads envelope of one standard Freedom Station rack (91.4 × 105.4 × 203.3 centimeters), which provides a user volume of 1.3 cubic meters. Approximately 0.8 cubic meters can be used for the plant growth chamber, with the remainder being occupied by support hardware and a small germination/sprout growth chamber. The total plant growth area (2.8 square meters) consists of four rectangular shelves (76 × 94 centimeters) each with an area of 0.7 square meters. Other overall system constraints include using standard low power rack resources, minimizing the heat transferred into the surrounding environment, containing the nutrient solution, and recycling the plant transpiration water. In addition, cabin air containing CO_2 will be introduced into the Salad Machine whenever the unit's CO_2 levels fall below 300 parts per million. Oxygen-enriched air from the plant growth volume will have water vapor, particulates, and organic volatiles removed before being returned to the cabin environment.

These general requirements are intended to keep the Salad Machine as transparent to Space Station Freedom systems as possible, and to minimize the effect of the Salad Machine input and output on other Space Station Freedom facility operations. As long as the broad, general plant growth requirements are satisfied in conjunction with these general system constraints, the Salad Machine has been conservatively estimated to be capable of producing 600 grams of edible biomass (fresh weight) per week.

A "continuous production" system where vegetables are planted and harvested on a regular basis is planned for the Salad Machine. Such a system maximizes light utilization, minimizes the growing area required, and maintains a relatively constant nutrient composition and water requirement for the entire system.

Ames-Moffett contact: B. MacElroy
(415) 604-5573 or FTS 464-5573
Headquarters program office: OSSA

ORIGINAL PAGE
BLACK AND WHITE PHOTOGRAPH

Life Support Database System

William E. Likens

A Life Support Database has been developed, which provides a centralized, readily accessible source of high-quality, standardized information for use in a wide range of life support research and technology development efforts. The Life Support Database is intended to be very broad in scope and include recycling process equipment specifications, chemistry, materials, missions and standards information, etc. The source of all data entries is recorded and available for display to facilitate maintenance of a high degree of data traceability and quality control.

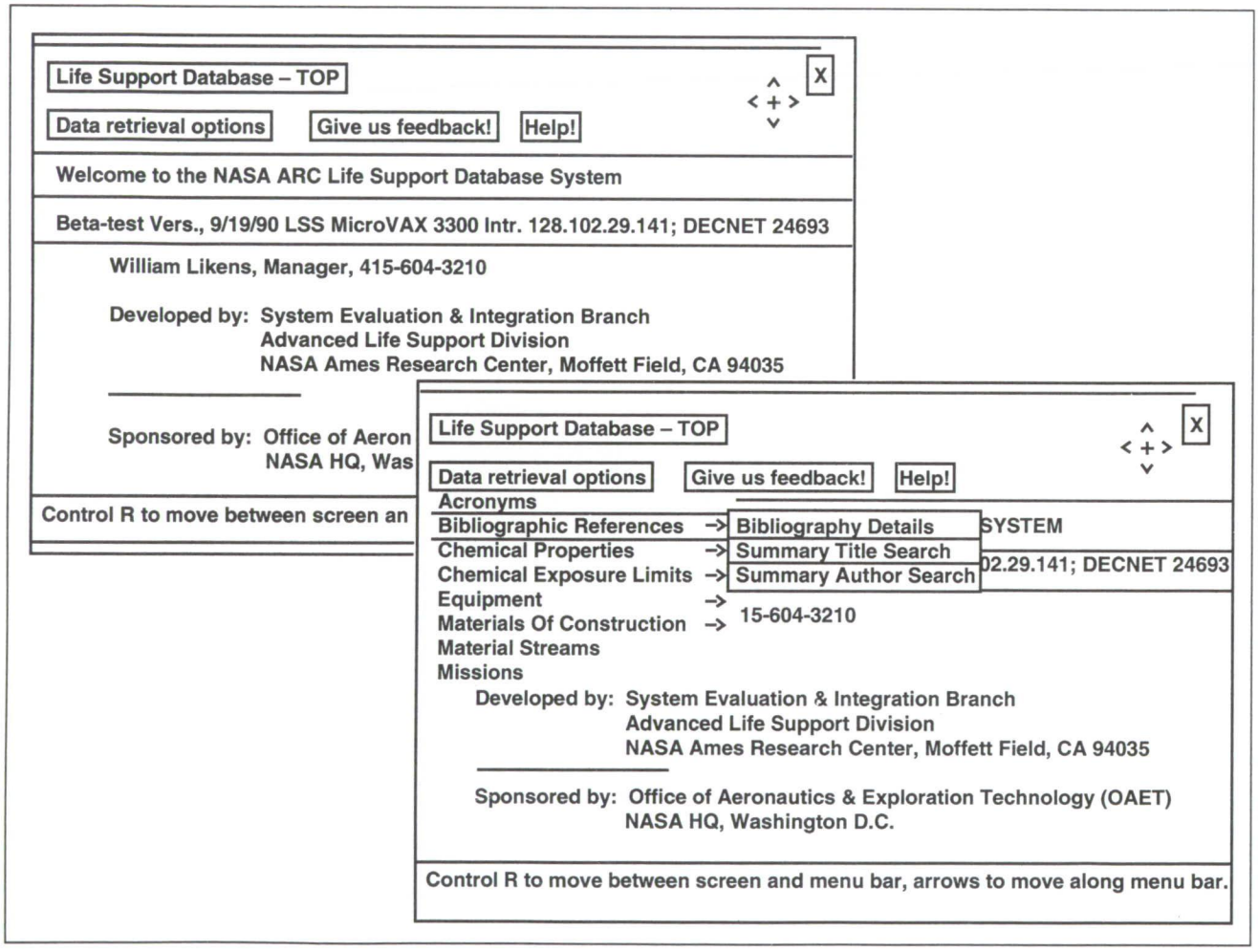


Fig. 1. Arrow-key driven format and pull-down menu of the Life Support Database

Some of the many applications of the database include: modeling and simulation analysis, trade-off studies and assessments, preparation of subsystem and system designs, and the planning of experiments and testing programs. The database is designed in a manner that will both preserve essential information for continued use and allow rapid and easy future expansion as new data are gathered via ongoing research and development.

The database has been implemented as a central archive that is remotely accessible over NASA networks. The host computer for the Life Support Database is a DEC VAX 3300 located at Ames Research Center. The host is connected to the NASA Space Physics Analysis Network (SPAN), a network using DECNET protocols, and the NASA Science Internet Network (NSI). The database is built upon Sybase Relational Database Management System (RDMS) software. The user interface for the database was designed by Ames staff, using tools provided within the Sybase RDMS. Users need not be acquainted with computer databases or computer data communications to use this menu-driven system. The figure shows an arrow-key driven pull-down menu.

A test release version of the system has been completed and is being evaluated by users at Ames, the Jet Propulsion Laboratory, Johnson Space Center, and Marshall Space Flight Center. Formal release of the operational system is planned for early 1991.

Ames-Moffett contact: W. Likens
(415) 604-3210 or FTS 464-3210
Headquarters program office: OAET

A Direct Interface Fusible Heat Sink for Astronaut Cooling

Curtis Lomax

Astronaut cooling during extravehicular activity (EVA) is a critical design issue in developing a portable life support system (PLSS) that meets the requirements of a space station mission. Two of these requirements are that the cooling device be easily regenerable and non-venting during operation. In response to this, a direct interface fusible heat sink prototype with freezable quick-disconnects has been developed for which two patents have been applied.

A proof-of-concept direct fusible heat sink prototype has been constructed and tested. It consists of an elastic container filled with normal tap water using two quick-disconnects embedded in a wall of the device. These quick-disconnects are designed so that they may be frozen in the ice and yet still be joined to the cooling system, thereby allowing an immediate flow path. Using this approach, the following inherent difficulties in a direct interface heat sink have been overcome: (1) establishment of an initial flow path, (2) avoidance of low flow freeze-up, and (3) rates of heat transfer inadequate at the end of the melting process.

During EVAs, crew members generate metabolic heat and equipment produces mechanical heat. Of the metabolic heat, 90% is excess. The excess heat must be removed from the body to enhance the comfort and performance/productivity of the crew member. Once removed from the body, the heat may be either stored or rejected, or some combination of the two. On orbit, heat rejection occurs only by radiation or mass transfer. Storage is generally accomplished by inducing a phase change in a substance or by causing an endothermic reaction to take place. Any self-contained system that attempts to control the thermal condition of a space-suited astronaut will be limited by either the capacity of heat transfer or the rate of heat transfer, assuming the necessary power is available. For instance, a storage system will be limited by capacity, as will a mass transfer system. A radiation system will be limited by rate of heat transfer.

Thermal regulation of astronauts during EVAs has been studied in some detail. In the past, cooling of space-suited crew members has been accomplished by using a sublimator as well as umbilical supply. These approaches provide both adequate capacity and rate, while being compact and lightweight. The disadvantages are venting of water and subsequent loss of water during operation or, in the case of umbilical supply, awkward umbilicals to manage. Future PLSSs will require thermal regulatory systems that are non-venting, regenerable, and self-contained.

A non-venting, regenerable, and self-contained thermal regulatory proof-of-concept prototype has been developed. The prototype uses the phase change properties of water to store the waste heat. The device is a direct interface fusible heat sink.

If the requirement for cooling is 11,680 British Thermal Units (BTUs) per EVA, and ice cooled to 0°F and warmed to 40°F is used as a phase change material, then approximately 70 pounds of water will need to be included in the full capacity device. This corresponds to 1.12 cubic feet for water and 1.25 cubic feet for ice. Conservatively estimating 30 pounds for hardware, this gives a total weight of 100 pounds for the thermal regulatory system. The device is made possible by using specially designed freezable quick-disconnects that both allow the heat sink to be connected into the cooling loop and provide for a flow path.

A direct interface fusible heat sink has been constructed and tested. It performed adequately when judged by two criteria: (1) attainable heat transfer rate during any time of the melt (2000 BTUs/hour, 586 watts), and (2) start-up operations. It is believed that a flight quality heat sink would weigh approximately 100 pounds (45.3 kilograms). The system is a viable method of thermal regulation and should be developed further for use during Space Station Freedom EVAs.

Ames-Moffett contact: C. Lomax
(415) 604-3344 or FTS 464-3344
Headquarters program office: OAET

An Experimental and Computational Study of Unsteady Facilitated Transport

Ted Wydeven, Alicia Yum, Sanford Davis

Supporting human-in-space activities for long periods requires advanced environmental control systems. For example, carbon dioxide must be separated from the surrounding air to prevent toxic concentrations from occurring. Semipermeable passive membrane systems are under active investigation for gas separation and purification. These systems require no external power sources and offer advantages unobtainable from other methods.

An attractive enhancement to passive membranes is the process of facilitated transport whereby permeation through either a liquid or polymeric membrane is chemically augmented thereby significantly improving membrane performance and overall system efficiency. Probably the best known example of facilitated transport is the key role of hemoglobin in facilitating the uptake and rejection of oxygen by red cells in the human circulatory system.

In this study, the facilitated transport experiment first considered by others for transport of nitric oxide (NO) across a thin liquid membrane of formamide containing anhydrous ferrous chloride is investigated using a new computational model. The earlier work of others is re-examined with emphasis on the transient nature of facilitated transport as well as the final steady-state response. The figure shows a comparison between computational and experimental results. The results shown are derived from this study and a study done by W. J. Ward.

A numerical solution of the equations governing facilitated transport can be used to directly compute the flux of NO and to compare this with an experiment using the same nominal system as previously investigated by others. By comparing computation with experiment, it was shown that the inclusion of transient effects places a greater demand on an accurate determination of the transport coefficients when predicting the unsteady transport of the permeant.

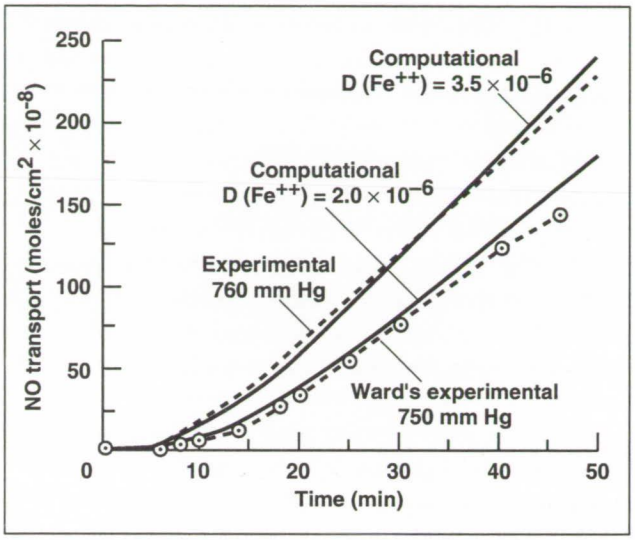


Fig. 1. Facilitated transport—comparison of computational and experimental results

In summary, a simple model of facilitated transport has been shown to generally predict transient effects in facilitated transport. An exact and fully predictive model of facilitated transport must await further refinements in determining the relevant parameters. This situation is quite common in many areas of applied research, such as turbulence modeling (the transport of momentum) and thermal diffusion (the transport of heat). In these fields, the underlying equations are well established but the transport coefficients are not well defined. Determining the relevant parameters still represents a fertile sub-field by itself.

Ames-Moffett contact: T. Wydeven
(415) 604-5738 or FTS 464-5738
Headquarters program office: OSSA

High Purity GaAs as a Far-Infrared Photoconductor

Jam Farhoomand

High purity gallium arsenic (GaAs) exhibits excited state far-infrared photoconductivity in the temperature range from 2 Kelvin to 4.2 Kelvin. The response is characterized by an exceptionally sharp peak which is magnetically tunable over a broad range. This dominant peak, at 279 micrometers, belongs to the 1s-2p transition of the residual shallow level impurities, and its intensity is over an order of magnitude above the continuum.

We are studying the performance of such a detector under low-background conditions. The sample under test was prepared by liquid phase epitaxial growth. The purpose of this study is to ascertain the suitability of this detector for low-background astronomy.

Because of the relatively shallow energy levels of a far-infrared photoconductor, thermally generated carriers as well as the carriers generated by spurious radiation pose severe problems. Therefore, for low-background operation it is absolutely critical to take every precaution to ensure a light-tight environment. Such an environment is established using cold filters and cold apertures. In addition, the detector is placed in two baffle boxes both painted with infrared-absorbing black paint developed at Ames Research Center. As a calibrated radiation source, an internal blackbody is used for all the measurements. The detector signal is processed through a low-noise transimpedance amplifier with a balanced, cold front end.

The basic parameters of interest in characterizing a detector are the responsivity and the noise equivalent power (NEP). Some parameters, such as the quantum efficiency and the photoconductive gain, are more fundamental. They are related to responsivity and are generally more difficult to measure. We also have to determine the optimum operating condition of the detector in terms of temperature, spectral response, bias, and speed or electrical bandwidth. Linearity, leakage current, and radiation hardness are also of concern.

The responsivity is a measure of how much electrical signal a detector generates for a certain amount of incident radiation. This parameter is measured at different detector temperatures and bias levels to find the optimum operating point. Our preliminary measurements show a peak responsivity of about 2 amps/watt at 3.5 Kelvin temperature and 350 millivolt bias.

The NEP is a measure of the detector's noise characteristics and indicates the system sensitivity. Like the responsivity, this parameter is measured as a function of temperature and bias level. But it has the added variable of the electrical bandwidth. The NEP, therefore, is measured as a function of frequency (f) and, for the sample under test, has a strong 1/f dependence. The minimum NEP at 100 hertz, 3.5 Kelvin, 350 millivolt bias is measured to be 2×10^{-16} Watt/$\sqrt{\text{hertz}}$.

The preliminary measurements of the fundamental parameters of a high purity GaAs protoconductor under low-background conditions indicate that this detector shows at least comparable performance to the existing state-of-the-art far-infrared detectors. A more comprehensive set of data is required to establish its suitability for low-background astronomy.

Ames-Moffett contact: J. Farhoomand
(415) 604-3412 or FTS 464-3412
Headquarters program office: OAET

Compressed Video for Remote Animal Monitoring

Robert W. Jackson, Richard F. Haines

When groups of animals are maintained in a laboratory, good husbandry practice requires that all animals be observed every day to monitor their health. For animals that are maintained in Space Station Freedom, television signals can be used to allow ground personnel to share the monitoring responsibility with the on-board crew members.

A study has been performed to evaluate the use of reduced-bandwidth television signals for monitoring the health and status of groups of rodents. Standard television cameras were used to prepare video tapes of groups of rodents from fixed and hand-held mountings. The video tapes were then processed through commercial bandwidth-reduction equipment to prepare short samples of reduced-bandwidth video. The reduced-bandwidth samples were viewed by groups of biologists and engineers and rated for their usefulness in monitoring the health and status of the animals.

Results of the ratings are shown in the table: for the fixed camera, the samples were generally acceptable at all reduced bandwidths, for the hand-held camera, the lowest bandwidth samples were unacceptable.

Compressed Video Ratings

Compressed bit rate (kilobits per second)	384	448	576	768	1152	1536
Test condition	Percentage of viewers rating video sample acceptable					
Hand-held camera	0.0	0.1	0.1	0.3	0.6	0.8
Fixed camera	0.7	0.7	0.9	0.8	0.8	0.9

This study has shown that the use of reduced-bandwidth television signals holds promise for monitoring the health and status of rodents and that fixed cameras will allow greater bandwidth reduction than movable cameras. Additional work is needed to derive ground monitoring requirements for use with Space Station Freedom.

Ames-Moffett contact: R. Jackson
(415) 604-5921 or FTS 464-5921
Headquarters program office: OSSA

Space Qualified ^{3}He Cooler

ORIGINAL PAGE
BLACK AND WHITE PHOTOGRAPH

Peter Kittel

Existing space qualified cooler technology has been limited to temperatures above 1.5 Kelvin. This was the stored superfluid helium technology used on Infrared Astronomical Satellite (IRAS) and Cosmic Background Explorer (COBE). A number of important scientific applications require lower temperatures. One application is high-performance infrared bolometers. The performance of bolometers improves as $T^{5/2}$. Hence their sensitivity will increase by a factor of 50 on cooling from 1.5 Kelvin to 0.3 Kelvin. Other applications that would be enabled by a sub-Kelvin cooler include the study of critical phenomena at the ^{3}He/^{4}He tricritical point in the absence of gravitational mixing (near 0.87 Kelvin) and the optimization of high-stability clocks for navigation and relativity experiments (0.5-0.8 Kelvin).

These sub-Kelvin temperatures can be reached by the evaporation of liquid ^{3}He. (^{3}He is a rare isotope of helium.) The principal technical challenge was to develop a technique of controlling the location of the boiling liquid in the absence of gravity. The technique used for controlling liquid ^{4}He on IRAS could not be used because ^{3}He is not a superfluid at these temperatures. If the location of the cryogen was not fixed, then the temperature of the scientific instrument could not be maintained. Other technical challenges involved the development of a compact closed cycle pumping system that could operate efficiently at low temperatures.

A technique of using surface tension was developed to confine the liquid cryogen in a porous (20 micrometer pores) copper matrix. This technique was perfected in a series of laboratory demonstrations at Ames Research Center and at the University of Oregon using –1 g. During these tests the liquid was held at the top of a chamber by surface tension. The surface tension forces were strong enough to contain the boiling cryogen while gravity tried to pull the liquid out.

To further verify this technology, a cooler was flight qualified and successfully flown on a sounding rocket in the fall of 1989. This cooler is shown in the figure. The vapor from the boiling cryogen is pumped

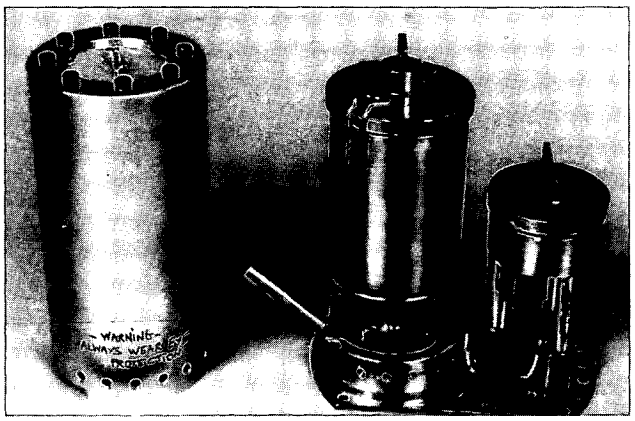


Fig. 1. Spaceflight qualified ^{3}He cooler: The right-hand chamber contains the sintered copper for containing the liquid ^{3}He. Next to it is the sorption pump containing activated charcoal. To the left is a thermal radiation shield that fits over the pump. The cooler is filled with 55 atmospheres of ^{3}He gas at room temperature through the stem on the left of the pump and then sealed

by a small sorption pump. A 1.5- to 2-Kelvin precooler is required. This is supplied by a superfluid helium tank of the type used in IRAS. The ^{3}He cooler is bolted to the tank and is operated by a single electrical heater on the sorption pump. The cooler operated normally during launch and during the 10 minutes of 0 g in flight. The flight cooler was developed through a cooperative agreement with the University of California at Berkeley.

This technology is applicable to other cryogens. This technology is being extended to cryogens with lower surface tension, in a dilution cooler that will operate at temperatures below 0.1 Kelvin.

Ames-Moffett contact: P. Kittel
(415) 604-4297 or FTS 464-4297
Headquarters program office: OAET

Low-Background and Radiation Environment Evaluation of Infrared Detector Arrays

Mark McKelvey

During FY 90, investigations of the performance characteristics of Hughes Aircraft Company 58- by 62-element direct readout (DRO) extrinsic silicon infrared (IR) detector arrays were continued. This array technology is being studied for use in general space-based astronomical observations, and directly for application in the Infrared Array Camera of the Space Infrared Telescope Facility (SIRTF). Testing in FY 90 concentrated on the characterization of these devices in radiation environments simulating those to be experienced in Earth orbit.

Laboratory characterization of this array type has been previously conducted, determining basic performance levels with an eye toward the use of these devices in orbiting observatories. In this earlier work we have demonstrated that these sensors can be used for low-background infrared astronomical imaging with extremely high sensitivity, and we have also identified areas where the technology needs further development. Our effort in FY 90 concentrated on the complex problem of learning how the ionizing particles found in Earth orbit modify the performance levels measured in our earlier tests. Radiation-environment testing was emphasized to assess the suitability of this array technology for use on platforms at altitudes up to 100,000 kilometers.

Small (millicurie) sources of gamma- and x-radiation have been used in the Ames Research Center IR Detector Lab to simulate the on-orbit environment, in terms of both radiation field and low-IR background. In addition, proton-environment tests have been conducted using the 74-inch cyclotron at the Davis campus of the University of California. Dose rates at the Davis facility can be varied over a wide range to simulate the majority of anticipated on-orbit ionizing particle fluxes. The devices have shown substantial sensitivity to proton fluxes, with significant shifts in their radiometric calibration after irradiation. We have also found methods which can be used to recover the pre-irradiation performance characteristics. Our goal is the identification of the determining mechanisms and parameters of the observed radiation effects, to control and minimize them.

In FY 90 a "bare" (i.e., lacking a detector substrate) version of the 58 × 62 multiplexer was evaluated to isolate radiation effects endemic to the readout circuitry, without the sometimes confusing influence of the detector elements themselves. Testing of the bare multiplexer showed that its basic operating characteristics were not altered by radiation doses expected on Earth orbit (e.g., few rads), and that the basic technology used to produce this device could deliver reliable flight hardware from a radiation-environment standpoint.

A cooperative effort between Ames and NASA's Goddard Space Flight Center in early FY 90 yielded pioneering infrared astronomical observations, using an integrated detector array at a wavelength of 20 micrometers. The Ames Si:Sb array was used at NASA's Infrared Telescope Facility to image NGC 7027 and the galactic center, with a preliminary attempt to observe the apparent disk of material surrounding the star Beta Pictorus. In addition to the astronomical data obtained, this demonstration helped us to better understand the strengths and limitations of the device.

In FY 91 we are conducting tests on Impurity Band Conduction (IBC) versions of the 58- by 62-element array. The IBC detector architecture promises improved radiation hardness and fewer anomalous effects. Our continuing research will allow a final judgment to be made on the suitability of this technology for SIRTF and other orbiting IR telescope platforms.

Ames-Moffett contact: M. McKelvey
(415) 604-3196 or FTS 464-3196
Headquarters program office: OAET

Biological Research Laboratory for Space Station Freedom

Joel Sperans, Roger D. Arno, John J. Givens

The Space Station Freedom will provide a wealth of new opportunities for life sciences research in the microgravity environment of Earth orbit. A comprehensive systems design study has been completed which details a concept for providing a flexible, multi-functional research facility for conducting a variety of life science experiments on-board the Space Station Freedom in a laboratory-type environment. Such research will require the long-term housing of plant and animal subjects, as well as cell and tissue culture support systems. A natural adjunct to such a set of microgravity vivaria in space is a centrifuge which can expose the same specimens to variable gravity levels, simulating Earth, Lunar, Mars, or other gravity levels depending upon different scientific experiment protocols. The figure shows the general configuration of some of the major Biological Flight Research Laboratory components.

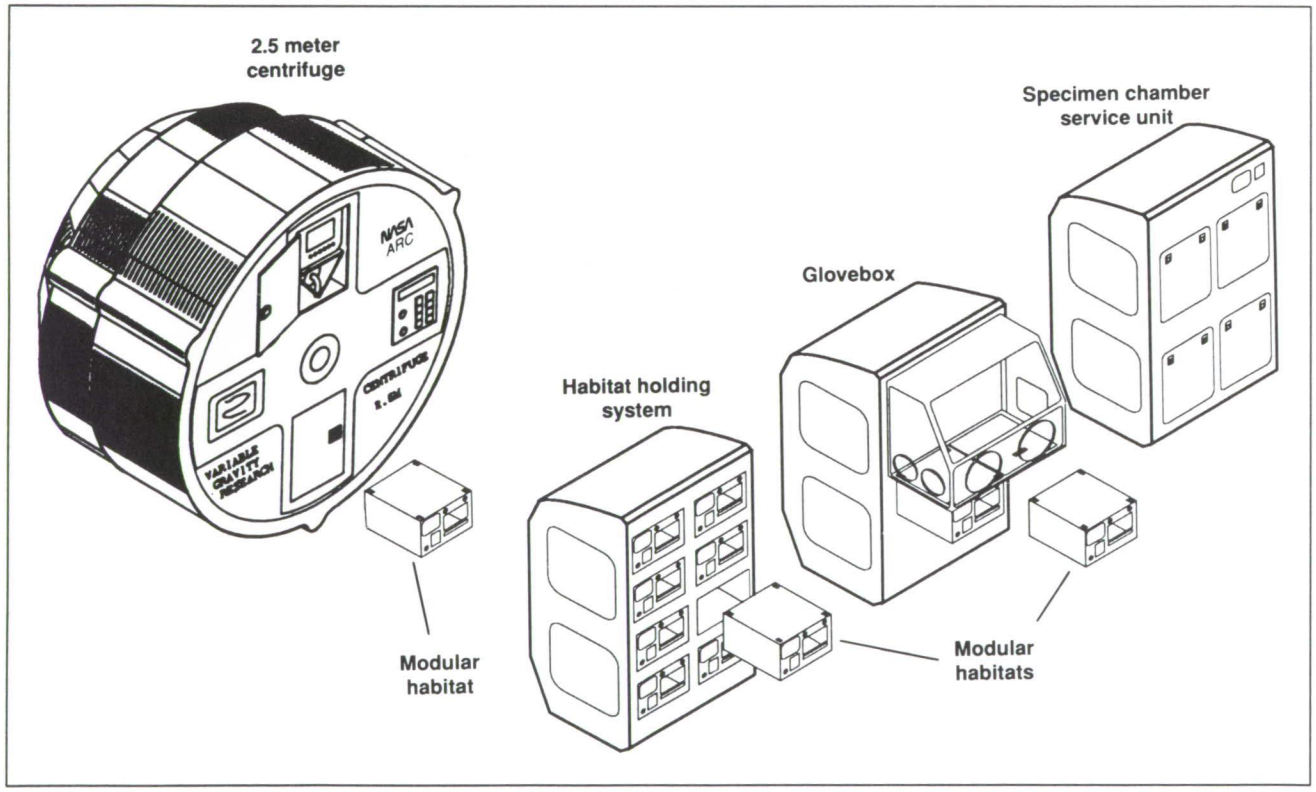


Fig. 1. Centrifuge facility equipment suite

The modular habitats, about the size of standard file drawers, provide a controlled specimen chamber environment for plants and animals. Modular habitats support animals or plants in a low stress environment. The external structure provides a primary level of bioisolation and houses the specimen chamber. Surrounding the specimens, the specimen chamber offers a second level of bioisolation. It is configured to accommodate specific requirements of the species studied. Functional units supply food, water, lighting, waste management, environmental control, video observation, and data collection. The modular habitat interfaces with other laboratory systems for power, air circulation, and most controls and data storage. It is, however, self-sufficient for up to an hour, providing for transport between facility systems. Data collected from modular habitats are tagged with the source, including habitat, specimen, and sensor identification and habitat location.

These transportable modular habitats fit in custom racks, called habitat holding units, that supply long-term environmental control and life support, power, cooling fluids, waste handling, contamination control, instrumentation, and digital command and data links.

To provide a range of gravity levels, modular habitats are installed at the periphery of the centrifuge with the floors oriented outward so that rotation of the wheel produces artificial gravity. The centrifuge provides the same services as the 0-g holding units while rotating at selectable rates to offer a range of gravity levels. It can accommodate a mixed group of plant and animal modular habitats, providing consumables and functional service required to support specimens and meet the requirements of scientific experiments. Food and water reserves supply animals for 14 days and plants for up to 90 days without resupply. Momentum compensation limits changes in total system angular momentum caused by starting or stopping the centrifuge as well as removing or replacing modular habitats. The system also accommodates mass distribution during normal centrifuge system operation.

For use on orbit, the habitats mate with the glovebox workstation which provides a fully enclosed environment for all specimen handling and experiment protocols requiring crew support.

A specimen chamber service unit provides for resupplying specimen chambers as appropriate in support of science experiments.

The ultimate reward of this flight research laboratory is to enable "use of the unique characteristics of the space environment, particularly microgravity, as a tool to advance knowledge in the biological sciences; to understand the role of gravity in the biological processes of both plants and animals; and to understand how plants and animals are affected by and adapt to the space flight environment, thereby enhancing our capability to use and explore space." Such a capability not only has a tremendous potential for terrestrial applications in medicine, agriculture, and ecology, it will also enable a permanent human presence in space and support the exploration of the moons and planets of the solar system.

Ames-Moffett contact: E. Bauer
(415) 604-5695 or FTS 464-5695
Headquarters program office: OSSA

Pilot Land Data System

Gary Angelici, L. Popovici, Jay Skiles, C. Wong

The Pilot Land Data System (PLDS) is a limited scale, distributed information system designed to explore scientific, technical, and management approaches to satisfy the needs of NASA's land science community now and into the next century. The goal of the PLDS is to develop and implement a state-of-the-art data and information system to support research in the land-related sciences that will lead to a permanent research tool.

The PLDS is based on a distributed architecture that will use microcomputer workstations, supercomputers, and high-speed digital communications to form an operational capability with intelligent and useful services. From a local computer or terminal, an investigator can access a PLDS computer, conduct a complete search of the PLDS (and other) data holdings, and locate and possibly retrieve desirable data sets. Access to electronic mail, data analysis, super computer, on-line help, and file transfer capabilities are offered as additional services to scientists by the PLDS. The PLDS is managed by Goddard Space Flight Center (GSFC), with Ames Research Center, Jet Propulsion Laboratory (JPL), and the university community participating.

The Ecosystem Science and Technology (ECOSAT) Branch at Ames is contributing to the development of the PLDS in the construction and operation of a data and information system that serves the needs of two basic communities within the land science community: the community that uses aircraft imagery to accomplish its research objectives, and the ecosystem science community.

A data base of remotely sensed imagery collected by various instruments mounted on high and medium altitude aircraft based at Ames has been constructed and made available to land scientists via dial-up connection and national networks. Over 600 Daedalus Thematic Mapper Simulator (TMS), NS001 TMS, Thermal Infrared Multispectral Scanner (TIMS), airborne sunphotometer, and aerial photographic entries are inventoried on a Sun 4 computer at Ames using ORACLE data base management software. After the testing and evaluation phase, the PLDS data base and software will be expanded to handle new data sets and to exploit new windowing technologies.

The effort of PLDS at Ames to serve the ecosystem science community was expanded greatly by collaboration with an ecosystem science project being conducted by scientists in the branch and outside institutions. The Oregon Transect Ecosystem Research (OTTER) project is collecting a wide variety of data obtained from sensors on satellites, on aircraft, and on the ground. To date, PLDS at Ames has created an inventory of approximately 300 OTTER aircraft flight lines (consisting of Daedalus TMS, NS001, and TIMS data) and 400 OTTER field sunphotometer entries. OTTER scientists are able to access the data and information using the PLDS user friendly data and information querying and ordering capabilities. A transparent connection to OTTER project meteorological and chemical data being managed at a long-term ecological research site in Oregon has been provided from the PLDS Sun computer at Ames.

Ames-Moffett contact: G. Angelici/J. Skiles
(415) 604-5947/3614 or FTS 464-5947/3614
Headquarters program office: OSSA

A Cryogenic Absorption Cell for Gas Phase Spectroscopy

Charles Chackerian, Jr., James E. McGee

We have constructed a coolable 30-centimeter path length 50-millimeter-diameter absorption cell for carrying out spectroscopic studies of gases at reduced temperatures. The cell is suitable for use with Fourier Transform Spectrometers or various laser sources.

The cell has a copper body with an acid-resistant stainless steel liner, and the modular outer vacuum jacket is easily expandable to accommodate longer cold cells. We have cooled the cell to 37 Kelvin and it cools from ambient temperature to 150 Kelvin in about 45 minutes. Three air-filled rubber bellows prevent vibration from being transferred from the cryogenic refrigeration unit to the body of the cell. The cell is equipped with resistive heaters that are used in a feed-back loop to control the temperature to ±0.3 Kelvin. Silicon diode temperature sensors at the center and ends of the cell indicate the excellent thermal conductivity of the cell.

Ames-Moffett contact: C. Chackerian, Jr.
(415) 604-6300 or FTS 464-6300
Headquarters program office: OSSA

Computer Simulations Help Unravel Origins of Tropospheric Ozone Hill

Robert Chatfield

In the last decade scientists have gradually recognized alteration of a large segment (approximately 20%) of the global troposphere, exhibiting high levels of carbon monoxide and ozone. Ozone in the troposphere is a primary greenhouse gas, and both ozone and carbon monoxide are primary controls on the hydroxyl radical, which is the Earth's main self-cleaning agent for many greenhouse gases. Less dramatic than the "Antarctic ozone hole" in the stratosphere, this tropospheric phenomenon of a high level of ozone already affects the inhabited equatorial regions of the world. We now believe that the "tropospheric ozone hill" is primarily due to the external combustion of agricultural waste and other biomass including the destruction of tropical forests, and it is directly related to food production.

Both ozone and carbon monoxide are produced from other primary emissions via complex "smoggy" chemical interactions, and have important natural sources that could be localized in the same portion of the tropics; namely tropical Africa, tropical South America, and the Atlantic Ocean stretching between them. To simulate the situation and understand causes, a model must include detailed meteorological transport, fine resolution of the reacting flow in space and time, many chemical reactions and the thermal and ultraviolet radiation field driving them, a knowledge of the patterns of burning, and a large variety of physical and chemical land-surface boundary conditions. In principle, detailed spatial resolution of all these factors in an extremely large computer simulation is necessary to simulate the nonlinear chemistry correctly. For some questions, many hundreds of interacting chemical species must be modeled that represent many thousands of points in space. These restrictions demand intensive supercomputer simulations using judicious combinations of many complex subcodes.

An effort initiated at Ames Research Center involves performing simulations of relatively simpler tracers of the effects of fires, with the aim of integrating increasingly sophisticated chemistry so as to handle the more intricate questions of tropospheric ozone production and modification. Basic results presented at international scientific forums highlight the importance of the correct simulation of the dry winds originating from desert and scrub areas of the tropics in the process of polluting the middle atmosphere for weeks and months on end. This study concentrates on the most visible and easily studied effects of this ozone pollution. Similar alterations probably also occur in the global nitrogen cycle, and can lead to progressive changes in the global environment of oxidizing gases and also global temperature through the greenhouse effect.

Ames-Moffett contact: R. Chatfield
(415) 604-5490 or FTS 464-5490
Headquarters program office: OSSA

Boundary Delineation of Agricultural Lands by Graphics Workstations

Tom Cheng , Robert Slye, Matt Ma, Gary Angelici

The National Agricultural Statistics Service (NASS) of the U.S. Department of Agriculture (USDA) uses a manual delineation method to select sample sites on paper-based materials, photographs, and maps, in its surveys of agricultural commodities. The area of interest (e.g., a county) is divided or delineated into contiguous parcels that can be easily located on the ground. This procedure is slow, labor-intensive, and sometimes inaccurate. Four Ames Research Center scientists: T. Cheng, R. Slye, M. Ma, and G. Angelici, are responsible for transferring the image-processing technology to NASS by designing, developing, and maintaining a computer-assisted boundary delineation procedure to aid the collection of agricultural information.

NASS and Ames have worked together for more than 10 years to integrate remote sensing technology into the procedures employed by NASS in its information gathering activities. The latest cooperation is a NASS-sponsored research task for the development of a software and hardware system to create and edit boundaries of agricultural lands on graphics workstations. A 3-year proposal was awarded by NASA, starting in 1988, through the Earth Observation Commercial Application Program for additional hardware and personnel.

Prototype software for this computer-assisted boundary delineation procedure was completed and tested in FY 89. The software system is called Computer Assisted Stratification and Sampling (CASS) that stratifies and randomly samples land parcels, by using image processing systems. With a background display of Landsat Thematic Mapper imagery and the corresponding USGS Digital Line Graph data on a monitor, operators use a cursor to delineate agricultural lands into polygons, called primary sampling units (PSU), based on land-use and land-cover types. Selected PSUs are randomly chosen from each interested area and further delineated into ultimate sampling units, or segments. The segments are then randomly selected and field surveyed for predicting agricultural statistics.

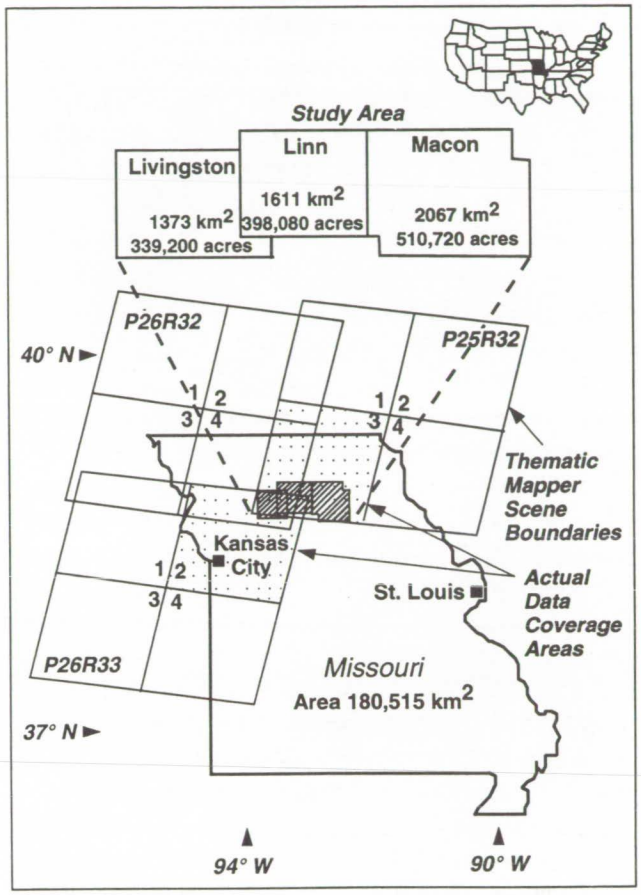


Fig. 1. Study area

After a test using three Missouri counties (see both figures), NASS applied CASS to 21 Michigan counties as a semi-operational procedure starting in FY 90. Previous analysis indicated that CASS used only one-fifth of the time relative to the manual techniques in creating sampling units.

Current efforts are directed toward completion and upgrading of the software, and implementation of an operational hardware system. A Hewlett-Packard (HP) 9000 Model 375 TurboSRX Graphics workstation was used at Ames as a display station.

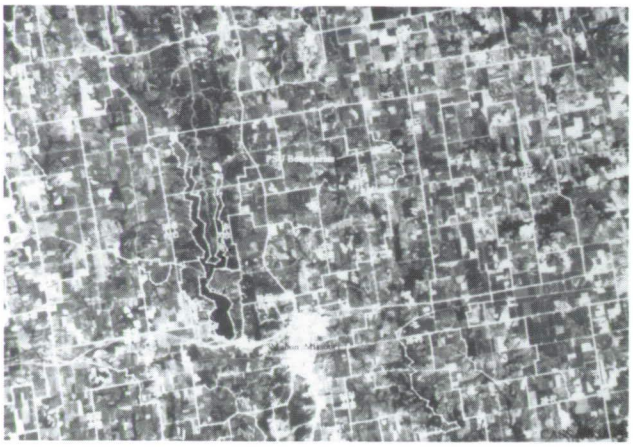


Fig. 2. Digital Line Graph (DLG) and primary sampling unit (PSU) boundaries. A 1024- by 1280-pixel window of Thematic Mapper image of Macon County, Missouri, was displayed using channel 1, 3, and 5 in blue, green, and red, respectively. The highly vegetated area appears to be bright red. Using two graphic overlay planes, DLG roads were overlaid in blue, and the PSUs boundaries were overlaid with strata labels in white (see color plate 15 in Appendix)

The HP system renders 24 million instructions per second of computing power with 16 megabytes of random access memory. It has more than 800 megabytes of on-line storage including a rewritable optical disk drive with 650 megabytes (both sides) per platter capacity. The TurboSRX display subsystem provides 1024 by 1280 display with 24-bit color depth, with four overlay planes for graphics display. A high-quality color printer is being considered to enhance the effectiveness of field survey of the procedure. The final configuration of the operational system at NASS, to be completed in 1991 and based on Ames recommendations, will consist of up to five HP display stations networked to a data server.

Ames-Moffett contact: T. Cheng
(415) 604-3326 or FTS 464-3326
Headquarters program office: OSSA

Remote Sensing and Paleoecology

Hector D'Antoni

The study of paleoclimate by pollen analysis entails four main steps: (1) Fossil pollen recovery from stratified sediments, (2) regional studies on modern pollen dispersal and deposition, (3) calibration of models to predict temperature and precipitation from modern pollen and climate data, and (4) prediction of paleoclimate. This has been successfully used in the eastern United States and Canada, but it has limited possibilities at the global scale because of the paucity of climate data in many regions. This is the case of Patagonia, a region that encloses many clues to explain the role of the Antarctic ice on the global climate through time.

I decided to supplant the climate data by remote sensing data. Advanced Very High Resolution Radiometer (AVHRR) data were used for the first trial. Modern pollen data of 74 sampling sites located between 45° and 54° South were used to generate the models and a sequence of fossil pollen data taken at 45°28' South (first figure) served to predict (hindcast) the radiometric data.

The two best multiple linear regression models were selected from a group of 180. Model 1 (first table) predicts the values of band 1 (0.58-0.68 micrometers) calibrated as percent of albedo. Its main statistics are: R – Square = 0.79; Mallows' CP = 2.73 (4 regressors); standard error of estimates = 0.76%. Model 2 (second table) predicts band 2 (0.725 to 1.100 micrometers) as percent of albedo. R – Square = 0.72; Mallows' CP = 13.76 (9 regressors); standard error of estimates = 0.02.

The hindcasted values (part (a) of the second figure) are usual for a desertic region. The trend lines outlined show a neat increment of albedo for the last 3,000 years, suggesting an increment of the desert conditions for the same period. Part (b) of the second figure shows the Normalized Difference Vegetation Index (NDVI = (Ch2 – Ch1) /(Ch2 + Ch1)) computed from the hindcasted data of Channels 1 and 2 only for samples not containing animal excrements that may contribute amounts and types of pollen not at random. The NDVIs show a corresponding trend to lower values. These results support my previous interpretation based on pollen



Fig. 1. Location of Alero de las Manos Pintas

Predictive Model for Albedo Values of Channel 1

Variable name	Regression coefficient	Standard error
Intercept	6.72603	0.209825
Caryophyllaceae** 0.5	0.160624	0.0999231
Chenopodiineae** 0.25	0.716582	0.161962
Compositae tub.** 0.5	0.268262	0.0723546
Nassauvia spp.** 0.5	0.374852	0.0542450

Note: ** = power.

Predictive Model for Albedo Values of Channel 2

Variable name	Regression coefficient	Standard error
Intercept	3.93915	0.0948580
Compositae tub.** 0.5	–0.0348575	0.0948580
Cyperaceae	–0.0162453	0.0049650
Ephedra spp.	–0.0056123	0.0033118
Gramineae** 0.5	–0.0492848	0.0107064
Gunnera sp.	–0.0421968	0.0180176
Misodendrum sp.** 0.5	–0.0947309	0.0283862
Nassauvia spp.	–0.0058178	0.0020203
Polygala sp.	–0.0344669	0.0116809
Solanaceae	–0.1362710	0.0169869

Note: ** = power.

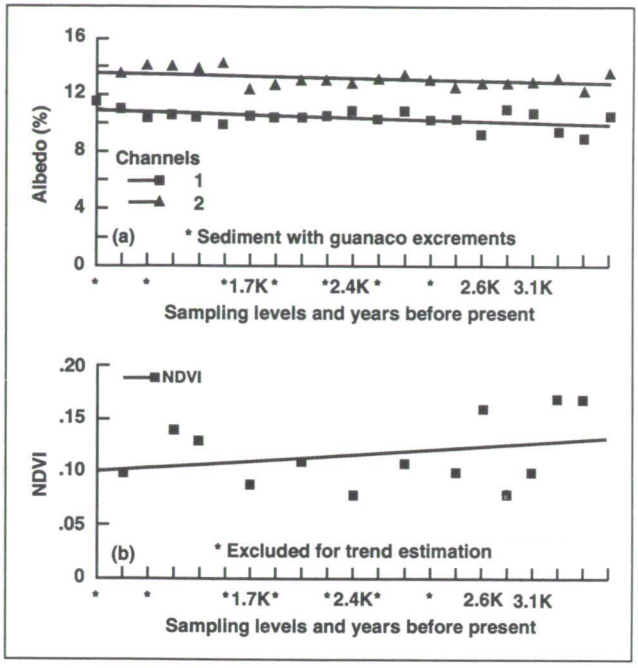


Fig. 2. Desertic region. (a) Predicted albedo values for the sedimentary profile of Alero de las Manos Pintadas (approximately 3,500 years ago to present). Trends (solid lines) to higher albedo are shown for both channels. (b) Normalized Difference Vegetation Index predicted values and trend toward lower values (solid line)

data alone. The predictive models based on AVHRR data allow fossil samples to fit on modern vegetation belts as viewed on satellite imagery. The hindcasted values describe the vegetation process through time, and vegetation is a direct synoptic representation of the climate of a region.

Calibration of pollen data in terms of remote sensing data is consistent: the synoptic description of vegetation by both pollen analysis and remote sensing (AVHRR) data is consistent in terms of scale. Thus, remote sensing data make a quasi material model for paleoclimatology and paleoecology.

This work shows the link between long and short time scales by predicting the past in terms of the modern relationships between pollen dispersal and albedo values. Vegetation cover seems to have decreased in the last 3,000 years around Alero de las Manos Pintadas. This might reflect an advance of the extremely dry central sector on the moderate subandean and western sector of Patagonia. More stratigraphic work is necessary to verify this hypothesis.

Ames-Moffett contact: H. D'Antoni
(415) 604-5149 or FTS 464-5149
Headquarters program office: OSSA

Airborne Arctic Stratospheric Expedition Results

Steve Hipskind, Estelle Condon

Early results from the 1989 Airborne Arctic Stratospheric Expedition (AASE) were published in March 1990. The AASE was conducted from Stavanger, Norway, in winter 1988-1989 to study the ozone production and loss mechanisms in the north polar stratospheric environment with particular emphasis on the effect of polar stratospheric clouds (PSCs). The entire dataset, including aircraft and related data, from the AASE was published on compact disc (CDROM) in July 1990.

The aircraft data consist of the measurements taken on both the NASA ER-2 and DC-8 which each flew 18 missions, including the ferry flights to and from the deployment location. The DC-8 carried a suite of 10 instruments, and the ER-2 carried a suite of 13 instruments measuring chemical, meteorological, and cloud physical parameters. Related data include that from both Total Ozone Mapping Spectrometer (TOMS) and Stratospheric Aerosol Measurement (SAM II), which are on board the Nimbus 7 satellite, as well as balloon-borne ozonesonde data.

In addition to the standard aircraft data, which for the in situ instruments is generally recorded at a 1-hertz frequency, a separate CDROM was published which contains the data from the Meteorological Measurement System (MMS) on the ER-2 aircraft recorded at a frequency of 5 hertz.

Both discs are available from the author at Ames Research Center, Moffett Field, CA 94035-1000.

Ames-Moffett contact: S. Hipskind
(415) 604-5076 or FTS 464-5076
Headquarters program office: OSSA

Estimating Regional Carbon Flux in High Latitude Ecosystems

Gerald Livingston, Leslie A. Morrissey, James R. Podolske

Whether mankind is inducing global climatic change is the subject of much current debate, particularly as the decade ending in 1990 was the warmest in recorded history. One potential cause of the observed global warming is the dramatic and continuing increase in the atmospheric concentrations of various "greenhouse" gases as a result of agricultural and industrial activities during the past century. To predict with confidence the impact of these increases on the Earth's climate and atmospheric chemistries, the present day global sources and sinks of these gases must be quantified in detail. Biological and chemical feedback mechanisms, which may increase or decrease rates of emissions or atmospheric chemical reactions, must be considered in this effort to predict the potential impact and magnitude of climatic change.

Methane is one of the most chemically and radiatively active of the greenhouse gases, participating in both tropospheric and stratospheric chemistries and significantly contributing to the Earth's energy balance. The atmospheric concentration of methane has increased during the past century directly in proportion to that of the human global population, and is continuing to increase at a rate of about 1% per year. Sources of methane are diverse, globally distributed and, as yet, poorly quantified, although the major *natural* source is the anaerobic bacterial decomposition of wet, organic-rich soils.

The northern high latitude tundra (treeless wetlands) and taiga (forested) ecosystems are expected to be particularly important global sources of methane due to their extensive areal coverage, the vast carbon resources currently stored in the peatlands and frozen soils of these ecosystems, and the anticipation that climatic warming will be most evident in northern high latitudes. As a consequence, climatic change leading to warmer summer soil temperatures, a change in the hydrological dynamics, or a change in the length of the growing season for these ecosystems, could result in dramatically increased biogenic methane emissions from the northern high latitudes and potentially even greater climatic warming.

Supported by NASA's Terrestrial Ecosystems, Interdisciplinary Research in Earth System Science, and Advanced Technology Development Programs, efforts are under way at Ames Research Center within the Ecosystem Science and Technology Branch to quantify regional and seasonal methane emissions from selected northern tundra and taiga ecosystems and to address the potential impacts of climatic change on methane emissions. Our approach integrates in situ measures of ecosystem parameters such as, soils, hydrology, vegetation, and emissions, with regional landscape characterizations derived from satellite remote sensing observations. Parallel studies include isotopic ratio measures of C^{12} and C^{13}, development of a prototype instrument integrating laser spectroscopy and micrometeorological instrumentation to measure carbon flux using eddy correlation techniques, and development of advanced spatial statistical approaches.

Results to date have demonstrated that rates of methane emissions and the biological and physical processes controlling those emissions can be effectively stratified both spatially and seasonally by using satellite-borne multispectral observations. The first figure represents 1987 mid-summer methane emission rates projected from empirical data for a segment of a 200,000-square-kilometer area from the Alaska North Slope. Moreover, observations between 1987 and 1990 provide initial insight into the local and regional scale responses of Arctic tundra to increased climatic temperatures and to the environmental interactions regulating methane emissions.

The effect of increased atmospheric temperatures on methane emissions from northern wetlands will increase both total emissions and interannual and seasonal variability. The magnitude of this effect will be determined by the resultant soil temperatures and those factors affecting the areal distribution of methane emission rates through regulation of the regional water table. Regional scale projections for the North Slope, based upon observed interannual temperature differences between 1987 and 1989, indicate mid-summer emissions will increase

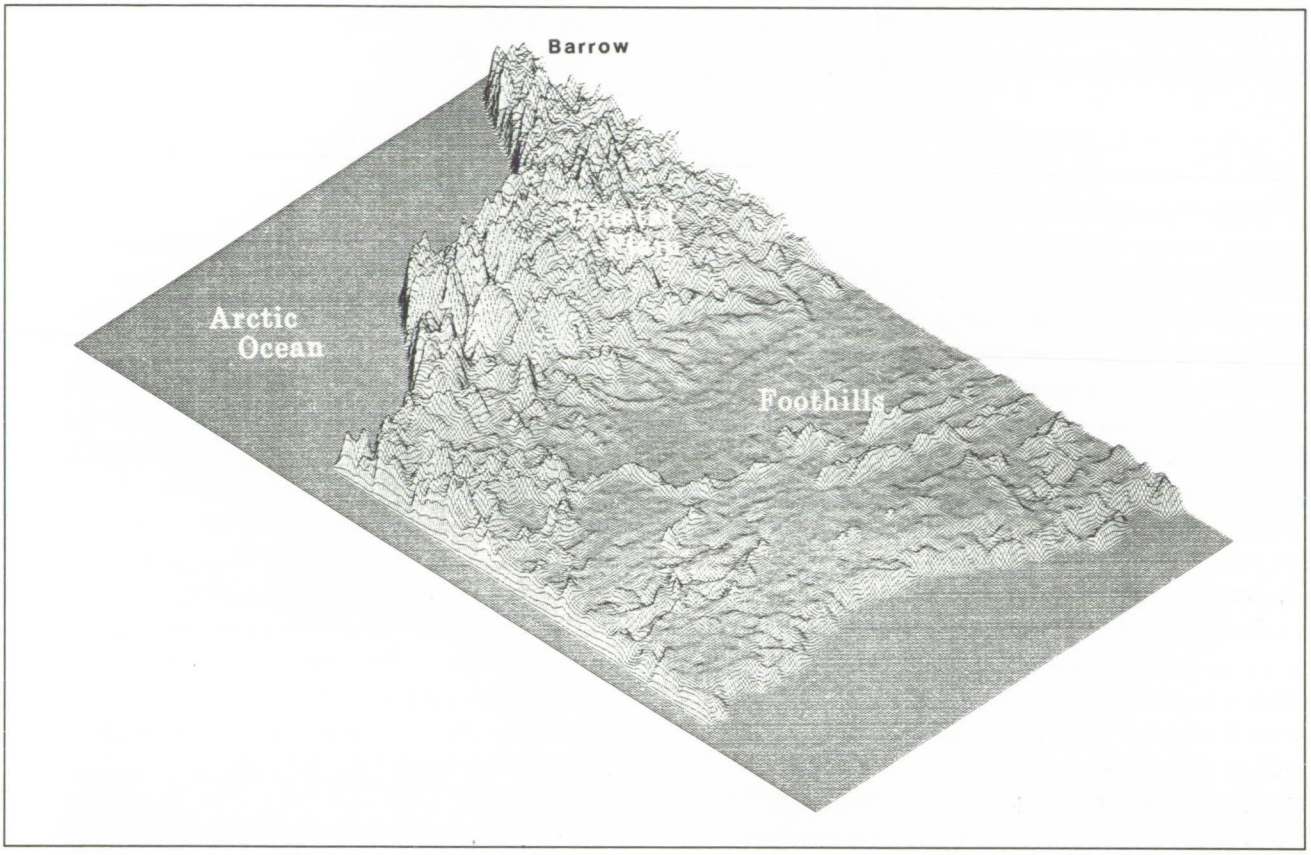


Fig. 1. 1987 mid-summer methane flux from the Alaska North Slope near Barrow

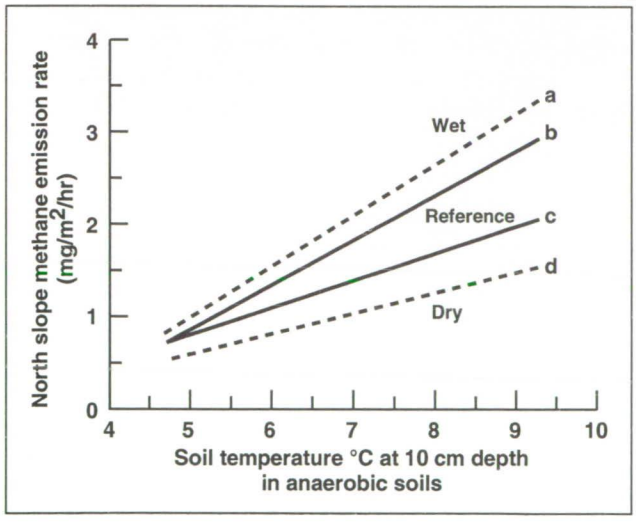


Fig. 2. Projected average methane emission rates for the Alaska North Slope under selected climatic regimes. Area of the North Slope is approximately 196,000 square kilometers. Reference projections are based upon observed temperature differences between 1987 and 1989 and simulated variations in the hydrological status of these peatlands

approximately linearly with soil temperature (see second figure).

Simulations of moderately drier environmental conditions than present suggest regional methane emissions may more than double, whereas wetter conditions could lead to emissions 4 to 5 times those of the 1987 regional mean of 0.72 milligram m^{-2} hr^{-1}. In comparison, the length of the biologically active season for these northern latitudes derived from 30-year climate records has varied by only a factor of 2. As such, although the global impact of climate change on growing season length is expected to be significant, these results demonstrate that the magnitude of summer soil temperatures may be as significant or more significant in determining the rate of methane emissions from northern ecosystems. The climatic impact of these projected increases in emissions is still under study.

Ames-Moffett contact: G. Livingston
(415) 604-3232 or FTS 464-3232
Headquarters program office: OSSA

Contributions of Tropical Forests and Land Use Change to Global Nitrous Oxide Emissions

Pamela Matson, Carol Volkmann, Tina Billow

Nitrous oxide, a trace gas whose atmospheric concentrations have increased 0.2-0.3% per year for the last 20-30 years, is one of several important greenhouse gases. In addition to absorbing infrared energy radiated from Earth's surface, nitrous oxide also catalyzes the breakdown of ozone in the stratosphere. Because of these roles, considerable attention has been directed to understanding the changing sources and sinks of this gas. Our research has elucidated the importance of tropical ecosystems, and tropical land use change, as sources for the global increase.

Results from studies at a range of sites selected along gradients of soil fertility and climate suggest that 2.4 teragrams per year of nitrous oxide are emitted from humid and wet tropical forests, and that another 1 teragram per year is emitted from seasonally dry tropical forests. Thus, undisturbed tropical forests represent the largest background source of nitrous oxide globally.

Tropical forests are being disturbed at very rapid rates: 8-10 million hectares are cleared and permanently converted to other uses each year. Our research in cattle pastures in Brazil indicates that rain forest conversion to pasture results in threefold increases in annual fluxes over undisturbed forests. Thus, clearing in these humid tropical environments may account for up to 25% of the annual global increase in nitrous oxide in the atmosphere. Studies of land conversion in the dry tropics suggest that upland pastures there may not have elevated fluxes; land use change in those environments may not result in increased emissions. Finally, our ongoing studies in intensive tropical agricultural systems in Hawaii and Mexico indicate that major increases in gas fluxes may occur with fertilization and intensive management.

Further research is under way to estimate the importance of tropical agriculture in the increasing global emissions of nitrous oxide.

Ames-Moffett contact: P. Matson/C. Volkmann
(415) 604-6884/3228 or FTS 464-6884/3228
Headquarters program office: OSSA

Remote Sensing of Canopy Chemistry and Herbivory in Mangrove Forests

David L. Peterson, Roy A. Armstrong

Using remote sensing, the relationship between canopy nitrogen and tannin and herbivory by insects in red mangrove (Rhizophora mangle) forests is under study. A field spectroradiometer was used with an integrating sphere to obtain hemispherical reflectance from red mangrove leaves during initial field work, which was completed in December 1990, in southwestern Puerto Rico. The mangrove leaves were sampled for nitrogen and tannin content and percent herbivory. These measurements are being used to test the hypothesis that herbivory in red mangroves is positively related to nitrogen content and inversely related to tannin content. The spectral data are being analyzed to develop statistical models for quantifying foliar nitrogen and tannin.

Also during December, a new analytical method for measuring proanthocyanidins (condensed tannins) was developed in collaboration with Mr. Lehel Telek from the Tropical Agriculture Research Station of the U.S. Department of Agriculture in Puerto Rico. Previously reported analytical methods were found to be of limited use due mainly to unsuitable standards, interference from other plant ingredients, and by lack of reproducibility. In this method the condensed tannins are strongly absorbed by nylon powder from aqueous acetone extractions of fresh leaf material. After a series of steps, the nylon is dissolved in acid and heated in a boiling water bath. The absorbance of the resulting red solution is measured at maxima against a nylon blank in a spectrophotometer. Two papers describing the method and the variability in mangrove tannins are being prepared for publication.

An overflight has been requested over Puerto Rico to acquire Airborne Visible Infrared Imaging Spectrometer data. These data will be used to infer the large-scale patterns of canopy chemistry and herbivory in mangrove ecosystems.

Ames-Moffett contact: R. Armstrong
(415) 604-5912 or FTS 464-5912
Headquarters program office: OSSA

Regional Extrapolation of Ecosystem Models of Evapotranspiration and Net Primary Production

David L. Peterson, Jennifer Dungan

Much of the current understanding about the way that forest ecosystems process water, energy, and nutrients has grown from the use of ecosystem models based on data collected at small study sites. To extend this understanding from the site scale to regional or continental scales, thereby improving the understanding of effects on and influence of global change on all ecosystems, there is a need to spatially extrapolate these models beyond the individual site.

This project will extrapolate a forest stand model beyond the conifer stands for which it was developed to a regional scale. This effort, in collaboration with the University of Montana and the University of Toronto, uses remote sensing data to provide criteria for the model, and a means of separating the data into functional ecosystem units. Work is focused on the mountainous terrain of western Montana, where the functional ecosystem unit is being defined as a hill-slope at a given scale.

The model includes daily meteorological conditions at a base station (maximum and minimum temperature, incoming solar radiation, and precipitation). These data are extrapolated from the base station to specific sites with a mountain climatology model. Characteristics of the canopy (such as leaf area index derived from remote sensing data) and soil (such as soil water-holding capability derived from soil survey maps) are used in the simulation of canopy evapotranspiration (ET), net photosynthesis, and net primary productivity (NPP).

Our initial simulations of a small fluvial watershed (15 square kilometers), partitioned from 2 to 66 landscape units, show that annual watershed estimates of ET and NPP are independent of scale from 6 to 66 units. Area-perimeter calculations of this watershed as a function of partition size produce a fractal behavior with a fractal dimension of 1.23, indicative of fluvial-geomorphology. These results suggest functional similarity under certain organizing principles, showing how small watershed measurements may be related to large regional estimates.

Data for all variables are provided to the model processor for a single landscape unit, the processor simulates changes in state variables over time using a fixed time increment, and results on a subset of variables are sent to a file which is later used for data visualization (in the form of bar charts, time series plots, or maps). As long as number of units is small, these computations can usually be done efficiently on a desktop computer. As the number of units begins to reach the thousands or hundreds of thousands, as is the case when remote sensing data are used, simulations become prohibitively time consuming in current environments. A primary goal in this project is to move the model to computer platforms that will operate on instructions in parallel, rather than in serial, to accomplish simulation at the regional scale. The model is being rehosted and optimized for the Connection Machine, CM2, at Ames Research Center. We plan to conduct simulations across a broad range of spatial resolutions and aggregations up to 250 × 250 kilometers and to compare our ecophysiological results to those of global circulation models.

Ames-Moffett contact: D. Peterson
(415) 604-5899 or FTS 464-5899
Headquarters program office: OSSA

Advanced Technology for Remote Sensing the Biochemical Content of Plant Canopies

David L. Peterson, Scott G. Hubbard

As part of NASA's efforts in FY 89 to develop a Global Change Technology Initiative, Ames Research Center scientists identified the scientific problem of the remote sensing of the biochemical composition of plant canopies as a major technology challenge. Recent research had shown that the potential exists for the estimation of these plant properties from imaging spectrometry, but that technology may not be optimum for solving this problem. What was needed was a fresh look at the nature of the problem and at the advanced technology which could enable the successful estimation of these properties from spacecraft sensors.

A workshop sponsored by the Office of Aeronautics, Exploration, and Technology examined this topic. The goal of the workshop, held in the summer of 1990, was to determine what the measurement requirements were and whether such measurements were feasible now or with further advancements in sensor technology such as detectors, optics, and materials.

Workshop attendees established the following goal statement:

> To obtain quantitative information about the concentration of recyclable materials in plant canopies via remote sensing.

By "recyclable," we mean the transfer of organic material to inorganic or mineral forms as part of the biogeochemical cycling of the elements within ecosystems. The critical materials are: proteins containing nitrogen which transform into nitrate and ammonium in the soil; lignin and cellulose which regulate the rate of leaf decomposition and thus the rate of nitrogen release; chlorophylls involved in photosynthesis and also containing nitrogen; labile carbohydrates such as starch and sugars which indicate energy sources; and water in plant tissues.

Remote sensing of plant biochemistry from space is feasible, provided (a) sufficient science definition can be advanced, (b) atmospheric and plant architectural/biomass effects which have both spectral and albedo influences on reflected canopy radiance can be systematically removed or corrected in the data, and (c) sensor sensitivity required by the measurement requirements can be achieved.

Measurement Requirements	
Spectral bands/regions	500-1000 nanometers 1100-1300 nanometers 1500-1600 nanometers 1700-1800 nanometers 2000-2400 nanometers
Spectral resolution	8 nanometers at 2-nanometer spectral sampling intervals
Spatial resolution	200 meters
Signal:noise performance	1000 at 20% albedo for 8 nanometers (1.5-2.4 micrometers)
Accuracies	Absolute radiometric Vis-NIR: 5% SWIR: 3%
Stability	0.1 to 1% repeatability
Swath width	At least one global coverage per month

The measurement requirements were specified at the workshop and are summarized in the table.

A broad range of sensing alternatives and design tradeoffs was considered. Among the candidates were grating or prism dispersive approaches including the use of a spectral wedge, an imaging interferometric approach with fixed gratings, a variety of detector array materials including pyroelectric detectors, and on-board signal processing including the use of Z-plane integrated circuits attached to the arrays. Initial calculation indicated that the desired performance, especially the required signal:noise, may be achievable with modest extensions of current technology.

Ames-Moffett contact: D. Peterson
(415) 604-5899 or FTS 464-5899
Headquarters program office: OSSA

Oregon Transect Ecosystem Research Project

David L. Peterson, Michael A. Spanner, Pamela A. Matson, Lee Johnson, Gary Angelici, Jay Skiles, Jennifer Dungan, Tina Billow

Oregon Transect Ecosystem Research (OTTER) is an interdisciplinary research project to measure and to model the major fluxes of carbon, nitrogen and water through temperate coniferous forest ecosystems in Oregon. Several models of ecosystem processes, FOREST-BGC, MT-CLIM, and Bioclimatology, have been developed by OTTER scientists in recent years to use variables derived from remote sensing for estimating key ecosystem fluxes. At the same time, scientists from this research team have developed quantitative relationships between key ecosystem parameters and various data obtained from remote sensing systems.

The goal of OTTER is to test and to validate the predicted fluxes and to biologically regulate these fluxes as simulated in these models by studying a range of control and fertilized forests in Oregon lying across an east-west climatic gradient. At the same time, the project will test how well the key model-driving variables can be retrieved from remotely sensed data through the use of correlative and radiative transfer models. And, by using NASA's Pilot Land Data System (PLDS) for data management and control, OTTER will test that system for studying ecosystem problems.

The integrated ecosystem model, FOREST-BGC, provides daily, seasonal, and annual estimates of photosynthesis, transpiration, above- and below-ground productivity, as well as nitrogen cycling through litterfall, decomposition, nitrogen mineralization, and root uptake. Meteorological data from six field stations, absorbed photosynthetic active radiation, leaf area index, total biomass, and foliar biochemical contents will be derived to drive the model. Seasonal changes in canopy leaf area, photosynthetic capacity, stomatal conductance, biochemical composition, litterfall, and other components of plant production will be used to examine the regulation of these processes.

The general approach is to concentrate upon six forested areas along a temperature-moisture gradient across west-central Oregon. Two of these sites have ongoing fertilization treatments under way to modify plant production. The sites are: (1) a coastal forest of western hemlock and Sitka spruce at Cascade Head and a nearby clear-cut site regrowing with the nitrogen-fixing pioneer tree, red alder; (2) a mature forest of Douglas fir near Corvallis in the Coast Range; (3) two dense stands of second-growth Douglas fir near Scio in the western Cascade Mountains, one being fertilized; (4) a mixed species forest of mountain hemlock, subalpine fir, Engelmann spruce and lodgepole pine at Santiam Pass on the Cascade crest; (5) a split-thinned stand of Ponderosa pine, one part being fertilized, near the Metolius River east of the Cascades; and (6) a low-density stand of western juniper near Bend in the Oregon high desert. Leaf area is highest on the western end and in the western Cascades where the environmental conditions are more favorable. Virtually all of the forests, except perhaps the coastal site, tend to be water-limited in the late summer and all have some limitation due to nitrogen availability.

Four times during 1990, a multi-sensor aircraft campaign was conducted to obtain the remotely sensed data from aircraft. The four data acquisitions permit us to examine the dynamical variations in plant physiology, biophysics, biochemistry, ecological processes, and nutrient cycling which occur in these forests.

The sensors being used and the associated aircraft are (1) NASA ER-2: Daedalus Thematic Mapper Simulator, Airborne Visible Infrared Imaging Spectrometer (AVIRIS), Thermal Imaging Multichannel Scanner (TIMS); (2) NASA C-130: TIMS, Advanced Solid-state Array Spectrometer, NS-001 Thematic Mapper, and the sun-tracking sunphotometer; (3) NASA DC-8: Synthetic Aperture Radar; (4) Oregon State University's ultralight aircraft: Spectron SE590 and SE393 spectroradiometers, Barnes MMR spectrometer, Air Infrared Thermometer and stereo video camera; (5) Canadian aircraft: Fluorescence Line Imager and the Compact Airborne Spectrographic Imager; and (6) University of Minnesota aircraft: Spectron instrument. In addition, satellite data are being acquired from the Advanced Very High Resolution Radiometer (daily clear coverage) and the Total Ozone Mapping Spectrometer (daily).

During 1989, five meteorological stations were installed near each of the first five sites and continuous recordings of the surface meteorology were begun. Two flights of the ER-2 with AVIRIS aboard were obtained in 1989. Maximum concentration of effort occurred throughout 1990 with all aircraft involved in a June and August deployment and only the ER-2 in February/March and October. The 1990 campaign was successfully completed and ground measurement of the reference and biological components completed, as well as sunphotometer measurements of the atmospheric turbidity coinciding with the overflights. The PLDS and Oregon State University's Forest Science Data Base have been linked to ingest and manage the gigabits of data now flowing into them.

This project involves scientists from around the country and Canada. Principal investigators include: Richard Waring, David Myrold, Richard McCreight, and Barbara Yoder of Oregon State University; Steven Running, University of Montana; and Samuel Goward, University of Maryland, in addition to the scientists listed from Ames' Ecosystem Science and Technology Branch.

Collaborators include: Steven Durden, Jet Propulsion Laboratory; Alan Strahler, Boston University; John Miller, York University in Canada; Carol Wessman, University of Colorado; and Susan Ustin, University of California at Davis.

With the intense data collection of 1990 complete, this team and many graduate students and assistants will begin analyzing the data in preparation for the simulations by the models in 1991. Several additional aircraft flights are planned for 1991 to fill in missing acquisitions as well as to continue many of the field measurements. The findings from OTTER will be used to help NASA plan the next and much larger ecosystem study, that of Canada's boreal forests for the mid-1990s.

Ames-Moffett contact: D. Peterson
(415) 604-5899 or FTS 464-5899
Headquarters program office: OSSA

NASA Remote Sensing Links Dinosaur Extinction to Asteroid Impact

Kevin O. Pope, Adriana C. Ocampo, Charles E. Duller

The northern plain of the Yucatan Peninsula is a region of youthful karst limestone development. Karst development here is controlled largely by fractures in the flat Tertiary period limestone surface, which also control ground water flow. Two main fracture systems occur in the plain. The north-south trending Holbox Fracture Zone is in the east. In the west is a system whose salient feature is a semi-circular boundary between fractured and unfractured rock, along which is a chain of sink holes (see the figure), named the Cenote Ring. Cenote is the local Spanish word for sink hole, adapted from the Yucatec Maya word, dz'onot.

The Cenote Ring was discovered with Landsat Thematic Mapper imagery during an archaeological remote sensing survey of ancient and modern surface water sources in 1987, but its origin remained unexplained. We now propose that its origin is related to a buried impact crater dating geologically to the Cretaceous/Tertiary boundary.

The Cenote Ring forms a nearly perfect 170-kilometer-diameter semicircle, truncated by the ocean and centered beneath the village of Chicxulub, for which the feature is named. Cenotes here are roughly circular water bodies approximately 50-500 meters in diameter, from 2 to more than 80 meters deep. Density and width of the ring varies from about 3 cenotes per square kilometer along a 3-kilometer-wide portion in the southwest to a chain of single cenotes 3 kilometers apart in the southeast.

The Cenote Ring must be a structural anomaly, for no combination of stresses from the region's fault systems (see the figure) could produce such a nearly perfect circular feature. The ring correlates with circular gravimetric and magnetic anomalies which others have speculated reflect a buried asteroid or comet impact feature.

A gravimetric and magnetic high lies at the center of the ring, while a gravimetric and magnetic low is found just outside the ring. The 170-kilometer-diameter region within the Cenote Ring corresponds to the floor of the proposed buried crater, while the actual crater diameter is suspected to be over 200 kilometers. The subsurface geology and

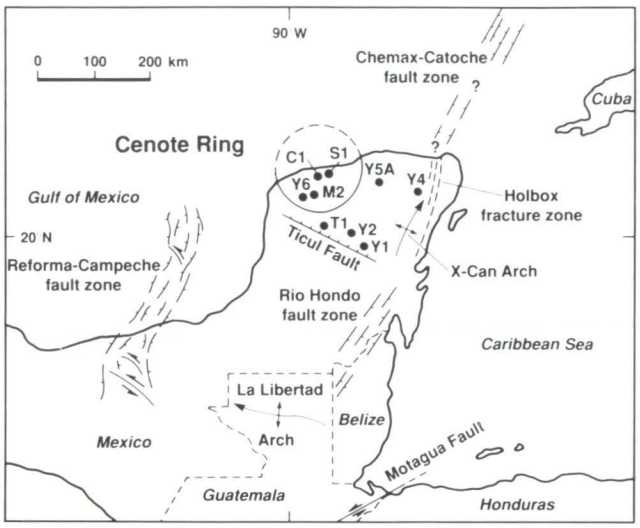


Fig. 1. Tectonic features of the Yucatan Peninsula. Locations of exploratory well cores studied are identified as C1, M2, Y5a, etc.

magnetic and gravimetric anomalies of the region support the interpretation that the fracturing that created the ring is related to slumping in the rim of a buried impact crater.

We examined data from nine exploratory oil wells in the vicinity (see the figure). The well data show that the ring interior corresponds with a Late Cretaceous structural low filled with Tertiary sediments. A large body of evidence now exists, supporting the hypotheses (1) that a major comet or asteroid impact occurred in the Caribbean region at the end of the Cretaceous period, and (2) that such an impact is responsible for the mass extinction of many floral and faunal species (including the large dinosaurs) that marks the end of the Cretaceous period. Until now, the remains of such an impact crater have escaped discovery. The Cenote Ring, discovered through NASA Remote Sensing Technology, offers a prime candidate for the impact site of a global catastrophic event.

Ames-Moffett contact: C. Duller
(415) 604-6031 or FTS 464-6031
Headquarters program office: Director's Discretionary Fund

Advanced Aircraft for Earth Science

Philip B. Russell, Max Loewenstein, Steven Wegener

Stratospheric science and, indeed, Earth science in general have always required a variety of experimental approaches, including satellite, balloon, aircraft, and ground-based studies. All indications are that this need for an integrated approach will continue indefinitely. Ames Research Center is assessing the requirements, feasibility, and optimal means of providing advanced aircraft to complement the progress planned in other approaches.

There is a real need for improved aircraft capabilities for stratospheric science alone. A workshop conducted by Ames in 1989 showed that stratospheric science requires both in situ and remote measurements from a very-high-altitude aircraft. The vertical resolution of passive remote measurements benefits greatly from increased platform altitude. Atmospheric-science missions proposed by the workshop are

1. to explore the Polar Vortex to determine the causes of ozone loss above Antarctica,
2. to determine high-altitude photochemistry in tropical and middle latitudes,
3. to understand the transport of chemical species by the general circulation of air and how it is chemically processed and transmitted to midlatitudes,
4. to study the relationship between volcanic, stratospheric cloud/aerosol, greenhouse, and radiation balance.

Recent studies of the status of aircraft technology conclude that state-of-the-art knowledge in the critical engineering disciplines would provide the necessary technology for a scientific aircraft operating subsonically at 30 kilometers (100,000 feet). However, to sustain a level cruise or even use a jump-up or zoom maneuver to attain 37 kilometers (120,000 feet) (subsonically) is problematic and may not be achievable with current technology. Subsonic flight at 40 kilometers (130,000 feet) will require major technological advances.

The above-mentioned scientific and correlative-measurement goals require the development of a higher-flying, longer-range complement to the ER-2, i.e., a multi-investigator, facility platform capable of accessing any spot on the globe in any season. Key specifications include a cruise altitude of 30 kilometers (100,000 feet), a subsonic cruising speed, a range of 6,000 nautical miles with vertical profiling capability down to 10 kilometers (33,000 feet) and back at remote points, and a payload capacity of 3,000 pounds. A capability to jump up to 35 or 40 kilometers altitude (115,000-130,000 feet), even with a considerably reduced payload, is highly desirable. The required range, and the requirements to fly in the polar night and in an unrestricted manner over oceans, often from commercial airports and in sensitive airspaces, imply a need for both unmanned and manned operations.

Ames is developing an approach for melding the above-mentioned stratospheric-science platform requirements with those of other Earth-science disciplines. The goal is to define the most cost-effective path to satisfying the critical needs of Earth science for advanced airborne platforms. This task entails collaboration with a variety of Earth-science disciplines and agencies, as well as with aeronautical experts and research facilities, to determine the optimal path.

Ames-Moffett contact: P. Russell
(415) 604-5404 or FTS 464-5404
Headquarters program office: OSSA and OAET

Remote Sensing Data Prove Useful for Disease Vector Modeling

Joan S. Salute, Byron L. Wood

In 1990, the Biospheric Monitoring for Disease Prediction Project completed studies on data collected in northern California. The data were analyzed to determine if remote sensing and geographic information system technologies could be used to distinguish high-mosquito-producing rice fields from low-mosquito-producing rice fields. With 90% accuracy, the study successfully identified high-producing fields 2 months before peak mosquito production. The 2 months lead time is important for allowing the direction and application of control measures.

Vector-borne diseases—such as malaria which is carried and spread by the anopheline mosquito—continue to be a risk to over half of the Earth's human population, primarily in the tropical regions. Although malaria is not present in California, the anopheline freeborni mosquito (the western malaria vector) is abundant in flooded California rice fields and was chosen for investigation. Rice fields vary greatly in their mosquito production, and this investigation was carried out to determine if remotely sensed aircraft or satellite data, in conjunction with geographic information system (GIS) technologies, could be used to differentiate relative production rates.

The tools used in this investigation included multi-temporal remote sensing data acquired by the Ames Research Center High Altitude Aircraft and the Landsat satellites, land use maps incorporated in a GIS, and field studies of vegetation and actual mosquito larval production. Several methods of statistical analysis were employed to determine that these tools could be used to differentiate between high- and low-mosquito-producing fields.

The rice fields which had early season (May-June) rapid canopy development supported higher larval production than those that developed later in the season (July). This results from higher plant tiller densities, as well as leaf area, which may provide more favorable habitat for successful anopheline oviposition. Vegetation canopy development is easily detected and measured with appropriately timed remote sensing data acquisition and analysis.

The digitized land use maps and GIS analysis tools were used to calculate the distance from each of the investigated rice fields to the nearest livestock pasture. Livestock pastures provide blood meals for the mosquitoes, and female mosquitoes require a blood meal before and after each egg-laying cycle. It was found that rice fields within 3 kilometers of a livestock pasture produced higher larval populations than rice fields more than 3 kilometers from livestock pastures. These measurements can be automatically calculated given appropriate inputs to the GIS.

By statistically combining the spectral (remote sensing) and spatial (GIS) analyses, high-mosquito-producing fields were identified with 90% accuracy using May and June data. These results show tremendous potential for extending these methods to other rice-growing areas where malaria remains a significant human health problem. Worldwide, more than 140 million hectares are devoted to irrigated rice. Rice production is expanding in tropical and sub-tropical regions of Asia, Africa, and the Americas where malaria is endemic, and the total number of cases has increased very significantly during the last decade. It is anticipated that remote sensing and GIS technologies will eventually be used in an operational mode for the surveillance of habitats supporting vector-borne diseases, and will play an important role in the control of these diseases.

Ames-Moffett contact: J. Salute
(415) 604-5596 or FTS 464-5596
Headquarters program office: OSSA

Airborne Tropospheric Chemistry Studies

Hanwant B. Singh

Chemical composition of the atmosphere is changing. A major goal of the NASA Global Tropospheric Experiment (GTE) is to understand the composition and chemistry of the atmosphere so that a realistic assessment of the consequences of these changes can be made. To achieve this goal, airborne GTE studies have been performed at midlatitudes over the Pacific (1986), in the Brazilian tropics (1987), and in the Arctic (1988 and 1990). An important objective of these studies has been to understand reactive nitrogen and ozone chemistry of the troposphere.

At Ames Research Center, we have developed and flown a highly sensitive peroxyacetyl nitrate (PAN) measuring instrument that can detect PAN (as well as other organic nitrogen compounds) to low parts per trillion by volume (10^{-12} by volume) concentrations. These experiments have shown that PAN, a specific tracer of nonmethane hydrocarbon (NMHC) and nitrogen oxides chemistry, is a major component of reactive nitrogen and a reservoir for nitrogen oxides in the global troposphere. Acetaldehyde and acetone are key intermediate products of NMHC oxidation and precursors for PAN formation.

We have built an instrument to measure these aldehydes (and ketones) to low parts per trillion by volume levels. These capabilities have been integrated into a single experiment to measure tropospheric concentrations of PAN and its aldehyde/ketone precursors (PANAK). The integrated PANAK instrument flew for the first time in the Atmospheric Boundary Layer Experiment over northern Canada. The experiment is substantially computer controlled, and organic nitrogen and carbonyl analyses are performed every 6 minutes and 12 minutes. Statistical techniques and photochemical models are used to analyze and interpret these data.

Ames-Moffett contact: H. Singh
(415) 604-6769 or FTS 464-6769
Headquarters program office: OSSA

Telescience as a Tool for ER-2 Investigators

Steven S. Wegener

The high-altitude ER-2 aircraft is used primarily as a platform for scientific missions to investigate regions in the atmosphere (up to 20 kilometers) inaccessible by other aircraft or satellites. The aircraft can accommodate several in-situ and/or remote sensing instrument packages supporting atmospheric, geophysical, oceanographic, and meteorological research experiments. With an objective of enhancing the scientific productivity of the ER-2 atmospheric missions, studies were conducted to determine the feasibility of using telemetered data to provide the investigators on the ground a real-time capability to direct the aircraft to probe the interested atmospheric phenomena.

In the fall of 1990, an ER-2 flight over the northern Sierras collected meteorological, aerosol, and trace gas data in the stratosphere. These data were down-linked via line-of-sight telemetry for remote, real-time analysis. Observed products such as aircraft position, meteorological parameters, vertical temperature profiles, ozone concentration, particle size, and density distributions were displayed along with forecasted products provided by the National Meteorological Center. This combined data set was reviewed by the mission scientist and could provide the basis to direct the aircraft to a new, more clearly defined target of scientific interest. This experiment demonstrated the power of real-time analysis to provide guidance to enhance the scientific productivity of future ER-2 missions.

Use of a two-way aircraft satellite communication link is being investigated. We have initiated the development of requirement documents for the use of the NASA Tracking and Data Relay Satellite to support ER-2 flights worldwide. Data rates range from 50 kilobits per second to 10.7 megabits per second.

A telescience concept using two-way communication and real-time analysis provides a powerful tool for atmospheric scientists and many others who can benefit from a remote presence on the ER-2. Future ER-2 applications range from disaster assessments to test bedding of satellite instrumentation such as the Earth Observing System. Applications are obvious in any environment that is hostile or simply inconvenient to human presence.

Ames-Moffett contact: S. Wegener
(415) 604-6278 or FTS 464-6278
Headquarters program office: OSSA

Modeling Forest Fire Smoke Plumes

Douglas L. Westphal, Owen B. Toon

While many theoretical studies of the impact of aerosols on climate and weather have been conducted by other researchers, the accuracy of the numerical models used in these studies is uncertain. Observations of changes in climate or weather have not been available to validate these theoretical calculations, except for a few cases involving large volcanic eruptions. However, recent in situ and satellite observations have shown that the presence of large amounts of smoke in the atmosphere has measurable effects on atmospheric radiative heat transfer and the surface energy budget. Smoke can also induce atmospheric heating rates comparable in magnitude to other diabatic processes, thereby modifying the atmospheric circulation.

We have developed a numerical model of meteorology, aerosols, and radiative transfer and have studied the impact of forest fire smoke on atmospheric processes. In particular, we have compared theoretical simulations of the properties and meteorological effects of a large smoke plume with observations following a large forest fire in western Canada which burned 180,000 hectares (1800 square kilometers) over a period of several months during the summer of 1982. Most significantly, the Eg Fire, so called because of its origin near the Egnell Lakes, British Columbia (59.8°N, 127.7°W), burned 72,000 hectares on July 29, creating a smoke cloud that was detected for more than a week in satellite imagery.

The visible wavelength satellite imagery for 1948 UTC 31 July showing the smoke plume is presented in the first figure. The smoke plume can be seen streaming southeastward out of Alberta, then over southern Saskatchewan and Manitoba, the eastern Dakotas, much of Minnesota, and the Great Lakes. The smoke was transported out over the Atlantic Ocean on subsequent days and arrived over Europe on August 5-6.

Our first objective has been to use the model for a 2-day simulation of the magnitude, duration, spatial extent, and diurnal pattern of the observed smoke transport and smoke-induced weather

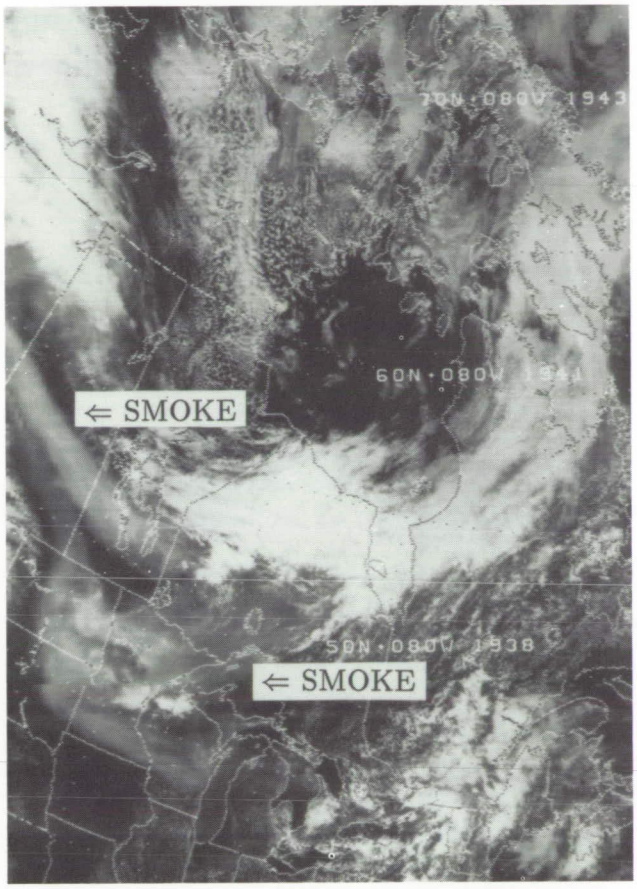


Fig. 1. Satellite image at 0.63-micrometer wavelength showing the Eg Fire smoke plume at 1948 UTC 31 July 1982

modification. Although some observations of the Eg Fire smoke plume were made, a complete data set of the optical and physical properties of forest fire smoke was not obtained. Thus the second objective has been to analyze a variety of measurements of smoke made in the Eg Fire smoke plume and several other smoke plumes and to use these measurements along with our microphysical simulation to develop conceptual models of the evolving properties of the particles in a large forest fire smoke cloud.

ORIGINAL PAGE
BLACK AND WHITE PHOTOGRAPH

The distribution of simulated smoke optical depths at 0.63 micrometer at 18 hours into the simulation is shown in the second figure and are in agreement with the distribution of smoke seen in the first figure; optical depth values are as high as 3.8. The smoke had an albedo of 35%, or more than double the clear-sky value, and cooled the surface by as much as 5 Kelvin, thus demonstrating the first climatological importance of forest fire smoke.

The best agreement with the observations of surface cooling was obtained when a fuel loading more than 10 times that previously suggested was used to calculate the initial smoke mass load. The previous estimate considered only the small surface fuels that control fire spread rates. Apparently more fuel is available for combustion in large intense forest fires than had previously been assumed, and estimates for the smoke production from biomass burning following a nuclear war should be revised accordingly.

Although laboratory tests suggested that the imaginary refractive index of forest fire smoke may be a large as 0.1, the model simulations indicated that a value of 0.01 yields results which closely match the observed cooling, single scattering albedo, and spectral dependence of optical depth. A simulation with a smoke imaginary refractive index of 0.1, typical of smoke from urban fires, produced 9 Kelvin cooling.

Direct measurements of the size distribution in the Silver Fire smoke plume, the sunphotometer data for the Eg Fire smoke plume, and the model simulations showed that coagulation occurs within forest fire smoke plumes in such a way that mean particle size and the specific extinction and absorption increase with time. During the 2-day simulation the geometric mean radius by number increased from the initial value of 0.08 micrometer to a final value of 0.15 micrometer, while the specific extinction and absorption increased by 40% and 25%, respectively. At 42 hours into the simulation, these

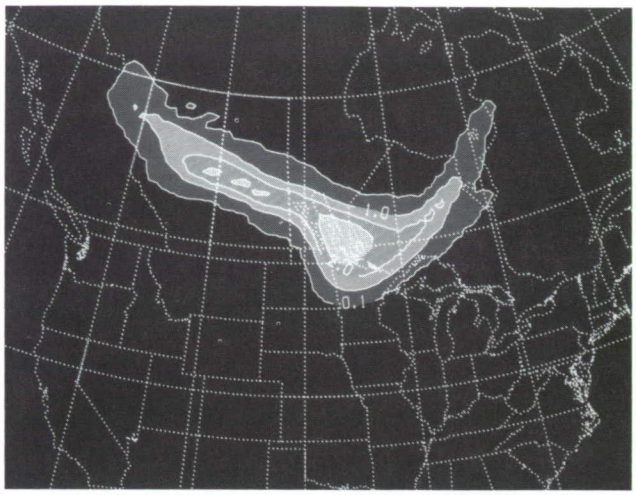


Fig. 2. Simulated optical depth at 0.63-micrometer wavelength at 1800 UTC 31 July 1982

changes in the smoke optical properties led to a 32% increase in optical depth and an 11% increase in surface cooling over that found in a simulation in which coagulation was not allowed.

In the model, 47% of the smoke was removed by scavenging as it was incorporated into a frontal zone over the Great Lakes, while dry deposition removed an insignificant fraction of the smoke. Self-lofting of the smoke in a direct, smoke-induced circulation, was observed in the baseline simulation and was particularly strong in the urban smoke simulation. The self-lofting process increased the relative humidity and precipitation, and therefore removed more of the smoke, acting as a negative feedback. However, water clouds were transparent to solar radiation in this version of the model, so the self-lofting results must be viewed with caution.

Ames-Moffett contact: D. Westphal/O. Toon
(415) 604-3522/5971 or FTS 464-3522/5971
Headquarters program office: OSSA

Advanced Automation of Mass Spectrometric Systems for Life Support Systems

Carla M. Wong, Peter T. Palmer

Ames Research Center has joined with the University of Florida and Finnigan Corporation, San Jose, California, in a pioneering agreement under the American Technology Initiative Program (AmTech-8801) to investigate the feasibility of an artificial intelligence, mass spectrometric-based system for monitoring closed-loop life support systems.

The University of Florida has performed the research on instrument design and analytical chemistry. Finnigan Corporation has focused on design and engineering analyses. Research at Ames has involved the development of an expert system to control the various steps of the chemical analysis and identification of volatile compounds.

Not only must the system address the identification and quantitation of target or known compounds, but it must also indicate the presence and attempt the identification of unknown or potentially hazardous compounds. Thus, it must allow for symbolic reasoning on and autonomous control of the analytical processes used by human experts in the field of mass spectrometry. The expert system must encode knowledge on method selection, experimental design, instrument control, data processing, data interpretation, and conflict resolution. More importantly, it must allow for feedback of results from previous experiments to guide the selection of new experiments.

The expert system has been implemented on a DECstation computer using CLIPS, an expert system shell developed at Johnson Space Center. It includes a variety of knowledge bases and over 130 rules which embody knowledge on various aspects of mass spectral analysis. The tasks of data processing and display are achieved by external software modules developed by Finnigan Corporation, which are invoked directly from the rules. Custom software has been developed to integrate these modules into the expert system and to automate a variety of other tasks, which have not been encoded into commercially available software.

Finnigan Corporation's Ion Trap technology was chosen for generating the mass spectral data because of its small size, low weight, low power requirements, high sensitivity, inherent flexibility, and potential for miniaturization. An Ethernet link has been installed and a communication protocol developed to allow the expert system to specify the experiments to be performed and the Ion Trap control computer to return the desired data.

As it is currently implemented, the system addresses target compound identification through the use of a data-driven approach which is based on three different types of mass spectrometric experiments. It is capable of indicating the presence of unknowns and can often give some indication of their identity through the use of molecular weight information and spectral matching results. The system's capabilities for autonomous chemical analysis were successfully demonstrated on the Biomass Production Chamber at Kennedy Space Center in September 1990.

Ames-Moffett contact: E. Sheffner
(415) 604-6565 or FTS 464-6565
Headquarters program office: OSSA

Implementation of Signal Processing Algorithms in the Search for Extraterrestrial Intelligence

D. Kent Cullers, Peter Backus

The goal of the Search for Extraterrestrial Intelligence (SETI) Microwave Observing Project (MOP) is to search for signals produced by technological civilizations on distant planets. Although the modern concept of SETI dates back 30 years, and more than 50 searches have been conducted in that time, the SETI MOP represents a tremendous increase in capability over all previous searches combined.

In the targeted search portion of the MOP, SETI researchers will examine the nearly 800 known Sun-like stars, out to a distance of 80 light years, for both pulsed and continuous wave (CW) signals that are either steady in frequency or may drift by as much as one part in 10^9. The search will be conducted over the range of frequencies from 1 Gigahertz to 3 Gigahertz with six simultaneous resolutions of 1, 2, 4, 7, 14, and 28 Hertz. A Multichannel Spectrum Analyzer (MCSA) divides a 10-Megahertz bandwidth of the spectrum into these fine resolutions. A Signal Detection Subsystem processes the output of the MCSA in real time with a one-observation-cycle delay.

Several significant strides have been made in the development of the signal detectors for SETI. Preliminary designs of both pulse-detection and CW detection modules have been developed using commercially available computer components. The pulse-detection algorithm processes different frequency bands and resolutions in parallel using the same microcode. Though its sensitivity is within 3 decibels of an ideal pulse detector, it runs 10,000 times faster. It searches the data for groups of three pulses with a common spacing that may be part of a regularly spaced pulse train. Each pulse triplet is found in less than a microsecond, on the average. This algorithm converts a task which, in its ideal form, is too large for any existing supercomputer into one sized for a modest commercial machine using four i860 processors.

Of particular importance to the SETI MOP is the development of an algorithm for enhanced sensitivity to non-drifting CW signals. This class of signal is considered to be particularly likely as an interstellar beacon. Directed transmissions, or those from unaccelerated platforms in space, may be extremely stable in frequency. The constant drift detector mixes every channel of the spectrometer against itself. If a signal of constant drift is present in any channel, it is converted to a slowly oscillating sinusoid that can be directly integrated. Only a signal with constant drift will grow in this process and the sensitivity to such signals is about twice that of power accumulation, the technique used for rapid drifts.

The drifting CW detector integrates signal energy along any path possible for a constantly drifting signal, even those that change by as much as one channel per spectrum. For every starting frequency, the number of allowed drifts grows in proportion to the observation length. An algorithm that approximates the ideal integration paths converts this n^2 accumulation into an *n log n* process, thereby saving a factor of 100 in processing at the cost of about 1 decibel in sensitivity. A special-purpose board design allows this task to be accomplished using commercial chips. Although the accumulation task is memory intensive, the algorithm can be performed using low-cost disk memory.

Another problem faced by the SETI MOP is that of distinguishing between a potential signal from an extraterrestrial civilization and the more mundane signals produced by our own technological society. These radio frequency interference (RFI) signals will have many of the characteristics that the signal-processing algorithms are designed to detect. To better understand the problem, a series of observations has been made at potential observing sites around the world. These data analyzed at Ames Research Center have shown that the RFI mitigation task is challenging, but not overwhelming. Examination of data with small antennas, over many directions in the sky, and using a catalogue, should allow elimination of most candidates immediately after detection. This will remove the need for lengthy reobservation.

Ames-Moffett contact: D. Cullers
(415) 604-6019 or FTS 464-6019
Headquarters program office: OSSA

Gravitational Effects on Regional Distribution of Calcium in the Adult Human Skeleton

Sara Arnaud

The sensitivity of calcium in the body to space flight is primarily the consequence of its primary location in bone (99%), an organ system that functions for support, locomotion, and as a reservoir of calcium. Calcium distribution is affected not only by gradients that enhance deposition of bone mineral in the gravity-dependent areas of the skeleton, but also by forces imposed on it through muscle activity. The signals that promote the deposition, removal, and relocation of mineral in bone at the local level are unknown. To identify the skeletal sites where these processes are most active, we have studied the distribution of mineral in adult bone in a model of weightlessness and during higher-than-normal gravitational loads.

We have used dual photon absorptiometry, through collaboration with Malcolm Powell, Nuclear Diagnostics, San Francisco, and Robert Marcus, Department of Medicine, Stanford University. We evaluated whole body and regional distribution of calcium (see the first figure for regions) in adult male volunteers in two separate studies. The first study used a micro-gravity model (bed rest in a position with the head 6° lower than the feet (HDT) for periods up to 30 days) that shifts headward the normal gravitational forces on the skeleton. The second used habitual levels of physical activity, quantified by a method developed by Rod Whalen (Ames Research Center), and descriptive criteria to separate the effects of normal and higher than normal skeletal loads at 1 g on the distribution of mineral in the skeleton.

During one month of HDT bed rest, there was no loss of total body calcium, but there was a trend for redistribution of mineral to the gravity-dependent regions of the skeleton. Bone density in 11 adult men showed increases in all regions of the body above the pelvis, with a 10% increase in the skull ($p < 0.05$). This pattern suggests an influence of gravity on the entire skeleton possibly mediated through hydrostatic column pressures (see the second figure).

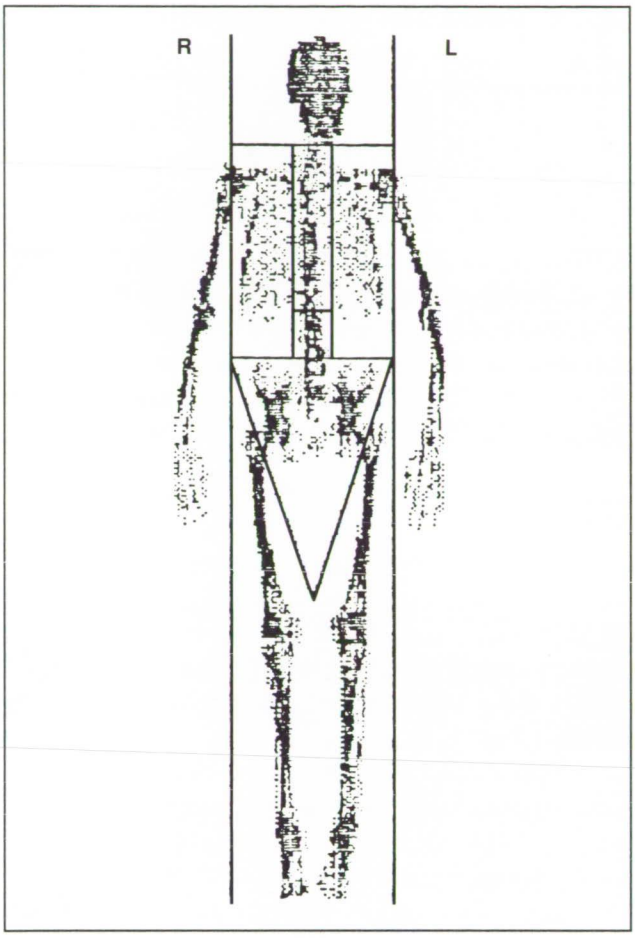


Fig. 1. Skeletal regions quantified by dual photon absorptiometry: skull, arms, thoracic spine, lumbar spine, pelvis, and legs

The influence of recreational sport activity habitually carried out twice a week (exercisers) on regional bone density in adult men was assessed by comparison to men whose activity did not include regular participation in sports (non-exercisers). Exercisers showed higher total body calcium content (8.8%) than non-exercisers; higher densities in lumbar spine, skull, legs, and arms of exercisers accounted for their higher total bone mineral. There was considerable variation and no differences in rib,

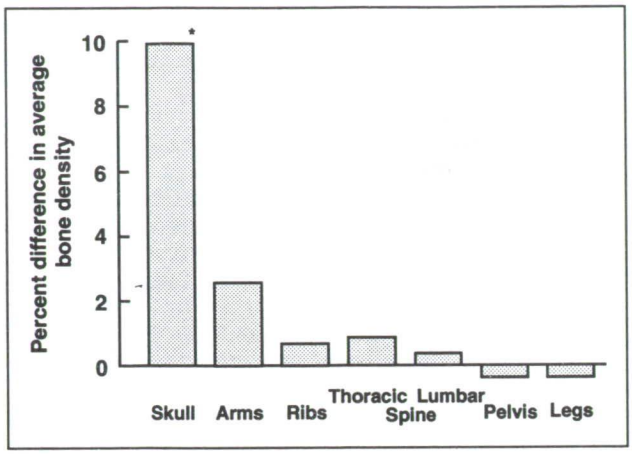


*Fig. 2. Average differences in the regional bone mineral density in 11 men before and after a 30-day HDT bed rest study. * indicates statistical difference of mineral density in one region before and after bed rest, $p < 0.05$*

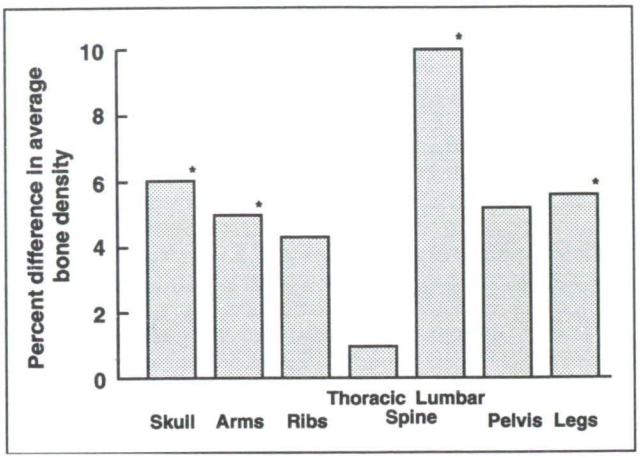


*Fig. 3. The regional areas of the skeletons showing higher mineral density in 27 exercisers than in 22 non-exercisers. * indicates statistical difference in mean regional density values in the two groups, $p < 0.05$*

thoracic spine, and pelvic regions of the skeleton in the two groups. The higher loads imposed on the bone by the exercisers, doing a variety of sports, such as jogging, cycling, and weight-lifting, affected the lumbar spine, skull, and peripheral skeleton, primarily (see the third figure). Whether higher skull density in the exercisers is related to external or internal forces is not clear.

These studies indicate that the distribution of bone mineral in adult men is changeable, and highly sensitive to gravity, operating through hydrostatic column pressures (fluid flow, volume, or pulsation), contraction of skeletal muscles during activity, and/or other factors. To maintain an Earth-ready lower skeleton during spaceflight, it will be important to determine the nature and magnitude of forces applied to bones of the pelvis, legs, and feet; the relationship of bone mineral to bone strength; and the minimum amount of activity needed to maintain both.

Ames-Moffett contact: S. Arnaud
(415) 604-6561 or FTS 464-6561
Headquarters program office: OSSA

Perceptual and Behavioral Adaptation to Altered Gravitational-Inertial Forces

M. M. Cohen, R. Welch

Perceptual illusions and disruptions of precise psychomotor performance have been reported during and immediately following exposure to the altered gravitational-inertial conditions encountered during launch, orbital insertion, orbital flight, and re-entry. Because the illusions and disruptions of behavior are of both significant theoretical and practical interest, and because they also represent potential dangers for space operations, we have undertaken a more comprehensive investigation to increase our understanding of these effects and help lead to their amelioration.

The study described here is one of a series in which we examined changes in perception and perceptual-motor behavior that result from exposure to altered gravitational-inertial forces (GIF). Our studies all use a particular research strategy: the systematic alteration of the gravitational-inertial field in which perception and motor behavior take place. We explicitly assume that, by carefully observing how perception and motor behavior are altered by controlled perturbations of GIFs, we will be able to delineate the range over which normal perception and behavior remain unaffected by specific gravitational-inertial inputs. We will also describe and predict quantitatively how various parameters of perception and behavior are altered by systematic changes in the gravitational-inertial field.

In general, we regard both hypogravity and hypergravity as arbitrarily selected points along a continuum. By viewing GIFs as a continuum, and by systematically varying the GIFs over a wide range of conditions, both with respect to their directions and their magnitudes, we can systematically examine the effects of altered GIFs on perception and behavior.

The terrestrial environment provides a baseline GIF that cannot be eliminated experimentally, except for extremely brief periods (1-3 seconds) in a vertical accelerator, or for more moderate durations (<60 seconds) in high performance jet aircraft flying Keplerian trajectories. Not only are these techniques limited in the amount of time that they can provide hypogravity, but the periods of hypogravity are always preceded and followed by brief periods of hypergravity, which can introduce additional complexities in interpreting experimental results.

Although long-term exposure to true microgravity can be obtained only in orbital or interplanetary flight, the careful segregation of activity during specific phases of parabolic flight might enhance the value of parabolic flight as a simulation or training technique. For example, an individual permitted to act only during the hypogravity phase of parabolic flight will generate and receive motor-sensory feedback that is uniquely characteristic of that condition alone. If it is the nature of the feedback that determines adaptation to specific environmental conditions, one might expect directionally opposite effects in an individual who is permitted to act only during the hypergravity phase of parabolic flight. We conjectured that adaptation to specific altered GIFs could be made to cumulate across several parabolas if an individual is permitted to act only during a single phase (hypergravic or hypogravic) of each parabola. This process of segregating activity to specific phases of parabolic flight to achieve different adaptive states was explored in the study reported here.

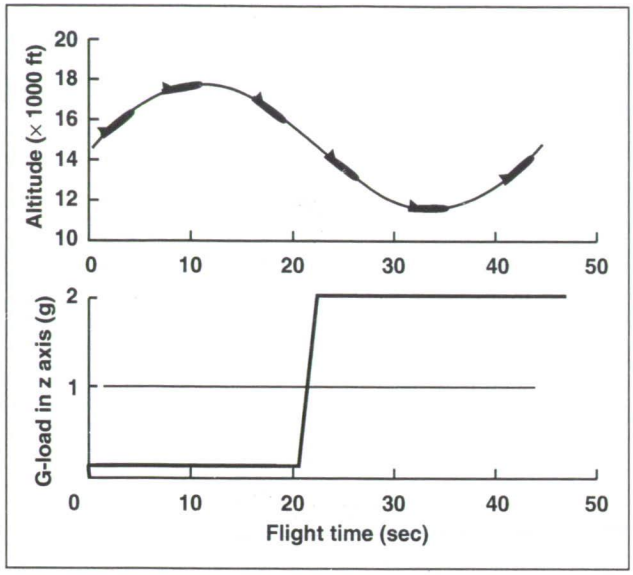


Fig. 1. Idealized flight and gravitational profiles as a function of time

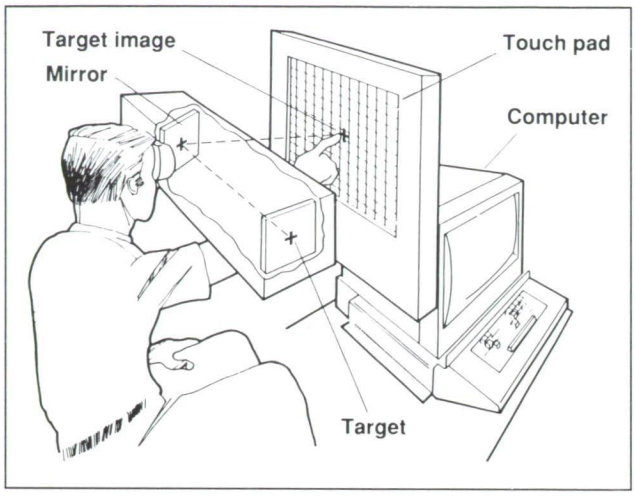


Fig. 2. Hand-eye coordination apparatus

The Learjet aircraft (NASA#705), based at Ames Research Center, was used to provide each of nine experimental subjects with sets of five 50-second parabolas that were preceded and followed by periods of straight and level flight. The first figure illustrates the G-loading effects of a single parabola.

As illustrated in the second figure, the subjects used their right index finger to indicate the position on a touch pad where a dimly illuminated target appeared to be located; the target image was approximately 50 centimeters from the subject's eyes, and both X and Y coordinates of each pointing response were registered on a digital computer. The subjects were trained to reach out rapidly and repeatedly, at intervals of approximately 2.5 seconds, and data collection did not commence until it was clear to the experimenter that the subjects were using rapid ballistic responses which would allow for little or no mid-course corrections. There were 10 pointing responses obtained in straight and level flight before the parabolas were initiated; 10 responses were obtained during either the hypergravic or hypogravic phase of each parabola, yielding a total of 50 responses in parabolic flight for each phase; 10 responses were obtained in straight and level flight immediately after the fifth parabola was completed.

As shown in the third figure, pointing responses did not begin to segregate until after the sixth trial of the first parabola, where it first became apparent that reaching movements made in hypergravity were higher than those made in hypogravity. This difference continued to manifest itself throughout the remaining parabolas. When the subjects again returned to level flight, they initially pointed above or below the target, depending on whether they had previously made reaching movements during the hypogravity or the hypergravity phase of the parabolas. If responses were made exclusively during the hypergravity phase, there was an initial post-parabola error of reaching above the target. If responses were made exclusively during the hypogravity phase of the parabolas, the initial errors were below the target. All of these initial post-parabola errors rapidly diminished.

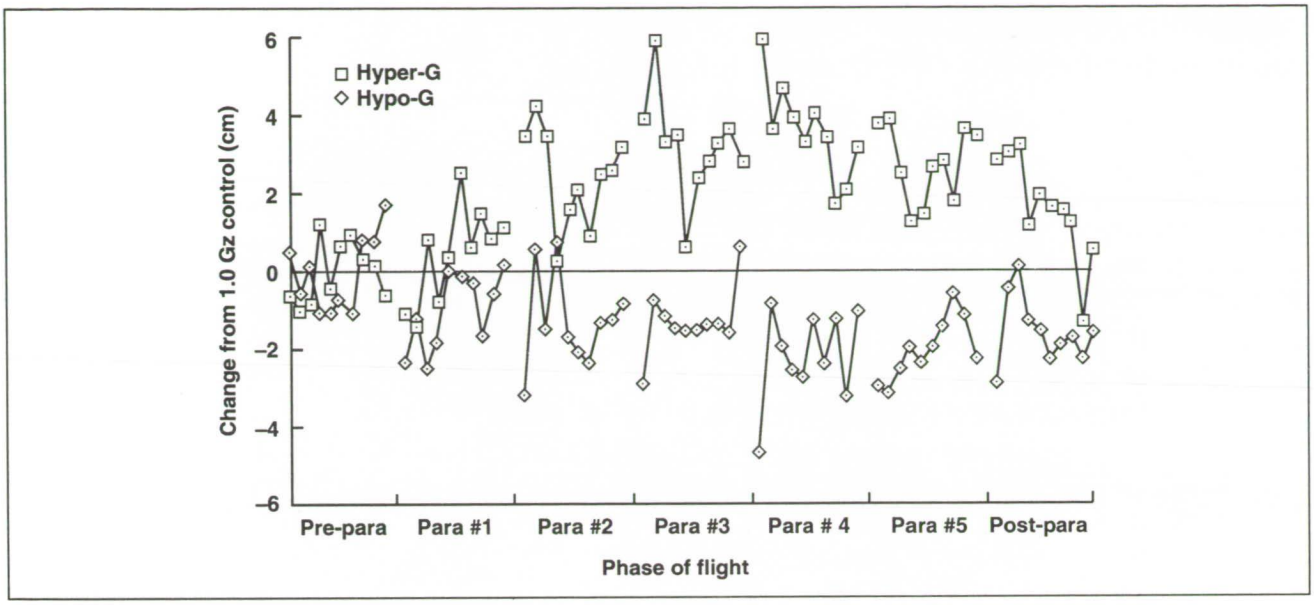


Fig. 3. Pointing to a mirror-viewed target during single phase of parabolic flight

These data suggest that changes in hand-eye coordination under altered GIFs depend not on the environment per se, but on the specific conditions of feedback that are provided by reaching movements in the environment. We intend to explore these effects in greater detail and will attempt to develop training procedures that can allow rapid and specific adaptation to the altered GIFs encountered in flight.

Ames-Moffett contact: M. Cohen/R. Welch
(415) 604-6441/5749 or FTS 464-6441/5749
Headquarters program office: OSSA

Autogenic-Feedback Training: Countermeasure for Orthostatic Intolerance

P. Cowings

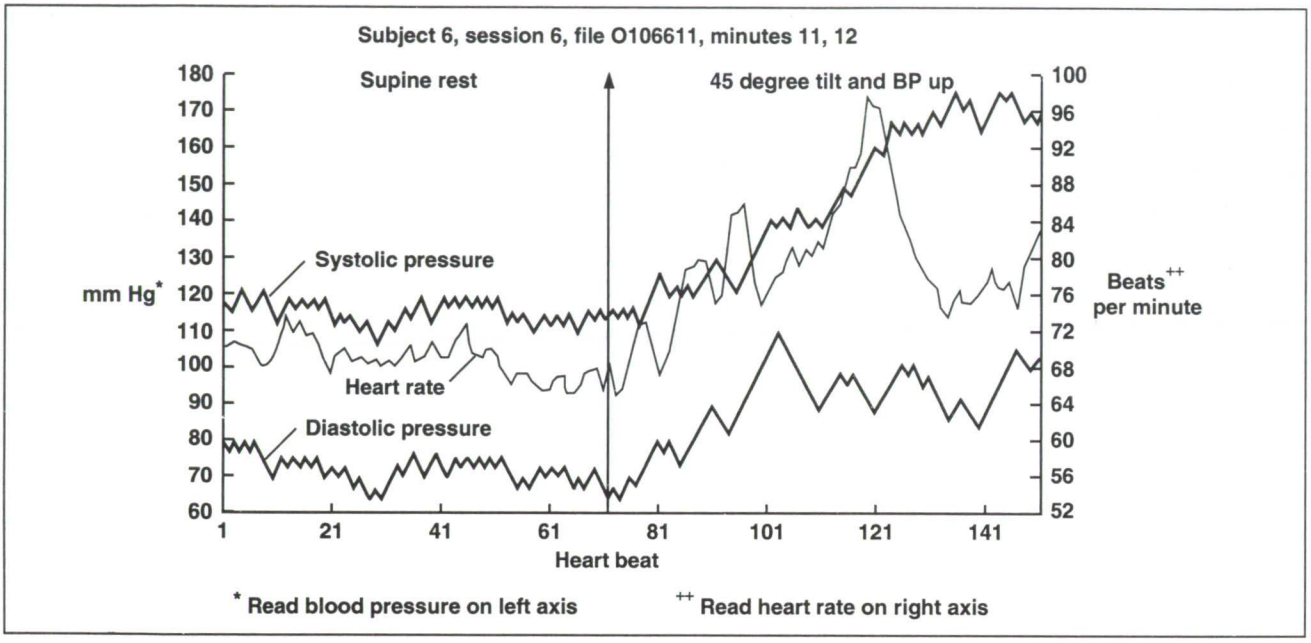


Fig. 1. A 2-minute sample of data from one subject practicing blood pressure increases during head-up tilt

NASA has identified cardiovascular deconditioning that can lead to the inability to adequately perform physical work as a serious biomedical problem associated with long-duration exposure to microgravity in space. High priority has been given to the development of countermeasures for this disorder and the resulting orthostatic intolerance (standing-induced fainting) experienced by crew members upon their return to Earth's gravity.

The present study was designed to examine the feasibility of training human subjects to control their own cardiovascular responses to gravitational stimulation (i.e., a tilt table). Using an operant conditioning procedure, Autogenic-Feedback Training (AFT), we would determine if subjects could learn to increase their blood pressure voluntarily. Clinical research has demonstrated that similar procedures have been used to successfully prevent orthostatic intolerance in patients with generalized bodily paralysis.

A primary criterion for this type of training is that the individual must be presented with ongoing information about his own responses in real time (e.g., displaying heart rate on a digital panel meter). For the present study, a computer-controlled blood pressure monitoring system was developed, which provided continuous "feedback" of both systolic and diastolic blood pressure on every beat of the heart.

Six men and women participated in this study. Each subject was given four to nine training sessions (each lasting 15-30 minutes). The figure shows the data of one of these subjects. The left side of this graph shows 1 minute of resting blood pressure and heart rate, followed by a voluntary increase of blood pressure of up to 50 mm Hg during tilt. This study demonstrates that learned control of blood pressure by normotensive individuals is possible. This skill could be a valuable adjunct to other countermeasures (e.g., inflight fluid loading and exposure to lower body negative pressure) in preventing standing-induced fainting upon return to Earth.

Ames-Moffett contact: P. Cowings
(415) 604-5724 or FTS 464-5724
Headquarters program office: OSSA

Autogenic-Feedback Training: Preventing Space Motion Sickness on SL-J

P. Cowings

Space motion sickness (SMS) affects 50% of all people exposed to the microgravity of space. These motion-sickness-like symptoms have proven resistant to pharmacological interventions and often produce unacceptable side effects.The effectiveness of a physiological conditioning method as an alternative to pharmacological management was examined.

This conditioning method, Autogenic-Feedback Training (AFT), involves training human subjects to voluntarily control several of their physiological responses. AFT has been tested on over 250 individuals in ground-based tests of motion sickness and has successfully enabled 80% of these people to significantly reduce, or suppress entirely, symptoms of motion sickness. Previously flown on STS 51-C and STS 51-B, in 1985, the preliminary results from space indicate that AFT may prove to be an effective treatment for SMS as well.

The AFT experiment has been manifested on Spacelab-J, which is scheduled for launch in 1992. In support of this experiment, five American and Japanese crew members (prime and back-up) as well as two "surrogate" crew members were given 6 hours of AFT for control of motion sickness symptoms. The number of rotations tolerated in a motion sickness test was increased after the administration of AFT (see the figure).

All subjects showed improvement in their ability to suppress motion sickness symptoms.

The hypotheses of the AFT flight experiment are

1. preflight AFT for the control of motion sickness will be an effective preventive and/or countermeasure for SMS.

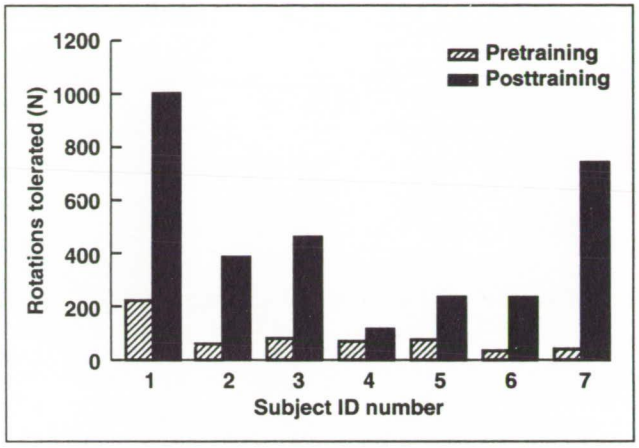


Fig. 1. Number of rotations tolerated before and after receiving initial training for seven subjects

2. the physiological data collected in space will enable objective indications of the effect of AFT and will provide information on crew member's physiological reactions to the microgravity environment.
3. the crew member's performance during preflight training for symptom control can be used to predict their susceptibility to SMS.

Ames-Moffett contact: P. Cowings
(415) 604-5724 or FTS 464-5724
Headquarters program office: OSSA

Autogenic-Feedback Training: Aid to Cockpit Peak Performance

P. Cowings

Significant Improvement Following AFT

	Variable
1.	Crew coordination/Communication checklist/Execution
2.	Planning and situational awareness–Taxi/Take-off
3.	Aircraft handling–Taxi/Take-off
4.	Procedures checklist callouts initial cruise
5.	Planning and situational awareness touch and go
6.	Stress management–Touch and go
7.	Aircraft handling–Touch and go
8.	Crew coordination–Cruise/SAR
9.	Aircraft handling–Cruise/SAR
10.	Crew coordination/Communication emergency initiation
11.	Stress management–Emergency approach and landing
12.	Overall performance–Emergency approach and landing
13.	Crew coordination–Briefing, communication, anticipation
14.	Crew coordination–Timely, relevant, complete COMS
15.	Crew coordination–Interpersonal relations/group climate
16.	Crew coordination–Prep/Planning for in-flight activities
17.	Crew coordination–Workload distributed and communicated
18.	Crew coordination–Overall technical proficiency
19.	Overall rating–Overall knowledge of aircraft/handling
20.	Overall rating–Overall technical proficiency
21.	Overall rating–Overall motivation
22.	Overall rating–Overall performance

Airline crashes attributed to pilot error are sometimes associated with "autonomous mode" behavior. In such cases, the pilot, in a high state of psychological and physiological arousal, tends to narrowly focus on a particular problem, often ignoring other, more critical information. This stress-induced dissociation can cause a pilot to fail to carry out critical crew coordination activities, which leads to fatal errors.

The present study examined the effect of training in physiological self-regulation as a means of improving crew cockpit performance. Autogenic Feedback Training (AFT) is a physiological conditioning procedure which has been used as a countermeasure for motion sickness. Motion sickness is characterized by large changes in physiological response levels; i.e., the heart beats faster and sweating increases. AFT enables subjects to learn to detect and to voluntarily regulate these physiological response levels and thereby reduce the symptoms of motion sickness. It was hypothesized that other stressful situations produce similar bodily responses; therefore, AFT may be useful in enhancing crew task performance.

Research was done under operational conditions at Coast Guard Air Station Barbers Point, Hawaii. Two randomly assigned groups of pilots (N-17) in HC 130 Hercules aircraft and HH-65 Dolphin helicopters participated in this study. During airborne scenarios, physiological data were recorded and individual crew performance was rated by an independent flight instructor. Then, half of the crew members received 12 40-minute sessions of AFT, while half did not. All crew members were again subjected to airborne scenarios and crew performance was re-evaluated. The results of this study outlined in the table indicate improved flight performance following AFT.

Ames-Moffett contact: P. Cowings
(415) 604-5724 or FTS 464-5724
Headquarters program office: OSSA

Investigating Neural Adaptation to Altered Gravity

N. Daunton, F. D'Amelio, R. Fox,
M. Corcoran, M. Ross, L-C. Wu

To ensure crew health, safety, and productivity during and following long-duration spaceflight, investigations of the changes in nervous system structure, biochemistry, and physiology that underlie adaptation to altered gravitational environments are being conducted. Knowledge of the types of changes that take place during the process of adaptation will make it possible to develop methods, both pharmacological and behavioral, to facilitate the process. These methods could also minimize or counteract those changes that may prevent astronauts from returning to a fully functional life on Earth or adapting to a planetary gravitational field following long periods of exposure to microgravity.

Research by investigators in the Life Science Division focused on the identification of neuromorphological and neurochemical changes in the neuromuscular and vestibular systems and the relationship of these changes to alterations in function. Thus, in recent studies rats have been exposed to hypergravity (2 g) produced by centrifugation, or to simulated microgravity produced by hindlimb suspension, for periods up to several weeks. Using image analysis, modeling, immunocytochemical, autoradiographic, and kinematic techniques, data obtained immediately following altered-g exposure and during recovery from this exposure have been analyzed. Changes in structure, neurochemistry, and function of the hindlimb neuromuscular system and of the gravity-sensing otolithic portion of the vestibular system were identified.

Preliminary findings from vestibular system studies indicate that changes in number and types of synapses in the otolithic endorgans are induced by 14-day exposures to 2 g. These neuromorphological changes are accompanied by several changes in vestibular function. For example, immediately following, and up to 2 days after removal from the centrifuge, a significantly greater percentage of centrifuged rats, as compared to control rats, were unable to perform the righting reflex, indicating general vestibular dysfunction. A significantly greater percentage of centrifuged animals than control animals also showed signs of disorientation in a swimming test, indicating abnormal otolith system function. However, after a week of recovery from centrifugation both righting and orientation responses returned to normal.

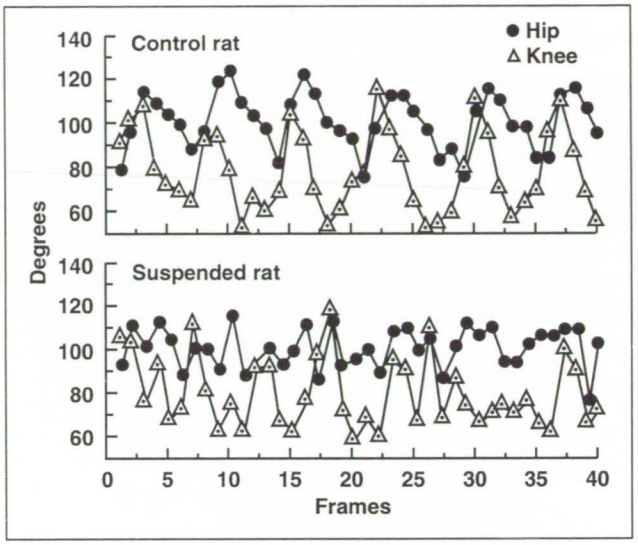


Fig. 1. Results of preliminary kinematic analysis of hip and knee joint angles during swimming for representative control and suspended animals

Analysis of data from neuromuscular system studies indicates that exposure to simulated hypo-g (hindlimb suspension) results in muscle atrophy and degeneration of motor end-plates in hindlimb antigravity muscles. Using the swim test, functional changes have also been found in this neuromuscular system following 14 days of hindlimb suspension. Suspended rats were found to be inefficient swimmers as compared to control animals, covering significantly shorter distances per unit time than controls, and swimming at a steeper angle than controls. These differences between suspended and control animals were still apparent 24 hours after removal from suspension.

Inefficiency of swimming may be attributed to disrupted patterns of coordinated hindlimb movements in suspended animals compared with control animals, as shown in the figure. Results illustrate that the normal, regular phase relationship between

hip and knee flexion/extension cycles seen in the control animal was disrupted in the suspended animal. In addition, the suspended rat showed a restricted range of hip movements as compared with that in the control animal.

Neuromorphological and neurochemical data on the effects of hyper-g exposure on the neuromuscular system are not yet available. However, studies of neuromuscular system function following centrifugation have indicated that exposure to 2 g leads to a disruption of normal step sequencing during beam walking in rats. This suggests that changes occur in the neural coordination of limb movements, as was found following exposure to hind-limb suspension. Preliminary analysis indicates that step sequencing returns to normal after 8 days of recovery from hyper-g exposure.

Future studies will investigate the effects of longer periods of exposure to suspension and hyper-g, and will begin to evaluate the effects of various pharmacological agents on the rate of functional recovery following long-term altered-g exposure. In addition data on neuromorphological and neurochemical changes obtained in these studies will be compared with data obtained by the same research team members from Cosmos and Spacelab flight experiments. Such comparison of flight and ground control data should enable validation of ground-based simulation models.

Ames-Moffett contact: N. Daunton
(415) 604-4818 or FTS 464-4818
Headquarters program office: OSSA

Astronaut Rehydration Fluid Formulations

J. Greenleaf, L. Keil

Total body water is divided arbitrarily into that contained within (intracellular water) and outside (extracellular water) body cells. Extracellular water is composed of that located outside of the vascular system (interstitial water) and inside the vascular system (plasma water). Chronic reduction of body water (hypohydration) from the extracellular, and probably the intracellular compartments, occurs in astronauts exposed to microgravity. This natural adaptive response does not appear to compromise physical or psychological performance unless compounded by additional excessive fluid and electrolyte losses from vomiting, diarrhea, or sweating. The most critical point in a mission when astronaut performance may be compromised is during reentry and immediately after landing. Then, the reduced total body water can lead to degradation in physical and psychological performance.

The purpose for the present research project is to design and evaluate rehydration fluid formulations that astronauts can drink a few hours before reentry and immediately after landing to restore total body water and plasma volume, in particular. These new formulations would replace the salt (NaCl) tablets and water currently being used. To be optimally effective, salt tablets and water need to be taken in a ratio of 1 gram of salt to 100 milliliters of water. This procedure is inconvenient for astronauts when they are secured in their seats prior to reentry. Excessive salt intake without an appropriate volume of water can accentuate the total body hypohydration by raising NaCl concentration in the blood plasma. Premixed fluid formulations of a proper composition will negate this potential problem.

Two studies were completed. In the first study healthy men, previously dehydrated for 24 hours, drank 6 fluid formulations (one per week) and then sat for 70 minutes. This procedure simulated hypohydrated astronauts preparing for reentry. Changes in their plasma volumes were calculated from the blood hematocrit [(plasma volume/total blood volume) × 100] and hemoglobin concentration (see the first figure).

The second study followed this same protocol except that the men exercised in the supine position on a cycle ergometer at a moderately heavy load (71% of their maximal aerobic work capacity) for 70 minutes. Changes in their plasma volumes were calculated (see the second figure). This procedure simulated hypohydrated astronauts preparing for and performing extravehicular activity. The formulations were (a) water + aspartane (asp, non-caloric sweetener); (b) 19.6 milliequivalents per liter (mEq/l) NaCl + asp.; (c) 157 mEq/l NaCl-Na citrate + asp.; (d) 19.6 mEq/l NaCl +9.7% glucose; and two commercial drinks; and (e) P and (f) PS containing various types of carbohydrates and electrolytes.

In the resting study (first figure) the change of plasma volume (PV) after drinking the formulations ranged from –3.8% ($p < 0.05$) at 3 minutes to +7.6% ($p < 0.5$) at 70 minutes. Plasma volume decreased ($p < 0.05$) during the initial 9 minutes with drinks b, d and e, and PV was unchanged with a, c and f. At 70 minutes PV changed by +1.1% to +1.5% (NS, like water) with drinks a, b and d; and increased ($p < 0.05$) by +3.1% (drink f), by +4.6% (drink e), and

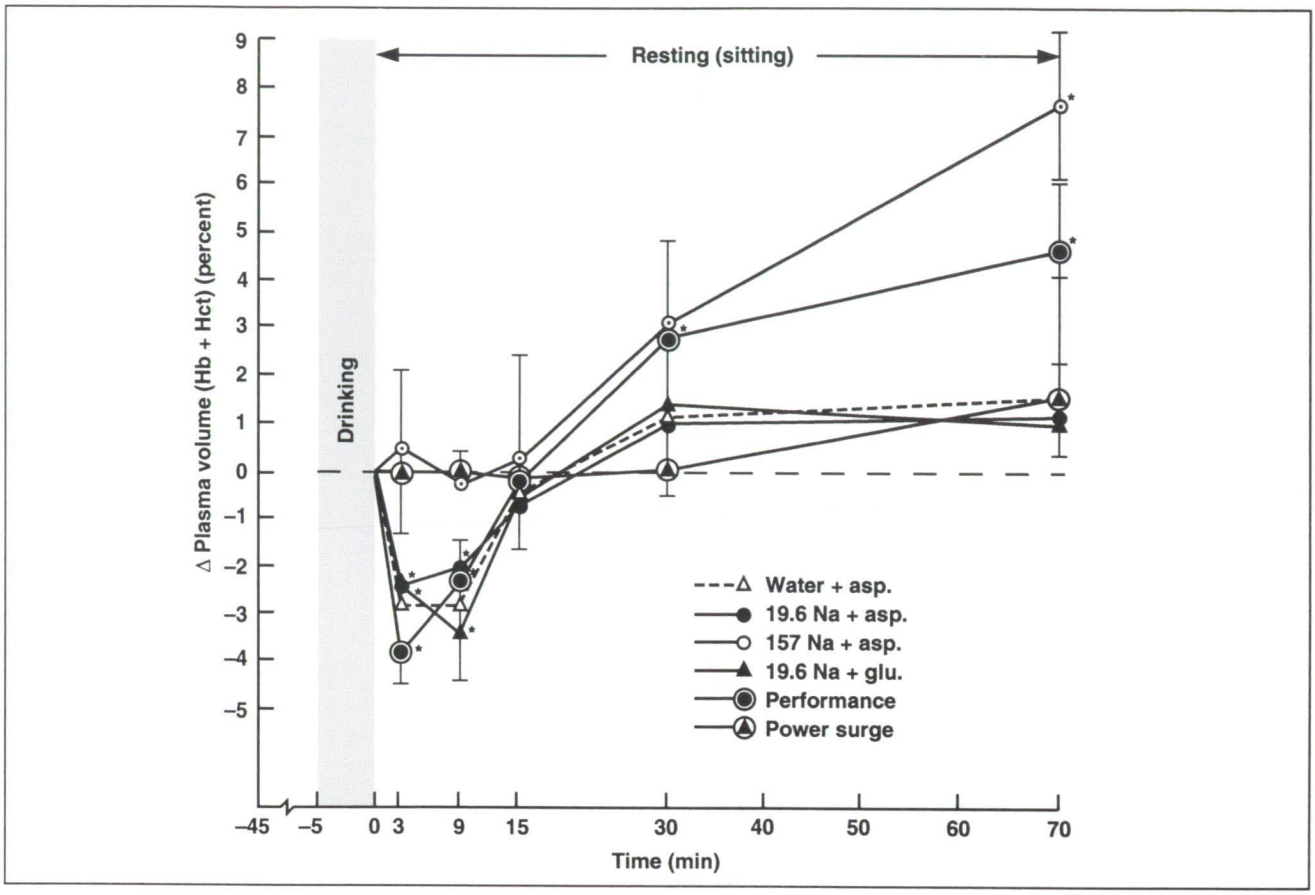


*Fig. 1. Mean (±SE) percent changes in plasma volumes of 5 men during 70 minutes of sitting, after consuming 6 fluid formulations (12 ml/kilogram of body weight). PV changes were calculated from the blood hemoglobin (Hb) and hematocrit (Hct). The osmotic pressure of the formulations is mOsm/Kg H_2O. *p < 0.05 from zero*

by +7.6% (drink c). Thus, fluid formulations containing sodium compounds near isotonic concentrations (i.e., the same concentration as blood plasma) seem better than more dilute solutions for restoring and increasing plasma volume in resting, hypohydrated men.

In the exercise study, changes in PV occurred (second figure); all 6 drinks resulted in depression of PV from –5.2% to –14.0% at 70 minutes. With no fluid intake, the reduction in PV at 70 minutes with this moderately heavy exercise load would have been about 12%. Changes in PV with the drinks were similar to this non-drinking PV response. Thus, performance of intensive exercise immediately after drinking these fluids appears to inhibit fluid transfer from the gastrointestinal system into the vascular system.

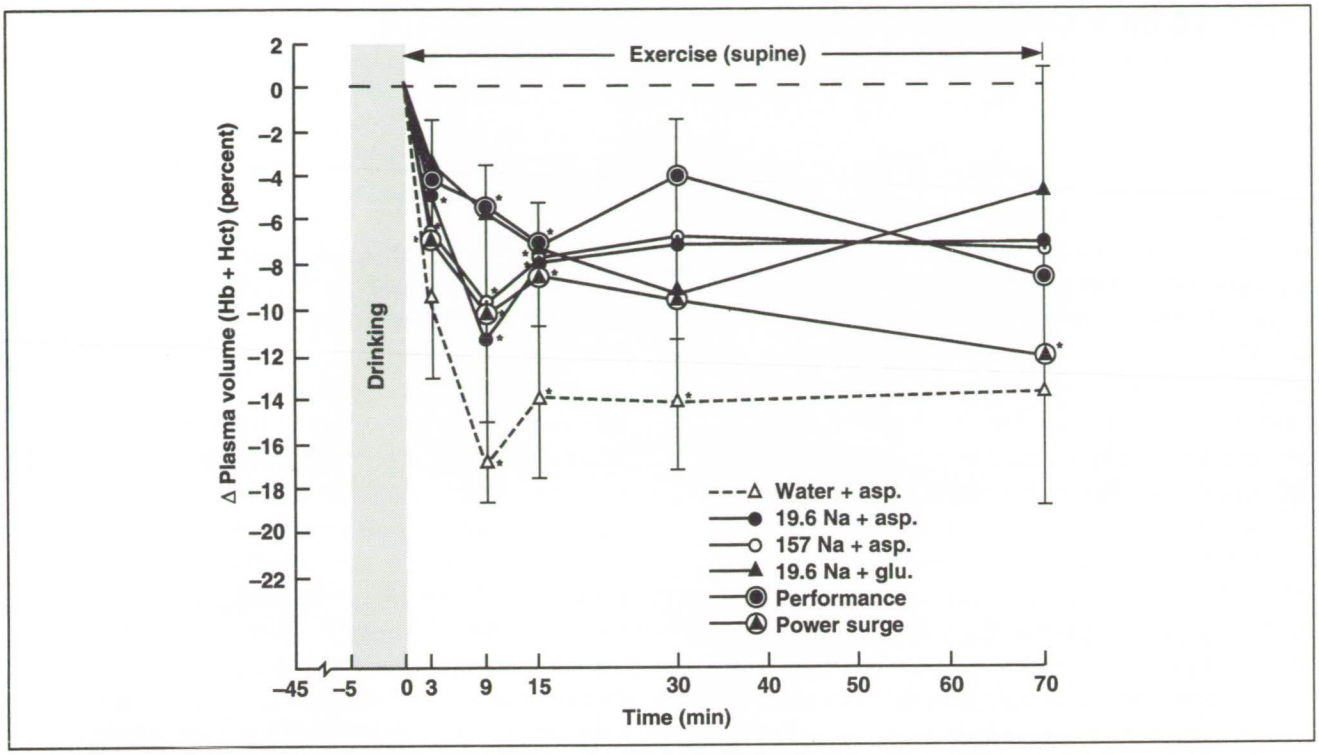


*Fig. 2. Mean (±SE) percent changes in plasma volumes of 4 men during 70 minutes of intensive cycle ergometer leg exercise at 71% of aerobic capacity in the supine position, after consuming 6 fluid formulations (12 ml/kilogram of body weight). PV changes were calculated from the blood hemoglobin (Hb) and hematocrit (Hct). The osmotic pressure of the formulations is mOsm/Kg H_2O. *p < 0.05 from zero*

Fluid formulations from these ground-based experiments, that provide significant increases in plasma volume, will be proposed for testing in flight for their efficacy in restoring or increasing plasma volume. The goal is to provide one or more fluid formulations, having generally high astronaut acceptability, that will provide a better countermeasure for microgravity-induced hypohydration than salt tablets and water, so that performance will not be compromised during reentry and landing of the Space Shuttle.

Ames-Moffett contact: J. Greenleaf/L. Keil
(415) 604-6604/6378 or FTS 464-6604/6378
Headquarters program office: OSSA

Exercise as a Countermeasure of Muscle Wasting in Long-Term Hindlimb Suspension

R. Grindeland

In the growing rat, certain muscles (soleus, adductor longus) waste (atrophy) and other muscles (e.g., gastrocnemius, plantaris, extensor digitorium longus, tibialis anterior) show reduced growth during spaceflight. In more mature animals all of these muscles atrophy. In addition to the decrease in mass, protein, and fiber size, the muscles of flight rats also show conversion from slow to fast twitch fiber types, changes in enzyme (aerobic and anaerobic) complement, and degeneration of the motor end plates, the nerve interaction with the muscle. Contractile protein, and strength, are lost more rapidly than total proteins. Thus, these muscles lose strength and control. Hindlimb suspension (HS) appears to mimic spaceflight effects on skeletal muscle except for a slower conversion to fast twitch fibers and a reduced fat deposition in muscles.

Procedures intended to prevent or lessen the muscle atrophy have included pharmacological interventions, electrical stimulation, exercise, and centrifugation. The pharmacological and electrical treatments have proved to be essentially ineffective. Although flight and HS rats show marked decreases in plasma bioassayable growth hormone concentrations, administration of growth hormone (GH) to HS rats has not alleviated the atrophy. Centrifugation on the Cosmos 936 mission protected muscle mass but introduced other problems, perhaps due to the small radius centrifuge used.

One group found that the use of centrifugation as a countermeasure did not ameliorate the atrophy induced by HS. Exercise of human beings in space is thought to have some value; however, there is a paucity of definitive data to support that view. Exercise of HS rats has yielded variable results. Most exercise regimens (human or animal) are of questionable efficacy, are extremely inefficient, and probably are not acceptable to most astronauts. In HS rats, which are allowed to ambulate for one 8-hour or four half-hour periods per day, atrophy of the soleus is virtually prevented. Whether the gastrocnemius and other muscles were also protected is unknown. Another group found that short periods of heavy exercise (carrying a load up a 1-meter ladder inclined at 85°) was much more effective and efficient than endurance-type training in HS rats.

Working with this group, we have found that carrying 60% of body weight up a ladder as many as 30 times per day ameliorated the atrophy. Fifteen climbs appear to be about as effective as 30; fiber analyses have not been completed, so a conclusion cannot yet be drawn. Secondly, we found (in six experiments) that exogenous GH given in various regimens (doses, times) to intact HS rats was ineffective. GH given to HS hypophysectomized (hypox) rats evoked 60% as much growth as in ambulatory hypox rats. Muscle growth in the GH-treated hypox rats was directly proportional to body-weight gain. Recently, we achieved a major breakthrough by combining slight exercise (three bouts of five climbs carrying 20% of body weight) with the administration of GH (1 milligram/kilogram/day).

The effect on the muscles is shown in the table. The important conclusions are (1) exercise alone had no effect, (2) GH administration had a limited effect, (3) GH + exercise had a much greater effect than GH alone ($p < 0.05$), and (4) muscle weights increased more than body weight in GH + exercise rats. The effects were also seen in the tibias; in which, again, exercise had no effect, GH had some effect, but GH + exercise had a greater effect ($p < 0.05$).

We have also shown that insulin-like growth factor 1 (IGF-1) receptors in muscle increase (absolute and relative) in HS rats. Also, during HS IGF-1 levels in plasma remain constant so atrophy is not due to a deficit in IGF-1 or its receptors. Whether tissue IGF-1 levels are changed is unknown. Measurement of GH receptors has been more difficult with differing results obtained with different labeled GH preparations; resolution of this problem is continuing.

Effect of Exercise and/or Growth Hormone on Absolute Weights of Skeletal Muscles of Suspended Rats Bilaterally (mg), (R + L/2), Mean ± S.E.

	Soleus	Tibialis Anterior
Presusp (t = 0)	97.03 ± 3.79	553.09 ± 29.30
Ambulatory		
+ Saline	98.46 ± 4.17	398.47 ± 5.85
+ GH	102.12 ± 1.66	479.98 ± 15.58
Suspended		
+ Saline	81.43 ± 2.99	384.62 ± 9.63
+ GH	84.72 ± 2.50	449.34 ± 10.09
+ Exercise	78.83 ± 1.62	392.68 ± 10.87
+ GH + Exer	99.64 ± 1.97	471.79 ± 15.06

	Medial Gastroc.	Adductor Longus
Ambulatory		
+ Saline	519.20 ± 4.93	53.85 ± 1.27
+ GH	626.11 ± 21.97	56.13 ± 2.22
Suspended		
+ Saline	464.15 ± 11.00	42.05 ± 1.11
+ GH	496.60 ± 9.21	45.48 ± 2.84
+ Exercise	454.18 ± 5.66	40.58 ± 1.95
+ GH + Exer	550.83 ± 14.89	44.52 ± 2.40

Research will continue to determine the optimal exercise-GH regimen in hypox HS rats and then in intact HS rats. Receptors for IGF-1, IGF-2, and GH will also be measured in muscles of HS rats, and related hormones in their plasma will be assayed. We shall look particularly at regimens to protect the red muscles which showed relatively little benefit in the study cited above. Once the optimal treatment is established we hope to do a 6-month suspension study to further establish long-term effects of HS on muscle and the efficacy of the treatment.

Ames-Moffett contact: R. Grindeland
(415) 604-5756 or FTS 464-5756
Headquarters program office: OSSA

Physiologic Mechanisms of Fluid Shifts in Humans During Acute, Simulated Microgravity

A. R. Hargens, S. E. Parazynski, M. Aratow

An understanding of mechanisms for local fluid shifts during microgravity is a major research effort of the Life Science Division. It was postulated that in microgravity, blood was somehow shifted toward the head, thereby causing headache, facial swelling, and nasal congestion. These symptoms are common complaints of astronauts in flight. Recent investigations yield new insights into the origins and time course of this headward fluid shift in human subjects. In these studies, microgravity was simulated by 6° head-down tilt, while micropressure measurements were performed to monitor local fluid movement.

All four forces that govern fluid transfer between the microcirculation and tissues were directly measured for the first time in the head and neck in eight normal volunteers. One of these forces, called capillary blood pressure, filters blood out of small vessels. This pressure previously had not been measured in the upper part of the human body. Using a microscope and microscopic pipet, a painless procedure was developed at Ames Research Center to record this pressure in the lip.

Capillary blood pressure increased and remained elevated during head-down tilt (see the figure). This increase in local capillary pressure caused more filtration of fluid from the blood into tissues of the head, producing facial swelling. Forehead skin blood flow at the capillary level also increased during head-down tilt as measured by laser Doppler flowmetry. Higher capillary blood flow also could contribute to facial swelling and other fluid-shift symptoms associated with the microgravity environment. In other studies of head-up tilt compared to head-down tilt, skin blood flow was regulated in capillaries of the foot much better than that in the head.

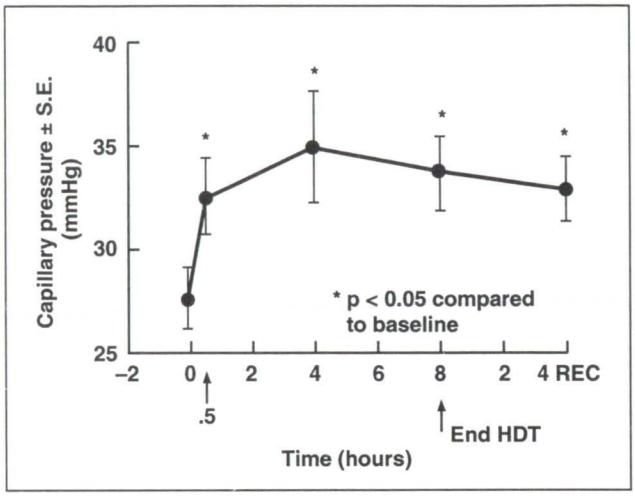


Fig. 1. Capillary blood pressure in the head (normally 27.5 millimeters (mm) Hg in upright posture) increases during 8-hour head-down tilt (HDT) to 33-35 mm Hg and remains elevated in the 4-hour upright recovery period

Overall, these local blood pressure and flow changes explain the rapid facial swelling of astronauts when they are exposed to microgravity.

Ames-Moffett contact: A. Hargens
(415) 604-5746 or FTS 464-5746
Headquarters program office: OSSA

Lower Body Negative Pressure Provides Load Bearing for Humans Exposed to Microgravity

A. R. Hargens, R. T. Whalen, D. E. Watenpaugh, G. Murthy, D. F. Schwandt

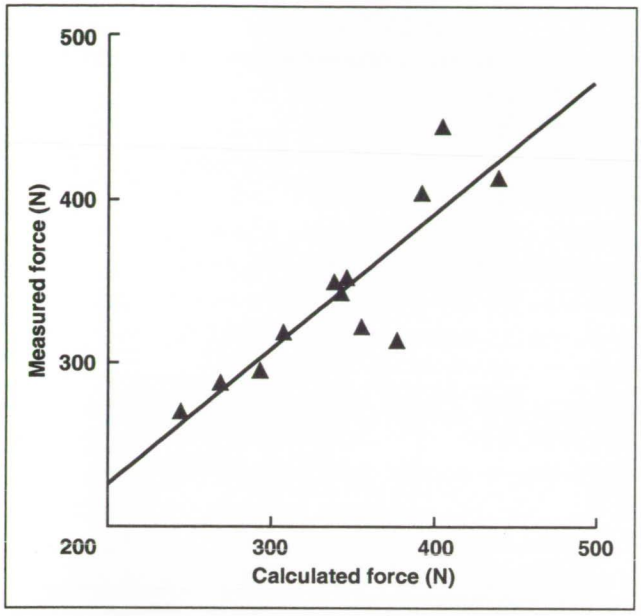


Fig. 1. As an example, measured forces in Newtons developed by 50 mm Hg LBNP correlated well with calculated forces

Presently, exercise protocols and equipment requirements for spaceflight are undefined. We hypothesized that lower body negative pressure (LBNP) produces a footward force equal to the product of the pressure differential and body cross-sectional area at the waist seal. This would provide adequate loads that may maintain musculoskeletal mass and cardiovascular tone during spaceflight. (See article titled "Musculoskeletal Loading with Lower Body Negative Pressure" by R. T. Whalen, A. R. Hargens, D. E. Watenpaugh, D. F. Schwandt.)

In our recent studies, aimed at validating the use of LBNP as a method for axially loading the body, 12 male volunteers, each weighing between 68-87 kilograms, were sealed at the superior iliac crest in upright or supine LBNP chambers. The force due to LBNP was transmitted to the feet of our subjects. Each subject was exposed to 10 millimeter (mm) Hg increments of LBNP, up to 70 mm Hg (standing) or to 50-100 mm Hg (supine), depending upon individual tolerance. Static reaction force was measured at each increment. Subsequently, foot and leg exercises were performed to determine the

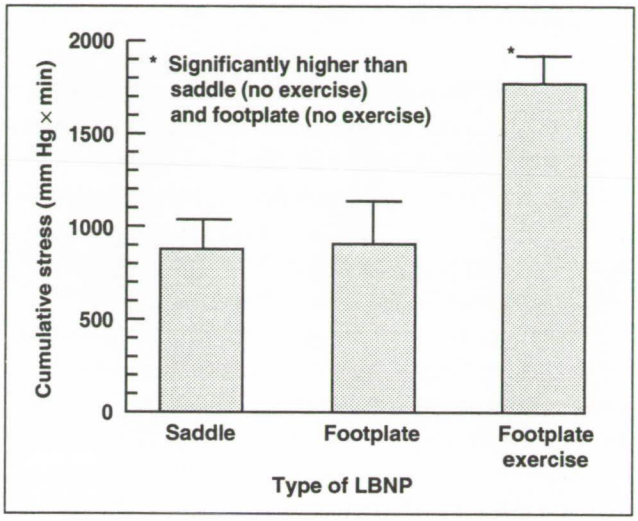


Fig. 2. Tolerance to LBNP is increased by exercise. Cumulative stress is defined as the product of LBNP amplitude and duration

inertial loading effects of exercise within the supine LBNP chamber and to assess the effect of exercise on LBNP tolerance.

An additional static force approximately equivalent to 1% Earth body weight was generated against the feet by each mm Hg of LBNP either during upright standing or supine posture. Furthermore, the forces measured agreed well with forces calculated from the cross-sectional areas of our subjects' waists (see first figure).

Exercise within the LBNP chamber produced high and low inertial forces that corresponded to the expected cycle of activity and doubled LBNP tolerance relative to static LBNP (see second figure).

These results indicate that exercise in microgravity against 100 mm Hg LBNP will produce static and inertial forces similar in magnitude to those occurring on Earth at +1 g. This gravity-independent technique may help maintain musculoskeletal and cardiovascular systems of crew members during short-term and prolonged exposure to microgravity.

Ames-Moffett contact: A. Hargens
(415) 604-5746 or FTS 464-5746
Headquarters program office: OSSA

Gravity and Skeletal Growth

E. Morey-Holton

Decreased bone formation has been reported in growing rats flown on Soviet Cosmos biosatellites. Bone labels were given to these animals before flight to directly assess the amount of bone formed during flight. On Cosmos 1887 and 2044, bone labels could not be given and data obtained suggest that significant bone changes may be masked when bone formation is measured indirectly.

The Soviet Cosmos biosatellite 1887 was complicated by an unexpected postflight processing time of more than 2 days after landing. To assess the extent of such extended recovery due to delayed access to the animals postflight, Cosmos 2044 was launched with experiments identical to those previously flown on Cosmos 1887. Each flight lasted about 14 days; however, the rats on Cosmos 2044 were almost 1 month older than the animals on Cosmos 1887. Animals on the ground served as synchronous controls. Shafts of tibial bones from both flight and control rats were shipped to the United States where they were processed, and area and perimeter measurements were determined using a computerized histomorphometry system.

Visual observations of tibial cross sections under brightfield or polarized light did not show any obvious differences. Histomorphometric measurements did not show any significant differences between flight and corresponding ground controls; the differences from the basal group on Cosmos 1887 indicate that bone growth did occur during the flight period. No obvious bone growth was found in the Cosmos 2044 animals.

Data from Cosmos 2044 are difficult to compare with data from Cosmos 1887 because of the age difference. Larger bones on Cosmos 2044 agree with the older age of the rats. The lack of any increase in bone mass during the flight period indicates that the animals were adults and that bone mass was not accumulating as rapidly in either flight or ground control, unlike some animals in Cosmos 1887. Larger, adult rats may require a longer flight period to demonstrate bone changes particularly in cortical bone because the skeleton is accumulating more slowly. The data also suggest that bone changes may not be readily obvious if only the total cross-sectional bone mass is observed. Administration of bone labels may be necessary on shorter flights to directly monitor changes in bone formation in growing rats; when bone formation is measured indirectly, using cross-sectional bone area, significant changes may be missed.

Ames-Moffett contact: E. Morey-Holton
(415) 604-5471 or FTS 464-5471
Headquarters program office: OSSA

Effects of 24 Hours of Reloading on Bone Metabolism after 6 or 11 Days of Hindlimb Unloading

E. Morey-Holton, C. Cone, D. Bikle

Investigation of bone metabolism requires radioisotope injections, usually given the last day of the experiment. Rats in shuttle middeck lockers cannot be handled in flight and injections must be given postflight. To determine if bone metabolism changes within 24 hours of reloading, an experiment was conducted using the ground-based flight-simulation rat model.

Male, growing rats were used. The experimental groups (in which the hindquarters were raised off the ground) were studied at the end of either 6 or 11 days, with or without 24 hours of readaptation/load-bearing. Normal load-bearing littermates served as controls at each time period (controls were fed the average daily amount of food consumed by the flight-simulation animals). Rats were injected intraperitoneally with ^{3}H-proline (10 microcuries/100 grams) and ^{45}Ca (1 microcurie/100 grams), approximately 24 hours before euthanasia. The humerus, tibia, and femur were removed and cleaned. Parameters measured included body mass, bone mass, and ^{3}H-proline and ^{45}Ca uptake and calcium in bone and serum. Radio-labeled proline measures metabolism of the organic portion of bone while radioactive calcium indicates turnover of the inorganic portion (bone mineral metabolism).

Body mass increased similarly in all groups; this finding is very important because different growth rates make an experiment very difficult to interpret. In all bones measured, bone mass and calcium content were significantly correlated, suggesting that calcium content may be estimated from bone weight. In the control groups, 5 days' growth was reflected by an increase in bone mass and bone calcium and a decrease in bone metabolism. In the unloaded limbs, accumulation of bone mass and calcium was slower than controls for the first 6 days with return to control levels within 11 days; calcium isotope uptake at 11 days was essentially identical to control values at 6 days, suggesting the bones were 5 days younger. Bone mass and calcium content reduction after 6 or 11 days of unloading were not altered by 24 hours reloading, but most metabolism parameters did recover within 24 hours. Metabolism in the femur appears to recover more rapidly than the tibia with reloading. The recovery from unloading is more rapid after 6 days than after 11 days.

Ames-Moffett contact: E. Morey-Holton
(415) 604-5471 or FTS 464-5471
Headquarters program office: OSSA

Neurocomputer Development Based on Experimental Data at the Vestibular Research Facility

A. J. Pellionisz, D. L. Tomko

For experimental investigation of the vestibular neural apparatus, Ames Research Center's Vestibular Research Facility (VRF) provides the scientific community with unique, state-of-the-art equipment and techniques unavailable elsewhere. The vestibular neural apparatus is a relatively simple and ancient neural mechanism that maintains equilibrium and balance (e.g., in navigation and flight control of animals). Because of this, the vestibular system and the closely related cerebellum have become a center of interest of neurocomputer research and development, not only in the neuro-science community but also in information science and technology development. This interest is logical, because the vestibular neural network is nature's best known massively parallel "neurocomputer" whose functional principles (e.g., in flight control) could have a direct impact on primary missions of NASA.

To combine ongoing vestibular experimentation with mathematical-computer research and development, two major projects were initiated in the VRF in the Life Science Division during FY 90. The projects involved investigators from New York University and Philipps University of Marburg (Germany).

First, a computer-modeling approach was started, which aims at three-dimensional modeling of the head-neck-eye system whose movements are controlled by the vestibular neural network's gravity and angular acceleration receptors (see figure). This computer model is derived from data of experiments on gravity receptor control of eye movements, and provides an heuristic tool for interpreting the experimental data and predicting other aspects of vestibular control function that are amenable to empirical testing.

A second project was initiated in neurocomputing (cosponsored by Ames Director's Discretionary Fund and the Alexander von Humboldt Prize for Scientific Research) "to develop an electronic 'brain' to study the brain." That is, the project was to build and write software for a functional parallel-processing computer that is capable of both (1) processing massively parallel (multi-unit) recordings from the vestibular neural net in a fast on-line manner, and (2) providing neuroscientists and computer experts with a prototype of an electronic equivalent of a structurally and functionally well-identified

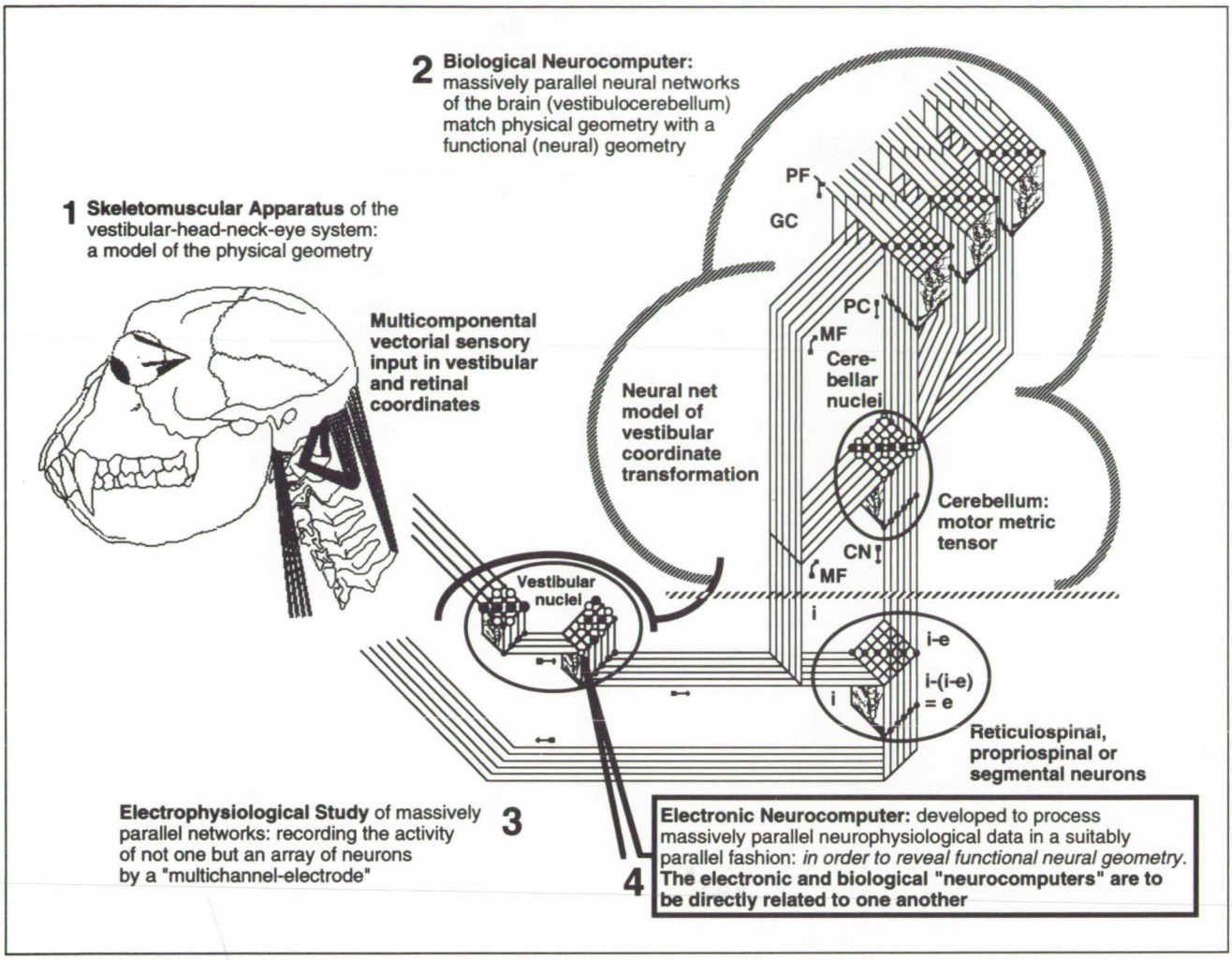


Fig. 1. Vestibular head-neck-eye neural stabilization as an existing neurocomputer: a prototype for electronic neurocomputers

subsystem of the biological brain. Vestibular computer modeling and neurocomputer research are connected to experimentation as well as to one another, thereby providing an integrated approach.

Ames-Moffett contact: A. Pellionisz
(415) 604-4821 or FTS 464-4821
Headquarters program office: OSSA

Biological Neural Networks as a Basis for Improved Computer Technology and Chip Design

M. Ross

Biological neural networks are highly successful computational systems that function as massively parallel, distributed processors of information. To study the principles of their architecture, utricular and saccular macula, which receive and transmit vestibular impulses, are serially sectioned for study. Electron micrographs are assembled as montages of the serial sections. In this way, every receptor cell (type I and type II hair cells), each terminal (calyx) of the vestibular nerve fibers, and afferent and efferent processes can be identified and labeled.

Tracings of terminals and their receptive fields, consisting of hair cells synapsing with calyces or afferent processes, are digitized into a PC. Digitized data are then transferred to a Silicon Graphics IRIS high-performance workstation for reconstruction as shaded solids, and for animation. The montages are also used to produce abstract maps of the connectivities of that part of the network present in the series. The results have been used to produce terminal/receptive field organizations by Monte Carlo simulations, using constraints deduced from the montages.

Findings are incorporated into symbolic, two- and three-dimensional, dynamic models of a functioning macula to learn more about the meaning of constrained randomness in wiring, redundancy, and feed forward-feedback loops in parallel distributed processing of information. Most recently, we have produced symbolic block diagrams of functioning receptive fields as a prelude to electronic circuit diagrams, network simulation, and design of a chip based on principles derived from study of nature's accelerometers.

Our findings indicate that the basic functional organization of natural neural sense organs and neural networks can be understood and can be reproduced for applications in computer technologies. A chief observation is that biological neural systems are distinctly non-modular. They appear to use highly directed, channeled inputs and lateral, distributed modifying circuitry with some local control to achieve meaningful neuronal output. It is the disturbed, modifying portion of the network that is expected to be most altered by adaptive processes when the network is challenged by new operational environments, such as space. Redundancy and constrained randomness in wiring may underlie system robustness. A further observation is that neural network architecture differs from one site to another, most likely for functional purposes, even though the network itself is continuous.

Simulations based on the biological principles we and others have uncovered will be useful in exploring the basis of neural adaptation, learning, and fault tolerance for applications in parallel-processing computer technologies. Further contributions will occur in the area of bionic or biomimetic devices for use as sophisticated, miniaturized (chip) sensors, and motor controllers in both medicine and robotics. These and other technological applications based on neural functioning suggest that neurotechnology will be the powerful new science to emerge from the next decade and to usher in the new century.

Ames-Moffett contact: M. Ross
(415) 604-5757 or FTS 464-5757
Headquarters program office: OSSA

The Role of Visual-Vestibular Interactions in the Perception of Motion

L. Stone

The perception of motion is critical to the performance of visually guided navigation and movement. Motion information is available to perception from the visual, vestibular, and oculomotor systems. A clear understanding of how motion information is processed within all three of these systems and how these three systems interact is crucial for (1) modeling human performance in tasks that require motion processing, and (2) anticipating how microgravity environments may adversely affect perception and performance.

Current research has focused on visual perception of motion specifically related to how the accuracy and precision of human visual perception of speed and direction depends on parameters of the stimulus. Contrast has been found to have a profound effect on motion perception.

First, a lower-contrast grating appears to move more slowly than a comparable higher-contrast reference grating. We are now examining whether certain models of primary visual cortex can explain this result.

Second, if a plaid (the sum of two gratings of different orientations) is composed of gratings with different contrasts, the direction of motion is misperceived and is biased in the direction of the higher-contrast grating. We are quantitatively examining the two results to determine whether plaid-direction bias is the direct result of an underlying misperception of grating speed.

Third, the precision in direction and speed of a moving plaid can often be predicted from the precision in the perception of orientation and speed of its component gratings. This result sheds light on how the extrastriate visual cortex of the brain extracts the speed and direction information from moving patterns.

Future studies will be extended in a number of ways. First, three-dimensional motion (that which is generated when the viewer moves within a structured environment) will be examined, as well as simpler grating and pattern motion. Second, eye movement measurements will be made to examine the oculomotor response. Third, the perception of motion during vestibular stimulation will be examined. Finally, the long-term goal is to use combined visual and vestibular stimulation to examine how all of these factors (vision, vestibular sensation, and eye movements) interact in the perception of motion.

Ames-Moffett contact: L. Stone
(415) 604-4252 or FTS 464-4252
Headquarters program office: OSSA

Gravity Receptor Physiology Research at the Vestibular Research Facility

D. L. Tomko

During head movement, vestibular sensors provide signals of head position, as well as linear and angular velocity, in inertial space. These sensors are biological linear and angular accelerometers, whose outputs are used by the brain to produce eye movements that compensate for head movements. This keeps the eyes and the visual world stable in inertial space. Vestibular linear acceleration receptors play a critical role in control of eye movements during pitch, roll, or linear oscillation of the head. They code not only head position relative to Earth's gravity, but also respond to translational acceleration. Exact eye movement control mechanisms are not understood, especially how these position and rate sensors are integrated in the brain, how linear accelerations produce eye movements, and how linear acceleration is differentiated from head tilts by the brain.

Human brain mechanisms that use gravity receptor outputs to reflexively control eye position and stabilize visual space are affected by microgravity exposure because of the removal of Earth gravity effects. To better understand how linear accelerations and gravity receptor stimulation control eye movement, experiments have been conducted on the low-vibration Vestibular Research Facility (VRF) linear sled. Effects of gaze position and angle on eye movement control during linear acceleration (VSLVOR) have been extensively studied, and have been found to significantly impact eye movements produced by linear acceleration.

A summary of the effects of measured ocular convergence angle on VSLVOR amplitude are

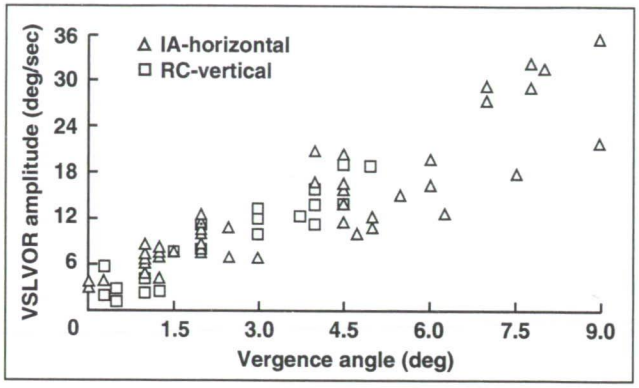


Fig. 1. VSLVOR amplitude and vergence

shown in the figure: linear oscillations at 5.0 hertz (0.36 g) produced oscillatory vertical eye movements during head-to-tail (RC) oscillations, and horizontal eye movements during left-to-right (IA) oscillation. Eye movement aptitude increases dramatically as convergence angle increases (near visual targets) and decreases with distant targets requiring little or no vergence.

These data illustrate the physiological mechanism underlying the common advice to "look at the horizon" to reduce vestibular motion sickness symptoms, since looking at distant targets reduces or eliminates eye movements produced by linear oscillation.

Ames-Moffett contact: D. Tomko
(415) 604-5723 or FTS 464-5723
Headquarters program office: OSSA

Vestibular Research Facility for Ground-Based Studies

D. L. Tomko, T. Wynn

The Vestibular Research Facility (VRF) in the Life Science Division at Ames Research Center provides NASA and the space research community with a suite of unique, state-of-the-art equipment and techniques for: (1) sophisticated ground-based investigating of vestibular function in 1 g and hypergravity; (2) defining critical scientific questions for microgravity research and providing a facility for obtaining baseline data for this research; and (3) defining equipment and methods required for conducting research in space. The VRF consists of a multiaxis centrifuge, two air-bearing linear sleds (12 feet and 30 feet in length), and supporting neurophysiological laboratory equipment and personnel. Both the VRF centrifuge and linear sleds are able to deliver stimuli at extremely low levels of vibration, which provide unprecedented and unequalled opportunities for investigations of the vestibular system.

Accomplishments using the VRF facility during FY 90 include the completion of the Operational Readiness Review for the centrifuge; design, installation, and test of a 10-foot prototype DC linear motored control system; and completion of two scientific studies, one on the centrifuge and the other on the short linear sled. In addition, in March, a multiagency review was conducted to certify the VRF hardware and scientific accomplishments as a unique national resource, leading to an interagency agreement to open the facility for use by other Federal agencies.

Ames-Moffett contact: D. Tomko
(415) 604-5723 or FTS 464-5723
Headquarters program office: OSSA

Postflight Fainting, Blood Pressure Control, and Countermeasures

Joan Vernikos

Head-down bedrest (–6°) has proven to be an excellent analog for studying the effects of microgravity on the cardiovascular system and its regulation. It further allows us to conduct such investigations under controlled conditions, not possible during flight. We have therefore used head-down bed rest extensively (1) to determine the long-term changes in the regulation of blood pressure, blood flow, and blood volume, which underlie the orthostatic intolerance (feeling of faintness) often seen on return to Earth's 1 g and (2) to develop and test practical and effective countermeasures.

Two such studies have been completed by the Life Science Division at Ames Research Center in collaboration with investigators at Kennedy Space Center (KSC). The first study investigated the time course of the changes in blood volume over 30 days of –6° bed rest and examined the effects of such simulated weightlessness on specific blood pressure reflex control mechanisms of vascular resistance that have not been examined in controlled ground-based studies.

Technologies adapted by the KSC team afforded us this unique opportunity. Results showed that blood volume decreased promptly on assuming the head-down position and then continued to decline more slowly during the 30 days. The carotid cardiac baroreflex did not parallel the changes in blood volume, but showed a delayed response and became less sensitive with time (only after the 12 days of bed rest). This decreased responsiveness of the baroreflex, which persisted through at least 5 days of ambulatory recovery, was correlated with post-bed-rest fainting episodes, whereas the change in blood volume was not. The blood pressure responses to metered doses of Angiotensin-II were also dampened, in parallel with the baroreflex changes.

Results of the first study indicated that the vasomotor regulatory deficits after relatively short exposures of just a few days may be more readily compensated for by techniques that expand blood volume, whereas more prolonged missions may require additional countermeasures directed at restoring baroreflex sensitivity.

The second, recently completed study was of 7 days (bed rest) duration. The study was designed to compare the current procedure of ingesting salt tablets and water to expand blood volume before re-entry with that of ingesting fluorocortisone tablets, a drug used extensively clinically in patients suffering from orthostatic hypotension (fainting episodes upon standing). Additional information on the onset and regulation of the blood pressure changes were obtained in this study. They showed that the function of both sympathetic and parasympathetic chains of autonomic control of blood pressure are already impaired by 7 days of exposure to the effects of simulated microgravity. Very preliminary results suggest that fluorocortisone may provide advantages over the salt/water load currently used in preventing orthostatic intolerance.

Ames-Moffett contact: J. Vernikos
(415) 604-3736 or FTS 464-3736
Headquarters program office: OSSA

Adaptation to Altered Gravito-Inertial Environments

R. Welch, M. M. Cohen

Exposure to altered gravito-inertial environments (hyper- and hypogravity) causes initial disruptions of both perception and performance. These effects include the mislocalization of visual objects, errors in hand-eye coordination, alteration in the gain of the vestibulo-ocular reflex, and disturbances of postural equilibrium and locomotion. Although astronauts' experiences during orbital missions suggest that many of these problems (as produced by hypogravity) dissipate after a short period of time, it is important that both these effects and the adaptive process by which they are overcome be understood. The current research aims to accomplish this goal.

The research involves a three-pronged approach: (1) to identify, verify, and quantify the initial effects of altered gravito-inertial states on human perception and perceptual-motor performance; (2) to determine the time-course of adaptation to these states; and (3) to devise a training procedure by which the adaptive processes may be facilitated.

One set of ongoing experiments entails exposing human subjects to hypergravity (1.75 g) in Ames Research Center's 20-g centrifuge for a period of 20-30 minutes. Mislocalization of a visual target (the "elevator illusion") and errors in hand-eye coordination are measured at the onset of the exposure period. Subjects are then allowed to point at a target and are provided with both visual and proprioceptive/kinesthetic feedback about their errors. Periodically, they are measured on the strength of the elevator illusion. It is expected that both hand-eye coordination and (more importantly) visual localization will become more accurate over the course of the hypergravic exposure period.

Of particular interest will be the possibility that repeated alternation between hypergravity and normal gravity, distributed over a period of weeks or perhaps months, will lead to the acquisition of simultaneous adaptations to both gravitational environments. Such potential "dual adaptations" would thus allow subjects to move between the two situations with little or no disruption of perception or performance.

A second set of experiments is examining the issue of dual adaptations by means of an "analog experiment." That is, instead of altering the gravito-inertial environment, a rearrangement of hand-eye coordination (a visual tracking task) is being used. Human subjects are provided with the experience of alternating between a normal tracking task and one involving a 108° rotation between movements of the hand and movements of a visual cursor viewed on a video monitor. Results confirm that dual adaptations can be produced and that the primary cue "informing" subjects about which environment they are in at a given time is feedback from their initial interactions with the environment. Ongoing experiments are examining the possibility that repeated alternation between the two visual tracking tasks produces a generalized ability to perform altered hand-eye relationships never previously experienced.

Ames-Moffett contact: R. Welch
(415) 604-5749 or FTS 464-5749
Headquarters program office: OSSA

Influence of Physical Activity Level on Bone Density

R. Whalen, T. Tamanaha, T. Hutchinson

On Earth the body is subjected daily to high musculoskeletal forces, particularly in the axial skeleton and lower limbs, during normal activities such as walking, running, and lifting. Body segment weight by itself is a small component of the total force when compared to the muscle forces required to stabilize and move the body or limb in the gravitational field of Earth. The levels of force in muscle, bone, and tendon are scaled by the strength of the gravitational field, body size, body shape, and the "intensity" of activity. The cumulative influence of the muscle and bone forces developed during daily activity, in combination with endocrine, metabolic, and genetic factors, maintains the mass and structure of muscle and bone.

The goal of our research, in the Life Science Division, is to gain a better understanding of the influence of mechanical forces on musculoskeletal homeostasis and functional adaptation. The objective of the first phase of our recent study was to assess the range in the level of daily activity in a group of 53 normal, astronaut-age males. Activity logs and the number of walking steps taken each day, monitored with calibrated stepmeters, were recorded during a consecutive 10-week period.

Results indicate that a "normal" lifestyle is, in fact, quite sedentary. The mean of 8,000 steps taken is equivalent to about 6.5 kilometers walking, or less than 80 minutes walking per day at a normal pace of 1.4 meters/step. An interesting finding was that heel bone mineral density was not significantly related to the number of daily steps, yet individuals engaged in exercise activities generating high musculoskeletal forces maintained higher levels of bone mineral density than non-exercisers. This has important implications for the optimization of exercise countermeasures in space.

In the second phase of the study, the gait of each subject was video-taped and the ground reaction forces were measured with a forceplate embedded in a walkway. This information is being processed and will be combined with a biomechanical model to obtain more accurate estimates of the forces and average daily loading histories exerted on the heel of each subject. These data will then be used to validate and refine current mathematical models that relate bone density to the daily history of forces exerted on the bone.

Ames-Moffett contact: R. Whalen
(415) 604-3280 or FTS 464-3280
Headquarters program office: OSSA

Musculoskeletal Loading with Lower Body Negative Pressure

R. T. Whalen, A. R. Hargens, D. E. Watenpaugh, D. F. Schwandt

The probable cause of bone demineralization and muscle atrophy in space is the reduction in the levels of muscle force required to perform exercise and other daily activities. Other factors, unique to "microgravity" environments, such as the loss of fluid hydrostatic pressure gradients, may also exert a systemic influence. We have proposed a novel way of imposing a high external axial force on the body using lower body negative pressure (LBNP) which, when coupled with exercise, shows promise as a simple and reliable way of developing physiological levels of bone-on-bone and muscle forces in the lower body in "microgravity" environments. (See article titled "Lower Body Negative Pressure Provides Load Bearing for Humans Exposed to Microgravity" by A. R. Hargens, R. T. Whalen, D. E. Watenpaugh, G. Murthy, and D. F. Schwandt.)

The concept of loading the body is illustrated in parts (a) and (b) of the figure in which the lower limbs are enclosed in a chamber that isolates them from the upper body by a flexible, vacuum seal at the waist. The seal allows "frictionless" movement in the axial (z-axis) direction. As air is evacuated from the chamber, a resultant external force, equal to the product of the pressure differential (Δp) and waist cross-sectional area (A_{xy}), is applied to the body at the centroid of the cross-section. This force, along with body weight (on Earth) and the inertial force of accelerating the center of mass of the body, contribute to the total vertical ground reaction force (GRF_z). The magnitude of the vertical component of the ground reaction force provides a good estimate of the lower limb musculoskeletal forces developed during "upright" activities.

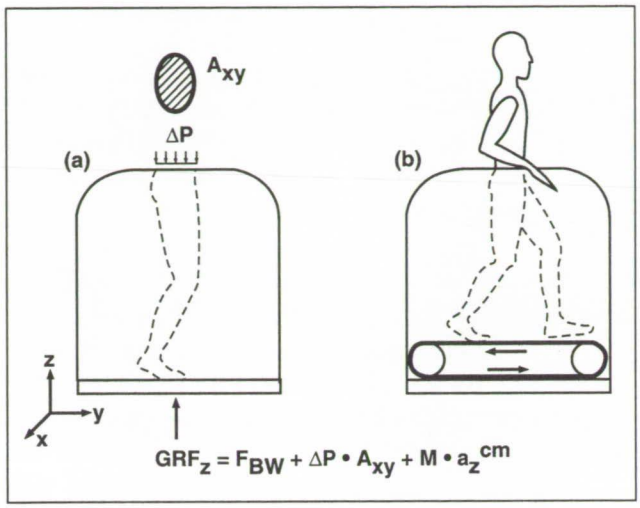


Fig. 1. Differential pressure as a means of applying an axial force on the body during exercise. (a) Force from the pressure difference ($DP \times A_{xy}$) and the vertical component of the ground reaction force (GRF_z), composed of body weight (F_{BW}), the pressure force, and the inertial force of accelerating the mass of the body ($M \times a_z^{cm}$), are illustrated; (b) treadmill, mounted inside the chamber, and a negative chamber pressure of 100 millimeters Hg will be used to approximate 1-g walking and running in space

Waist and hip cross-sectional areas for a wide range of body sizes were estimated from anthropometric data in current scientific literature and were used to calculate the range in pressure required to produce a force equivalent to one Earth body weight. With the vacuum seal located between the hip and

waist, predicted pressures were nearly independent of body size and approximately equal to 13.3 kilopascals (or 0.13 atmosphere).

Although not a body force like gravity, the force resulting from the air pressure resembles the action of gravity in several important ways. Most importantly, the center of pressure, the location of the resultant force, is at or very near the center of mass of the body (and center of gravity on Earth) during "upright" activities. Also, the applied force throughout the gait cycle should be nearly constant even without pressure regulation, since the displaced volume during exercise is small compared to the total chamber volume. If the chamber seal is air-tight, the device acts like a constant force, energy-conserving spring. And finally, since the air pressure is uniformly distributed over the surface of the body, the force is not detected as a localized force pulling down (or pushing) on the body.

The dynamics of walking and running (and related activities) performed in the chamber in "microgravity," and the musculoskeletal forces in the lower limbs, are anticipated to be similar to normal activity on Earth, even in the absence of body segment weights and gravitational moments of force. This is an important consideration since tissue stress histories in space may need to be comparable or equivalent to tissue stress histories on Earth to avoid musculoskeletal tissue loss and diminished motor coordination.

Ames-Moffett contact: R. Whalen
(415) 604-3280 or FTS 464-3280
Headquarters program office: OSSA

Characterization of Neurospora Circadian Rhythms Experiment

ORIGINAL PAGE
BLACK AND WHITE PHOTOGRAPH

Randy Berthold

The Characterization of Neurospora Circadian Rhythms Experiment (CNCR) was successfully flown as a mid-deck experiment on the Space Shuttle Columbia, January 9-19, 1990. For almost 2 months, the Principal Investigator (PI), Dr. J. Ferraro, Southern Illinois University, and the Secondary Payloads Project team worked around slips, scrubs, poor weather, and a multitude of obstacles to finally fly what Johnny Carson quipped was "NBC commissary mold!"

The team drew on its collective experience to overcome some interesting "challenges." There were facilities problems with power outages and runaway environmental temperatures. Real-time changes had to be made to in-flight operations. Even new flight foam inserts for the locker were built and certified in 8 hours.

The mission achieved its goals and objectives and the CNCR experiment may have actually accomplished more than what was originally defined.

By performing various real-time changes to the in-flight operations, the PI feels extra data points and a phase response curve may have been obtained. The flight specimens, after extensive computer analysis, indicated that the biological clock was slowed after exposure to microgravity. This implies that the human biological clock can be either advanced or delayed, depending on microgravity-specific environmental factors.

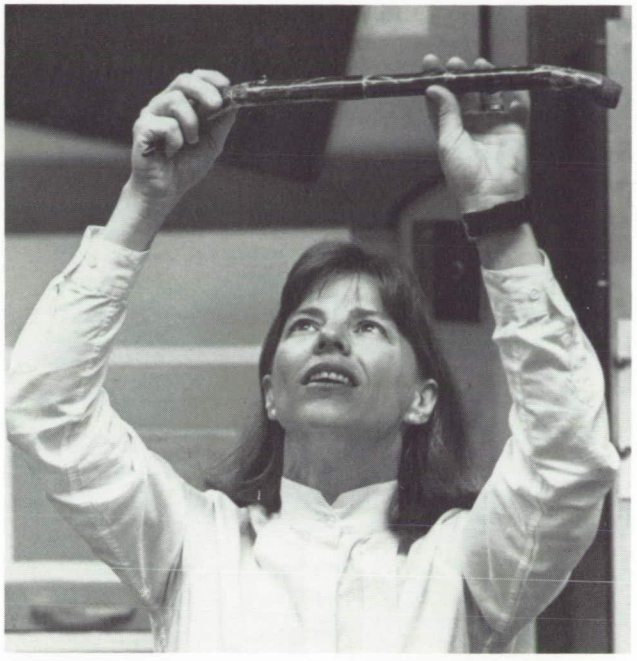


Fig. 1. Astronaut B. Dunbar establishing the growth front of the experiment to be flown on STS 32

Ames-Moffett contact: C. Winget
(415) 604-5753 or FTS 464-5753
Headquarters program office: OSSA

Growth Hormone Concentration and Distribution in Plants

Randy Berthold

The Growth Hormone Concentration and Distribution in Plants experiment flown on Space Transportation System 34 from October 13-23, 1989, was based on the hypothesis that the concentration and distribution of the plant growth hormone, Indoleacetic Acid (IAA), would be affected by microgravity. To study the effects of zero gravity on the distribution of IAA, the experiment required that plant seedlings (*Zea mays*, or corn) be grown in complete darkness in zero gravity.

At Kennedy Space Center Hangar L Pre-flight Facility, the seeds were prepared in a hood for placement into the flight canisters. No unusual or dangerous chemicals were used for this procedure. During pre-flight activities, the passive liquid nitrogen freezer (GN_2) was also prepared for flight. This involved a NASA procedure that has been used on previous Shuttle flights. The GN_2 freezer was charged with several liters of liquid nitrogen under strict safety guidelines and then decanted.

The plants were grown from seeds planted inside four hollow stainless steel canisters 18 hours prior to flight. During flight, the plants grew for 4 days. Two canisters were placed inside the gaseous nitrogen freezer to arrest plant growth and preserve the IAA inside the plant tissue. Two other plant canisters remained untouched for a post-flight analysis of continued growth. A detailed analysis of IAA concentration and distribution in the plant will be made of frozen samples.

Post-flight, the frozen canisters were placed into a dry ice (frozen carbon dioxide) shipping container that was sent to the Principal Investigator's laboratory. Post-flight synchronous control data analysis is not complete. However, an extensive analysis of flight data indicates that the microgravity environment affects plant growth. This implies that growth of plants on long-duration missions (e.g., space station) will need further study. These results also may provide information relevant to plant growth on Earth.

Ames-Moffett contact: C. Winget
(415) 604-5753 or FTS 464-5753
Headquarters program office: OSSA

Spacelab Life Sciences-1: 1990 Events

Bonnie P. Dalton

FY 90 was a year of watchful waiting and practicing for the Ames Research Center Spacelab Life Sciences (SLS)-1 Project. Major pieces of rack-mounted hardware were delivered to the Kennedy Space Center (KSC) during the previous 2 years and were fully integrated by the conclusion of 1989. These included the Research Animal Holding Facility (RAHF), the General Purpose Work Station (GPWS), and the Refrigerator/Incubator Module (R/IM). Due to the lack of flight racks at a development center, we experienced a fit problem when transferring the GPWS from the Ames ground rack to the KSC flight rack. The less than 1/8-inch interference with the flight rack structure required careful cutting into the cabinet frame to ensure fit without damage.

Ames continued to provide major design engineering support following integration of the GPWS to rectify negative margins discovered during the Marshall Spacelab analyses. As a result of the effort, the two overhead lockers located in the GPWS had to be removed and were replaced by a solid panel.

The GPWS is a self-contained unit providing approximately 10 cubic feet of interior working space and manipulation of biologicals including aldehyde fixatives. It will be maintained within its same flight rack structure from SLS-1 into Spacelab J where it will be used by both American and Japanese investigators.

The RAHF has been refurbished from its maiden flight on Spacelab 3 (1985) to ensure particulate containment. Though capable of sustaining 24 rodents, only 20 rodents will be maintained within the RAHF on SLS-1. Two double-cage compartments will be outfitted to test particulate containment during the flight. Modification of the cages includes addition of a single pass auxiliary fan (which pulls particulates within the module), reformulation of the rodent food bar for less crumbling, and overall "structural tightening" to ensure containment.

The R/IM has flown on STS 26, 29, and 35. The unit will be used in SLS-1 to maintain a 28°C environment for a jellyfish experiment.

Stowage items were sent on a locker-by-locker basis to Johnson Space Center (JSC) where the foam infrastructure was cut and then processed on to KSC. Stowage items, though significantly smaller in size than rack-mounted items, require a high level of coordination between engineering and training personnel because optimal use of the items is subject to orientation within the stowage compartment. Stowage items ranged in size from an Olympus camcorder and its mounting brackets, a Zeiss microscope, Zero boxes, an Animal Enclosure Module (AEM) water refill box, and a General Purpose Transfer Unit which can contain an RAHF cage, to small battery packs, disposable gloves, masks, wipes, and pen markers.

The AEMs have been used many times, since their inception, in the Student Shuttle Involvement Program with STS 8. The units on SLS-1 will differ in that they have automatic lighting control and a water box that can be refilled "in flight." SLS-1 will provide the only opportunity to date to compare data from animals group-housed within the AEM versus single housing in the RAHF.

Flight hardware function was verified during the Level IV and III/II Mission Sequence Tests and the Health Checks at KSC. Flight crew (mission and payload specialists) and Ames ground crew (Payload Operations Control Center members) training and hardware tests were conducted during the nine Mission Integrated Training Simulation sessions conducted at JSC with mock-up hardware. The year ended with the science and logistics ground crew furthering their training during a 2-week simulation of pre-flight Hangar L operations at KSC in December. The simulation included not only the Ames SLS-1 cadre, but all Ames SLS-1 investigators and their team members, a total of 83 people.

Ames-Moffett contact: B. Dalton
(415) 604-6188 or FTS 464-6188
Headquarters program office: OSSA

Astrophysical Simulation and Analysis Facility

Louis Allamandola, Farid Salama, Scott Sandford, William Schutte, Robert Walker

Experimental studies of materials produced under conditions similar to those in interstellar space—comets, some planets and their satellites—are performed to provide the fundamental data needed to design future space missions and to interpret the measurements made with existing NASA telescopes and satellites. The principal goals are to (1) discover the composition of these very different celestial objects and, with this information, deduce the evolutionary history of these objects; and (2) describe the role these materials play in determining the physical and radiative properties of these objects.

Currently, we are able to measure the ultraviolet, visible, and infrared spectroscopic properties of these materials at temperatures ranging from a few degrees above absolute zero to room temperature. By detailed comparisons of these spectral properties with astronomical spectra measured from telescopes, one is able to determine the composition of the astronomical objects.

In addition to our projects, we collaborate with many other researchers on other projects, both in and outside of NASA. Recent collaborations include the first measurement of the ultraviolet and visible spectroscopic properties of the ionized PAH, naphthalene, isolated in neon. This information, the first of its kind on a PAH that is truly isolated as in space, has direct applications in several areas. In particular, this will be used to determine how interstellar ultraviolet and visible radiation is so efficiently converted into infrared radiation. The chemical evolution of PAHs in different radiation environments, and the detailed dependence of their infrared emission properties on size and structure has also been successfully modeled. This model will now be used to deduce how PAHs are distributed throughout many different interstellar objects.

In addition to work on PAHs, studies of interstellar, planetary, and cometary ices are also under way. For example, our detailed spectroscopic observations of the interstellar medium revealed the ubiquity of an absorption band, which is characteristic of a general class of hydrocarbons.

The detailed comparison (first figure) of this interstellar band with the hydrocarbon band produced

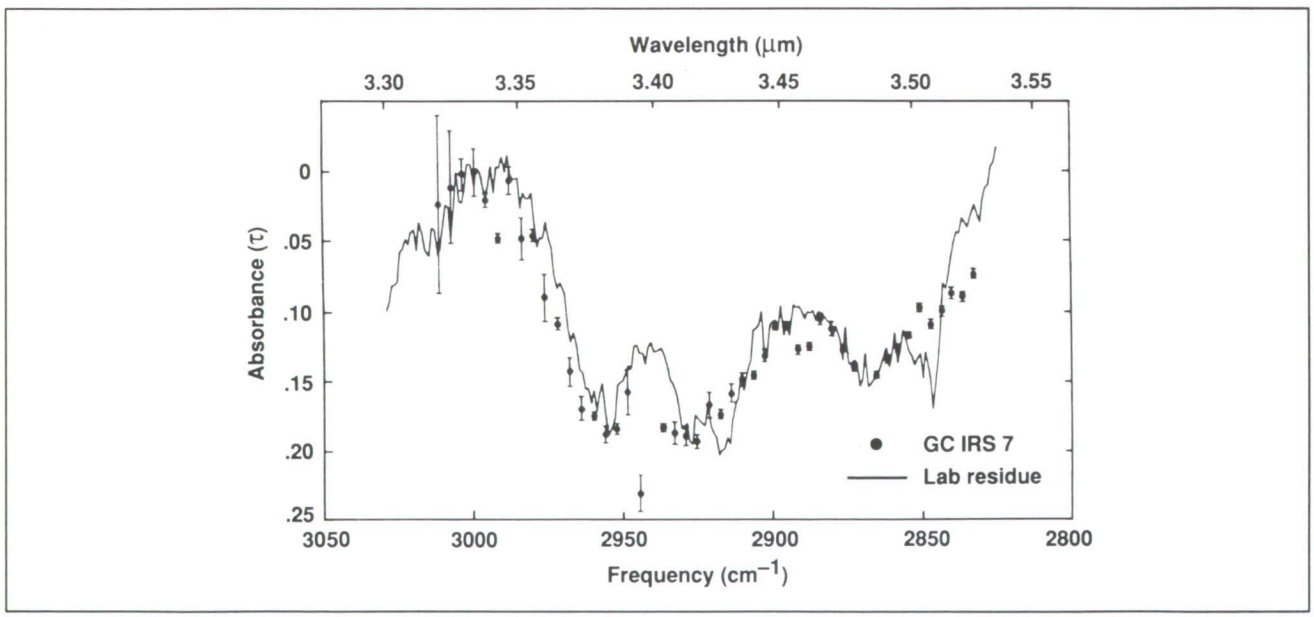


Fig. 1. Comparison of the hydrocarbon spectral fingerprint toward the Galactic Center with that produced in the laboratory. The excellent fit implies that this type of material is common throughout space.

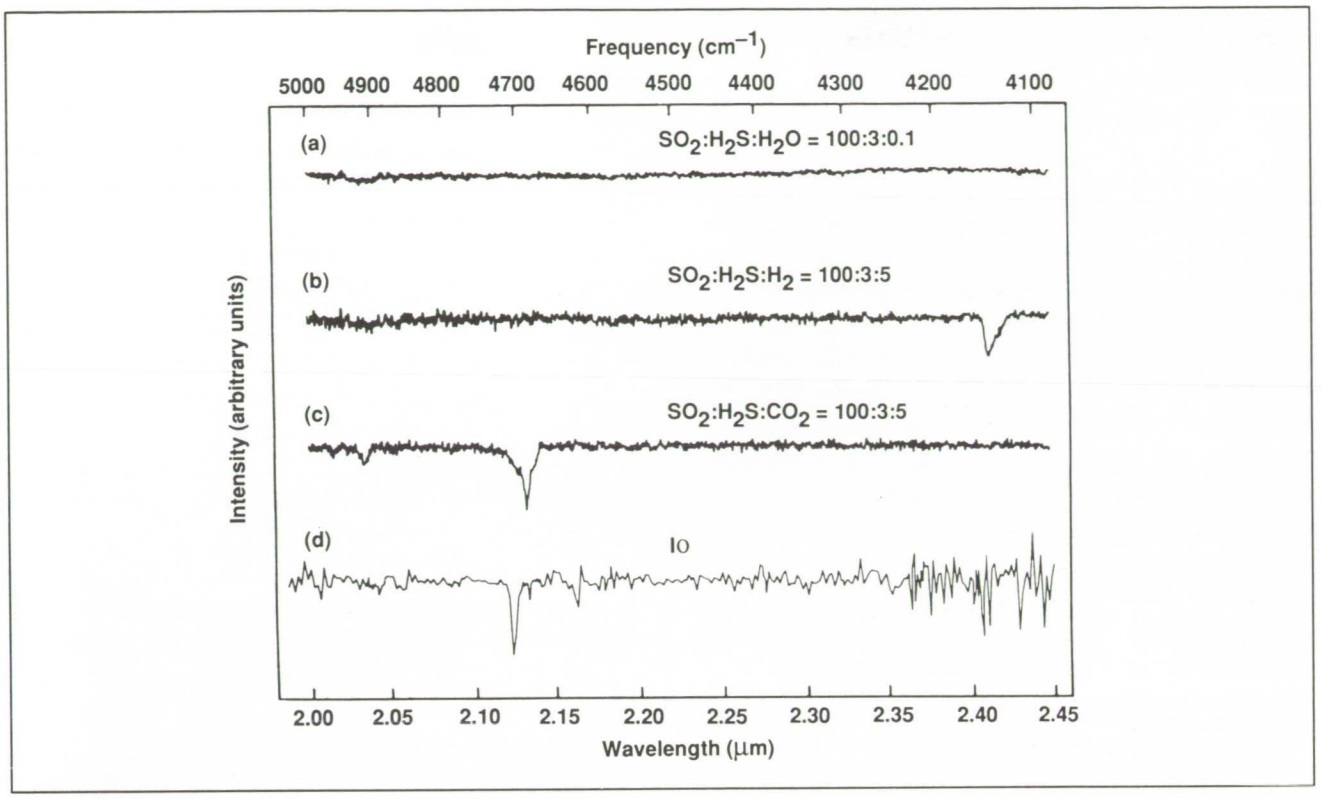


Fig. 2. Comparison of the spectral features of several Io ice analogs with the newly discovered absorption band on Io. The close match between the spectrum of the CO_2 containing ice with the Io spectrum suggests that CO_2 may be present on Io.

in laboratory simulations of the radiative processing of interstellar/pre-cometary ice analogs has given great insight into the chemical and physical nature of this complex, organic, interstellar material. This work also shows how much cosmic carbon is in this molecular form, and reveals the evolutionary processes which produced it. These materials will now be analyzed chemically and will be searched for on the Comet Rendezvous and Asteroid Flyby mission.

Finally, an extensive set of laboratory experiments was carried out to determine the spectral properties of CO_2 frozen in many different ices. This data base will be invaluable in analyzing spectra obtained by space-borne infrared telescopes. Furthermore, the comparison of these spectra (second figure) with the newly discovered infrared absorption on Io (a moon of Jupiter) suggests that CO_2 may be present. If this is verified with subsequent studies, this will be the first evidence for carbon on this satellite.

Ames-Moffett contact: L. Allamandola/
S. Sandford
(415) 604-6890/6849 or FTS 464-6890/6849
Headquarters program office: OSSA

Search for Planet Formation Debris Signatures

Dana E. Backman, Fred C. Witteborn

Planetesimals (small precursors to planets) are believed to have formed by the rapid accumulation of dust and gases orbiting very young stars. Collisions between orbit-crossing planetesimals are expected to destroy many of them, generating giant debris clouds that slowly spiral into the star or are swept up by the surviving planetesimals. These eventually become the full-sized planets. While it is not presently feasible to detect planets around distant stars, debris clouds are much easier to detect because they have enormously large surface areas, even when they are of relatively low mass (as low as 1% of the mass). The thermal emission is expected to peak in the 5-20 micrometer range for debris associated with terrestrial planet formation. Thus, we can look for evidence of planet formation by studying excess (i.e., nonstellar) infrared radiation from the vicinities of young stars.

In preliminary work aimed at this search, we have studied co-added Infrared Astronomical Satellite (IRAS) survey data on 176 A-F main sequence stars in four nearby open clusters with ages less than 10^9 years. IRAS photometry was not accurate enough to discern individual stars later than class "A" in three of the clusters studied. However, statistical statements can be made about the presence or absence of small infrared excesses in the cluster stars considered as groups.

In the figure it can be seen that there is clearly greater than 12-micrometer luminosity from "A" stars in the two younger clusters (α Persei and Pleiades,

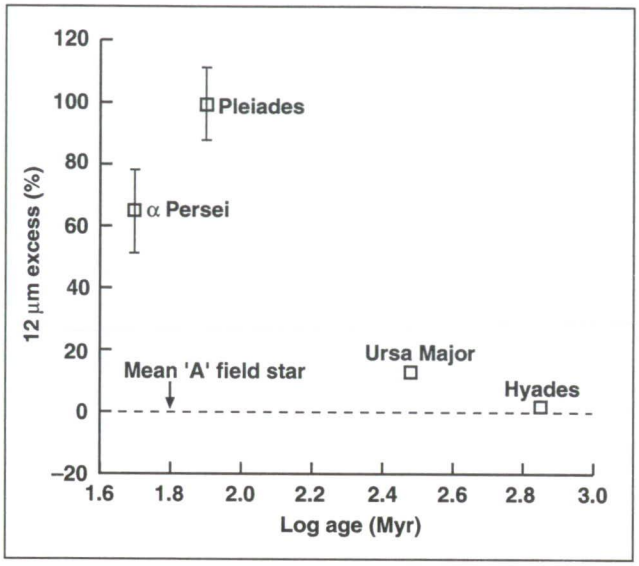


Fig. 1. Average cluster "A" star infrared excess versus age

t = 50-80 million years (Myr)) than in the older two (Ursa Major and Hyades, t = 300-700 Myr). There is no comparable significant trend, at the IRAS co-added survey sensitivity level, in the F and G stars. This may be because the clusters are too distant for this type of study on those spectral types, which will have to await proposed observations on the Multiple Mirror Telescope, Mt. Hopkins, Arizona, and NASA's Infrared Telescope Facility, Mauna Kea, Hawaii.

The Hyades stars, with ages approaching half the typical main sequence lifetimes of "A" stars appear to have visual-to-infrared colors very close to those of average field stars. The somewhat younger Ursa Major stream stars are close enough to Earth to allow photometric precision such that their small excess relative to field stars is still significant.

It is likely that the excess in the "A" stars is due to solid debris at temperatures on the order of 200 Kelvin, to account for the observed contrast relative to the stellar photospheres at 12 micrometers. The 12/25 micrometer ratios indicate that the excesses cannot be due to free-free emission or companion stars. The presence of significant excesses in Pleiades "A" stars was not correlated with the presence of reflection nebulosity, so the material in the thin molecular cloud that the Pleiades appear to be passing through is unlikely to be the cause of the excesses in that cluster. The trend with cluster age indicates that the grains are progressively destroyed or swept up.

The amount of solid mass indicated in the Pleiades per star is roughly 10% of the mass of Earth if the particles are imagined to have (1) grain size distribution following a power law in radius with exponent –3.5, (2) a size range from 0.1-micrometer to 50-kilometer radius, and (3) spatial and mass distributions like the solid planetary material in our solar system.

Subsequent work will be directed at isolating individual stars exhibiting infrared excesses and measuring their infrared spectra to find characteristic signatures of silicates and other expected debris constituents.

Ames-Moffett contact: D. Backman
(415) 604-4216 or FTS 464-4216
Headquarters program office: OSSA

Detection of Nanophase Lepidocrocite in Iron-Smectite Mars Soil Analog Materials

Amos Banin, David F. Blake

Smectite clays were suggested as important components of the Mars soil on the basis of various spectral, chemical, and geological evidence. Specifically, iron-enriched smectite clays were shown to simulate many of the findings of the Viking Labeled Release experiments on Mars, and to have spectral reflectance in the visible range, strongly resembling the bright regions on Mars (see first figure). The mineralogical nature of the iron phases of these Mars analog-clay systems has not yet been fully characterized. The iron phases were found to be virtually amorphous using X-ray powder diffractometry; to possess extremely small particle size; and to have high specific surface area and high reactivity in the catalytic decomposition of certain organics.

In conjunction with T. Ben-Shlomo, of the Hebrew University in Rehovot, Israel, we have employed thermodynamic, selected area electron diffraction (SAED), and micro-analytical methods to characterize the nano-size iron phases in Mars soil analog materials (MarSAM) iron-enriched smectite clays. We have found that the major crystalline phase is lepidocrocite (γ-FeOOH). The presence of less crystalline phases such as the double-hydroxy salts of Fe(II)-Fe(III) ("green rust"), ferrihydrite ($Fe_5O_7(OH)O4H_2O$) and completely "amorphous" iron oxides and oxyhydroxides cannot be ruled out.

Lepidocrocite (γ-FeOOH) has been suggested in the past as the major iron mineral in Mars soil mainly on the basis of speculations on the weathering scenarios of rocks at a fluctuating water table. Another geological scenario, supported by laboratory experiments, suggested oxidative weathering of iron sulfide minerals by acidic ground water leading to the formation of goethite(α-FeOOH) and jarosite ($(M)Fe_3(SO_4)_2(OH)_6$). Nanophase hematite (α-Fe_2O_3) has also been suggested as the major iron-oxide mineral in the weathered surface materials on Mars. This was based on similarities between laboratory measurements of the spectral reflectance of certain mixtures of nanophase hematite with other matrix minerals, and the spectral reflectance of Mars measured from Earth.

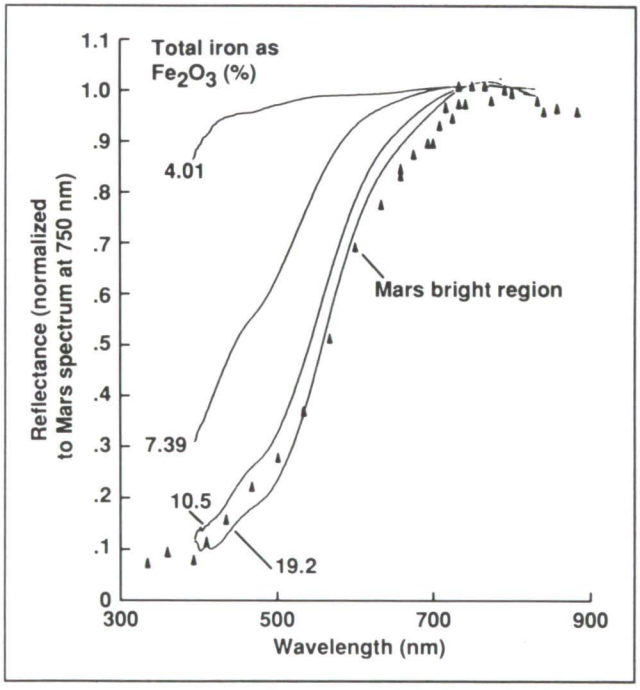


Fig. 1. Spectral reflectance of MarSAM and of the bright regions on Mars in the visual to near-infrared (VIS-NIR) range

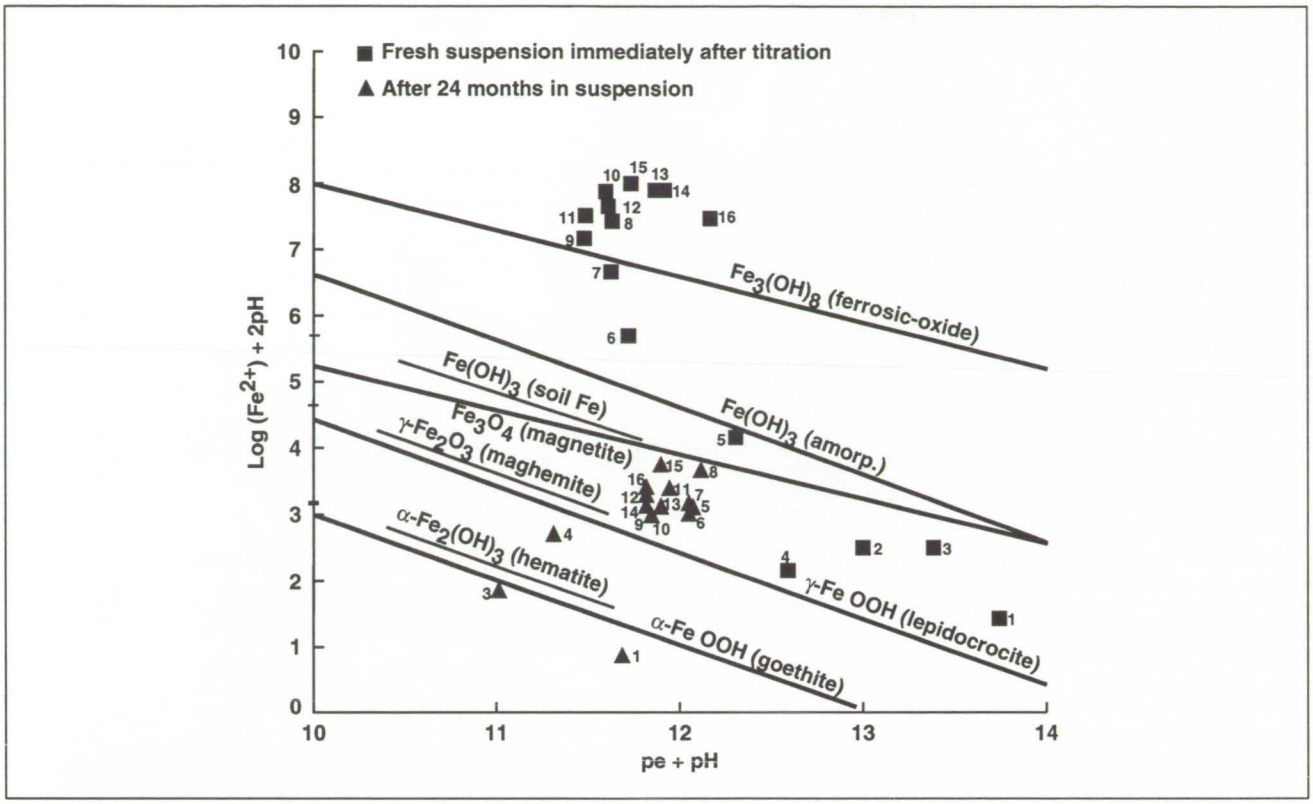


Fig. 2. Solubility relationships of iron oxide and oxyhydroxide minerals and of iron-enriched Mars soil analogs

The second figure shows solubility relationships of iron oxide and oxyhydroxide minerals and of iron-enriched Mars soil analogs. Smectite clays were treated with increasing amounts of $FeCl_2$ solutions (1-16). Measurements of pH, Eh, and Fe^{2+} in solution were taken immediately, and after 24 months of storage at 5°C (pe = Eh(mV)/59). Ferrosic-oxide ($Fe_3(OH)_8$) seems to have been formed in the fresh suspensions in samples 7 to 16. Aging caused slow transformation into more stable crystalline iron oxides, involving completion of iron oxidation. After 24 months, iron solubility was apparently controlled by a solid slightly more soluble than lepidocrocite and maghemite and less soluble than $Fe(OH)_3$ and soil Fe.

Our findings show that iron-enriched smectites, mineral systems that display spectral and chemical similarity to Mars soil, contain nanophase lepidocrocite and not nanophase hematite. We conclude that the spectral reflectance method may not be efficient and discriminating enough to identify nanophase iron oxide minerals that seem to prevail on the surface of Mars. Studies continue to characterize nanophase iron oxyhydroxides in MarSAM and to suggest better mineralogical protocols for their identification in Mars soil and dust.

Ames-Moffett contact: A. Banin
(415) 604-6631 or FTS 464-6631
Headquarters program office: OSSA

Global Properties of the Heliosphere

A. Barnes, P. Gazis, J. Mihalov

The Pioneer and Voyager spacecraft are situated in an excellent configuration for exploring the global properties of the outer heliosphere. Pioneer 10 is now nearly 50 astronomical units (au) from the Sun near the solar equatorial plane; Pioneer 11 and Voyager 2 are at nearly the same heliocentric distance (about 30 au) and longitude, but Pioneer 11 is about 17° north of Voyager 2 in latitude (see figure). All three spacecraft have working plasma analyzers, so that intercomparison of data from these spacecraft provides important information about the global character of the outer solar wind.

The morphology of the heliosphere varies with the solar cycle, and in ways that are, at best, only partly understood. During the period around the past solar minimum (1985-1987) Pioneer 11 at 17° North heliographic latitude was observing fast solar wind, characteristic of the high latitude corona; whereas Pioneer 10 and Voyager 2 near the ecliptic were observing relatively slow wind from near-equatorial regions of the corona. During this period the current sheet associated with the interplanetary magnetic field lay below the latitude of Pioneer 11. In contrast, during the subsequent period (1987-present) of increasingly high solar activity, the strong latitudinal gradient in solar wind speed has disappeared. In fact, there are occasional signs of a reverse gradient (higher velocities near the solar equator). The magnetic polarity of the Sun is expected to reverse this year or next. A number of transient high-speed flows have been observed in the distant heliosphere; these are presumably associated with violent coronal events. A study to identify the source events and associated inner-heliospheric disturbances is under way.

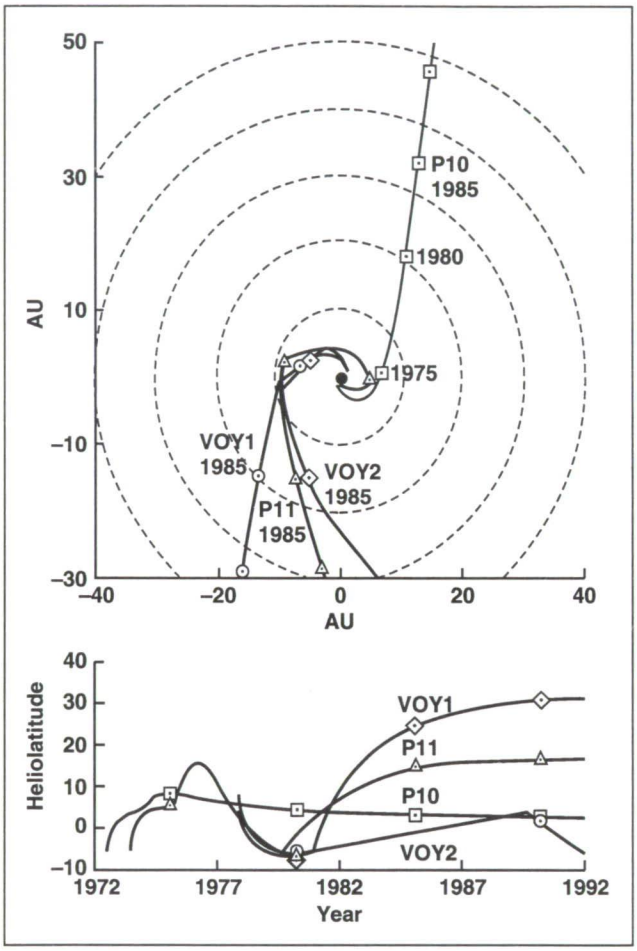


Fig. 1. Pioneer and Voyager Spacecraft trajectories

As far out as 48 au, the averaged solar wind velocity continues to exhibit its well-known variation with solar cycle: average velocities are highest near solar minimum, and lowest near solar maximum.

The solar wind density continues to drop as expected with increasing heliocentric distance, and the temperature shows no sign of rising at great heliocentric distance, as might be expected from interaction with the interstellar medium.

The detailed structure of the solar wind is similar to what was seen during the last solar maximum. For much of the time, the solar wind is characterized by "pressure waves," i.e., correlated enhancements of density and temperature associated with nearly constant solar wind speed. At other times, the solar wind contains long-term velocity enhancements, nonperiodic disturbances that persist for long time periods (less than or comparable to 100 days).

No indication of the presence of a heliospheric terminal shock has been detected to date.

Ames Research Center scientists participating in this research are A. Barnes, P. Gazis, and J. Mihalov.

Outside collaborators participating in various aspects of this activity are A. Hundhausen, High Altitude Observatory; A. Lazarus, Massachusetts Institute of Technology; F. McDonald, University of Maryland; J. Simpson, University of Chicago; E. Smith, Jet Propulsion Laboratory; J. Van Allen, University of Iowa.

Ames-Moffett contact: A. Barnes
(415) 604-5506 or FTS 464-5506
Headquarters program office: OSSA

Plasma Environment of Venus

A. Barnes, P. Gazis, J. Mihalov

The Pioneer Venus Orbiter (PVO) with most of its instruments operating well, including Ames Research Center's Orbiter Plasma Analyzer (OPA), continues to monitor the plasma environment of Venus. Using OPA data, we conducted a study of superthermal ion fluxes on the night side of the planet, in the energy range 10-250 electronvolts. These flows, which consist of singly ionized O^+ escaping from the planet, are found in about 5% of the nightside periapsis observations in the altitude range 800-2200 kilometers. In one exceptional period (1982, altitude 1100-1400 kilometers) ion escape was enhanced, appearing in about 15% of the observations.

In FY 90, measurements were repeated at similar altitudes, but at a time of higher solar activity and lower solar wind dynamic pressure. During this period the escape flux was reduced. The data from the earlier period (with enhanced escape fluxes) show individual episodes suggesting enhancement of flux with solar wind dynamic pressure. The mean flux escaping from the night side has not been observed to exceed 2×10^6 cm^{-2} s^{-1}, corresponding to a loss of not more than 10^{24} ions/second from the nightside of the planet.

One expects that at Venus, in analogy with Earth and Jupiter, solar wind ions can be reflected (or accelerated) at the planet's bow shock back into the solar wind. We have looked for such ions in data from the OPA, during those seasons when periapsis of PVO was high and when substantial portions of periapsis passages near noon were outside of Venus' bow shock. During these periods, sustained fluxes of ions (more energetic than those measured in the upstream solar wind), streaming away from the bow shock, were acquired. The observations suggest that these energetic ions (1) are protons that originate at the shock and (2) are energetic enough to travel upstream of the bow shock along the interplanetary magnetic field, as far as ~0.5 Venus radii. They maintain a beam-like character, when conditions are favorable, with the field intense and steady enough.

It is widely accepted that the observed nightside ionosphere of Venus is maintained by direct transport of ionospheric material from the dayside. In particular, high velocity (actually supersonic) nightward flows are observed by PVO near the terminator at altitudes higher than about 250 kilometers. We completed a theoretical study of such transport. In particular, we show that any transport from the high-pressure dayside to the low-pressure nightside can occur only if the flow passes through a transition to the supersonic regime. This condition implies substantial convergence of the subsonic streamlines, corresponding to a slow upwelling of the dayside ionosphere. At high altitudes this plasma is accelerated horizontally, is constricted, and undergoes a supersonic transition near the terminator. Beyond the terminator the flow remains supersonic, but the flow speed is below escape velocity, so that the accelerated plasma cannot escape from the planet. This plasma must therefore be incorporated into the nightside ionosphere, probably undergoing a shock transition.

Ames Research Center scientists participating in this research are A. Barnes, P. Gazis, and J. Mihalov.

Outside collaborators participating in various aspects of this activity are L. Brace and R. Theis, Goddard Space Flight Center; C. Russell, University of California, Los Angeles; and K. Moore and D. McComas, Los Alamos National Laboratory.

Ames-Moffett contact: A. Barnes
(415) 604-5506 or FTS 464-5506
Headquarters program office: OSSA

Stable Isotope Analysis Using Tunable Diode Laser Spectroscopy

Joe Becker, Todd Sauke

Measurements of ratios of stable isotopes are used in such diverse fields as petroleum prospecting, medical diagnostics, and planetary exploration. The development of semiconductor laser technology has progressed to the point where tunable diode lasers can be realistically considered for a reliable, lightweight, high-resolution molecular spectrometer, suitable for flight hardware.

Ratios of $^{13}C/^{12}C$ in carbon dioxide have been measured using our tunable diode laser spectrometer to a present accuracy of better than 0.4%. These results were made possible by using state-of-the-art, high-temperature tunable diode lasers, an etalon and wavenumber calibration technique, high-speed assembly language controlled data acquisition, and the ratioing of absorbances from simultaneously acquired sample and reference data scans. Increased accuracy will result from improving temperature stabilization of the gas cells and by incorporating the instrument response function into the data-fitting model to account for known instrumental distortions.

Data for an individual ratio determination are obtained over a time of less than 1 minute, while the sequence of 20 pairs of spectra was obtained over a time of about 30 minutes. The length of time required to acquire the data can be drastically reduced by more efficient data file handling and by using a faster computer. Because the accuracy of the present measurement is limited by systematic rather than statistical errors, the number of co-added scans per spectrum can be reduced to speed up the data acquisition without seriously compromising accuracy. In fact, faster data acquisition may improve accuracy by limiting the time during which system drifts can occur. Overall optimization in choice of sample pressure, scanning repetition rate, number of scans to signal average, and other experimental details should yield further improvements in accuracy and speed.

It is expected that these and other improvements in technique that are now being implemented, in collaboration with Max Loewenstein (Atmospheric Chemistry and Dynamics Branch), will allow determinations of isotopic ratios to better than 0.1% for measurement times substantially shorter than 1 minute, perhaps several seconds. Using this laser technique, isotopic ratios can be measured without the extensive sample purification required for mass spectrometric analysis; many of the commonly expected impurity gases can be present in the sample without adversely affecting the measurement. By optimizing sample cell configuration, the amount of carbon required to make an isotopic ratio determination can be less than a microgram.

The rugged, lightweight and reliable, tunable diode laser is ideally suited for use in instruments both in the laboratory and in the field. Tunable diode laser spectroscopy should be a useful technique for in situ measurements of isotopic ratios in such diverse fields as medical diagnostics using expired CO_2 in human breath, petroleum exploration, and planetary exploration missions.

Ames-Moffett contact: J. Becker
(415) 604-3213 or FTS 464-3213
Headquarters program office: OSSA

Phase Relationships in Low-Temperature Mixed Ices

ORIGINAL PAGE
BLACK AND WHITE PHOTOGRAPH

David Blake, Louis J. Allamandola

Comets are thought to be the most primitive objects in the solar system, containing pristine remnants of the solar nebula and perhaps of the interstellar molecular cloud that preceded it. From remote observations, it is known that cometary bodies contain mostly water ice with varying amounts of other volatiles, rocky materials, and prebiotic organic matter. A knowledge of the phases and components of cometary ice will provide insight into extraterrestrial prebiotic organic chemistry, as well as providing ground truth for proposed cometary missions (e.g., Comet Rendezvous Asteroid Flyby). We have modified an electron microscope to allow for the vapor deposition, thermal processing, and in situ observation of mixed ices in the temperature range 12-200 Kelvin (K). We report here observations of a simple mixed ice (2:1 H_2O:CH_3OH).

When a 2:1 H_2O:CH_3OH mixture is vapor-deposited onto a thin carbon substrate held at 85 K inside the microscope, an amorphous solid is formed (see first figure). Diffraction patterns show two diffuse maxima similar to amorphous water ice (part A, second figure). As the ice is warmed, a phase separation occurs at about 129 K (see third figure). Two phases can be characterized by electron diffraction. One of the phases appears to be cubic water ice (part B, second figure). The second phase has not been identified but it has a relatively high symmetry, possibly cubic. When this two-phase assemblage is further warmed, the unidentified phase sublimes at about 150 K, leaving a porous microstructure of hexagonal ice (part C of second figure and the fourth figure).

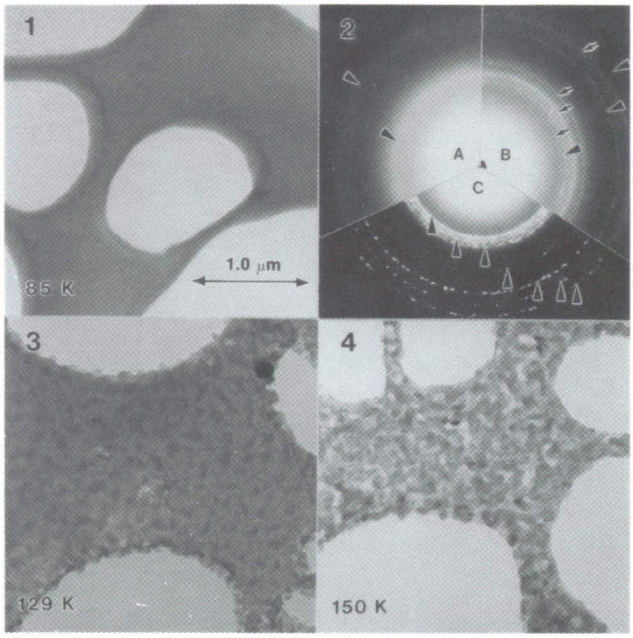


Fig. 1. Transmission electron microscope (TEM) micrograph of 2:1 H_2O:CH_3OH ice deposited onto holey carbon film. Note the apparent absence of structure in the ice (28,000 X magnification)

Fig. 2. Collage of diffraction patterns from Figs. 1, 3, and 4. (A) Amorphous pattern from as-deposited ice, 85 K. Arrows mark diffuse maxima typical of amorphous ice. (B) Diffraction pattern from sub-solidus phase separation at 129 K. Large arrows mark maxima for cubic water ice, small arrows mark maxima for a second, unidentified phase. (C) Diffraction pattern from hexagonal water ice after apparent sublimation of the unidentified second phase, 150 K. Large arrows mark maxima for hexagonal water ice

Fig. 3. Bright field TEM micrograph of 2:1 H_2O:CH_3OH ice after eutectoid phase separation at 129 K

Fig. 4. Bright field TEM micrograph of 2:1 H_2O:CH_3OH ice after warming to 150 K. The ice appears to be a porous microstructure of single-phase hexagonal water ice

Two observations can be made, which have relevance to the mechanical and gas release properties of comets. First, sub-solidus phase separations (those taking place in the solid state) are capable of imparting a wide range of mechanical properties to solids. The most well-known reaction of this type occurs in the system Fe-C, in which small amounts of carbon and other alloying elements, along with thermal annealing, produce the varied properties of steels. Second, solid-state phase separations produce a complex microstructure which, upon heating and sublimation of one of the phases, may result in a highly permeable microporous architecture. The presence of such microstructures in cometary ice may, in part, explain the observed variations in volatile release from comets as they enter the solar system. A knowledge of the mechanical and gas release properties of comets (and ultimately, a direct analysis of cometary ice by spacecraft) will allow scientists to unravel the origin and the thermal and chemical processing history of comets.

Ames-Moffett contact: D. Blake
(415) 604-4816 or FTS 464-4816
Headquarters program office: OSSA

Robotic Telescope Search for Other Planetary Systems

William J. Borucki

Although many lines of logic suggest that most stars are accompanied by planets, direct supporting evidence has been elusive. Determining if stars are accompanied by planets is of both scientific and human interest for a number of reasons. From a scientific viewpoint, if we knew what proportion of stars had planetary systems, what types of stars tended to be accompanied by planets, and what the sizes and orbital characteristics of the planets were, we would be able to more fully understand how stellar and planetary systems form and evolve.

Investigators have shown that high-precision photometric methods potentially could detect planets by searching for variations of stellar brightness and color that occur when a planet transits its star. The magnitude of brightness reduction is proportional to the ratio of the planet's and star's areas. For the solar system, the decrease in light amounts to 1% for giant planets, such as Jupiter and Saturn; 0.1% for planets like Uranus and Neptune; and 0.01% for Earth-sized planets. A highly characteristic color change caused by differential limb darkening, with an amplitude approximately 0.1 of that for the brightness reduction, would also accompany the transit. This could be used to verify that the source of brightness variation was a planetary transit rather than another phenomenon such as star spots. The photometric results should provide the planet size, period of orbit, and additional information about the activity cycles of the star.

Because the photometric method works only for objects whose orbital plane is near the line of sight between the Earth and the central star, the probability of observing a transit during a single observation is small. Hence the search program must be designed to continuously monitor hundreds of stars to attain a significant discovery rate.

To monitor hundreds of stars night after night for several years, in a careful and consistent manner, requires a robotic telescope. Recently, completely automatic photometric telescopes were developed and are in routine operation for a number of research programs. At Mt. Hopkins, Arizona, four 0.75-meter-aperture robotic telescopes specifically designed to do automatic photometry, are housed under one large roll-off roof in a totally automated observatory. The telescopes slew rapidly, find each star and center it with an electronic (CCD) camera, and check that each star has the correct magnitude and color index. Because the telescopes are designed for automatic photometry only, they readily make over 600 observations a night, even during the short nights of summer. Although robotic telescopes can make the many observations required, unless they can also make each observation with very high photometric precision, a photometric search will not be successful.

Space-based radiometric measurements of the Sun already detect changes as small as 0.001% and could readily detect transits by Earth-sized planets if the instrument sensitivity were large enough. However, ground-based photometers, which must observe through the terrestrial atmosphere, routinely attain a precision of only 1%. Nevertheless, because placing instruments in space is difficult and expensive, it is worth considering what could be done from a ground-based system using the latest technology. If a photometric precision of 500 or larger can be obtained routinely, then a ground-based search for large planets should be practical.

In FY 90, the Smithsonian Institution's 0.75-meter-aperture robotic telescope on Mt. Hopkins was used to determine the photometric accuracy of current systems. Two of the stars monitored were reported to be the least variable of all stars observed. A special effort was made to frequently observe the target stars, closely matched comparison stars, check stars, and extinction stars, and to operate in a consistent manner. Observations over a 3-month period showed a season-to-season precision of 0.17%. Such precision is adequate for determining the rotation rates of many stars and for detecting transits by Jupiter-sized objects from ground-based telescopes. These results show that it has become practical to conduct a ground-based photometric search for other planetary systems.

Ames-Moffett contact: B. Borucki
(415) 604-6492 or FTS 464-6492
Headquarters program office: OSSA

Search for Venusian Lightning

William J. Borucki, John W. Dyer,
James R. Phillips, Phan Pham

Lightning in planetary atmospheres is expected to cause the formation of trace gases and prebiological molecules. From optical measurements of the planetary flash frequency, the energy of the flash, the optical efficiency, and the molecular yields, it is possible to calculate the production of various molecular species. Three spacecraft experiments have provided evidence suggesting the occurrence of lightning activity in the venusian atmosphere: radio detection from Veneras 11, 12, 13, and 14; an optical detection of a single storm by the Venera 9 orbiter; and the low-frequency electric field variations detected by the Pioneer Venus orbiter electric field detector. However, a search by optical detectors on balloons floating in the clouds of Venus found no lightning activity.

The detection of lightning is somewhat of a surprise in that the meteorological conditions necessary to produce the lightning activity don't appear to be favorable on Venus. Theories of terrestrial lightning indicate that the presence of a large number density of precipitation particles with diameters of 1 millimeter or larger, and strong convective activity, is necessary for charge generation and separation before lightning can begin. Volcanism sometimes produces lightning, but again, only when large amounts of particulate matter are raining out in the presence of strong convective activity. Most volcanic activity produces no lightning.

Spacecraft entry probes descending through the atmosphere of Venus show the clouds to be composed of micrometer-sized particles rather than large particles, to have no convective activity, and to have a lower atmosphere free of dust. Although the clear lower atmosphere doesn't prove that there is no volcanic activity, it does indicate that violent volcanic activity isn't common.

Ames-Moffett contact: B. Borucki
(415) 604-6492 or FTS 464-6492
Headquarters program office: OSSA

Long Duration Exposure Facility Post-Retrieval Evaluation of Exobiology Interests

T. E. Bunch

The successful recovery of the Long Duration Exposure Facility (LDEF) will have many special rewards for space engineers and scientists who need to know the effects of long-term space erosion and the level of space contamination. Moreover, LDEF has functioned as a hard collector of interplanetary dust particles (IDP), also known as cosmic dust. Although particles that have collided with LDEF will not be in pristine condition, expectations are that some material will remain which can provide information as to the compositional character of the particle. LDEF samples are just now becoming available for study. We have developed experimental techniques to determine the effects of impact (particularly temperature) on carbonaceous materials.

Cursory examination of LDEF shows the existence of thousands of impact craters, of which less than one-third exceed 0.3 millimeter in diameter; the largest crater is 5.5 millimeters. All craters larger than 0.3 millimeter have been imaged and recorded into a data base by the preliminary examination team (the "A-Team"). Various portions of LDEF surfaces are contaminated by out-gassed materials from experimenters' trays, in addition to LDEF autocontamination, and impact with orbital debris not of extraterrestrial origin. Few craters show oblique impact morphology (low impact angle) and, surprisingly, only a low number of craters have recognizable impact debris (ejecta spray patterns, crater interior impactor residue). Study of this debris could be of interest to exobiology in terms of carbon content and carbonaceous materials.

Because IDPs nominally impacted LDEF at velocities greater than 3 kilometers/second, the potential for intact survival of carbonaceous compounds is mostly unknown. Calculations show that for solid phthalic acid (a test impactor), complete molecular dissociation into molecular fragments and atomic species would not necessarily occur below 3 kilometers/second, if all of the impact energy was directed at breaking molecular bonds; which is not the case. Most of the energy is used for crater formation and impactor disruption.

To confirm our expectations that some organic compounds (e.g., phthalic acid) can survive the lower hypervelocity impact regime, we performed impact experiments (LDEF analogs) by using Ames Research Center's Vertical Gun Range. Grains of phthalic acid and the Murchison meteorite (part a of the figure), grain diameter = 0.2 millimeter for both, were fired into an Al plate at 2.1 and 4.1 kilometers/second, respectively. Laser ionization mass spectrometry (LIMS) microanalyses of the impactor residues, performed by Filippo Radicati of Charles Evans & Assoc., confirm that phthalic acid molecules remain intact on impact at 2.1 kilometers/second (parts c and d of the figure) and some of the carbonaceous compounds in the Murchison meteorite retain their molecular integrity on impact at 4.1 kilometers/second.

We assume that some of the LDEF craters were formed at impact velocities less than 5 kilometers/second and conclude that meaningful biogenic element and compound information can be obtained from IDP impacts on LDEF. We recently received two LDEF crater samples with intact IDP debris (part d of the figure) and we expect to publish results on these and other samples in the near future.

Ames-Moffett contact: T. Bunch
(415) 604-5909 or FTS 464-5909
Headquarters program office: OSSA

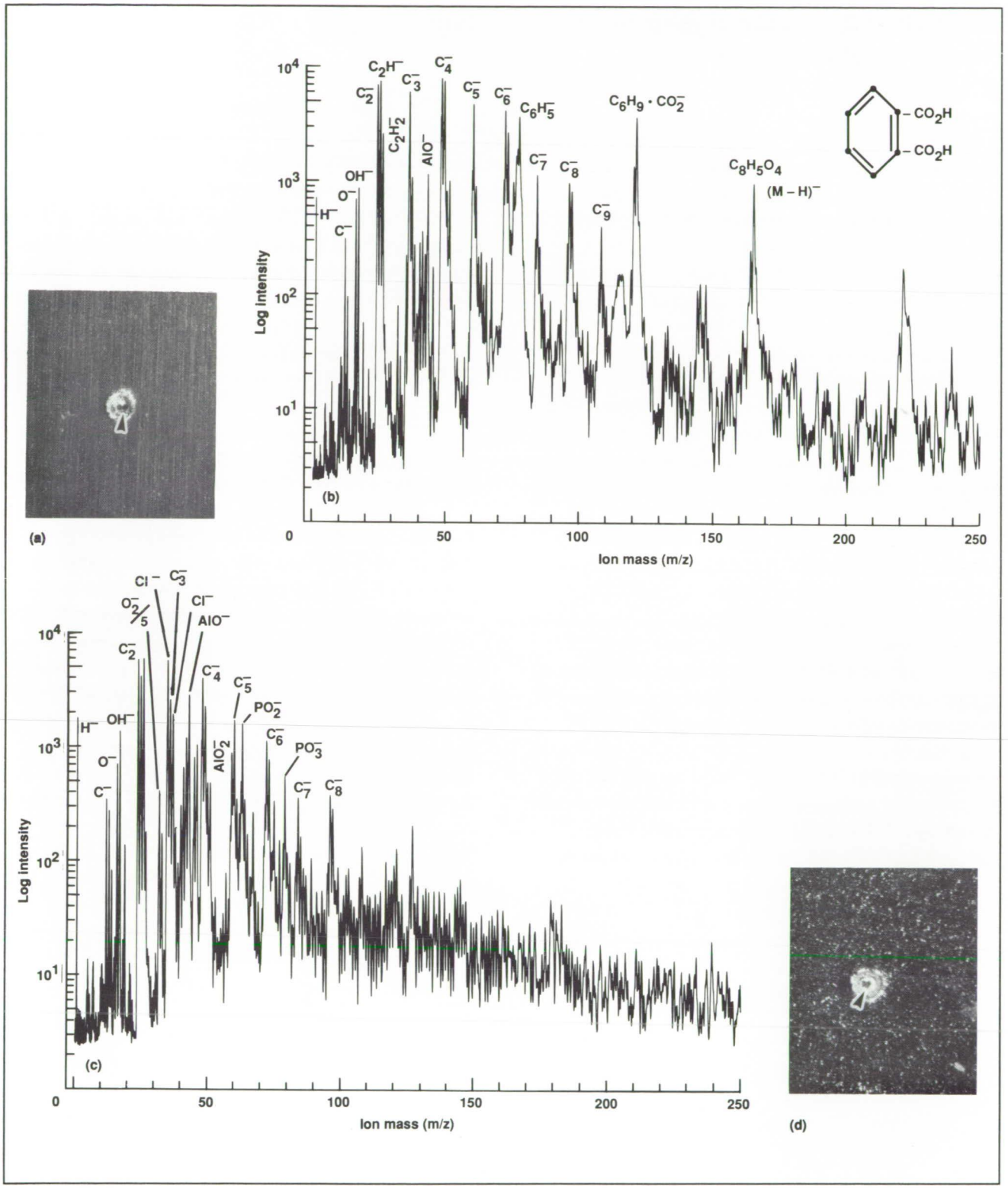


Fig. 1. (a) Vertical Gun Range test crater made by impacting a 0.2-millimeter Murchison meteorite particle at 4.1 kilometers/second. Note residue (arrow), crater diameter = 0.3 millimeter. (b) Laser microprobe spectrum of a phthalic acid impact crater showing the intact integrity of the acid molecule (arrow 1) and a minor molecular fragment (arrow 2). The remainder of the spectrum is attributed to contamination from gun powder, which is shown in (c). (d) LDEF crater with impacting particle residue (arrow), crater diameter = 0.120 millimeter.

Polycyclic Aromatic Hydrocarbon Molecules around Evolved Stars

Richard H. Buss, Jr., Alexander Tielens

After some stars evolve, they become rich in carbon and blow material into space as a shell around the star. In collaboration with Michael Werner and Martin Cohen, we observed some of these stellar shells in the infrared to learn more about the type of material in the shell. In particular, to discover if a certain class of molecules, polycyclic aromatic hydrocarbons (PAH), were in the shells, we obtained infrared spectra with Ames Research Center's Kuiper Airborne Observatory. We worked with Fred Witteborn's Faint Object Grating Spectrometer and group (Astrophysics Branch), including Jesse Bregman, Dianne Wooden, Amara Graps, Scott Sandford, and Dave Rank (Lick Observatory). In addition, spectra from the Infrared Astronomical Satellite (IRAS) Spectral Database obtained by Martin Cohen at Ames were used to study the circumstellar shells.

First, Buss, Tielens, and Ted Snow (University of Colorado) studied the mid-infrared IRAS spectra of cool carbon-giant stars with hot companion stars to search for infrared emission bands from PAHs in the shells of the carbon stars. One carbon giant with a hot companion, HD 38218, has a strong PAH-like 8-micrometer emission band. It is likely that the hot star companion excites the circumstellar PAH molecules of the cool carbon star shell, producing the observed 8-micrometer feature. Moreover, because the circumstellar PAHs appear to absorb both visible and ultraviolet light, they might be large compared to some interstellar PAH molecules. Since other carbon giant shells are likely to harbor PAH molecules, large circumstellar carbonaceous grains might form from PAH molecules.

Secondly, we took infrared spectra of two more evolved, warm carbon-rich stars known as transition stars. These warm transition stars (IRAS 22272 and 07134) show weak 3.3- and 6.2-micrometer emission bands and strong emission in 6.9- and 12-micrometer bands, as well as a strong, broad 6 to 9-micrometer plateau (see the figure). We attribute the 3.3- and 6.2-micrometer bands to circumstellar PAH molecules, and the 6- to 9-micrometer plateau and the 12- and 6.9-micrometer bands to larger aromatic hydrocarbon clusters. The observed emission band energy strengths suggest that relatively large PAH materials (>100 carbon atoms) are present around these warm transition stars and that material generally present in the space between stars might also have PAH emission similar to the evolved carbon-rich star PAH emission, as does the very evolved star shell, NGC 7027 (see the figure).

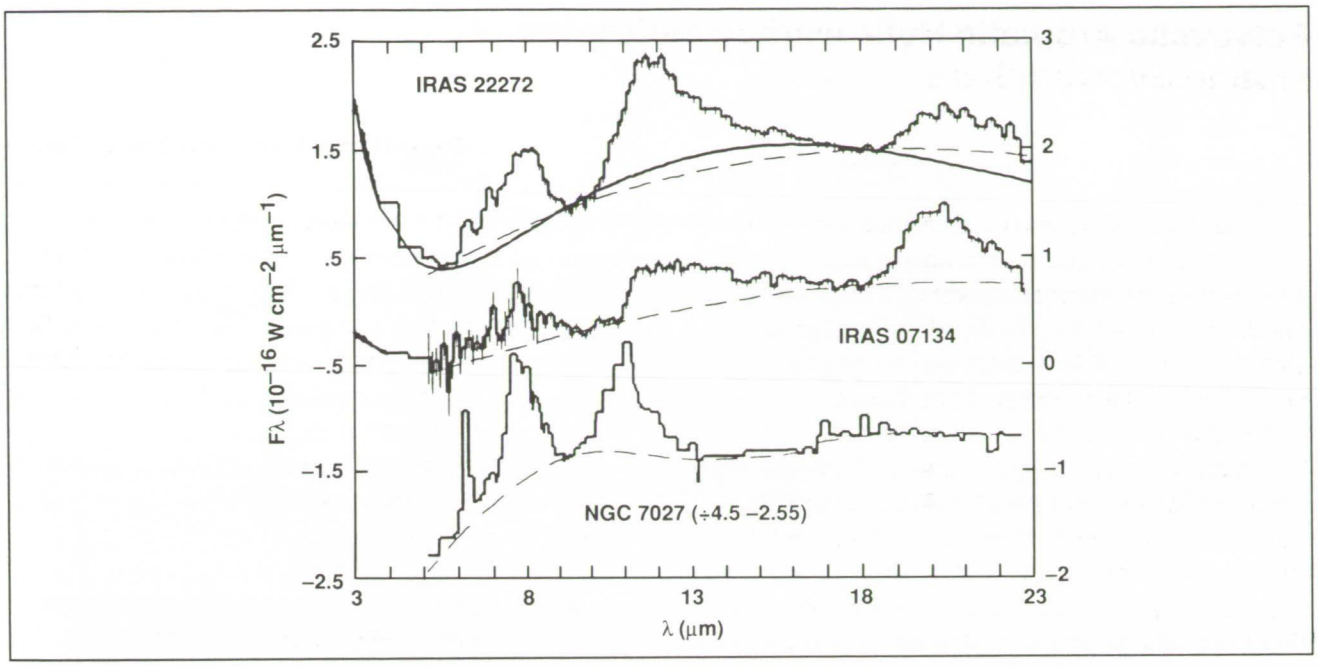


Fig. 1. The infrared spectrum of the transition branch objects IRAS 22272 and 07134 are compared to that of the planetary nebula NGC 7027. All 5-8 micrometer spectra have been obtained from the Kuiper Airborne Observatory. The longer wavelength spectra were taken by the Infrared Astronomical Satellite. In addition to the 12- and 21-micrometer emission bands, these objects exhibit aromatic hydrocarbon emission bands and plateaus from 6 to 9 micrometers.

Thus, during the course of FY90's research, we have found that some carbon-rich evolved-star shells harbor PAH materials, which may resemble and evolve into interstellar PAH materials. This link is important because cosmic PAHs might closely resemble organic materials on Earth.

Ames-Moffett contact: R. Buss
(415) 604-6857 or FTS 464-6857
Headquarters program office: OSSA

Sedimentary Records of Atmospheric O_2 Levels

D. E. Canfield

Although atmospheric O_2 is rapidly cycled through marine and terrestrial organisms, it is the burial and preservation of chemically reduced compounds in sediments that allow O_2 to accumulate in the atmosphere. The most important of these reduced substances is organic carbon, with pyrite (FeS_2) of somewhat lesser significance. Conversely, the weathering of organic carbon and pyrite acts as an O_2 sink. Levels of atmospheric O_2 have indeed changed over geologic time; over a long time scale, the atmosphere has evolved from an early reducing state to an oxidized one. This important transition likely resulted both from a decreased flux of reduced gases from the Earth's mantle and from an increased burial flux of organic carbon and pyrite into sediments. In collaboration with R. A. Berner at Yale University, we have determined that over Phanerozoic time (the past 570 million years) changes in the relative rates of burial and the weathering of reduced compounds probably created fluctuating O_2 levels.

Our approach has been to combine average values for the organic carbon and pyrite sulfur content of various sedimentary rock types (including marine clastics, continental redbeds, and coals) with the rates of burial of these rock types over time.

Important findings include the following: enhanced rates of O_2 production led to elevated atmospheric O_2 concentrations in the Cretaceous period (65-135 million years before present (mybp)), and the Permo-Carboniferous (~270-340 mybp). High O_2 production rates were the result of vast organic-rich coal deposition. During the Triassic (190-225 mybp), global climate was particularly arid, and coal-swamps gave way to the deposition of sediments, such as redbeds, which had little organic carbon and pyrite. The burial rates of reduced compounds were low (lower than their rates of weathering from older sedimentary rocks) and levels of atmospheric O_2 likely fell in response.

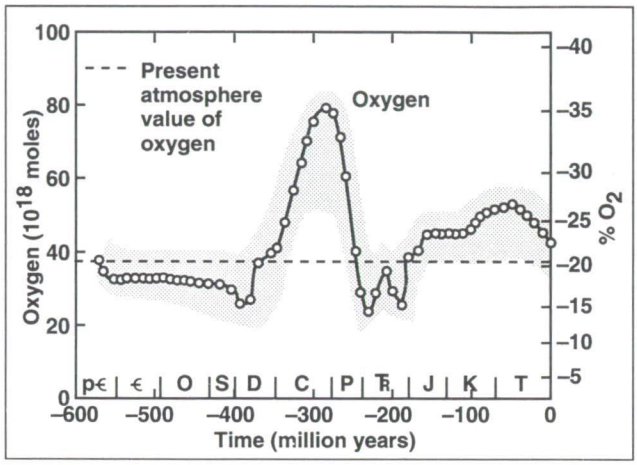


Fig. 1. Estimate of O_2 versus time through the Phanerozoic. The values of O_2 should be considered in a qualitative to semi-quantitative sense. The shaded "error" zone results from a sensitivity analysis of the various parameters used in the model. The dashed line represents the present atmospheric value

In principle, a similar modeling approach could be extended back in time to predict the timing and most important causes of the first appearance of appreciable O_2 in the atmosphere. To do this, however, we need additional information, including the chemical composition of sedimentary rocks deposited in the Precambrian Era (before 570 mybp), as well as a better idea as to when sulfate reduction arose as an important process of carbon oxidation.

Ames-Moffett contact: D. Canfield
(415) 604-5748 or FTS 464-5748
Headquarters program office: OSSA

Sulfate Reduction in Modern and Ancient Sediments

D. E. Canfield, D. J. Des Marais

Sulfur has likely played a key role in the evolution of life on Earth. In fact, Earth's first organisms might have obtained energy for growth from the chemical oxidation of reduced sulfur compounds emanating from thermal springs. Also, sulfur is common in the coenzymes and proteins used for energy transfer in modern organisms, and was probably involved in the earliest energy transfer systems. The central role of sulfur for life on Earth suggests that sulfur might have been equally important for life evolving elsewhere; such as Mars, where abundant sulfur has been detected on the regolith.

As Earth's ancient atmosphere and oceans became more oxidizing, dissolved sulfate accumulated in the oceans, and bacteria evolved that could gain energy by coupling the reduction of sulfate to the oxidation of organic matter. Sulfate reduction is also the most efficient anaerobic decomposition process. Sulfate reducers liberate more inorganic nutrients (N and P) than do, for example, methane-producing bacteria. This means that the evolution of sulfate-reducing bacteria allowed for a more dynamic and rapid cycling of carbon than was possible before their emergence. Sulfate reduction may be a very ancient process; evidence from molecular phylogeny suggests that sulfate-reducing bacteria are as old as cyanobacteria, which were likely the first oxygen-evolving organisms on Earth.

We are accumulating geochemical evidence for the antiquity of sulfate reduction on Earth. To do so, it is necessary to understand the geochemistry of sulfur in modern sediments that are the best homologs to ancient sediments as preserved in the rock record. Cyanobacterial mats, laminated microbial communities which are widespread but not particularly abundant on the modern Earth, are perhaps the best such homologs.

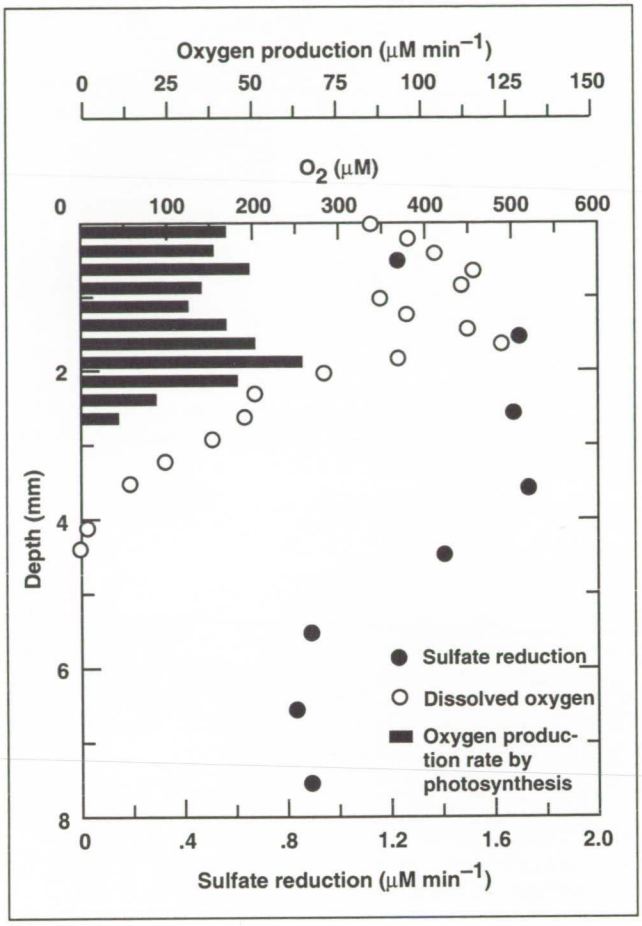


Fig. 1. Daytime depth distribution of sulfate reduction, dissolved O_2, and O_2 production rate by photosynthesis measured in cyanobacterial mats from Guerrero Negro, Baja California Sur, Mexico

In our studies of microbial mats from Guerrero Negro, Baja California Sur, Mexico, which are dominated by the cyanobacterium Microcoleus chthonoplastes, we find that sulfate reduction is very

important because it is responsible for 75% of the organic matter oxidation in the mats. Also, rates of sulfate reduction are extremely rapid and among the highest rates ever measured. Even with such rapid rates, the sulfide produced from sulfate reduction is highly fractionated isotopically; its $^{34}S/^{32}S$ value is about 5% lower than that of seawater sulfate. This sulfide forms the mineral pyrite. Thus the search for isotopically depleted pyrites in ancient rocks from a similar environment may constrain the timing of the emergence of sulfate reduction as an important organic carbon mineralization process.

Microscale studies of these same mats reveal that rapid rates of sulfate reduction are found during the day in the aerobic zone of the mat, where photosynthesis produces elevated levels of O_2. This finding challenges the conventional view that sulfate reduction is a strictly anaerobic process. We have not yet identified the biochemical pathway that promotes aerobic sulfate reduction. However, we suspect that sulfate-reducing bacteria exploit the tremendous reducing power (H_2 gas and dissolved organics) created by cyanobacteria during photosynthesis. Aerobic sulfate reduction may be an ancient phenomenon in cyanobacterial communities. This underscores the close association between sulfate-reducing bacteria and cyanobacteria in both time and space.

Ames-Moffett contact: D. Canfield
(415) 604-5748 or FTS 464-5748
Headquarters program office: OSSA

High Molecular Weight Polycyclic Aromatic Hydrocarbons and Fullerenes in Carbonaceous Meteorites

Sherwood Chang, Etta Peterson

The chemistry of aromatic carbonaceous material in meteorites lies at the intersection of lines of investigation coming from two other research areas: the role of polycyclic aromatic hydrocarbons (PAH) in interstellar chemistry and the laboratory synthesis and the characterization of soccerball-shaped "Buckminsterfullerenes" (e.g., C_{60}, "Buckey ball," and C_{70}). Although sizes of interstellar PAHs have been estimated to range from C_{20} to $>C_{50}$, the higher molecular weight fullerenes have also been suggested as interstellar species. Insofar as evidence already exists for organic matter of interstellar origin in meteorites, the nature and origin of meteoritic PAHs and the possible occurrence of fullerenes in meteorites are of considerable interest.

Typically, analyses of discrete PAHs in carbonaceous meteorites show the presence of species up to 20 carbon atoms (e.g., benzopyrene, $C_{20}H_{12}$), but mostly of species $<C_{16}$. Compounds containing 26 carbon atoms have been reported in the Allende meteorite, but molecular identifications were limited to species $<C_{20}$. Together with collaborators M. S. deVries, H. R. Wendt, and H. Hunziker (IBM Almaden Research Center, San Jose), we have detected and identified the highest molecular weight PAHs thus far observed. These species were found in carbonaceous residues obtained by acid dissolution of Murchison and Allende meteorite samples. We also note an intriguing correlation between the meteoritic products and those obtained by laser ablation of graphite in the presence of various amounts of H_2.

Samples derived from acid residues of the Murchison and Allende meteorites were analyzed by two-step laser desorption-photon ionization mass spectrometric (LD-PIMS) analysis. Vacuum sublimates of the residues were collected on a gold-plated sampling bar at three different temperatures (300, 450, and 600°C). The bar was then transferred to the LD-PIMS apparatus in which each of three spots of sublimed material was desorbed by pulses from a KrF laser. The desorbed molecules were entrained in a supersonic expansion, which was intersected downstream by light from an ArF laser for ionization. The ions were detected with a time-of-flight mass spectrometer. Analysis of the sampling bar between the sublimate spots gave no evidence of PAHs.

Part (a) of the first figure shows the mass spectra of sublimates from a Murchison sample. The most prominent peaks indicate the presence of PAHs such as anthracene and penanthrene (mass 178), pyrene (202), perylene (252), benzoperylene (276), and coronene (300). The spectra also show numerous higher mass peaks differing by multiples of 14 mass units from the unsubstituted PAHs. Ions from these alkylated derivatives may contribute to the envelope of masses on which the more prominent ions are superimposed.

This is the first time that PAHs of such high mass and carbon number have been observed in meteorites. The presence of coronene ($C_{24}H_{12}$) and its alkyl derivatives is particularly interesting because the main infrared emission bands of coronene appear to fit some of the unidentified interstellar emission bands in the infrared.

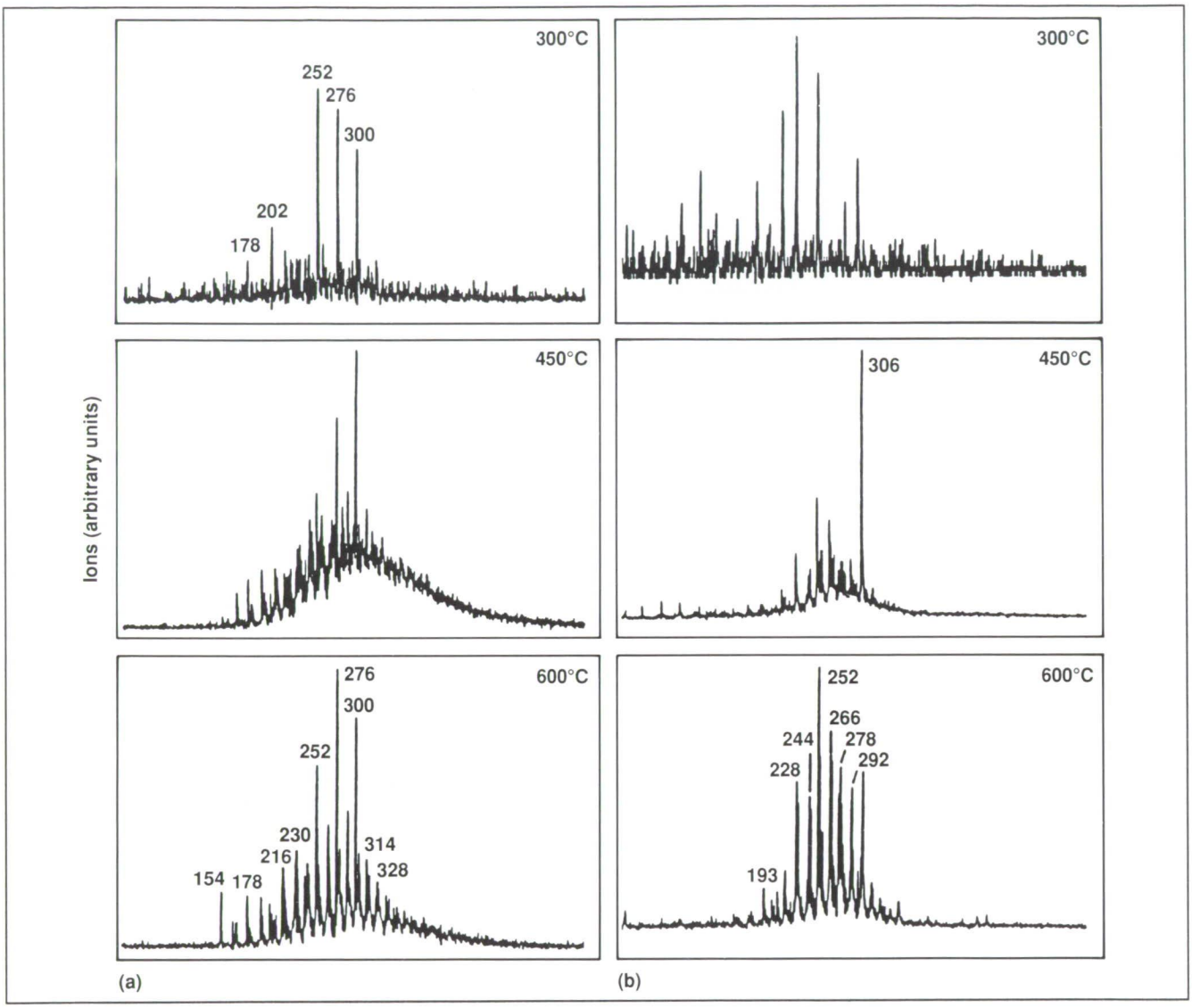


Fig. 1. Time-of-flight mass spectra obtained from samples collected at different temperatures by sublimation of (a) Murchison and (b) Allende acid residue samples

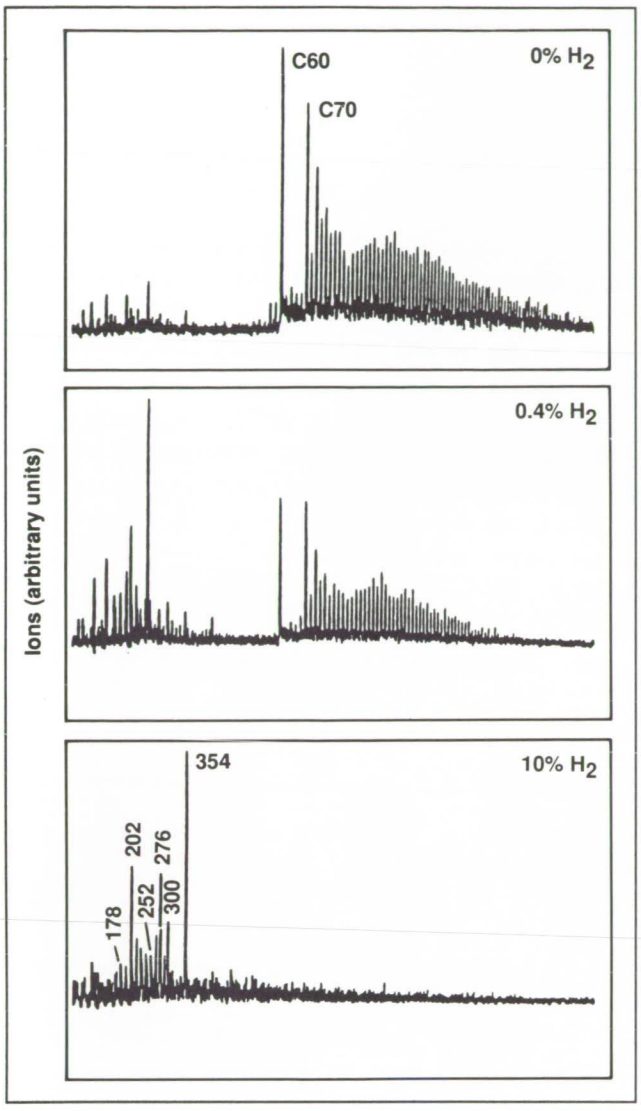


Fig. 2. Time-of-flight mass spectra of products of graphite ablation in Ar with different concentrations of H_2. Peaks above C_{70} in the top panel are 24 Atomic Mass Units apart

Part (b) of the first figure shows the results from an Allende sample. Generally, when analyzed under identical conditions, the Allende samples yielded less sublimate than did Murchison samples. PAHs are evident in the spectra, but they are less abundant; they exhibit a somewhat different PAH composition; and they appear to be relatively depleted in the more volatile species relative to Murchison PAHs. Fullerenes, however, have not been detected thus far.

Results shown in parts (a) and (b) of the first figure can be compared with analyses of material synthesized in the laboratory by laser ablation of graphite in 500 torr of Ar. Ablation products collected on a sample bar and analyzed in the LD-PIMS apparatus yielded the results shown in the second figure: a wide range of fullerene clusters with C_{60} and C_{70} most prominent. The other panels of the second figure show the effect of adding hydrogen to the Ar buffer gas. With increasing concentration of H_2, the production of fullerenes decreases, while synthesis of PAHs increases. At 10% H_2, fullerenes are no longer produced.

Remarkably, graphite ablation yields PAH distributions similar to those found in the meteorite samples. These results suggest that cosmic abundances of H_2 in circumstellar or interstellar environments may preclude the synthesis of fullerenes, but not the production of other PAHs.

Ames-Moffett contact: S. Chang
(415) 604-5733 or FTS 464-5733
Headquarters program office: OSSA

Organic Material on Solar System Bodies

Dale Cruikshank

Many of the small bodies of the outer solar system have surfaces that are very low in reflectivity. These surfaces are thought to be black because they contain carbon-rich material, probably the same as that in black carbonaceous meteorites. A new analysis of the infrared reflectance of a number of black asteroids, two comets, the rings of Uranus (known to be composed of black particles), and one hemisphere of Saturn's satellite, Iapetus, reveals a weak absorption band at 2.2-2.3 micrometers, which is identified as an overtone of the XCN fundamental (near 4.7 micrometers).

Ames Research Center researchers, D. P. Cruikshank and L. J. Allamandola (Astrophysics Branch), collaborated with W. K. Hartmann (Planetary Science Institute, Tucson), D. J. Tholen (University of Hawaii), R. H. Brown (Jet Propulsion Laboratory), and C. N. Matthews (University of Illinois, Chicago) in a study of this cyano-group absorption in solid materials in the laboratory and on various solar system bodies.

The presence of cyano-group molecules in solids gives clues to the role of water in the history of the surfaces on which it occurs. This molecular material is thought to originate in interstellar clouds and to be incorporated in the nebula from which the Sun and the planets formed. This study is the first to find a chemical link among a wide variety of types of solid bodies in the solar system.

Ames-Moffett contact: D. Cruikshank
(415) 604-4244 or FTS 464-4244
Headquarters program office: OSSA

Particle Gas Dynamics in the Protoplanetary Nebula

Jeffrey N. Cuzzi

During the last decade, a number of theoretical and observational studies have demonstrated the likelihood that flattened disks of dust and gas will form as a natural byproduct of stellar formation, and they have established their global thermal and dynamical properties. Collisional accretion of comet-sized planetesimals leads to the growth of solid planetary cores, followed by hydrodynamical accretion of nebula gas to form jovian-type planets in the outer solar system. However, poorly understood stages connect these landmark events, and earlier stages of accretion are even less well understood. For instance, accretion of the planets has long been thought to result from the settling of particulates into a sufficiently flattened layer that gravitational instability may occur. However, gas drag and turbulent shear in and around the particle layer may result in diffusional spreading of the particle layer, and may prevent gravitational instability.

We have developed a detailed numerical model of the early nebula environment that adequately treats the processes occurring in a medium containing two distinct phases (gas and particles). These phases obey different forcing functions, but are coupled by aerodynamic drag and are therefore able to influence each other's dynamical properties.

We have found that diffusive expansion of the particle layer, preventing gravitational instability, indeed continues until the particle sizes are considerably larger than previously expected. That is, we can show that particles must accrete to sizes approaching planetesimals themselves (tens to hundreds of meters, depending on their density) before they can become gravitationally unstable.

For the first time, we have also demonstrated in detail the dynamics and mean motion of the gas and particle phases. A radial outward flow is set up in the gas in the vicinity of the particle layer. There is also an associated inward drift of the particle phase, caused by momentum transfer between the particle layer and the intermingled gas.

In FY 90, we have implemented several alternative formulations for the viscosity of the particle phase itself, which allowed us to explore much denser particle layers—those with a mass density over one hundred times that of the surrounding gas. We also ran model evolutions at two different distances from the early Sun—the current distance of the Earth (1 astronomical unit (au)) and of Saturn (10 au). The entire gas and particle disk at 10 au is considerably more vertically distended than at 1 au, but not sufficiently so to cause the particles to be more stable against early gravitational instability.

In collaboration with Stuart Weidenschilling, Planetary Science Institute (Division of SAI International, Tucson, Arizona, we wrote a review chapter for "Protostars and Planets II." In this chapter new results for particle accretion in the nebula are included, which incorporate our numerical results in a parametrized way. These particle growth calculations (nine at 1 au) allow the particles to grow as porous fractal particles, and show that growth to 10- to 100-meter size is quite rapid (takes only a few thousand years). This is considerably less than the accretion timescale one infers from meteorite data; however, perfect sticking is assumed in these first model efforts and this growth rate must be regarded as an upper limit. It is more likely that collisions produce different combinations of accumulation and destruction, stretching out the period of planetesimal accretion.

Ames-Moffett contact: J. Cuzzi
(415) 604-6343 or FTS 464-6343
Headquarters program office: OSSA

Planetary Ring Dynamics and Morphology

Jeffrey N. Cuzzi

Planetary rings as a class share many structural similarities, and presumably similar controlling processes. Obviously, there are great differences in detailed structure between the broad, opaque rings of Saturn; the nearly transparent rings of Jupiter; the dark, narrow rings of Uranus; and the incomplete ring-arcs of Neptune. On the other hand, these systems are quite similar in their combinations of diffuse rings of material interspersed with belts or ensembles of mountain-sized "moonlets."

We hope to understand these similarities and differences in terms of the conditions of formation and the operation of similar processes in different environments. Since the Voyager encounters of Jupiter (1977), Saturn (1980-81), Uranus (1986), and Neptune (1989), our understanding of ring structure has been greatly enhanced. From an understanding of the structure and dynamics of planetary rings, we hope to gain insight into the process by which planets form from their own protoplanetary particle disks.

One of our major accomplishments this year has been the first truly realistic modeling of the process by which material gets redistributed within ring systems following meteoroid bombardment. This work is a collaborative effort with R. Durisen at Indiana University.

The coupled transport of mass and angular momentum, combined with the normal viscous processes acting in particle disks, can result in complex and nonintuitive structures such as small-scale fluctuations; systematic buildup or erosion of material near certain kinds of edges; and other structures similar in many ways to features observed in the rings. This modeling is a major numerical effort, as it needs to account for the angular and velocity distribution of the ejected material in a realistic way.

We have recently determined that, when the angular and velocity distribution of the ejecta is well modeled, and the viscosity of the ring material is simultaneously treated, structure is observed at the inner boundary of a region of large optical depth (where it adjoins a region of lower optical depth). This is highly reminiscent of a structure observed at the inner boundaries of both the A and B rings of Saturn. This structure consists of a 1000-kilometer-wide linear "ramp" of material extending inward of the boundary, and the generation of an "irregular" structure on several-hundred-kilometer lengthscales outward of the boundary. Each length scale reflects a different facet of the transport process.

In a related study, Cuzzi and Jet Propulsion Laboratory collaborator Linda Horn have shown that the apparently "irregular" structure within Saturn's B ring indeed has definite preferred scales, which vary throughout the rings. In the inner B ring, the preferred scale is about 100 kilometers, and in the outer two-thirds of the B ring the preferred scale is about 300 kilometers. In light of the above mechanism, one suspects that these scale lengths constrain ejection velocities (and therefore surface properties) and/or ring viscosity (which acts to diffuse structure).

One other very exciting development during FY 90 was the discovery by our Stanford University collaborator Mark Showalter of a new moon embedded within a gap in Saturn's rings. The moon had been predicted by Cuzzi and Jeffrey Scargle of Ames Research Center in 1985. It was discovered by Showalter, using inferences of the precise orbital and geometrical parameters for the moon derived from a model that we constructed collaboratively in 1986. The moon, tentatively named Pan (the Greek god of shepherding, which is the generic term in popular use for ring confinement by local moons) is about 10 kilometers in radius and sufficiently bright to be an icy object. The presence of such an object within Saturn's rings where it would have great difficulty accumulating (it lies within an empty gap) strongly favors the idea that rings derive from preexisting moons, and not the other way around.

Finally, we have concluded a major study of the properties of Saturn's E ring. This work is primarily that of Showalter. This work integrated six major data sets with a common geometrical and radiative transfer modeling approach for the first time. The E ring was found to have a very peculiar particle-size distribution, entirely dominated by a very narrow range of micron-sized particles. The reason for this is not known, but these tiny particles must be replenished, probably from the geologically young-looking satellite Enceladus, on a timescale of decades or centuries.

Ames-Moffett contact: J. Cuzzi
(415) 604-6343 or FTS 464-6343
Headquarters program office: OSSA

Microbial Mats, Stromatolites, and the Rise of Molecular Oxygen in Earth's Early Atmosphere

David J. Des Marais

The size of our atmosphere's molecular oxygen (O_2) inventory reflects a balance between a source principally from oxygenic photosynthesis and from sinks (which include oxygen respiration and the weathering of reduced materials in sediments and rocks).

Microbial mats are stratified communities which grow within the environmental microgradients situated at the surfaces between water and a solid substrate. Stromatolites, the fossils of layered accumulations of microbial mats, occur in rocks as old as 3.5 billion years. Because these mats are therefore quite ancient, and because many mats contain oxygen-producing (oxygenic) photosynthetic microorganisms, we have explored the role of microbial mats in the accumulation of O_2.

Oxygenic photosynthesis very likely first appeared in ancient microbial mats. The early evolution of the primitive nonoxygen-producing photosynthetic bacteria created a diverse array of light-harvesting photosynthetic pigments, such as the chlorophylls and carotenoids. This diversification was driven, at least in part, by competition for light within microbial communities.

Working in collaboration with B. Jorgensen (Aarhus University, Denmark), our group has shown that a typical photosynthetic microbial mat exhibits steep light gradients within a few millimeters of its surface. In collaboration with A. Palmisano (now with Procter and Gamble Corp.), we have documented

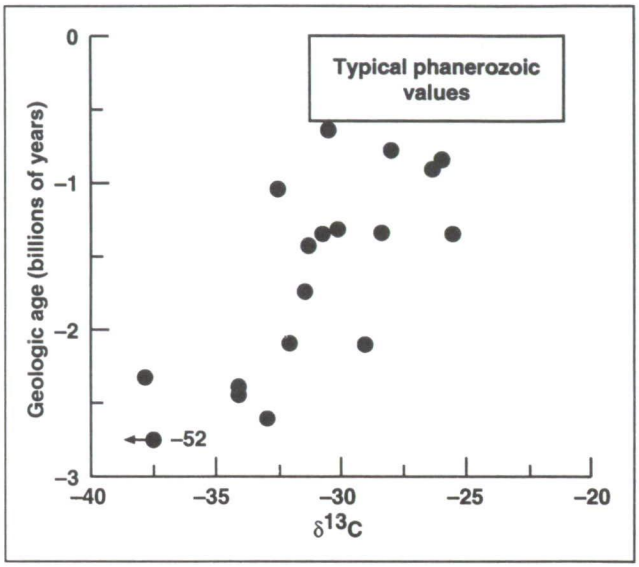


Fig. 1. Carbon isotopic composition of stromatolitic organic matter versus its age. The term $\delta^{13}C$ on the horizontal axis represents a sample's $^{13}C/^{12}C$ value, relative to a "PDB" limestone standard ($^{13}C/^{12}C$ = 0.0112372), as follows:

$$\delta^{13}C = (((^{13}C/^{12}C)sample/(^{13}C/^{12}C)standard) - 1)1000$$

Data point at lower left represents a $\delta^{13}C$ value of –52, plotting offscale to the left. Box labeled "Typical Phanerozoic" depicts the range of $\delta^{13}C$ values observed for all samples of sedimentary organic carbon from that age interval

dramatic millimeter-scale variations with depth in the composition of pigments. Such an environment in the mat has compelled the bacteria to share the available light energy by harvesting different wavelengths at various depths. This depth stratification might have provided the incentive for diversification of the light-harvesting apparatus, leading ultimately to oxygenic photosynthesis.

The size of the ancient atmospheric O_2 reservoir increased because its photosynthetic source was larger than its sinks. This imbalance occurred because some of the reduced organic carbon produced during oxygenic photosynthesis escaped reoxidation by being buried in sediments. The burial of other reduced species, such as ferrous iron and sulfides, also enhanced O_2 levels. However, organic carbon was, and still is, by far the largest reduced reservoir in the Earth's crust.

Working in collaboration with H. Strauss (University of Bochum, Germany) and J. Hayes (Indiana University), we estimated the relative amounts of the reduced (organic) and oxidized (carbonate) carbon in stromatolites of Proterozoic age, 2.7 to 0.6 billion years old. These estimates were obtained from measurements of the stable carbon isotopic composition of well-preserved organic matter and carbonates (limestones, dolomites, etc.). Using our previous knowledge of the average isotopic composition of crustal carbon and also the present-day size of these two crustal carbon reservoirs, we performed mass-balance calculations which indicated that the reduced carbon reservoir increased between 2.5 and 0.8 billion years ago.

The trend implies that the crust-ocean-atmosphere system increased its inventory of oxidized species such as sulfates, ferric iron, and O_2. This finding corroborates independent evidence (obtained by other laboratories from their analyses of ancient soils, iron ores, and evaporite deposits) that these oxidized species indeed became more abundant during this time interval.

This work improves our understanding of the processes controlling the oxidation state of Earth's surface environment. It also increases our confidence that we will someday be able to reconstruct, with greater precision, the timing and magnitude of past changes in the composition of Earth's atmosphere.

Ames-Moffett contact: D. DesMarais
(415) 604-3220 or FTS 464-3220
Headquarters program office: OSSA

Planetary Protection Issues and the Future Exploration of Mars

Don L. DeVincenzi

A primary scientific theme for the Space Exploration Initiative (SEI) is the search for life, extant or extinct, on Mars. Because of this, concerns have been raised with respect to Planetary Protection (PP), the prevention of biological cross-contamination between the Earth and Mars (or other planets) during solar system exploration missions.

A workshop, "Planetary Protection Issues and the Human Exploration of Mars," in July 1990 addressed these concerns. It was organized by Donald L. DeVincenzi; co-chaired by Harold P. Klein (University of Santa Clara, Santa Clara, CA) and John Bagby (Missouri State Department of Health); and administered by Sara E. Bzik (SETI Institute). The necessity for, and impact of, planetary protection requirements on both unmanned and human missions to Mars comprising the SEI were assessed. Participants included chemists, microbiologists, and geologists as well as attorneys, journalists, and environmentalists.

The following ground-rules were adopted as working assumptions for discussions:

1. The information needed to assess PP issues must be obtained during the unmanned precursor mission phase before any human landings on Mars;
2. Samples returned from Mars will be considered biologically hazardous until proven otherwise;
3. Deposition of terrestrial microbes and materials on Mars, and exposure of the crew to martian materials are inevitable consequences of human landings on Mars; and,
4. Human landings on Mars will occur only after no harmful effects of martian materials on terrestrial life forms are demonstrated.

A conservative PP strategy was developed for precursor missions to Mars. Key features of the proposed strategy addressed concerns to prevent both forward contamination (Mars contamination by terrestrial materials) and back contamination (Earth contamination by materials from Mars).

To prevent forward contamination, it was proposed that all orbiters follow Mars Observer PP procedures for assembly, trajectory, and lifetime; and that all landers follow Viking PP procedures for assembly, microbial load reduction, and bioshield. To prevent back contamination, it was proposed that all sample-return missions have PP requirements which include fail-safe sample sealing; a protocol for breaking the contact chain with the martian surface; and containment and quarantine analyses in an Earth-based laboratory.

In addition to scientific and technical issues, workshop attendees made several recommendations for forward- and back-contamination non-scientific concerns, including legal issues and public health. Attendees recognized that the general public could have significant concern over the importation of potentially hazardous nonterres-trial materials. It was suggested that NASA strive for greater public education and consent and also establish a reputable and open advisory structure to deal with these issues.

Our experience with the Apollo program indicates that legal, treaty, and other considerations (ranging from the level of local statutes to international agreements) must be examined. This is in addition to the general public reaction to the cross-contamination potential.

Responsibilities for these issues of public concern would range far beyond the scope of NASA and the SEI. Varied Government agencies such as the Public Health Service, the Department of Agriculture, the Environmental Protection Agency, and the Department of the Interior, and international bodies such as the World Health Organization would be involved.

It was also recommended to (1) do more studies on the possibility of survival and growth of terrestrial organisms under martian environmental conditions; (2) emphasize precursor missions acquiring much more detailed information on Mars' environmental properties; and (3) develop additional life detection tests for future Mars lander vehicles.

Ames-Moffett contact: D. DeVincenzi
(415) 604-5251 or FTS 464-5251
Headquarters program office: OSSA

Far Infrared Emission from the Galactic Center Filaments

Ed Erickson, Sean Colgan, Jan Simpson

NASA's Kuiper Airborne Observatory was used to measure lines of [S III] 19 and 33 micrometers, [O III] 52 and 88 micrometers, [N III] 57 micrometers, [Si II] 35 micrometers, [O I] 63 and 145 micrometers, and [C II] 158 micrometers, and the adjacent continuum in a 45-inch (1.8 parsec) beam from the radio continuum peak G0.095 + 0.012 near the end of the E2 thermal filament. An H II region excited by about 10 zero-age main sequence stars of T_{eff} approximately equal to 35,000 Kelvin and L approximately equal to 4×10^4 L_O per beam fits the available data characterizing the ionized gas. The emission from these stars also would be consistent with the infrared thermal continuum luminosity. The fluxes of [O I] and [C II] suggest that they originate in a photo-dissociation region (PDR), but the ([Si II] 35 micrometer)/([O I] 63 micrometer) line flux ratio is 8—the highest yet seen in any source—suggesting extensive grain destruction and self-absorption in the [O I] line.

The E2 filament was probed at eight positions along its length with measurement of both [O III] lines and the [S III] 33-micrometer line. The data show the radio peak and the E2 filament are similar in nature. Moving northward along the filament: (1) the ionized gas radial velocity is constant to about 10 kilometers/second; (2) the electron density in the O^{++} emitting gas is approximately constant at 250 centimeters^{-3}, much lower than the approximately 2×10^4 centimeters^{-3} density of the nearby molecular gas; (3) the excitation decreases slowly; (4) the luminosity decreases by a factor of about 2; and (5) the grain temperature is roughly constant.

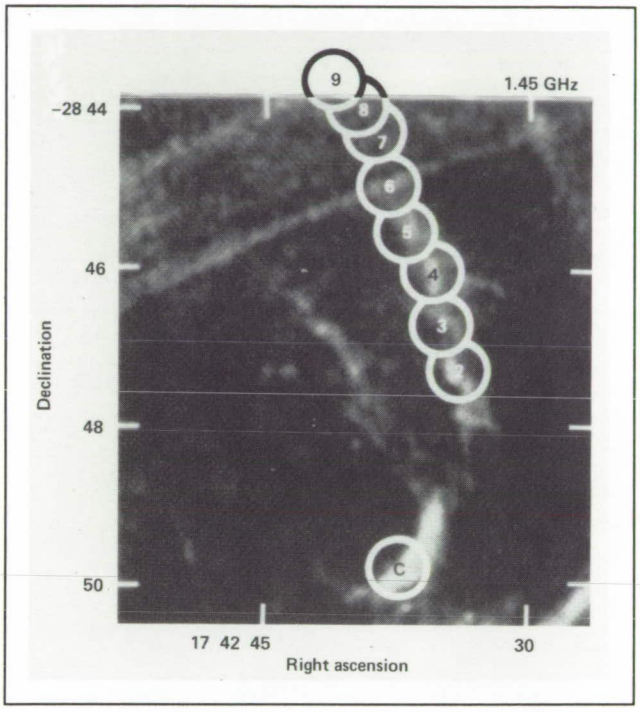


Fig. 1. Locations of infrared observations overlaid on a very large array continuum radiograph. The circles indicate the beam size

ORIGINAL PAGE
BLACK AND WHITE PHOTOGRAPH

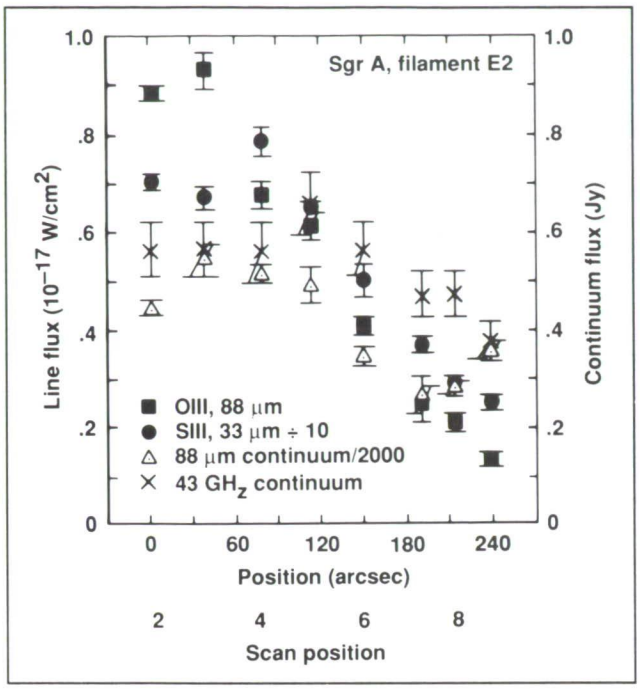


Fig. 2. Measures [O III] 88 micrometers, [S III] 33 micrometers, 88-micrometer continuum, and 43 gigahertz radio continuum versus distance along the E2 filament. The horizontal values ("0" and "240") correspond to positions 2 and 9 in the first figure, respectively

Comparison with the radio data indicates the filament is roughly tubular with an approximately 10:1 length to diameter ratio. The infrared lines and continuum are compatible with the H II region/PDR model, but it is difficult to understand why stars would be distributed to produce the filament structure. A magneto hydrodynamic model of collisional ionization also matches most of the observations fairly well, but has difficulty matching the radio recombination lines, and can generate only a small fraction of the total far-infrared luminosity.

Ames-Moffett contact: E. Erickson
(415) 604-5508 or FTS 464-5508
Headquarters program office: OSSA

Stratospheric Observatory for Infrared Astronomy

Ed Erickson, Ted Dunham, Jackie Davidson

The Stratospheric Observatory for Infrared Astronomy (SOFIA) is a proposed 2.5-meter-diameter airborne telescope to be developed jointly by NASA and the West German Science Ministry. It is intended to fill the need for a larger collection area for high-resolution spectroscopy throughout the infrared-submillimeter range and for improved spatial resolution at wavelengths of 30 millimeters and longer. It will replace the Kuiper Airborne Observatory (KAO).

KAO users and other members of the infrared community have been consulted to establish the scientific requirements for this facility, which is expected to function for 20 years. Like the KAO, it will be a gyrostabilized, open port, Cassegrain telescope with an oscillating secondary mirror. A tertiary mirror will direct collected radiation through a spherical air bearing to instruments which will be directly accessible in the cabin (see the figure).

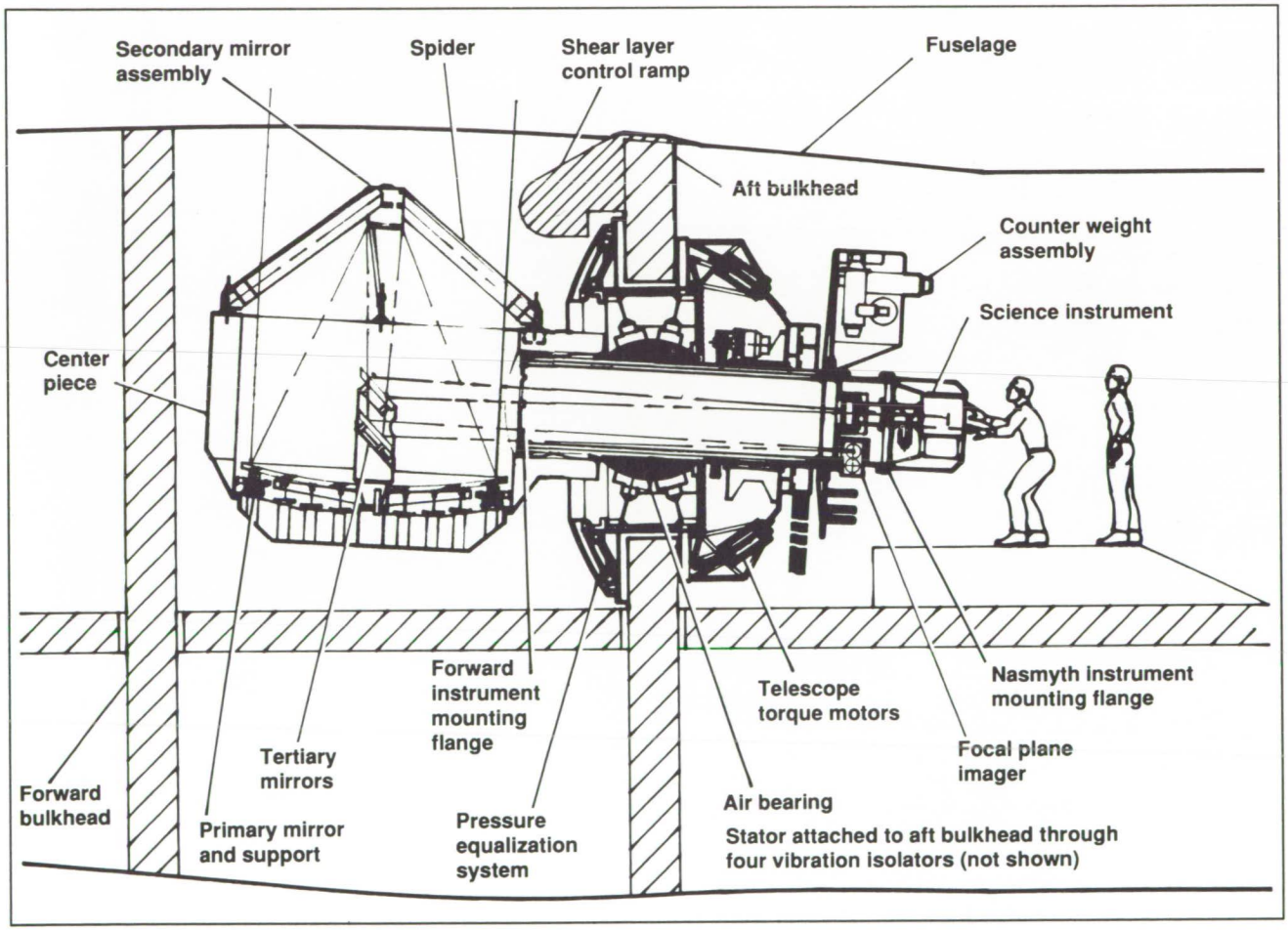


Fig. 1. Conceptual drawing of the Stratospheric Observatory for Infrared Astronomy telescope

The telescope will be mounted in a Boeing 747SP aircraft, which will permit 7 hours of continuous observation at 41,000 feet altitude. This will allow observations in most of the wavelengths obscured from ground-based observation by atmospheric water vapor and from locations all over the Earth.

The telescope instrument complement, provided largely by the investigators, is expected to include photometers, array cameras, polarimeters covering the 0.3 to 3.50-micrometer range, and spectrometers with resolutions as high as 1 kilometer/second covering the 0.9-micrometer to 1.5-millimeter spectral range. Each year, it is hoped to support 120 flights, and to serve 15 instrument teams and 25 guest investigator teams. SOFIA will be based at Ames Research Center, as is the KAO.

SOFIA's definition phase studies have been completed, and two Non-Advocate Reviews have concluded that the project is ready for development. Current plans are for development to begin in FY 93, which will lead to operations in 1998.

Ames-Moffett contact: E. Erickson
(415) 604-5508 or FTS 464-5508
Headquarters program office: OSSA

Exobiology Intact Capture Experiment

Mark Fonda, Glenn Carle

The Exobiology Intact Capture Experiment (Exo-ICE) instrument, selected as an attached payload for the Space Station Freedom, will combine the most recent advances in underdense media-collection technology with acoustic/thin film trajectory-sensor technology for intact capture and accurate tracking of hypervelocity cosmic dust particles. The Solar System Exploration Branch, in the Space Science Division at Ames Research Center, is developing the Exo-ICE instrument.

This instrument consists of four identical and completely independent instrument modules, each with a 1-square-meter collecting area, resulting in a total collection surface of 4 square meters. Each module consists primarily of Aerogel, an intact capture collection media, with thin film velocity sensors and acoustic impact detectors.

The instrument will directly measure the particle trajectory with sufficient accuracy to enable the reconstruction of particle size and will also measure orbital parameters to allow astrophysical source area determinations. It will collect cosmic dust while maintaining less than 1 in 1000 total biogenic elemental contamination throughout the experimental sequence. Further, the Exo-ICE instrument will collect particles in the 50 to 200-micrometer size range with a minimum 25% mass recovery from four primary source regions from which cosmic dust particles may have evolved: (1) comets, (2) asteroids, (3) interstellar clouds, and (4) stellar condensates. The instrument is expected to capture at least 200 particles in the desired range over a 2-year period, or around 40 particles per harvesting period. Standard mechanical attach points for easy integration into the Johnson Space Center Cosmic Dust Collection Facility will be provided.

The Exo-ICE instrument, unlike atomized capture techniques, will preserve all of the desired information pertinent to exobiology. That is, the analysis results from the Exo-ICE will bear directly upon major scientific issues of the origin and evolution of comets, as well as the evolution of the solar system, planets, and life itself. The analytical data obtained will substantially broaden our knowledge in the following areas: (1) elemental, molecular, and isotopic composition, and mineralogical, morphological, and phasal characteristics of cosmic dust, including abundances and distribution of the biogenic elements (hydrogen, carbon, nitrogen, oxygen, phosphorus, and sulfur) and their compounds; (2) relationships among comets, cosmic dust, meteorites, asteroids, and interstellar grains; (3) conditions in the solar nebula during solar system formation and post-formational alteration; and (4) the relationship of cosmic dust to volatiles on the terrestrial planets.

Ames-Moffett contact: M. Fonda
(415) 604-5744 or FTS 464-5744
Headquarters program office: OSSA

Olivine—Surprises from Below the Continents

Friedemann Freund, Minoru M. Freund, François Batllo, Rodney C. LeRoy

Olivine is a green mineral that has been cherished since antiquity as a semi-precious stone under the name of peridot. Olivine is the main mineral constituent of the upper mantle—that layer of high-density rock on which the continents float and drift following the dictates of plate tectonics. Olivine crystals make up nearly 90% of the common upper mantle rocks. Their composition, $(Mg,Fe)_2SiO_4$ with typically about 10% ferrous iron (Fe^{2+}), testifies to the pervasively reducing conditions that characterize the upper mantle—a reminiscence of the highly reducing nature of the solar nebula from which our planet accreted some 4.5 billion years ago.

One question of interest to planetary science relates to the interaction between rocks and gases in the depth of the Earth; for instance, water (H_2O). We have been able to show that, despite their overall reducing appearance, olivine crystals from the upper mantle contain oxygen in an unusual oxidation state, namely –1 instead of –2. Most minerals, including olivine, are made up of O^{2-} anions, which compensate for the positive charges centered on the metal cations. The fact that oxygen is present as O^- indicates oxidation. Normally, such an oxidation would only affect the cations; for instance, changing Fe^{2+} into Fe^{3+} and causing olivine crystals to turn yellow. We discovered that this is not the whole story. The olivine structure seems to "hide" its more oxidized oxygen in the form of peroxy moieties; e.g., two O^- joined together to form O_2^{2-}. At low temperatures these peroxy moieties are stable, even in the presence of Fe^{2+}. If the temperature is raised, they fall apart, releasing electronic defects, so-called "positive holes," which act as highly mobile charge carriers propagating through the olivine structure.

The figure shows the reversible increase/decrease of the dielectric susceptibility as a function of temperature for an olivine single crystal from San Carlos, Arizona. The dielectric susceptibility is a measure for the concentration of mobile charges. The set of curves in the figure documents the appearance of mobile charges in olivine at 1 bar between 500–600°C; an observation that has never before been made, mainly because of a lack of an appropriate measuring technique. This technique is now available at Ames Research Center and we are measuring "positive holes" charge carriers in a wide variety of mineral samples.

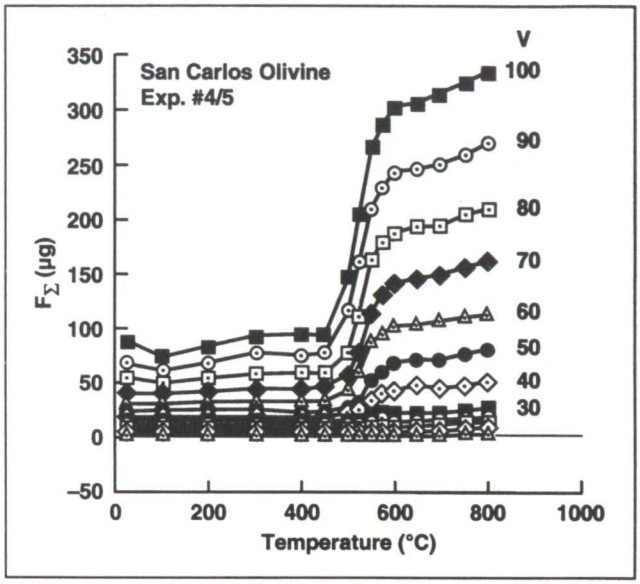


Fig. 1. The dielectric susceptibility of a single olivine crystal from San Carlos, Arizona, increases and decreases reversibly during heating and cooling through the temperature interval 500–600°C at 1 bar pressure

The appearance of O^- charge carriers in olivine upon heating, and their disappearance upon cooling, sheds new light on the electric properties of upper mantle rocks. Since the upper mantle is a region where powerful electric currents flow at certain depth levels, these new findings may have a profound impact on our current understanding of magnetotellurics, the science of the fleeting electric and magnetic anomalies in the Earth.

But how are the peroxy moieties introduced into the olivine structure in the first place? Here we are still in a stage of inference and speculation. Work on structurally simpler crystals, in particular MgO, suggests that traces of dissolved "water" (which normally form OH^- anions) undergo an internal redox reaction by which they split pairwise into hydrogen molecules plus peroxy moieties: $OH^- + OH^- = H_2 + O_2^{2-}$. If the H_2 molecules diffuse away (which they easily do because of their small size), the mineral structure clandestinely acquires a complement of peroxy moieties. This process, if substantiated through further work, may be at the root of a number of anomalies in the realm of geology/geophysics that are still poorly understood.

Ames-Moffett contact: F. Freund
(415) 604-5183 or FTS 464-5183
Headquarters program office: OSSA

Schroedinger's Radial Equation: Solution by Extrapolation

David Goorvitch, David C. Galant

We have adapted an extrapolation method to solve a one-dimensional radial Schroedinger's equation. This algorithm lays the foundation for solving the coupled Schroedinger's equation appropriate for the radical OH. This important molecule plays a role in interpreting observations from the microwave to the visible part of the spectrum in astronomical sources, the interstellar medium and in the Earth's atmosphere. As such, it is vitally important to obtain accurate wave functions so that accurate Einstein A coefficients can be calculated.

Knowledge of the intrinsic spectral properties of the emitting species is necessary to unravel the chemical and physical state of a stellar atmosphere. Usually, the transition frequencies can very accurately be calculated using a matrix formulation of the Hamiltonian that includes several interacting states. Equally important is knowledge of the strength of the transitions. The strength of a diatomic transition depends upon an accurate expectation value for the transition moment. For electronic transitions, an additional requirement is the Franck-Condon factor, which is the overlap integral between the initial and final electronic vibrational states.

The method we use combines a finite difference method with iterative extrapolation to the limit. This numerical procedure has several distinct advantages over the more conventional methods, such as Numerov's method or the method of finite differences without extrapolation. The advantages are

1. initial guesses for the term values are not needed
2. the algorithm is simple to implement, has a firm mathematical foundation, and provides error estimates
3. the method is less sensitive to round-off error since a small number of mesh points are used and, hence, can be implemented on small computers
4. the method is faster for equivalent accuracy

We demonstrate the advantages of the present algorithm by solving Schroedinger's equation with an analytical as well as a numerical potential function. For the analytical potential function, we use a Morse potential function appropriate for HCl. For the numerical potential function, a Rydberg-Klein-Rees potential function for the $X\ ^1\Sigma$ state of CO is used. A direct comparison of the results for the $X\ ^1\Sigma$ state of CO is made with results obtained by using the Numerov or predictor-corrector method.

Ames-Moffett contact: D. Galant
(415) 604-4851 or FTS 464-4851
Headquarters program office: OSSA

Molecular and Atomic Shocks in the Interstellar Medium

Michael R. Haas, Ed Erickson, David J. Hollenbach

Shocks waves are generated by the supersonic injection of mass into the interstellar medium by young stellar objects, winds from OB stars and the expansion of their associated HII regions, red giant outflows, planetary nebulae ejection, Wolf-Rayet winds, and supernovae. As illustrated in the figure, these shocks play a major role in the formation and destruction of interstellar clouds, in the heating of the hot phase of the interstellar medium, and in triggering star formation.

Depending on the type of shock and the physical conditions in the pre-shock gas, a large fraction of the input mechanical energy is converted into heat and radiated away as line emission. This emission characterizes the physical conditions in the ambient interstellar gas, thereby permitting the determination of important physical parameters, such as the pre-shock density, the shock velocity, the composition, the magnetic field strength, the overall source geometry, and the energetics of the flow.

We have measured [SiII] (34.8 micrometer) and [SI] (25.2 micrometer) line emission from Orion's BN-KL region using a cryogenic grating spectrometer aboard NASA's Kuiper Airborne Observatory.

The [SiII] observations were made with a 34-inch aperture and were spaced every 15 inches in a line through the shocked H_2 v = 1-0 S(1) peaks 1 and 2. The bulk of the [SiII] emission in Orion is believed to originate in photodissociated gas at the interface between the HII region and its parent molecular cloud. However, there is a twofold enhancement in [SiII] near IRc2, which we attribute to a fast, dissociative jump shock where the wind from IRc2 impacts slower-moving material. From model fits, we estimate the gas-phase depletion near IRc2 to be ∂_{Si} of approximately 0.3-1.0, relative to solar. The spatial distribution of the [SiII] emission has a centralized peak; unlike the H_2 and [OI] emissions, which exhibit a double-lobed structure. A possible explanation is that the gas-phase silicon abundance is significantly larger near IRc2, where higher velocity shocks have destroyed more of the silicate grains.

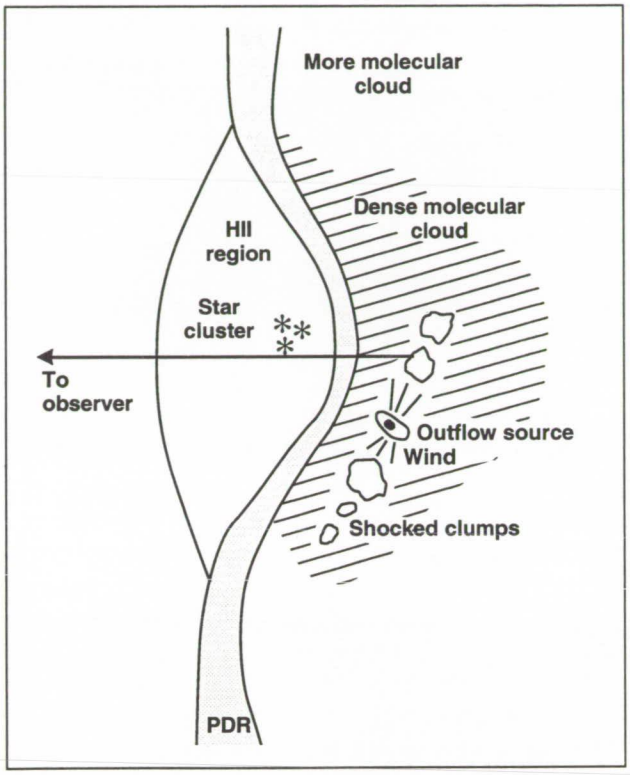


Fig. 1. Cartoon illustrating a blister geometry for a star-forming region on the face of a molecular cloud

We have measured the 25.2-micrometer line of S^0 at two locations near H_2 peak 1 in a 29-inch aperture. This is the first unambiguous detection of the [SI] line in any source. Unlike the other far-infrared fine structure lines and radio recombination lines observed to date, no appreciable contribution to the [SI] line is expected from the photodissociation region, where the sulfur is primarily S^+. Hence, this line is an important new diagnostic of shocked gas. The observed intensity is consistent with recent models of fast, dissociative jump shocks if H_2 reforms on grains in the post-shock gas and the preshock density is approximately 10^5 centimeters^{-3}.

The [OI] (63 micrometer) fine-structure line was observed in the supernova remnant IC 443. These are the first reported observations of far-infrared line emissions from a supernova remnant. The peak [OI] flux occurs at the same location as the shock-excited molecular hydrogen emission peak. Comparison with the Infrared Astronomical Satellite (IRAS) far-infrared emission shows that the [OI] line emission is an important contributor to the 60-micrometer band, with estimates ranging from approximately 40% to 75% of the total band flux. This is the first region of this type to be discovered in the IRAS data set. The distribution of the [OI] line emission appears to be similar to that of the molecular hydrogen 1-0 S(1) line. We consider the possibility of X-ray or far-ultraviolet excitation of the emission, but we conclude that the [OI] line emission is shock-excited.

The infrared emission is modeled using a variety of continuous and jump shocks. We find, based on our current theoretical understanding of shock processes, that continuous shocks with a distribution of shock velocities from 10 to 45 kilometers/second are present. The low velocity shocks provide most of the [OI] line emission and the higher velocity shocks produce most of the 1-0 S(1) line emission.

This model cannot, however, explain why the [OI]/H_2 1-0 S(1) and H_2 1-0 S(1)/2-1 S(1) line ratios appear to remain relatively constant across the source, unless the ad hoc assumption is made that the distribution of shock velocities is the same in every beam. However, by relaxing certain theoretical assumptions, a partially dissociative jump shock model with v_s of approximately 10 to 20 kilometers/second can explain the observations. It has to be assumed that the shock is indeed jump-type, despite suspicions that the physical parameters of the flow are appropriate to continuous shocks and that the oxygen chemistry is suppressed so that H_2O and OH are not formed.

The far-infrared shocked line emission ([OI], H_2O, CO) may well dominate the total emission in the IRAS 60- and 100-micrometer bands. Thus, previous models involving collisionally heated grains to explain the IRAS emission from the shocked molecular region may be unnecessary.

Ames-Moffett contact: M. Haas
(415) 604-5511 or FTS 464-5511
Headquarters program office: OSSA

Mars Climate Studies

Robert M. Haberle

The current climate of Mars is characterized by the interacting seasonal cycles of dust, water vapor, and carbon dioxide—the principal atmospheric constituent. Each summer, for example, the seasonal covering of carbon dioxide frost in the northern polar regions disappears and exposes to the atmosphere an underlying water-ice cap that is a source of atmospheric water.

During the Viking mission, almost 7×10^{14} grams of water was observed to appear in the northern hemisphere after the residual cap was exposed. Yet it was not clear whether the cap was the sole source of this water, since it would require significant equatorward transport by the atmosphere to prevent the polar regions from becoming greatly saturated (widespread cloudiness was not observed).

During FY 90, work was carried out at Ames Research Center in collaboration with Bruce Jakosky at the University of Colorado, to estimate the equatorward transport and, hence, the potential contribution to the observed increase in atmospheric water vapor due to sublimation from the residual polar cap. Results indicated that the high-latitude circulation was too sluggish during summer to move water very far from the Pole. Consequently, it was estimated that the residual cap supplied about half the observed increase and the remainder came from the mid-latitude regolith.

As a follow-on to that study, work was initiated with Aaron Zent (National Research Council) and Howard Houben (Space Physics Research Institute) to determine the ability of the regolith to make up the difference. Efforts focused on the development of a coupled boundary layer/regolith model to investigate the exchange process. The model simulates the vertical movement of water through the soil (where it can exist as vapor, ice, or sorbate) and into the atmosphere (where it is transferred to the free atmosphere by turbulence within the boundary layer). The model results showed that the mid-latitude regolith could readily supply the observed increase, while the high-latitude regolith could not.

During FY 90, work was also carried out to better characterize the dust cycle. Micrometer-sized particles become suspended in the martian atmosphere by dust storms that range in size from local to global. Mapping the thermal inertia of the martian surface during the Viking mission revealed a bi-modal distribution of particle sizes that was not consistent with theories of aeolian processes. In particular, the large particles, which are thought to initiate saltation, were inferred to be about 500 micrometers in diameter—much larger than that expected for the most easily mobilized particles. Similarly, the small particles, which presumably represent sinks for atmospheric dust, were estimated at 50 micrometers—much larger than the 1- to 10-micrometer-sized particles that settle out of the atmosphere.

However, the methods used to determine the thermal inertia, and hence the particle sizes, were based on models which did not account for the atmospheric effects on radiation at the surface. Instead, they assumed that because the martian atmosphere was so thin, all of the sunlight arriving at the planet reaches the surface unattenuated and that the amount of infrared energy radiated by the atmosphere to the surface was a constant, and a small fraction of the noontime solar insolation. Using sophisticated atmospheric radiation models, we were able to show that these assumptions led to an overestimate of the inferred thermal inertias and hence the corresponding particle sizes.

When the previously determined thermal inertias are corrected for atmospheric effects, the large and small particle modes are shifted downward to 150 and 5 micrometers, respectively. These particle sizes are in much better agreement with theories of sand and dust movement on Mars.

Ames-Moffett contact: R. Haberle
(415) 604-5491 or FTS 464-5491
Headquarters program office: OSSA

Evolution of the ATP Synthase Complex

Lawrence Hochstein, Helga Stan-Lotter

The Archaea constitute a third Domain (the highest biological taxon) whose evolutionary status is equivalent to that of the Eucarya (formerly the plant and animal Kingdoms) and the Bacteria (all other microorganisms recognized as bacteria). The Archaea, which diverged at a very early time during the evolution of life, occupy highly specialized ecological niches that are characterized by a relatively limited species diversity. As a consequence, competitive pressures in such environments are low relative to what occurs in most ecosystems. Since this situation would be expected to favor the retention of primitive properties, the Archaea may be used to study the early evolution of life.

The ATP Synthase Complex is a membrane-bound enzyme associated with the synthesis of adenosine triphosphate, the essential energy currency of all living cells. This complex is remarkable in that it is ubiquitous and is highly conserved among organisms with respect to structure and function. This suggests that the complex had an early origin, a notion that is inconsistent with its molecular and structural complexities. Therefore, Ames Research Center has been seeking evidence for more primitive examples of the ATPase Complex and postulated that if such examples exist, they would occur in the Archaea.

In collaboration with Helga Stan-Lotter, of the University of Vienna and the Search for Extraterrestrial Intelligence (SETI) Institute, we have studied the ATPase from the salt-loving organism, Halobacterium saccharovorum, which is an extremely halophilic member of the Archaea. The data suggest that while this enzyme has a number of properties in common with ATP Synthases, it is more closely related to the proton-pumping vacuolar ATPases found in the Eucarya. Evidence now establishes that the halobacterial ATPase is not related structurally to the ATP Synthase Complex.

We previously demonstrated that the halobacterial enzyme was inhibited by dicylcohexylcarbodiimide (DCCD) under conditions that inhibit the ATPase function of the ATP Synthase. Inhibition is associated with the binding of the inhibitor to the β subunit of the catalytic moeity. In the case of the halobacterial enzyme, inhibition is associated with the binding of DCCD to subunit II, which we suggest is analogous to the β subunit. The amino acid sequence about the DCCD-binding site of the β subunit is highly conserved; that is, the sequence is uniform among the enzymes from many types of organisms (see the figure).

Sequence	Source
-**ILEU-GLU*-LEU**-VAL-LEU-THR-VAL-ALA-VAL-PHE-VAL-GLU-	Halobacterial
-ALA-GLY-VAL-GLY-GLU-ARG-THR-ARG-GLU-GLU-ASN-ASP-LEU-TYR-**HIS-GLU*-MET**-	Animal
-ALA-GLY-VAL-GLY-Glu-ARG-THR-ARG-GLU-GLY-ASN-ASP-LEU-TYR- **MET-GLU*-MET**-	Plant
-GLY-GLY-VAL-GLY-GLU-ARG-THR-ARG-GLU-GLY-ASN-ASP-PHE-TYR- **HIS -GLU*-MET**-	Bacterial

The asterisk (*) represents the residue (GLU) to which DCCD is bound. The relevant tripeptide sequence is represented in boldface.

Fig. 1. Amino acid sequences around the DCCD-binding site in the beta subunit of 3 ATP synthases and the ATPase from halobacterium saccharovorum

We postulated that if the halobacterial enzyme were related to the ATP Synthase, the amino acid sequence about the halobacterial DCCD binding site would show a high degree of conservation relative to the DCCD binding site sequence found in the β subunit from the ATP Synthase.

We recently determined the sequence about the DCCD binding site. This was accomplished by incubating the halobacterial enzyme in the presence of radioactive DCCD, isolating the subunit to which the DCCD was bound, and preparing peptide fragments by enzymatic digestion. The fragment containing radioactivity was sequenced. This sequence is shown in the figure and compared to the sequences from the β subunit of the ATP Synthases from animal, plant, and a bacterium.

Without question, there is no structural homology (similarity in amino acid sequences) between the halobacterial sequence and the other binding sites. Therefore, the halobacterial ATPase does not seem to have evolved, at least not structurally, along the same evolutionary line that gave rise to the ATP Synthase. Understanding how the halobacterial ATPase is related to the general class of proton-pumping ATPases in general, and the ATP Synthase in particular, awaits clarification of the function of the halobacterial enzyme.

Ames-Moffett contact: L. Hochstein
(415) 604-5938 or FTS 464-5938
Headquarters program office: OSSA

Center for Star Formation Studies

David Hollenbach

The Center for Star Formation Studies, a consortium of scientists from the Space Science Division at Ames Research Center, and the Astronomy Departments of the University of California at Berkeley and Santa Cruz, conducts a coordinated program of theoretical research on star and planet formation. The Center, under the directorship of D. Hollenbach, supports postdoctoral fellows, senior visitors, and students who meet regularly at Ames to exchange ideas and to present informal seminars on current research, host visits of outside scientists, and conduct a week-long workshop on selected aspects of star formation each summer. The Center's grant was renewed in FY 90, guaranteeing its continuation through 1993.

Research at the Center has helped to develop the following picture of star and planet formation. Stars form from the gravitational contraction of interstellar molecular clouds; the inflowing gas and dust fall supersonically onto the forming protostar and the orbiting protoplanetary disk of gas and dust, gradually building up the mass of the protostar and disk over a period of about a million years. The disk material partially spirals into the protostar, partially fragments and coalesces to form planets, and is partially dispersed back into interstellar space. The protostar eventually develops a strong wind, which may help to terminate the accretion phase. Low-mass stars (those with masses comparable to our Sun) and high-mass stars (those with masses 10 to 100 times the solar mass) share this common evolution. High-mass stars have the additional characteristic of producing intense fluxes of ultraviolet radiation, which ionizes, dissociates, heats, and pressurizes the surrounding gas, causing expansion and disruption of the circumstellar material.

The theoretical research of the Center in FY 90 included work on many of these aspects of low- and high-mass star formation. D. Lin (University of California at Santa Cruz) and S. Murray (University of California at Santa Cruz) showed how thermal instabilities cause the rapid fragmentation and gravitational collapse of huge galactic clouds of gas and dust, leading to the formation of large bound clusters of millions of stars called "globular clusters." F. Shu (University of California at Berkeley), F. Adams (Harvard College Observatory), S. Ruden (University of California at Irvine), P. Cassen (Ames), and L. Tomly (San Jose State University) showed how massive protoplanetary disks become gravitationally unstable, and how these instabilities lead to viscous dissipation, heating of the disk, and the spiraling of material into the protostar. J. Pollack (Ames), S. Ruden, W. Cabot (Stanford University), O. Hubicky (University of California at Santa Cruz), and P. Cassen studied the evolution of the disks subject to turbulent viscosity. F. Shu, S. Ruden, J. Nagita (University of California at Berkeley), and A. Glassgold (New York University) have modeled the origin of protostellar wind as arising from the interaction of a rapidly rotating, magnetic protostar with the partially ionized gas accreting onto the star from the protoplanetary disk. These winds were shown to be largely neutral, with high abundances of CO and atomic hydrogen.

Results on high-mass star formation obtained in FY 90 included those of D. Hollenbach, A. Tielens (Ames), M. Wolfire (Smithsonian Astrophysical Observatory), M. Burton (Ames), and T. Takahashi (St. Norbert's College, De Pere, Wisconsin) who modeled the effect of the ultraviolet radiation on neutral circumstellar gas and the resultant infrared and millimeter emission from this gas. C. McKee (University of California at Berkeley) showed that the ultraviolet radiation from the young massive stars produces a small, but significant, amount of ionization in galactic molecular clouds. This ionization level controls the rate of low-mass star formation in the galaxy, and the typical column density of material in molecular clouds.

In FY 91, work will focus on the evolution and dispersal of disks, a comprehensive theory of the origin of protostellar winds, the physics of accretion shocks (and shocks driven by the protostellar winds), and the formation of high-mass stars.

Ames-Moffett contact: D. Hollenbach
(415) 604-4164 or FTS 464-4164
Headquarters program office: OSSA

Small-Particle Research on Space Station Freedom

Judith Huntington, David Stratton, Mark Fonda

A wide range of fundamental scientific questions involving interactions between small (micrometer-sized) particles could be addressed by conducting particle experiments in the low-gravity (microgravity) environment of Space Station Freedom. Example experiments which have been suggested by scientists at Ames Research Center include the following:

1. particle-aggregation studies relevant to hypotheses concerning nuclear winter, species extinction due to climatic changes, and martian dust storms
2. investigations of the synthesis of amino acids and other complex organic compounds on the surfaces of growing particles
3. determination of the growth, optical properties, and chemical composition of the organic aerosols produced in Titan's atmosphere by simulating Titan's atmospheric organic hazes
4. studies of dipolar grain coagulation and orientation as a possible mechanism for polarization of starlight shining through interstellar dust clouds
5. simulation of radiative emission by particles in various astrophysical environments such as circumstellar shells, planetary nebulae, and protostellar disks

Experiments have also been suggested by other NASA and university scientists representing diverse disciplines such as exobiology, planetary science, astrophysics, and atmospheric science. The suggested experiments have in common the requirement that they be performed in an extremely low-gravity environment. In many cases microgravity is required because the experiments must (1) suspend aggregates for times substantially longer than possible in ground-based laboratories, (2) require a convection-free environment, or (3) propose to grow and study fragile aggregates that are gravitationally unstable on Earth.

Ames is developing an interdisciplinary research facility, the Gas-Grain Simulation Facility (GGSF), for conducting research in the microgravity environment of Space Station Freedom. The GGSF is specifically designed to facilitate experiments that simulate and study fundamental chemical and physical processes involving particles in the submicrometer to millimeter size range. Processes such as nucleation, growth, coagulation, condensation, and low-velocity collisions will be studied with this facility. The 1-cubic-meter GGSF will provide the following: a 15- to 20-liter experiment chamber; environment control subsystems; mechanisms for particle production, positioning, and removal; measurement equipment (e.g., video cameras, optical particle counters, spectrometers, and photometers); and energy sources.

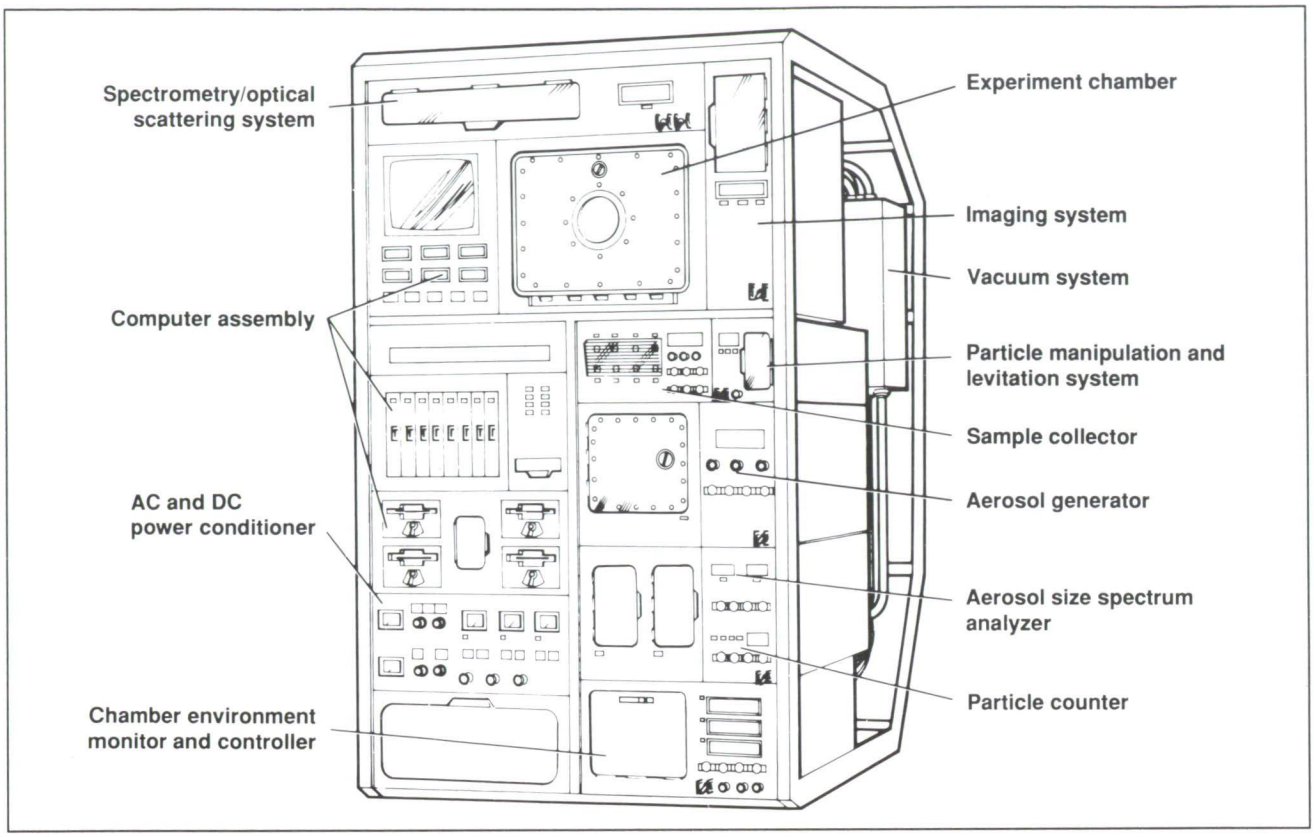


Fig. 1. Gas-Grain Simulation Facility

A NASA Research Announcement will allow members of the GGSF science community to initiate ground-based concept studies for GGSF-related experiments. In-house studies of a data base of candidate experiments have resulted in a GGSF Level I Science and Technical Requirements Document (Phase A). There have also been several advances on the GGSF design and engineering front. In addition to in-house engineering studies that have produced a conceptual design and cost estimate of the facility, a NASA Small Business Innovative Research grant has been awarded to Femtometrics, Costa Mesa, California, to develop and test a cascade impactor instrument for measuring aerosol particle mass concentrations within a number of aerodynamic particle size ranges. A 2-year Phase A engineering study for the entire GGSF will be awarded early in FY 91 to develop a facility reference design and a bread-board of a GGSF precursor instrument for the Space Shuttle.

Ames-Moffett contact: J. Huntington
(415) 604-3675 or FTS 464-3675
Headquarters program office: OSSA

An Isotopic Signature of Carbon Cycling in Paleoenvironments

Linda L. Jahnke, Roger E. Simmons, David J. DesMarais

The recycling of carbon in contemporary ecosystems is a complex process. Contributing to that recycling are many microbially mediated aerobic and anaerobic processes, some of which result in the deposition of sedimentary organic matter. Analysis of this organic material and its degradation products (kerogen) can provide insights into the microorganisms and metabolic mechanisms responsible for its recycling and deposition.

Two important biogenic signatures that tend to survive degradation can be sought in the analysis of sedimentary organic material: "biomarker" molecules (which are characteristic of particular biochemical processes), and patterns of stable carbon isotope abundance (which arise during enzymatic conversion of substrates to cell matter). Studies of such signatures in modern day ecosystems and sediments can serve as the basis for interpreting ancient signatures preserved in the geological record of life on Earth, thus increasing our understanding of the evolution of ancient microbial ecosystems.

It is widely recognized that the first life on Earth evolved within anaerobic communities, and that little, if any, free oxygen was available for respiratory or metabolic processes as is so common today. Within such anaerobic systems, recycling of the major elements depended solely upon anaerobic processes. Analysis of the carbon isotopic ratios of the organic matter preserved in sedimentary rock has shown that the principal mechanism for biological carbon fixation during this period was carbon dioxide assimilation by an enzyme similar to the ribulose-bisphosphate carboxylase found in extant organisms. After the development of oxygenic photosynthesis, the presence of molecular oxygen in such ecosystems probably resulted in dramatic changes, both in biochemistry and in the microbially mediated cycling of carbon.

Kerogens, which are greatly enriched in the light isotope (^{12}C) of carbon, are found during the Late Archean (approximately 2.8 to 2.5 billion years old). It has been hypothesized that these isotopically light kerogens resulted from a two-step process accompanied by isotopic fractionation that enriched the ^{12}C isotope at each stage. The stages are the microbial assimilation of CO_2 to form methane (CH_4) as a by-product, and also the conversion of this isotopically light CH_4 into cell material by another group of bacteria known as methanotrophs. This is of particular importance because methanotrophic bacteria require oxygen for assimilating CH_4 into biomass. Thus the isotopic record suggests that methanotrophs may have been among the first aerobic microorganisms.

We have shown that methanotrophic bacteria synthesize relatively large amounts of a class of lipid biomarker (triterpenoids) that is known to be preserved in sediments. During aerobic methane oxidation, ^{12}C is known to be oxidized more rapidly to organic matter than ^{13}C, leaving the unconsumed methane isotopically "heavy." We have also found that ^{12}C is preferentially incorporated into biomass and lipid constituents synthesized from methane. The ^{12}C enrichment in biomass relative to the starting methane was greater in cells grown at low oxygen (0.5% O_2) than in cells grown at high oxygen (10% O_2). Further enzymatic reactions operating on the intracellular carbon pool resulted in even greater ^{12}C enrichment in the resulting terpenoid biomarkers. Such isotopic fractionations should allow for the unambiguous distinction between biomarkers of the methanotroph and those of other bacterial triterpenoids, thereby providing a rigorous method for detecting methane cycling in paleoenvironments.

Ames-Moffett contact: L. Jahnke
(415) 604-3221 or FTS 464-3221
Headquarters program office: OSSA

Prebiotic Polynucleotide Synthesis: Hot or Cold?

Anastassia Kanavarioti, Sherwood Chang

In collaboration with Prof. C. F. Bernasconi of the University of California at Santa Cruz, we have investigated template-directed polynucleotide syntheses in which chemically activated mononucleotides react on a polynucleotide template and form a strand complementary to the template. Our interest arose (1) because the template-directed reactions provide a mechanism that could have been used on prebiotic Earth to form polynucleotide precursors of nucleic acids and (2) because these reactions are the basis for polynucleotide self-replication in biology. In this context, the study of template-directed reactions may shed some light on questions of chemical evolution and the origin of life.

One of the most efficient, prebiotic polynucleotide-synthesizing reactions is the polymerization of guanosine 5'-phosphate 2-methylimidazolide, abbreviated 2-MeImpG, in the presence of polycytidylate, poly(C), acting as the template. In the absence of the template the major reaction pathway of 2-MeImpG is hydrolysis which leads to the unreactive guanosine 5'-phosphate. In contrast to that, in the presence of the template guanosine-oligomers, $(pG)_n$, up to n = 40 units long are formed (eq. 1, M = 2-MeImpG, k_n = bimolecular rate constant for step n).

$$M \xrightarrow{k_2[M]} (pG)_2 \xrightarrow{k_3[M]} (pG)_3 \xrightarrow{k_4[M]} (pG)_4 \xrightarrow{k_5[M]} (pG)_5 \xrightarrow{k_6[M]} (pG)_6 \rightarrow\rightarrow\rightarrow (pG)_n \qquad (1)$$

Recently, we studied the kinetics of these reactions at three different temperatures, 6°C, 23°C, and 37°C, in an attempt to elucidate the effect of temperature on this polymerization. A long-standing assumption was that temperatures close to freezing would (1) stabilize stacking interactions among the mononucleotides and therefore facilitate their reaction, (2) stabilize association between the template and the growing polynucleotide strand for more accurate information transfer, and (3) minimize the deactivation of the activated monomer by slowing down its hydrolysis. However, it was also expected that lower temperatures would most likely slow down the polymerization reaction, and it was unclear whether this factor would be important enough to override the beneficial effects of the other three factors.

A better understanding of the effect of temperature on template-directed reactions can be gained by comparing the results obtained by the polymerization of 2-MeImpG at 6°C and 37°C. Analyses of the oligomeric products according to length were performed on a high-performance liquid chromatograph. In part (a) of the figure, one sees that samples of poly(C) and 0.02 M 2-MeImpG (kept at 6°C for approximately 2.5 hours) form a series of oligomers up to 6 units long. Because 2-MeImpG is being consumed both by the polymerization process as well as by concurrent hydrolysis, we stopped the reactions at an early stage to facilitate kinetic analysis of the data. Hence, in most cases oligomeric products no longer than the 10-mer were observed. It is noticeable that the yield in a specific oligomer decreases with increasing oligomer length. This result is consistent with chemical intuition for a polymerization like equation (1) where formation of oligomer, n, cannot occur before formation and accumulation of the shorter one, n-1. Similar behavior, although not identical, is observed in the same reaction performed at 37°C (part (b) of the figure). Here formation of the trimer is slower than formation of the tetramer and pentamer, and longer oligomers form even faster.

What is striking, however, is that the same reaction performed at the two different temperatures seems to yield roughly the same amount of products or, in other words, to proceed with almost the same overall rate. This observation implies that at the higher temperature, the enhancing effect on the polymerization rate counterbalances the diminishing influence of the stabilizing interactions. These qualitative observations are confirmed by determining each bimolecular rate constant k_n, with

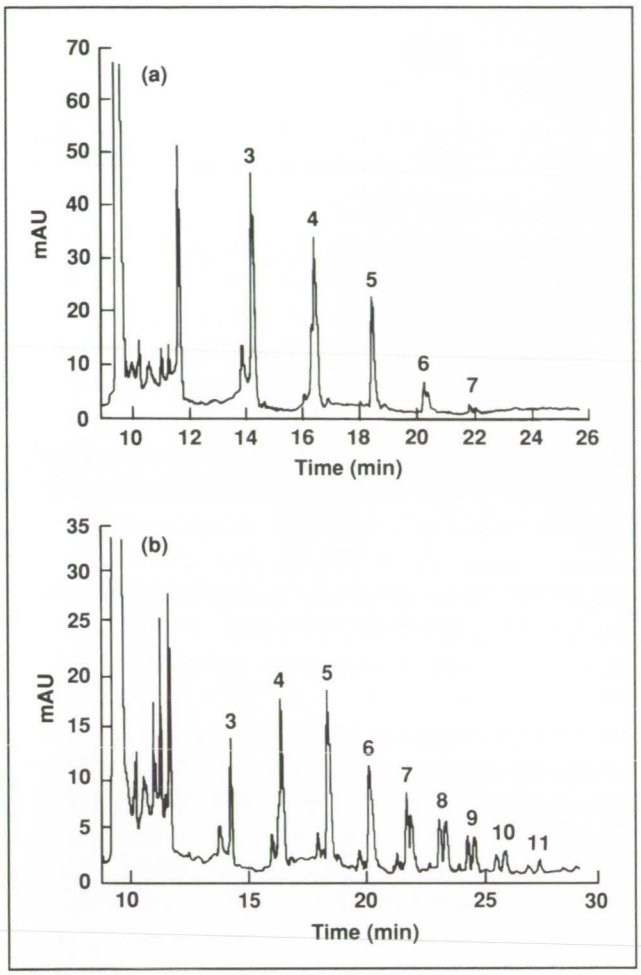


Fig. 1. High-performance liquid chromatography profiles: Effect of temperature on yield and length of oligomeric products in the template-directed polymerization of 2-MeImpG (3 stands for trimer $(pG)_3$; 4 stands for trimer $(pG)_4$, etc.). (a) 6°C, 0.02 M 2-MeImpG after 2.44 hours; (b) 37°C, 0.02 M 2-MeImpG after 2.48 hours

$2 \leq n \leq 10$, at all three temperatures. In addition to that, the results indicate that in the early stages of the reaction, different processes compete in such a way as to give rise to a larger fraction of longer oligomers at the higher temperature, and a larger fraction of shorter oligomers at the lower temperature. This competition suggests that for a constant supply of activated monomer, the polymerization process would favor longer oligomers at the higher temperature.

Our results cannot yet be generalized to other systems. It is likely that a template-directed reaction based on other nucleotides may behave differently. The question remains unclear whether prebiotic polynucleotide synthesis was favored in a hot or in a cold environment. Many more template-directed reactions need to be investigated before the effect of temperature on these reactions can be clearly understood. Interestingly, recent models of the prebiotic Earth favor the higher rather than the lower temperatures.

Ames-Moffett contact: A. Kanavarioti
(415) 604-5733 or FTS 464-5733
Headquarters program office: OSSA

Use of the Shuttle External Tank as a Gamma-Ray Imaging Telescope

David G. Koch

High-energy gamma-ray astronomy has been hampered by the absorption of the atmosphere. The low fluxes require long integration times and low-angular resolution, thereby limiting the ability to recognize point sources of radiation. In FY 91 NASA will be launching the Gamma Ray Observatory (GRO), which will help progress in this field of research. However, even with GRO most of the sources detected will have positions with large uncertainties, and the long exposures required to detect the sources will make it impossible to observe short-term variations which could lead to an understanding of the emission mechanisms.

A concept for a much more sensitive detector, that has been investigated by David Koch, uses a spent shuttle external tank (ET) as a low-pressure vessel for a large area gas Cherenkov telescope. This Gamma-Ray Imaging Telescope System (GRITS) would have an order of magnitude greater collecting area than GRO. The background that such a telescope would experience has been investigated in collaboration with E. Barrie Hughes at Stanford University. It was concluded that the GRITS design would not have any undue instrumental background problems. Mission and systems design work has been led by Max Nein of Marshall Space Flight Center and has also been supported by Martin-Marietta, Michoud, Louisiana. Analyses have shown that the reuse of an ET for this purpose is feasible and that GRITS could be assembled on-orbit in two shuttle missions. Assembly also could be based at the Space Station Freedom. A major challenge to the success of GRITS is providing for space debris and micrometeoroid protection.

Ames-Moffett contact: D. Koch
(415) 604-6548 or FTS 464-6548
Headquarters program office: OSSA

Small Explorer Mission to Measure Chemical Species Important in Star Formation Processes

David G. Koch, David Hollenbach

The processes that lead from quiescent molecular clouds to the formation of stars and planets are not well understood. The ability of dense interstellar clouds to radiate energy, and thereby collapse, depends on their chemical composition, which is uncertain. A direct determination of the abundance of species that have been predicted to be gas coolants in the clouds will address such critical issues as (1) stability of clouds against collapse; (2) variations in star formation efficiencies in different regions; and (3) the processes whereby energy is removed, permitting stars and planets to form.

The submillimeter wavelength region is particularly useful for making observations of five important species: O_2 (487.249 GHz), CI (492.162 GHz), ^{13}CO (550.926 GHz), H_2O (556.936 GHz), and $H_2{}^{18}O$ (547.676 GHz). These species were selected because the conditions required to excite each line are sufficiently different to ascertain the thermal balance within dense clouds. Due to atmospheric absorption, these measurements are virtually impossible from within the atmosphere. Combining these measurements with ground-based measurements at longer wavelengths of CO, and airborne and space-based measurements in the infrared of OI, C^+, and OH, should also lead to a direct determination of the primary reservoirs of interstellar carbon and oxygen.

As part of the small explorer program, NASA selected the Submillimeter Wave Astronomy Satellite (SWAS) to carry out these observations. A Scout-class instrument is being developed for launch in FY 95. The team will be headed by Gary Melnick (Smithsonian Astrophysical Observatory) as the Principal Investigator, with Co-Investigators at Ames Research Center (D. Hollenbach and D. Koch), the University of Cologne, Johns Hopkins University, University of Massachusetts-Amherst, and the National Air and Space Museum. The instrument will be built by Ball Aerospace Systems Group, with receivers built by Millitech Corporation, and an acousto-optical spectrometer built by the University of Cologne. The spacecraft bus is being developed by NASA Goddard Space Flight Center. SWAS will be used to conduct a high-spectral-resolution survey of galactic molecular clouds of species critical to an understanding of the chemistry and thermodynamics in star-forming regions.

Ames-Moffett contact: D. Koch
(415) 604-6548 or FTS 464-6548
Headquarters program office: OSSA

Microvolume Metastable Ionization Detector for Analyzing Planetary Atmospheres

Dan Kojiro, Fritz Woeller, Nori Takeuchi, Don Humphry

Analytical instrumentation for use aboard spacecraft or planetary probes for determining the chemical composition of planetary atmospheres and surfaces must operate with extremely limited resources. Emphasis is placed not only on successfully performing the required analyses, but also on minimizing the size, weight, and energy consumption of the instrument. Often the analyses performed under these conditions require the separation and identification of several components at concentration levels down to the part-per-billion level or lower.

The Metastable Ionization Detector (MID), which uses metastable helium to ionize sample molecules, is a powerful and sensitive gas chromatographic detector used in flight analytical instruments. Helium, in the presence of a strong electric field, can be excited to a metastable state through collisions with beta particles emitted by a radioactive source. These excited molecules, metastable helium, can then ionize molecules with ionization potential below 19.8 electron volts. This results in a nearly universal sample ionization mechanism with great sensitivity.

The Cometary Ice and Dust Experiment (CIDEX), set to fly on the Comet Rendezvous and Asteroid Flyby (CRAF) Mission, uses MIDs with internal volumes of about 200 microliters. A miniaturized version, the micro-volume MID (μMID) (see figure), has been developed with an internal volume of less than 20 microliters.

The brass body plate of 21 × 17 × 5 millimeters has a 1.6-millimeter-diameter hole lengthwise at the center axis. The middle section of this hole forms an 11-millimeter long detector cavity between two gas ports. Each end contains a 5-millimeter-long insulator made from Coors AD-99 double-bore alumina rod. Each insulator holds one electrode and also gives support to the tip of the other one pointing in the opposite direction. The electrodes are made from 0.25-millimeter-diameter stainless steel wire, and the gap between them measures 0.4 millimeter. Fastening and sealing is achieved externally by applying cyanoacrylate adhesive. An 11-millimeter-diameter flat hole is milled in 2 millimeters deep and orthogonal to the electrode position, far enough to break through and create a 0.6-millimeter slit in the top of the cavity. The Nickel-63 layer on the source foil is placed against this slit. A press-fitted disc of Teflon®, 11 millimeters in diameter and 2 millimeters thick, backs the foil and is secured by a steel plate. The standoff between the source and either electrode is 0.6 millimeter.

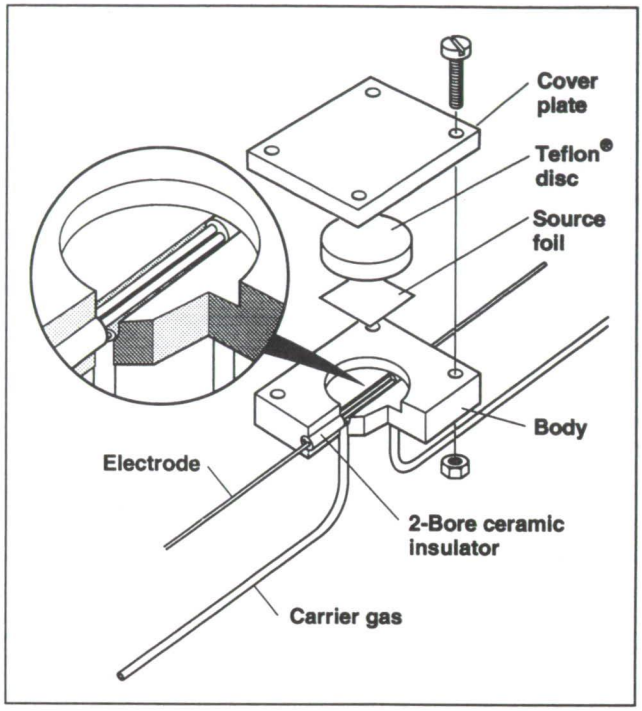


Fig. 1. Microvolume Metastable Ionization Detector. Dimensions are given in text

The performance of the μMIDs was similar to the CIDEX MIDs. However, the much smaller internal volume of the μMID allowed the use of carrier gas flow rates of 2 standard cubic centimeters a minute, nearly an order of magnitude less than the usual MID carrier flow rate. The low flow rate greatly reduces the amount of carrier gas required for a given experiment and also eliminates the need for make-up gas if capillary columns are used. The compatibility of this μMID with the modulated voltage circuits that are used to expand MID response ranges is now being investigated.

Ames-Moffett contact: D. Kojiro
(415) 604-5364 or FTS 464-5364
Headquarters program office: OSSA

Severe Downslope Windstorms on Mars

Julio A. Magalhães, Richard E. Young

Global and local dust storms in the atmosphere of Mars, and observable changes in the distribution of dust on the planet's surface, indicate that surface winds are sufficiently intense to raise dust from the surface at particular times and locations. However, models of the global atmospheric circulation predict surface wind speeds which are generally significantly less than the speeds required to raise dust. Dark streaks associated with localized topographic obstacles, such as hills and craters, provide a well-documented example of dust removal from the Martian surface. The association of these features with topographic obstacles suggests that the interaction of the regional atmospheric flow with the obstacle may yield significantly enhanced winds in the lee of obstacles. This may be an important mechanism for raising dust on Mars.

The required surface wind amplifications produced by interaction with the obstacles must be large (factor of 5-10) so the physical nonlinearity of the fluid dynamics must be included in the analysis. During calendar year 1990 we studied steady, two-dimensional, smooth, incompressible, inviscid flow over an infinite ridge. By transforming the equations of motion for such a fluid into an equation for the streamline displacement, we were able to preserve the physical nonlinearity of the problem while obtaining a mathematically linear equation. Observations and modeling of severe downslope windstorms in the lee of mountain chains on Earth suggest that the windstorms result from the interaction of a smooth, high-speed surface flow capped by a stationary well-mixed turbulent layer, which traps the disturbance in the vertical direction.

On Mars at the time and location of the formation of the dark streaks, the atmospheric circulation yields near-surface (approximately 1-2 kilometers above the surface) mean wind reversals, which cause vertically propagating atmospheric waves to become convectively unstable near the level of the wind reversal. Therefore, a turbulent upper layer, which traps the disturbance, was assumed as an upper boundary condition.

The theory we have studied describes the combinations of upstream surface wind, wind reversal height, upstream atmospheric stratification, and obstacle height. These combinations produce large surface wind increases in the lee of the obstacle. Surface wind speed enhancements of up to a factor of 4 can be produced. Using the mean atmospheric conditions predicted by circulation models of Mars, we find that during nighttime conditions of atmospheric stratification, the large surface wind amplifications can be produced for the obstacle heights associated with the dark surface streaks.

The existence of a mean wind reversal at a height that is approximately equal to the height of the near surface atmospheric layer, which undergoes large diurnal variations in stratification, allows the Martian atmosphere to "tune" itself to conditions favorable to the production of large surface wind amplification at the season and location of dark streak formation. In calendar year 1991, we plan to investigate the conditions favorable to the production of the turbulent layer that caps the laminar high-speed, near-surface flow, and is essential to the existence of the severe downslope windstorms.

Ames-Moffett contact: J. Megalhães
(415) 604-3116 or FTS 464-3116
Headquarters program office: OSSA

Biomarkers and the Search for Extinct Life on Mars

Rocco Mancinelli, Lisa White

We have been conducting ecological studies regarding the abiotic/biotic relationship in microbial ecosystems. These studies have been performed to determine how one might interpret data in an ecological context from exobiology experiments conducted during future Mars missions. The research includes laboratory experiments and field experiments focusing on theoretical calculations regarding the stability of organic matter that might be buried on Mars, the study of the physiology of nitrogen fixation, microbial activity in evaporitic salt crusts, and studies of the impact of various abiotic factors on nitrogen and carbon cycling in microbial ecosystems. The ecosystems used for this work are those that have been suggested as possible analogs of early Mars. They include desert endolithic microbial ecosystems, microbial mat ecosystems, and microbes inhabiting evaporites.

From our studies we have concluded that the nitrogen cycle of the cryptoendolithic microbial ecosystem inhabiting the Antarctic dry valleys is incomplete. Biological nitrogen fixation, denitrification, and nitrification do not occur in nature within this ecosystem. All of the fixed nitrogen is supplied exogenously. If the abiotic portion of the ecosystem is changed by the elimination of fixed nitrogen, or by decreases in O_2, the biota changes. This leads to a change in the ecosystem. The nitrogen cycle of the endoevaporitic microbial community inhabiting a natural mixed crust of halite and gypsum also exhibits an incomplete nitrogen cycle. This endoevaporitic community, however, does exhibit nitrogen fixation; but neither nitrification nor denitrification could be detected. The microbial community inhabiting these ecosystems performs the least number of transformations of nitrogen of any ecosystem reported to date, and therefore may represent the simplest nitrogen cycle in nature. Both of these communities, however, fix carbon photoautotrophically, and appear to possess a complete carbon cycle (C-fixation $\rightarrow$ respiration).

In contrast, benthic microbial mats carry out complete nitrogen and carbon cycles in nature. The mat inhabiting Lake Hoare, a perennially ice-covered lake in Taylor Valley, Antarctica, exhibits an incomplete nitrogen cycle during the mid to late austral summer (no N_2-fixation), and a complete nitrogen cycle during late spring and early summer before melt water from the Canada Glacier runs into the lake. In the microbial mats inhabiting a hypersaline pond, in Baja, California, the nitrogen cycle appears always to be complete. The pattern of nitrogen and carbon fixation and denitrification varies diurnally in the hypersaline microbial mats. Data suggest that this phenomenon in the hypersaline microbial mats is due to diurnal changes in nutrient demand.

Results of these studies allow us to place, conceptually, the Antarctic dry valley cryptoendolithic microbial community (which we have shown to have, essentially, no biological nitrogen cycle) at one end of a continuum. Microbial mat ecosystems (which have a complete nitrogen cycle) are at the other end. Ecosystems lying along such a continuum and exhibiting incomplete to complete biological cycling of nutrients show that the greater the dependence of the organisms on the abiotic components of their ecosystem, the more vulnerable they may be to changes in the environment (e.g., drying out and decreases in nutrient availability, as might have occurred on early Mars). Studying such simple systems provides data for a more complete understanding of the relationship between the biotic and abiotic components of an ecosystem.

Ames-Moffett contact: R. Mancinelli
(415) 604-6165 or FTS 464-6165
Headquarters program office: OSSA

Definition of Exobiology Experiments for Future Mars Missions

Rocco Mancinelli, Lisa White

The ecology of microbially dominated ecosystems was studied to determine what might be important to measure during missions to Mars, and how one might interpret data from such simple systems when analyzed using mission candidate analytical techniques. Results of these studies, combined with knowledge of practical mission constraints, led to the selection of differential thermal analysis/gas chromatography (DTA/GC). As an analytical technique, it shows promise for its applicability to conduct exobiology experiments on a Mars mission.

We compared the analyses of a variety of substances important to exobiology using pyrolytic GC, DTA and DTA/GC. The substances tested included organic compounds (proteins and amino acids), inorganic compounds (NO_{3-}, CO_3^{2-}, and NO_{2-} salts), clays (montmorillonite, kaolinite, and nontronite), non-clays (palagonite), and various mixtures of these substances. In addition, we analyzed samples collected from the Antarctic endolithic microbial ecosystem. Data thus far suggest that of all of the techniques tested, DTA/GC is the most promising for its applicability to Mars exobiology experiments.

The data from pyrolytic GC only allows one to directly identify substances volatilized from the sample after it has been combusted. Using pyrolytic GC techniques where the sample was placed in a tube, evacuated, and then heated to 700°C, we could not distinguish between montmorillonite and palagonite. We could, however, determine if H_2O, organics, and CO_3^{2-} were in the sample. It was only possible to distinguish between adsorbed H_2O and H_2O of hydration when the heating occurred in a step-wise fashion with increments not greater than 100°C. It was not possible to identify unequivocally the parent organic compound from its volatilized components.

Differential thermal analysis yields more information than pyrolytic GC. For example, from DTA analysis alone it is easy to distinguish between the thermal signature of montmorillonite and kaolinite (parts (a) and (b) of the first figure), and to detect adsorbed H_2O (the endothermic peak at 100°C in part (a)). Parts (a) and (b) of the first figure depict the thermal analysis signatures of 50 milligrams of montmorillonite and 50 milligrams of kaolinite, respectively (obtained from the soil standards laboratory, University of Missouri, Columbia). The characteristic thermal signatures of kaolinite and montmorillonite both have important features that occur above 700°C, indicating that differential scanning calorimetry (DSC) is not the method of choice for distinguishing these clays.

Part (c) of the first figure illustrates the thermal signature of 50 milligrams of glycine, which decomposes at 450°C and has an endothermic peak at 250°C due to decomposition (the endothermic peak at ~100°C is due to adsorbed H_2O). In parts (a), (b), and (c), the DT endotherm due to free water vaporizing occurs at 125°C.

The DTA signature of a mixture of 1% glycine in 50 milligrams of kaolinite is depicted in part (d). The endothermic peak occurring at 250°C is due to the decomposition of glycine seen at 450°C, and the remainder of the curve is the thermal signature of kaolinite. The general curvature of the baseline seen in DTA analyses is due to changes in heat capacity of the sample.

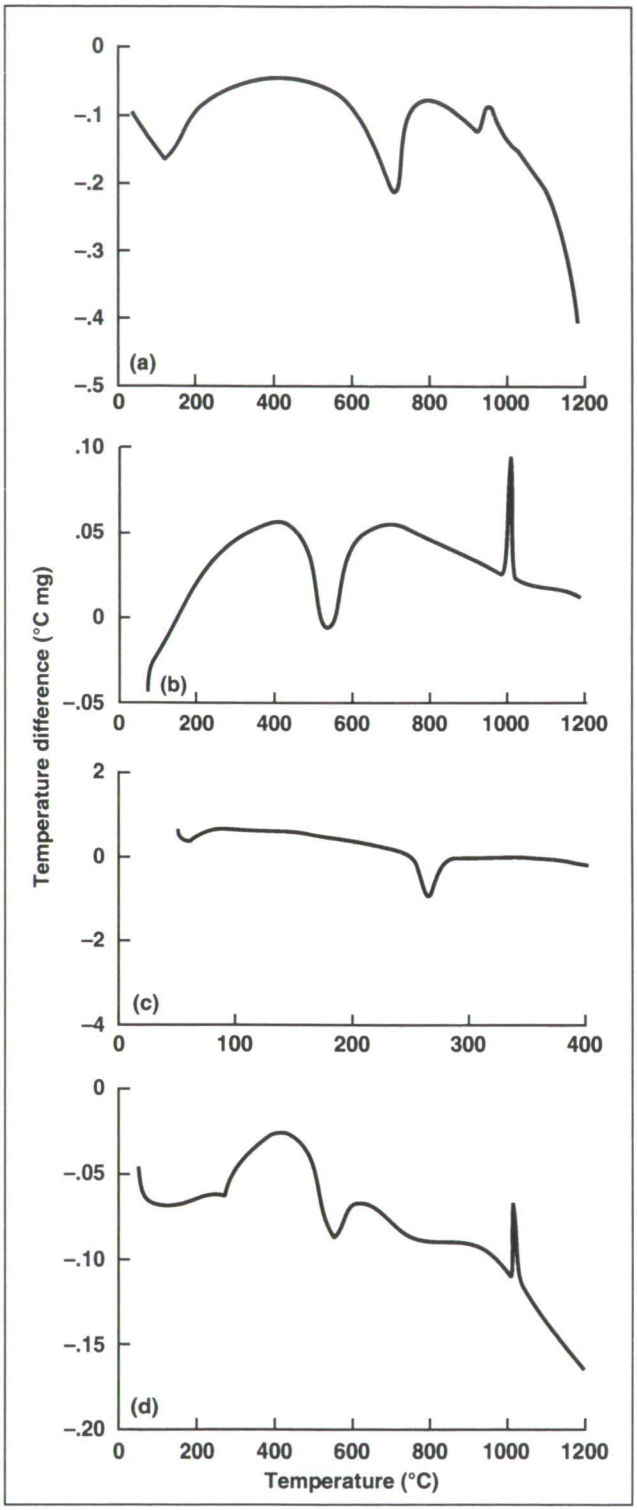


Fig. 1. Typical DTA analyses of clays and organics. Analyses were performed on a Dupont model 1600 DTA. Samples were heated from ambient room temperature (22°C) to 1200°C at a rate of 10°C min^{-1}. The reference was 30 milligrams of aluminum oxide

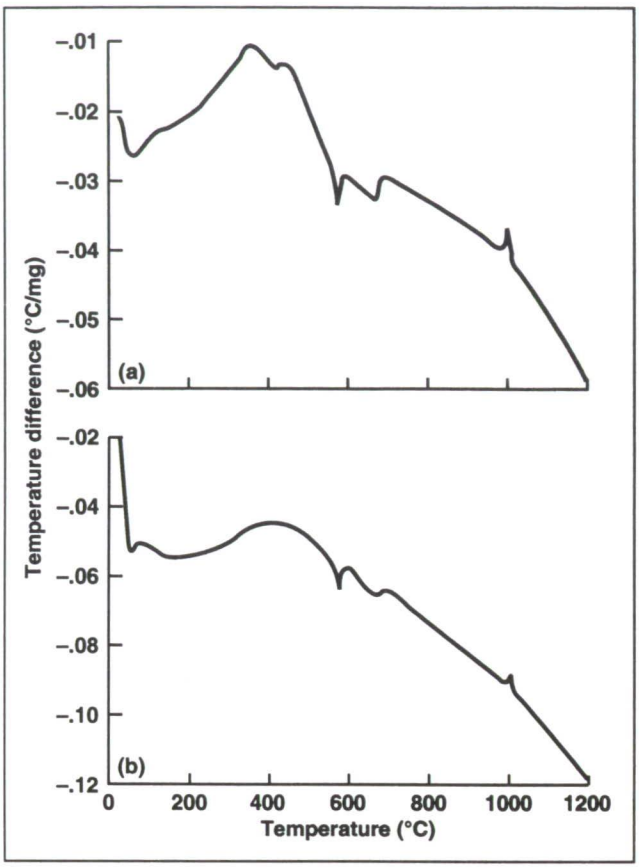


Fig. 2. Results of DTA analyses of Beacon sandstone from the Dry Valley region of Antarctica (a) uninhabited and (b) inhabited by cryptoendolithic lichens. Analyses were performed on a Dupont model 1600 DTA. Samples were heated from ambient room temperature (22°C) to 1200°C at a rate of 10°C min^{-1}. The reference was 30 milligrams of aluminum oxide

We are beginning to gather data from samples of some microbial ecosystems. For example, preliminary data suggest that the DTA/GC signature of the Antarctic Dry Valley Beacon sandstone that is uninhabited (part (a) of the second figure) is distinct from the same sandstone that is inhabited by cryptoendolithic microorganisms (part (b) of the second figure).

In part (a) of the second figure, the exothermic peaks observed at 350 and 485°C are due to the transition of γ-Fe203 $\rightarrow$ α-Fe_2O_3, and are unaccompanied by gas evolution. The endothermic event occurring at 600°C is due to the transition of

α-quartz to β-quartz, and is not associated with gas evolution. The 700°C endotherm is accompanied by the evolution of H_2O vapor, and is due to a dehydration reaction. The exothermic peak at 1100°C is due to a transition reaction characteristic of kaolinites.

In part (b) of the second figure the thermal analysis curve of the inhabited sample is similar to that of the uninhabited rock. The transition of γ Fe203 → α-Fe_2O_3 (350-485°C) is somewhat masked by the broad exothermic peak (400-500°C) caused by the decomposition of organics and accompanied by evolution of hydrocarbons.

The distinction between the signatures of the uninhabited and inhabited sandstone appears to be due to the abundance of organics and the abundances and oxidation states of nitrogen and iron. Uninhabited rocks contain greater quantities of oxidized iron and oxidized nitrogen species than inhabited rocks. The amount of iron in the inhabited zone of the rock is significantly less, probably as a result of microbial activity (this characteristic lack of iron remains long after the organisms have died).

The total amount of nitrogen is greater in the inhabited rock. The nitrogen data seem to correlate well with what we know about the nitrogen transformation reactions within this ecosystem (i.e., slow turnover, no biological nitrogen-fixation, no loss of nitrogen through denitrification, and no oxidation via nitrification (see article titled "Biomarkers and the Search for Extinct Life on Mars")). Further investigation of these data is proposed.

Ames-Moffett contact: R. Mancinelli
(415) 604-6165 or FTS 464-6165
Headquarters program office: OSSA

Wind Tunnel Experiments Enable Prediction of Magellan Spacecraft Findings

John R. Marshall

On August 10, 1990, the Magellan spacecraft was placed in orbit around the planet Venus. During the following months, its radar mapping activities produced remarkable high-resolution images of the planet's surface that are providing planetologists with clues to past and present geological and climatic activity. Geological experiments conducted at Ames Research Center with the Venus Wind Tunnel enabled some of the Magellan findings to be predicted before the spacecraft arrived at Venus.

The Venus Wind Tunnel is a closed-circuit, high-pressure boundary-layer tunnel that enables the simulation of conditions at the surface of Venus where the atmospheric pressure is nearly 100 times greater than that on Earth. The wind tunnel experiments showed that the wind on Venus should produce surface features such as dunes with the characteristics of sand deposits found under water. The (inferred) similarity between wind action on Venus and water action on Earth derives from the fact that both water and the carbon dioxide atmosphere of Venus are dense enough to transport sand in a way that promotes the formation of sand structures responsive to fluid forces; they deter the formation of structures (e.g., sand ripples) related to ballistic (grain impact) processes.

Having established this similarity for small-scale (20-centimeter-long) sand structures in the wind tunnel experiments, it was possible, using terrestrial analogs, to predict that Venus should have giant (>100 meters) sand waves forming in trains transverse to the wind direction. Magellan radar images do indeed portray surface features that are suggestive of such sand structures according to Magellan team members Raymond Arvidson and Ronald Greeley. The structures are observed where there are thought to be loose surface materials; they are transverse to the dominant wind direction, and the spacing between them is on the kilometer scale.

Ames-Moffett contact: J. Marshall
(415) 604-4983 or FTS 464-4983
Headquarters program office: OSSA

Titan's Atmosphere

Christopher P. McKay, James B. Pollack,
Jonathan I. Lunine, Régis Courtin

We have been conducting a research program directed at understanding the processes that control the thermal structure of Titan's atmosphere and its evolution in time. We find that a one-dimensional radiative-convective model can simulate Titan's current atmospheric temperature profile within ~10%. These results are shown in the first figure. Lately, we have used our model to investigate the evolution of Titan over the last 4 billion years.

To model Titan's evolution, it was necessary to include in our model the effects of the ocean presumed to exist on Titan. The presence of an ocean is inferred from the presence of methane in Titan's atmosphere. Since methane is destroyed by sunlight over a time that is short compared to the history of Titan, there must be a mechanism, such as an ocean, that can resupply methane to the atmosphere. Over geological time the initially pure methane ocean would be converted to ethane and, hence, would become smaller. As this occurred, the amount of nitrogen that could be dissolved in the ocean would decrease and the total mass of nitrogen in the atmosphere would increase—providing an enhanced greenhouse effect. In addition, during the last 4 billion years the Sun has become about 30% more luminous. Together, these effects suggest that Titan should have been even colder in the past than it is today.

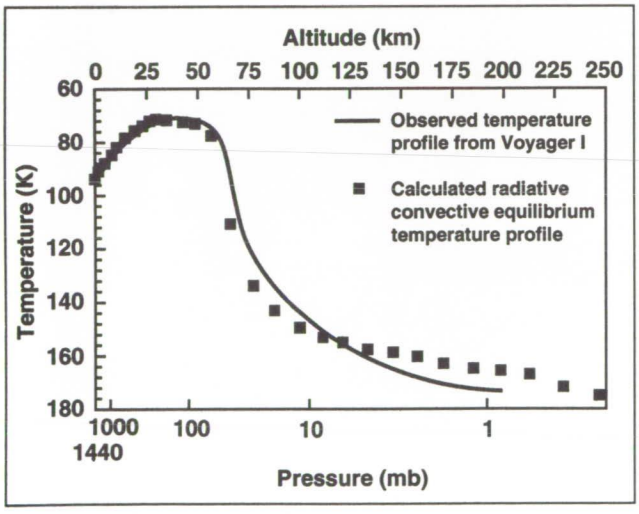


Fig. 1. Titan atmospheric temperature profile. Comparison of Voyager data (solid line) and results of the radiative-convective model of Titan's atmosphere (squares)

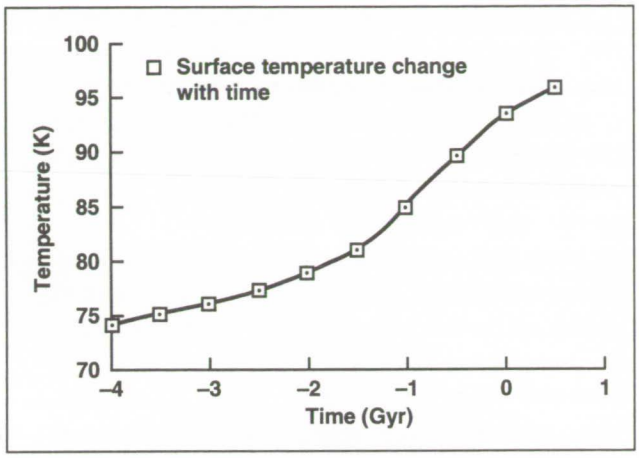


Fig. 2. Titan's surface temperature change with time

The second figure shows the time history of Titan's surface temperature determined from our coupled atmosphere-ocean model.

Ames-Moffett contact: C. McKay
(415) 604-6864 or FTS 464-6864
Headquarters program office: OSSA

Impact Constraints on the Environment for Chemical Evolution and the Continuity of Life

Verne R. Oberbeck, Guy Fogleman

Early in their histories, the Moon and Earth were heavily bombarded by planetesimals and asteroids that were capable of interfering with chemical evolution and the origin of life. We have calculated the frequency of giant terrestrial impacts capable of stopping prebiotic chemistry in the probable regions of chemical evolution.

The limited time available between impacts disruptive to prebiotic chemistry at the time of the oldest evidence of life suggests the need for a rapid process for the chemical evolution of life. The classical hypothesis for the origin of life through the slow accumulation of prebiotic reactants in the primordial soup in the entire ocean may not be consistent with constraints imposed by the impact history of Earth. On the other hand, rapid chemical evolution in cloud systems and lakes, or other shallow evaporating water bodies, would have been possible because reactants could have been concentrated and polymerized rapidly in this environment.

Thus, life probably could have originated near the surface between frequent surface-sterilizing impacts. There may not have been continuity of life depending on sunlight because there is evidence that life, existing as early as 3.8 billion years ago, may have been destroyed by giant impacts. The first such organisms on Earth were probably not the ancestors of present life.

Ames-Moffett contact: V. Oberbeck
(415) 604-5496 or FTS 464-5496
Headquarters program office: OSSA

Prebiotic Chemistry in Clouds

Verne R. Oberbeck, John Marshall, Thomas Shen

In the traditional concept for the origin of life, prebiotic reactants became slowly concentrated in the primordial oceans and life evolved slowly from a series of highly protracted chemical reactions during the first billion years of Earth's history. However, chemical evolution may not have occurred continuously because planetesimals and asteroids impacted the Earth many times during the first billion years, sterilized the planet, and required the process to start over. A rapid process of chemical evolution may have been required for life to appear at or before 3.5 billion years ago. Thus, a setting favoring rapid chemical evolution may be required.

A chemical evolution hypothesis by C. R. Woese (University of Illinois) accomplished prebiotic reactions rapidly in droplets in giant atmospheric reflux columns. However, Siegfried Scherer (Universität Konstanz, Konstanz, Germany) raised a number of objections to Woese's hypothesis and concluded that it was not valid.

We propose a mechanism for prebiotic chemistry in clouds that satisfies Scherer's concerns regarding the Woese hypothesis and includes advantageous droplet chemistry.

Prebiotic reactants were supplied to the atmosphere by comets, meteorites, and interplanetary dust, or synthesized in the atmosphere from simple compounds using energy sources such as ultraviolet light, corona discharge, or lightning. These prebiotic monomers would have first encountered moisture in cloud drops and precipitation. We propose that rapid prebiotic chemical evolution was facilitated on the primordial Earth by cycles of condensation and evaporation of cloud drops containing clay condensation nuclei and nonvolatile monomers. For example, amino acids supplied by (or synthesized during entry of) meteorites, comets, and interplanetary dust would have been scavenged by cloud drops containing clay condensation nuclei. Polymerization would have occurred within cloud systems during cycles of condensation, freezing, melting, and evaporation of cloud drops.

We suggest that polymerization reactions occurred in the atmosphere as in the Woese hypothesis, but that life originated in the ocean as in the Oparin-Haldane hypothesis. The rapidity with which chemical evolution could have occurred within clouds accommodates the time constraints suggested by recent astrophysical theories.

Ames-Moffett contact: V. Oberbeck
(415) 604-5496 or FTS 464-5496
Headquarters program office: OSSA

Comet Ice and Dust Gas Chromatograph Instrument

Bonnie O'Hara

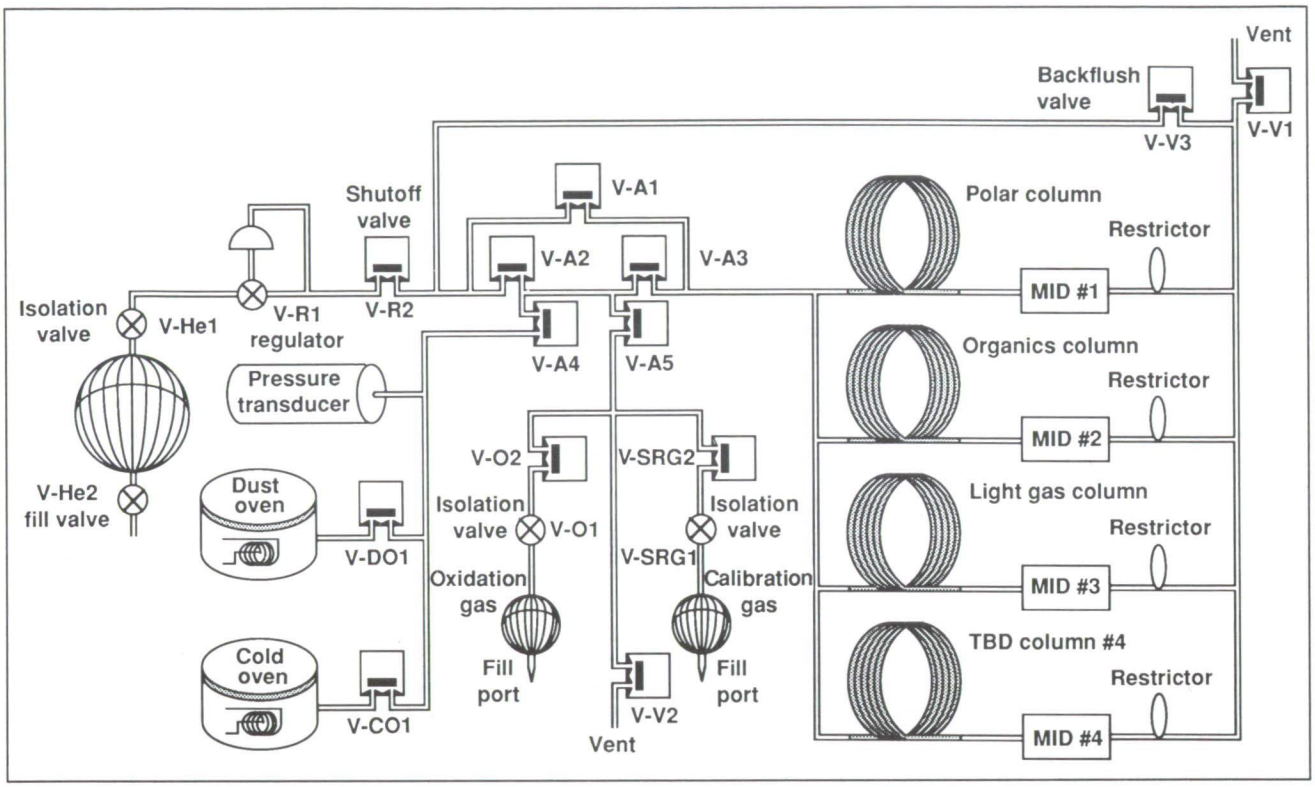


Fig. 1. Block diagram of Cometary Ice and Dust Experiment gas chromatograph

The Cometary Ice and Dust Experiment (CIDEX), an integrated gas chromatograph (GC)/ X-ray fluorescence spectrometer instrument, has been selected for inclusion on the Comet Rendezvous Asteroid Flyby (CRAF) mission. This instrument will measure the elemental and molecular constituents of collected dust grains, resulting in a greater understanding of the nature of the dust.

The GC, using modulated voltage metastable ionization detectors and a suite of columns, will measure the volatile compounds of the biogenic elements (C, H, O, N, and S) thermally released from collected ice and dust grains. Four columns, operated in parallel, have been selected to separate (1) light gases, i.e., N_2, CO, CO_2; (2) organics and sulfur gases, i.e., alkanes (C6), alkenes (C4), alkynes (C3), COS, H_2S, CS_2; and (3) polar gases (2), i.e., H_2O, alcohols (C2), aldehydes (C2), nitriles (C3), NH_3, CH_3NH_2. The fourth column, the TBD (or Confirmation) column, will also separate the polar gases and some organic gases.

As seen in the figure, control of gas and vapor flow within the GC instrument is performed by 13 miniature latching solenoid valves, for example V-A1, V-DO1. Requirements for low-power, low-weight, low-leakage, and high reliability led to the development by Parker Hannifin Corporation of a miniature latching solenoid valve weighing less than 30 grams and having an internal leak rate less than 3×10^{-8} standard cubic centimeters/second. A test gas sample valve manifold (including miniature latching solenoid valves V-A1, V-A2, V-A3, V-A4, V-A5) is being fabricated by Martin-Marietta Space Systems and will be tested to establish its GC performance characteristics.

Ames-Moffett contact: B. O'Hara
(415) 604-5770 or FTS 464-5770
Headquarters program office: OSSA

Spectroscopy and Reactivity of Mineral Analogs of Martian Soil

Jim Orenberg, Ted Roush

The objective of these investigations is the elucidation of the mineral content of the martian soil. Throughout geologic time, the martian soil has participated in surface-atmosphere interactions, volatile balances, and geological land-forming processes. As a result, the soil holds important clues to the processes that shaped the early geological history of Mars, to the amount of liquid water once present, and to extinct or extant life on the planet. Exobiologists need to thoroughly understand the geochemical and physical aspects of the martian soil to better understand similarities and differences between the early environments on Earth and Mars, and thus to answer a primary question in comparative planetology as to why life developed on Earth to its rather complex level and why, apparently, this did not occur on Mars.

Mixtures of palagonite and iron-rich montmorillonite clay (16 weight % iron as ferric oxide) were evaluated as Mars surface mineralogical models by characterization of the diffuse reflection spectrum. The presence of the 2.2-micrometer absorption band in the reflectance spectrum of clays, and its absence in the Mars spectrum, have been interpreted to indicate that highly crystalline clays cannot be a major mineral component of the soil on Mars. Palagonite does not show this absorption band feature in its spectrum. In mixtures of these two materials (parts (a) and (b) of the figure), the 2.2-micrometer clay band is not differentiated from the absorption spectrum of palagonite below 15 weight % montmorillonite. This prompts the conclusion that iron-rich montmorillonite clay may be present in the soil on Mars, up to 15 weight % in combination with palagonite, and remain undetected in remotely sensed spectra of Mars.

To extend the information contained in the laboratory spectral reflectance measurements to grain sizes or viewing geometries different from those actually observed, we are pursuing theoretical spectral modeling, based upon the equations of radiative transfer. This allows the calculation of the reflectance of a particulate surface, given the refractive indices of the component materials. The refractive indices, which describe how energy is scattered or absorbed by the particles, are limited or nonexistent for materials proposed as Mars soil analogs, such as clays and palagonite. Thus, one effort focused upon obtaining these values and, as a result, mid-infrared (5-25 micrometers) optical constants were derived for (1) the layer lattice silicates, kaolinite, serpentine, and pyrophyllite; (2) the smectite clays, montmorillonite, and saponite; and (3) palagonite, a silica-rich weathering product of basaltic glass.

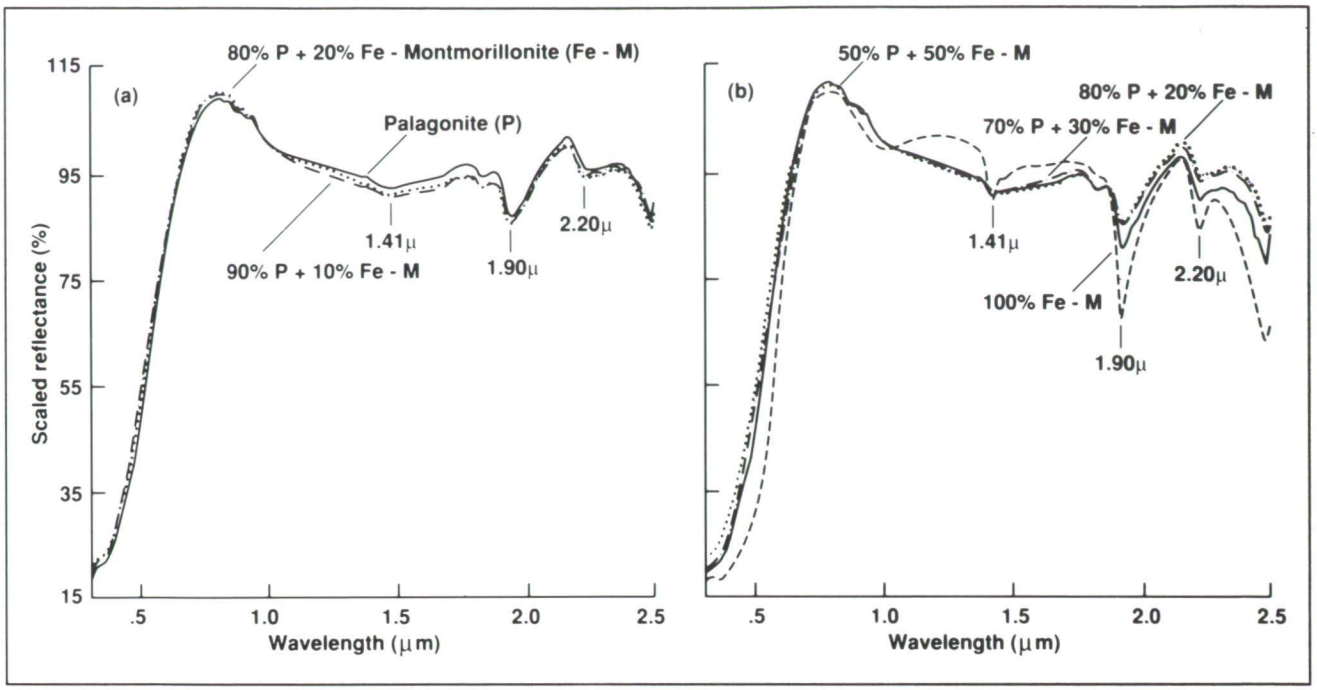


Fig. 1. A comparison of the diffuse reflectance spectra of different weight % mixtures of palagonite and Fe-montmorillonite (15.8 ~ 0.8 wt % Fe as Fe_2O_3). All spectra are scaled to unity at 1.02 micrometers

Future research includes deriving optical constants of carbonates, nitrates, sulfates, and additional silicates; and using these values in the theoretical models to constrain the composition of Mars soil materials.

The best spectral mineral analogs of the martian soil should also conform to Viking biology results. Palagonite and iron-rich montmorillonite and their weight % mixtures will be tested in the laboratory under the conditions of the gas exchange experiment, GEX, performed on Viking. A GEX apparatus consisting of a gas reaction manifold with 10 sample cells was fabricated and attached to a simple gas chromatograph; it is almost complete and ready for testing with mineral analog samples.

Ames-Moffett contact: G. Carle
(415) 604-5765 or FTS 464-5765
Headquarters program office: OSSA

Cavities in Liquids and Hydrophobic Solubilities

Andrew Pohorille, Lawrence R. Pratt

The tendency for nonpolar solution components to be sequestered from an aqueous environment—the hydrophobic effect—is the driving force for the formation of the simplest organized mesoscopic structures in aqueous solutions, namely micelles and bilayer membranes. Hydrophobic effects undoubtedly provided the dominant stabilizing factor for the self-assembly of organic materials during prebiotic evolution. One of the central goals of the NASA Exobiology Program is understanding the prebiological conditions necessary for the formation of protocells, which can execute a variety of the functions of modern cells.

Since water is ubiquitous, the issue of solubilities of nonpolar materials in aqueous phases affects an amazing variety of biological and technological problems. For example, the incorporation of nonpolar gases in ices plays a role in the formation and behavior of comets, as well as the inventory of greenhouse gases above Antarctica. It is widely appreciated that hydrophobic effects provide a major contribution to the stability of proteins. The utility of surfactants in industrial applications ranging from detergency to tertiary recovery oil to controlled drug delivery depends crucially on the hydrophobic effect.

In recent years, solubility models have led to a suggestion that the characteristic differences between nonaqueous solvents and liquid water are not due to the structure of liquid water. Instead, it was suggested that they are due principally to the comparatively small size of the water molecule. This physical picture had not been directly tested previously. Moreover, this was a picture that could be clarified by accumulating data on the structures of liquids and by attending to basic issues of the theory of liquids. For these reasons, a study based upon computer experimentation was made of a basic feature of solubility in liquids: the likelihood of finding a molecular-size cavity that could accommodate the solute.

This study showed that the frequencies of occurrence of molecular-size cavities in liquid water can be reliably calculated and that those results differed markedly from similarly computed quantities for common organic solvents. It was observed that water has a larger fractional free volume, but that free volume is distributed in smaller packets. The work to form cavities in these liquids was also obtained. Comparison of the cavity formation work for water to the same property for a simple nonpolar reference solvent indicated that the nonpolar liquid finds more configurations that can accommodate an atomic solute of substantial size and, thus, would be a better solvent for hydrophobic species.

In conjunction with previous experimental and theoretical results, these computations indicated that molecular-size cavities should be considered submacroscopic. This is important because common descriptions of hydrophobic solutes are based upon macroscopic parameters such as the thermodynamic tension of the water liquid-vapor interface. Thus, our observations provide a significant restriction on approximations involved in biomolecular modeling.

This work shows how information on the abilities of water to organize solution materials available on the early Earth can be extracted from computer simulation studies. Future directions for this research include development of improved solubility models and of software tools to provide hydrophobic maps of large-scale structures, such as macromolecules, in aqueous solution.

Ames-Moffett contact: A. Pohorille
(415) 604-5759 or FTS 464-5759
Headquarters program office: OSSA

Development of the Mid-Infrared Spectrometer for the Infrared Telescope in Space

T. L. Roellig

The Mid-Infrared Spectrometer (MIRS) is one of four instruments that will fly aboard the orbiting Infrared Telescope in Space (IRTS). This telescope is a joint NASA/Japanese Space Agency (ISAS) project that is scheduled for a spring 1994 launch aboard a Japanese expendable launch vehicle and subsequent retrieval by the Space Shuttle. The telescope itself is liquid helium-cooled and will survey approximately 12% of the sky before its cryogen runs out and it begins to warm up. The four infrared instruments that share a common focal plane on the telescope are being built by groups in both Japan and the United States. The MIRS was developed by a group at the University of Tokyo with a group here at Ames Research Center. The MIRS is a low-resolution survey instrument, operating between 4.2 and 11.6 micrometers, optimized for background-limited studies of the solid state features in low-surface brightness diffuse sources. A cold shutter and an internal calibration source will allow absolute flux measurements of the astronomical sources.

During FY 90 the flight model of the MIRS was assembled and is now being tested and calibrated. The dispersive optics, instrument housing, and warm readout electronics were built in Japan under the direction of Dr. T. Onaka of the University of Tokyo. These parts were then shipped to Ames where they were integrated with the detectors, field optics, and cold pre-processing electronics that were developed by the Ames group.

Preliminary measurements of the MIRS performance have indicated that the instrument sensitivity is as high as was originally designed. This means that the MIRS sensitivity will be limited only by the natural background from the zodiacal dust emission throughout its entire spectral range. Extrapolating from the IRAS mission, this means that the MIRS should be able to measure the spectra of at least 30,000 different discrete point sources as well as measure the spectra from broad areas of diffuse regions.

The present schedule is for the MIRS to undergo another 2 months of calibration and testing at Ames, after which it will be shipped to ISAS in Japan for further testing and integration into the telescope with the other instruments. Performance and interference tests will then be conducted with the complete telescope and instrument assembly. This instrument/telescope assembly is then scheduled to be delivered to the spacecraft assembly point for testing and integration in early FY 92.

Aside from the Si:Bi infrared detectors, which were supplied by Aerojet ElectroSystems, Inc., all of the other U.S.-supplied components of the MIRS were constructed at Ames. In addition to the work done by the Space Science Division professional and technical staff, we have had assistance in this project from M. Savage and T. McMahon of Sterling Software Corp. as well as from T. Gustavson of California Institute of Technology, and N. Jennerjohn of San Francisco State University.

Ames-Moffett contact: T. Roellig
(415) 604-6426 or FTS 464-6426
Headquarters program office: OSSA

Evolution of Biological Carbon Fixation and the Search for Life on Mars

Lynn J. Rothschild

Biological carbon fixation (primary production) was a crucial innovation in early evolution because it liberated life from abiotically produced organic carbon. Biological carbon fixation permitted the development of the biogeochemical carbon cycle, the evolution of a complex community structure among living organisms and, indirectly, the formation of an aerobic environment on Earth through oxygenic photosynthesis. Both morphological fossils and the stable carbon isotope record suggest biological carbon fixation arose very early in the evolution of life, at least by 3.5 billion years ago. Oxygenic photoautotrophy, the subject of this research, may have evolved as early as 2.9 billion years ago, or possibly even 3.5 billion years ago.

My studies address the question, "Were rates of biological carbon fixation, particularly in photoautotrophs, different in the past?" To answer this question, I have experimentally manipulated modern organisms (microbial mats) that serve as analogs for ancient communities (stromatolites). The mats studied are found in Baja, California; one in a hypersaline pond of a salt company, and the other in the intertidal zone of Laguna Ojo de Liebre. To determine rates of carbon fixation, inorganic carbon ($NaH^{14}CO_3$) was added to samples of mat in the field with and without supplemental nutrients (i.e., bicarbonate, nitrate, ammonia, or phosphate).

These studies revealed a diurnal pattern of carbon fixation that rises with the Sun, dips during midday, peaks again in the early afternoon, and drops to essentially zero by sunset. In these mats, the diurnal pattern of carbon fixation is influenced primarily by the availability of light and inorganic carbon, and secondarily by the availability of nitrogen. In contrast, total daily carbon fixation is strongly influenced by temperature.

Carbon fixation in many other photoautotrophic organisms, from cyanobacteria to plants, is limited by the levels of inorganic carbon available today. During the history of the Earth, the availability of inorganic carbon is thought to have decreased dramatically while many other environmental variables are thought to have remained essentially constant in the marine environment.

In a novel approach to both evolutionary and carbon fixation studies, Rocco Mancinelli and I determined experimentally the effect of different levels of inorganic carbon on carbon fixation using the mat communities to reconstruct carbon fixation rates in stromatolites from their origin (~3.5 billion years ago) to the present. The results suggested that carbon fixation in such communities has been carbon-limited for much of their history. This carbon limitation may at least partially explain the virtual disappearance of stromatolites from the fossil record during the last 600 million years after being dominant for over 2 billion years.

In a related study, R. Mancinelli, M. White, L. Giver (University of California, Berkeley), and I showed that cyanobacteria living in an evaporite crust can fix carbon and nitrogen in situ. Because the evaporite is composed of the salts gypsum and halite, I suggested that such communities could exist on Mars. This suggestion has clear implications for future exobiological investigations of Mars. For example, there could be experiments in dried lake beds where evaporites are thought to occur.

Ames-Moffett contact: L. Rothschild
(415) 604-6525 or FTS 464-6525
Headquarters program office: OSSA

Experimental Study of Aerosol Formation in Titan's Atmosphere

Thomas W. Scattergood

The atmospheres of all of the planets, Saturn's satellite Titan, and Neptune's satellite Triton are known to contain aerosols (clouds and hazes). For the outer planets and Titan, these aerosols are the products of active chemistry involving simple compounds in their atmospheres. The presence of aerosols can have profound effects on the chemistry and radiation balance of the atmosphere and can influence the nature of the sunlight that is reflected back to Earth. Future entry probes, e.g., the Galileo probe to Jupiter in 1996 and the Cassini-Huygens probe to Titan in 2003, can directly examine atmospheric aerosols. Until then, the only methods for studying the atmospheric aerosols of the outer planets and of Titan are analysis of planetary spectra and experimental and theoretical simulation.

To help understand the nature of the aerosols found in the atmosphere of Titan and how the aerosols are formed, an experimental program is under way at Ames Research Center to study the formation of particles in Titan-like gas mixtures and to examine the chemical and physical properties of these particles. These studies are being done by Tom Scattergood (SUNY at Stony Brook/Ames), Brad Stone and Ed Lau (San Jose State University), and Verne Oberbeck (Ames).

In these experiments, the particles are formed by exposing various mixtures of acetylene (C_2H_2), ethylene (C_2H_4), and hydrogen cyanide (HCN), all known components of Titan's atmosphere, in molecular nitrogen (N_2), the dominant component, to 1850Å ultraviolet light (UV) emitted by a low-pressure mercury lamp. Ultraviolet light is considered to be the dominant source of energy for driving chemistry in outer planetary atmospheres. The reactant gas (or gases in some experiments) is decomposed by the UV light, and reactions of the products eventually lead to the formation of particles suspended in the gas. After a few hours, the particles settle out onto clean plates placed at the bottom of the photolysis vessel. These plates are then removed and placed in a scanning electron microscope so that the size distributions of the collected particles can be determined. Also, samples of the gases from which the particles were formed can be analyzed by gas chromatography to determine the identities of the molecules which may have led to particle formation.

In all of the experiments done thus far, particles were formed as evidenced by the scattering of light from the beam of a helium/neon laser. Examination of particles collected on the plates showed the basic particles to be spheres of 0.1 to 1.4 micrometers, with a mean radius of about 0.6 micrometers. A typical photograph of the aerosols formed from the photolysis of 1 torr C_2H_2 in 58 torr N_2 is shown. As can be seen in the photograph (and as found in the other photographs taken), many of the particles collected on the plates consist of roughly linear aggregates of the spheres, some containing as many as 10 units.

These results are consistent with those obtained by A. Bar-nun, I. Kleinfeld, and E. Ganor (Tel Aviv University) who did similar experiments but with 20 torr of C_2H_2. It is interesting to note that the mean size (0.6 micrometers) is consistent with the mean size (0.5 micrometers) of Titan's aerosols as determined from analysis of Titan's visible spectrum. However, recent analyses presented at the 1990 meeting of the Division of Planetary Sciences of the American Astronomical Society indicate that Titan's aerosols are not spherical, but must be elongated. The results of our experiments support this conclusion.

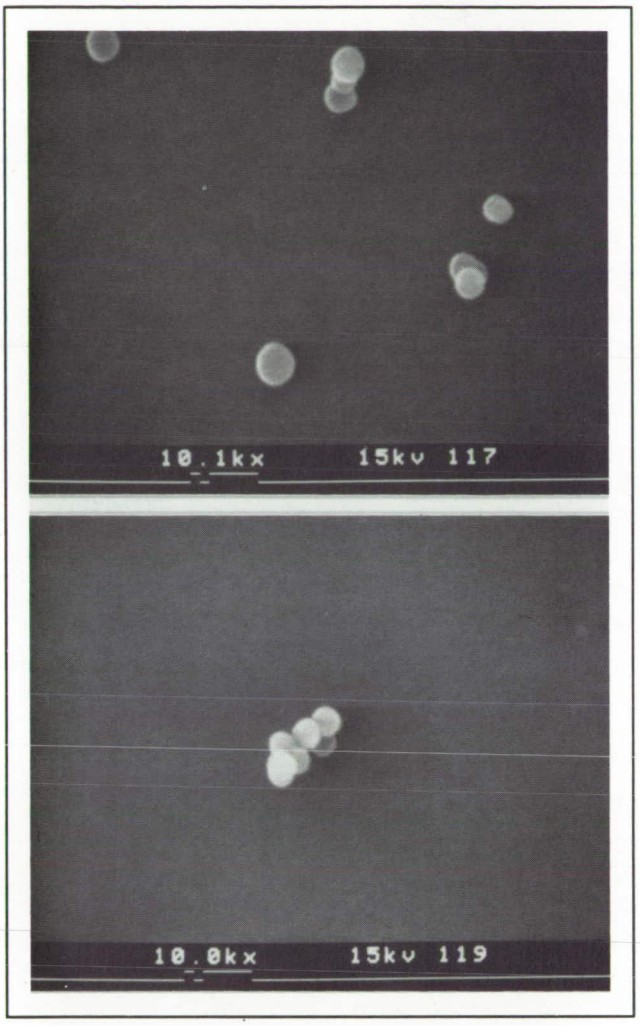


Fig. 1. Photopolymer produced from 1849 Å photolysis of C_2H_2. Mixture: 1 torr C_2H_2, 58 torr N_2

Future work will include mixtures with lower pressures of the reactant gases, which are more realistic models of Titan's upper atmosphere where the photoaerosols are made. This work will include measurements of the production rates of the aerosols as functions of reactant gas pressure and photolysis time. Also, evaluation of the suitability of these experiments for the Gas Grain Simulation Facility, to be flown aboard Space Station Freedom, and initial determination of the hardware needed to perform these experiments will be made.

Ames-Moffett contact: T. Scattergood
(415) 604-6163 or FTS 464-6163
Headquarters program office: OSSA

ORIGINAL PAGE
BLACK AND WHITE PHOTOGRAPH

Mineral Crystals as Biomarkers in the Search for Life on Mars

Deborah E. Schwartz, Rocco L. Mancinelli

By 3.5 billion years ago, life on Earth appeared to be widespread and to have developed sophisticated ecological communities. Thus, life must have originated prior to 3.5 billion years ago; but tectonic processes, substantial weathering, and biological activity on Earth make unlikely the discovery of evidence of this early life. Geologic and climatologic models have shown that conditions on Earth may have been similar to those on Mars during this early period. Therefore, the events leading to the origin of life, which we know occurred on Earth, may have also occurred on Mars. Subsequent planetary development, however, seems to have maintained habitable conditions only on Earth.

Climatic, atmospheric, and chemical changes on Mars may have led to the extinction of life forms that might have once existed. The apparent absence of tectonism, present-day hydrologic cycles, and biological activity allows us to speculate that traces of early life forms, if they existed, may remain in subsurface materials. An objective of exobiology is to search for traces of possible extinct life forms on Mars. To attain this objective, universal signatures or biomarkers indicative of past (or present) biological activity must be identified, and used in the search for life on Mars.

Several potentially applicable biomarkers have been identified and include: organics (e.g., specific classes of lipids and hopanes), suites of compounds (reduced carbon, sulfur, reduced nitrogen), as well as the isotopic ratios of C, N, and S. All of these biomarkers can have either biologic or abiotic origins and, thus, the discovery of any one of them alone will not give absolute indication of past (or present) biological activity.

We have been investigating the use of minerals resulting from biologically controlled mineralization processes as biomarkers because they have crystallographic, morphologic, and isotopic characteristics distinguishable from abiotically produced minerals of the same chemical composition. Biomineralization is phylogenetically diverse occurring almost universally throughout the biosphere. Additionally, biominerals have been found in the fossil record as far back as the Precambrian, and are stable over long periods of time. Some biologically produced minerals, such as the siliceous frustules of diatoms, are abundant, widely distributed, and play an important role in the geologic record.

The discovery of a biologically produced mineral, as with the discovery of a fossil, can provide direct, definitive evidence for life. The technology needed to discern biologically produced minerals exists; such an experiment could be flown and used on future Mars missions or performed in the laboratory following a sample return.

Ames-Moffett contact: D. Schwartz
(415) 604-3668 or FTS 464-3668
Headquarters program office: OSSA

Silicone Gas Chromatographic Column Development

Thomas Shen

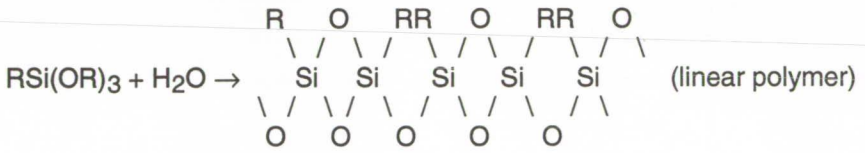
In situ analyses of planets and their atmospheres and of other solar system bodies, such as comets, require highly sensitive and specialized instrumentation. These flight instruments must be highly accurate and precise. They also must be able to perform meaningful analyses on small sample amounts under very restricted conditions.

Gas chromatography (GC) has been successfully used in the Viking and Pioneer Venus Missions. It has also been proposed for use on future missions, such as Comet Rendezvous Asteroid Flyby and Cassini, which require the determination of low concentrations of polar and nonpolar chemicals at a part-per-billion level.

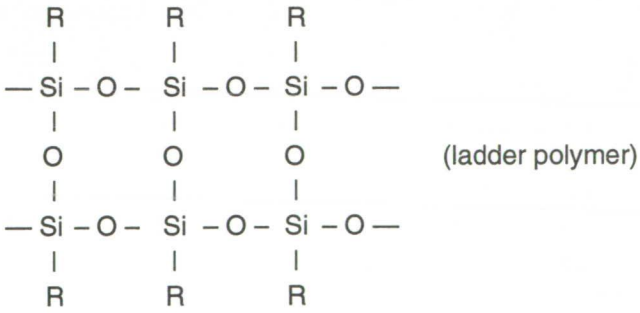
The GC consists of two important components, columns and detectors. A highly sensitive detector/spectrometer combination (the metastable ionization detector, MID, and the ion mobility spectrometer, IMS) was developed for future missions. These detectors, however, are extremely sensitive to column bleed, which occurs with conventional liquid phases coated on solid supports, and yield chromatograms with very noisy baselines. However, the use of silicone liquid phases on solid supports provides good separation of polar as well as nonpolar compounds.

As a result of problems experienced when using the conventional column, we recently synthesized highly crosslinked silicone polymer packed columns. These columns not only separate amines and alcohols of polar compounds, but also resolve the nonpolar compounds, such as alkanes, alkenes, and alkynes.

Generally, silicone condensation polymerization gives low or noncrosslinking polymers that are soluble in organic solvents. This reaction can be explained in the following equation:



or



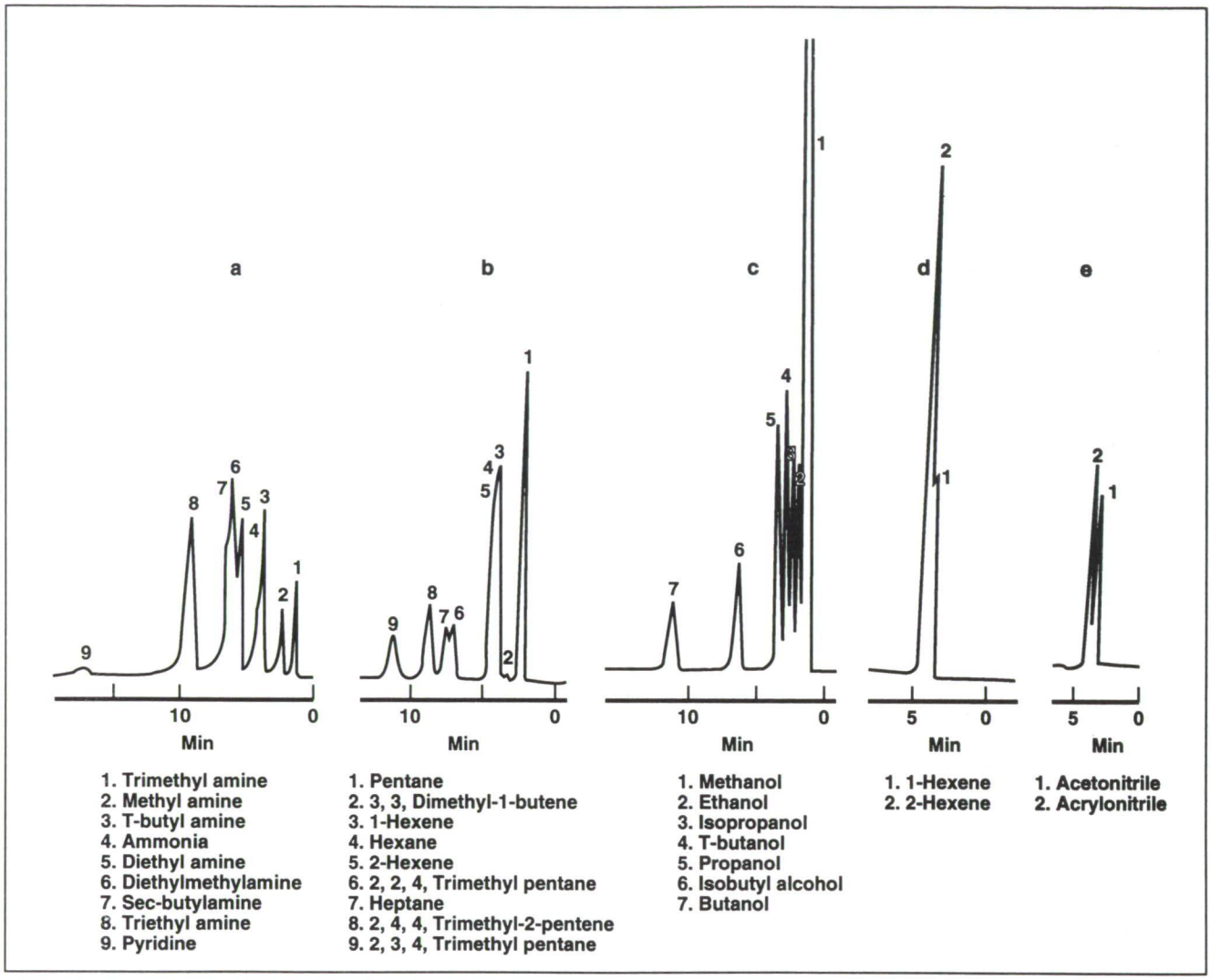


Fig. 1. GC chromatograms of various compounds using a vinyltriethoxylsilane/octadecyltrichlorosilane column (6-feet × 1/16-inch stainless steel) at 107°C and 13 milliliters/minute helium

Both linear and ladder polymers are soluble in organic solvents, such as heptane and THF, and are not useful for GC column applications. To make highly crosslinked polymers, vinyl groups were included and a free radical polymerization was further applied. Condensation polymerization and free radical polymerization of vinyltriethoxylsilane with octadecyltrichlorosilane forms highly crosslinked polymers that are not soluble in most solvents. Analysis of separated hydrocarbons, amines, and alcohol mixtures using these copolymers gives sharp peaks as shown in both figures.

Parts (a) through (e) of the first figure shows the separation of different organic chemical groups, hydrocarbons, alcohols, amines, and nitriles. The second figure demonstrates that no bleeding was detected when IMS and MID detectors were used.

This newly synthesized silicone column, made from the copolymer of vinyltriethoxylsilane and octadecyltrichlorosilane with a molar ratio of 2 /1, is useful for separating polar and nonpolar chemicals with short retention times at low operation temperatures. These features make such a column useful for flight missions. In addition, this column may be used

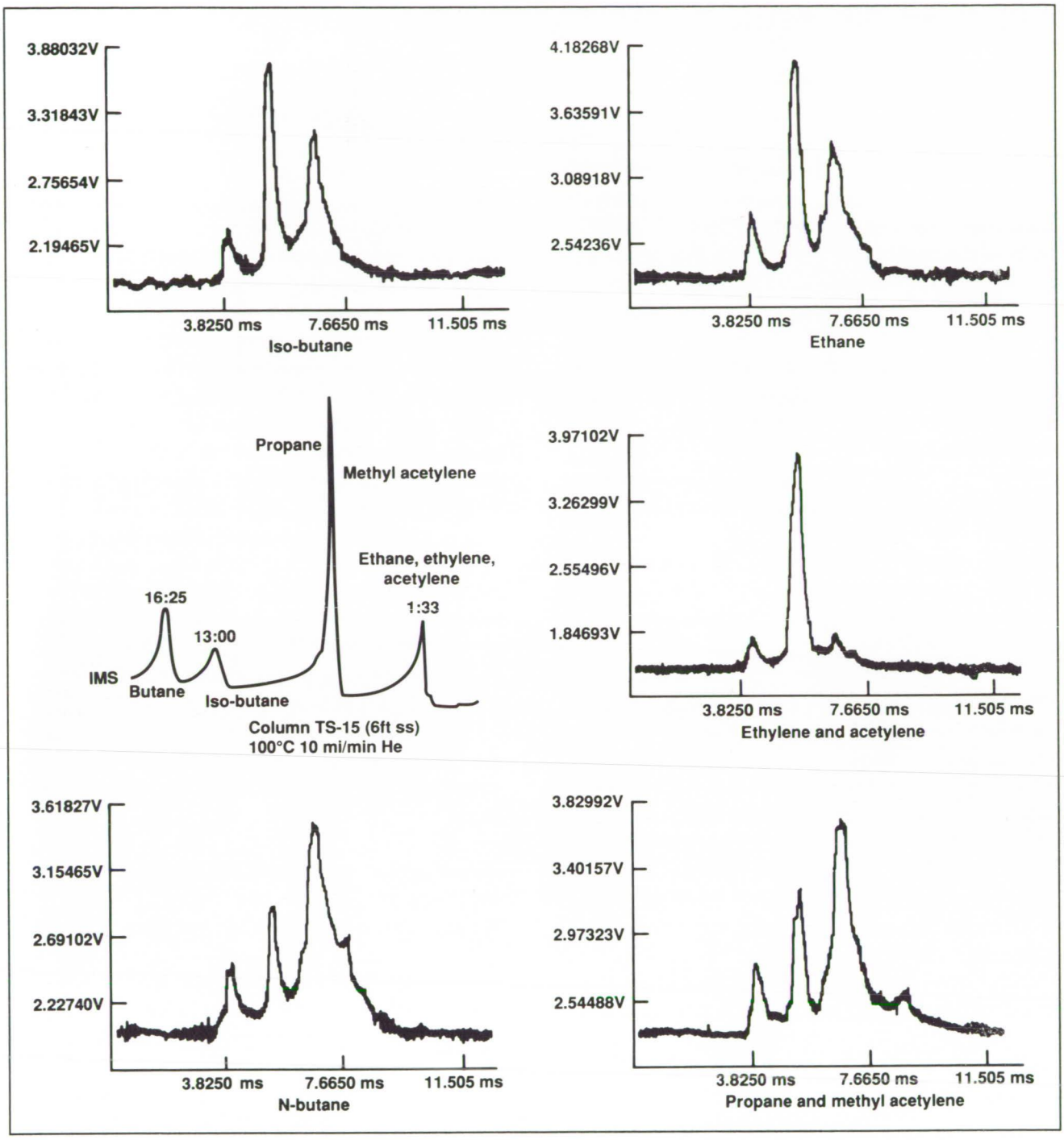


Fig. 2. Collecting electrode current shows total ion current regardless of drift time. Different IMS spectra are then produced from each GC peak

as a universal GC column if a temperature programing oven or an IMS or Gas Chromatograph-Mass Spectrometer detector is used. A patent disclosure will be filed.

Ames-Moffett contact: T. Shen
(415) 604-5769 or FTS 464-5769
Headquarters program office: OSSA

A Planetary Rings Data Center

Mark R. Showalter, Jeffrey N. Cuzzi

The Planetary Data System (PDS) is charged with restoring, cataloging, and archiving all planetary data. The motivation behind the program is to improve the distribution of planetary data sets, accompanied by the ancillary information needed for their analysis. Responsibility for the data applicable to various scientific disciplines has been divided among a number of institutions, which were selected through a competitive process in late 1989. Ames Research Center was chosen as the site for the PDS "Rings Node."

Our collaborators include J. B. Pollack of Ames, G. L. Tyler and E. A. Marouf of Stanford University, and P. D. Nicholson of Cornell University. During our first year of activity, our primary emphasis has been on setting up our initial facilities. However, several of our accomplishments in FY 90 illustrate the research aspects of the PDS.

One ongoing project is the development of an image catalog, so that one may quickly sort through the enormous suite of Voyager images and identify that subset most relevant to a particular study. Ultimately, users will be able to constrain the search based on the specific ring features depicted, the viewing and lighting geometry, timing, and other image properties. In July, Mark Showalter used a prototype of this catalog to identify the images in which he discovered Saturn's 18th moon, now designated 1981S13.

Our node also supported a comparative study of Saturn occultation data sets by P. D. Nicholson at Cornell, which has contributed significantly to the reliability and scientific value of these data. The Voyager 2 photopolarimeter (PPS) observed the brightness of a star as it was occulted by Saturn's rings, yielding a radial profile of ring opacity with 100-meter resolution. A comparable data set was provided by the Voyager 1 radio science (RSS) experiment, in which radio transmissions from the spacecraft were received at the ground as Voyager passed behind the rings. After processing, the RSS opacity profiles have radial resolution comparable to that of the PPS. Unfortunately, these two data sets have shown a persistent radial offset, such that circular ring features fall at different radial positions within each profile. Nicholson has now corrected a timing error in the PPS data set and solved for a revised Saturn ring plane orientation, which brings these two data sets into proper alignment.

These FY 90 accomplishments represent two examples of the scientific contributions that we anticipate under the auspices of the PDS Rings Node.

Ames-Moffett contact: M. Showalter
(415) 604-3382 or FTS 464-3382
Headquarters program office: OSSA

Mineralogy of Mercury, the Moon, and Asteroids

Ann L. Sprague

Very little is known regarding the composition of Mercury's surface. The few locations observed show less iron content than lunar basalts. On asteroids, compositional information regarding the presence of olivine-, pyroxene-, iron-, and water-bearing rocks is known through the study of visible and near-infrared reflectance spectroscopy. The Moon's mineralogy is better known; samples from seven locations have been returned to Earth and analyzed in the laboratory, and extensive ground-based remote sensing has provided considerable information regarding regional compositional differences.

A National Research Council postdoctoral fellow (Ames Research Center) Ann L. Sprague, and her colleagues Fred Witteborn, Dale Cruikshank (Ames), and Richard Kozlowski (University of Arizona) have successfully obtained thermal infrared spectra of Mercury, the Moon, and a suite of diverse but well characterized asteroids using the Faint Object Grating Spectrometer developed by Fred Witteborn, Jesse Bregman (Ames) and Dave Rank (Lick Observatory).

These thermal infrared spectra reveal emissivity maxima and minima determined by the principal absorption bands of constituent minerals. By analyzing these spectra it has been determined that the composition of Mercury at three locations is more feldspathic than basaltic or anorthositic locations on the Moon. The spectrum of Vesta indicates it is more mafic (contains more iron, magnesium, and calcium) than any location observed in the thermal infrared on the Moon so far.

Continued analyses are aimed at providing the first map of Mercury to show rock type and at providing another effective way of determining regolith composition of asteroids.

Ames-Moffett contact: A. Sprague
(415) 604-6857 or FTS 464-6857
Headquarters program office: OSSA

Physics of the Lunar Alkali Atmosphere

Ann L. Sprague

Neutral sodium and potassium atoms are two newly discovered components to the lunar tenuous atmosphere. National Research Council postdoctoral fellow (Ames Research Center) Ann L. Sprague and her colleagues Donald Hunten and Richard Kozlowski (University of Arizona) have illustrated that the different distributions of sodium and potassium about the planet can in part be explained by the way the atoms absorb visible light while they are momentarily adsorbed on surface materials.

Sodium has a distribution characterized by a higher temperature than that of potassium. Both constituents have nonthermal distributions; that is, they do not have the velocity distribution expected from the lunar surface temperature. The study of the tenuous lunar atmosphere may make important contributions to understanding the relationship of planetary outgassing to atmospheric composition and to the inventory of volatile elements in the interior and regolith of solid solar system bodies.

Continued observations are planned to determine the variability of sodium and potassium and what effects, if any, location and phase have on the quantity of atoms in the atmosphere. Resonant emissions from the atoms as they bounce around the surface in sunlight are observed with a high-resolution echelle spectrograph at the Mt. Bigelow Observatory.

Ames-Moffett contact: A. Sprague
(415) 604-6857 or FTS 464-6857
Headquarters program office: OSSA

Telepresence for Planetary Exploration

Carol Stoker, Michael McGreevy, Christopher McKay, Owen Gwynne

The fundamental limiting factor in the scientific exploration of Mars by human crews is the range of human mobility. Even with the most ambitious and technologically capable program, astronaut time will always be at a premium. The ability of Mars crew members to conduct field science will be limited by the capabilities of the transportation system that gets them to the field site, the time they can spend at the field site, the time they can spend outside of a protected habitat, and limitations on manual dexterity imposed by their pressure suits.

A human in a space suit may not be the most capable sample acquisition system on Mars, but a trained scientist is certainly the best system for conducting science. The role of the human in field science is not simply intelligent sample selection, but rather one of formulating and testing hypotheses by interacting with the environment. However, unless the range of human mobility can be significantly expanded, science will proceed at an unacceptably slow pace.

Telepresence is a promising technology which can be used to expand the range over which humans can interact with the martian environment. Stated simply, telepresence is a form of remote control which projects the senses of the human operator into a distant work site. In practice, telepresence is a high-fidelity form of teleoperation in which the machine senses are directly projected into the senses of the human operator and where the machine is servo-controlled by actions performed by the human operator. Ideally, the human operator of a telepresence system should feel present in the environment. Using telepresence on Mars will allow detailed exploration of a much larger region than would be possible otherwise.

Telepresence offers many advantages for facilitating human exploration of Mars. A suite of telerobots could be deployed at a variety of locations on Mars, allowing the Mars explorers to expand the number and diversity of sites examined. Mars science crews could use their time with maximum effectiveness to perform science tasks which require a high level of real-time interaction with the environment.

Furthermore, using telepresence would provide superhuman sensory capabilities, such as multispectral vision to aid in the identification of minerals. Expanded data-gathering capability (compared to that available to an unaided field scientist), combined with data handling to make the information accessible, could vastly improve the quality of field work. Another attractive advantage afforded by telepresent science is the capability of recording the entire field experience with high fidelity, thereby keeping the most accurate possible record of the data.

In addition, telepresence and recording capabilities, combined with virtual environment simulation, would allow the data and the field experience to be shared with others on Earth. This would facilitate not only the involvement of an expanded scientific community, but it could be used as a tool for education to allow the general public to share in the experience of Mars exploration.

The focus of this project is to develop telepresence technology for use in scientific field work. Our approach has been to establish a core team of scientists and technology researchers, to conduct field studies in scientifically interesting environments, to observe what the scientist does when present, and then to step back incrementally. Teaming the planetary science users with the exploration technologists early in the research and development phase ensures that a critical focus on developing technology that meets real scientific needs is maintained.



Fig. 1. Artificial vision system

In FY 90, the first of a series of field studies was performed in the Amboy lava field in the southern California Mojave Desert, April 7-9, 1990. This site was chosen because of its scientific relevance to Mars geoscience exploration problems, and because it had been extensively studied by members of our scientific team. The object of this study was to degrade the geoscientists' natural sense of presence by providing the field scientist with an artificial vision system of limited visual quality. The scientist then tried to perform normal field tasks using this visual system. The figure is an illustration of the artificial vision system.

By interviewing the subjects and documenting their reactions and preferences while trying to use the system, we gained considerable insight into the needs and requirements for telepresence systems. The results of the Amboy study provide a rich source of concrete observations of exploration behavior that are applicable to the design of telepresence systems.

Ames-Moffett contact: C. Stoker
(415) 604-6490 or FTS 464-6490
Headquarters program office: OSSA

ORIGINAL PAGE
BLACK AND WHITE PHOTOGRAPH

Science Strategy for Human Exploration of Mars

Carol Stoker, Christopher McKay,
Robert Haberle, Owen Gwynne

Human exploration of Mars represents an unprecedented scientific challenge. A human presence on Mars would open up new possibilities in terms of the breadth and detail of scientific exploration of that planet. The level and scope of scientific activity on Mars would be a valid rationale for the expenditures necessary to accomplish the program.

During FY 90, we have worked in support of the Space Exploration Initiative to develop a scientific rationale and strategy for the human exploration of Mars. To support this effort, we held several workshops to solicit input from the broad scientific community, and we worked with several groups within and outside of NASA who were studying mission design options to gain a perspective on the technologically possible strategies for human exploration of Mars. The key results of this analysis are described here.

The scientific objectives of Mars exploration can be framed within the overarching theme of exploring Mars as another home for life, both for evidence of past or present life on Mars, and as a potential future home for human life. The two major areas of research within this theme are (1) determining the relationship between planetary evolution, climate change, and life; and (2) determining the habitability of Mars. Within this framework, we have analyzed the exploration objectives for exobiology, climatology, atmospheric science, geology, and martian resource assessment.

Simply stated, exploration and science are the acts of discovery and understanding. The workshop concluded that there is a level of science and exploration accomplishment which, in itself, is a valid rationale for performing the exploration. Each of the proposed mission profiles was examined from this viewpoint. Missions that fall into the class of "sprint" or "flags and footprints" are generally characterized by individual missions with short stay times and do not reach that level of accomplishment. Missions which have an extended stay time (more than 1 year), but limited mobility range, can do significant science and exploration for a few years if the landing site is carefully selected. However, to accomplish a level of science and exploration that truly justifies the investment, the program will require decades of exploration with surface access over a regional area with at least a 4000-kilometer radius.

Human exploration of the scope described is likely to proceed in four major phases: (1) Precursor phase, that will obtain environmental knowledge necessary for human exploration; (2) Emplacement phase, that includes the first few human landings where crews will explore the local area of the landing site; (3) Consolidation phase, when a permanent base will be constructed and crews will be capable of detailed exploration over regional scales; (4) Utilization phase, in which a continuously occupied permanent Mars base exists and humans will be capable of detailed global exploration of the martian surface.

The phases of exploration differ primarily in the range and capabilities of human mobility. In the Emplacement phase, mobility is likely to be via an unpressurized rover, similar to the Apollo lunar rover, which will have a range of a few tens of kilometers. In the Consolidation phase, mobility will be via a pressurized all-terrain vehicle capable of expeditions from the base site lasting several weeks. In the Utilization phase, humans will be capable of expeditions several months long to any point on the martian surface by using a suborbital rocket equipped with habitat, lab, and return vehicle. Because of human mobility limitations, it is important to extend the range and duration of exploration in all phases by using teleoperated rover vehicles. The development of a telepresence capability to operate remote vehicles on Mars and perform surface field science is the subject of a study described in the article titled "Science Strategy for Human Exploration of Mars."

Site selection for human missions to Mars must consider the multi-decade time frame of these four exploration phases. We suggest that operations in the first two phases be focused in the regional area containing the Coprates Quadrangle and adjacent areas.

Ames-Moffett contact: C. Stoker
(415) 604-6490 or FTS 464-6490
Headquarters program office: OSSA

An Instrumentation Technique to Measure Water Vapor in the Martian Atmosphere

José Valentin, Kirsten Hall, John Phillips

The technique of selective thermal modulation (STM) has been proven feasible for monitoring water vapor in the martian atmosphere. Since water vapor is the only component modulated, the need for a gas chromatographic column is eliminated.

The STM system used in this work is shown in the first figure. It consists of a modulator and a thermal conductivity detector. The modulator is a piece of tubing coated with sorbitol which produces a change in water concentration resulting in a change in the detected signal. The water vapor modulation system was calibrated using both helium and carbon dioxide (i.e., carbon dioxide, the main component of the martian atmosphere, is used to emulate the martian environment) as the carriers, followed by signal averaging of the data to improve the sensitivity of the detector for water.

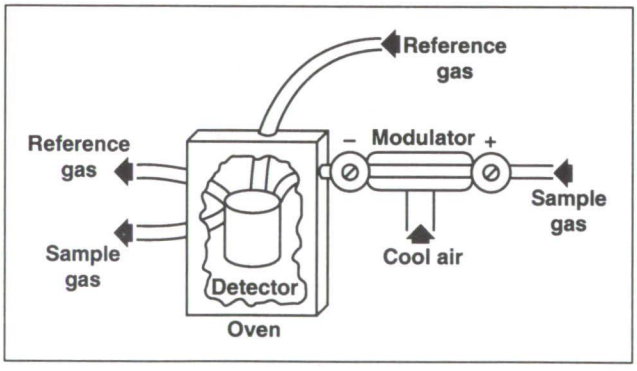
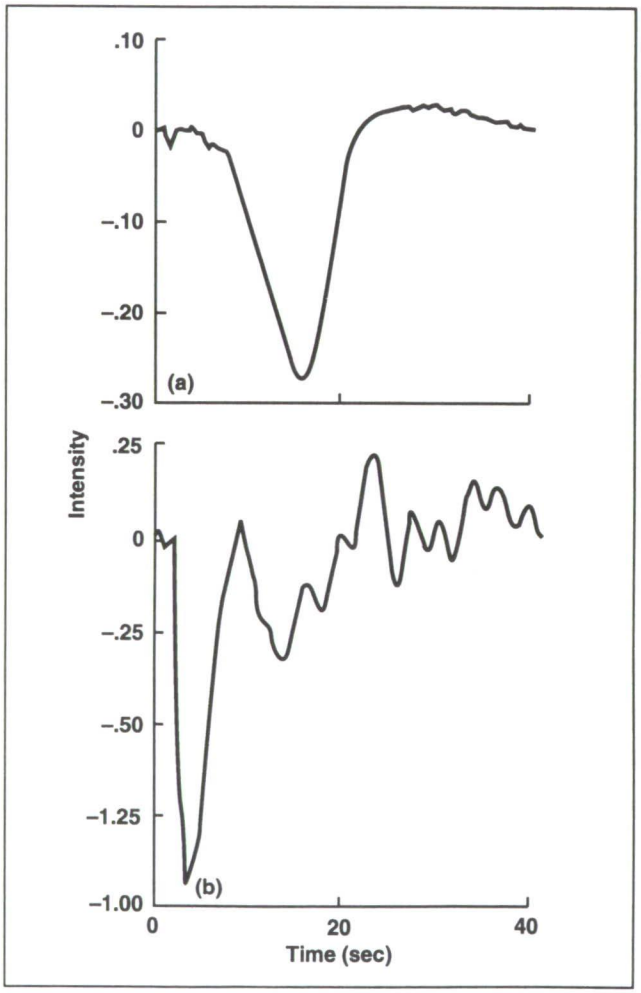


Fig. 1. Major components of the selective thermal desorption modulation system

The second figure represents the signals obtained after performing signal averaging computations using the sample mixture containing 41.5 ± 0.8 parts per million of water vapor in helium (part (a) of the second figure) and the mixture containing 100.9 ± 2.0 parts per million of water in carbon dioxide (part (b) of the second figure).



Flg. 2. Response obtained from signal averaging of water vapor in (a) helium, and (b) carbon dioxide. The data acquisition rate is 2 points/second and the detector oven is maintained at 105°C. The water concentrations are (a) 41.5 ppm (47 modulations), and (b) 100.9 ppm (95 modulations)

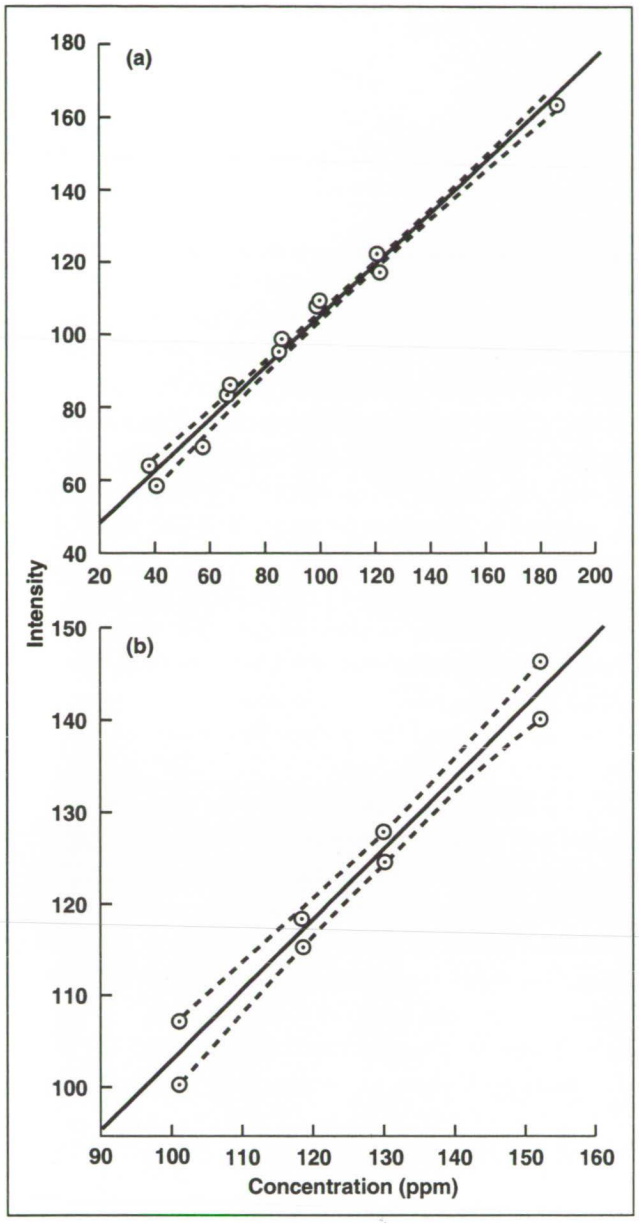


Fig. 3. Calibration curves illustrating the linear increase in signal intensity with increasing concentrations of water vapor in (a) helium, and (b) carbon dioxide. Each point represents (a) 32 minutes, and (b) 60 minutes of data averaged together

The small peak present in both signals at time = 5 seconds is the result of a voltage surge initiated by turning the electric switch on and off, controlling the flow of cold air.

Part (a) was generated from 32 minutes of data acquisition. The signal-to-noise ratio for water in helium improved by a factor of 13.5 as a result of signal averaging, lowering the detection limit from 17.3 parts per million for one pulse signal to 1.3 parts per million for the averaged pulse signal.

Part (b) was generated from 60 minutes of data acquisition. The signal-to-noise ratio for water in carbon dioxide improved by a factor of 8.1 as a result of signal averaging, lowering the detection limit from 460.8 parts per million for one pulse signal to 56.7 parts per million for the averaged pulse signal. Here the signal-to-noise ratio is worse than in part (a) because of the similarity in thermal conductivity between water vapor and carbon dioxide at room temperature.

The third figure represents the calibration curves for water in helium (part (a)) and water in carbon dioxide (part (b)) proving the feasibility of this technique.

The STM technique can easily be developed for use in any application that requires quantitative analysis of water vapor concentration. The power of this technique lies in its simplicity. It consists of only a few components. These advantages may one day allow the STM technique to be widely used in the analysis of gases, specifically in analyzing water vapor in the martian atmosphere from a land rover or a descending spacecraft.

Ames-Moffett contact: J. Valentin
(415) 604-5766 or FTS 464-5766
Headquarters program office: OSSA

Galileo Mission to Jupiter

Richard E. Young

Galileo is the first planetary mission designed to conduct extended observations of one of the giant outer planets, in this case Jupiter, and is the first mission to directly sample the atmosphere of one of the giant planets.

The spacecraft consists of an orbiter and atmospheric entry probe. The orbiter will conduct an extensive (approximately 10 orbits during a 22-month period) survey of the Jovian system, including the planet, its satellites, and its magnetosphere. The entry probe will directly sample the composition, structure, and meteorological state of Jupiter's atmosphere. The spacecraft was launched October 18, 1989, aboard the Space Shuttle Atlantis, and will encounter Jupiter on December 7, 1995. During the trip to Jupiter, Galileo will make scientific observations of Venus, the Earth-Moon system, and obtain the first closeup views of an asteroid.

The atmospheric entry probe represents one of the most difficult and demanding aspects of Galileo. The probe was designed and built by Hughes Aircraft under the supervision of Ames Research Center. At encounter with Jupiter, the probe's speed relative to the Jovian atmosphere exceeds 100,000 mph, and peak deceleration due to atmospheric entry is equivalent to 350 g. Bow shock temperature is 28,000° F, and two-thirds of the heat shield ablates away during deceleration to Mach 1. The probe carries six scientific instruments and will measure atmospheric winds, composition, structure, radiative heating distribution, aerosol distribution, helium abundance, and lightning.

As of mid-January 1991, the spacecraft is in good health, and there have been no major problems. The Venus flyby occurred in February 1990, and the planned Venus observing sequence was carried out successfully. Preliminary analysis of the data, which was telemetered to Earth in November 1990, indicates that the data is of high quality and will produce some important results concerning the dynamics, chemistry, and clouds of Venus. Images taken in the ultraviolet and near-infrared parts of the spectrum show features in the clouds which can be used to give information on dynamics and cloud structure. Spectral results indicate that water vapor probably decreases near the planet surface. There appears to be a polar dipole feature in the southern hemisphere similar to the one previously observed in the northern hemisphere.

In December 1990, Galileo flew by Earth, making observations of the Earth-Moon system. Images of the Earth and the far side of the Moon were obtained. Spectral measurements and particle and field measurements were also made. The main objective was to achieve a gravity assist from the Earth, which was completely successful.

Galileo is now heading toward an encounter with the asteroid Gaspra in October 1991. This will be the first close flyby of an asteroid, within a distance of about 1600 kilometers.

Ames-Moffett contact: B. Chin
(415) 604-6523 or FTS 464-6523
Headquarters program office: OSSA

Xenon Fractionation in Porous Planetesimals

Kevin Zahnle, James B. Pollack, James F. Kasting

Noble gas elemental and isotopic abundance patterns should, in principle, provide constraints on the formation and early evolution of the terrestrial planets and their atmospheres, but at present these patterns are poorly understood. One long-standing problem is that terrestrial xenon is isotopically much heavier than any of its supposed sources, including the solar nebula and carbonaceous meteorites. Yet by contrast terrestrial krypton (Kr), a lighter element than xenon (Xe), is not significantly fractionated. Moreover, the terrestrial Kr/Xe ratio is roughly 50% above solar, again quite distinct from other solar system materials. These observations pose a severe problem for single source models for planetary rare gases, since fractionation and loss processes act preferentially on the lighter gas. Thus, the fundamental problem of terrestrial xenology is how xenon became both fractionated and depleted, while krypton was left seemingly unaffected.

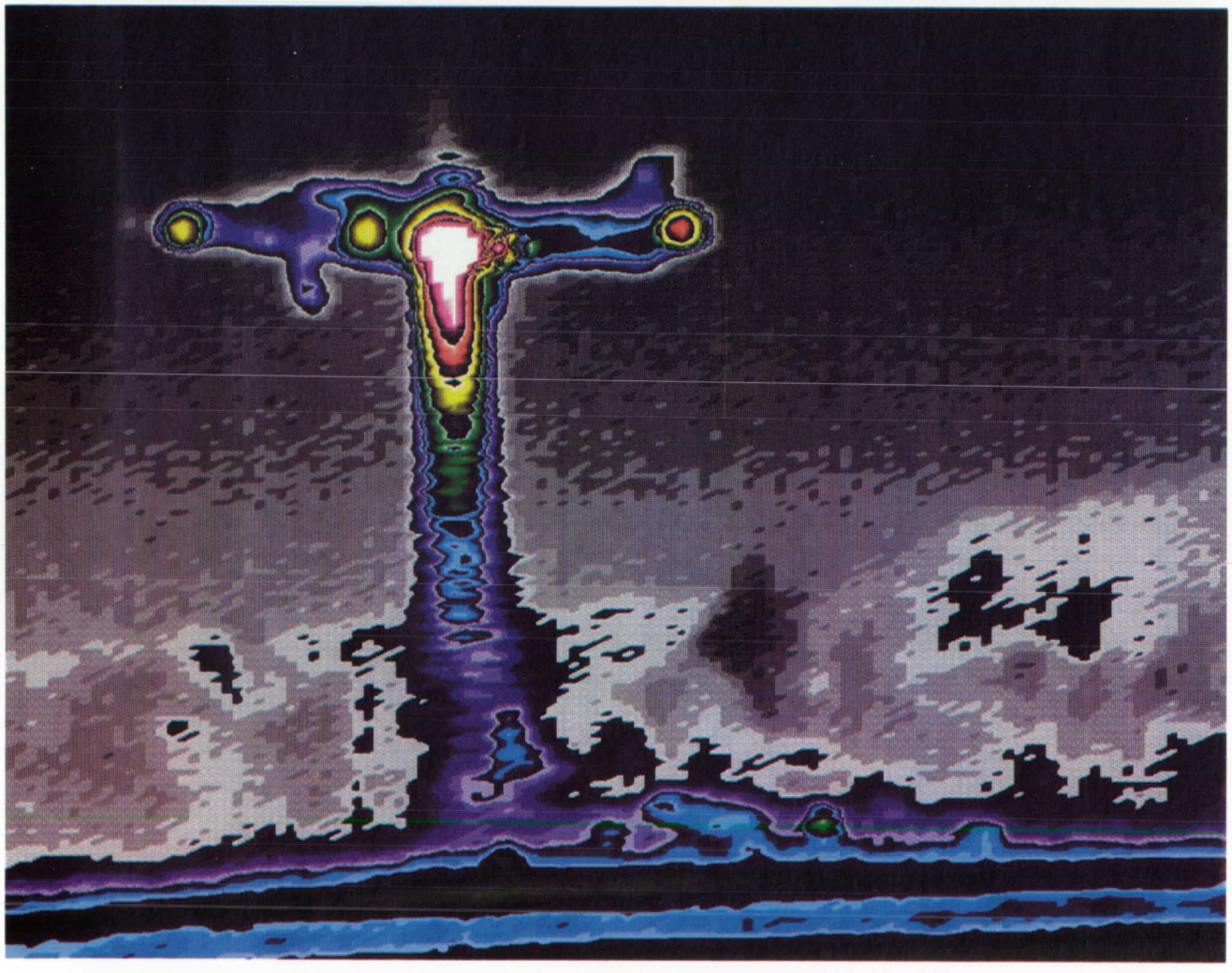
The detection of probable atmospheric gases trapped in meteorites from Mars has revealed a second solar system inventory broadly similar to Earth's, and dissimilar to solar or meteoritic inventories. The similarities between Earth and Mars imply a common source or sources for krypton and xenon. In this study we identify a mechanism that naturally produces a xenon-rich source material for both planets with the observed isotopic fractionation.

We hypothesize that xenon fractionation was caused by gravitational separation of adsorbed solar nebular gases inside large porous planetesimals. In our model, xenon is first adsorbed in small cold bodies in the nebula. These accumulate to form planetesimals large enough to have significant self-gravity. Inside the planetesimals, temperatures rise enough to release most of the adsorbed xenon. The gas phase xenon sinks and is diffusively separated and concentrated by gravity, with its heavier isotopes most greatly concentrated. We point out that xenon would have been trapped as the planetesimals grew and pores were squeezed shut by lithostatic pressure. The degree of fractionation is controlled by the lithostatic pressure at the pore-closing front (roughly 1-1.2 kilobars), and so would have been roughly the same for all large planetesimals.

The predicted degree of fractionation agrees well with that preserved in terrestrial and martian xenon. We also show that enough fractionated xenon to supply Earth could have been trapped this way. Relative to xenon, this source is strongly depleted in other noble gases. That a very similar process is observed to occur in terrestrial polar ice sheets, in which fractionated air is trapped at the transition between snow and ice, clearly shows that the mechanism is physically realistic.

Ames-Moffett contact: K. Zahnle
(415) 604-3148 or FTS 464-3148
Headquarters program office: OSSA

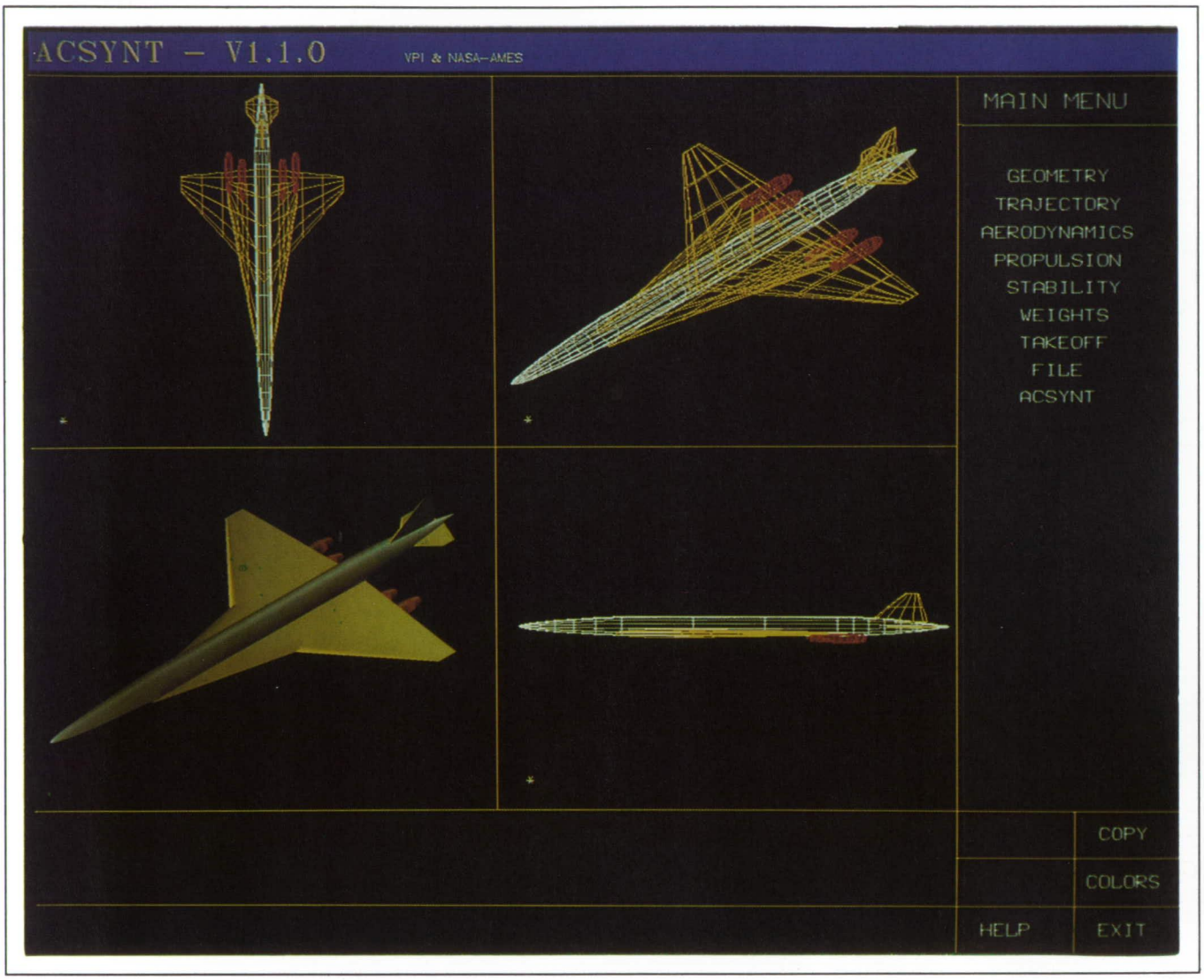
To amplify the details in the black and white photographs for some papers, the reader has been referred to corresponding special color plates in this appendix. Each caption provides the location of the corresponding paper.



Color plate 1. Infrared image of YAV-8B Harrier in hover (see fig. 1, page 4)

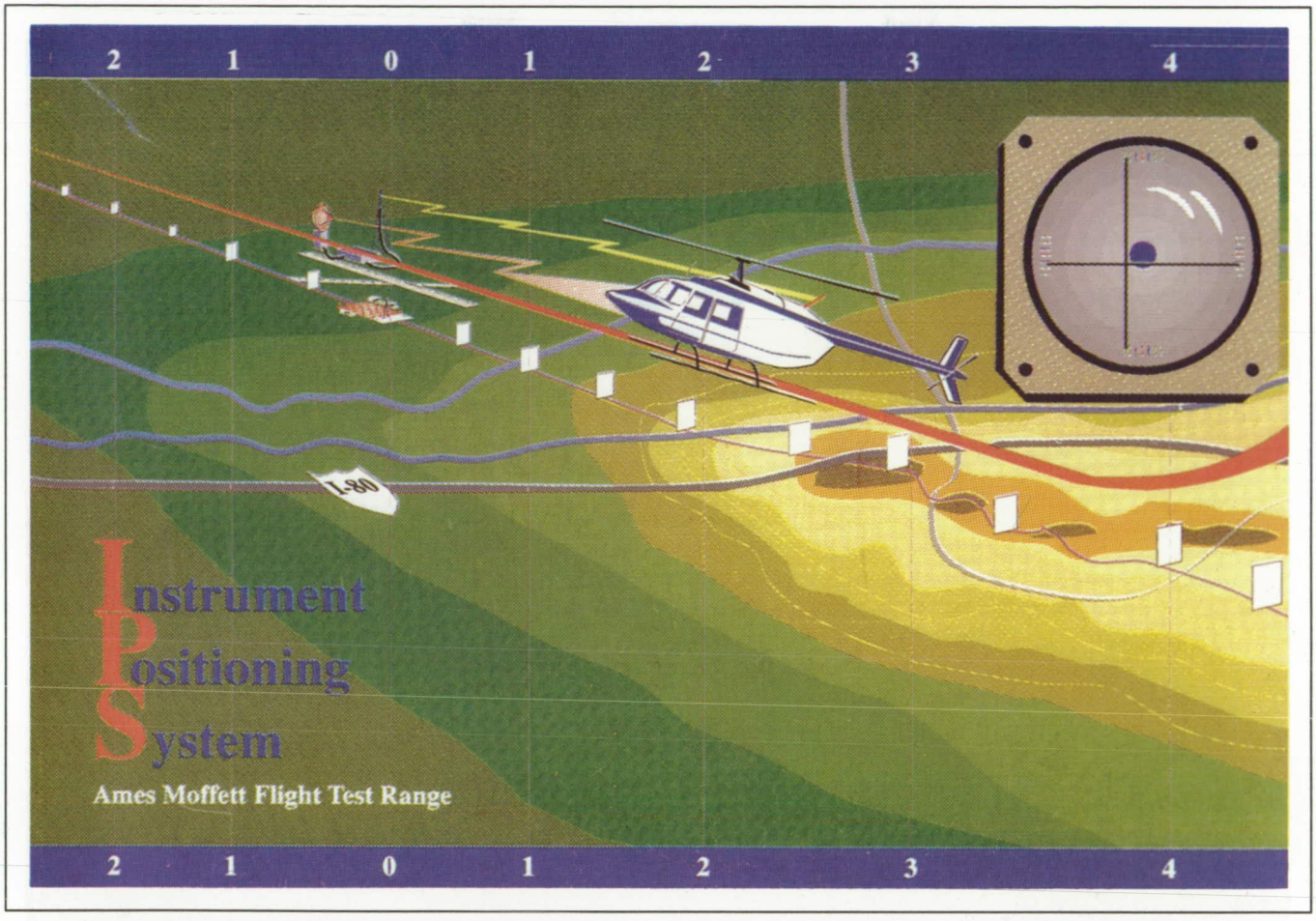
ORIGINAL PAGE
COLOR PHOTOGRAPH

PRECEDING PAGE BLANK NOT FILMED
450 INTENTIONALLY BLANK



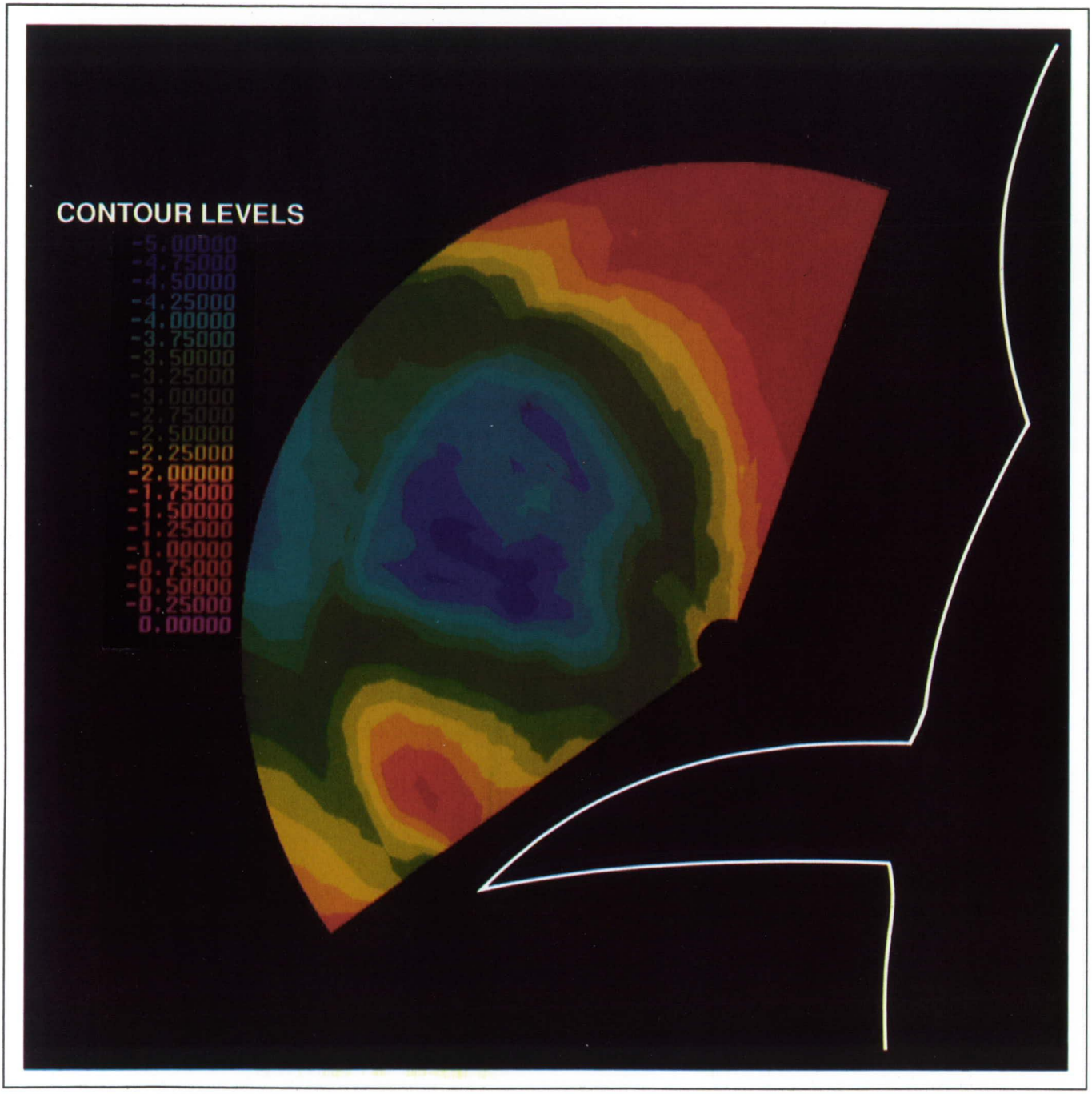
Color plate 2. ACSYNT geometry modeling interface (see fig. 1, page 12)

ORIGINAL PAGE
COLOR PHOTOGRAPH



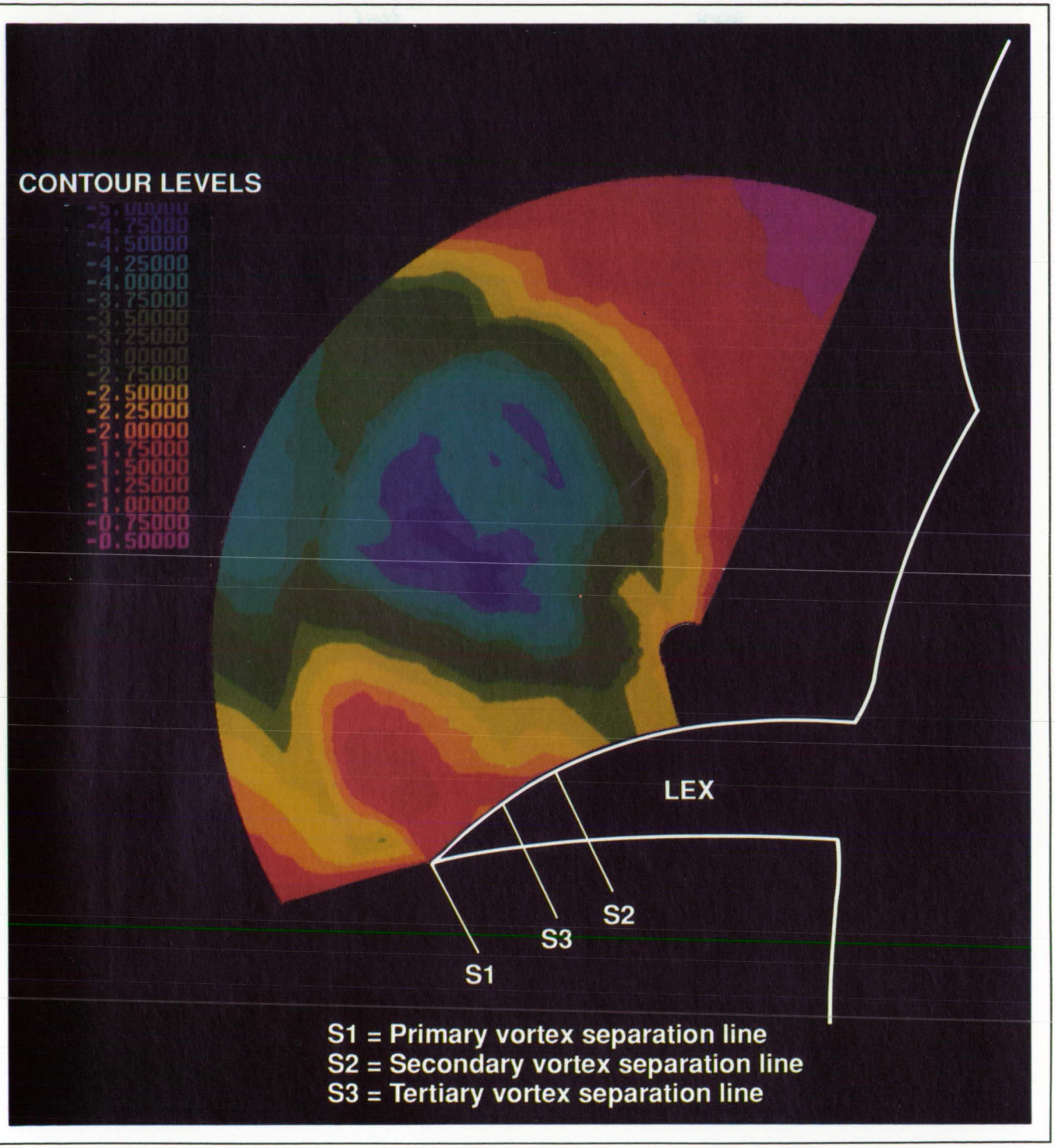
Color plate 3. Instrument positioning system at the Navy Crows Landing Facility (see fig. 1, page 25)

ORIGINAL PAGE
COLOR PHOTOGRAPH



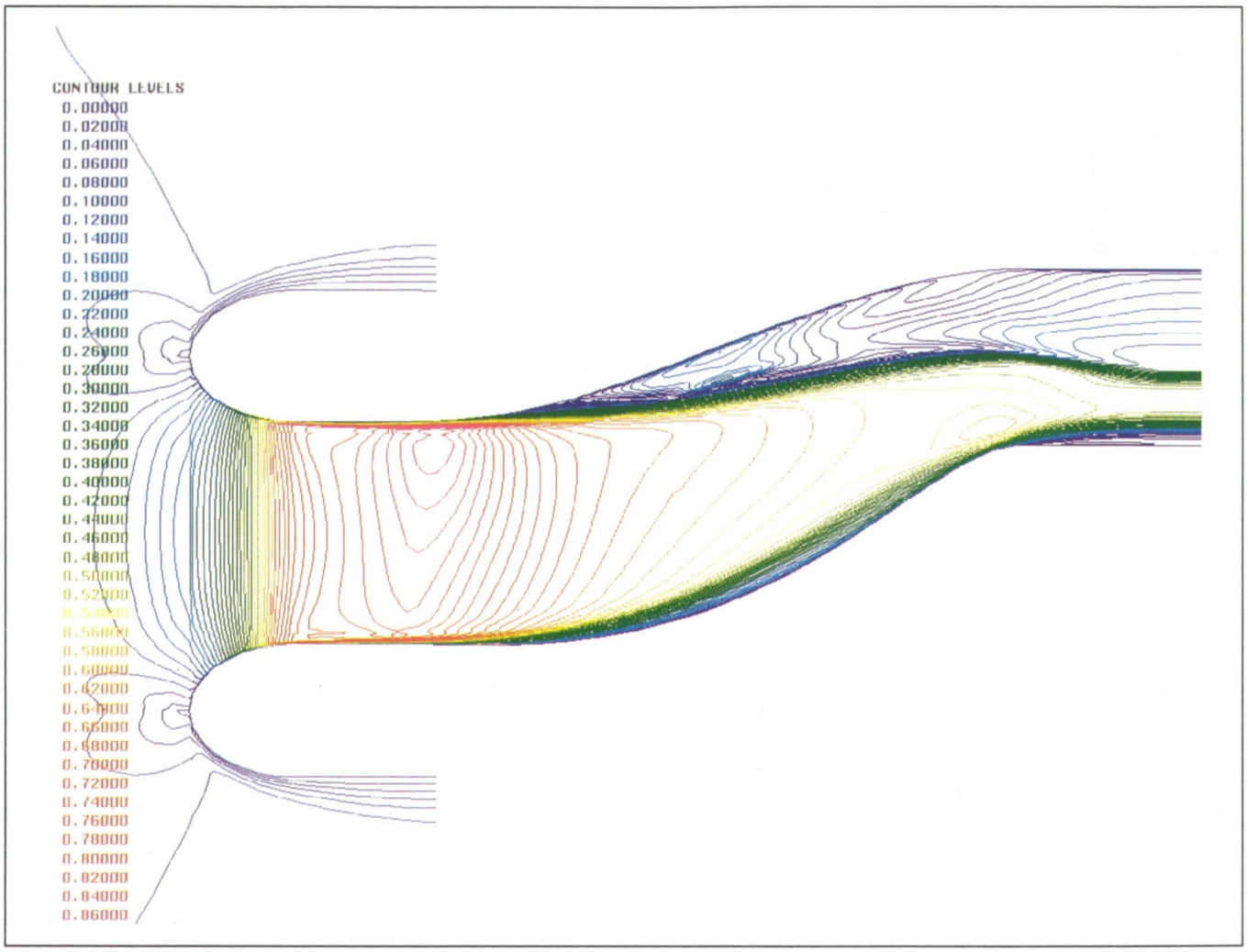
Color plate 4. Local static pressure measured through LEX vortex with LEX vortex survey rake (see fig. 3, page 228)

ORIGINAL PAGE
COLOR PHOTOGRAPH



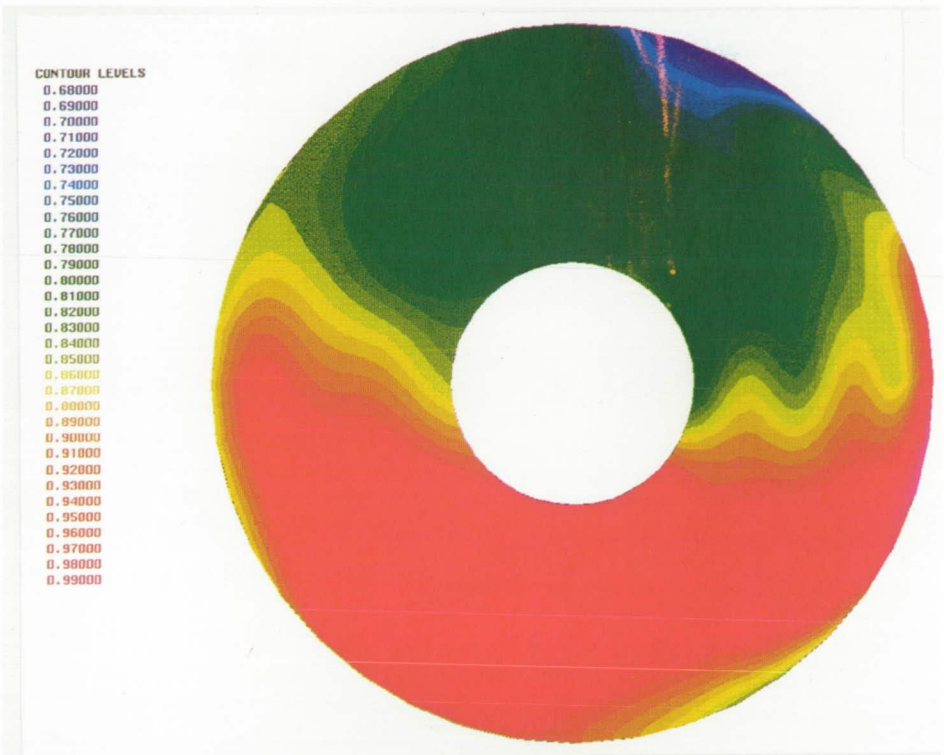
Color plate 5. Correlation of off-surface and surface LEX static pressure coefficients with surface flow visualization results (see fig. 4, page 228)

ORIGINAL PAGE
COLOR PHOTOGRAPH

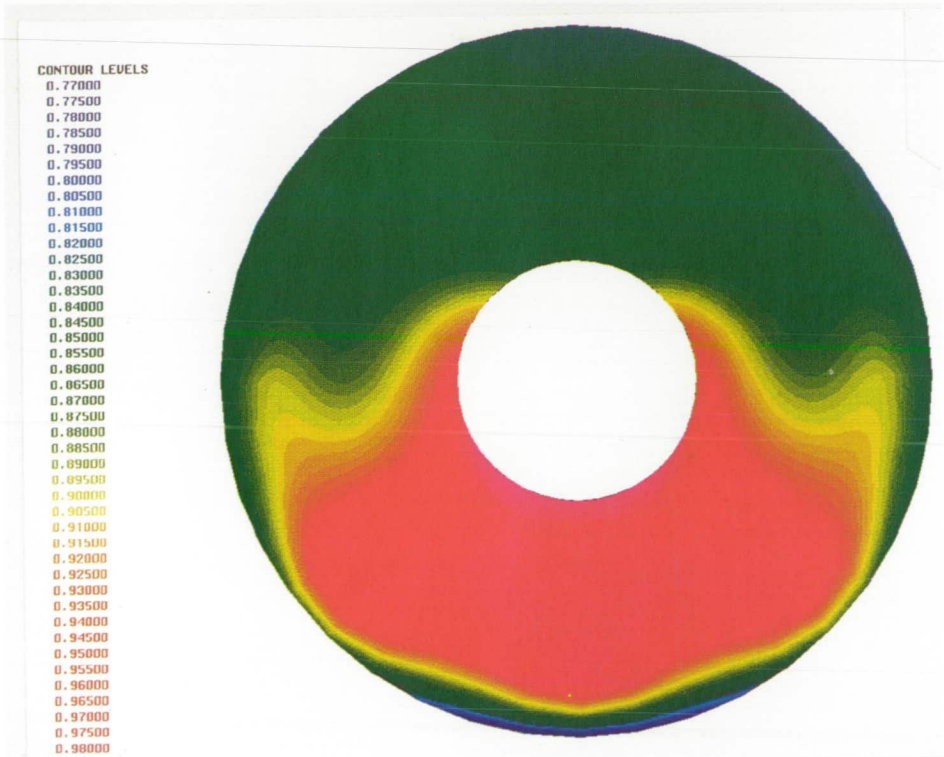


Color plate 6. Computed Mach contours, $p_{exit}/p_{\infty} = 0.8$ (see fig. 3, page 237)

ORIGINAL PAGE
COLOR PHOTOGRAPH



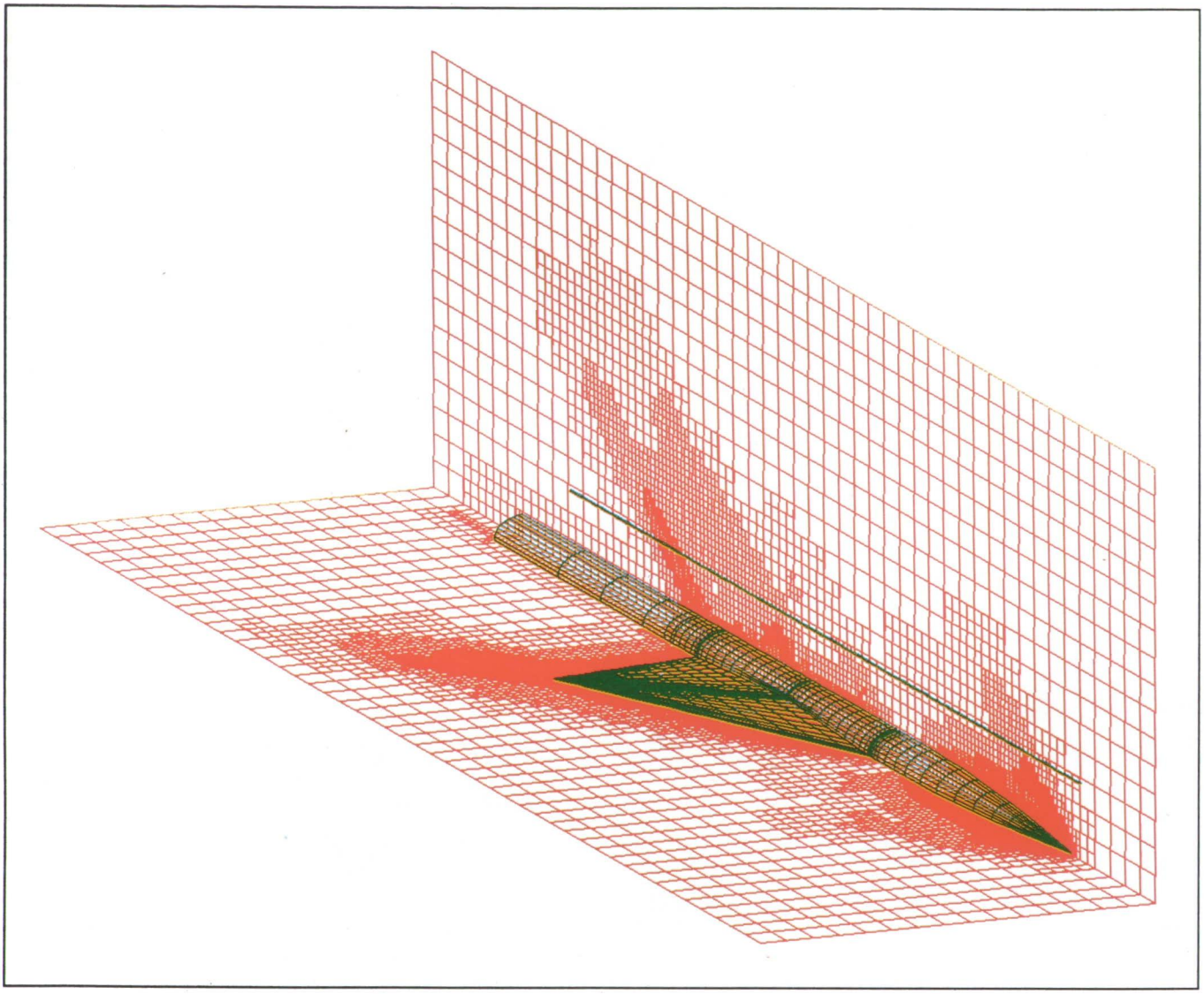
(a)



(b)

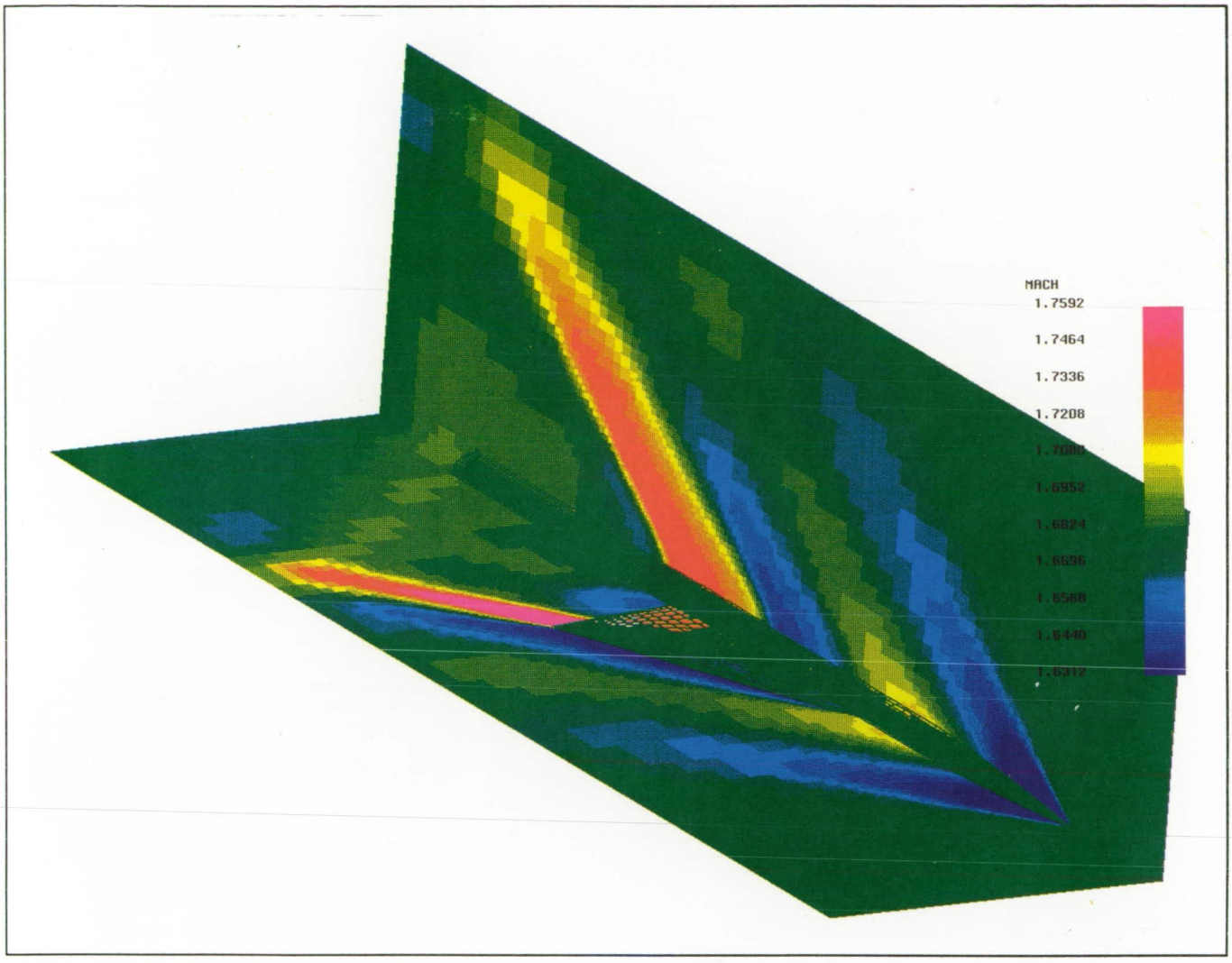
Color plate 7. Total pressure on engine face, $p_{exit}/p_{\infty} = 0.8$. (a) Computed, (b) experimental (see fig. 4, page 238)

ORIGINAL PAGE
COLOR PHOTOGRAPH



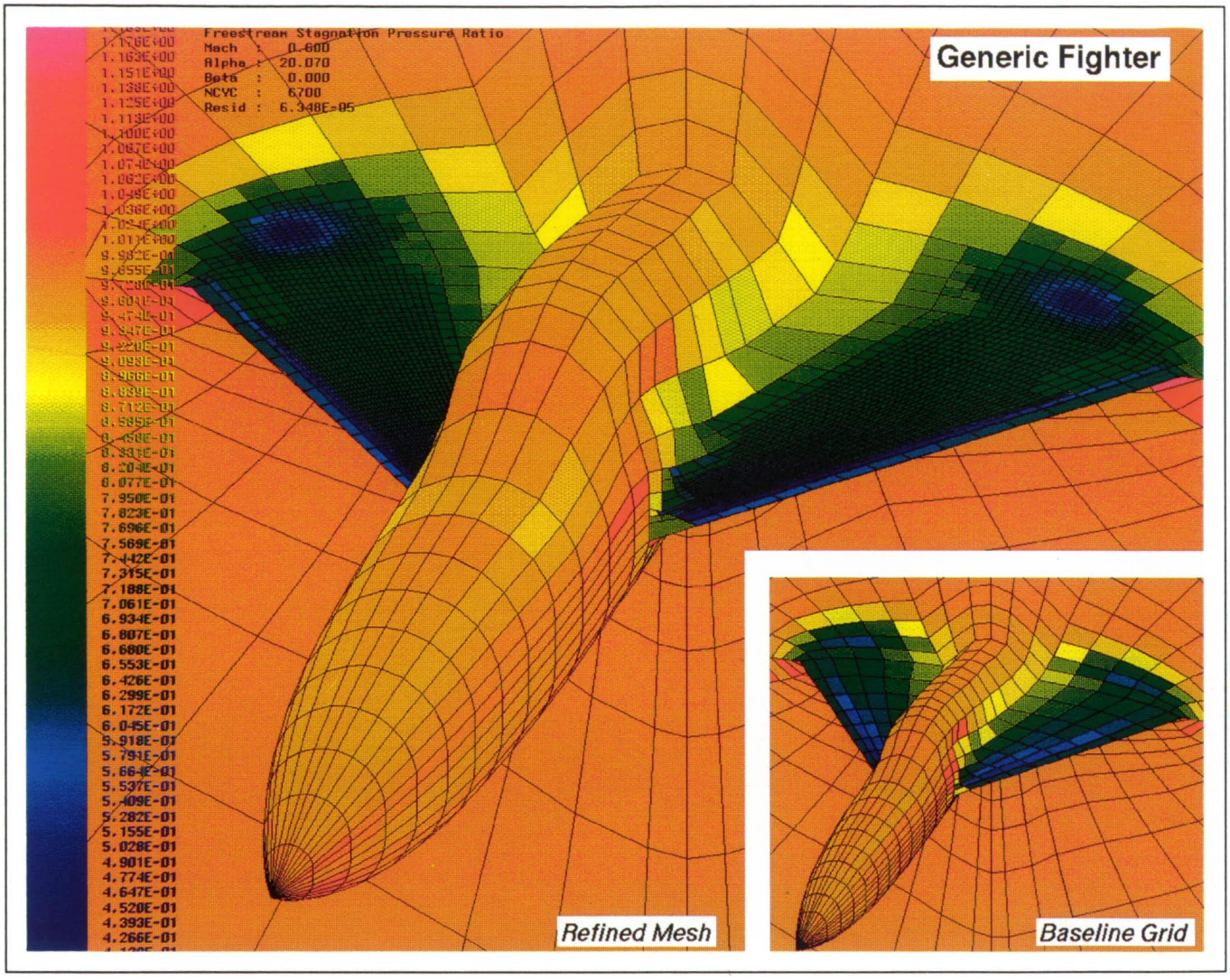
Color plate 8. Refined grid for wing/body geometry from TranAir (see fig. 1, page 245)

ORIGINAL PAGE
COLOR PHOTOGRAPH



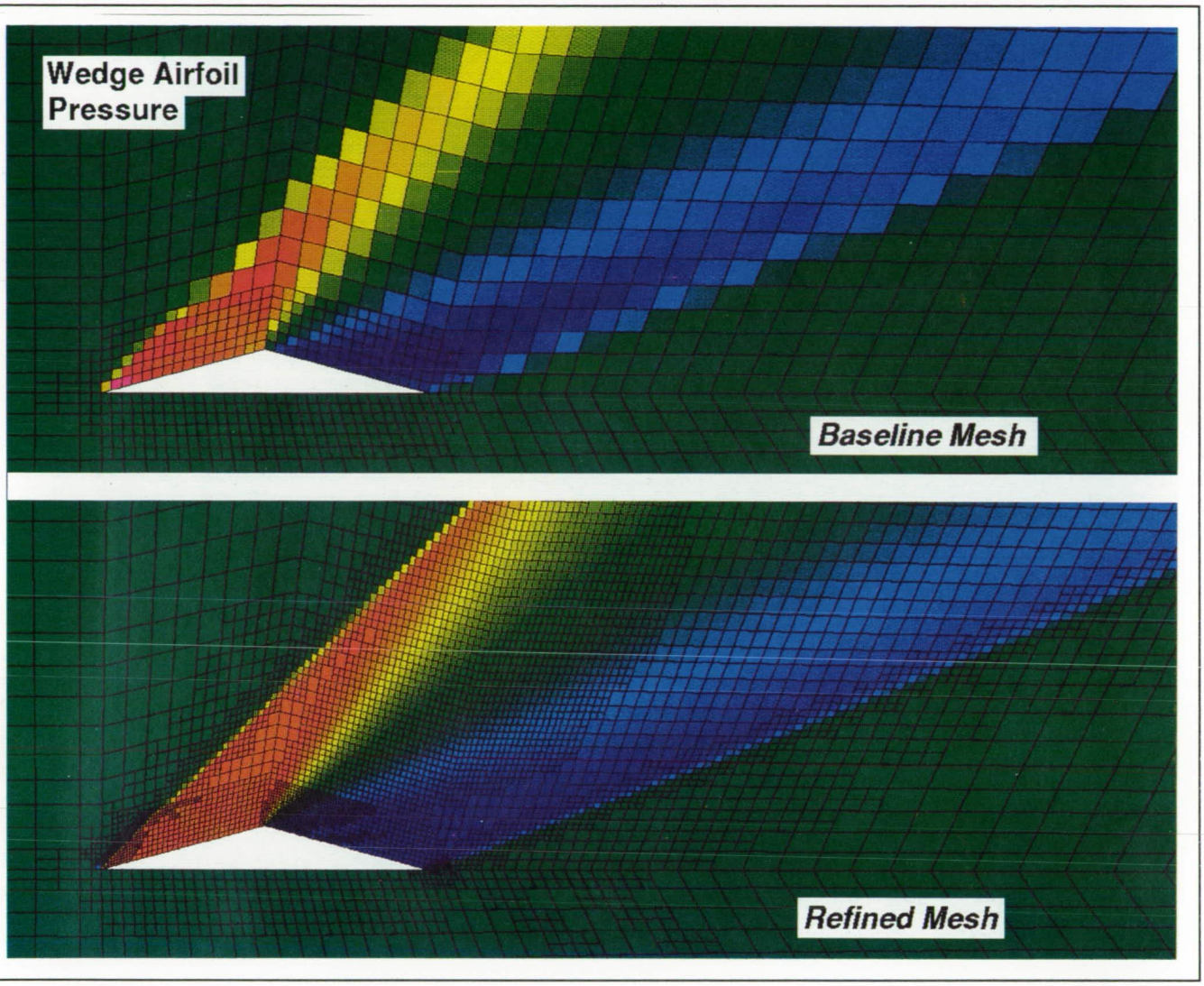
Color plate 9. Centerline Mach Number contours for wing/body geometry at M = 1.68 and α = 0 (see fig. 2, page 245)

ORIGINAL PAGE
COLOR PHOTOGRAPH



Color plate 10. Generic fighter (see fig. 1, page 247)

ORIGINAL PAGE
COLOR PHOTOGRAPH



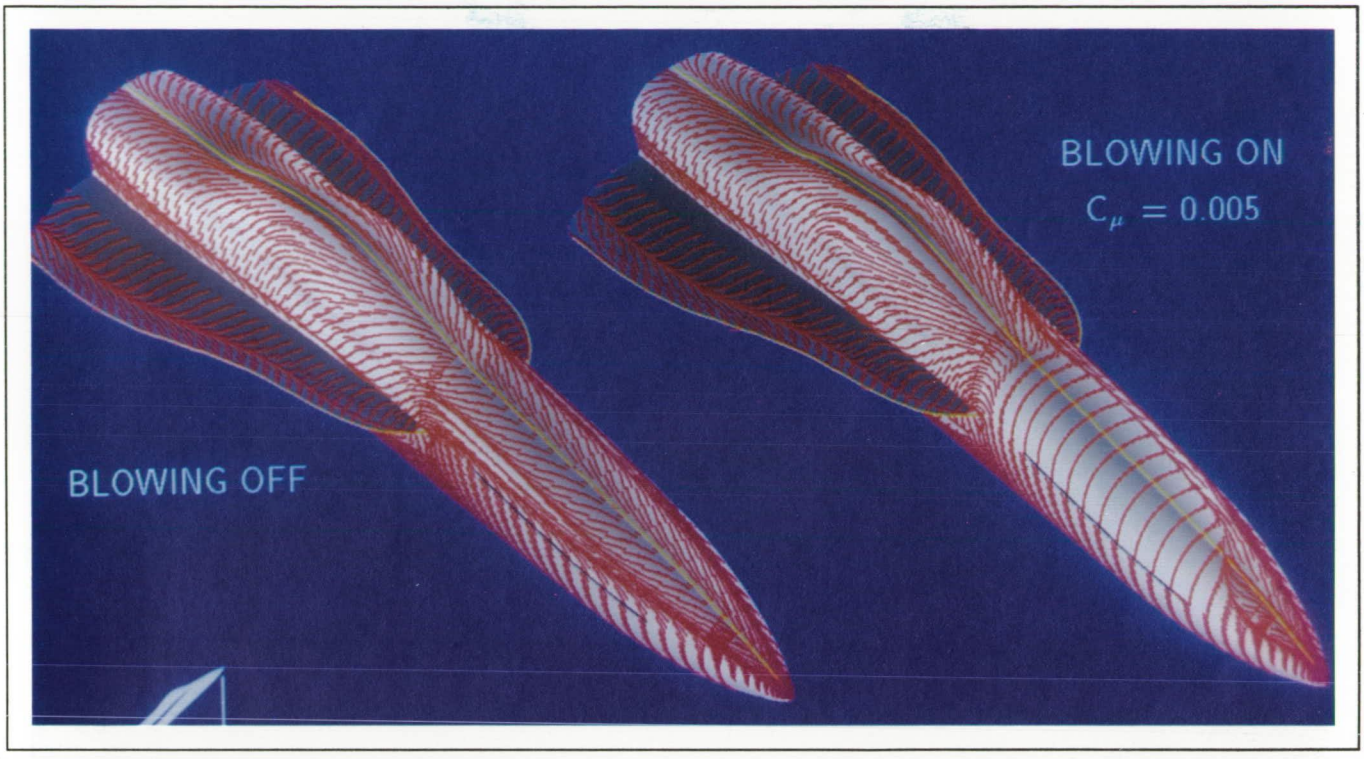
Color plate 11. Wedge airfoil pressure (see fig. 2, page 247)

ORIGINAL PAGE
COLOR PHOTOGRAPH



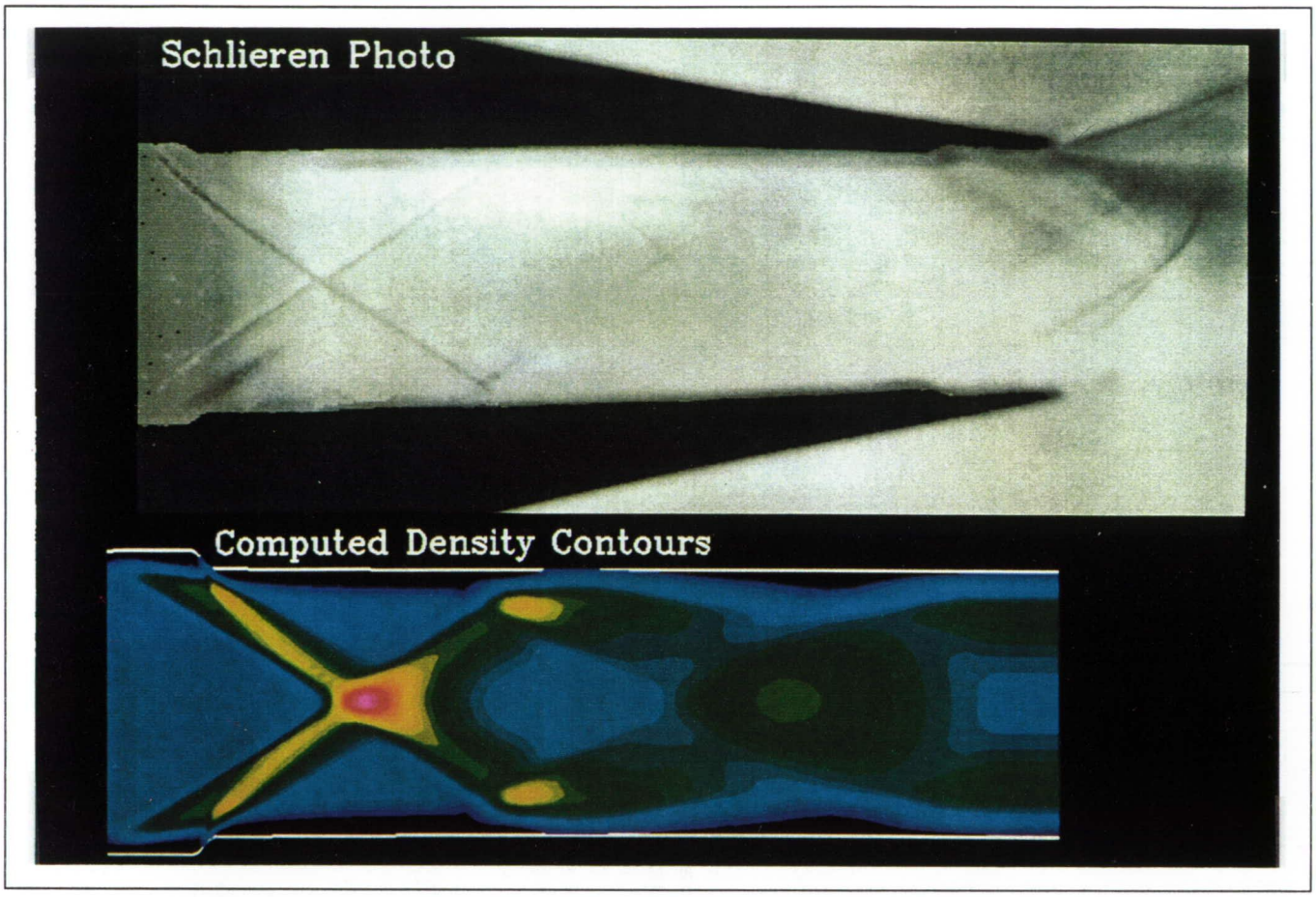
Color plate 12. Computed flow structures about F-18 wing and body, $M_\infty = 0.243$, $\alpha = 30.3°$, $Re_{\bar{c}} = 11.0 \times 10^6$ (see fig. 1, page 266)

ORIGINAL PAGE
COLOR PHOTOGRAPH



Color plate 13. Effect of asymmetric tangential blowing on the F-18 surface flow pattern, $M_\infty = 0.2$, $\alpha = 30°$, $Re_{\bar{c}} = 11.52 \times 10^6$ (see fig. 1, page 268)

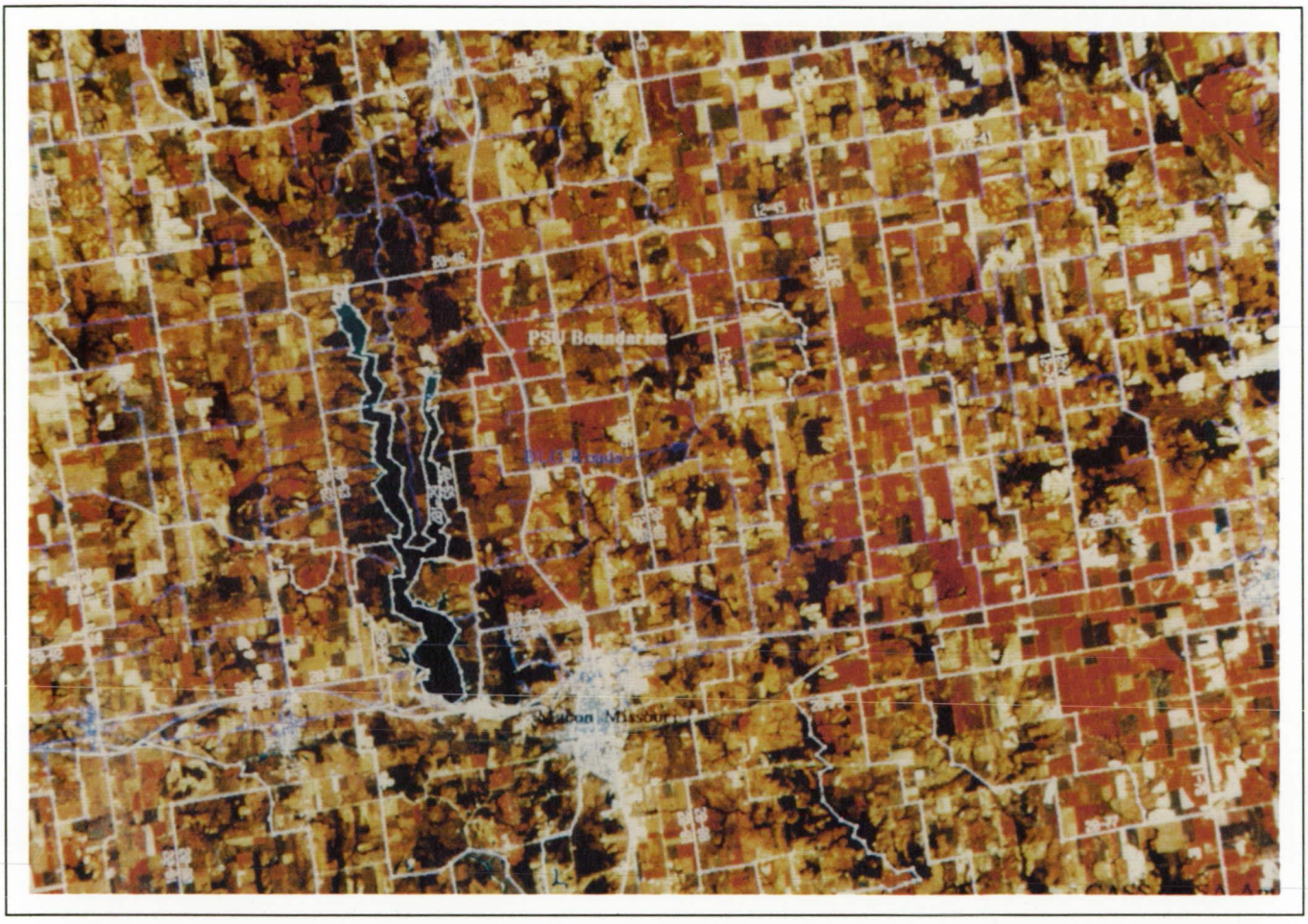
ORIGINAL PAGE
COLOR PHOTOGRAPH



Color plate 14. Comparison of observed and predicted wave patterns in a Proof-of-Concept supersonic diffuser (see fig. 2, page 270)

ORIGINAL PAGE
COLOR PHOTOGRAPH

C-6



Color plate 15. Digital Line Graph (DLG) and primary sampling unit (PSU) boundaries. A 1024- by 1280-pixel window of Thematic Mapper image of Macon County, Missouri, was displayed using channel 1, 3, and 5 in blue, green, and red, respectively. The highly vegetated area appears to be bright red. Using two graphic overlay planes, DLG roads were overlaid in blue, and the PSUs boundaries were overlaid with strata labels in white (see fig. 2, page 312)

ORIGINAL PAGE
COLOR PHOTOGRAPH

REPORT DOCUMENTATION PAGE

Form Approved
OMB No. 0704-0188

Public reporting burden for this collection of information is estimated to average 1 hour per response, including the time for reviewing instructions, searching existing data sources, gathering and maintaining the data needed, and completing and reviewing the collection of information. Send comments regarding this burden estimate or any other aspect of this collection of information, including suggestions for reducing this burden, to Washington Headquarters Services, Directorate for information Operations and Reports, 1215 Jefferson Davis Highway, Suite 1204, Arlington, VA 22202-4302, and to the Office of Management and Budget, Paperwork Reduction Project (0704-0188), Washington, DC 20503.

1. AGENCY USE ONLY *(Leave blank)*	2. REPORT DATE	3. REPORT TYPE AND DATES COVERED
	April 1992	Technical Memorandum – Fiscal Year 1990

4. TITLE AND SUBTITLE
Research and Technology 1990

5. FUNDING NUMBERS

6. AUTHOR(S)
Ames-Moffett and Ames-Dryden Investigators

7. PERFORMING ORGANIZATION NAME(S) AND ADDRESS(ES)
Ames Research Center
Moffett Field, CA 94035-1000

8. PERFORMING ORGANIZATION REPORT NUMBER
A-91054

9. SPONSORING/MONITORING AGENCY NAME(S) AND ADDRESS(ES)
National Aeronautics and Space Administration
Washington, DC 20546-0001

10. SPONSORING/MONITORING AGENCY REPORT NUMBER
NASA TM-103850

11. SUPPLEMENTARY NOTES
Point of Contact: Dr. Charles A. Smith, Executive Assistant to the Director, Ames Research Center, MS 200-1, Moffett Field, CA 94035-1000 (415) 604-5113 or FTS 464-5113
or the Ames telephone number(s) at the end of each article

12a. DISTRIBUTION/AVAILABILITY STATEMENT
Unclassified — Unlimited
Subject Category 99

12b. DISTRIBUTION CODE

13. ABSTRACT ***(Maximum 200 words)***

Selected research and technology activities at Ames Research Center, including the Moffett Field site and the Dryden Flight Research Facility, are summarized. These accomplishments exemplify the Center's varied and highly productive research efforts for 1990.

14. SUBJECT TERMS
Aeronautics, Space technology, Transatmospherics, Space sciences, Earth sciences, Life sciences, Research and technology

15. NUMBER OF PAGES
486

16. PRICE CODE
A21

17. SECURITY CLASSIFICATION OF REPORT	18. SECURITY CLASSIFICATION OF THIS PAGE	19. SECURITY CLASSIFICATION OF ABSTRACT	20. LIMITATION OF ABSTRACT
Unclassified	Unclassified		